STATE OF CALIFORNIA
The Resources Agency

Department of Water Resources

Bulletin No. 63-4

Sea-Water Intrusion:

AQUITARDS
IN THE COASTAL GROUND WATER BASIN
OF OXNARD PLAIN, VENTURA COUNTY

A Joint Study by
State of California
Department of Water Resources

and

University of California
Department of Civil Engineering
Geotechnical Engineering
Berkeley

SEPTEMBER 1971

STATE OF CALIFORNIA

The Resources Agency

Department of Water Resources

Bulletin No. 63-4

Sea-Water Intrusion:

AQUITARDS
IN THE COASTAL GROUND WATER BASIN
OF OXNARD PLAIN, VENTURA COUNTY

A Joint Study by

State of California
Department of Water Resources

and

University of California
Department of Civil Engineering
Geotechnical Engineering
Berkeley

SEPTEMBER 1971

FOREWORD

The purpose of this bulletin is to present information on one of the last unknown
res of ground water reservoirs: the aquitards. In many underground basins, these
tions, which are of low permeability, serve to separate the aquifer systems into water-
ng layers. Various studies have given hints of the capabilities, limitations, and com-
ties of aquitards, but, heretofore, no definitive study had been made. In recent years,
rowing interest in management of basins, in use of basins as storage and disposal sites,
n establishment of boat marinas that encroach upon coastal basins has made urgent our need
derstand the potentialities of aquitards.

With these thoughts in mind, the Department of Water Resources, using authority vested
 under Section 229 of the California Water Code, contracted with the University of California
dertake research into the nature of aquitards. This work was conducted by the Geotechnical
eering Group of the Department of Civil Engineering under the supervision of Dr. Paul A.
rspoon, as principal investigator, and Dr. James K. Mitchell, as co-investigator. It has
d as the project on which three of the University's graduate students have completed their
rates, one has developed a doctoral problem, and a fifth has completed work for his masters
e.

The agreement between the Department and the University, signed in 1967, specified that
nvestigation was to be of those aquitards within a coastal ground water basin. A coastal
 was selected because these basins in particular face possible degradation as their fresh
 is pumped out and sea water is drawn in. A number of artificial barriers have been tried
alting this trend, with varying degrees of success. But, investigators have suspected,
atural barriers--the aquitards--might be used if their characteristics were fully understood.

The Oxnard Plain of Ventura County seemed almost tailor-made for this research: its
d water basin consists of a number of layers of aquifers separated by aquitards, the upper
er is known to be intruded by sea water, and the basin as a whole has been extensively
ed in recent years.

The first indication of trouble in the aquifers of the Oxnard Plain came in the 1930's
water levels in the topmost aquifer were found to have declined to about 5 feet above sea
 in most of the basin and to below sea level in the vicinity of Port Hueneme. At that
sea-water intrusion was detected as much as a half mile inland. A wet period of approximately
ars brought a recovery of water level elevations and a temporary halt to the sea-water in-
on. But, by 1945, water levels were once again declining and, by 1949, they were as much
 feet below sea level. Since then, the front of the intruding sea water has moved further
d. By 1966, almost 6,100 acres were known to be underlain by water containing high
ides, which are regarded as indicators of the presence of sea water.

Meantime, the Department of Water Resources had undertaken a study of the extent of the
sion and of underground conditions; from this study came recommendations for measures that
 be taken to stem the intrusion. As a result, the State Legislature in 1965 appropriated
000 to construct and operate an experimental extraction-type barrier to attempt to control
ntrusion. A 2-year test proved the barrier is technically feasible, but it pointed up the
for additional study of underground conditions in the Oxnard Plain before a full-scale
er is constructed.

An important phase of this additional study, which is reported in this bulletin, is
rned with the aquitards. However, it has not only added to our understanding of conditions
n the Oxnard Basin, but it has also contributed materially to our knowledge of the nature
haracter of ground water basins in general.

William R. Gianelli.

William R. Gianelli, Director
Department of Water Resources
The Resources Agency
State of California

TABLE OF CONTENTS

TABLES

ABSTRACT

This report gives the results of a comprehensive program of investigation on aquitards, i.e., the fine-grained sediment that act as confining layers in ground water systems. Since little is known about the hydraulic properties of aquitard materials or methods for their investigation, a three-year program of research was set up under the joint sponsorship of the State of California, Department of Water Resources and the University of California, Berkeley, with the Oxnard Coastal Plain of Ventura County as a focal point. The overall objective was to develop a better understanding of aquitards in the coastal ground water basins of California and particularly their relationship to sea water intrusion.

Field, laboratory and theoretical analyses have helped to define the important role that aquitards play in controlling ground water movement in the Oxnard Basin. Contrary to the usual concept that aquitards are effective confining beds, the results of this work show that, at least in the Oxnard test area near Port Hueneme, these beds have a small but significant permeability. This basin is clearly a system of leaky aquifers. This was proven by a series of pumping tests and a new method of analyzing the field data. To support this method, a more complete theory than has heretofore been available for transient flow in leaky aquifers was developed. This new theory was used to support the "ratio" method of evaluating hydraulic properties of aquitards.

Using the ratio method, the aquitard overlying the Oxnard aquifer was found to have an average permeability of 0.025 gpd/ft^2; the aquitard underlying is somewhat more permeable, 0.042 gpd/ft^2. By contrast the permeability of the aquifer is 1,405 gpd/ft^2. The aquitard overlying the Oxnard aquifer has a specific storage coefficient of 2.4×10^{-1} ft^{-1}; the aquitard underlying is somewhat less, 1.0×10^{-4} ft^{-1}. These results, however are about a hundred times larger than the storage value obtained for the aquifer, 1.2×10^{-6} ft^{-1}.

An independent evaluation of aquitard materials in the Oxnard Basin was also made through laboratory studies on core samples. Selected samples were studied with regard to composition, consolidation, permeability, and effects of replacing the natural pore fluids by salt water. The aquitard sediments are predominantly in the silt size and are mainly composed of quartz and clay minerals. The clay content is generally less than 20 percent and is dominantly montmorillonite with lesser amounts of kaolinite and illite. Permeabilities vary erratically depending on grain size and range from 0.1 to less than 0.001 gpd/ft^2. Leaching the clay-rich fractions of these core samples with salt water having a NaCl concentration equal to that of sea water did not seem to have any significant effects on permeability.

A second theoretical study was also carried out on the mechanism and effects of chemico-osmotic diffusion. This study shows that when an aquitard is low in permeability because of a significant clay content (i.e. ~0.001 gpd/ft^2), diffusion becomes an important mechanism for moving salt ions through such beds. Whether such movement can cause degradation of fresh water layers will depend on the thickness of the aquitard and the presence of any hydraulic gradients that may have developed. However, if a coastal basin has aquitard permeabilities as high or higher than those found at Oxnard, the process most likely to cause significant amounts of non-potable waters to move across such aquitards will probably be that of convective movement due to a hydraulic gradient.

The implications of this work with regard to sea water intrusion, development of marinas, accumulation of poor quality waters in semiperched zones, ground water recharge, and rate of migration through aquitard layers are reviewed. All of these considerations lead to the more general problem of the level of field observation that is necessary in multiple aquifer systems where leakage across aquitards poses a threat to ground water resources. This will require further field and laboratory work similar to that of this investigation plus appropriate measurements of the hydraulic heads that can develop across aquitards.

It is concluded that in utilizing the ground water resources of coastal basins, such as those of California, the ability of aquitards to control water intrusion on the one hand, and to contribute to recharge on the other, must be carefully evaluated in any effective program of water resource management.

CHAPTER I. INTRODUCTION

P. A. Witherspoon

A. OBJECTIVES

The overall objective of this investigation is to develop a better understanding of the role of aquitards in the coastal ground water basins of California and particularly their relationship to sea water intrusion.

Since little is known about the hydraulic properties of aquitard materials or methods for their investigation, a comprehensive three-year program of research was set up under the joint sponsorship of the State of California, Department of Water Resources and the University of California, Berkeley, with the Oxnard Coastal Plain of Ventura County as a focal point. A general location map is shown in Figure I-1.

This research program had the following specific objectives:

(1) to develop improved field methods of evaluating hydraulic properties of aquitards

(2) to investigate the physical and hydraulic properties of aquitard materials in the laboratory

(3) to investigate the theory of flow in multiple aquifer systems

(4) to investigate the theory of coupled flow of salt and water ions in clay layers

B. IMPORTANCE OF AQUITARDS IN GROUND WATER MOVEMENT

1. Problems with Sea Water Instrusion

Traditionally, ground water geologists as well as hydrologists have tended to focus their attention on the more permeable layers of a ground water basin in developing water supplies. Obviously they need to locate the best aquifer conditions to provide wells that would be adequate for the long range needs of the consumer.

In the coastal ground water basins of California, there generally have been no serious problems in finding water. These basins usually contain thick deposits of highly productive sands and gravels that have been deposited as multiple-aquifer systems. Such systems, contain a series of aquifers that are separated by aquitards, i.e., confining layers of relatively low permeability clays and silts.
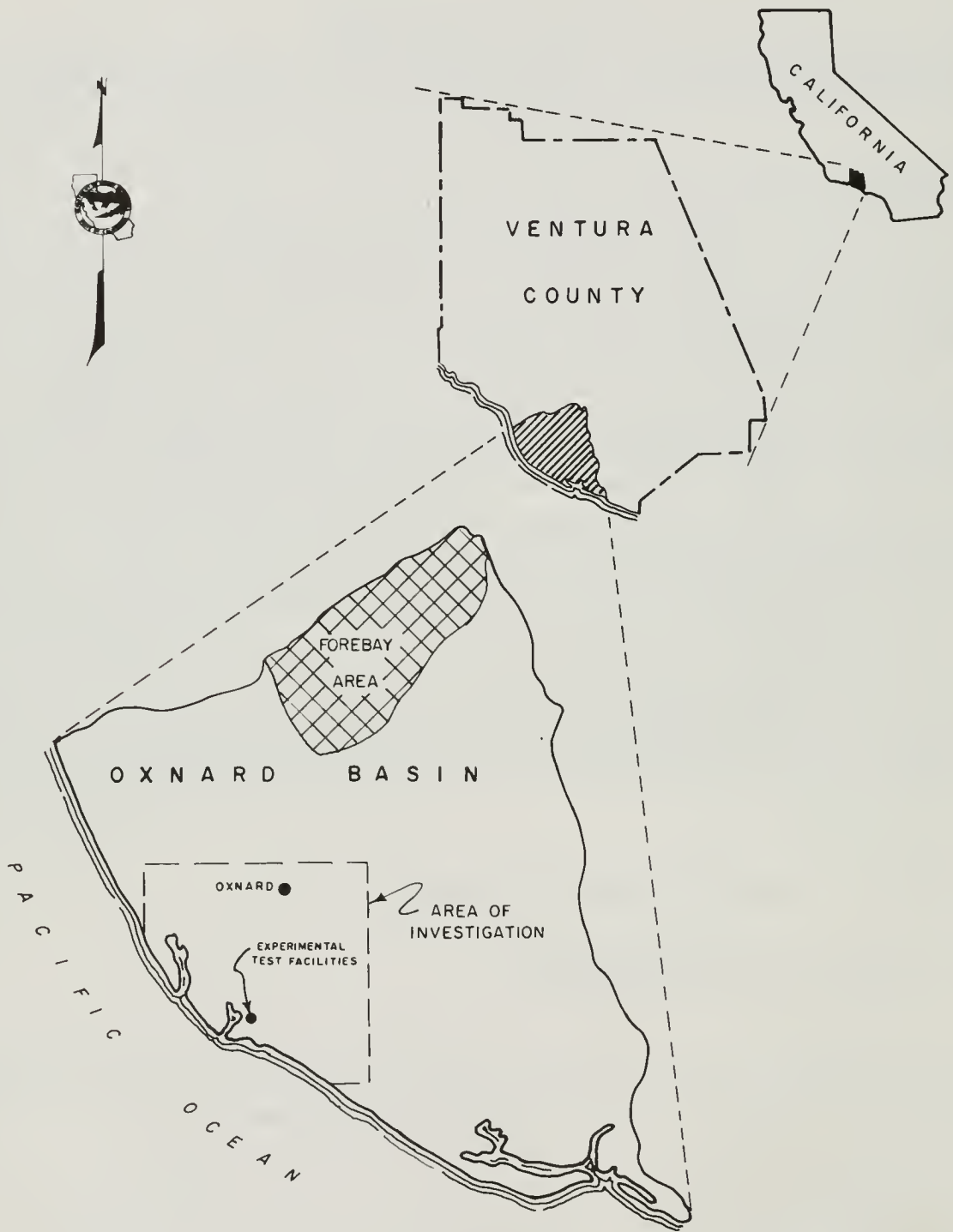
Fig. I-1. Location map

The problem in managing these coastal basins has been more that of determining the appropriate rate at which to produce water. Years ago when consumptive use of water was limited, demands were easily met. But as population and agricultural centers began to grow rapidly in the coastal areas of California, the water requirements increased enormously. For a time, these increasing needs could be met by simply drilling and equipping more wells. What was apparently not realized, however, was that the coastal aquifers were connected with the ocean by outcrops out on the continental shelf. Thus, one need only develop a sufficient hydraulic gradient landward and sea water inevitably invaded those coastal areas wherever excessive pumpage persisted.

Sea water intrusion in California has been well documented. The following is only a partial list of the reports that have been published by the State of California, Department of Water Resources:

(1) "Investigation of Ground Water Pollution of Bolsa Chica Mesa-Sunset Beach, California," Office Report, January 1958;

(2) "Sea-Water Intrusion in California," Bulletin No. 63, November 1958;

(3) "Quality of Ground Waters in California, 1955 through 1959," Bulletins Nos. 66-55 through 66-59, June 1958 through February 1963;

(4) "Intrusion of Salt Water into Ground Water Basins of Southern Alameda County," Bulletin No. 81, December 1960;

(5) "Sea-Water Intrusion, Oxnard Plain of Ventura County," Bulletin No. 63-1, October 1965;

(6) "Sea-Water Intrusion, Bolsa-Sunset Area Orange County," Bulletin 63-2, January 1968;

(7) "Sea-Water Intrusion, Pismo-Guadalupe Area," Bulletin No. 63-3, February 1970; and

(8) "Sea-Water Intrusion Lower Salinas Valley, Progress Report 1968-1969," June 1970.

Solutions to the disastrous effects of degradation by sea water have not been easy. Where shallow aquifers were developed as the first source of supply and brine concentrations became intolerable, the simplest solution has been to drill to deeper unaffected layers of fresh water. In other cases, the innovation of a hydraulic or dynamic barrier to prevent landward migration of sea water has been used, as in the case of the Los Angeles County Flood Control District [Bruington and Seares, 1965].

In employing these solutions, however, the role of the aquitards has largely been overlooked. For example, when the withdrawal of water is stopped from a degraded aquifer and simply started again in another aquifer beneath, a hydraulic gradient from the intruded toward the unintruded layer quickly develops. Since the permeability of the intervening aquitard is almost always unknown, how can one determine the rate at which sea water from a degraded zone may migrate vertically downward to an uninvaded zone? Such migration might take place long before horizontal intrusion by sea water from the relatively more distant outcrops out on the shelf could occur.

-3-

Another situation where the role of the aquitards in preventing sea water intrusion is largely unknown concerns the increasing development of marinas. Not only has an increasing population in California placed greater and greater demands on ground water resources, but the trend toward water sports has required the development of more and more shallow harbors for sea craft. The construction of such marinas requires the removal of some of the aquitard layers that normally have provided a natural barrier between the ocean and the fresh water aquifers beneath.

If the hydraulic head in such aquifers is reduced below sea level through local pumping, the same problem can develop of a gradient that moves sea water toward sources of fresh water. Thus, the question arises, how much of an aquitard layer can safely be removed during the construction of a marina? An accurate knowledge of aquitard properties is needed to have a reliable answer.

The above discussion has focussed on the movement of brine through aquitards under the influence of an hydraulic gradient, but it is also possible for salt ions to move through porous media by diffusion. In the presence of clay minerals, the coupled action of both hydraulic and chemical gradients must be considered to understand this migration. In those situations where one aquifer of a multiple-aquifer system has been intruded by sea water, there might not be any hydraulic gradient across an aquitard layer that confines the degraded zone, yet migration of salt ions toward fresh water would still occur. How rapidly can such migration take place, and just exactly what role does the aquitard play in this kind of mass transfer?

Problems of sea water intrusion are intimately concerned with the ability of aquitard materials to control migration, but the importance of these fine-grained sediments in controlling such phenomena is not well understood.

2. Problems with Regional Recharge and Subsidence

In developing a comprehensive program of management for a given basin, one should have a water budget that is applicable to the area under consideration. Such budgets require estimates of the magnitude of ground water recharge as well as overall use. Although such recharge is normally believed to take place in areas of aquifer outcrops, there is increasing evidence that the aquitards also play an important role. Gill [1969] has recently reported that substantial amounts of water being produced from the Potomac-Raritan-Mogothy aquifer system is coming through the aquitards within the system. Walton [1965] has also shown earlier how the Maquoketa Formation in Illinois, which is essentially a shale bed, serves as an effective transmitter of water between aquifers.

Furthermore, the contribution from storage in aquitards may far exceed that of the coarser grained sediments that make up the aquifers. As will be shown from the

results of both field and laboratory testing in the discussion that follows, the co-efficient of storage per foot of thickness (S_s) for the aquitards in the Oxnard basin is roughly two hundred times greater than that of the aquifers. Under such conditions, the local contribution of water from storage in the aquitards can be quite significant. The time for this phenomena to take place depends on the permeability of the fine-grained sediment, but this is another important aspect of the role of aquitards in multiple-aquifer systems.

At the same time that the aquitards give up some of their stored water, they also undergo another closely related phenomenon. The loss of water results in reduced pore pressures, which allows the structure of the fine-grained sediments to collapse to some degree. This collapse can lead to land subsidence that is practically irreversible. Poland and Davis [1969] have gathered a wealth of information on the relationship between land subsidence and water withdrawal from multiple-aquifer systems. Anyone attempting to predict such effects must understand the behavior of aquitard materials under the influence of pumping.

3. Problems with Underground Storage and Waste Disposal

For the past twenty years, aquifers at depths below 500 feet have been used for storing natural gas in the United States. One of the critical questions in such storage operations is the tightness of the aquitards that lie above these storage reservoirs. In this case, the main problem is that of determining the permeability of the aquitard layers, and it has been necessary to develop field methods to solve this problem [Witherspoon, et al. 1967]. Where the properties of the aquitards were not properly investigated, the gas industry has on occasion been witness to spectacular (and dangerous) effects of gas leakage.

It is also possible to store other kinds of fluids or to dispose of waste products underground provided such action does not lead to pollution of potable supplies of water. Proper protection of water resources requires that we understand the role of aquitards in these situations and develop reliable methods of testing the ability of the fine-grained sediments to act as barriers to migration.

4. Problems in Analyzing Pumping Tests

In analyzing results of water pumping tests, the well known Theis solution is customarily used to determine permeability and specific storage of the aquifer under investigation. As long as the aquitards do not leak significant amounts of water into the aquifer, this method of analysis produces reliable results.

However, groundwater hydrologists noted many years ago that deviations from the aquifer behavior as predicted by the Theis solution were not uncommon. Some of these deviations were caused by water leaking out of the confining beds, and this has led to the "leaky aquifer" theory of Hantush and Jacob [1955b]. This theory and its later modifications [Hantush, 1960a] relied only on an examination of aquifer behavior and attempted to relate such behavior to the properties of the adjacent aquitards.

Unfortunately, this theory has not been entirely satisfactory. When the degree of leakage is small, the method gives reliable results, but as leakage increases, certain errors are introduced. The errors are such that one tends to overestimate the permeability of the aquifer and underestimate the permeability of the confining beds. Furthermore, the theory does not provide a means of distinguishing whether the leaking beds lie above or below the aquifer being pumped. One tends to underestimate the importance of leakage and cannot identify the source completely. Here again, the role of aquitards in multiple aquifer systems must be understood if a reliable evaluation of the hydraulic properties of these fine-grained sediments is desired.

P. A. Witherspoon and J. K. Mitchell

A. REVIEW OF RESULTS

Field, laboratory and theoretical analyses have helped to define the important role that aquitards play in controlling ground water movement in the Oxnard coastal basin. These studies have led to several important findings. Contrary to the usual concept that aquitards are effective confining beds, our results show that, at least in the Oxnard test area near Port Hueneme, these beds have a significant permeability. This basin is clearly a system of leaky aquifers.

This was proven by a series of pumping tests and a new method of analyzing the field data. To support this method, a more complete theory than has heretofore been available for transient flow in leaky aquifers was developed. This theory is summarized in Chapter IV and the details are presented in Appendix A. This new theory was used to support the "ratio" method of evaluating hydraulic properties of aquitards.

1. Ratio Method of Analyzing Field Data

The ratio method relies upon measurements of drawdown in the aquitard while water is being pumped from an adjacent aquifer above or below. At any given time, drawdown at a known point in the aquitard, s', divided by drawdown in the adjacent aquifer, s, at the same radial distance from the pumping well provides the key factor, s'/s. This ratio has been shown from theory to be dependent on the permeability of the aquitard, K', and on the coefficient of storage per unit thickness of aquitard, S_s'. The specific relationship is shown by a family of curves on Figure IV-16. Examples of the application of the method to field data from this investigation are presented in Chapter V.

The ratio method has a distinct advantage over procedures that have been used in the past. By making measurements in the aquitard above or below an aquifer that is being pumped and comparing the effects in the aquitard with those in the aquifer, a simple and direct procedure for calculating hydraulic properties can be used. There is no ambiguity as to which aquitard is leaking. Previous methods relied only on measurements in the aquifer being pumped, and therefore, the megnitude of leakage from above or from below could not be ascertained. The ratio method eliminates this difficulty.

2. Field Pumping Tests

The ratio method was tested in this investigation by analyzing data obtained while pumping water from the Oxnard aquifer and simultaneously recording the transient response in the aquitards immediately above and below. The results are quite significant. The aquitard overlying the Oxnard aquifer has an average permeability of 0.025 gpd/ft^2 (1.1 x 10^{-6} cm/sec), and the aquitard underlying is somewhat more permeable, 0.042 gpd/ft^2 (1.9 x 10^{-6} cm/sec). By contrast the permeability of the aquifer in the test area is 1,405 gpd/ft^2 (6.4 x 10^{-2} cm/sec).

Results for the storage factors are also significant. The aquitard overlying the Oxnard aquifer has a specific storage coefficient, S_s', of 2.4 x 10^{-4} ft^{-1}, and the aquitard underlying is somewhat less, 1.0 x 10^{-4} ft^{-1}. These results, however, are about a hundred times larger than the value obtained for the aquifer, 1.2 x 10^{-6} ft^{-1}.

3. Laboratory Studies

An independent evaluation of the aquitard materials in the Oxnard Basin was also made during this investigation through laboratory studies on core samples. In the drilling operations, about 40 feet of core were taken from the aquitard overlying the Oxnard aquifer and about 30 feet, from the underlying aquitard. Selected samples were studied with regard to composition, consolidation, permeability, and the effects of replacing the natural pore fluids by salt water. The results are presented in Chapter VI.

The sediments throughout these aquitard layers are predominantly in the silt size and are mainly composed of quartz and clay minerals. The clay content is generally less than 20 percent and is dominantly montmorillonite with lesser amounts of kaolinite and illite. The aquitard beneath the Oxnard, however, has a much higher proportion of sand than the aquitard above. In general, these fine-grained sediments are moderately compressible, with compression index values ranging from 0.2 to 0.6.

Permeabilities as measured in the laboratory vary erratically with depth depending on grain size and range from 0.1 to less than 0.001 gpd/ft^2 (10^{-5} to 10^{-7} cm/sec). The laboratory results are generally in agreement with the results of the pumping tests, although many of the measured values are lower than was obtained in the field. This resulted from restricting the experimental work to clay-rich samples since these can be more reliably tested in the laboratory than samples containing too much sand. Leaching these clay-rich samples with salt water having a NaCl concentration equal to that of sea water did not seem to have any significant effects, although the results were inconclusive because of the aquitard variability.

4. Analysis of Chemico-Osmotic Diffusion

A second theoretical study was also carried out during this investigation on the mechanism and effects of chemico-osmotic diffusion. When sea water is on one side of an aquitard and fresh water in on the other, salt ions will tend to move toward the fresh water. This movement, however, is complex and depends on a number of factors. The results of a theoretical analysis for some assumed situations at Oxnard are presented in Chapter VII, and the details of the theory of chemico-osmotic diffusion are given in Appendix D.

These theoretical studies show that when an aquitard is low in hydraulic permeability because of a significant clay content (i.e. ~0.001 gpd/ft^2 or ~10^{-7} cm/sec), diffusion becomes an important mechanism for moving salt ions through such beds. Whether such movement can cause degradation of fresh water layers will depend on the thickness of the aquitard and the presence of any hydraulic gradients that may have developed. A discussion of this process as well as movement under the influence of a hydraulic gradient alone is presented in Chapter VIII.

B. IMPLICATIONS OF RESULTS

The importance of aquitards in controlling ground water movement has been discussed in Chapter I in terms of a number of problems that face the hydrogeologist as well as hydrologist. In view of the results of this investigation, what are the implications of our findings with regard to the role of aquitards in ground water systems?

1. Sea Water Intrusion

Clearly, the aquitards of the Oxnard coastal basin have sufficient permeability that they cannot be considered confining beds in the usual sense. If the permeability that was obtained in this study (~0.02 gpd/ft^2 or ~10^{-6} cm/sec) is typical of the basin, a substantial vertical migration of water from one aquifer to another is possible. For example, a gradient of 1 ft/ft can move 560,000 gpd vertically across an aquitard with this permeability over an area of one square mile.

Furthermore, if one of the shallow aquifers has been degraded by sea water intrusion, as is the case at Oxnard, pumpage from a second lower aquifer can lead to intrusion into this lower level. Whether such intrusion will lead to a significant degradation of potable waters will depend on the circumstances. This is a potential problem that cannot be ignored in coastal basins already subject to sea water intrusion.

Such migration also raises the question whether the initial intrusion in a coastal

aquifer is necessarily horizontal. If a sufficient vertical gradient develops offshore
across an aquitard separating ocean waters from a fresh water aquifer that extends onshore
the same argument can be made that the aquitard may provide a potential path for migration
to occur. Sea water would not have to move inland solely from an outcrop out on the con-
tinental shelf for intrusion to take place. Here again is a potential problem that cannot
be ignored when plans are being made to produce significant supplies of water from a
coastal basin.

2. Marinas

A comparable problem arises on a smaller scale when a marina is constructed in a
coastal basin. The excavation of a harbor removes some portion of the aquitard layers
that serve as a natural barrier between salt and fresh waters. If, in addition, the per-
meability of the aquitard is of the same order as that found at Oxnard, a reduction of he
in a fresh water aquifer lying beneath the marina can lead to vertical migration of marin.
waters into the fresh water system.

For example, if the marina covers an area of 100 acres, a vertical gradient of 1
ft/ft can move 87,000 gpd of sea water across an aquitard when the permeability is 0.02
gpd/ft^2. Whether this constitutes a problem will depend on the magnitude of dilution
that takes place once the salt water reaches the fresh water aquifer. This, of course,
depends on the hydraulic conditions that control movement within the fresh water system.
Obviously, migration of this kind is much more localized, and thus, only wells that pro-
duce in the near vicinity of the marina are in potential danger of intrusion by sea
water.

3. Poor Quality Water

Still another implication of this study concerns the problem of degradation from
poor quality waters that accumulate for one reason or another in semiperched aquifers over
lying fresh water systems. This can be especially critical if dangerous constituents such
as arsenic, boron, or nitrate happen to accumulate in abnormally high concentrations in th
shallow waters. Since the hydraulic head in the semiperched zones will usually exceed tha
of the fresh water aquifers beneath, the prevailing direction of movement will be downward
If the results found at Oxnard are typical, one can easily demonstrate that a small down-
ward movement of shallow water containing a concentration of undesirable elements that is
10 or more times the acceptable limit for potable water can lead to a serious problem (see
Chapter VIII).

4. Ground Water Recharge

Although the above discussion has focussed on the difficulties that arise from leaky aquitards, such beds also provide important paths for ground water recharge. For example, if the vertical gradient across the aquitard overlying the Oxnard aquifer is only 0.1 ft/ft and the permeability is 0.02 gpd/ft^2, the volume of vertical recharge per square mile of aquifer amounts to 56,000 gpd, or about 63 acre-feet per year. Spread over the 95 square miles of the Oxnard Basin, this inflow would amount to 6,000 acre-feet per year, which is about 13 percent of the reported ground water supply for the area (46,000 acre-feet per year). Thus, leakage through this aquitard could be a significant source of recharge to the basin.

Another source of water can come from storage in the aquitard layers. This is due to the fact that S_s, the coefficient of storage per foot of thickness, is generally much higher in fine grained sediments than in the coarse grained aquifers. As mentioned above in connection with the pumping tests, S_s for the Oxnard aquifer was found to be 1.2×10^{-6} ft^{-1}, whereas in the overlying aquitard, S_s was determined to be 2.4×10^{-4} ft^{-1}, or 200 times higher.

Drawdowns in the aquifer will always be greater than those in the aquitard, but it is obvious that a factor of 200 will more than offset such differences in terms of water release. This is not an important factor in the Oxnard Basin because hydraulic heads do not continue to fall year after year but fluctuate depending on the relative magnitudes of annual withdrawal and ground water recharge. In multiple-aquifer systems, however, where the withdrawals continually exceed the basin recharge and the total thickness of the aquitards far exceeds that of the aquifers, the contributions from storage in the fine grained sediments can be quite significant. Those who prepare hydraulic budgets should not overlook the role of aquitards either from the standpoint of their storage capacity or from the standpoint of the communication they provide with other parts of a multiple aquifer system.

5. Time Factor

In all of the above considerations, one must keep the time factor in mind. In other words, if the permeability of a key aquitard is of the order of 0.02 gpd/ft^2, how long will it take for sea water or some other non-potable fluid to move across such a bed? The answer depends on the magnitude of the hydraulic gradient that is maintained and the thickness of aquitard to be traversed.

If the vertical gradient is as high as 1 ft/ft, the velocity through an aquitard with a permeability of 0.02 gpd/ft^2 will be one foot per year. Thus, if the aquitards range in thickness from 10 to 50 feet, sea water could pass through them in from 10 to

50 years. On the other hand, if the vertical gradient is only one tenth as high (i.e. 0.1 ft/ft), the time factor would be increased ten times.

A period of 10 to 50 years is relatively short and happens to coincide with the time periods over which the various sea water intrusion problems in the coastal basins of California have occurred. One wonders whether the observed degradation has always followed the traditional concept of horizontal movement from the aquifer outcrops out on the continental shelf, or whether there might be some instances where aquitard leakage was a contributing factor. This could probably be checked by investigating compositional changes in the pore waters of offshore aquitards in those coastal basins where intrusion has occurred.

The picture changes considerably if the permeability is reduced by a factor of ten (i.e. to 0.002 gpd/ft^2 or 10^{-7} cm/sec). A decreased permeability implies a higher clay content and with it, the greater likelihood that chemico-osmotic diffusion must be considered. This kind of coupled flow is a non-steady process and is quite complicated. Details are given in Chapter VII where examples have been worked out for an aquitard having a permeability of 0.002 gpd/ft^2.

Movement of salt ions takes place by diffusion in such an aquitard whether a hydraulic gradient due to pumping is present or not. The rate of movement, however, is very slow; our theoretical studies show that salt ions will take about 800 years to move across an aquitard that is 30 ft thick. If, in addition, a hydraulic gradient of 1 ft/ft is also acting in the same direction as the diffusive movement, the time will be reduced appreciably to 170 years. Because this kind of movement is non-steady, the time factor decreases with the square of the thickness of the aquitard. Thus, if thickness in the above example is reduced to 10 ft, the above time factors are reduced to 80 and 19 years, respectively.

In summary, if a coastal basin has aquitard permeabilities as high or higher than those found at Oxnard, the process most likely to cause significant amounts of non-potable waters to move across such aquitards will probably be that of movement due to a hydraulic gradient. As the aquitards become clay-rich and their permeabilities fall to levels of the order of 0.001 gpd/ft^2, the migration will be controlled by chemico-osmotic diffusion. In this case, the only danger points will be those locations where the aquitards that must serve as barriers to movement are too thin. In either circumstance, careful control of hydrologic conditions must be maintained if sea water intrusion is to be eliminated.

6. Need for Field Observations

All of these considerations lead to the more general problem of the level of field observation that is necessary in multiple aquifer systems where leakage across aquitards poses a threat to ground water resources. Obviously, one must first know the magnitude

of the aquitard permeability; otherwise reliable estimates of leakage through such beds
will not be possible. This will require further field and laboratory work similar to that
of this investigation. As the range of permeabilities for aquitards becomes better known,
useful correlations can probably be developed that will provide a means of predicting
reliable values for permeability.

Once the permeabilities are established, appropriate measurements of hydraulic
head across the aquitard under consideration will provide the data needed to estimate
the rate of movement through such a bed. Locations where critical problems of fresh
water degradation may occur should be equipped with enough observation wells so there
can be no question concerning the magnitude of vertical communication. These wells should
be placed in the aquitard under consideration as well as in adjacent aquifers above and
below.

CONCLUSIONS

(1) The Oxnard coastal basin is clearly a multiple system of leaky aquifers.
(2) The ratio method described in this report provides a new field procedure for
     evaluating hydraulic properties of aquitards.
(3) A theory of transient flow in multiple aquifers systems has been developed that
     provides a scientific basis for the ratio method.
(4) A theory of chemico-osmotic diffusion through aquitard layers has been developed
     that provides an understanding of the controlling factors in this complex process.
(5) Movement of salt water through aquitards by chemico-osmotic diffusion becomes
     important when the permeability falls to levels of the order of 0.001 gpd/ft^2
     ($\sim 10^{-7}$ cm/sec).
(6) At higher permeabilities, movement through aquitards is largely controlled by the
     hydraulic gradients that result when water is being pumped from adjacent aquifers.
(7) Leakage through the aquitards of coastal basins is an important consideration in
     several facets of the general problem of degradation of fresh water systems.
(8) Those who prepare hydraulic budgets should not overlook the contributions to
     ground water recharge that can come from the aquitards.
(9) Aquitards play a far more important role in controlling ground water movement than
     has heretofore been realized.

RECOMMENDATIONS

(1) Further investigations on aquitards are needed so that the range in the hydraulic
     properties of these fine-grained sediments can be better established.
(2) The traditional concept of a horizontal intrusion of sea water into fresh water

-13-

aquifers needs to be re-examined to determine if aquitard leakage may also be a contributing factor.

(3) In utilizing the ground water resources of coastal basins, such as those of California, the ability of aquitards to control sea water intrusion on the one hand, and to contribute to recharge on the other, should be carefully evaluated in any effective program of water resource management.

CHAPTER III. OXNARD BASIN

P. A. Witherspoon

   To understand the hydraulic system of the Oxnard Basin requires a knowledge of the relationships between the various geologic units and their aquifers and aquitards. This chapter presents information on these relationships and on the recharge and withdrawal of ground water and the status of sea water intrusion.

A. GEOLOGIC SETTING

   During the Tertiary and Quarternary time, several thousand feet of sediments were laid down on a pre-Cretaceous basement of igneous and metamorphic rocks. Of these sediments, only the Quaternary deposits are important as a source of ground water, and only they will be discussed in this chapter. A generalized geologic column is given in Figure III-1.

AGE	GEOLOGIC UNIT	GRAPHIC LITHOLOGY	AQUIFER UNITS	MAXIMUM THICKNESS (IN FEET)	GENERAL LITHOLOGY AND WATER-BEARING CHARACTER OF SEDIMENTS
RECENT	(RECENT DEPOSITS)		SEMIPERCHED ZONE	80	FINE-TO MEDIUM-GRAINED SAND WITH SOME GRAVEL, INTERBEDDED SILT AND CLAY LENSES. UNDEVELOPED BY WELLS. LOCALLY DEGRADED BY RETURN IRRIGATION WATER.
			CONFINING CAP	150	SILT AND CLAY WITH FINE-TO MEDIUM-GRAINED SAND LENSES CONFINING MEMBER ABOVE OXNARD AQUIFER
			OXNARD	160	FINE-TO COARSE-GRAINED SAND WITH GRAVEL VARYING FROM GRANULE TO COBBLE IN SIZE INTERBEDDED SILT AND CLAY LENSES. HIGH PERMEABILITY. PRINCIPAL PRODUCING AQUIFER IN OXNARD BASIN SUBJECT TO SEA-WATER INTRUSION
			UNCONFORMITY		
LATE PLEISTOCENE	(UPPER PLEISTOCENE DEPOSITS)			150	SILT AND CLAY
			MUGU	250	FINE-TO COARSE-GRAINED SAND WITH GRANULES INTERBEDDED SILT AND CLAY LENSES. HIGH PERMEABILITY LOCALLY DEVELOPED BY WELLS IN OXNARD BASIN. SUBJECT TO SEA-WATER INTRUSION
				80	SILT AND CLAY
			UNCONFORMITY		
EARLY PLEISTOCENE	SAN PEDRO FORMATION (LOWER PLEISTOCENE DEPOSITS)		HUENEME	300	FINE-TO COARSE-GRAINED SAND WITH SILT AND CLAY LENSES, MODERATE TO HIGH PERMEABILITY. DEVELOPED BY FEW WELLS IN OXNARD BASIN MAY BE SUBJECT TO SEA-WATER INTRUSION
				170	SILT AND CLAY
			FOX CANYON	550	FINE-TO COARSE-GRAINED SAND WITH GRAVEL STRINGERS. INTERBEDDED SILT AND CLAY. MODERATE PERMEABILITY DEVELOPED BY FEW WELLS IN OXNARD BASIN MAY BE SUBJECT TO SEA-WATER INTRUSION
				40	SILT AND CLAY
	SANTA BARBARA FORMATION (LOWER PLEISTOCENE DEPOSITS)		GRIMES CANYON	1500+	FINE-TO COARSE-GRAINED SAND WITH GRAVEL INTERBEDDED SILT AND CLAY PROBABLE MODERATE PERMEABILITY DEVELOPED BY FEW WELLS IN OXNARD BASIN MAY BE SUBJECT TO SEA-WATER INTRUSION

Fig. III-1.   Generalized geologic column of water bearing sediments in Oxnard Basin

DEPARTMENT OF WATER RESOURCES, SOUTHERN DISTRICT, 1970

Recent Deposits

Recent deposits in the coastal plain were laid down during the post-glacial period, while the sea level was rising. The sediments consist of alluvial sands and gravels, lagoonal silts and clays, and dune sands. These deposits make up the Oxnard aquifer, the confining cap, and the semiperched zone. Maximum thicknesses in the Oxnard Basin for these zones are 160 feet, 150 feet, and 80 feet, respectively. The Recent deposits lie unconformably on the late Pleistocene deposits.

Late Pleistocene Deposits

The late Pleistocene deposits consist of interbedded sands, gravels, silts, and clays. They make up an aquitard that separates the Oxnard aquifer from the Mugu aquifer, and Mugu aquifer itself, and also a lower aquitard that separates the Mugu aquifer from the lower Pleistocene deposits. Maximum thicknesses in the Oxnard Basin are 150 feet for the upper aquitard, 250 feet for the Mugu aquifer, and 80 feet for the lower aquitard. In the forebay area, the Oxnard and Mugu aquifers merge. The upper Pleistocene deposits unconformably overlie the lower Pleistocene sediments.

Early Pleistocene Deposits

Although early Pleistocene deposits were not encountered during the drilling for this project, they are described here to complete the stratigraphy of the water-bearing sediments in Oxnard Basin.

Two formations form the lower Pleistocene deposits in Oxnard Basin. They are the San Pedro Formation, which conformably overlies the Santa Barbara Formation.

The San Pedro Formation comprises marine and continental deposits of sand, gravel, silt, and clay. Two water-bearing zones have been designated within this formation. They are the Hueneme and Fox Canyon aquifers. The Hueneme, which is the uppermost of the two, is separated from the Fox Canyon by an aquitard of silt and clay. Maximum thickness for the Hueneme aquifer is 300 feet, for the aquitard immediately below it, 170 feet, and for the Fox Canyon aquifer, 550 feet.

The Santa Barbara Formation is chiefly composed of marine clay, silt, sand, and gravel, and attains a maximum thickness of more than 1,500 feet in Oxnard Basin. The permeable sands and coarse gravels in the uppermost part of this formation have been termed the Grimes Canyon aquifer. This aquifer is separated from the Fox Canyon aquifer by a silt and clay aquitard that attains a maximum thickness of about 40 feet.

B. MULTIPLE AQUIFER SYSTEM

The water-bearing sediments in the Oxnard Basin are, in downward sequence:
the semiperched zone, the Oxnard aquifer, the Mugu aquifer, the Hueneme aquifer, the
Fox Canyon aquifer, and the Grimes Canyon aquifer. Following is a brief discussion
of these water-bearing units and their associated aquitards. Although emphasis is
placed on the upper aquifers, the three lower ones will be discussed to complete the
aquifer system.

Semiperched Zone

The semiperched zone is the uppermost water-bearing unit in the test area. It
is composed of fine to medium-grained sand with interbedded silty clay lenses. In the
study area, the average thickness is about 30 feet. Immediately below the semiperched
zone and overlying the Oxnard aquifer is the confining, or clay cap. It is made up of
predominately silty and sandy clays. Within the test area, the cap has an average
thickness of approximately 35 feet.

Oxnard Aquifer

The Oxnard aquifer, which is the most important water producer in the Oxnard
Basin, is composed of fine to coarse-grained sand and gravel. Within the study area
the average thickness is about 90 feet. The aquifer exhibits high permeabilities of
between 1,200 and 1,300 gallons per day per square foot (gpd/ft^2). Within the study
area, lithologic and electric logs of the pumping and observations wells show the
aquifer to be a single unit, with no prominent silt or clay lense interruptions.

Immediately below the Oxnard aquifer and separating it from the Mugu aquifer is
an aquitard that is composed of silty clay with some interbedded sandy clay lenses. The
average thickness of this aquitard in the test area is approximately 30 feet.

Mugu Aquifer

The material that forms the Mugu aquifer is fine to coarse-grained sand and
gravel with some interbedded silty clay. Within the study area, the average thickness
of this water-bearing zone is approximately 110 feet. Although no test was made for
permeability in this study, permeabilities in other parts of Oxnard Basin are rather
high with the range between 1,900 and 2,200 gpd/ft^2.

In the forebay area (see Figure I-1 for location), the Mugu aquifer merges with
the Oxnard aquifer. It is probably in hydraulic continuity with the ocean, although in

the immediate vicinity of the study area no evidence could be found of sea water moving laterally within this zone.

Underlying the Mugu is an aquitard composed of silty clay. In the study area, the thickness is not known, but within the Oxnard Basin it reaches a maximum of 80 feet. This aquitard is continuous except in the forebay area, where the Hueneme aquifer merges with the other water-bearing zones.

Hueneme Aquifer

The Hueneme aquifer is composed of irregularly interbedded sand, silt and clay, with some gravel. Its thickness ranges from 100 feet within the City of Port Hueneme to about 300 feet north of the City of Oxnard. Permeability for this water-bearing zone is estimated to be 400 to 600 gpd/ft^2. It is thought to be in hydraulic continuity with the ocean.

Separating the Hueneme aquifer from the underlying Fox Canyon aquifer is an aquitard that is composed of silt and clay. These sediments are absent only in the northern portion of the forebay area, where the Fox Canyon aquifer merges with the Hueneme aquifer. Although the thickness in the study area is not known, the aquitard's maximum thickness for the basin is approximately 170 feet.

Fox Canyon Aquifer

The Fox Canyon aquifer is composed of fine to coarse-grained sand with gravel stringers and interbedded silt and clay, and has a maximum thickness of approximately 550 feet in Oxnard Basin. Permeabilities for this water-bearing zone range from 200 to 400 gpd/ft^2. Besides merging with the Hueneme zone, the Fox Canyon is also in hydraulic continuity with the overlying Oxnard aquifer. The Fox Canyon is the second most important water producer after the Oxnard aquifer.

The aquitard that separates the Fox Canyon and the underlying Grimes Canyon aquifer is composed of silt and clay; it attains a maximum thickness of about 40 feet in Oxnard Basin.

Grimes Canyon Aquifer

Most of the information concerning the Grimes Canyon aquifer has been derived from oil well electric logs. Very few water wells are perforated in this water-bearing zone. These electric logs indicate that the aquifer is composed of fine to coarse-grained materials, with a maximum thickness of more than 1,500 feet. The areal extent of the Grimes Canyon aquifer is approximately the same as that of the Fox Canyon aquifer.

No tests have been conducted to determine its permeability range.

C. REGIONAL RECHARGE

Recharge water may enter the forebay area of Oxnard Basin in many ways. These are, not necessarily in order of importance: natural percolation of surface waters in the Santa Clara River, percolation of Santa Clara River water that is diverted to the spreading grounds in El Rio and Saticoy, subsurface inflow from Santa Paula Basin, and percolation of precipitation.

The principal recharge for the Oxnard Basin pressure area is by subsurface inflow from the forebay area. In addition, some subsurface water flows from West Las Posas Basin. If the piezometric elevations are below sea level, subsurface water flows into the aquifers from offshore.

D. HISTORY OF WATER WITHDRAWAL

Artesian conditions existed in the Oxnard Basin pressure area during years of ground water surplus. At that time ground water flowed to the ocean through the aquifers that outcrop offshore.

Deficient water conditions became apparent, however, as urban and agricultural economy expanded and annual extractions from the Oxnard Basin exceeded annual replenishment. This unbalanced condition caused piezometric levels to drop to elevations below sea level, with the result that the Oxnard aquifer was soon intruded with sea water. The most serious deficiency of ground water occurred during the latter part of 1947. Prior to this, during the wet period from 1937 to 1945, water levels in the Oxnard aquifer had recovered and had remained above sea level. The water levels started to decline in 1945 and remained at low levels because of decreased precipitation. Only in 1969 have water levels begun to recover because of increased precipitation.

E. SEA WATER INTRUSION

Sea water intrusion was first recorded in 1950, but was suspected as far back as the early 1930's. By 1952, three water wells located near the head of the Hueneme submarine canyon exceeded the recommended chloride ion concentration for most uses. Definite evidence of sea water intrusion in the Point Mugu area appeared about 1958. A total of 44 water wells (42 near Port Hueneme and 2 near Point Mugu) were affected by sea water intrusion by the summer of 1963.

By 1965, 169,000 acre-feet of usable storage capacity in the Oxnard Basin was lost to sea water. This consisted of approximately 91,000 acre-feet near Point Mugu

and 78,000 acre-feet near Port Hueneme. This, of course, does not include offshore storage capacity.

At present, the most serious threat to the quality of ground water in the Oxnard Basin is this intrusion of sea water at these two localities. Although little is known about the three lower aquifers, the Hueneme, the Fox Canyon, and the Grimes Canyon, very likely they also may be subjected to degradation by ocean water.

All the lateral movement of sea water in the Port Hueneme area has taken place in the Oxnard aquifer. However, in the Point Mugu area, sea water has invaded both the Oxnard and Mugu aquifers. This is probably because in the vicinity of Mugu Lagoon no aquitard separates the two aquifers and the Oxnard has no apparent clay cap.

CHAPTER IV. FLOW IN MULTIPLE AQUIFER SYSTEMS

S. P. Neuman and P. A. Witherspoon

A. INTRODUCTION

In dealing with non-steady flow of ground water to wells, it has been customary to treat the aquifer from which fluid is being withdrawn as an independent geohydrological unit. If the aquifer is confined from above and from below by layers that are effectively impermeable, then methods based on the well-known Theis solution are usually applicable. Quite often, however, the confining layers are not completely impermeable but act as conduits for vertical migration of fluid from one aquifer to another. If the confining layers are compressible, they can also release water from storage and thereby increase the supply available to the aquifer. The combined effect of these phenomena is known as leakage.

When the effects of leakage are detectable by observing drawdown in the aquifer being pumped, the confining beds are called "aquitards," and the aquifer is referred to as being "leaky." Where such effects are not easily detectable in the aquifer, the confining beds are called "aquicludes," and the aquifer is termed "slightly leaky" [Neuman and Witherspoon, 1968].

Since leakage means that there is hydraulic communication between aquifers that are separated from each other by a series of aquitards or aquicludes, the behavior of each aquifer is closely related to the behavior of all the other layers. Thus, instead of focusing attention only on the particular aquifer from which fluid is being withdrawn, it is necessary to study the behavior of a complex of layers which we call a "multiple aquifer system."

A rigorous approach to flow in multiple aquifer systems involves boundary conditions that are difficult to treat analytically. It has, therefore, been customary to simplify the mathematics by assuming that flow is essentially horizontal in the aquifers and vertical in the aquitards. The validity of this assumption for a system composed of two aquifers that are separated by an aquitard has been investigated using the finite element method, and the results are given in Appendix A (see Figures VI-11 to IV-14). It was found that when the permeabilities of the aquifers are more than two orders of magnitude greater than that of the aquitard, the errors introduced by this assumption are usually less than 5%. These errors increase with time, decrease

with radial distance from the pumping
well, and are smallest in the pumped
aquifer and greatest in the aquitard.
Since the permeability contrast between
aquifer and aquitard is usually more
than two orders of magnitude, it appears
that the above assumption can be used
with confidence.

     Consider now a confined system
of two aquifers that enclose an aquitard
as shown schematically on Figure IV-1.
A well of infinitesimal radius is com-
pleted in the lower aquifer and discharges
at a constant rate Q_1. If this system
reaches a steady state, then the assump-
tion of vertical flow in the aquitard

Fig. IV-1. Schematic diagram of
two-aquifer system

implies that the rate at which water leaks into the pumped aquifer is proportional to
the potential drop across the aquitard. Flow in the pumped aquifer can then be des-
cribed by the partial differential equation[*]

$$\frac{\partial^2 s_1}{\partial r^2} + \frac{1}{r}\frac{\partial s_1}{\partial r} - \frac{(s_1 - s_2)}{B^2_{11}} = 0 \qquad\qquad (IV\text{-}1)$$

[cf. Polubarinova Kochina, 1962]. Similarly, flow in the unpumped aquifer is governed
by

$$\frac{\partial^2 s_2}{\partial r^2} + \frac{1}{r}\frac{\partial s_2}{\partial r} - \frac{(s_2 - s_1)}{B^2_{21}} = 0 \qquad\qquad (IV\text{-}2)$$

Here B_{11} and B_{21} are known as "leakage factors". When the aquitard is impermeable
($K_1' = 0$) then $B_{11} = B_{21} = \infty$, the terms $(s_1 - s_2)/B^2_{11}$ and $(s_2 - s_1)/B^2_{21}$ vanish, and
the above equations reduce to Laplace's equation as expected for non-leaky aquifers.

    This approach to steady flow in leaky aquifers was first introduced into the
literature by DeGlee [1930] and was later used by Steggenventz and Van Ness [1939].
Additional work along these lines by Glebov [1940], Myatiev [1946, 1947], and Girinsky
[1947] has been summarized by Polubarinova-Kochina [1962] and Aravin and Numerov [1965].

[*]Explanation of symbols is given in Notation.

-22-

Jacob [1946] extended this approach to non-steady state by writing

$$\frac{\partial^2 s_1}{\partial r^2} + \frac{1}{r}\frac{\partial s_1}{\partial r} - \frac{s_1}{B_{11}^2} = \frac{S_{s1}}{K_1}\frac{\partial s_1}{\partial t} \qquad \text{(IV-3)}$$

where it is assumed that drawdown in the unpumped aquifer remains zero. However, it is important to recognize that this equation is still based on the assumption that leakage is proportional to the potential drop across the aquitard. While correct for steady state, under non-steady conditions such an assumption is tantamount to ignoring the possibility of water being released from storage in the aquitard. The assumption of zero drawdown in the unpumped aquifer is an additional limitation of Jacob's approach. Nevertheless, between the years 1949 and 1960, Hantush [1949, 1956, 1957, 1959] and Hantush and Jacob [1954, 1955a, 1955b, 1960] have used this approach to develop a large number of solutions to various problems involving flow in leaky aquifers.

In 1960 Hantush [1960a) published a modification of Jacob's approach in which, for the first time, consideration was given to the effect of storage in the aquitard. A detailed discussion of this modified approach is given in Appendix A, Chapter II-B. Although Hantush's modification constituted an improvement over Jacob's theory, it has never been used in subsequent work on leaky aquifers. Between 1961 and 1967, Hantush [1962, 1964, 1967a, 1967b] and DeWiest [1961, 1963] analyzed various problems involving flow in leaky aquifers, but in all of this work, storage effects in the aquitard were consistently neglected. In only one of these analyses has Hantush [1967b] allowed drawdown in the unpumped aquifer to vary with time. Yotov [1968] has extended the application of equation IV-3 to unconfined aquifers with delayed yield.

The assumption of linear potential drop across the aquitard (i.e., no storage in the aquitard) is obviously in error at early values of pumping time. At large values of time, such a situation may eventually be realized if the system approaches a quasi-steady state. The other assumption of no drawdown in the unpumped aquifer is valid at sufficiently small values of time, in which case the effects of this aquifer on the rest of the system can be ignored. However, these effects can be quite significant at large values of time. Therefore, proper consideration must be given to both storage and drawdown at all points in the flow region if one wishes to obtain a complete understanding of the nature of flow in a multiple aquifer system.

In an effort to provide a more complete description of the behavior of flow in such systems, we shall present below analytical solutions for non-steady flow in a confined two-aquifer system. However, in contrast to previous work, we shall consider the effects of storage in the aquitard and allow drawdown in the unpumped aquifer to vary with time.

B. THEORETICAL STUDIES

1. Analytical Solutions for a Two-Aquifer System

Consider again the two-aquifer system shown in Figure IV-1. As mentioned earlier, we shall assume that flow is vertical in the aquitard and horizontal in both aquifers. One apparent implication of this assumption is that the unpumped aquifer must be thin enough so that drawdown across its thickness at any time may be regarded as constant. The principle here is analogous to that of temperature distribution in a cooling fin. From a practical standpoint, however, we have found that the thickness of the unpumped aquifer has little effect on the applicability of our solutions (Appendix A, Chapter IV-A). Similarly, no restriction on the thickness of the pumped aquifer is necessary because the radial gradients induced by the well are much larger than the vertical gradients in this layer caused by inflow from the aquitard.

Using Hantush's modified approach to leaky aquifers, we shall formulate the problem as follows:

$$
\left. \frac{\partial^2 s_1}{\partial r^2} + \frac{1}{r}\frac{\partial s_1}{\partial r} + \frac{K_1{}'}{T_1}\frac{\partial s_1{}'}{\partial z} \right|_{z=0} = \frac{S_{s_1}}{K_1}\frac{\partial s_1}{\partial t}
$$

$$
s_1(r,\,0) = 0
$$

$$
s_1(\infty,\,t) = 0
$$

$$
\lim_{r \to 0} r\,\frac{\partial s_1}{\partial r} = -\,\frac{Q_1}{2\pi T_1}
$$

Aquifer 1 (pumped)   (IV-4)

$$
\frac{\partial^2 s_1{}'}{\partial z^2} = \frac{S'_{s_1}}{K'_1}\frac{\partial s_1}{\partial t}
$$

$$
s_1{}'(r,\,z,\,0) = 0
$$

$$
s_1{}'(r,\,0,\,t) = s_1(r,\,t)
$$

$$
s_1{}'(r,\,H_1{}',\,t) = s_2(r,\,t)
$$

Aquitard 1   (IV-5)

-24-

$$\left.\frac{\partial^2 s_2}{\partial r^2} + \frac{1}{r}\frac{\partial s_2}{\partial r} - \frac{K_1'}{T_2}\frac{\partial s_1'}{\partial z}\right|_{s\,=\,H_1'} = \frac{S_{S2}}{K_2}\frac{\partial s_2}{\partial t}$$

$$s_2(r, 0) = 0$$

$$s_2(\infty, t) = 0$$

$$\lim_{r \to 0} r\,\frac{\partial s_2}{\partial r} = 0$$

Aquifer 2
(unpumped)   (IV-6)

A rigorous solution to equations IV-4, IV-5, and IV-6 is obtained using Laplace and Hankel transforms. The details of this procedure are outlined in Appendix A (Chapter II-C). The results are expressed in terms of five dimensionless parameters: (a) β_{11} and r/B_{11} with reference to the pumped aquifer, (b) β_{21} and r/B_{21} with reference to the unpumped aquifer, and (c) t_{D_1}, dimensionless time with reference to the pumped aquifer. Drawdown in the pumped aquifer is given by

$$s_1(r, t) = \frac{Q_1}{4\pi T_1} \int_0^\infty (1 - e^{-y^2 \bar{t}_{D_1}}) \left\{ [1 + G(y)]\, J_o\,[\omega_1(y)] \right.$$

$$\left. + [1 - G(y)]\, J_o\,[\omega_2(y)] \right\} \frac{dy}{y}$$ (IV-7)

In the aquitard

$$s_1'(r, z, t) = \frac{Q_1}{4\pi T_1} \frac{2}{\pi} \sum_{n=1}^\infty \frac{1}{n} \sin \frac{n\pi z}{H_1'} \int_0^\infty \left[1 - e^{-n^2\pi^2 \bar{t}_{D_1}} + \frac{e^{-n^2\pi^2 \bar{t}_{D_1}} - e^{-y^2 \bar{t}_{D_1}}}{1 - y^2/(n^2\pi^2)} \right]$$

$$\left\{ \left[\frac{2(r/B_{21})^2 (-1)^n\, y}{F(y)\,\sin y} - G(y) - 1 \right] J_o[\omega_1(y)] \right.$$

$$\left. - \left[\frac{2(r/B_{21})^2 (-1)^n\, y}{F(y)\,\sin y} - G(y) + 1 \right] J_o\,[\omega_2(y)] \right\} \frac{dy}{y}$$ (IV-8)

In the unpumped aquifer

$$s_2(r, t) = \frac{Q_1}{4\pi T_1} \int_0^\infty \left(1 - e^{-y^2 \bar{t}_{D_1}} \right) \frac{2(r/B_{21})^2}{F(y)} \left\{ J_o\,[\omega_1(y)] - J_o\,[\omega_2(y)] \right\} \frac{dy}{\sin y}$$

(IV-9)

where $\bar{t}_{D_1} = t_{D_1} (r/B_{11})^4/(4\beta_{11})^2$ and $t_{D_1} = \dfrac{K_1 t}{S_{s_1} r^2}$ (IV-10)

$G(y) = M(y)/F(y)$ (IV-11)

$\omega_1^2(y) = \dfrac{1}{2}[N(y) + F(y)]$ (IV-12)

$\omega_2^2(y) = \dfrac{1}{2}[N(y) - F(y)]$ (IV-13)

$$F^2(y) = M^2(y) + \left[\dfrac{2(r/B_{11})(r/B_{21})y}{\sin y}\right]^2$$ (IV-14)

$$M(y) = \left[\dfrac{(r/B_{11})^4}{(4\beta_{11})^2} - \dfrac{(r/B_{21})^4}{(4\beta_{21})^2}\right] y^2 - \left[\left(\dfrac{r}{B_{11}}\right)^2 - \left(\dfrac{r}{B_{21}}\right)^2\right] y \cot y$$ (IV-15)

$$N(y) = \left[\dfrac{(r/B_{11})^4}{(r\beta_{11})^2} + \dfrac{(r/B_{21})^4}{(4\beta_{21})^2}\right] y^2 - \left[\left(\dfrac{r}{B_{11}}\right)^2 + \left(\dfrac{r}{B_{21}}\right)^2\right] y \cot y$$ (IV-16)

In all of these equations $J_o[\omega_1(y)]$ must be set to zero when $\omega_1^2(y) < 0$, and the same is true of $J_o[\omega_2(y)]$ when $\omega_2^2(y) < 0$. It should be mentioned that equations IV-7 through IV-16 could be expressed in simpler form as may be seen in Appendix A. However, we have chosen to use r/B and β because these parameters have been extensively employed in most work dealing with leaky aquifers.

It is of interest to note that when $K_1' \rightarrow 0$ (i.e., the aquitard is impermeable), equation IV-7 reduces to the Theis solution. This is shown in Appendix A (Chapter II-C).

2. Solutions for Case When Aquifers Have Identical Properties

If the hydraulic properties of both aquifers are the same, then $r/B_{11} = r/B_{21}$ $\beta_{11} = \beta_{21}$. As a result $G(y) = M(y) = 0$ and (IV-7), (IV-8), and (IV-9) simplify respectively to

$$s_1(r, t) = \dfrac{Q_1}{4\pi T_1} \int_0^\infty (1 - e^{-y^2 \bar{t}_{D_1}}) \left\{ J_o[\omega_1(y)] + J_o[\omega_2(y)] \right\} \dfrac{dy}{y}$$ (IV-17)

$$s_1'(r, z, t) = \dfrac{Q_1}{4\pi T_1} \dfrac{2}{\pi} \sum_{n=1}^\infty \dfrac{1}{n} \sin \dfrac{n\pi z}{H_1'} \int_0^\infty \left[1 - e^{-n^2\pi^2 \bar{t}_{D_1}} + \dfrac{e^{-n^2\pi^2 \bar{t}_{D_1}} - e^{-y^2 \bar{t}_{D_1}}}{1 - y^2/(n^2\pi^2)}\right]$$

$$\cdot \left\{ [(-1)^n - 1] J_o[\omega_1(y)] - [(-1)^n + 1] J_o[\omega_2(y)] \right\} \dfrac{dy}{y}$$ (IV-18)

-26-

$$s_2(r,\ t) = \frac{Q_1}{4\pi T_1} \int\limits_0^\infty (1 - e^{-y^2 \bar{t}_{D_1}}) \left\{ J_o [\omega_1(y)] - J_o [\omega_2(y)] \right\} \frac{dy}{y} \tag{IV-19}$$

where instead of (IV-14) and (IV-16), one now must use $F(y) = \dfrac{2(r/B_{11})^2 y}{\sin y}$ and

$$N(y) = \left[\frac{2(r/B_{11})^4}{(4\beta_{11})^2} \right] y^2 - 2(r/B_{11})^2 y \cot y$$

As before, the Bessel functions must be set to zero when the squares of their arguments are negative.

3. Asymptotic Solutions for Early Time

In his modified theory of leaky aquifers, Hantush [1960a] presented a solution in the pumped aquifer that applies to our problem at early time. His solution can be expressed as

$$s_1(r,\ t) = \frac{Q_1}{4\pi T_1} \int\limits_{\frac{1}{4t_{D_1}}}^\infty \frac{e^{-y}}{y} \, \mathrm{erfc} \left[\frac{\beta_{11}}{\sqrt{y(4t_{D_1} y - 1)}} \right] dy \tag{IV-20}$$

where $t_{D_1} \leqslant \dfrac{1.6\ \beta_{11}^2}{(r/B_{11})^4}$ \tag{IV-21}

A corresponding solution in the aquitard has been developed by the authors (see Appendix A, Chapter II-E):

$$s_1'(r,\ z,\ t) = \frac{Q_1}{4\pi T_1} \int\limits_{\frac{1}{4t_{D_1}}}^\infty \frac{e^{-y}}{y} \left\{ \mathrm{erfc} \left[\frac{\beta_{11} + y(z/H_1')4\beta_{11}/(r/B_{11})^2}{\sqrt{y(t_{D_1} y - 1)}} \right] \right.$$

$$\left. - \mathrm{erfc} \left[\frac{\beta_{11} + y(2-z/H_1')4\beta_{11}/(r/B_{11})^2}{\sqrt{y(4t_{D_1} y - 1)}} \right] \right\} dy \tag{IV-22}$$

If the thickness of the aquitard is sufficiently large, equation IV-22 can be further simplified by letting $H_1' \to \infty$. The resulting equation is

$$s_1'(r,\ z,\ t) = \frac{Q_1}{4\pi T_1} \int\limits_{\frac{1}{4t_{D_1}}}^\infty \frac{e^{-y}}{y} \, \mathrm{erfc} \left[\frac{\beta_{11} + y\sqrt{t_{D_1}/t_{D_1}'}}{\sqrt{y(4t_{D_1} y - 1)}} \right] dy \tag{IV-23}$$

which is identical with a solution previously developed by Hantush (personal communication, 1960).

4. Discussion of Results for a Two-Aquifer System

To study the nature of these analytical solutions, we have evaluated them numerically using the Zonneveld adaptation of the Adams-Moulton method of numerical integration. The asymptotic solutions require much less computer time than the more complicated general solutions and were therefore used whenever applicable, i.e., whenever

$$t_{D_1} \leqslant \frac{1.6\ \beta_{11}{}^2}{(r/B_{11})^4}$$

As a first approach, let us consider the case where both aquifers have identical geometry and hydraulic properties. If we choose $\beta_{11} = r/B_{11} = 0.01$ and $\beta_{21} = r/B_{21} = 0.01$, we can evaluate equations IV-7 through IV-9 (or equations IV-17 through IV-19) in terms of dimensionless drawdown, s_D, and dimensionless time with respect to the pumped aquifer, t_{D_1}.

The results are shown in Figure IV-2, as a family of five curves. The upper curve represents behavior in the pumped aquifer, the lower curve represents dimension-less drawdown in the unpumped aquifer, and the three intermediate curves show results for various elevations in the aquitard. The Theis solution is included for reference purposes. Results for the cases where β and r/B parameters are increased to 0.1 and 1.0 are shown on Figures IV-3 and IV-4, respectively.

The validity of these results was verified independently using the finite element method. A discussion of this method is given in Chapter III of Appendix A, and the particular finite element network used is also described. The finite element method is a numerical technique that enables one to analyze flow behavior in layered systems with arbitrary degrees of heterogeneity and anisotropy. A further advantage of the method is that systems with complicated geometry and boundary conditions are easily handled. The finite element method provides a realistic check on the analytical solutions because, contrary to these solutions, it does not assume that flow is horizontal in the aquifers and vertical in the aquitard.

Figures IV-2, IV-3 and IV-4 show the kind of correspondence that was obtained between the analytical solutions and the finite element results. Excellent agreement was obtained in all cases. At small values of time when vertical gradients in the aquitard are large, an extremely fine network is required in order to obtain acceptable results. The network used in our work was not always fine enough to accomplish this.
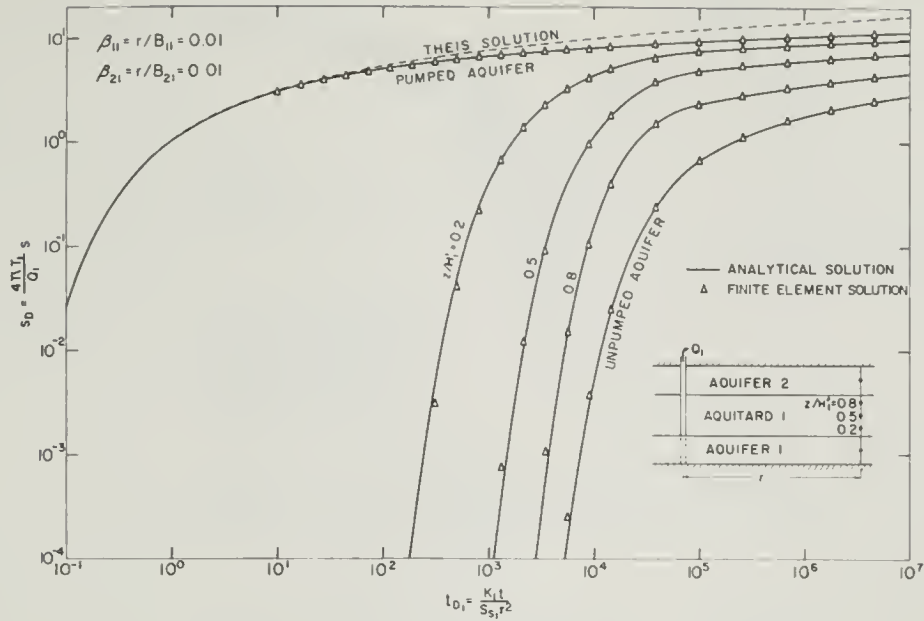
-28-

Fig. IV-2.   Dimensionless drawdown versus dimensionless
time in a two-aquifer system for $\beta_{11} = \beta_{21}$
$= r/B_{11} = r/B_{21} = 0.01$.
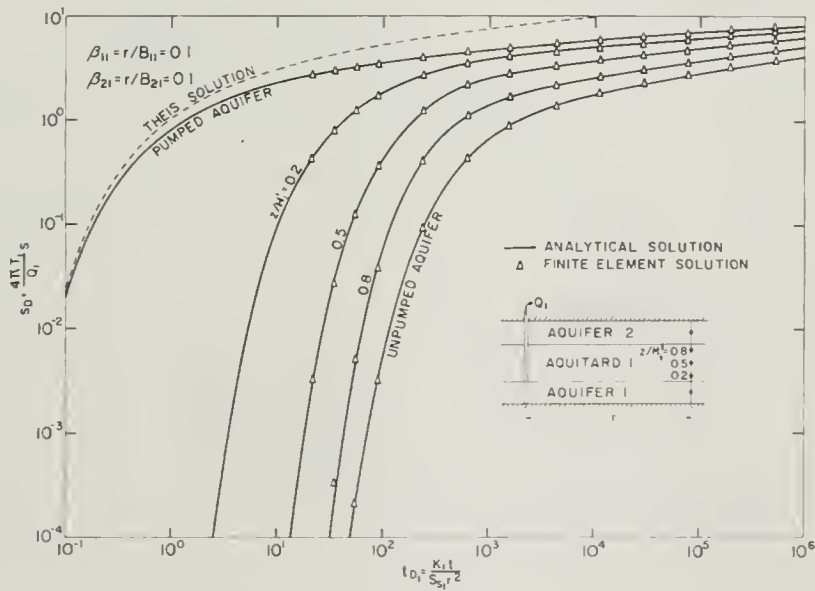
Fig. IV-3.   Dimensionless drawdown versus dimensionless
time in a two-aquifer system for $\beta_{11} = \beta_{21}$
$= r/B_{11} = r/B_{21} = 0.1$.
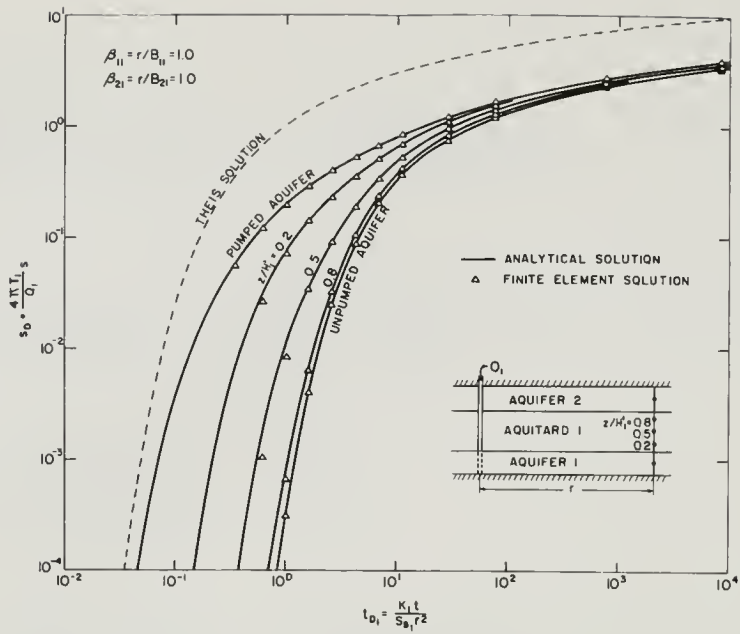
Fig. IV-4. Dimensionless drawdown versus dimensionless time in a two-aquifer system for $\beta_{11} = \beta_{21}$ $= r/B_{11} = r/B_{21} = 1.0$.
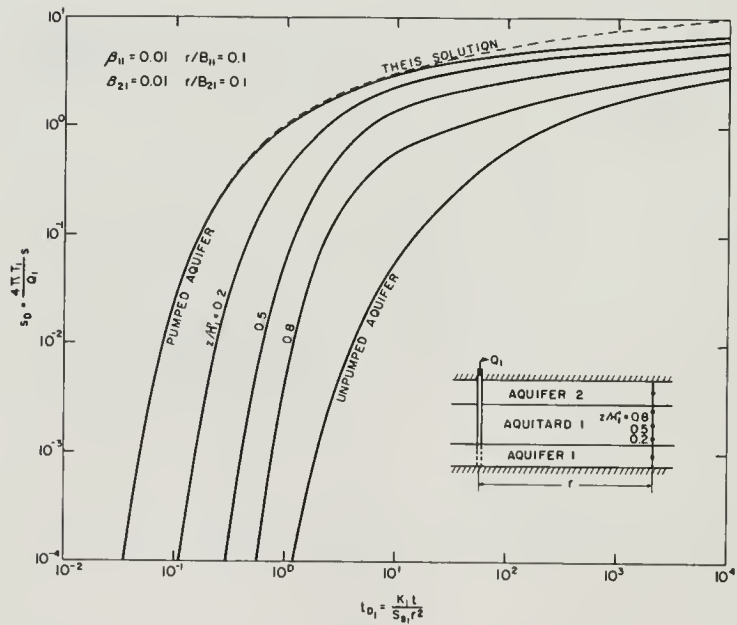
Fig. IV-5. Dimensionless drawdown versus dimensionless time in a two-aquifer system for $\beta_{11} = \beta_{21}$ $= 0.01$ and $r/B_{11} = r/B_{21} = 0.1$.

One must note, however, that our curves give data over a much greater range than is ordinarily available in the literature.

As another example, we shall now consider the case where $\beta_{11} = \beta_{21} = 0.01$ and $r/B_{11} = r/B_{21} = 0.1$ as shown on Figure IV-5. Further examples of the effects of these parameters may be found in Appendix A (Chapter IV).

A comparison of Figures IV-2 through IV-5 shows that (a) for a fixed ratio of $\beta_{11}/(r/B_{11})$, the spread between the curves decreases as the magnitudes of β_{11} and r/B_{11} are increased, and (b) for a given value of either β_{11} or r/B_{11}, the spread between the curves decreases as the ratio $\beta_{11}/(r/B_{11})$ decreases.

To explain the first relationship, we recall that

$$\frac{r/B_{11}}{\beta_{11}} = \frac{r\sqrt{\dfrac{K_1'}{K_1 H_1 H_1'}}}{\dfrac{r}{4H_1}\sqrt{\dfrac{K_1' S_{s_1}}{K_1 S_{s_1}}}} \tag{IV-24}$$

This shows that the ratio $(r/B_{11})/\beta_{11}$ remains constant while changing either r of K_1'/K_1. As radial distance increases, drawdowns in the pumped aquifer become smaller, and vertical gradients across the aquitard are also smaller. On the other hand, if K_1'/K_1 increases, the permeability contrast decreases, and again these vertical gradients are smaller. Thus, in both cases the net result is to cause the spread between the curves to diminish.

The second relationship is explained by noting that if β_{11} is fixed, r/B_{11} must increase for the ratio $(r/B_{11})/\beta_{11}$ to increase. Equation IV-24 shows that one obvious way to accomplish this is to decrease H_1'. Reducing the thickness of the aquitard will decrease the time for the disturbance to reach any given dimensionless elevation z/H_1' and, therefore, bring the curves closer together. On the other hand, fixing r/B_{11} implies that β_{11} must decrease for this ratio to increase. Reference to (IV-24) shows that one way of accomplishing this is to decrease H_1' and at the same time increase H_1. The effect is the same as before.

We have examined above only those cases where both aquifers have identical properties such that $\beta_{11} = \beta_{21}$ and $r/B_{11} = r/B_{21}$. Now we shall discuss the more general case where these properties are not identical. At early values of time, when $t_{D_1} \leqslant 1.6\,\beta_{11}^2/(r/B_{11})^4$, the solutions given by equations IV-20 and IV-22 are independent of β_{21} and r/B_{21}. Thus, the properties of the unpumped aquifer do not affect drawdowns in other parts of the system at sufficiently small values of time.

As time increases, however, drawdowns everywhere in the system become affected by the presence of the unpumped aquifer (i.e., by β_{21} and r/B_{21}). To show this, we shall consider a system where $\beta_{11} = r/B_{11} = 0.1$ and the properties of the unpumped aquifer vary
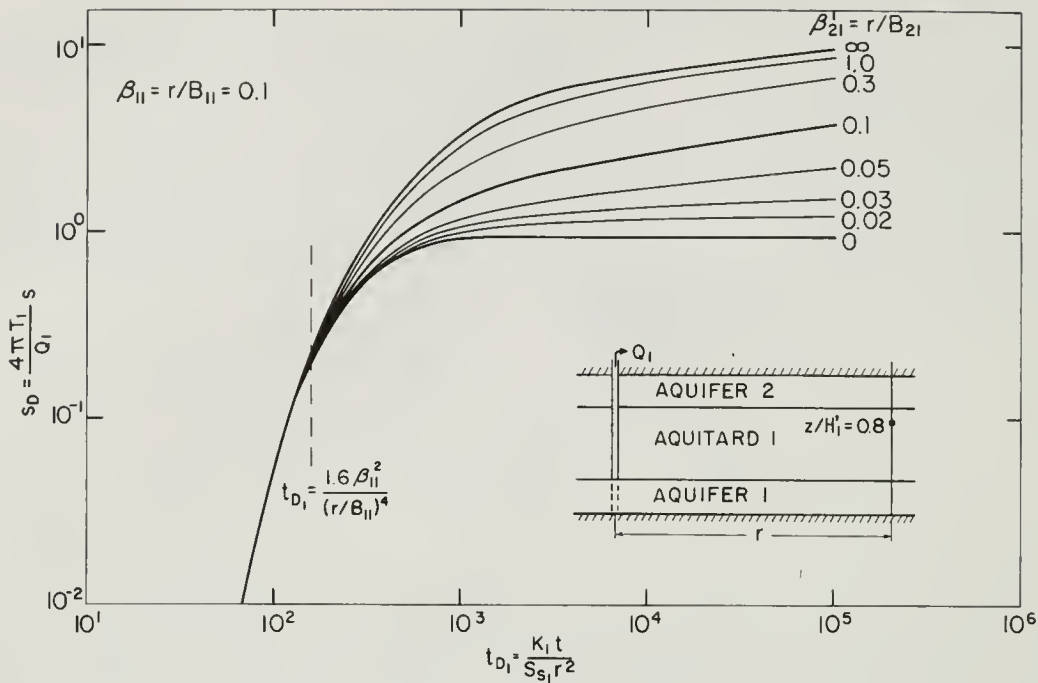
Fig. IV-6.   Effect of unpumped aquifer on dimensionless
drawdown in aquitard at $z/H_1' = 0.8$.
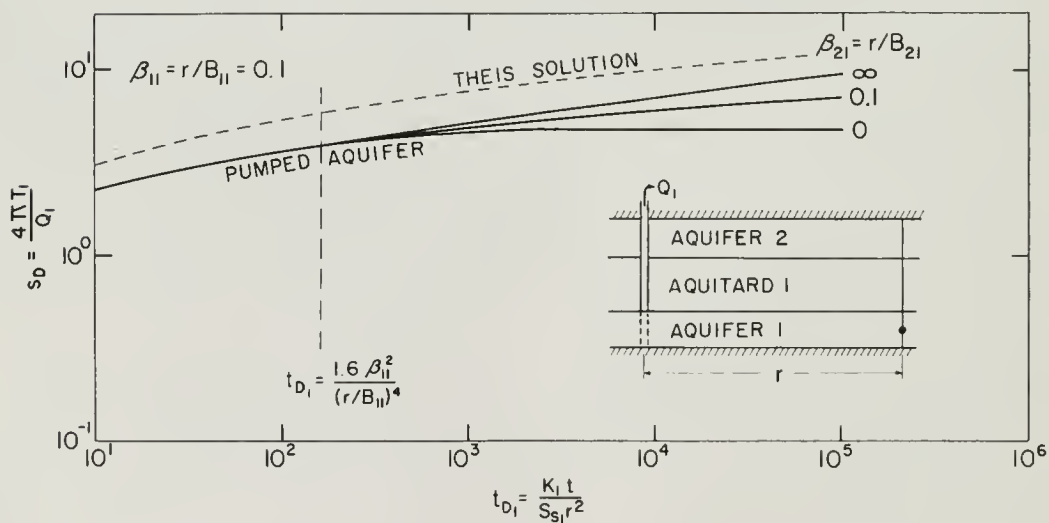
Fig. IV-7.   Effect of unpumped aquifer on dimensionless
drawdown in pumped aquifer.

in such a way that β_{21} and r/B_{21} range from zero to infinity. These situations correspond respectively to infinity and zero transmissibilities in the unpumped aquifer.

Figure IV-6 shows results for $z/H_1' = 0.8$ in the aquitard, and Figure IV-7 shows the effects in the pumped aquifer. Both results were obtained using the finite element method, but the particular curves for $\beta_{21} = r/B_{21} = 0.1$ and 0 were also checked using the analytical solutions. It should be realized that as the permeability of the unpumped aquifer approaches zero (i.e., $\beta_{21} = r/B_{21} \rightarrow \infty$), the assumption of vertical flow in the aquitard is no longer applicable at large values of time, and consequently the analytical solutions must be used with caution.

It can be seen in Figures IV-6 and IV-7 that when transmissibility of the unpumped aquifer becomes very large (i.e., $T_2 \rightarrow \infty$), drawdowns become constant as the quasi-steady state is reached. In this case, drawdown distribution across the thickness of the aquitard is linear at any given radial distance from the pumping well. These results further suggest that when $T_2 > 100\ T_1$ (i.e., $\beta_{21} < 0.1\ \beta_{11}$ and $r/B_{21} < 0.1\ r/B_{11}$) one is probably justified in neglecting drawdown in the unpumped aquifer. It should be noted that the spread in the curves, which reflects the effect of the properties of the unpumped aquifer, increases significantly with vertical distance from the pumped aquifer. This is to be expected because the closer the observation point is to the unpumped aquifer, the greater effect the properties of this aquifer will have.

5. Analytical Solutions for a Three-Aquifer System

Previously, our attention has been focused on a relatively simple system that consisted only of two aquifers and one aquitard. We shall now consider a more general situation where the system involves three aquifers that are separated from each other by two aquitards. Such a three aquifer system is illustrated in Figure IV-8.

We have solved this problem rigorously using essentially the same approach as that employed in analyzing the two-aquifer problem. The details of the mathematics are outlined in Appendix A (Chap. II-D). However, the solutions that were obtained are difficult to evaluate and therefore, were not used in
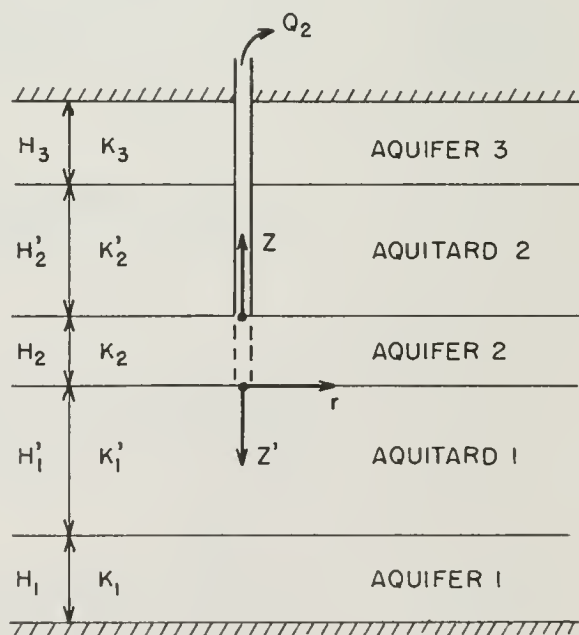
Fig. IV-8. Schematic diagram of three-aquifer system

studying the behavior of a three-aquifer system. Nevertheless, these solutions are important because they enable one to identify the dimensionless parameters β and r/B that control the behavior of a three aquifer system. Knowing the form of these parameters is very helpful in applying finite element or finite difference numerical methods to the study of flow in multiple-aquifer systems (see Appendix A, Chapter IV).

While rigorous solutions are difficult to evaluate, the same does not hold true for the asymptotic solutions at early values of time. When

$$t_{D_2} \leq \frac{1.6\,\beta_{21}^{\,2}}{(r/B_{21})^4} \quad \text{and} \quad t_{D_2} \leq \frac{1.6\,\beta_{22}^{\,2}}{(r/B_{22})^4} \quad ,$$

drawdown in the pumped aquifer is predicted by Hantush's [1960a] solution

$$s_2(r,\,t) = \frac{Q_2}{4\pi T_2} \int_{\frac{1}{4t_{D_2}}}^{\infty} \frac{e^{-y}}{y} \; \text{erfc}\left[\frac{\beta_{21} + \beta_{22}}{\sqrt{y(4t_{D_2}y-1)}}\right] \, dy \tag{IV-25}$$

We have also developed asymptotic solutions for the aquitards (see Appendix A, Chapter II-E) that can be expressed as

$$s_1'(r,\,z,\,t) = \frac{Q_2}{4\pi T_2} \int_{\frac{1}{4t_{D_2}}}^{\infty} \frac{e^{-y}}{y} \left\{ \text{erfc}\left[\frac{\beta_{21} + \beta_{22} + y(z'/H_1')4\beta_{21}/(r/B_{21})^2}{\sqrt{y(4t_{D_2}y-1)}}\right] \right.$$

$$\left. - \text{erfc}\left[\frac{\beta_{21} + \beta_{22} + y(2-z'/H_1')4\beta_{21}/(r/B_{21})^2}{\sqrt{y(4t_{D_2}y-1)}}\right] \right\} dy \tag{IV-26}$$

and

$$s_2'(r,\,z,\,t) = \frac{Q_2}{4\pi T_2} \int_{\frac{1}{4t_{D_2}}}^{\infty} \frac{e^{-y}}{y} \left\{ \text{erfc}\left[\frac{\beta_{21} + \beta_{22} + y(z/H_2')4\beta_{22}/(r/B_{22})^2}{\sqrt{y(4t_{D_2}y-1)}}\right] \right.$$

$$\left. - \text{erfc}\left[\frac{\beta_{21} + \beta_{22} + y(2-z/H_2')4\beta_{22}/(r/B_{22})^2}{\sqrt{y(4t_{D_2}y-1)}}\right] \right\} dy \tag{IV-27}$$

-34-

At sufficiently small values of time, or when the thickness of Aquitard 1 is large, equation IV-26 can be simplified by letting $H_1' \rightarrow \infty$. The result becomes

$$s_1'(r, z, t) = \frac{Q_2}{4\pi T_2} \int_{\frac{1}{4t_{D_2}}}^{\infty} \frac{e^{-y}}{y} \, \mathrm{erfc} \left[\frac{\beta_{21} + \beta_{22} + y\sqrt{t_{D_2}/t_{D_1}'}}{\sqrt{y(4t_{D_2}y-1)}} \right] dy \qquad (IV-28)$$

where $t_{D_1}' = \dfrac{K_1't}{S_{s_1}'z'^2}$. Similarly, if we let $H_2' \rightarrow \infty$, then (IV-27) reduces to

$$s_2'(r, z, t) = \frac{Q_2}{4\pi T_2} \int_{\frac{1}{4t_{D_2}}}^{\infty} \frac{e^{-y}}{y} \, \mathrm{erfc} \left[\frac{\beta_{21} + \beta_{22} + y\sqrt{t_{D_2}/t_{D_2}'}}{\sqrt{y(4t_{D_2}y-1)}} \right] dy \qquad (IV-29)$$

where $t_{D_2}' = \dfrac{K_2't}{S_{s_2}'z'^2}$.

Since the properties of the unpumped aquifers do not enter into equations IV-25 through IV-29, it is obvious that these equations will apply in multiple aquifer systems that are composed of an arbitrary number of layers. Another special case that leads to a relatively simple solution is one where drawdown in the two unpumped aquifers is assumed to remain zero. The solution in the pumped aquifer is given by

$$s_2(r, t) = \frac{Q_2}{4\pi T_2} \, 2\int_0^{\infty} (1 - e^{-t_{D_2}y^2}) \, J_0\,[\omega(y)] \, \frac{dy}{y} \qquad (IV-30)$$

where

$$\omega^2(y) = y^2 - 4\beta_{21} \, y \cot \left[\frac{4\beta_{21}\,y}{(r/B_{21})^2} \right] - 4\beta_{22} \, y \cot \left[\frac{4\beta_{22}\,y}{(r/B_{22})^2} \right]$$

and $J_0\,[\omega(y)]$ must be set to zero when $\omega^2(y) < 0$. In Aquitard 1 the solution is

$$s_1'(r, z, t) = -\frac{Q_2}{2\pi T_2} \, \frac{2}{\pi} \sum_{n=1}^{\infty} \frac{1}{n} \sin \frac{n\pi z'}{H_1'} \int_0^{\infty} \left[1 - e^{-\theta_{21}n^2\pi^2 t_{D_2}} \right.$$

$$\left. + \frac{e^{-y^2 t_{D_2}} - e^{-\theta_{21}n^2\pi^2 t_{D_2}}}{\dfrac{y^2}{\theta_{21}n^2\pi^2} - 1} \right] J_0\,[\omega^2(y)] \, \frac{dy}{y} \qquad (IV-31)$$

-35-

where $\theta_{21} = \dfrac{(r/B_{21})^4}{(4\beta_{21})^2}$.

The same equation can also be applied to Aquitard 2, provided that H_1' and θ_{21} are replaced by H_2' and θ_{22}, respectively. The details of the mathematics are outlined in Appendix A (Chapter II-F).

6. Theory of Flow in a Slightly Leaky System

When the pumped aquifer is confined between two aquitards that have a very low permeability (i.e. aquicludes), drawdown in the aquifer will usually follow the well-known Theis solution. This simply means that the amount of water contributed by the aquicludes is too small to show the usual effects of leakage and, therefore, one may refer to such a system as being "slightly leaky". Let us again consider a two aquifer system such as in Figure IV-1. Assuming that drawdown in the unpumped aquifer remains zero, flow in the aquiclude may be characterized by

$$\frac{\partial^2 s_1'}{\partial z^2} = \frac{1}{\alpha_1'} \frac{\partial s_1'}{\partial t} \tag{IV-32}$$

$$s_1'(r,\, z,\, 0) = 0 \tag{IV-33}$$

$$s_1'(r,\, 0,\, t) = \frac{Q_1}{4\pi T_1} \left[- \text{Ei} \left(- \left(\frac{1}{4t_{D_1}} \right) \right) \right] \tag{IV-34}$$

$$s_1'(r,\, H_1',\, t) = 0 \tag{IV-35}$$

It can be shown [Neuman and Witherspoon, 1968] that a solution to this problem is given by

$$s_1'(r,\, z,\, t) = \frac{Q_1}{4\pi T_1} \frac{4}{\pi} \sum_{n=1}^{\infty} \frac{1}{n} \sin \frac{n\pi z}{H_1'} \int_0^{\frac{n\pi z}{H_1'}\sqrt{t_{D_1}'}} \left[- \text{Ei}\left(- \frac{\left(\frac{n\pi z}{H_1'}\right)^2 t_{D_1}'}{4 t_{D_1}\left[\left(\frac{n\pi z}{H_1'}\right)^2 t_{D_1}' - y^2\right]} \right) \right] y e^{-y^2} dy \tag{IV-36}$$

At large values of time (or small values of z) one can assume that $t_{D_1}' \to \infty$, which means that the exponential integral in (IV-36) approaches $- \text{Ei}\,[-1/4t_{D_1}]$, The remaining integral approaches 1/2, and therefore (IV-36) becomes

$$s_1'(r, z, t) = \frac{Q_1}{4\pi T_1} \frac{2}{\pi} \left[- \text{Ei} \ (-1/4t_{D_1}) \right] \sum_{n=1}^{\infty} \frac{1}{n} \sin \frac{n\pi z}{H_1'}$$

$$= \frac{Q_1}{4\pi T_1} \left[- \text{Ei} \ (-1/4t_{D_1}) \right] (1 - \frac{z}{H_1'}) \qquad\qquad (IV-37)$$

Thus, the ratio between drawdown in the aquiclude at some given distance r and drawdown in the aquifer at the same radial distance from the pumping well is given by

$$\frac{s'}{s} = 1 - \frac{z}{H_1'} \qquad\qquad (IV-38)$$

Since we have assumed no drawdown in the unpumped aquifer, there will be a linear variation in the drawdown across the aquiclude as the quasi-steady state is approached.

At sufficiently small values of time, or when the aquiclude is relatively thick, one can obtain a simpler expression by letting $H_1' \to \infty$. In this case, boundary condition (IV-35) changes to

$$s_1'(r, \infty, t) = 0 \qquad\qquad (IV-39)$$

and the solution becomes [Neuman and Witherspoon, 1968]

$$s_1'(r, z, t) = \frac{Q_1}{4\pi T_1} \frac{2}{\sqrt{\pi}} \int_{\frac{1}{2\sqrt{t_{D_1}'}}}^{\infty} - \text{Ei} \left[- \frac{t_{D_1}' y^2}{t_{D_1}(4t_{D_1}' y^2 - 1)} \right] e^{-y^2} dy \qquad\qquad (IV-40)$$

At large values of time (or small values of z) the exponential integral in (IV-40) approaches $- \text{Ei} \ [-1/4t_{D_1}]$ such that

$$s_1'(r, z, t) = \frac{Q_1}{4\pi T_1} \left[- \text{Ei} \ (-1/4t_{D_1}) \right] \text{erf}(\infty) = \frac{Q_1}{4\pi T_1} \left[- \text{Ei} \ (-1/4t_{D_1}) \right] \qquad\qquad (IV-41)$$

Consequently, the ratio between drawdown in the aquitard and in the aquifer vertically below is unity, or

$$\frac{s'}{s} = 1 \qquad\qquad (IV-42)$$

This, of course, could have been anticipated from (IV-38) where H_1' is taken to be very large $(H_1' \to \infty)$.

It should be noted that all of the above equations are also valid for an aquitard that lies below the pumped aquifer, provided that z is measured downward from the bottom of this aquifer.

Equations IV-36 and IV-40 have been evaluated numerically using Zonneveld's adaptation of the Adams-Moulton method. Extensive tables of results for both finite and infinite aquitard have been published elsewhere [Witherspoon et al., 1967]. These results cover a practical range of dimensionless time and values of z/H_1' ranging from 0 to 0.9. For further discussion of these results, the reader is referred to Neuman and Witherspoon [1968].

C. APPLICABILITY OF EARLIER THEORIES OF FLOW IN LEAKY AQUIFERS

In discussing the evolution of theories dealing with flow in leaky aquifers, we mentioned the fact that it has always been customary to use one or both of the following two assumptions: (1) storage in the aquitards is negligible, and (2) drawdown in the unpumped aquifers remains zero. Since our new theory does not rely on any of these assumptions, it can be used to investigate the applicability of the simplifications introduced in the earlier approaches. To do this, we shall first consider a solution by Hantush and Jacob [1955b] that describes non-steady radial flow to a well completely penetrating an infinite leaky aquifer and discharging at a constant rate. This solution is of particular interest to us because it has been extensively tabulated [Hantush, 1956] and the resulting type curves are being widely used in evaluating the properties of leaky aquifers [Ferris et al., 1962; Walton, 1960, 1962; Slater, 1963; DeWiest, 1965; Narasimhan, 1968]. The results of this solution are usually presented in terms of the dimensionless parameter

$$r/B = r \sqrt{\frac{K'}{KHH'}}$$

which we note is a function of the permeability contrast between the pumped aquifer and an adjacent aquitard. We shall refer to this as the "r/B solution".

Subsequent to the r/B solution, Hantush [1960a] published his modified theory of flow in leaky aquifers where for the first time consideration was given to effects of storage in the aquitards. Assuming again that drawdowns in the unpumped aquifers remain zero, Hantush was able to develop asymptotic solutions for the pumped aquifer that apply only at small and large values of time. His solution for small values of time (see equations IV-20 and IV-25) has been extensively tabulated [Hantush, 1960b] in terms of the dimensionless parameter

$$\beta = \frac{r}{4H} \sqrt{\frac{K'S_s'}{K S_s}}$$

-38-

which we see differs from r/B in that the effects of storage are now included. We shall refer to this as the "β solution". His solution for large values of time can be written

$$s_1(r, t) = \frac{Q_1}{4\pi T_1} \int_{\frac{\delta_1}{4t_{D_1}}}^{\infty} \exp\left[-y - \frac{(r/B_{11})^2}{4y}\right] \frac{dy}{y} \qquad \text{(IV-43)}$$

where $\delta_1 = 1 + \frac{16\,\beta_{11}^2}{3(r/B_{11})^2}$ $\qquad$ (IV-44)

and his criterion for the validity of this solution can be expressed as

$$t_{D_1} \geqslant \frac{80\,\beta_{11}^2}{(r/B_{11})^4} \qquad \text{(IV-45)}$$

It is seen by virtue of the expressions given for δ_1 and t_{D_1} in (IV-20), (IV-44), and (IV-45) that (IV-20) and (IV-43) are functions of both β_{11} and r/B_{11}. In addition, it is evident from these limits on t_{D_1} that, for given values of β_{11} and r/B_{11}, these solutions cover the entire time domain except for an interval whose span is less than two log cycles.

A complete solution to this problem for all values of time has been developed in this work and is given in equation IV-30. For a two-aquifer system such as in Figure IV-1, this solution may be written

$$s_1(r, t) = \frac{Q_1}{4\pi T_1} 2 \int_0^{\infty} (1 - e^{-y^2 t_{D_1}}) J_o\,[\omega(y)]\,\frac{dy}{y} \qquad \text{(IV-46)}$$

where

$$\omega^2(y) = y^2 - 4\beta_{11}\,y\,\cot\left[\frac{4\,\beta_{11}y}{(r/B_{11})^2}\right]$$

and $J_o\,[\omega(y)]$ must be set to zero when $\omega^2(y) < 0$.

Equation IV-46 has been evaluated numerically and the results for values of β_{11} of 0.01 and 0.1 and various values of r/B_{11} are shown in Figures IV-9 and IV-10, respectively. In each figure, we see an envelope from which a family of r/B_{11} curves extend. The position of the envelope depends on the magnitude of β_{11}, and as this parameter increases in magnitude one sees that deviations from the Theis solution also
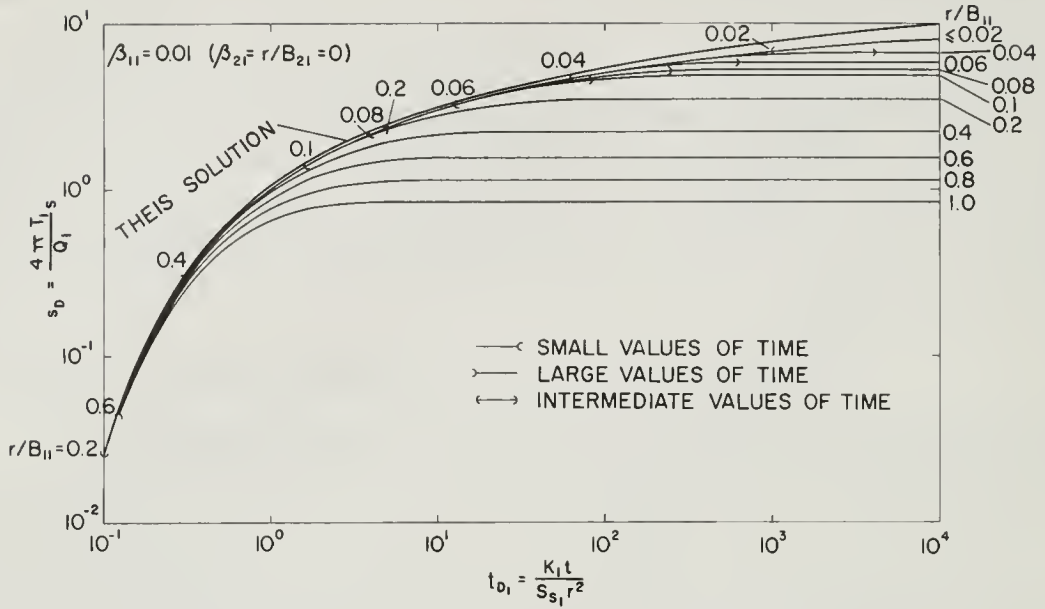
-39-

Fig. IV-9. Dimensionless drawdown in pumped aquifer
when drawdown in unpumped aquifer is zero
for $\beta_{11} = 0.01$.
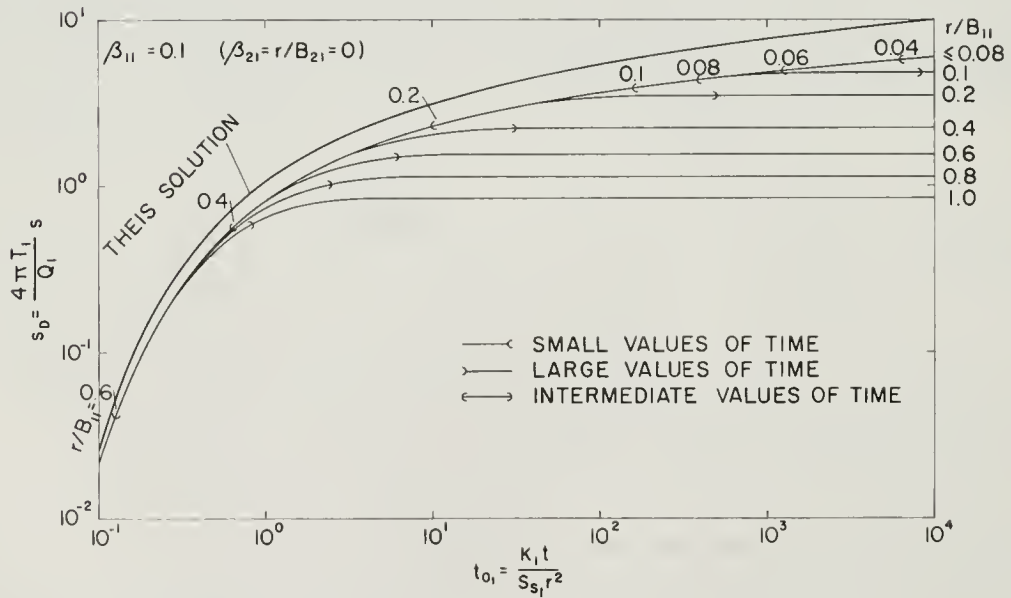
Fig. IV-10. Dimensionless drawdown in pumped aquifer
when drawdown in unpumped aquifer is zero
for $\beta_{11} = 0.1$.

increase. As r/B_{11} increases, the curves diverge from the envelope at earlier and earlier values of dimensionless time. These curves reach steady state values for dimensionless drawdowns that are identical with those obtained by Hantush [1956]. Additional graphs for other values of β_{11} are given in Appendix A (Chapter IV-A).

Each curve on Figures IV-9 and IV-10 has been divided by a set of parentheses into three sections. The section to the left of the parentheses corresponds to Hantush's [1960a] definition of small values of time (i.e., $t_{D_1} < 1.6 \ \beta_{11}^2/(r/B_{11})^4$) from his β solution. Our results as obtained from equation IV-46 are identical with his (as given by equation IV-20) over these same time intervals.

The section to the right of the parentheses on each curve corresponds to Hantush's solution for large values of time (equation IV-43). Again our results as obtained from equation IV-46 are identical with those evaluated by Hantush [1960a] from equation IV-43.

The section on each curve that is enclosed by parentheses, therefore, represents a time interval for which Hantush [1960a] stated his asymptotic solutions should not be used. Our results indicate that his criteria for the validity of his solutions are on the conservative side and could be relaxed somewhat.

1. Evaluating the Assumption that Storage in the Aquitard May Be Neglected

As indicated earlier, Hantush and Jacob [1955b] have solved the above problem of flow in a leaky aquifer by assuming that the storage capacity of the aquitard can be neglected. Their solution for all values of time can be expressed as

$$s_1(r, \ t) = \frac{Q_1}{4\pi T_1} \int_{\frac{1}{4t_{D_1}}}^{\infty} \exp\left[- \ y \ - \ \frac{(r/B_{11})^2}{4y}\right] \ \frac{dy}{y} \qquad (IV-47)$$

and has been referred to here as the r/B solution. One may note that if storage is to be neglected, then $\beta_{11} = 0$ in (IV-44), and equations IV-43 and IV-47 are identical.

Anyone familiar with the literature on leaky aquifers will immediately recognize that the family of curves shown in Figure IV-9 for $\beta_{11} = 0.01$ is almost identical with that of the r/B solution. The only difference is that the envelope of curves instead of coinciding with the Theis solution slowly diverges from it as time increases.

Thus if one is analyzing field data at large values of time for a system with $\beta_{11} = 0.01$, ignoring the effects of storage in the aquitard will only introduce a slight error as long as r/B_{11} is also small (i.e., $\leqslant 0.01$). From a practical standpoint,

however, it would appear that neglecting storage in the aquitard should not affect the solution for the pumped aquifer as long as $\beta_{11} \leq 0.01$.

An examination of Figures IV-9 and IV-10 shows that as β_{11} increases, the r/B solution becomes less and less representative of the actual behavior in the pumped aquifer. The errors involved in the r/B solution become significant when β_{11} reaches 0.1 and they are large when $\beta_{11} = 1.0$.

The nature of these errors for large values of β_{11} can be better understood by superposing the r/B solution on the $\beta_{11} = 1.0$ solution as shown in Figure IV-11. One sees immediately that the errors involved in the r/B solution increase as the magnitude of r/B_{11} decreases. However, from the convergence of the curves for the two solutions at large values of time, it is also apparent that these errors decrease with time and disappear altogether for those values of t_{D_1} given by (IV-45). We therefore conclude that with large values of β_{11} and zero drawdown in the unpumped aquifer, the r/B solution is subject to significant errors whenever $t_{D_1} \leq 80 \, \beta_{11}/(r/B_{11})^4$.

For the particular case of $\beta_{11} = 1.0$ as shown on Figure IV-11, this means that the entire non-steady state period of pumping cannot be analyzed using the r/B solution. In other words, the r/B solution would only be applicable to the steady state after drawdowns have become constant. It should be kept in mind that the steady state regions on all the curves of Figures IV-9, IV-10, and IV-11 are the result of the initial assumption that drawdown remains zero in the unpumped aquifer.

There is a simple physical explanation for the errors in the r/B solution when β_{11} is large. At small values of time, the disturbance created by withdrawing water has not yet significantly affected the unpumped aquifer. Most of the early leakage is derived from the aquitard, and the amount depends on the specific storage of this part of the system, i.e., on the magnitude of β_{11}. At this stage, disregarding storage in the aquitard is equivalent to neglecting leakage altogether. Thus the resulting curves for the r/B solution fail to show the true effects of leakage at early time.

As time increases, more and more leakage is being contributed by the unpumped aquifer, and the relative amount of water that comes from storage in the aquitard diminishes. By the time steady state is reached and drawdowns are constant, all of the leakage is supplied by the unpumped aquifer. The aquitard merely acts as a conduit for flow from one aquifer to another. The storage capacity of the aquitard has no influence on the behavior of the system, and therefore the r/B solution is applicable.

The assumption that storage in the aquitard may be neglected obviously fails completely if one is interested in the transient behavior of the aquitard itself.

2. Evaluating the Assumption that Drawdown in the Unpumped Aquifer May Be Neglected

As mentioned earlier, we have obtained a complete solution to the problem of
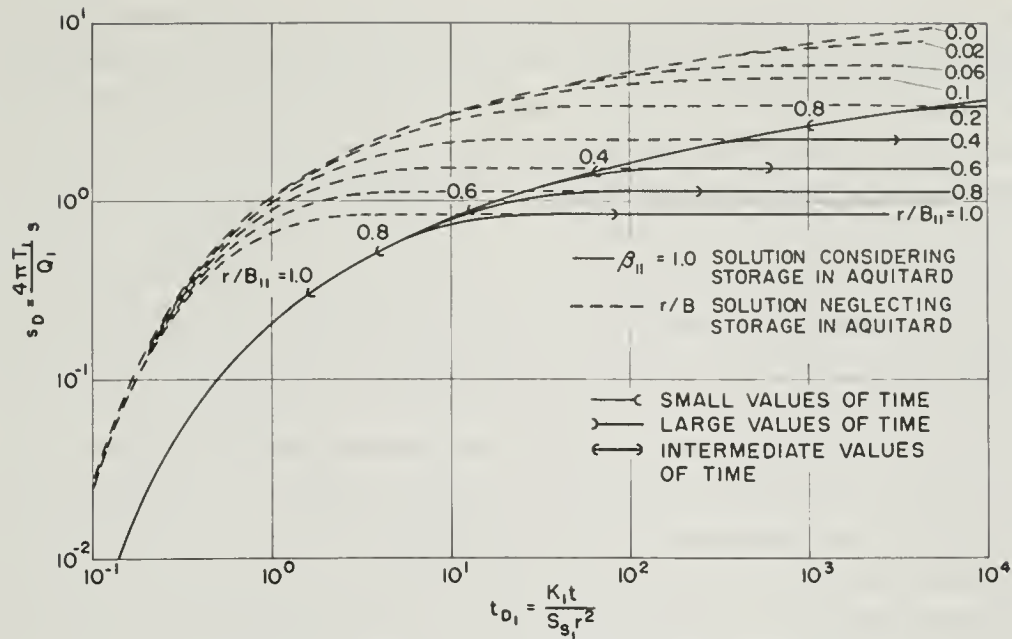
Fig. IV-11. Comparison of solution for pumped aquifer
when β_{11} = 1.0 with r/B solution.

flow in a two aquifer system for the case when drawdown in the unpumped aquifer is not
necessarily zero. The results are expressed in terms of the five parameters β_{11}, r/B_{11},
β_{21}, r/B_{21}, and t_{D_1}, and are given by equations IV-7 through IV-16. These solutions
have been evaluated for selected values of the controlling parameters, and some of the
results for the particular case when β_{11} = r/B_{11} = 0.1 are shown in Figure IV-6 and IV-7.

As might be expected, the results in the pumped aquifer are independent of β_{21}
and r/B_{21} at small values of time. In general we found that the transient behavior of
the pumped aquifer and the aquitard was not affected by conditions in the unpumped
aquifer as long as equation IV-21 is satisfied. However, transient effects in the
unpumped aquifer are dependent on β_{21} and r/B_{21} as well as on β_{11} and r/B_{11} at all
values of time. Thus the assumption that drawdown in the unpumped aquifer may be
neglected is valid at small values of time everywhere in the system except in the
unpumped aquifer itself.

At larger values of time when t_{D_1} > 1.6 $\beta_{11}^2/(r/B_{11})^4$, the behavior of the
unpumped aquifer may have a significant effect on drawdown in other parts of the
system. For example, reference to Figure IV-7 will show that the results for the
pumped aquifer that are uniquely defined for a given β_{11} and r/B_{11} at small values of
time become a family of curves at large values of time, depending on the values of β_{21}
and r/B_{21}.

A family with three branches is shown for the drawdown curve of the pumped
aquifer in Figure IV-7. The lower branch corresponds to the special case previously

-43-

discussed in connection with Figures IV-9 and IV-10, where it was assumed that there is no drawdown in the unpumped aquifer. A necessary condition for zero drawdown in the unpumped aquifer is that its transmissibility be infinitely large. Thus the lower branch of the curves for the pumped aquifer on Figure IV-7 corresponds to the special case where $T_2 = \infty$, which means $\beta_{21} = r/B_{21} = 0$.

When β_{21} and r/B_{21} are greater than zero, the assumption of no drawdown in the unpumped aquifer will no longer be valid. For example the middle branch of the drawdown curve for the pumped aquifer on Figure IV-7 represents another special case where the hydraulic properties of both aquifers are identical, i.e., $\beta_{11} = \beta_{21}$ and $r/B_{11} = r/B_{21}$. The upper branch represents the limiting case when $\beta_{21} = r/B_{21} = \infty$. This latter case implies that the permeability of the unpumped aquifer is zero ($K_2 = 0$) and means that a no-flow boundary exists at the interface between the aquitard and the unpumped aquifer. This corresponds to Hantush's [1960a] case 2 in his modified treatment of leaky aquifers. It is clear from Figure IV-7 that when the transmissibility of the unpumped aquifer is not infinitely large, as would usually be the case in the field, drawdown in the pumped aquifer does not reach steady state.

The assumption of zero drawdown in the unpumped aquifer can therefore lead to errors that will depend primarily on the magnitude of β_{11} and r/B_{11}. As is indicated on Figure IV-7 where $\beta_{11} = r/B_{11} = 0.1$, these errors increase with time as the ratios β_{21}/β_{11} and $(r/B_{21})/(r/B_{11})$ increase, i.e., as the transmissibility and storage capacity of the unpumped aquifer become less in relation to those of the pumped aquifer.

However, as the values of β_{11} and r/B_{11} decrease, the errors introduced by assuming zero drawdown in the unpumped aquifer will decrease for given ratios of T_2/T_1 and S_{s_2}/S_{s_1}. Theoretically these errors will not disappear completely unless the unpumped aquifer is replaced by a ponded body of water whose head remains constant. From a practical standpoint these errors can probably be neglected in analyzing drawdowns in the pumped aquifer when both β_{11} and $r/B_{11} < 0.01$ or when the ratios T_2/T_1 and S_{s_2}/S_{s_1} are sufficiently large. Our present work suggests that β_{21} and r/B_{21} should be about ten times smaller than β_{11} and r/B_{11}, respectively, in order for the errors to be negligible. This needs further investigation.

If we now turn our attention briefly to the aquitard, one would anticipate that the properties of the unpumped aquifer will have a much more profound effect on drawdown in the aquitard than we have just seen for the pumped aquifer. To illustrate this point we have included results on Figure IV-6 determined at only one location in the aquitard ($z/H_1' = 0.8$). Radial distance from the pumping well also becomes important, and these aquitard results are for a distance of more than twice the combined thicknesses of pumped aquifer and aquitard ($H_1 + H_1'$).

The aquitard results shown on Figure IV-6 for the limiting case of $\beta_{21} = r/B_{21} = \infty$ reveal an interesting result. It will be noted that dimensionless drawdown in the

-44-

aquitard coincides with that of the pumped aquifer at large values of time. This means that in this limiting case of a no-flow boundary on one side of the aquitard, flow in all parts of the system away from the immediate vicinity of the pumping well becomes radial at large values of time. Javandel and Witherspoon [1968] report the same effect has been noted for a well that partially penetrates a two-layered aquifer regardless of the permeability contrast.

Thus, since it has been customary to assume vertical flow in the aquitard in developing solutions for leaky aquifers, the special case of a no-flow boundary presents a problem because the direction of flow is essentially vertical only at early time and then slowly changes to become radial at large values of time, especially as distance from the pumping well increases. Hantush's [1960a] asymptotic solution at large values of time for case 2 in his modified approach to leaky aquifers does not take this into consideration. However, in checking his results for the pumped aquifer, we found that our solution, which in this case was obtained by the finite element method, is in good agreement with his, indicating that direction of flow in the aquitard at this stage does not affect the result in the pumped aquifer.

As mentioned earlier, Hantush [1967b] has also analyzed this two aquifer case and developed solutions for drawdown in both the pumped and the unpumped aquifers. However, he assumed that storage in the intervening aquitard could be neglected. It is therefore of interest to see how our results, which include the effects of storage in the aquitard, compare with his. If we choose $T_1 = T_2$ (e.g., $r/B_{11} = r/B_{21}$), then Hantush's equations 17 and 18 for the special case of equal diffusivities in both aquifers ($K_1/S_{s_1} = K_2/S_{s_2}$) may be written

$$s_1(r, t) = \frac{Q_1}{8\pi T_1} \int_{\frac{1}{4t_{D_1}}}^{\infty} \left\{ \exp(-y) + \exp\left[-y - \frac{2(r/B_{11})^2}{4y} \right] \right\} \frac{dy}{y} \qquad (IV-48)$$

$$s_2(r, t) = \frac{Q_1}{8\pi T_1} \int_{\frac{1}{4t_{D_1}}}^{\infty} \left\{ \exp(-y) - \exp\left[-y - \frac{2(r/B_{11})^2}{4y} \right] \right\} \frac{dy}{y} \qquad (IV-49)$$

Figure IV-12 shows a comparison of results for the pumped and unpumped aquifers as obtained using our solutions (equations IV-17 and IV-19) and as obtained using Hantush's solutions (equations IV-48 and IV-49). In both cases we arbitrarily chose $\beta_{11} = \beta_{21} = r/B_{11} = r/B_{21} = 0.1$. One may note that in the pumped aquifer our results differ somewhat from those of Hantush. His solution lies along the Theis solution at early time
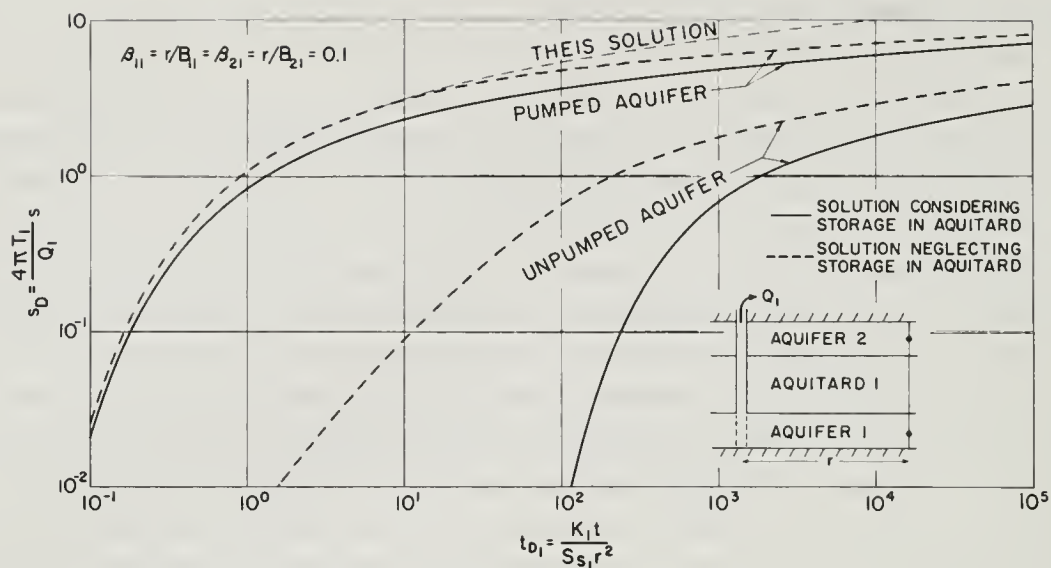
Fig. IV-12. Effect of neglecting storage in aquitard
on dimensionless drawdown in pumped and
unpumped aquifers.

and then diverges from it as time increases so as to lie between our solution and the
Theis curve. If we had chosen the case for $\beta_{11} = \beta_{21} = 1.0$, these differences would
be considerably greater.

It should be recalled that when we had zero drawdown in the unpumped aquifer,
errors due to neglecting storage in the aquitard did not disappear until steady state
was reached. Now we see from Figure IV-12 that when there is no steady state these
errors occur at all values of time.

For the unpumped aquifer, however, it is seen that there is a large difference
between our results and those of Hantush. His solution gives an earlier response and
a much greater drawdown than ours. This, of course, is to be expected because in our
system the aquitard contributes water from storage and therefore acts as a buffer
between the two aquifers. As might be expected the differences between our two solu-
tions for the unpumped aquifer will be even greater if $\beta_{11} = \beta_{21} = 1.0$.

This naturally raises the question whether the magnitude of the storage
coefficient for an aquitard is so small that it can be neglected. This question is,
of course, difficult to answer because of the scarcity of data on the hydrologic
characteristics of aquitards. One source of such data is a comprehensive report
containing a number of laboratory measurements on core samples from several different
aquitards of Central California [Johnson et al., 1968]. The materials range from
sandy silts to clays. Permeabilities range from 10^{-6} to over 10^{-3} gpd/ft^2, and
specific storage ranges from 3×10^{-6} to 5×10^{-4} ft^{-1}.

-46-

More recently Wolff [1970] has presented laboratory data for a shallow aquiclude in Salisbury, Maryland, composed primarily of clayey material. Permeabilities range from 2×10^{-4} to 5×10^{-2} gpd/ft^2 and specific storage ranges from 3×10^{-5} to 1×10^{-3} ft^{-1}. Our own laboratory measurements on samples taken from the Oxnard aquitards (see Table V-5) indicate values of specific storage that range from 1×10^{-4} to 6×10^{-4} ft^{-1}. These data show that the specific storage of unconsolidated aquitard materials is at least as large as that of most confined aquifer sands and gravels, if not significantly greater. Under these circumstances, it is not difficult to show that β may easily reach 0.1 and at times may exceed 1.0. If this is the case, our analysis indicates that, in general, storage in the aquitard must be taken into consideration when evaluating leaky systems.

3. Use of the r/B and β Solutions to Analyze Field Data

Several methods of using the r/B and β solutions to analyze the results of pumping tests have been proposed by Jacob [1946], Hantush [1956, 1960a], and by Narasimhan [1968]. The graphical curve matching methods of Jacob and Hantush are discussed in Appendix A (Chapter V-A), where it is shown that they are limited in application and may often lead to erroneous interpretations of the field data. The ratio method proposed by Narasimhan has an advantage because it eliminates errors due to individual judgment in the process of curve-matching. However, this method is also based on the r/B solution and is, therefore, subject to the same limitations as the r/B solution itself.

The following two examples of hypothetic field data will be used to illustrate the kind of errors that can arise when one uses the r/B curve matching procedure to analyze the results of a pumping test.

For the first example we shall assume a two aquifer system (Figure IV-13) where $H_1 = H_2 = 25$ feet, $H_1' = 100$ feet, $K_1 = 1800$ gpd/ft^2 and $S_{s_1} = 2 \times 10^{-6}$ ft^{-1} for the aquifer being pumped, and $K_1' = 0.5$ gpd/ft^2 and $S_{s_1}' = 8 \times 10^{-6}$ ft^{-1} for the overlying aquitard. We shall further assume that $T_2 \gg T_1$ such that $\beta_{21} \approx r/B_{21} \approx 0$, which means that drawdown in the unpumped aquifer is negligible.

If an observation well is completed in Aquifer 1 at a distance of $r = 300$ feet from the pumping well, the values of β_{11} and r/B_{11} become

$$\beta_{11} = \frac{r}{4H_1} \sqrt{\frac{K_1'S_{s_1}'}{K_1 S_{s_1}}} = \frac{300}{(4)(25)} \sqrt{\frac{(0.5)(8 \times 10^{-6})}{(1800)(2 \times 10^{-6})}} = 0.1$$
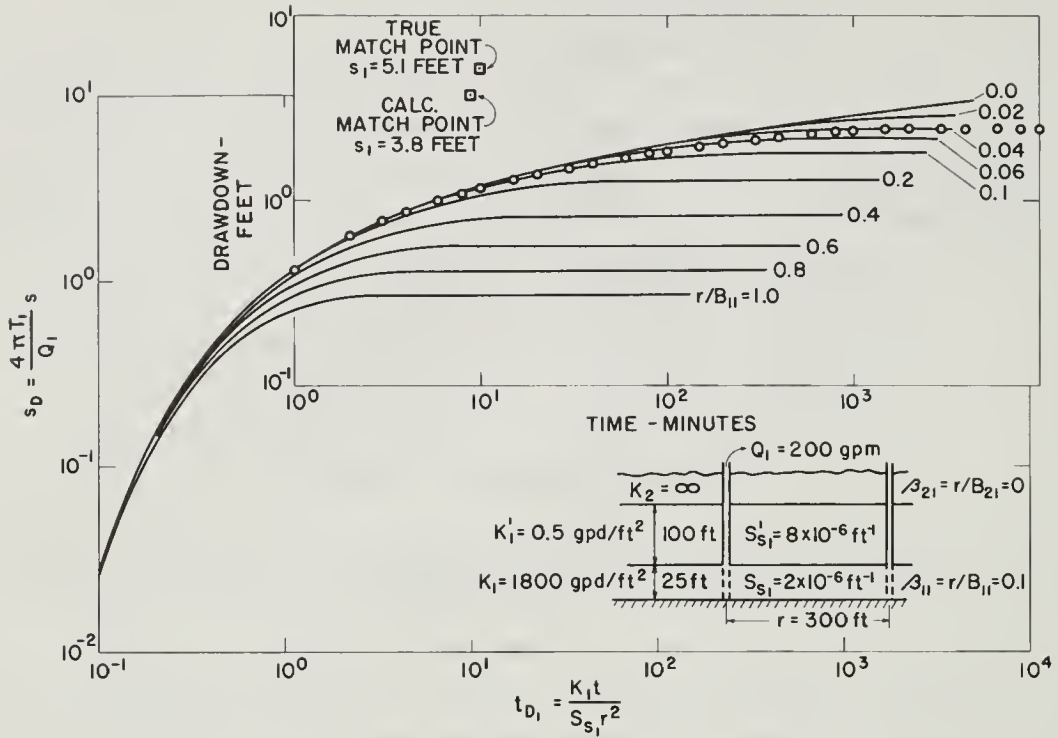
Fig. IV-13. Comparison of hypothetical field data
with r/B solution when drawdown in
unpumped aquifer is zero.

$$\frac{r}{B_{11}} = r \sqrt{\frac{K_1'}{K_1 H_1 H_1'}} = 300 \sqrt{\frac{0.5}{(1800)(25)(100)}} = 0.1$$

Under these conditions we shall assume that a pumping test is performed with $Q_1 = 200$ gpm, and the drawdown data at the observation well would of course follow the curve for $\beta_{21} = r/B_{21} = 0.0$ as shown on Figure IV-7. This fact, however, is unknown to the analyst, and in using the r/B solution he would obtain the best match with r/B = 0.04 (see Figure IV-13). Using the indicated match point at $s_D = 10$, where $s_1 = 3.8$ feet, he would then obtain

$$K_1 = \frac{114.6 \, Q_1}{H_1} \frac{s_D}{s_1} = \frac{(114.6)(200)(10)}{(25)(3.8)} = 2410 \text{ gpd/ft}^2$$

$$K_1' = \frac{(r/B_{11})^2 K_1 H_1 H_1'}{r^2} = \frac{(0.04)^2 (2410)(25)(100)}{(300)^2} = 0.11 \text{ gpd/ft}^2$$

-48-

Thus, we see that in using the r/B solution for this situation the calculated permeability is too high for the aquifer ($\approx 33\%$) and almost five times too low for the aquitard. The calculated permeability contrast would be $K_1/K_1' = 2410/0.11 = 21,900$, whereas the true value is only 3600.

If a second observation well were available at $r = 300$ feet, then drawdown data would follow the curve for $\beta_{11} = r/B_{11} = 1.0$ shown on Figure IV-11. If the analyst again used the r/B solution in the same manner as above, he would probably obtain the best match with $r/B = 0.3$. At the same match point of $s_D = 10$, where $s_1 = 1.5$ feet, he would then obtain

$$K_1 = \frac{(114.6)(200)(10)}{(25)(1.5)} = 6110 \text{ gpd/ft}^2$$

$$K_1' = \frac{(0.3)^2(6110)(25)(100)}{(30000)^2} = 0.15 \text{ gpd/ft}^2$$

From this second set of results, we see that the calculated permeability is three times too high for the aquifer and three times too low for the aquitard. The calculated permeability contrast is worse than before, $K_1/K_1' = 6110/0.15 = 40,700$, or over ten times the true value. This illustrates how the errors increase as β_{11} and r/B_{11} increase. The analyst could be badly misled from the results of this analysis by: (a) overpredicting the productivity of the aquifer, (b) underestimating the leakage contribution from the aquitard, and (c) concluding that the aquifer is radially inhomogeneous when the apparent increase in permeability with distance is due to a misinterpretation of the effects of leakage.

For the second example, we shall use the same two aquifer system as before, except that now we shall assume that the hydraulic properties of both aquifers are identical, i.e., $K_1 = K_2 = 1800$ gpd/ft^2 and $S_{s_1} = S_{s_2} = 2 \times 10^{-6}$ ft^{-1}. If the aquitard properties are the same as before, then an observation well at $r = 300$ feet would mean $\beta_{11} = \beta_{21} = r/B_{11} = r/B_{21} = 0.1$.

Under these conditions we shall assume that a pumping test is performed with $Q_1 = 200$ gpm, and the drawdown data would now follow the curve for $\beta_{21} = r/B_{21} = 0.1$ shown on Figure IV-7. This fact is again unknown to the analyst, and he might choose to match the field results with the r/B solution as indicated on Figure IV-14. If he does so, then at $s_D = 10$, $s_1 = 3.6$, and the permeability result for the aquifer would be $K_1 = 2540$ gpd/ft^2 or about 40% too high.

The result might be acceptable, but a more serious problem now arises in that one will have difficulty deciding what value of r/B to choose. The analyst who expects the drawdown data to flatten may be tempted to choose an r/B value at the end of the test period where he presumes the flattening is about to appear. However, the longer
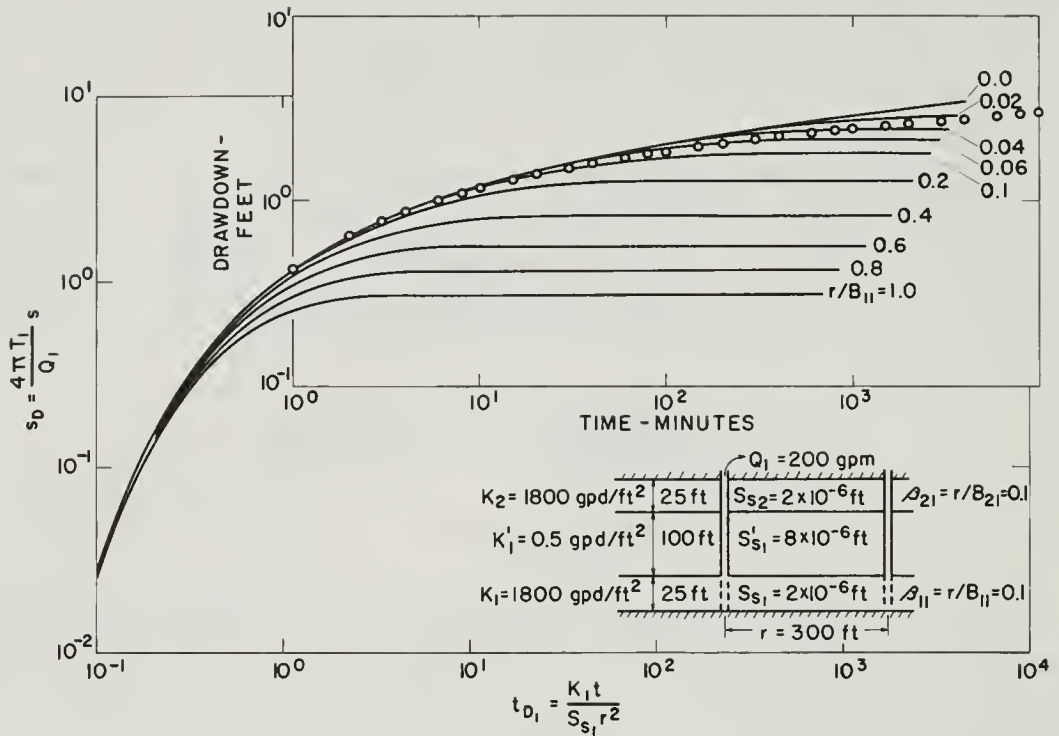
Fig. IV-14. Comparison of hypothetical field data
with r/B solution when properties of
aquifers are identical.

the test runs, the lower the value of r/B that will be selected, and the more the
result will be in error.

Another alternative for the analyst is to ignore the early drawdown data and
shift the plot of field data so as to force a match with the Theis solution. This
would yield even larger errors in K_1 and also lead to the erroneous conclusion that
there is no leakage.

We may, therefore, conclude that present methods of analyzing field data from
leaky aquifers need to be improved. These methods are based on two assumptions that
are not generally applicable. The assumption that storage in the aquitard is negligible
can lead to significant errors when β of the pumped aquifer is greater than 0.01. It
appears that large values of β of the order of 0.1 to 1.0 are certainly possible in
many field situations.

The second assumption of zero drawdown in the unpumped aquifer can also lead
to significant errors at large values of time. These errors cannot be neglected
unless the transmissibility of the unpumped aquifer is significantly greater than that
of the pumped aquifer. Since the r/B solution relies on both of these assumptions,
one must be cautious in using it to analyze field data.

Our discussion so far has been restricted to the case of a rather simple two

aquifer system. Obviously the problems of evaluating field data are further complicated by the fact that leakage may occur not only from above but also from below. This will tend to restrict further the applicability of the above two assumptions.

D. METHODS FOR DETERMINING HYDRAULIC CHARACTERISTICS OF MULTIPLE-AQUIFER SYSTEMS USING PUMPING TESTS

We have seen that all methods currently used by hydrologists to evaluate the results of pumping tests in leaky aquifers are based on certain simplifying assumptions which are not generally applicable. Our new theory of flow in multiple aquifer systems has eliminated the need for such assumptions and is therefore applicable to a wider variety of field situations. This theory shows that the behavior of drawdown in each layer is a function of several parameters, β_{ij} and r/B_{ij}, which depend on the hydraulic characteristics of the aquitards as well as on those of the aquifers. As a result, observation of drawdown in the pumped aquifer alone is not always sufficient to uniquely determine the values of β and r/B. For example, Hantush's β method (see Appendix A, Chapter V-A) is based on an analytical solution which we know is applicable at sufficiently small values of time. Nevertheless, since the method relies entirely on drawdown data from the pumped aquifer, it cannot be used to determine a unique value for β. Our theory indicates that one should be able to develop improved methods of analysis by installing observation wells not only in the aquifer being pumped, but also in the confining layers that enclose it. Indeed, as will be shown later, a series of observation wells in more than one layer is a prerequisite for any reliable evaluation of aquitard characteristics.

The idea of placing observations wells in a low permeability aquitard (i.e., aquiclude) overlying a slightly leaky aquifer was originally proposed by Witherspoon et al. [1962] in connection with underground storage of natural gas in aquifers. Their purpose was to determine how effective will a given aquiclude be in preventing leakage of gas from the intended underground storage reservoir to overlying sources of potable water and to the ground surface. Using results obtained from a finite difference simulation model, Witherspoon et al. were able to suggest a method for evaluating the hydraulic diffusivity of an aquiclude by means of a pumping test. Their method relies on the ratio between drawdown in the aquiclude and drawdown in the pumped aquifer, both measured at the same radial distance from the pumping well.

A theoretical analysis of flow in aquicludes adjacent to slightly leaky aquifers was first presented by Neuman and Witherspoon [1968] and has been reviewed above. This new theory led to an improved method for determining the hydraulic diffusivity [i.e. $\alpha' = k'/S_s'$] of aquicludes [Witherspoon and Neuman, 1967; Witherspoon et al., 1967, pp. 72-92] that is essentially similar to the method originally proposed by Witherspoon

et al. [1962]. Since the improved version is based on the ratio between drawdown in the aquiclude and the aquifer, we shall refer to it as the "ratio method." The ratio method has already been applied to several gas storage fields in Illinois and Minnesota and the results have proved to be very reliable. A detailed discussion of this method will be given later.

Another method for evaluating the hydraulic diffusivity of a confining layer was recently described by Wolff [1970]. In his analysis, Wolff assumed that at any given radial distance from the pumping well, and at a sufficiently large value of time, one can represent the drawdown in the pumped aquifer by a step function. Assuming also that drawdowns in the unpumped aquifers remain zero, Wolff arrived at a set of type curves which he recommended for aquitard evaluation.

Although this method gave satisfactory results for the particular site that was investigated by Wolff, it seems to us that the step function approach may lead to difficulties when applied to arbitrary multiple-aquifer systems. Fundamentally, drawdown in the pumped aquifer cannot be reliably represented by a step function unless a quasi-steady state is reached within a sufficiently short period of time. This will happen only if the transmissibility of the aquifer is large and if the observation wells are situated at relatively small radial distances from the pumping well. In order to minimize the effect of early drawdowns, the method further requires that the duration of the pumping test be sufficiently long and that the vertical distance between the pumped aquifer and the aquitard observation wells not be too small.

However, from our new theory of flow in multiple-aquifer systems, we now know that at large values of time, the results in the aquitard may be seriously affected by the influence of an adjacent unpumped aquifer. This is especially true for aquitard observation wells that have been perforated close to such an aquifer (see Figure IV-6). Thus, while the step function approach renders the method inapplicable at small values of time, the assumption of zero drawdown in the unpumped aquifers introduces an additional restriction at large values of time. In general, the method of Wolff [1970] seems to be applicable only at intermediate values of time.

In the special case where the thickness of the aquitard is known, one can determine its diffusivity directly from the step function type curves, without the need for a graphical curve matching procedure. Quite often, however, the effective thickness of the aquitard is unknown. For example, the aquitard may contain unidentified or poorly defined layers of highly permeable material that act as a buffer to the pressure transient and also act as a source of leakage. Another possibility is that the aquitard is situated below the pumped aquifer and that its lower limit has never been reached by a drill hole. For such cases, Wolff recommended a procedure that requires graphical matching of aquitard drawdown data with the type curves.

However, reference to Figure 10 in Wolff's paper [1970] will reveal that the

intermediate portions of these type curves are essentially parallel, and therefore, they cannot be matched uniquely with field results. On the other hand, neither the early nor the late portions of the type curves can be used with confidence. Thus, there may be an uncertainty when applying this method to real field situations.

Since all of the currently available methods appear to be limited in their application, there is an obvious need for a new approach that would enable one to determine the characteristics of multiple aquifer systems under a wide variety of field conditions. We shall demonstrate that a rational basis for such an approach is provided by our new theory of flow in multiple aquifer systems. Our discussion will be divided into two parts: In the first part, we shall show that the ratio method, which was originally developed for slightly leaky conditions (aquicludes), can also be used for very leaky conditions (aquitards). It will be shown that the ratio method offers many advantages over the step function approach and that it applies to both confined and unconfined systems. In the second part of our discussion, we shall recommend improved procedures for evaluating the transmissibility and storage coefficient of aquifers that are being supplied with leakage from above and/or below.

1. Method for Evaluating Aquitards

To develop a method for determining the hydraulic properties of aquitards, we shall consider first a two-aquifer system similar to that shown in Figure IV-1. We have seen that a complete solution for the distribution of drawdown in such a system is given by equations IV-7, IV-8, and IV-9. Each of these equations is dependent on five dimensionless parameters β_{11}, r/B_{11}, β_{21}, r/B_{21}, and t_{D_1}. Equation IV-8 for the aquitard involves one additional parameter, $z/H_1{}'$. This large number of dimensionless parameters makes it practically impossible to construct a sufficient number of type curves that would cover the entire range of values necessary for field application. For a set of type curves to be useful, one must usually require that they be expressed in terms of not more than two independent dimensionless parameters.

One way of significantly reducing the number of parameters is to restrict the analysis of field data to small values of time. In particular, we want to focus attention on those early effects that occur prior to the time when a pressure transient reaches the unpumped aquifer. At such early times, the unpumped aquifer does not have any influence on the rest of the system, and therefore drawdowns are independent of the parameters β_{21} and r/B_{21}. Furthermore, the aquitard behaves as if its thickness were infinite, which simply means that the parameters r/B_{11} and $z/H_1{}'$ also have no influence on the drawdown. Thus, the resulting equations will depend only on β_{11}, t_{D_1}, and an additional parameter,

$$t_{D_1}' = \frac{K_1't}{S_{s_1}'z^2} \qquad (IV-50)$$

In the pumped aquifer drawdown is then given by the asymptotic equation

$$s_1(r,\ t) = \frac{Q_1}{4\pi T_1} \int_{\frac{1}{4t_{D_1}}}^{\infty} \frac{e^{-y}}{y} \operatorname{erfc}\left[\frac{\beta_{11}}{\sqrt{y(4t_{D_1}y-1)}}\right] dy \qquad (IV-20)$$

In the aquitard the solution is

$$s_1'(r,\ z,\ t) = \frac{Q_1}{4\pi T_1} \int_{\frac{1}{4t_{D_1}}}^{\infty} \frac{e^{-y}}{y} \operatorname{erfc}\left[\frac{\beta_{11} + y\sqrt{t_{D_1}/t_{D_1}'}}{\sqrt{y(4t_{D_1}y-1)}}\right] dy \qquad (IV-23)$$

Theoretically equations IV-20 and IV-23 are limited to those small values of time which satisfy the criterion

$$t_{D_1} \leqslant \frac{1.6\ \beta_{11}^2}{(r/B_{11})^4} \qquad (IV-21)$$

Another way of writing this criterion is

$$t \leqslant 0.1\ \frac{S_{s_1}'H_1'^2}{K_1'} \qquad (IV-51)$$

indicating that the limiting value of time is independent of radial distance from the pumping well.

From a practical standpoint, the criterion given by (IV-21) or (IV-51) is overly conservative. For example, reference to Figures IV-2 through IV-9 in Appendix A reveals that the effect of the unpumped aquifer is felt in the rest of the system at times that are always greater than that predicted by equation IV-21 (which is indicated on these Figures by dashed vertical lines). It should be further noted on these figures that the effects of β_{21} and r/B_{21} are negligible as long as the log-log curve of drawdown versus time for the unpumped aquifer does not depart from its initial steep slope.

This can provide a useful criterion when analyzing field data to determine the time limit beyond which the asymptotic solutions may not be applicable. If an observation well can be provided in the unpumped aquifer, a log-log plot of drawdown versus time should enable the analyst to identify this time limit.

It should be recognized that there can be field situations where the above procedure may not be applicable. For example, when the transmissibility of the unpumped aquifer is large compared to that of the aquifer being pumped, drawdowns in the former will be too small to measure and one would not be able to determine the time limit as outlined above. Another example where this procedure may fail is when water levels in the unpumped aquifer are fluctuating during the pumping test due to some uncontrolled local or regional effects. In such cases, a more conservative estimate of the time limit can be established from drawdown data observed in one of the aquitard wells. In general, the smaller the distance z between this well and the pumped aquifer the more conservative is the time indicated by the above procedure.

Having established a practical method for estimating the time within which equations IV-20 and IV-23 are valid, we can now proceed to show how these equations can be used for aquitard evaluation. It will be recalled that Hantush's equation IV-20 by itself does not lead to a method for determining a unique value of β from field results. The same can be said of equation IV-23 because it involves three independent parameters, β_{11}, t_{D_1}, and t_{D_1}'. However, the usefulness of these two equations becomes immediately evident when one considers the ratio s_1'/s_1. This means the ratio of drawdown in the aquitard to that in the pumped aquifer at the same elapsed time and at the same radial distance from the pumped well.

Figure VI-15 shows the variation of s_1'/s_1 versus t_{D_1}' for a practical range of values for t_{D_1} and β_{11}. It may be seen that at $t_{D_1} = 0.2$ changing the value of β from 0.01 to 1.0 has practically no effect on the ratio s_1'/s_1. The same is true as t_{D_1} increases, and this is shown by the additional results for $t_{D_1} = 10^4$.
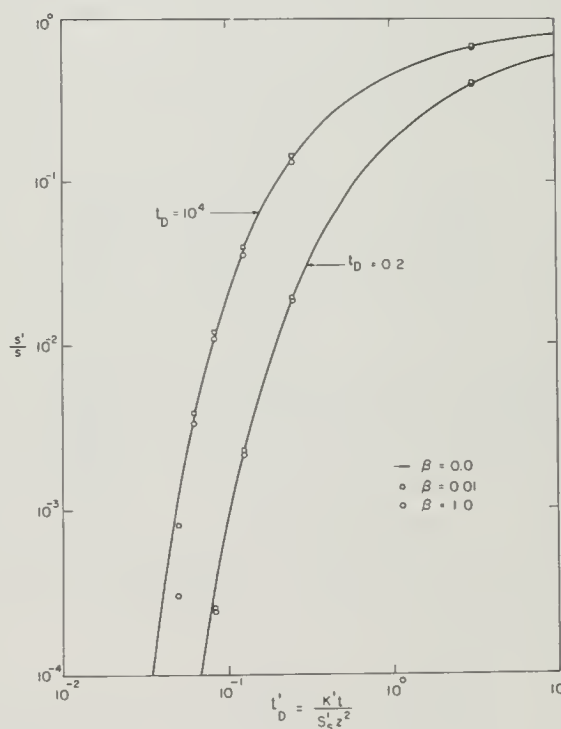
Fig. IV-15. Variation of s'/s with t_D' for various values of β

If we now utilize our theory for slightly leaky aquifers, where s_1' is given by equation IV-40 and s_1 is obtained from the Theis solution, we have in effect the special case where $\beta_{11} = 0$. This is represented by the two solid lines on Figure IV-15. We also examined the case where $\beta_{11} = 10$. and found that the values of s_1'/s_1 deviate significantly from those shown on this figure. These results thus indicate that the ratio s_1'/s_1 can be considered independent of β_{11} for all practical values of t_{D_1} and for $\beta_{11} < 1.0$. Since β_{11} is directly proportional to radial distance from the pumping well, its magnitude can be made less than unity simply by placing the observation wells close enough to the pumping well. A quick calculation will show that a distance of less than 100 feet will probably be satisfactory for most field situations.

This brings us to the very important conclusion that the ratio method, which we originally thought was restricted only to slightly leaky situations, can in effect be used to determine the hydraulic diffusivities of aquitards under arbitrary leaky conditions. We therefore decided to adopt the ratio method as a standard tool in evaluating the properties of aquitards.

The ratio method can be applied to any aquifer and its adjacent aquitards (above and below) in a multiple-aquifer system (see sketch on Figure IV-16). This method consists of measuring drawdown in the aquifer s and drawdown in either of the aquitards s', both at the same time and at the same radial distance from the pumping well. As has been discussed above, one can use our slightly leaky theory (see equations IV-34 and IV-40) to obtain a family of curves of s'/s versus t_D' for values of t_D ranging from 0.2 to 10^{10}. This is shown in Figure IV-16. These curves have been prepared from tables of values that were published by Witherspoon et al. [1967, Appendix G].

In the ratio method, one first calculates the value of s'/s at a given radial distance from the pumping well, r, and at a given instant of time, t. The next step is to determine the magnitude of t_D for the particular values of r and t at which s'/s have been measured. When $t_D < 100$, the curves in Figure IV-16 are sensitive to minor changes in the magnitude of this parameter and therefore a good estimate of t_D is desirable. When dimensionless time in the aquifer is greater than 100, these curves are so close to each other that they can be assumed to be practically independent of t_D. In this case, even a crude estimate of t_D will be sufficient for the ratio method to yield satisfactory results. A procedure for determining the value of t_D from drawdown data in the aquifer will be discussed later in connection with methods dealing with aquifer characteristics.

Having determined which one of the curves in Figure IV-16 should be used in a given calculation, one can now read off a value of t_D' corresponding to the computed ratio of s'/s. Finally the diffusivity of the aquitard is determined from the simple formula
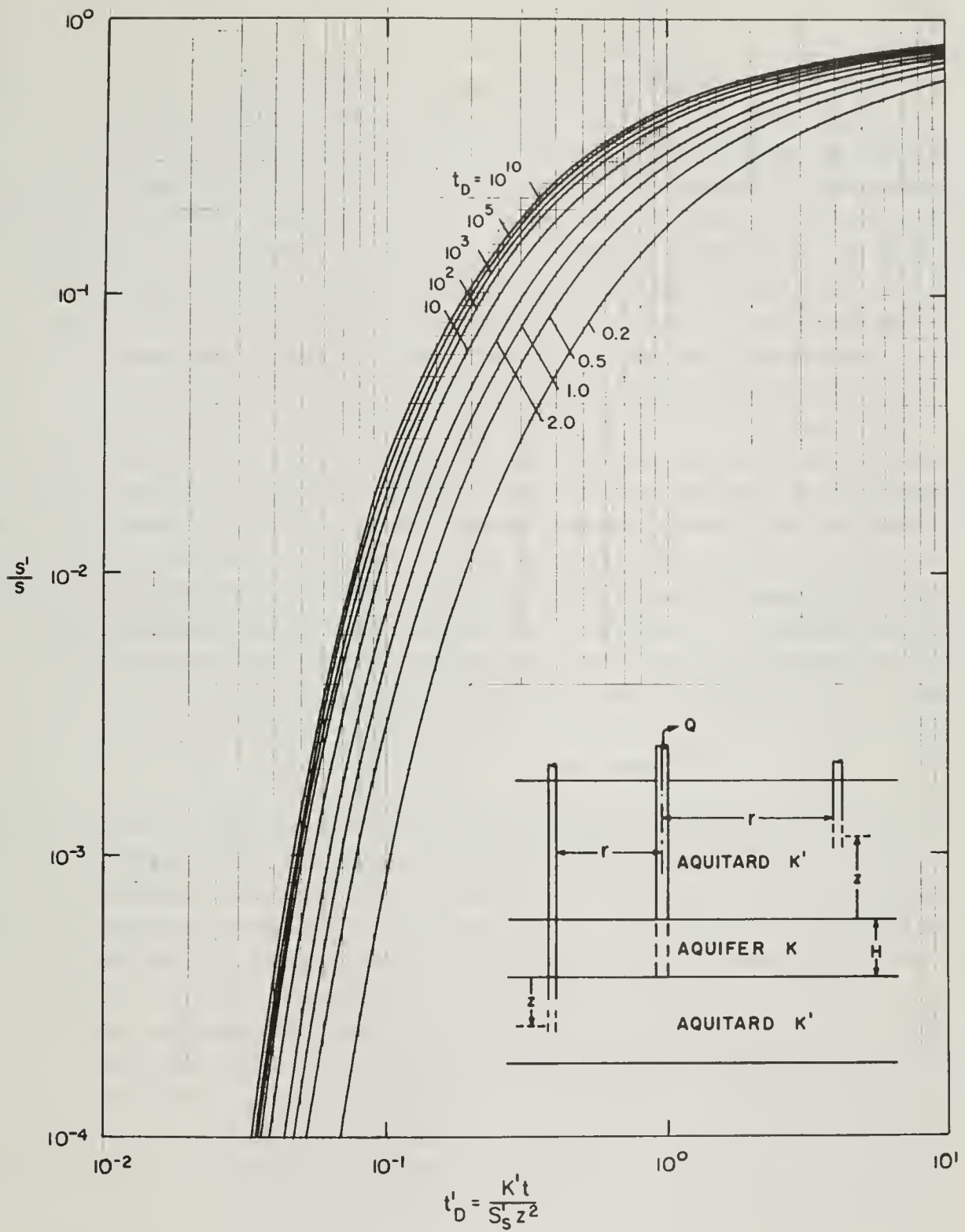
Fig. IV-16. Variation of s'/s with t_D' for semi-infinite aquitard.

-57-

$$\alpha' = \frac{z^2}{t} \, t_D' \tag{IV-52}$$

It is seen in Figure IV-16 that when s'/s is less than 0.1, the value of t_D' that is obtained by the ratio method is not very sensitive to the magnitude of s'/s. As a result, the value of α' that one calculates from equation IV-52 depends very little on the actual magnitude of the drawdown in the aquitard. Instead, the <u>critical quantity</u> that determines the value of α' at a given elevation z is the <u>time lag</u>, t, between the start of the test and the time when the aquitard observation well begins to respond. This is very important because it means that in using the ratio method one need not worry about having extremely sensitive measurements of drawdown in the aquitard observation wells. A conventional piezometer with a standing water column will usually give information that is sufficiently accurate for most field situations.

To evaluate the permeability and specific storage of an aquitard from its hydraulic diffusivity, one of these quantities must first be determined by means other than the ratio method. Experience indicates that permeability may vary by several orders of magnitude from one aquitard to another, and even from one elevation to another in the same aquitard. A much more stable range of values is usually encountered when dealing with specific storage. For these reasons, it is recommended that if core samples are available S_s' be measured in the laboratory. In many cases, such samples will not be available, and one will have to estimate S_s' from published results on similar sediments. When an average value for S_s' has been determined, K' is easily calculated from

$$K' = \alpha' \, S_s' \tag{IV-53}$$

We also studied the effects of aquitard heterogeneity and anisotropy on the value of K' that is obtained by the ratio method at a given elevation z. In our investigation, we used the finite element method to examine the behavior of a two-aquifer system under the following two conditions: (a) the aquitard is a homogeneous anisotropic layer with a horizontal permeability that may be as much as 250 times greater than the vertical, and (b) the aquitard consists of three different layers each of which is homogeneous and anisotropic. The results of this study indicated that for homogeneous, anisotropic aquitards, the ratio method will always give a value of K' which corresponds to the <u>vertical permeability</u> of the aquitard. In the case of a heterogeneous aquitard, K' is simply the average vertical permeability over the thickness z. If there are N layers of thickness H^n and vertical permeability K_v^n inside this interval, then K' represents the average value

$$K' = \frac{z}{\displaystyle\sum_{n=1}^{N} \frac{H^n}{K_v^n}} \tag{IV-54}$$

-58-

It is well known that at early values of time, drawdown in an unconfined aquifer can safely be approximated using the Theis solution provided that the storage coefficient is replaced by specific yield. At later values of time, drawdown may be affected by delayed yield and may therefore deviate from the Theis solution in a manner similar to that of confined leaky aquifers. This suggests that if the ratio method is applicable to aquitards that are adjacent to confined leaky aquifers, it should also be applicable to situations where the pumped aquifer is unconfined. This conclusion is further supported by the fact that the ratio method depends less on the actual values of drawdown in the aquifer than on the time lag observed in the aquitard. We were able to obtain data from Wolff [1970] for a pumping test where observation wells were placed in a confining layer underneath a water table aquifer. We analyzed these data using the ratio method and the results are in excellent agreement with those obtained by Wolff.

In showing that our slightly leaky theory is applicable to the so-called "leaky" aquifer, our previous discussion was restricted to a two-aquifer system. By now, however, the reader will recognize that such a restriction is not necessary and that the ratio method is actually applicable to arbitrary multiple-aquifer systems. As an example, let us consider a three-aquifer system such as in Figure IV-8. At small values of time, drawdown in the pumped aquifer is given by equation IV-25, and in the underlying aquitard by equation IV-28. These equations are completely analogous to (IV-20) and (IV-23) except that β_{11} has been replaced by $(\beta_{21} + \beta_{22})$, where now the first β parameter represents leakage from below and the second represents leakage from above. Thus, in order for the ratio method to be applicable, one only needs to arrange his observation wells such that the sum of the two values of β is less than unity (i.e., $\beta_{21} + \beta_{22} < 1$). From a practical standpoint, a radial distance of less than 100 feet from the pumping well will again be satisfactory for most situations that one is likely to encounter in the field.

In summary, it may be helpful to stress once again the following features of the ratio method:

(1) The method applies to arbitrary leaky multiple-aquifer situations.

(2) The pumped aquifer can be either confined or unconfined.

(3) The confining layers can be heterogeneous and anisotropic. In this case, the ratio method gives the average vertical permeability over the thickness z of the aquitard being tested.

(4) The method relies only on early drawdown data and therefore the pumping test can be of relatively short duration.

(5) The drawdown data in the unpumped aquifer or in the aquitard provide an insitu indication of the time limit at which the ratio method ceases to give reliable results.

(6) Since the method is more sensitive to time lag than to the actual magnitude

of s'/s, the accuracy with which drawdowns are measure in the aquitard
is not overly critical.

(7) The method does not require prior knowledge of the aquitard thickness.

(8) The ratio method is very simple to use and it does not involve any
graphical curve matching procedures. This is an advantage because
(a) curve matching is often prone to errors due to individual judgment,
and (b) a more reliable result can be obtained by taking the arithmetic
average of results obtained from several values of the ratio s'/s.

2. Method for Evaluating Aquifers

When the pumped aquifer is slightly leaky, one can evaluate its transmissibility
and storage coefficient by the usual procedures based on the Theis equation. When
leakage is appreciable, these procedures will not always yield satisfactory results.
Alternative methods for analyzing the results of pumping tests in leaky aquifers were
proposed by Jacob [1946] and by Hantush [1956, 1960a] and are outlined in Appendix A of
this report, (Chap. V-A). Still another method based on the r/B solution has recently
been proposed by Narasimhan [1968]. All of these methods rely on drawdown data from the
pumped aquifer alone. Their purpose is to determine not only the properties of the aquife
but also the so-called "leakage factors" r/B and β which depend on the characteristics of
the confining layers as well as on those of the aquifer. We have shown earlier that
these methods have limited application and that they can often lead to erroneous results.

Having introduced the ratio method as a means of evaluating aquitards, the only
remaining unknowns that need to be determined by other than this method are the aquifer
transmissibility T, and the storage coefficient, S. When the aquifer is leaky, the use
of methods based on the Theis solution will lead to errors whose magnitude is a function
of β and r/B. Reference to Figures IV-2 through IV-5, IV-9 and IV-10 will reveal that
the smaller are the values of β and r/B, the less the drawdowns in the pumped aquifer
deviate from the Theis solution. Therefore, the less are the errors introduced by such
methods. At this point, it is important to recognize that although β and r/B have been
termed "leakage factors", their magnitude does not necessarily reflect the amount of
water that leaks into the aquifer. In fact, both of these parameters are directly
proportional to r, which simply means that their magnitude in a given aquifer varies
from nearly zero at the pumping well to relatively large values further away from this
well. This implies that the extent to which leakage can affect the behavior of the
drawdown in any given aquifer is a function of radial distance from the pumping well.
Thus, the closer one is to this well, the smaller are the deviations of drawdown from
the Theis curve. On the other hand, the rate of leakage is obviously greatest near
the pumping well where vertical gradients in the aquitard are largest and diminishes as

the radial distance from this well increases. Therefore in a given system, β and r/B increase with radial distance while the actual rate of leakage decreases. The term "leakage factor" is obviously misleading and in our opinion should be considered a misnomer.

At first glance, it may appear as if we were faced with a paradox: the greater is the leakage, the less are the deviations from the non-leaky Theis solution. However, a closer examination of the flow system will show that there is a simple physical explanation for this phenomenon. Referring to the cross-sections shown on Figures IV-11 through IV-14 in Appendix A, the reader will recognize that while vertical gradients in the aquitard do not vary appreciably with radial distance from the pumping well, the same cannot be said about drawdown in the pumped aquifer. As a result, the rate of leakage per unit area relative to this drawdown is negligibly small in the immediate vicinity of the pumping well, but it becomes increasingly important at larger values of r. In addition to this, the water that leaks into the aquifer at smaller values of r tends to act as a buffer to the pressure transient. This transient cannot propagate as fast as it otherwise might have had there been no increase in aquifer storage. The effect is to further reduce the drawdown at points farther away from the pumping well. The net result is a situation where larger values of r are associated with less leakage but also with greater deviations from the Theis curve.

This brings us to the important conclusion that it is possible to evaluate the transmissibility and storage coefficient of a leaky aquifer using conventional methods of analysis based on the Theis solution. The errors introduced by these methods will be small if the data are collected close to the pumping well, but they may become significant when the observation well is placed too far away. This means that a distance drawdown analysis based on the Theis curve is not generally applicable to leaky aquifers and should therefore be avoided whenever possible.

Ideally, the values of T and S should be evaluated using drawdown or build-up data from the pumping well itself because here the effect of leakage is always the smallest. We recommend this approach whenever the effective radius of the pumping well is known (e.g., wells in hard rock formations). However, when a well derives its water from unconsolidated materials, its effective radius usually remains unknown due to the presence of a gravel pack. In these situations the above approach can still be used to evaluate T, but it cannot be used to determine S. As a general rule, early drawdown data are affected by leakage to a lesser degree than are data taken at a later time. We therefore feel that in performing the analysis, most of the weight should be given to the earliest data available, provided of course that there is confidence in their reliability.

Once S and T have been determined, one can calculate the dimensionless time at any given radial distance from the pumping well by the simple equation

$$t_3 = \frac{Tt_1}{St}$$

(IV-55)

This result can then be used in connection with the ratio method, as described earlier.

CHAPTER V. FIELD PUMPING TESTS

S. P. Neuman and P. A. Witherspoon

Two field pumping tests were performed, as part of this investigation, to gather specific data on the aquitards that lie above and below the Oxnard aquifer. Since the Oxnard basin has been subjected to sea water intrusion over a period of years (see Chapter III) we wanted to determine how effectively the aquitards of this basin are able to prevent vertical migration from one aquifer to another.

A. LOCATION

The State of California, Department of Water Resources had previously investigated the Oxnard sea water intrusion problem and had constructed several wells at various locations in the basin. The particular location described below was selected for our field studies because a large capacity pumping well (OPE-1) was available to produce from the Oxnard aquifer and was surrounded by several aquifer observation wells. The location of the test area outside Port Hueneme is shown on Figure V-1. The location relative to the rest of the state is shown in Figure I-1.

The pumping well, in the City of Oxnard, lies 3,400 ft east of Saviers Road, 350 ft south of Pleasant Valley Road, and 48 ft east of the Ventura County Railway (Figure V-1). When the well was drilled in October 1963, the elevation of the site stood approximately 10 ft higher than at present (1970). The well now lies within a concrete-lined channel excavated by the Ventura County Flood Control District. Two numbers designate this well: State Well No. 1N/22W-22J5 and field number OPE-1.

Just north and slightly west of this well, California Department of Water Resources personnel in June 1968 drilled five observation holes. They placed a single piezometer in holes 2, 3 and 5 and two piezometers in holes 1 and 4. All seven piezometers lie on the west bank of the flood control channel (Figure V-2).

B. CONSTRUCTION AND COMPLETION METHODS

Drilling of the observation holes began June 11, 1968; construction of piezometers ended June 29. A Failing 1,500 rotary rig drilled all holes. The rig used a 5 by 6 Gardner-Denver duplex mud pump equipped with a jet-type mud mixer. A shaker screen removed all drill cuttings. Table V-1 provides construction data.
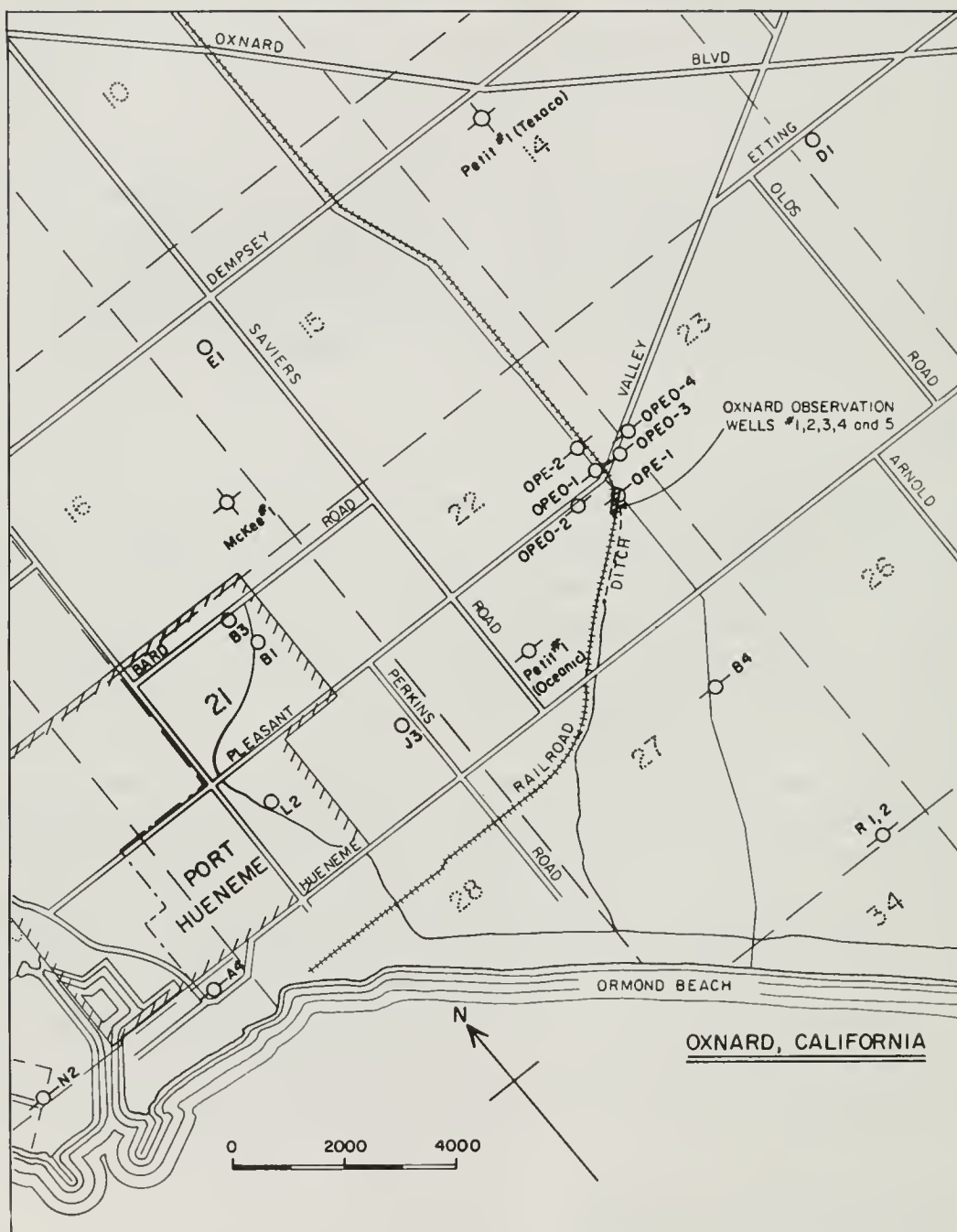
Fig. V-1. General location map of Oxnard field pumping test.
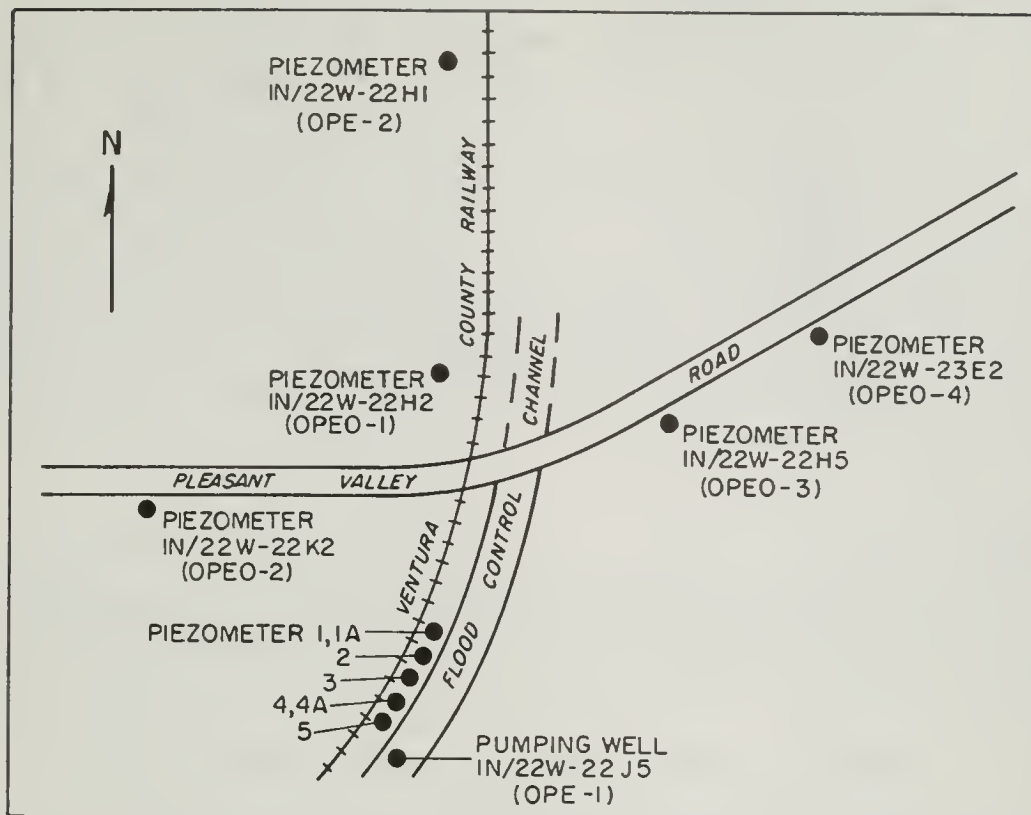
Fig. V-2. Location of piezometers used
in field pumping tests.

First Hole

A 6 3/4-inch tricone, soft-formation rock bit was used to drill the first hole.
To substantiate the lithologic log prepared during drilling, the Go-Western Company ran
an electric log and a copy is reproduced in Figure V-3.

After correlating lithologic and electric logs, the well was equipped with two
piezometers: No. 1 in the upper (Oxnard) aquifer, and No. 1A in the lower (Mugu) aquifer.
These correlations also indicated the depths where cores of the aquitards could be taken
in drilling the second observation hole.

The completed well contained a neat-cement plug from the bottom at 370 ft to 260
ft, a gravel pack from 260 to 226 ft, and a second neat-cement plug from 226 to 126 ft.
A second gravel pack was placed from 126 to 101 ft, and the remainder of the hole was
cemented to the surface.

Piezometer 1 passed through the upper cement plug and consisted of 116 1/2 ft
of nominal 2-inch diameter plastic pipe (Schedule 80 PVC, Type 2) fastened to a 3 1/2-

foot well point. Piezometer 1A passed through the upper two cement plugs into the lower gravel pack, and consisted of 235 1/2 ft of blank pipe fastened to a second 3 1/2-foot well point. The well points not only provided communication with the aquifers; they also added weight to the plastic tubing. Twenty-foot sections of tubing were connected by Ventura flush joints with modified acme threads.

After the observation hole had been drilled, the emplacement of piezometers generally followed a set procedure. With the bottom section cemented off, piezometer 1A was positioned and the drilling mud was displaced with water to allow the gravel to settle more easily. This water circulation continued slowly and was directed down the tubing and up the annulus while gravel (nominal 3/8-inch, well rounded) was shoveled in the hole. After the intervening cement plug was set, the second piezometer 1 was installed in a similar manner.

Second Hole

The second observation hole was drilled to 227 ft in the same manner as the first using a 9-inch tricone, soft-formation rock bit. Drilling was continuous except

Table V-1. Data on Observation Holes and Piezometers

Hole Data				Piezometer Data				
Observa-tion Hole	Distance from OPE-1[1] ft	Total Depth ft	Bit Size in	Piezom-eter	Depth ft	Pipe		Vertical Dist. z^2 ft
						Plastic	Steel	
1	100	370	6 3/4	1	120	x		–
				1A	239	x		–
2	91	227	9	2	225		x	-26^3
3	81	205	9	3	205		x	–6
4	72	95	9	4	95		x	+11
				4A	58.5	x		+50
5	62	84	9	5	84		x	+22

Note: [1]Pumping well

[2]Distance above top of Oxnard aquifer at 105 ft or below bottom at 199 ft

[3]Failed to operate satisfactorily

for two intervals, 60.4 to 104.9 and 198.0 to 227.4 ft, which were cored using a Pitcher Barrel coring tube (Figure VI-2). The hole was reamed each time after coring using the 9-inch bit. Piezometer 2 for this well was opened in the lower aquitard and consisted of 225 ft of 4-inch steel pipe (1/8-inch wall) with the bottom end sealed off by a flat plate. The bottom foot (224-225 ft) was slotted by cutting vertical perforations, 1/8-inch wide and 2 1/2-inches long, eight slots around in a set and three sets per foot. Gravel packing followed the same procedure as described earlier but extended only to 223 ft, i.e., only one foot above the top of the perforations. A 1-foot sand pack was placed on top of the gravel followed by a short cement plug. These precautionary steps were designed to prevent plugging the short

Fig. V-3. Electric log from first exploratory hole.

gravel pack. After the cement plug had set, the balance of the annulus was filled with cement. This procedure worked well on all piezometers but No. 2, which did not perform satisfactorily.

Third Hole

The third observation hole was drilled to 205 ft and equipped with a 4-inch piezometer in the same manner as the second hole. The perforations extended from 204 to 205 ft, and the gravel pack from 203 to 205 ft. Piezometer 3 was also open in the lower aquitard.

Fourth Hole

The fourth observation hole was drilled to 95 ft and equipped with a 4-inch piezometer in the same manner as the second hole except that a second smaller piezometer was placed in the annulus. Piezometer 4 was open to the upper aquitard from 94 to 95 ft and the gravel pack was placed from 93 to 95 ft.

After filling the annulus up to 58 1/2 ft with cement, 2-inch plastic pipe with a 3 1/2-foot well point was positioned opposite the semiperched aquifer that overlies

the Oxnard (Fig. V-3). In addition, the bottom 3 1/2 ft of plastic pipe were also perforated with four 3/32-inch diameter holes per set and eight sets per foot, alternating at 90° from each other. Piezometer 4A was completed by gravel packing from 58 1/2 to 51 1/2 ft and cementing to the surface in the usual manner.

Fifth Hole

The fifth observation hole was drilled to 84 ft and equipped with a 4-inch piezometer in the same manner as the second hole. Piezometer 5 was open to the upper aquitard from 83 to 84 ft and the gravel pack was placed from 82 to 84 ft.

Development

Airlift methods were employed in developing the piezometers. A trailer-mounted compressor provided the necessary air supply and water was added to those piezometers in the aquitards that produced too slowly. By positioning a 1/4-inch air hose opposite the perforated intervals, a satisfactory communication was established and the gravel packs were stabilized.

C. ANALYSIS OF PUMPING TEST RESULTS

Two pumping tests were performed in the field. The purpose of these tests was twofold: (a) to determine the hydraulic characteristics of the Oxnard aquifer and the confining layers that lie above and below using the new approach that was outlined in Section D of Chapter IV, and (b) to confirm the applicability of our new theory to the multiple-aquifer system of the Oxnard Basin. The five layers in which piezometers had been installed can be viewed as a three-aquifer subsystem of the Oxnard Basin, similar to the one shown on Figure IV-8. At the center of this subsystem is the Oxnard aquifer from which water was withdrawn at a constant rate, Q. The upper aquitard separates the pumped aquifer from the unpumped perched aquifer above. The lower aquitard lies between the Oxnard and the unpumped Mugu aquifer below.

As described earlier, seven new piezometers were installed to monitor the response at various elevations in the subsystem. Of these, two piezometers were open in the upper aquitard (Nos. 4 and 5), two in the lower aquitard (Nos. 2 and 3), and one piezometer in each aquifer (No. 1 in the Oxnard, No. 1A in the Mugu, and No. 4A in the perched zone). Unfortunately, piezometer 2 in the lower aquitard became clogged before the pumping tests started and had to be abandoned. Four additional piezometers (22H2, 22H5, 22K2, and 23E2) were used to monitor water levels in the Oxnard aquifer at radial distances ranging between 502 and 1060 ft.

Ideally, the seven new piezometers should have been arranged along a circular arc with its center at the pumping well, so as to give responses at various elevations at only one unique value of r. However, this was not possible under the local conditions and we therefore had to design the well field according to the scheme shown in Figure IV-2.

Water levels in these observation wells were measured mainly with the aid of a steel tape and with a fluid-conductivity probe suspended on an electric cable. The accuracy of the readings with both instruments was approximately ± 0.01 foot. Automatic Stevens recording devices were originally installed in piezometer 3 and some of the Oxnard observation wells to monitor water levels prior to the first pumping test. These recorders were not used during the test itself. Appendix B gives a tabulation of draw-down data from the first pumping test that were used in following analyses.

1. Results of First Pumping Test

For several months prior to the first pumping test, water levels everywhere in the Oxnard basin were continuously rising. Figure V-4 shows the variation in fluid levels in each part of the three-aquifer subsystem during portions of the two-month period prior to the test. Initially, water levels in the Oxnard and Mugu aquifers were rising steadily at a rate of 0.3 to 0.5 feet per day. A similar rise occurred in the lower aquitard which is situated between these two aquifers. In the perched aquifer the rise was relatively slow (less than 0.04 feet per day), while in the upper aquitard the rates progressively, increased from top (i.e. near the perched zone) to bottom (i.e. near the Oxnard).

Toward the second half of February, 1970, the water levels started to stabilize, and in March, these levels were nearly static. These conditions were ideal for a pumping test, and on March 6, 1970 the first test began. With the exception of a 25-minute power failure that occurred on March 11, 1970, the pump continued to
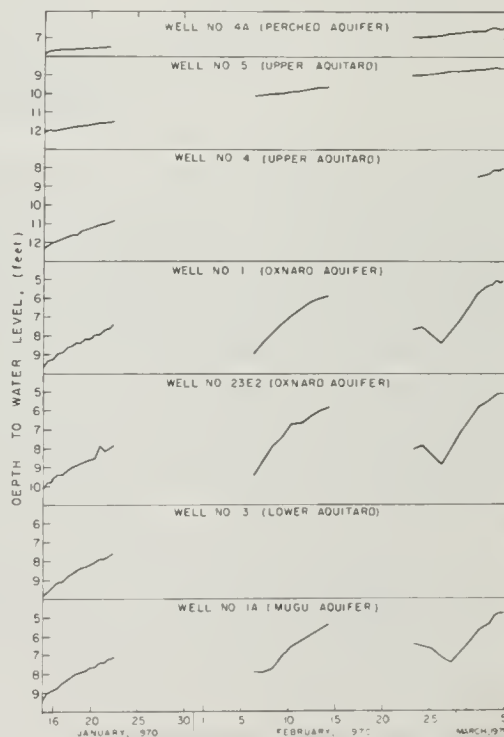
Fig. V-4.   Fluid levels in piezometers prior to first pumping test

-69-
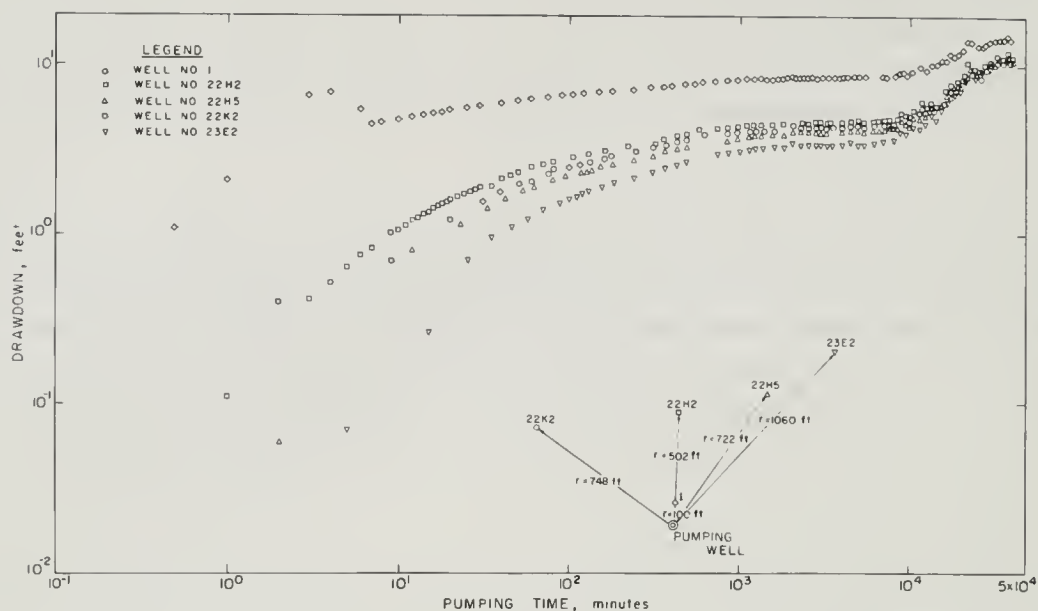
Fig. V-5.   Fluid levels in Oxnard piezometers
during first pumping test

operate at a constant rate of approximately 1000 gallons per minute for almost a month.
The test ended on April 3, 1970, when the pump was shut off and the water levels were
allowed to recover.   Appendix B lists the drawdowns in all piezometers for the entire
period of the first test.   Figure V-5 shows the response in the Oxnard aquifer at
various radial distances from the pumping well.   Piezometer 1, which is nearest to the
pumping well, demonstrates an anomalous behavior during the first 6 minutes of pumping.
This is apparently due to a surging effect in the pumping well.   At about 6,000 minutes,
the entire basin started experiencing a general fall in water levels probably due to the
beginning of intermittent pumping for irrigation at this time of the year.

        We have shown in Section D of Chapter IV that in order to obtain the best esti-
mate for transmissibility and storage coefficient in an aquifer, one should analyze the
early drawdown data from a piezometer nearest the pumping well using a method based on
the Theis solution.   However, the early drawdowns from piezometer 1 cannot be used to
obtain such a result.   The rest of these data lie on an almost flat curve that cannot
be used to match to the Theis solution without some uncertainty.   In fact, none of
the curves in Figure V-5 has a sufficiently well defined early portion to eliminate
such uncertainties.   An example of this is shown in Figure V-6, where the drawdowns
from piezometer 22H2 are matched to the Theis solution.   One notes immediately that
the early data are above the Theis curve for some reason, and after about 100 minutes,
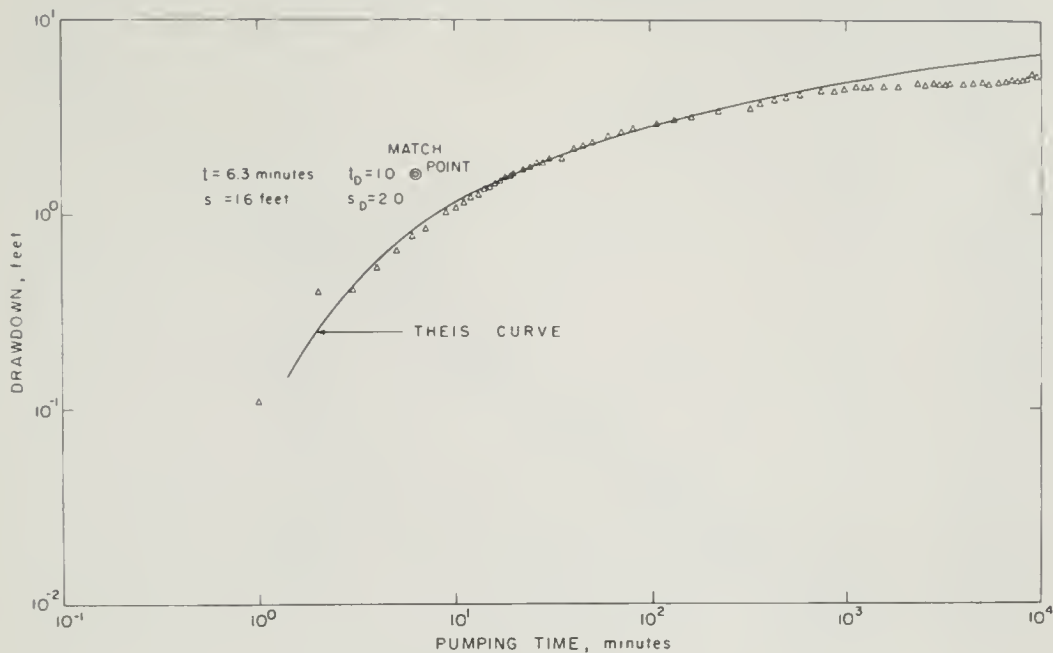
Fig. V-6.   Effect of leakage on drawdown data and
            comparison with Theis curve

there is definite evidence of leakage.

In cases such as this when the aquifer transmissibility is so high that the
steep portion of the drawdown curve is poorly defined, a more reliable result can be
obtained using Jacob's semi-logarithmic approach.   Figure V-7 shows an example of a
plot of drawdown versus time for piezometer 22H2 in the Oxnard aquifer.   It may be
seen that part of the data fall on a straight line, from which values of T and S can
readily be computed.   The early data fall above this line as predicted by theory and
the later data fall below due to effects of leakage.

According to Jacob's method, a straight line is drawn through the data, as
shown on Figure V-7.   From this line, one determines s_{10}, or the drawdown over one log
cycle, and t_0, or the time in minutes where this line intersects the horizontal co-
ordinate $s = 0$.   T and S can be calculated from

$$T = \frac{264\ Q}{s_{10}} \tag{V-1}$$

and

$$S = \frac{2.081 \times 10^{-4}\ T\ t_0}{r^2} \tag{V-2}$$

-71-
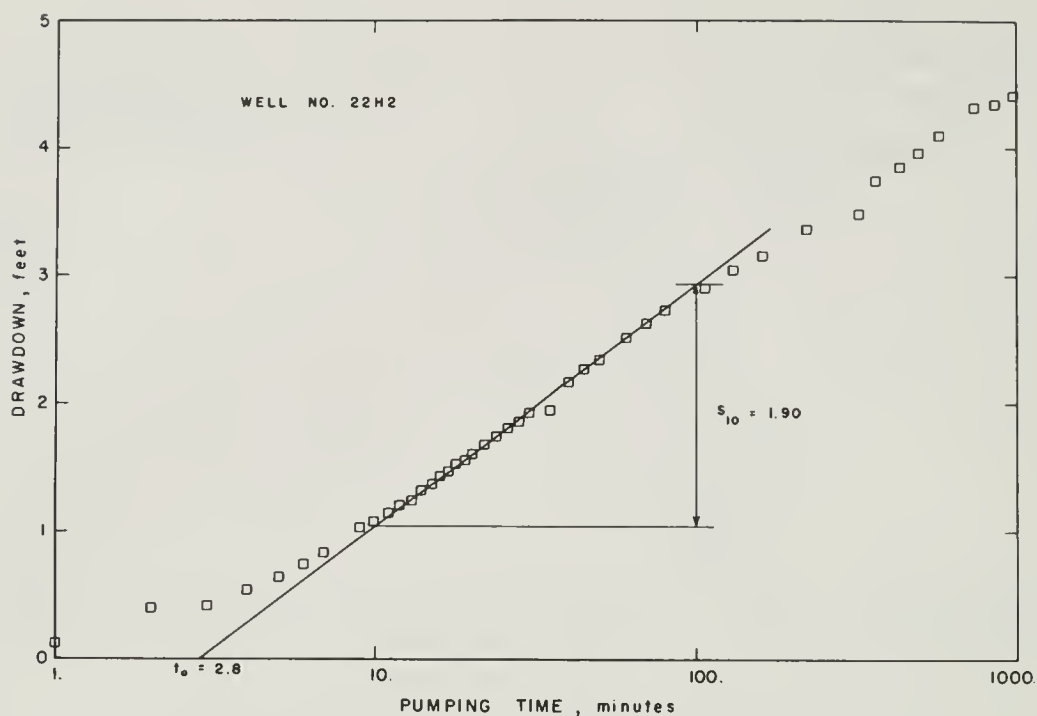
Fig. V-7. Plot of drawdown data for Oxnard piezometer
22H2 according to Jacob's method

where s_{10} and r are in feet, Q is in gallons per minute (gpm), T is in gallons per day
per foot (gpd/ft), and S is a dimensionless quantity. The results of the calculations
are given in Table V-2.

Table V-2. Results for Oxnard aquifer using Jacob's semi-log method

Well	r, ft.	T, gpd/ft.	S
1	100	130,600	1.12×10^{-4}
22H2	502	139,000	3.22×10^{-4}
22H5	722	142,600	3.08×10^{-4}
22K2	748	136,700	2.48×10^{-4}
23E2	1060	157,000	2.53×10^{-4}

In the event that log-log matching technique is used, T and S are calculated from

$$T = \frac{114.6 \ Q \ s_D}{s} \qquad (V-3)$$
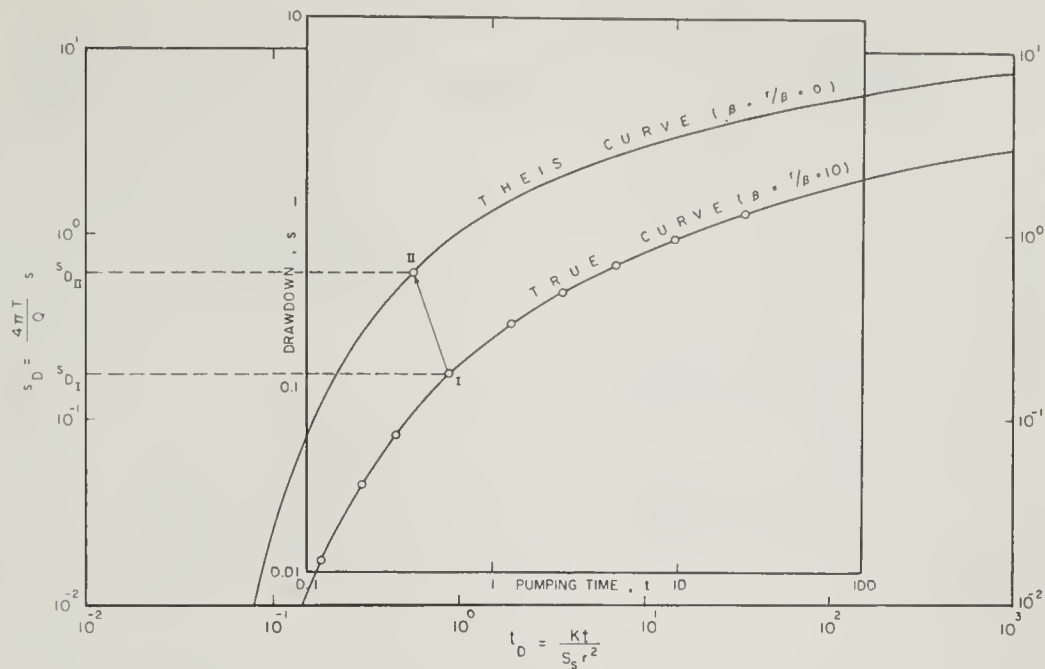
Fig. V-8. Comparison of hypothetical field data
with leaky and non-leaky type curves

$$S = \frac{9.28 \times 10^{-5} \ Tt}{r^2 \ t_D} \tag{V-4}$$

where the units are the same as in equations V-1 and V-2.

Table V-2 shows that, in general, the values of T become progressively larger
as r increases. This can be explained as follows. Since the Oxnard aquifer is ob-
viously leaky, the actual drawdown curve at any given well will lie below the Theis
solution, as shown diagrammatically in Figure V-8. To demonstrate this, we shall
choose a particular point on the data curve that corresponds to some given value of
s and t. If we were able to match the data to the true type curve where β and r/B
are not zero, we would obtain the true value of s_{D_1} for the point chosen.

However, such type curves were not available for this investigation, and we
used a method which is essentially equivalent to matching the field data to the Theis
curve. This means that the field data are being shifted upward from their true position
and our chosen point will now indicate an apparent value of $s_{D_{11}}$ which is greater than
s_{D_1}.

Referring to equation V-3, it is clear that since s remains unchanged, the
effect is to increase the value of T. The greater the radial distance r, the more
β and r/B become, and therefore the larger is the difference between the true type

-73-

Fig. V-9. Response of piezometers in lower aquitard
(No. 3) compared to that of Oxnard (No. 1)
and Mugu (No. 1A) aquifers during first
pumping test

curve and the Theis curve. This simply means that as r increases, the magnitude of T
should become more and more exaggerated, which is exactly what we see on Table V-2.

With regard to errors in S, the shifting of field data as indicated on Figure
V-8 may either be to left or to the right. Thus, the effect on the calculated values
of S is not predictable. This also is seen in Table V-2. With this in mind, we
decided to select the results from piezometer 1 of T = 130,600 gpd/ft and S = 1.12 x
10^{-4} as being most representative of the Oxnard aquifer, at least in the area of the
pumping test.

Having estimated the properties of the pumped aquifer, we shall now consider
the results from other parts of our three-aquifer subsystem. Figure V-9 shows the
response at one particular point in the lower aquitard (No. 3) as well as in the Oxnard
above (No. 1) and the Mugu below (No. 1A). Figure V-10 shows the response at two
different elevations in the upper aquitard (Nos. 4 and 5) as well as in the overlying
semiperched aquifer (No. 4A). Since piezometer 1 is located farthest from the pumping
well, we do not have the response in the pumped aquifer directly below the piezometers
where drawdowns in the upper aquitard were measured. However, from distance-drawdown
curves in the Oxnard aquifer and from the behavior of·piezometer 4 we concluded that
the aquifer response was approximately as shown by the dashed curve on Figure V-10.

Fig. V-10.   Response of piezometers in upper aquitard
            (Nos. 4 and 5) and semiperched aquifer
            (No. 4A) during first pumping test

It should be remembered that the new ratio method described above for evaluating aqui-
tards is more sensitive to the time lag than to the actual magnitude of drawdown in the
aquifer. For this reason, the dashed curve in Figure V-10 can be considered sufficiently
accurate for our purposes. It should be noted that the general form of the curves in
Figures V-9 and V-10 and their relationships to each other is similar to that of the
theoretical curves on Figure IV-2 through IV-5. This is encouraging because it suggests
that the particular multiple-aquifer system with which we are dealing behaves at least
qualitatively as our theory would predict. Therefore, the ratio method should be
applicable to this system, and we can proceed to evaluate the hydraulic properties of
the two aquitards that enclose the Oxnard aquifer.

To evaluate the lower aquitard, we shall determine the ratio s'/s at two early
values of time, $t = 80$ minutes and $t = 200$ minutes. At $t = 80$ minutes, one can read
on Figure V-9 that $s' = 0.078$ and $s = 6.6$ feet. The ratio is simply

$$\frac{s'}{s} = \frac{0.078}{6.6} = 1.18 \times 10^{-2}$$

-75-

To obtain t_D, we first rewrite equation V-4 as

$$t_D = \frac{9.28 \times 10^{-5} \; Tt}{r^2 S} \qquad (V\text{-}5)$$

where T is in gpd/ft, t is in minutes, and r is in feet. Then, using the known values of T and S and noting from Table V-1 that at piezometer 3, r = 81 feet, we can calculate

$$t_D = \frac{(9.28 \times 10^{-5}) \; (130,600) \; (80)}{(81)^2 \; (1.12 \times 10^{-4})} = 1.32 \times 10^3$$

Referring to Figure IV-16, we find that these values of s'/s and t_D correspond to $t_D' = 0.086$. From the definition of t_D', one can verify the formula

$$\frac{K'}{S_s'} = 1.077 \times 10^4 \; t_D' \; \frac{z^2}{t} \qquad (V\text{-}6)$$

where K'/S_s' is in gpd/ft, z is in feet, and t is in minutes. We note on Table V-1 that for piezometer 3, z = 6 feet and therefore

$$\frac{K'}{S_s'} = \frac{(1.077 \times 10^4) \; (0.086) \; (6)^2}{(80)} = 4.17 \times 10^2 \; \text{gpd/ft}$$

To compare this with the laboratory results, it is convenient to express K'/S_s' in cm^2/sec, in which case the formula becomes

$$\frac{K'}{S_s'} = 15.48 \; t_D' \; \frac{z^2}{t} \qquad (V\text{-}7)$$

From the data for piezometer 3, one then has

$$\frac{K'}{S_s'} = \frac{(15.48) \; (0.086) \; (6)^2}{(80)} = 5.99 \times 10^{-1} \; \frac{cm^2}{sec}$$

At t = 200 minutes, one can read on Figure V-9 that s' = 0.52 and s = 7.2 feet, from which

$$\frac{s'}{s} = \frac{0.52}{7.2} = 0.0722$$

Using equation V-5

$$t_D = \frac{(9.28 \times 10^{-5}) \ (130,600) \ (200)}{(81)^2 \ (1.12 \times 10^{-4})} = 3.3 \times 10^3$$

and therefore Figure IV-16 indicates that

$$t_D' = 0.175$$

Equations V-6 and V-7 give

$$\frac{K'}{S_s'} = \frac{(1.077 \times 10^4) \ (0.175) \ (6)^2}{(200)} = 3.39 \times 10^2 \ \text{gpd/ft}$$

and

$$\frac{K'}{S_s'} = \frac{(15.48) \ (0.175) \ (6)^2}{(200)} = 4.88 \times 10^{-1} \ \frac{\text{cm}^2}{\text{sec}}$$

Here, we note the calculated values of K'/S_s' decrease as t increases. The most reliable result is obtained at small values of time, and we shall therefore adopt

$$\frac{K'}{S_s'} = 4.17 \times 10^2 \ \text{gpd/ft} = 5.99 \times 10^{-1} \ \frac{\text{cm}^2}{\text{sec}}$$

as being representative of the top 6 feet in the lower aquitard.

A similar analysis can be made on the upper aquitard, assuming that the response in the pumped aquifer can be represented by the broken curve shown in Figure V-10. For piezometer 4 at t = 400 minutes, we find s' = .095 and s = 12.0 feet, from which

$$\frac{s'}{s} = \frac{0.095}{12.0} = 7.92 \times 10^{-3}$$

The magnitude of t_D at r = 72 feet is obtained using (V-5).

$$t_D = \frac{(9.28 \times 10^{-5}) \ (130,600) \ (400)}{(72)^2 \ (1.12 \times 10^{-4})} = 8.35 \times 10^3$$

From Figure IV-16, $t_D' = 0.075$ and using equations V-6 and V-7 for z = 11 feet, one has

$$\frac{K'}{S_s'} = \frac{(1.077 \times 10^4) \ (0.075) \ (11)^2}{(400)} = 2.44 \times 10^2 \ \text{gpd/ft}$$

and

-77-

$$\frac{K'}{S_s'} = \frac{(15.48)\ (0.075)\ (11)^2}{(400)} = 3.51 \times 10^{-1}\ \frac{cm^2}{sec}$$

It is interesting to note that had we used the drawdown in piezometer 1 as shown on Figure V-9 instead of that indicated by the dashed line in Figure V-10, we would have obtained a value of

$$\frac{K'}{S_s'} = 2.7 \times 10^2\ gpd/ft$$

which is very close to the original result. This shows how insensitive the ratio method is to the actual magnitude of the drawdowns. Again using the data on Figure V-9, it can be shown that at t = 800 minutes, K'/S_s' for piezometer 4 is 2.44×10^2 gpd/ft, which in this case, is the same as the result computed at t = 400 minutes.

Turning to piezometer 5, where z = 22 feet, one can determine that at t = 3,000 minutes, s' = 0.041 and s = 13.8 feet. One can quickly determine that $K'/S_s' = 1.02 \times 10^2$ gpd/ft, or 1.47×10^{-1} cm^2/sec. This is about half the value that was obtained from piezometer 4 and suggests that the average diffusivity of the aquitard decreases as the thickness of the section being tested increases. This is to be expected because the thicker the section under consideration, the more chance there is that it will include clay layers of low permeability and high specific storage. Consequently, the effect is to reduce the overall vertical diffusivity of the aquitard. The results that were adopted as representative for both aquitards are summarized in Table V-3.

Table. V-3. Results for hydraulic diffusivity of aquitards from first pumping test

Layer	Section tested	K'/S_s' gpd/ft	K'/S_s' cm^2/sec
Upper Aquitard	Bottom 22 feet	1.02×10^2	1.47×10^{-1}
	Bottom 11 feet	2.44×10^2	3.51×10^{-1}
Lower Aquitard	Top 6 feet	4.17×10^2	5.99×10^{-1}

It is important to note that the diffusivity of the Oxnard aquifer is

$$\frac{K}{S_s} = \frac{T}{S} = \frac{130,600}{1.12 \times 10^{-4}} = 1.17 \times 10^9\ gpd/ft$$

-78-

which is more than one million times the values that were obtained for the aquitards that enclose this important water source.

2.   Results of Second Pumping Test

After the completion of the first pumping test on April 3, 1970, the producing well was left idle for a period of 50 days. During this time, the basin was pumped intensively for irrigation and therefore water levels in the observation wells were unable to recover. Figure V-11 shows the variation in fluid levels in each part of the three-aquifer subsystem during the last four days prior to the second pumping test. It may be seen that in the Oxnard aquifer the water levels were fluctuating with a frequency of approximately one cycle per day, and with a maximum amplitude of more than one foot. Piezometer 4 was the only observation with a stable water level when the producing well was started again on May 22, 1970. From May 22 through May 31, 1970, the pump was operated at a constant rate of approximately 800 gallons per minute.

Fig. V-11. Fluid levels in piezometers prior to second pumping test.

Figure V-12 shows the response in the Oxnard aquifer at various radial distances from the pumping well. It is clear from this figure that the results were strongly affected by disturbances that originated outside the area of the test, and therefore these data do not yield reliable results. On the other hand, Figure V-13 shows that, despite the variable behavior in the aquifer, the response in the lower part of this subsystem was essentially similar to that observed during the first test. To see how insensitive the ratio method is to such disturbances, let us again calculate the diffusivity of the lower aquitard using data from piezometer 3. At t = 150 minutes, one can observe on Figure V-13 that s' = 0.17 and s = 6.3 feet, so that the ratio becomes

$$\frac{s'}{s} = \frac{0.17}{6.3} = 2.7 \times 10^{-2}$$

Using equation V-5 and adopting the values of T and S from the first test, we obtain

$$t_D = \frac{(9.28 \times 10^{-5}) \ (130,600) \ (150)}{(100)^2 \ (1.12 \times 10^{-4})} = 1.62 \times 10^3$$

-79-

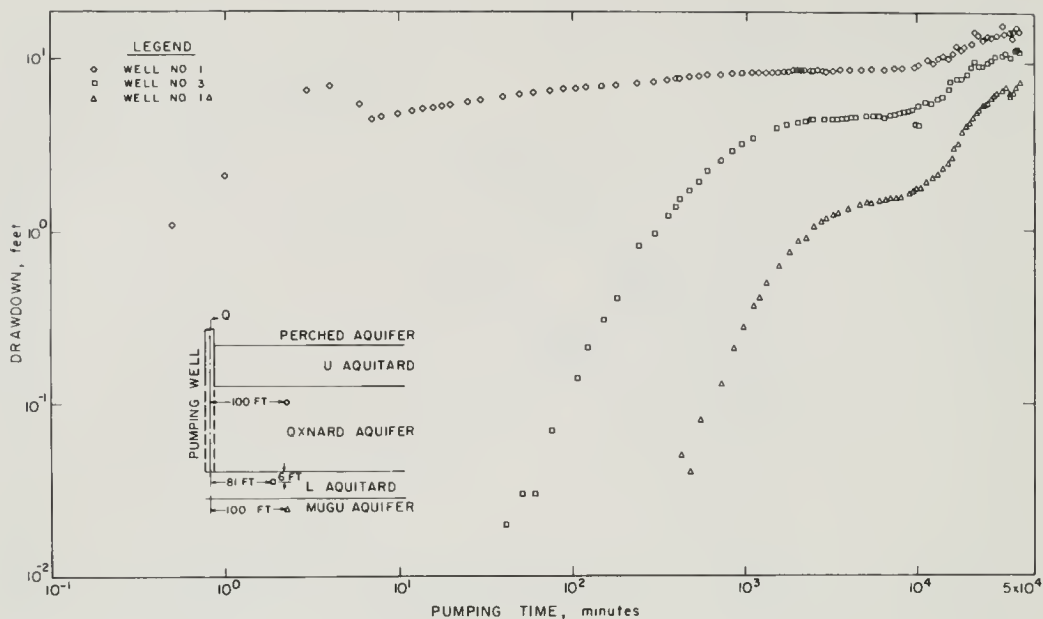Fig. V-12. Fluid levels in Oxnard piezometers during
second pumping test.
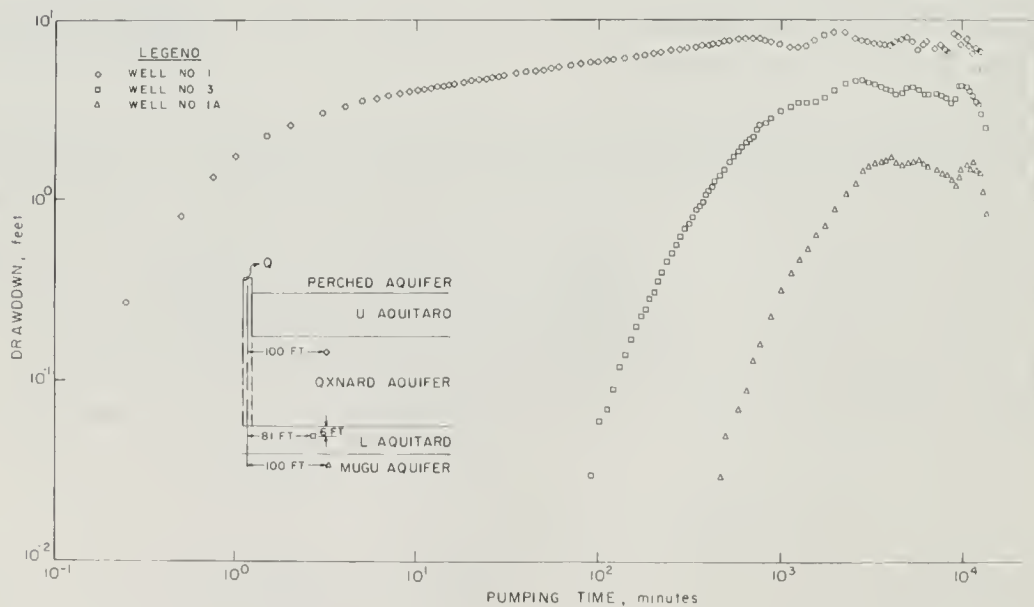
Fig. V-13. Response of piezometers in lower aquitard (No. 3)
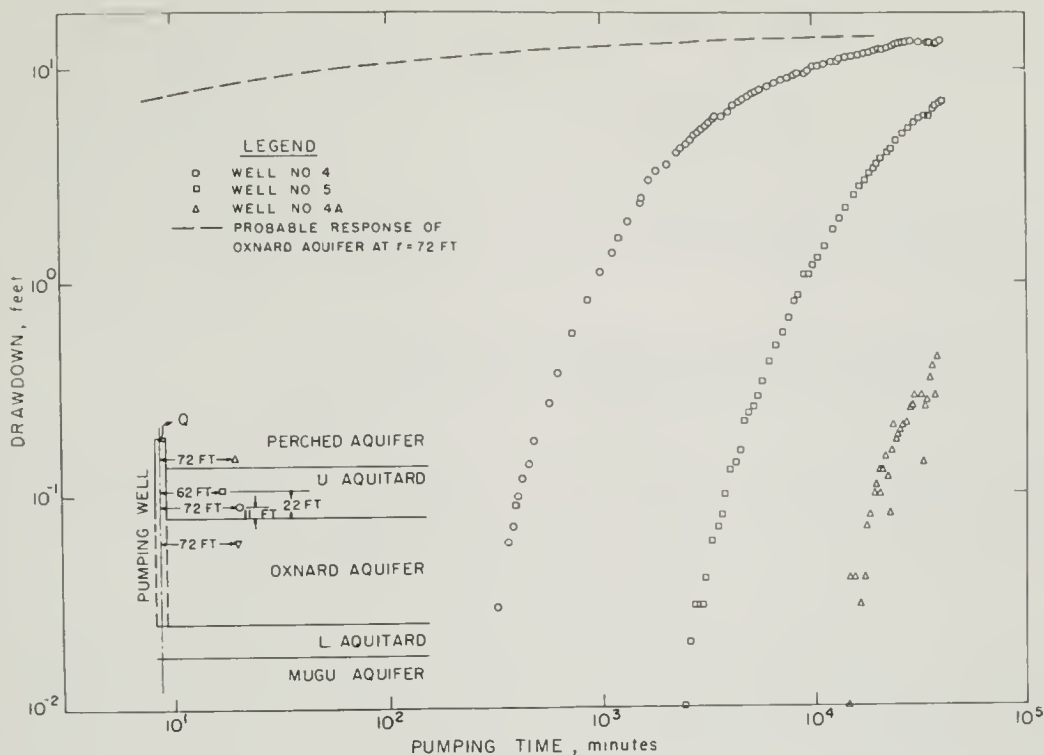compared to that of Oxnard (No. 1) and Mugu (No.
1A) aquifers during second pumping test.
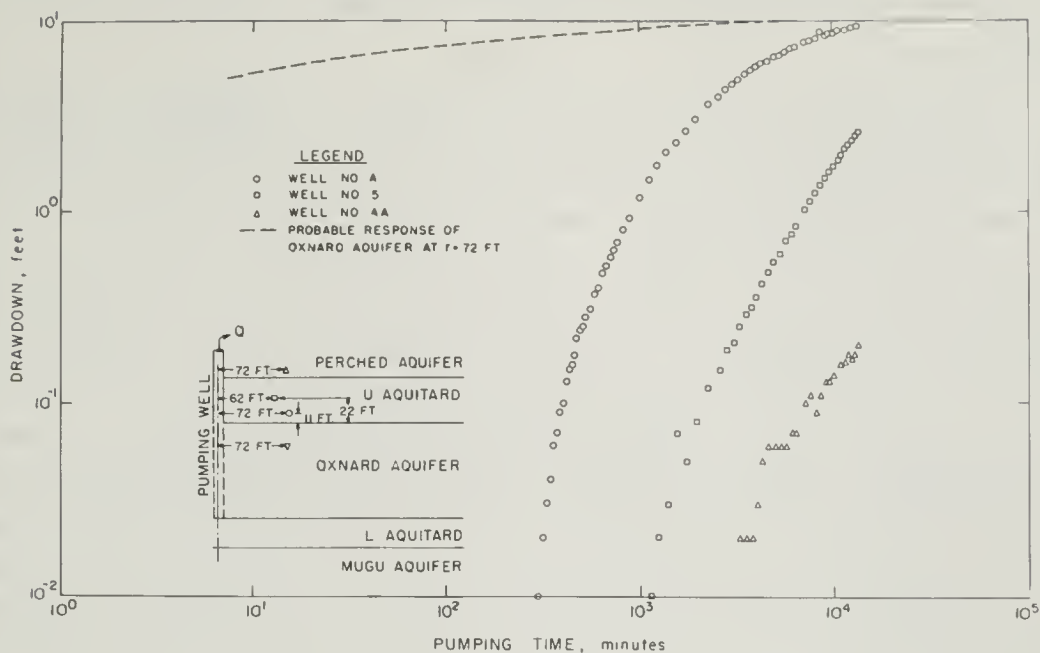
Fig. V-14.   Response of piezometers in upper aquitard
(Nos. 4 and 5) and semiperched aquifer
(No. 4A) during second pumping test.

referring to Figure IV-16, we see that these values of s'/s and t_D correspond to t_D' = 0.113.   Equation V-6 then gives

$$\frac{K'}{S_s'} = \frac{(1.077 \times 10^4) \, (0.113) \, (6)^2}{(150)} = 2.92 \times 10^2 \text{ gpd/ft}$$

which is somewhat less than the result obtained from the first pumping test (see Table V-3).

Figure V-14 shows the response in the upper aquitard as well as in the two aquifers that enclose it, and again the pattern is quite similar to that observed during the first test. However, since piezometer 4 was the only one where the water level was initially stable, it also results in the only curve which has exactly the same shape as it had during the first test. Choosing a small value of time, say t = 400 minutes, we find from Figure V-14 that s' = 0.1 and s = 8.5 feet, from which one can determine that K'/S_s' = 2.74 x 10^2 gpd/ft. This is very close to the result obtained in the first pumping test (see Table V-3). Finally for piezometer 5 at t = 3,000 minutes, K'/S_s' = 1.33 x 10^2 gpd/ft which again is very close to the result of the first pumping test.

In conclusion, it seems that although the second pumping test was performed under adverse conditions, it gives results which in general confirm the findings of the first

-81-

test. Obviously, the results of the first test appear to be more reliable and will therefore be adopted as being representative of the actual conditions in this part of the Oxnard basin.

3. Determination of Aquitard Properties Using Field and Laboratory Results

Having determined the average values of K'/S_s' for both aquitards as given in Table V-3, the next step is to evaluate the permeability, K', and the specific storage, S_s', in each aquitard. To do this, we shall utilize the laboratory measurements that are described below in Chapter VI. Referring to Figure VI-11, it is clear that permeabilities in the confining layers vary over a range of three orders of magnitude, and possibly more. Since the tests were conducted only on a limited number of samples, it would be practically impossible to obtain a representative average permeability from these data for either of the two aquitards. On the other hand, a relatively small range of values is obtained from the laboratory results for S_s', as will be shown below.

Let e be the void ratio and a_v, the coefficient of compressibility at any given elevation in the aquitard. If γ_w is the unit weight of water, then the coefficient of consolidation, c_v, is given by

$$c_v = K' \frac{(1 + e)}{a_v \, \gamma_w} \tag{V-8}$$

and is equivalent to the hydraulic diffusivity

$$\alpha' = \frac{K'}{S_s'} \tag{V-9}$$

comparing equation V-8 and V-9 shows that specific storage is related to e, a_v, and γ_w according to

$$S_s' = \frac{a_v \, \gamma_w}{1 + e} \tag{V-10}$$

If a_v is given in cm^2/kg, and S_s' in reciprocal feet, then (V-10) becomes

$$S_s' = 3.048 \times 10^{-2} \, \frac{a_v}{1 + e} \tag{V-11}$$

where γ_w was taken to be 1.0 g/cm^3. This last equation can now be used to obtain S_s' fr measured values of a_v and e as given in Table VI-8.

The results of such calculations are given in Table V-4 where it is seen that the variation in specific storage is much less than that observed for c_v and K' (see

-82-

Table V-4. Values of specific storage for aquitard
samples calculated from laboratory data

Layer	Sample depth, feet	Soil type	a_v cm^2/kg	e	S_s' $feet^{-1}$
Upper Aquitard	72.1	Clayey silt	2.9×10^{-2}	1.60	3.40×10^{-4}
	80.2	Clayey silt	5.0×10^{-2}	1.43	6.27×10^{-4}
	87.8	Silty clay	3.8×10^{-2}	1.07	5.59×10^{-4}
	98.0	Clayey silt	3.0×10^{-2}	0.96	4.66×10^{-4}
	98.1	Organic clayey silt	1.6×10^{-2}	1.02	2.41×10^{-4}
	103.5	Stiff clay	2.2×10^{-2}	0.92	3.49×10^{-4}
Lower Aquitard	202.5	Silt	6.0×10^{-3}	0.67	1.09×10^{-4}
	203.0	Silty fine sand	6.0×10^{-3}	0.71	1.07×10^{-4}
	221.1	Silty clay	6.0×10^{-3}	0.85	9.88×10^{-5}
	222.8	Silty fine sand	6.1×10^{-3}	0.39	1.34×10^{-4}
	226.0	Clay	1.5×10^{-2}	0.91	2.39×10^{-4}

Table VI-8). However, it must be remembered that all the laboratory tests were biased
in favor of the clays, i.e. the finest grained materials in each core sample. Therefore
these results represent only the highest values of S_s' in each aquitard. Since these
confining beds are largely made up of silty materials with relatively little clay (see
Table VI-2), the effective overall specific storage is probably on the low side of the
values listed on Table V-4. We therefore decided to adopt values of $S_s' = 1.0 \times 10^{-4}$
ft^{-1} for the lower aquitard and 2.4×10^{-4} ft^{-1} for the upper aquitard.

To compare these values of S_s' with the results of other workers, we examined
the data of Johnson et al. [1968] and Wolff [1970]. Johnson et al. give results for a
large number of core samples from several California locations on which they performed
consolidation tests. Although their values for hydraulic diffusivity (or coefficient of
consolidation) range from 1.4×10^{-2} to 1.5×10^{1} gpd/ft, their results for the coefficient
of storage are almost entirely within the range of 0.1 to 3×10^{-4} ft^{-1}. In other words,
K'/S_s' varies over three orders of magnitude because K' varies widely, while S_s' varies
only over one order of magnitude. It should be realized that their samples cover a wide
range of clay contents (10% to 80%). Wolff [1970] has obtained somewhat higher values
for S_s' ranging from 2.0 to 10×10^{-4} ft^{-1}. It is apparent that the results that were
selected above from Table V-4 are in good agreement with the work of others. It is also

evident that the coefficient of storage is not as sensitive to changes in lithology as is permeability.

Using $S_s' = 1.0 \times 10^{-4}$ ft^{-1} for the lower aquitard and 2.4×10^{-4} ft^{-1} for the upper aquitard, we can now convert the values of hydraulic diffusivity given in Table V-3 to obtain permeability from

$$K' = \frac{K'}{S_s'} \, S_s'$$ (V-12)

The results are given in Table V-5.

Table V-5. Hydraulic properties of aquitard layers

Layer	Section tested	Spec. Storage, S_s'		Permeability, K'	
		cm^{-1}	ft^{-1}	cm/sec	gpd/ft^2
Upper Aquitard	Bottom 21 ft	7.88×10^{-6}	2.4×10^{-4}	1.11×10^{-6}	2.45×10^{-2}
	Bottom 11 ft	7.88×10^{-6}	2.4×10^{-4}	2.66×10^{-6}	5.85×10^{-2}
Lower Aquitard	Top 6 ft	3.28×10^{-6}	1.0×10^{-4}	1.89×10^{-6}	4.17×10^{-2}

A comparison of these permeabilities with those on Table VI-7 indicates that these results are well within the range obtained by laboratory measurement. The field results are on the high side of the range of values obtained in the laboratory, because the latter represent only the least permeable members of the aquitards. Thus, it is concluded that there is reasonable agreement between laboratory and field results.

It is interesting to compare the specific storage and permeability of the aquitard with those of the Oxnard aquifer. Assuming that the thickness of the aquifer is 93 feet (105 - 198 ft), we have

$$K = \frac{T}{H} = \frac{130,600}{93} = 1,405 \text{ gpd/ft}^2$$

and

$$S_s = \frac{S}{H} = \frac{1.12 \times 10^{-4}}{93} = 1.20 \times 10^{-6} \text{ ft}^{-1}$$

Thus, the permeability of the aquifer is more than four orders of magnitude greater than that of the aquitards. The specific storage is at the lower end of the range normally

-84-

found for high permeability aquifers, but the important thing to note is that S_s is two orders of magnitude less than S_s' in the aquitards above and below it. In other words, for the same change in head, a unit volume of aquitard material can contribute about 100 times more water from storage than a similar volume in the aquifer. This further points to the necessity for considering storage in the aquitards when evaluating leaky aquifers (see Chapter IV-6).

CHAPTER VI. LABORATORY INVESTIGATIONS

J. K. Mitchell, J. A. Greenberg, J. H. Hardcastle, and D. T. Y. Wan

A. INTRODUCTION

As has been discussed in Chapter V, a series of core samples of the aquitard
sediments were collected during the drilling of the second observation hole (see Figure
V-2) which later was equipped as piezometer 2. These samples were needed for the lab-
oratory investigation phase of this study. Undisturbed samples were taken from 60 ft to
the top of the Oxnard aquifer at 105 ft and from the bottom of the Oxnard at 198 ft to a
total depth of 228 ft. Details of the drilling conditions are given in Section B of
Chapter V.

This report includes the results of laboratory measurements of the physical,
compositional, and hydrological properties of the core samples taken above and below the
Oxnard aquifer as well as the changes in these properties which result from leaching the
sediments with sodium chloride solutions in the laboratory. Part of the data presented
was published previously in "Physical and Hydrological Properties of the Aquitard Layers
in the Oxnard California Area," by James K. Mitchell [1969]. These data are included
herein along with additional results in order to facilitate the analysis of the response
of the sediments to leaching by sea water, and to provide the complete results of the
laboratory program under one cover. Laboratory methods are not described in detail in
this report except where methods were used which have not been standardized. However,
unless otherwise indicated, standard soil mechanics and soil science methods were used;
e.g., Lambe [1951], American Society of Agronomy [1965]. Johnson, et al. [1968] present
a detailed description of soil mechanic test methods and their application to the study
of the physical and hydrological properties of water-bearing deposits in subsiding areas
of Central California.

B. GENERALIZED STRATIGRAPHIC SECTION AND SAMPLING OPERATIONS

The general sequence of strata as given by the driller's log for first observation
hole is shown in Figure VI-1. Fine-grained sediments* were reported between depths of

---

*The designations "clay" and "sandy clay" are those of the driller. The results of
 classification tests presented subsequently indicate that the fine-grained layers
 contain very little clay, and are predominantly silt.

about 65 ft and 105 ft and between 198 ft and 246 ft, which marked the top of the Mugu aquifer. Fine-grained materials were encountered again below a depth of 330 ft. Two sample tubes were recovered from first observation hole at depths of 350.0 and 352.8 ft and 352.8 ft to 355.6 ft. These samples were taken primarily to test the suitability of the sampling equipment and procedures proposed for the detailed sampling scheduled in the second observation well.

Undisturbed samples were taken in the second observation hole in the fine-grained material between depths of 60.4 ft and 104.9 ft and 198.0 ft and 227 ft. The upper set of samples are representative of the fine-grained material which serves as the confining member above the Oxnard aquifer. The deeper samples were presumed to be representative of materials in the aquitard separating the Oxnard and Mugu aquifers. Subsequent study of these samples indicated that these deeper samples were almost entirely cohesionless (see Figure VI-3), and thus only limited information could be obtained in this study relative to the properties of any clay beds that may separate the Oxnard and Mugu aquifers. The bore hole was drilled through the sand formations and between points of sampling in the fine-grained materials using a rotary drill and bentonite drilling mud. Undisturbed samples were obtained using a Pitcher sampler. The operation of this device, which is particularly well suited for sampling in deposits containing successive layers of soft and hard consistency, is shown in Figure VI-2.

The thin-walled tube is suspended from the rotating cutter barrel, and drilling fluid circulates down through the tube and flushes the cuttings from the bottom of the previously drilled hole while the sampler is being lowered. When the sample tube reaches the bottom of the hole, the cutter barrel moves downward relative to the tube. The drilling fluid is then diverted into the annular space between the tube and the barrel, under the rotating cutter barrel, and upward along the barrel. In soft materials the compression in the spring above the sampling tube keeps the cutting edge of the tube below the cutter barrel and the tube penetrates the sediment in a manner similar to that for ordinary thin-walled sampling. In hard materials the spring compresses until the cutting edge of the tube is above the bottom of the cutter barrel. Rotation of the

DEPTH RANGE FOR UNDISTURBED SAMPLING IN OBSERVATION HOLE 2
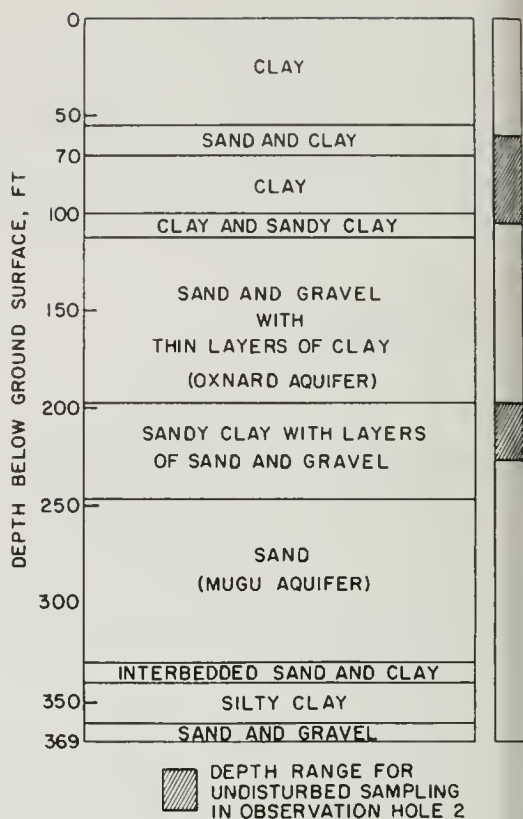
Fig. VI-1. Driller's log for first observation hole

-88-

barrel cuts an annular ring leaving a cylinder
of soil over which the tube can slide. Thus
the Pitcher sampler can adapt itself to the
consistency of the sediment, and it was found
to work very well in the materials encountered
in this investigation.

A total of twenty undisturbed samples,
ranging from medium sand to lean clay were
obtained. The sample tubes were 2.8 inches
in inside diameter and 2.8 feet long. Full
sample recovery was obtained in almost all
cases. All sample tubes were sealed imme-
diately after recovery, transported to the
Soil Mechanics and Bituminous Materials
Laboratory at the University of California,
Berkeley, and stored in a humid room.

C. CLASSIFICATION PROPERTIES OF AQUITARD
   SEDIMENTS

Figure VI-3 shows the variation of
in-situ water content, liquid limit, and
plastic limit with depth for the two major
fine-grained sediments encountered in obser-
vation hole 2. It may be seen that (1) there
is a rather wide variation in properties with
depth, (2) the in-situ moisture content is, in

Fig. VI-2. Schematic diagram of
Pitcher sampler
(after Terzaghi and
Peck, 1967)

general, substantially less than the liquid limit, which would be expected for samples
from large depth, and (3) the sediments tested were predominantly silts, silty clays and
clayey silts according to the Unified Soil Classification System.*

The data used in Figure VI-3 are listed in Table VI-1. Two to four values of
liquid limit are listed for a number of samples. These values represent liquid limit
test results obtained on different samples taken from the same sample tube and further
illustrate the range of variability, even over the relatively short vertical distances
contained within any one tube.

From Table VI-1 it may be noted that samples between depths of 200.7 and 219.0
ft are non-plastic. All core tube samples from the presumed aquitard underlying the

---

*Engineering soil classifications are described in most soil mechanics texts; Lambe and
 Whitman (1969) present the Unified System in some detail.

-89-
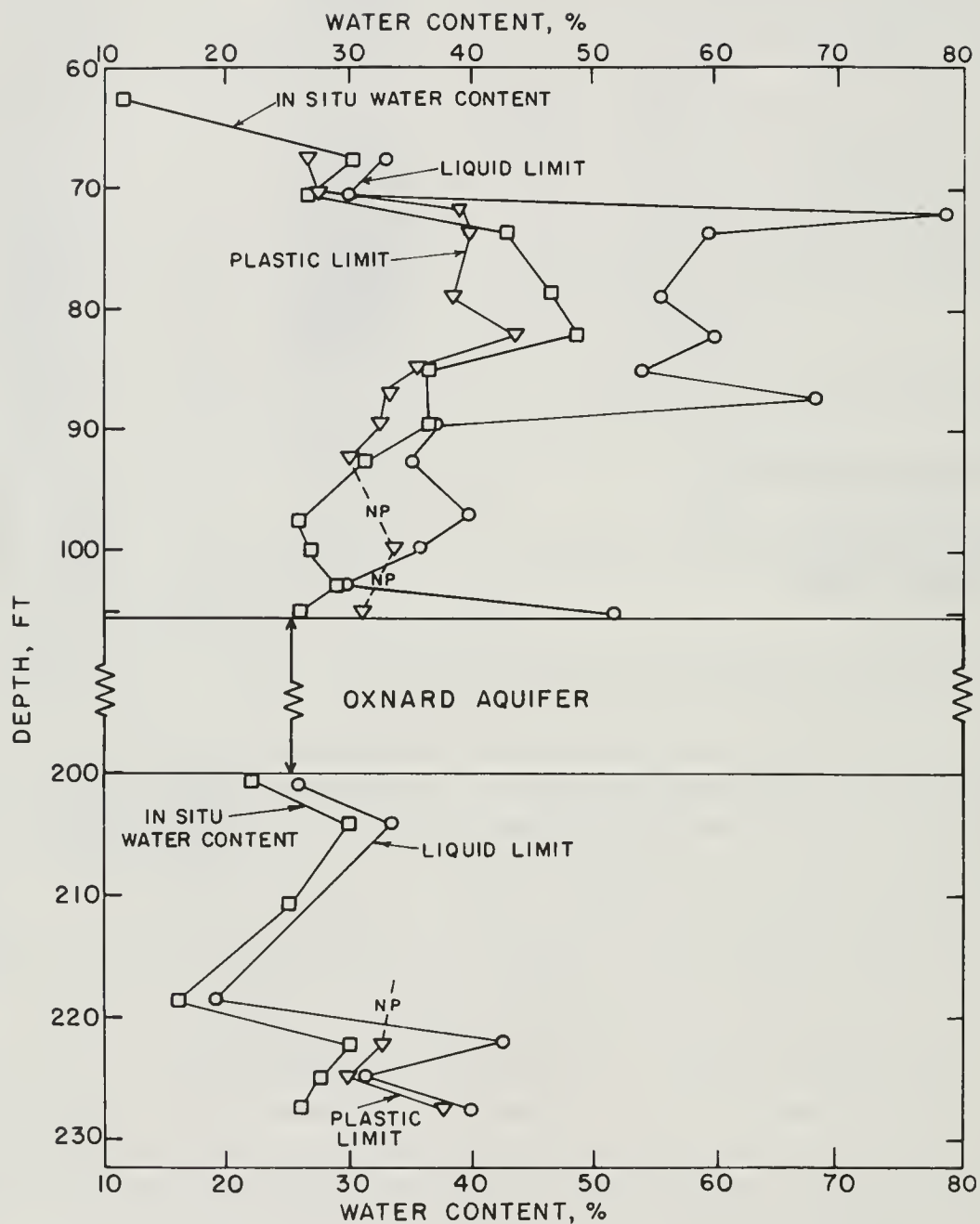
Fig. VI-3. Water content and plasticity profiles
in Oxnard aquitard materials

Table VI-1. Atterberg limits, in-situ water content and
classification data, Oxnard observation hole 2

Depth, ft.	Unified Classification		Liquid Limit, %		Plastic Limit (%)	In-situ Water Content %	Specific Gravity of Solids
			Range of Values for Different Samples from Same Tube	Aver-age			
62.0-62.5	Gravelly sand	(SW)	–	–	NP	11.6	
67.0-67.5	Clayey silt	(ML)	33.0	33.0	26.8	30.5	
70.0-70.3	Clayey silt	(ML)	30.0	30.0	27.6	26.7	
70.3-73.1	Clayey silt	(MH)		78.7	39.4		
72.5-73.1	Clayey silt	(MH)	64.0; 63.5; 51.1	59.5	39.9	43.6	
78.4-78.8	Clayey silt	(MH)	50.7; 52.7; 63.1	55.5	38.5	46.8	
81.0-81.6	Clayey silt	(MH)	50.9; 60.0; 69.1	60.0	43.5	48.5	
83.7-84.4	Clayey silt	(MH)	49.0; 53.0; 54.0; 58.4	53.6	35.3	36.5	
86.4-89.2	Clayey silt	(MH)		69.0	33.5		
88.8-89.2	Clayey silt	(ML)	37.2	37.2	32.6	36.6	2.68
91.5-92.0	Clayey silt	(ML)	33.4; 37.0	35.2	30.3	31.3	
96.0-96.5	Clayey silt	(ML)	37.0; 42.4	39.7	NP	26.7	2.68
96.5-99.3	Clayey silt	(ML)		40.0	29.6		
99.0-99.3	Clayey silt	(ML)	35.7	35.7	33.0	27.0	
101.6-102.1	Silt	(ML)	25.7; 32.4	29.0	NP	29.1	
102.1-104.9	Clay	(CL-CH)		51.9	27.7		
104.3-104.9	Clay	(CL-CH)	44.4; 49.3; 61.8	51.8	27.5	25.9	
200.7-201.0	Silty-fine sand	(ML)	25.5	25.5	NP	22.4	
203.6-204.0	Silt	(ML)	33.2	33.2	NP	29.8	
211.0-211.5	Silt	(ML)	–	–	NP	25.0	
218.5-219.0	Silt	(ML)	18.8; 19.4	19.1	NP	16.0	
221.5-221.8	Clayey silt	(ML)	42.6	42.6	32.7	30.0	
224.1-224.6	Clayey silt	(ML)	25.5; 36.7	31.1	29.8	26.8	
226.7-227.4	Clayey silt	(ML)	37.1; 41.0; 42.4	40.1	37.6	25.9	2.60[1]

[1]Sample observed to contain visible amounts of organic matter.

Oxnard aquifer have been examined. Figure VI-4 shows the profile of sediments between 198.0 and 227.4 ft depths. This figure shows that the profile is highly stratified and further that most of the material is sand. Those samples for which classification data are shown in Figure VI-3 and Table VI-1 are biased in favor of the most fine-grained materials encountered in the observation hole. Although the boring log for the second observation hole suggested that the aquitard separating the Oxnard and Mugu aquifers begins at a depth of about 200 ft, the results shown in Figure VI-4 suggest that the Oxnard may in fact extend to a depth of almost 225 ft. Since no samples were taken from depths greater than 227.4 ft, no definitive conclusions are possible relative to either the thickness of the aquitard separating the Oxnard and Mugu formations or its average properties.

In view of these findings, the need for additional undisturbed sampling beneath the Oxnard aquifer is evident if reasonable analyses of the influences of sea water intrusion and pumping are to be made.

The specific gravity of solids has been determined for four samples, giving the values listed in Table VI-1. With the exception of one of the samples from the 226.7 to 227.4 ft depth range, which contained a significant quantity of organic matter, all samples had specific gravity values of 2.68. This value of specific gravity is consistent with the fact that most of the aquitard sediments are composed predominantly of quartz particles, with lesser amounts of clay minerals and other non-clays. The specific gravity of quartz particles is 2.67; whereas, the clay minerals are generally heavier, with values of the order of 2.70 to 2.75.

A plasticity chart has been prepared for these materials and the results are shown in Figure VI-5. With the exception of the material
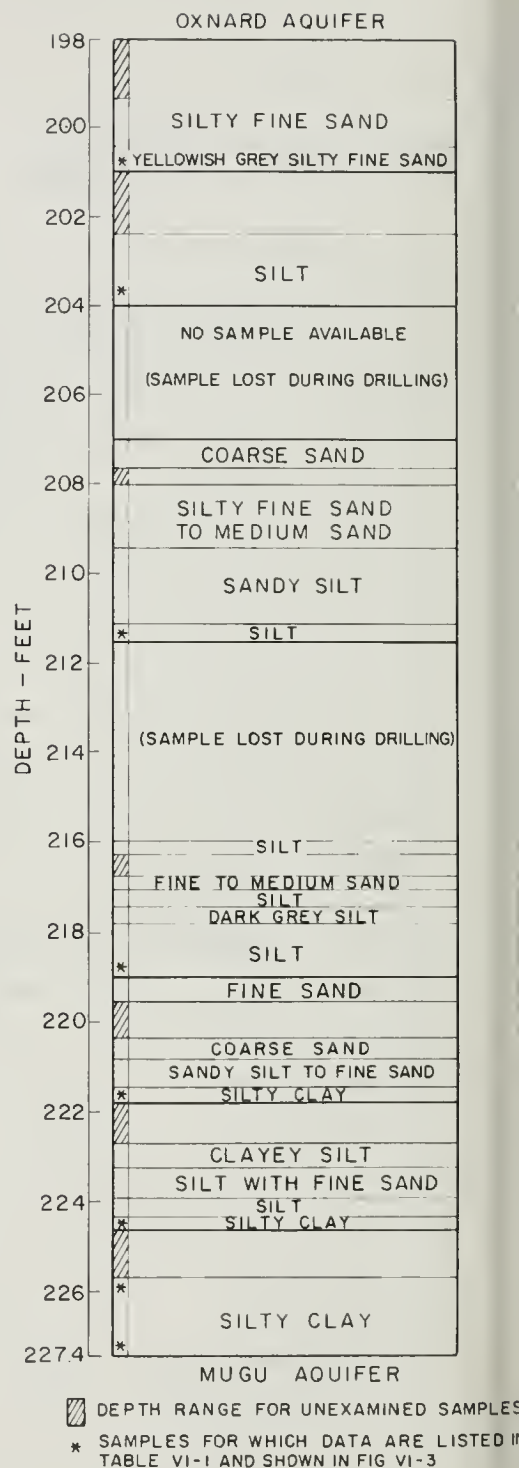
Fig. VI-4. Detailed profile of sediments between 198 and 225 ft depths - observation hole 2

-92-
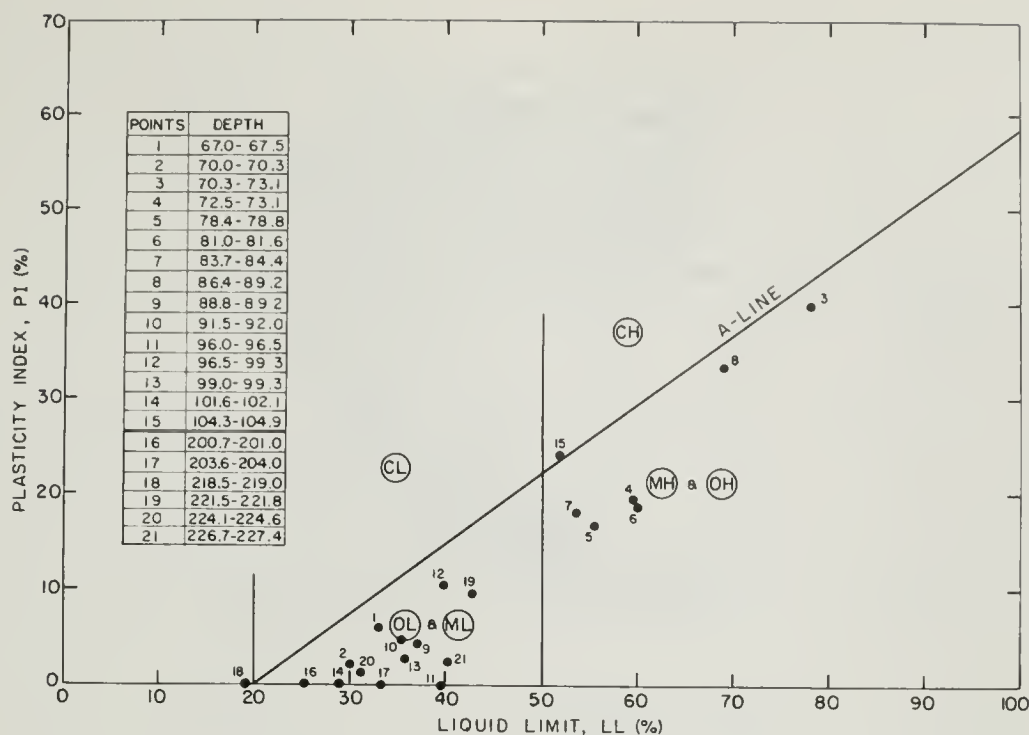
Fig. VI-5. Plasticity chart for Oxnard aquitard samples

at a depth of 104.3 to 104.9 ft, all samples plot well below the A-line in the zones characteristic of silts and organic materials.

As indicated in the Introduction, data on aquitard soils in California are meager; however, the comprehensive study reported by Johnson et al., [1968] includes rather detailed information on the sediments in three major subsidence areas of California; i.e., the Los Banos-Kettleman City area, the Tulare-Wasco area, and the Santa Clara Valley. Data in their report pertain mainly to properties, as determined in the laboratory, of the finer-grained materials encountered in holes drilled to depths as great as 2200 ft below ground surface.

Plasticity data for sediments from each of the three areas studied by Johnson et al., are shown in Figure VI-6. Comparison between Figures VI-5 and VI-6 shows that the Oxnard aquitard materials resemble most closely the sediments from the Los Banos-Kettleman City area with respect to plasticity characteristics, although the Oxnard sediments appear to be somewhat less plastic.

Figure VI-7 shows a photograph of partially dried material taken from a depth of 80.5 ft and trimmed to expose details of stratification. The darker zones represent areas of high clay content relative to the lighter regions. Some shrinkage cracking, which formed during the drying of the sample from its natural moisture content, may be noted. The material shown in this photograph is typical of the sediments encountered

-93-

(CH) INORGANIC CLAYS — HIGH PLASTICITY

(CL) INORGANIC CLAYS —LOW TO MEDIUM PLASTICITY,
GRAVELLY CLAYS, SANDY CLAYS, SILTY CLAYS, LEAN CLAYS

(OH) ORGANIC CLAYS — MEDIUM TO HIGH PLASTICITY

(OL) ORGANIC SILTS AND SILT CLAYS — LOW PLASTICITY

(MH) MICACEOUS AND DIATOMACEOUS FINE SANDY AND SILTY
SOILS, ELASTIC SILTS

(ML) INORGANIC SILTS AND VERY FINE SANDS, ROCK FLOUR,
SILTY OR CLAYEY FINE SANDS WITH SLIGHT PLASTICITY

$I_p = 0.73 (W_l - 20)$ "A" LINE

A. LOS BANOS – KETTLEMAN CITY AREA

CORCORAN CLAY
MEMBER OF
TULARE FORMATION

B. TULARE – WASCO AREA

PLASTICITY INDEX

LIQUID LIMIT

C. SANTA CLARA VALLEY

Fig. VI-6.   Plasticity characteristics of
sediments (after Johnson et
al., 1968)

-94-

Table VI-2. Grain size analysis of samples from
Oxnard observation hole 2

Unified Soil Classification and
Percent of Various Sizes [1]

Depth	Classification	Clay[2] Content %	Silt[3] Content %	Sand[4] Content %
62.0-62.5	Gravelly sand (SW)	0.2	3.8	96.0
69.8-70.3	Clayey silt (ML)	4.2	82.8	13.0
70.3-73.1	Clayey silt (MH)	48.0	50.0	2.0
72.5-73.1	Clayey silt (MH)	19.0	71.0	10.0
78.4-78.8	Clayey silt (MH)	(1) 2.0 (2) 22.0	93.0 77.6	5.0 0.4
83.6-84.4	Clayey silt (MH)	(1) 0.2 (2) 18.0	93.8 76.0	6.0 6.0
86.4-89.2	Clayey silt (ML)	33.0	65.0	2.0
91.0-92.0	Clayey silt (ML)	(1) 7.0 (2) 6.0	80.0 81.0	13.0 13.0
96.0-96.5	Clayey silt (ML)	13.0	67.0	20.0
96.5-99.3	Clayey silt .(ML)	13.0	60.0	27.0
98.7-99.3	Clayey silt (ML)	6.0	78.0	16.0
102.1-104.9	Clay (CL-CH)	33.0	59.0	8.0
104.0-104.9	Clay (CL-CH)	(1) 32.0 (2) 34.0	53.0 52.0	15.0 14.0
203.4-204.0	Silt (ML)	6.5	80.5	13.0
218.5-219.0	Silt (ML)	4.8	14.2	82.0
221.0-221.5	Clayey silt (ML)	15.0	63.0	22.0
224.0-224.6	Clayey silt (ML)	10.0	78.0	12.0

[1] All percentages are by weight of dry soil

[2] Finer than 2 microns (.002 mm)

[3] Between 2 microns and 74 microns (200 mesh sieve)

[4] Coarser than 74 microns
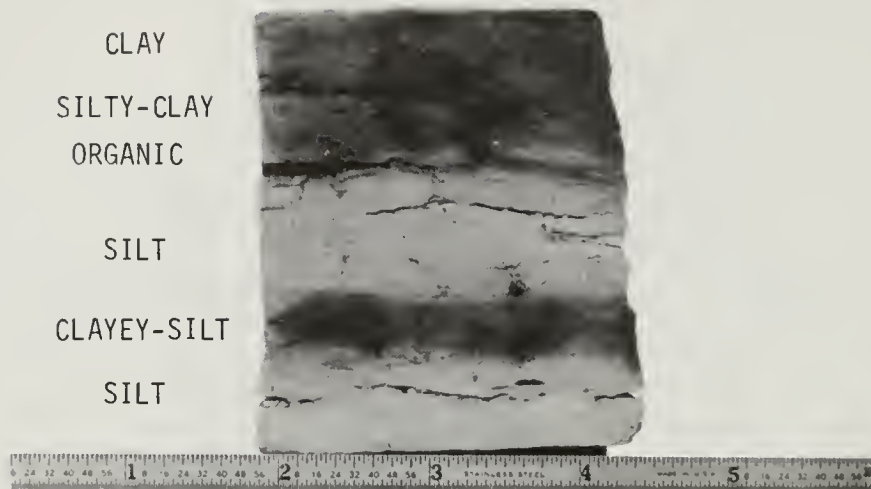
Fig. VI-7. Partially dried material from depth
of 80.5 ft showing stratification

and emphasizes the great variability of characteristics within small vertical distances.

Grain size distribution values have been obtained for a number of samples of the finer material using the hydrometer method of sedimentation analysis. Grain size distribution curves are presented in Appendix C. The results are summarized in Table VI-2 in the form of a listing of the percent (by weight) of clay, silt and sand sizes. Particles coarser than 200 mesh sieve (74 microns) are considered sand, particles between 200 mesh and 2 microns are silt, and clay size material is finer than 2 microns. Again it should be pointed out that the data for 204.0 to 224.6 ft depths are for samples representative of the finest materials encountered. It is clear from the results in Table VI-2 that the greatest proportion of particles are in the silt size range for almost all samples. These values as well as the shapes of the grain size distribution curves (Appendix C) indicate most samples to be quite uniform rather than well graded. The proportion of clay material is, in nearly all cases, quite low.

These findings are consistent with the plasticity data and confirm that the aquitard layers in the Oxnard area are composed predominantly of silty materials rather than clays.

A comparison of these results with those reported by Johnson et al., [1968] for sediments in the Los Banos-Kettleman City, Tulare-Wasco, and Santa Clara Valley areas shows that the Oxnard sediments fall within the ranges of grain size distributions exhibited by the sediments from the other areas. It appears, however, that the Oxnard materials overall are somewhat coarser grained with lower clay contents than those from the other areas.

D. COMPOSITION OF AQUITARD SEDIMENTS

The binocular microscope, X-ray diffraction analysis, and several types of chemical analysis were used to determine the composition of the aquitard sediments. The microscope was used to study the non-clay fraction of samples taken from tubes corresponding to depths of 73.1 ft, 96.5 ft, 219.0 ft and 221.8 ft. Study of silt and fine sand particles yielded information relative to particle size, particle shape, surface texture, and mineralogy.

1. Non-Clay Fraction

The non-clay fraction of the material in the confining bed overlying the Oxnard aquifer (samples from 73.1 ft and 96.5 ft depth) is composed of medium to fine particles and is uniform. Both bulky (predominantly quartz with some dark minerals) and platy particles were found. The platy particles were identified as mica. The bulky particles varied from angular and rough textured to rounded with smooth surfaces.

The non-clay fraction (silt and fine sand) of samples taken from the aquitard underlying the Oxnard aquifer was also composed mainly of quartz and mica particles. Large variations in surface texture - from smooth to rough - was observed. A wider range of particle sizes appears to exist in these samples than was found in the samples taken above the Oxnard aquifer.

Small amounts of organic matter were found in all samples examined. The titration method proposed by Rankin (1968) was used for quantitative estimation of the amount of organic matter. In this method the organic matter is oxidized using potassium dichromate and sulfuric acid. After additional of phosphoric acid and barium diphenylamine sulfonate indicator solution, the amount of potassium dichromate consumed in reaction with the organic matter can be determined by titration with ferrous sulfate. A separate set of samples was also examined which had been pre-treated with sodium hypochlorite (NaOCl) and hydrogen peroxide (H_2O_2) for the purpose of breaking down organic tissues prior to the titration test. The results of the organic matter determinations are given in Table VI-3.

These results show that while organic matter is present in all samples, the amounts are very small, in all cases less than 1%. It may be noted also in Table VI-3 that in all cases the pretreated samples gave slightly greater values of organic matter than the untreated soils. This probably reflects the greater ease with which broken down tissue can be oxidized by the dichromate solution. The presence of these small amounts of organic matter are not likely to be of great importance in influencing the behavior of these soils[*].

---

[*]Subsequent to these tests some samples have been found which contain larger amounts of organic material, some of which is in nearly undecomposed form.

Table VI-3. Organic matter content of
Oxnard aquitard materials

Sample Depth ft.	Organic Content, % by Weight	
	Pretreated Samples	No Pretreatment
72.1-72.5	0.69	0.48
83.2-83.6	0.89	0.14
98.3-98.7	0.80	0.47
203.0-203.4	0.89	0.71
226.4-226.7	0.25	0.22

Tests for carbonate minerals using hydrochloric acid showed that significant amounts of these minerals are not present.

2. Clay Minerals

X-ray diffraction was used to determine the mineralogy of the clay fraction of samples from depths of 72.5 - 73.1 ft and 96.0 - 96.5 ft in the confining bed overlying the Oxnard aquifer, and from 218.5 - 219.0 and 221.0 - 221.5 ft in the sediments presumed to separate the Oxnard and Mugu formations.

A Norelco diffractometer equipped with goniometer and automatic recorder was used. Filtered copper radiation with a wave length, λ, of 1.542Å was used for all tests. Samples of clay containing all particles finer than 2 microns were sedimented on glass slides and air dried. This produced samples in which most platy clay particles were oriented with their faces parallel to the slide and enhanced the basal reflections in the X-ray patterns obtained, thus facilitating the identification of the clay minerals. X-ray diffraction patterns were obtained for air-dried samples after treatment with ethylene glycol, and after heat treatment to 500°C. Comparison of the diffraction patterns obtained after each of these treatments provides a basis for positive identification of the different clay mineral types. A typical X-ray diffraction pattern is shown in Figure VI-8 for a sample from the 218.5 - 219.0 ft depth range after glycol treatment. The spacing, d, of the atomic plane associated with each diffraction peak and the intensity, I, of each peak relative to the strongest peak on the pattern are indicated.

All samples were found to contain montmorillonite, a kaolin group mineral, illite or hydrous mica, and quartz. It was not clear from the results whether the kaolin group mineral is kaolinite or halloysite. These two minerals cannot always be distinguished by means of X-ray diffraction. Although halloysite should probably not occur in such
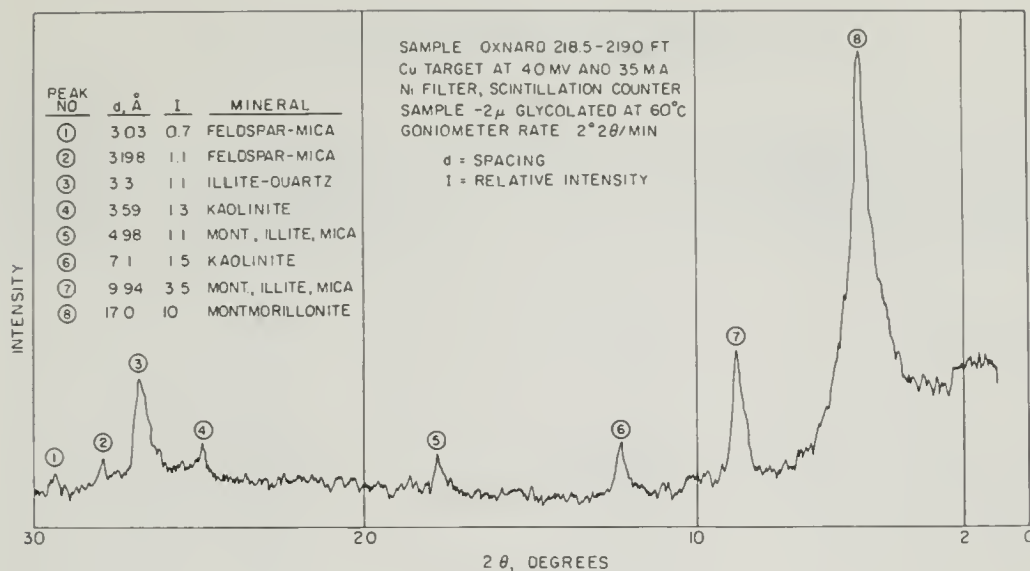
Fig. VI-8. Typical X-ray diffraction pattern
of clay-size fraction

sediments as these, an attempt was made to make more positive identification of the kaolin mineral using the electron microscope; however, the results were inconclusive.

A rough estimate of the relative amounts of each mineral was made based on the relative intensities of the diffraction peaks. Quantitative analysis on the basis of X-ray diffraction is tenuous at best; thus the values obtained are rough approximations. The results of this analysis are given in Table VI-4. It may be seen that in each case montmorillonite is the dominant mineral in the clay fraction. It is important to note, however, that in each case the amount of clay in the whole soil is quite small, amounting to only a few percent. Thus while montmorillonite is the most active of the clay minerals and may undergo substantial changes in characteristics if subjected to alteration in its chemical environment, as might be the case if the clay layers confining the Oxnard aquifer are invaded by salt water, the effect of this on the behavior of the aquitard layer as a whole may be limited.

3. Cation Exchange Capacity

The cation exchange capacity of several samples was obtained using the ammonium acetate method described by Chapman (1965). The results of these tests, expressed in milliequivalents of exchangeable cation per 100 grams of dry soil, are given in Table VI-5. Determination of the exchange capacities of samples of the whole soil were made first. The values obtained, 21.0 to 43.2 meq/100 gm, were considered quite high for sediments with such small amounts of clay size material. Consequently, additional

-99-

Table VI-4. Mineralogy of the clay-size fraction
from Oxnard aquitard samples

Sample Depth ft.	Amount of Soil <2μ, % by Weight	Mineral	Approximate Amount in <2μ Fraction % by Weight[1]	Approximate Amount in Whole Soil % by Weight
72.5-73.1	19	Montmorillonite Kaolin Mica or Illite Quartz	64 19 6 10	12 4 1 2
96.0-96.5	13	Montmorillonite Kaolin Mica or Illite Quartz	63 12 12 12	8 1.5 1.5 1.5
218.5-219.0	5	Montmorillonite Mica or Illite Kaolin Quartz	56 17 11 17	3 1 <1 1
221.0-221.5	15	Montmorillonite Kaolin Mica or Illite Quartz	55 11 11 22	8 1.5 1.5 3

[1]Based on diffraction peak intensities. Values indicated are very approximate.

determinations were made using the only silt size fractions (74μ-2μ) or clay size fractions (<2μ). The results shown in Table VI-5 indicate that the cation exchange capacity of the clay fraction ranges from 90 to over 100 meq/100 gm, a result compatible with montmorillonite clay mineral domination of the clay fraction. More surprisingly, the exchange capacity of the silt size fraction was found to range from 13 to 23 meq/100 gm. Such high values are not ordinarily associated with such particle size ranges, since the mineralogy is predominantly of the non-clay type. This high exchange capacity is possibly associated with the mica-like minerals that were observed microscopically in the silt sizes. Barshad [personal communication, 1969] has indicated that silts of high exchange capacity, probably ascribable to vermiculite minerals, have been found in California soils. If proportions of the silt and clay exchange capacities are combined based on the amounts of each size range present in the soil, then a value consistent with that measured for the whole sample is obtained.

Each entry in Table VI-5 represents a separate determination. Agreement between results for separate samples from the same depth is considered good, except for silt fraction from 83.2 - 83.6 ft depth. A pure sample of kaolinite, indicated by Hydrite UF,

Table VI-5. Cation exchange capacity values
for Oxnard aquitard samples

Sample Depth ft.	Exchange Capacity, meq/100 gm		
	Whole Sample	Clay Fraction	Silt Fraction
72.1-72.5	43.2		
83.2-83.6	35.4	118	23.3
	39.2	93	13.2
98.3-98.7	27.5		
	29.0		
103.5-104.0		121	23.2
203.0-203.4	21.0		
226.4-226.7	25.3	98	13.0
	26.5		
Hydrite UF		6.4	

was tested for comparison purposes and is included in the table.

A later section of this report will discuss the effects on the physical properties of a change in type of exchangeable cation.

4. Pore Fluid Composition

The quantity of soluble salts (equivalent NaCl) in the pore fluid of the Oxnard aquitard materials was determined using an electrical conductivity method. A slurry of 2 parts water to 1 part dry sediment was prepared and centrifuged to obtain clear supernatant fluid. The electrical resistivity of the fluid was measured using an AC Wheatstone Bridge and compared with values for standard solutions. The concentrations obtained were adjusted to account for the water content difference between the slurry and the in-situ sediment. The results of these determinations are given in Table VI-6.

These values, which are in the range of 1340 to 1920 ppm, indicate that sea water from the Oxnard aquifer has not yet invaded the aquitard layers to any significant extent at the site of the observation hole. Fresh water is generally considered to contain less than 1500 ppm total dissolved salts.

Analysis of pore water extracted from the soils was carried out by flame photometer and atomic absorption analyzer and indicated the dominant cations to be calcium and magnesium, with small amounts of sodium and potassium.

Table VI-6. Pore fluid salt content for
Oxnard aquitard materials

Sample Depth ft.	Equivalent NaCl Content		
	gm/liter	Normality	ppm
72.1-72.5	1.89	.0324	1890
83.2-83.6	1.34	.0238	1340
98.3-98.7	1.92	.0328	1920
203.0-203.4	1.81	.0310	1810
226.4-226.7	1.51	.0269	1510

E. PERMEABILITY OF AQUITARD SEDIMENTS

The present hydraulic permeabilities of 19 undisturbed samples from the confining beds above and below the Oxnard aquifer were determined in the laboratory. While the samples from above the Oxnard can be considered representative of the confining layer, those from below were more representative of the finest grained material encountered. Suitable undisturbed specimens of the coarser materials could not be prepared for permeability testing. In each case, the sample was recompressed prior to the permeability measurement to an effective consolidation pressure approximately equal to that originally acting on the material in-situ. The appropriate value of consolidation pressure for use in the permeability tests was determined by the product of the buoyant unit weight (water table assumed at the ground surface) and the sample depth.

The undisturbed specimens were contained in a consolidation ring having a diameter of 2.5 inches, and the initial sample height in the direction of flow was about one inch. Full saturation of the specimens was maintained by applying back pressure to the pore water. Hydraulic flow rates were determined using the procedures and apparatus described by Mitchell, Hooper, and Campanella (1965). The hydraulic pressure drop across the samples was maintained at a value of less than 15 percent of the effective consolidation pressure.

Several permeability determinations at differing hydraulic gradient magnitude were made on each sample and the results averaged. Table VI-7 presents a listing of these results, and Figure VI-9 shows the variation of permeability with depth. Permeabilities are given in terms of cm/sec and gpd/ft^2. It may be seen that local variations in permeability of as much as nearly three orders of magnitude are encountered in these deposits, which again reflects the rather substantial nonhomogeneous character of these sediments as shown earlier in Figure VI-3 for water content and plasticity. The assignment of an average value of permeability for use in the analysis of seepage through the aquitard layers will be difficult.
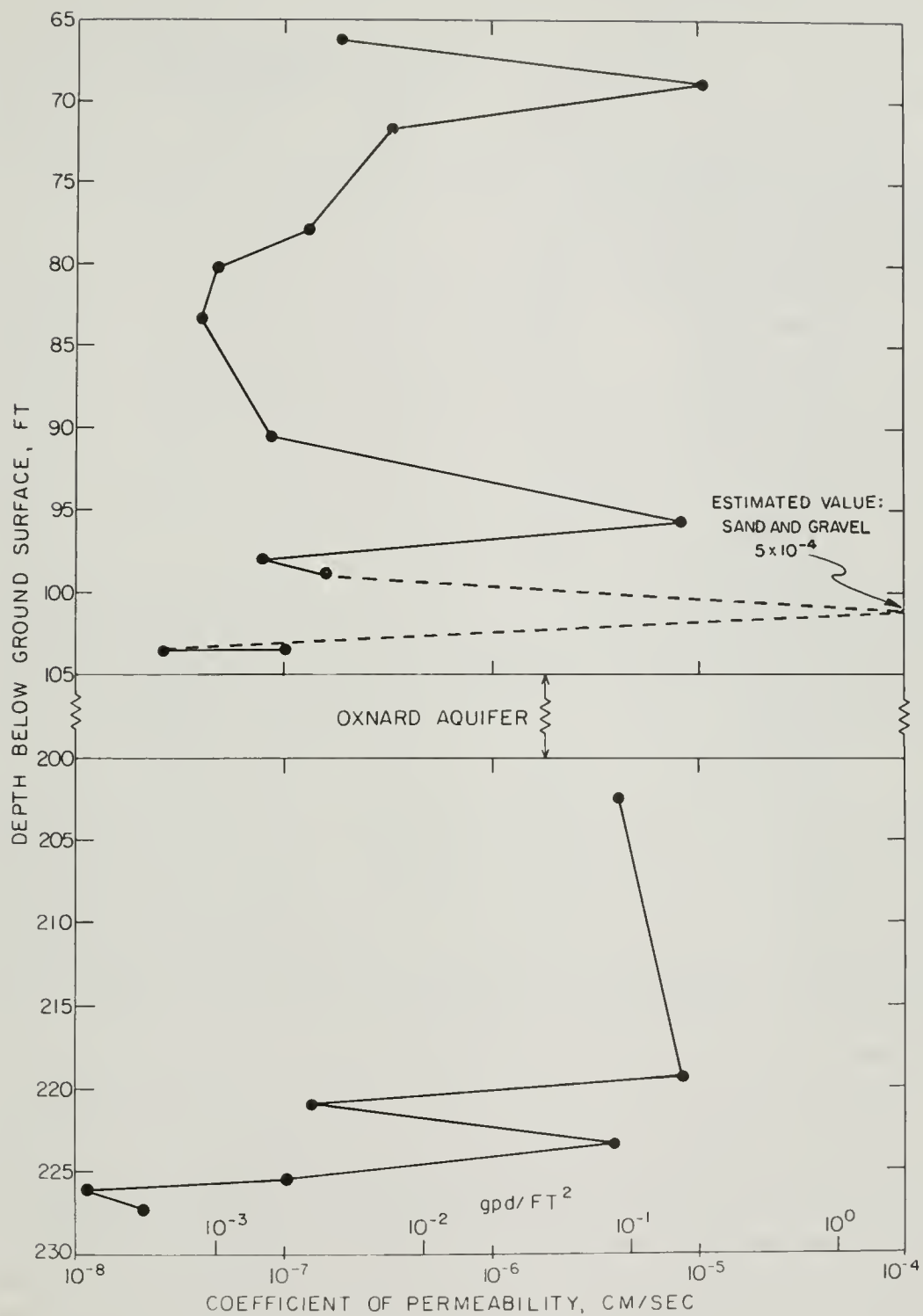
Fig. VI-9. Variation of permeability with depth.

Table VI-7. Permeability of undisturbed samples
of aquitard sediments

Sample Depth ft.	Soil Type	Water Content %	Effective Overburden Pressure kg/cm^2	Coefficient of Permeability[1]	
				cm/sec	gpd/ft^2
66.5	Clayey silt	45.0	2.0	1.93×10^{-7}	4.1×10^{-3}
69.3	Silty fine sand	26.0	2.0	1.09×10^{-5}	2.3×10^{-1}
72.1	Clayey silt	40.0	1.7	3.37×10^{-7}	7.1×10^{-3}
77.8	Clayey silt	45.0	1.9	1.31×10^{-7}	2.8×10^{-3}
80.2	Clayey silt	54.0	2.0	0.48×10^{-7}	1.0×10^{-3}
83.0	Clayey silt	36.7	2.0	0.40×10^{-7}	8.5×10^{-4}
91.0	Clayey silt	27.0	2.3	0.89×10^{-7}	1.9×10^{-3}
95.5	Silt	29.0	2.3	0.82×10^{-5}	1.7×10^{-1}
97.0	Clayey silt	43.0	2.4	0.80×10^{-7}	1.7×10^{-3}
98.0	Clayey silt	38.0	2.5	1.67×10^{-7}	3.4×10^{-3}
103.0	Stiff clay	32.0	2.5	0.26×10^{-7}	5.5×10^{-4}
103.4	Stiff clay	36.4	3.1	1.06×10^{-7}	2.3×10^{-3}
202.5	Silt	21.6	4.0	5.60×10^{-6}	1.2×10^{-3}
219.0	Sand with clay	23.5	5.25	8.81×10^{-6}	1.9×10^{-1}
221.1	Silty clay	31.2	6.0^2	1.35×10^{-7}	2.9×10^{-3}
223.6	Silt	25.5	5.44	4.48×10^{-6}	9.5×10^{-2}
225.9	Clay	32.4	6.77	1.05×10^{-7}	2.2×10^{-3}
226.0	Clay	32.0	8.0^2	0.16×10^{-7}	3.4×10^{-4}
226.4	Clay	27.0	5.49	0.39×10^{-7}	8.3×10^{-4}

[1] Average of at least two determinations on samples reconsolidated to effective in-situ overburden pressure and saturated using back pressure.

[2] Actual effective stress corresponding to value of permeability given.

In all cases, the direction of flow was in a vertical direction relative to the bedding planes of the sediments in-situ. The vertical permeability is, of course, of most interest from the standpoint of vertical migration of sea water. Experience shows that invariably the hydraulic permeability is several times greater in the horizontal direction than in the vertical direction for naturally deposited materials. Johnson et al. [1968] found from the results of a large number of tests on California sediments that the horizontal permeability was two to three times greater than the vertical permeability on the average. The horizontal to vertical permeability ratios ranged from unity to 200
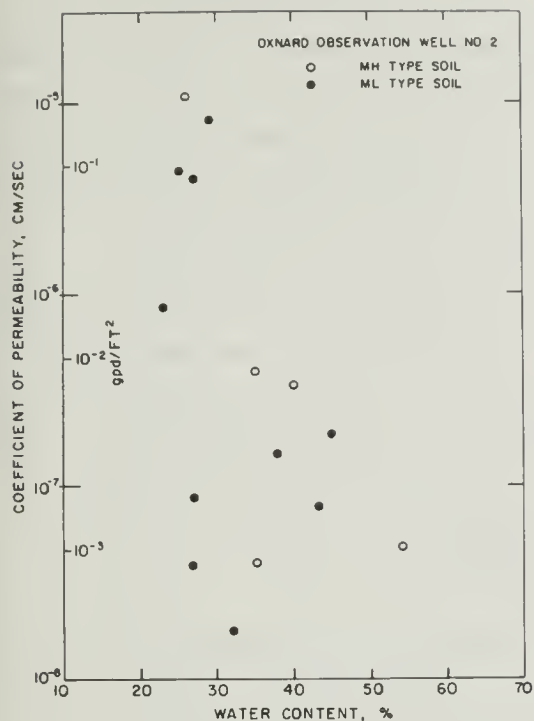
Fig. VI-10. Permeability for low
and high plasticity
materials.
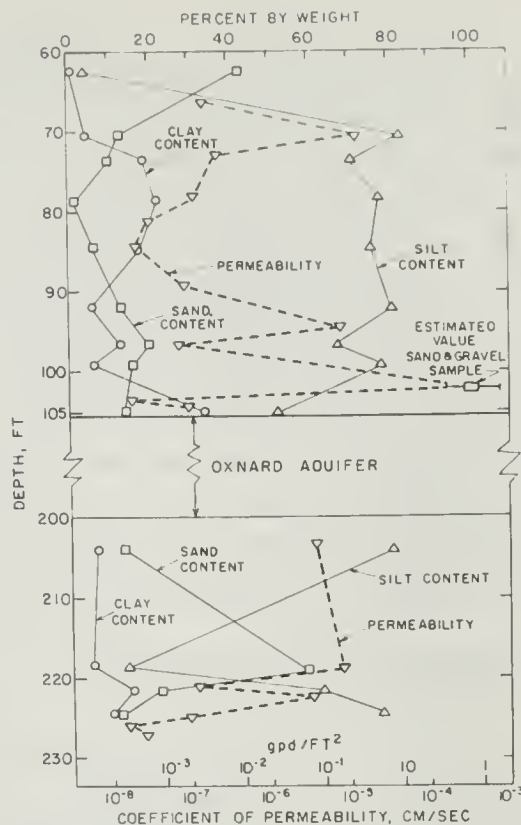
Fig. VI-11. Permeability and
size fraction
profiles.

for different samples, however. The fact that the horizontal permeability exceeds the
vertical permeability is usually a consequence of stratification of the sediments. It
may be influenced to some extent also by preferred orientation of clay particles.

Because the Oxnard sediments are in some respects similar to those studied by
Johnson et al., there is every reason to believe that they will also exhibit anisotropic
permeability characteristics.

Figure VI-10 was prepared in an attempt to determine if any sort of relationship
existed between permeability and water content. In this figure, the solid points refer
to clayey silts of low plasticity; whereas, the open points represent clayey silts of
high plasticity. No relationship appears to exist on this basis.

In Figure VI-11, the variations of permeability, sand content, silt content, and
clay content with depth are shown. From the shapes of these relationships there appears
to be some correlation between the relative amounts of the different size fractions and
permeability for the material overlying the Oxnard aquifer. A decrease in permeability
with increase in clay and silt content and decrease sand content is evident. Such a
relationship is not evident in the material underlying the Oxnard aquifer.

-105-

Since permeability of a fine-grained soil is a complex function of many factors; e.g. particle size, particle shape, size distribution, particle arrangement, and physico-chemical influences on the finer particles, the lack of any simple correlation between permeability and only one or two variables as in Figures VI-10 and VI-11 is not surprising.

Johnson et al., [1968] made a large number of permeability determinations on samples of deep sediments from three subsidence areas of California. Samples from core holes in the Los Banos-Kettleman City area had coefficients of vertical permeability ranging from 0.00007 to 370 gpd per sq. ft. Most samples had permeabilities in the range of 0.001 to 0.0. gpd per sq. ft. Samples from the Santa Clara Valley showed permeabilities in the range of 0.0001 to 0.03 gpd per sq. ft, with most values in the range of 0.0001 to 0.01 gpd per sq. ft. While these ranges may seem very large, it should be pointed out that Johnson et al., studied both coarse- and fine-grained samples. In the present study samples only of the fine-grained sediments were taken. The permeabilities of these materials, Table VI-7, compare favorably with those for the finer-grained samples tested by Johnson et al.

F. COMPRESSIBILITY CHARACTERISTICS OF AQUITARD SEDIMENTS

The compression characteristics of samples of undisturbed material from the aquitards above and below the Oxnard aquifer have been determined using standard consolidation testing procedures [Lambe, 1951]. The results of these tests are shown in Figure VI-12 for samples taken above the Oxnard aquifer and Figure VI-13 for samples from below 200 ft depth in the form of void ratio versus log effective vertical pressure. The laboratory consolidation characteristics have been determined for seven samples from the aquitard layer overlying the Oxnard formation; and five tests have been made on the material presumed to separate the Oxnard and Mugu aquifers. It is this latter material which is of the greater interest in this project, but unfortunately, most of the sediment from the zone samples is nearly cohesionless, as indicated earlier, so that preparation of satisfactory samples for consolidation testing was not possible in many cases.

The maximum preconsolidation pressure acting on these samples was determined using the procedure suggested by Casagrande [1936]. These values are compared with the existing effective overburden pressure in Figure VI-14. This pressure was estimated by assuming a submerged unit weight of sediment equal to 60 lb per cu ft. This is consistent with an average in-situ water content of 27.5% over the entire profile. Although the data are somewhat limited, the comparison on Figure VI-14 indicates that these sediments are over-consolidated; i.e., the present overburden pressure is less than the greatest stress to which the soil has been consolidated in its history.

No definite relationship is defined by the maximum past pressure values shown in the upper part of Figure VI-14, although a trend is indicated by the dashed curve. If in fact this curve is representative of the past pressure variation with depth, it would
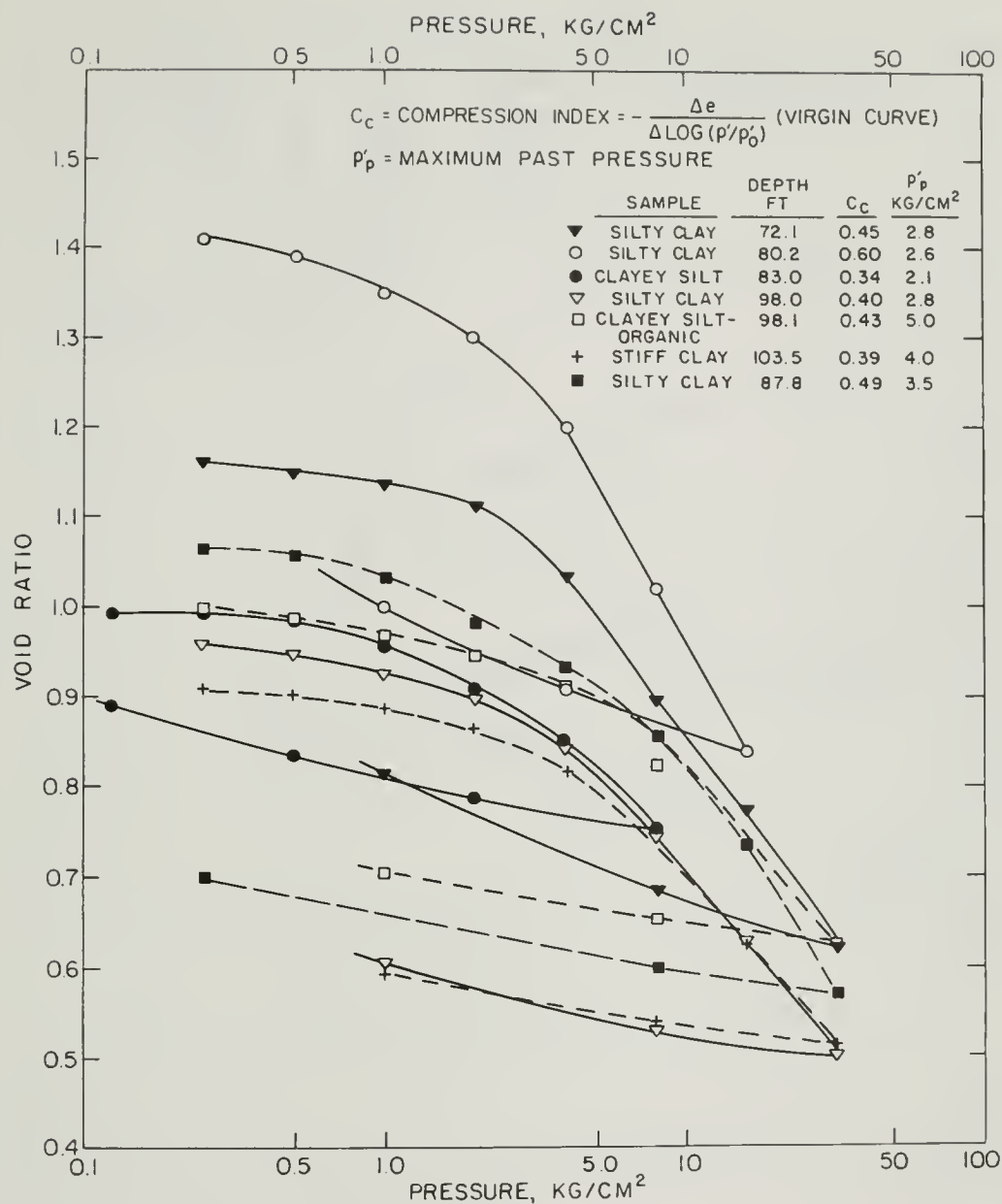
Fig. VI-12.   Compressibility characteristics of aquitard
              sediments overlying Oxnard aquifer

indicate that at some time in its history this layer had been partially consolidated under
a pressure considerably greater than the present overburden effective stress.   This con-
solidation would have involved drainage both upwards and down into the Oxnard aquifer;
i.e., the shape of the dashed curve suggests drainage at both aquitard boundaries.   A
considerable number of additional consolidation tests will have to be run before the past
pressure relationship can be defined with more certainty.
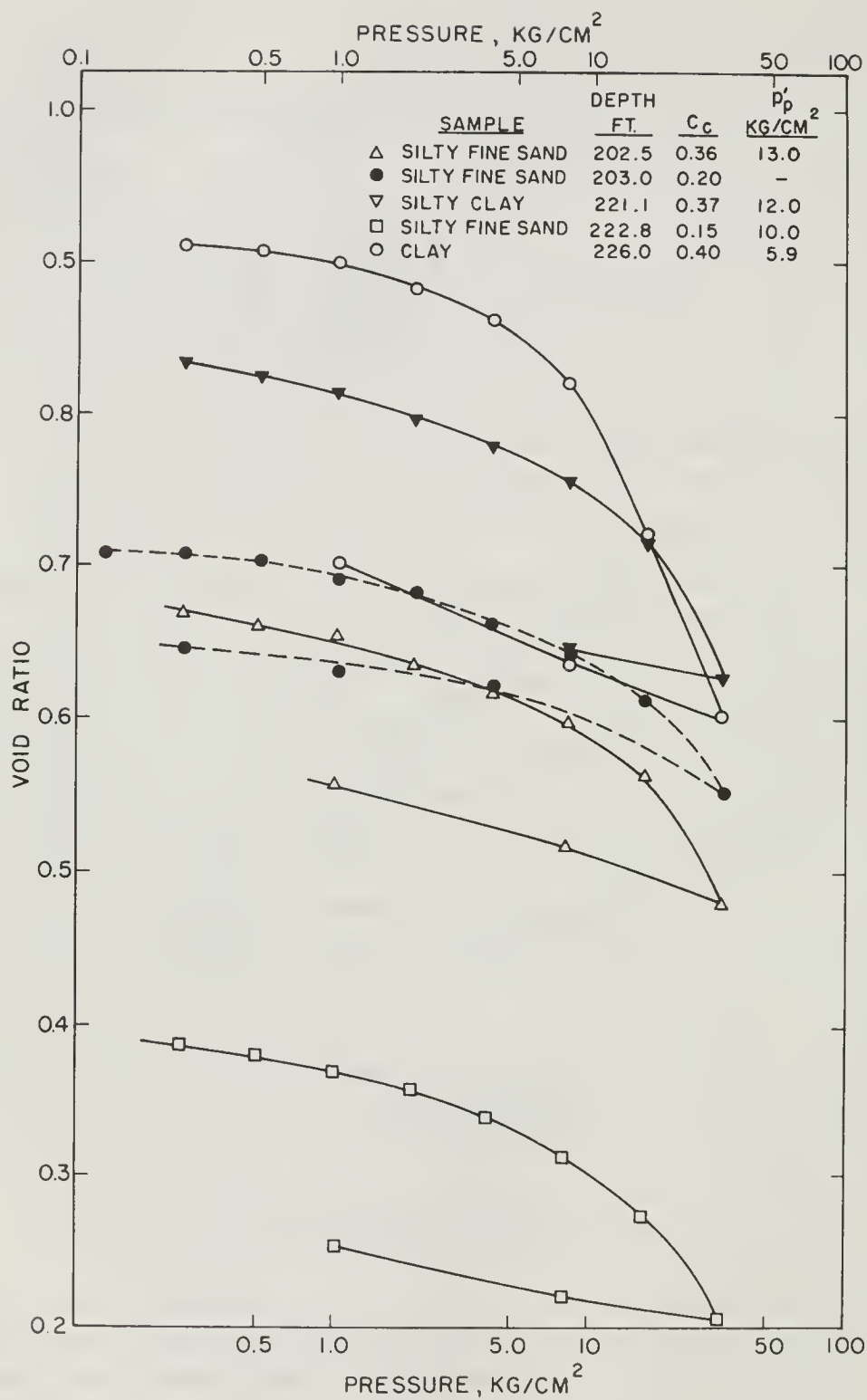
Fig. VI-13. Compressibility characteristics of aquitard
sediments underlying Oxnard aquifer
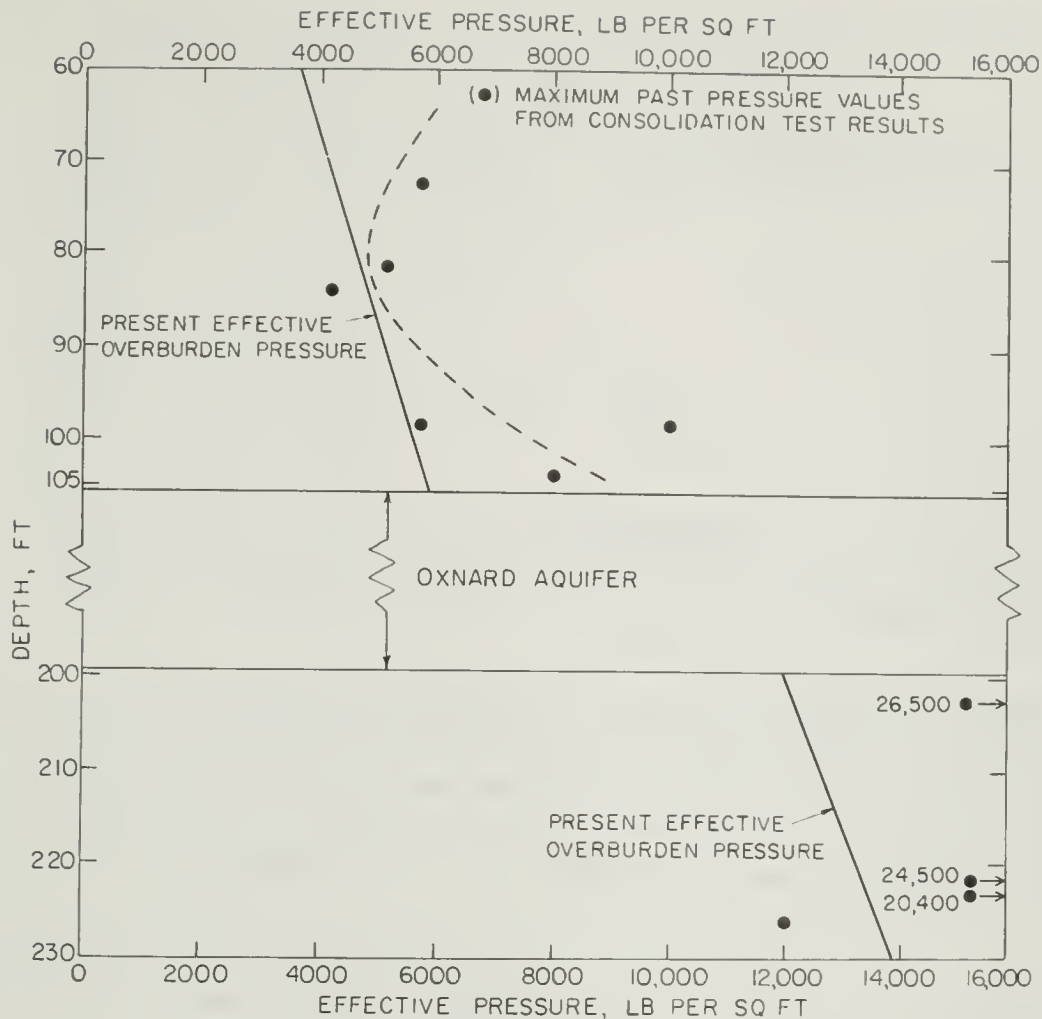
Fig. VI-14. Comparison between present effective overburden
and maximum preconsolidation pressures

The compression index values (change in void ratio per 10 fold change in consol-
idation stress) are in the range of 0.2 to 0.6. This represents a moderate compressibility
and is typical of values for silty materials.

Data of the type shown in Figures VI-12 and VI-13 are reproduced in a later section
of this report for use in comparing the compression characteristics of the existing sed-
iments from the same depth ranges which have been leached with sodium chloride solutions.
Such comparisons allow the estimation of surface settlements which might develop as a
result of changes in pore water pressures, cation type, and electrolyte concentrations
in the Oxnard and Mugu aquifers. The results of consolidation tests on unleached (as
received) samples are summarized in Table VI-8. Values of the coefficient of consolida-
tion are listed in Table VI-8 as well. The physical significance of this parameter is
given in the next section.

Table VI-8. Consolidation characteristics of aquitard sediments

(All samples from observation hole 2)

Sample Depth ft.	Soil Type	Initial Water Content %	Compression Index C_c [1]	Maximum Past Pressure kg/cm^2	Approximate Present Overburden Pressure kg/cm^2 [2]	Coefficient of Consolidation c_v cm^2/sec	Coefficient of Compressibility a_v cm^2/kg	Insitu Void Ratio e	Computed Permeability k [3] cm/sec
72.1	Clayey silt	43.8	0.45	2.8	1.8	1.1×10^{-2}	2.9×10^{-2}	1.60	1.3×10^{-7}
80.2	Clayey silt	54.0	0.60	2.6	2.0	7.7×10^{-4}	5.0×10^{-2}	1.43	1.6×10^{-8}
83.0	Clayey silt	37.0	0.34	2.1	2.0	6.0×10^{-3}	–	–	–
87.8	Silty clay	38.0	0.49	3.5	2.2	3.1×10^{-3}	3.8×10^{-2}	1.07	5.7×10^{-8}
98.0	Clayey silt	38.0	0.41	2.8	2.5	5.8×10^{-3}	3.0×10^{-2}	0.96	8.9×10^{-8}
98.1	Organic Clayey silt	34.4	0.43	5.0	2.5	4.2×10^{-2}	1.6×10^{-2}	1.02	3.3×10^{-7}
103.5	Stiff clay	35.0	0.40	4.0	2.6	5.6×10^{-3}	2.2×10^{-2}	0.92	6.4×10^{-8}
202.5	Silt	21.6	0.36	13.0	5.0	–	0.6×10^{-2}	0.67	–
203.0	Silty fine sand	26.6	0.2±	–	5.0	–	0.6×10^{-2}	0.71	–
221.1	Silty clay	31.2	0.37	12.0	5.5	–	0.6×10^{-2}	0.85	–
222.8	Silty fine sand	22.2	0.15	10.0	5.5	–	0.6×10^{-2}	0.39	–
226.0	Clay	32.0	0.40	5.9	5.7	1.7×10^{-3}	1.5×10^{-2}	0.91	1.3×10^{-8}

Note: [1] Change in void ratio per tenfold increase in pressure for pressures greater than the maximum past pressure; i.e., $C_c = -\dfrac{de}{d(\log p)}$

[2] Average values corresponding to present overburden pressure

[3] Computed from consolidation data; i.e., $k = c_v a_v \gamma_w / (1 + e)$

Finally, it should be noted that the substantial differences between void ratios for different samples subjected to the same consolidation pressure again reflect the large variability in sediment characteristics with depth throughout the aquitard layers.

G. EFFECT OF CONSOLIDATION ON THE PERMEABILITY OF AQUITARD SEDIMENTS

In five of the consolidation tests the hydraulic permeability was determined by direct measurement at the end of consolidation under each load increment. The results of these tests provide information concerning the change in permeability that accompanies a change in void ratio due to consolidation. Where possible, permeability values for these samples were also determined by computation from time-consolidation data obtained during each load increment using the Terzaghi theory for one-dimensional consolidation [Taylor, 1948]. Because of assumptions in the theory and deviations in actual soil behavior from that predicted by the theory, only approximate agreement can be anticipated between directly measured values of permeability and those determined theoretically.

The general procedure for analysis of consolidation test data for determination of permeability is as follows. For each load increment during a consolidation test, the change in sample thickness with time is recorded. Figure VI-15 is typical of the relationship obtained and shows the sample thickness change (in terms of dial indicator reading) as a function of time for a sample from a depth of 226.0 ft subjected to a pressure increment from 8.0 to 16.0 kg per sq. cm. The logarithm of time fitting method [Taylor, 1948] is used to relate the laboratory curve to a theoretical dimensionless curve for degree of consolidation versus time factor given by the Terzaghi theory. From the
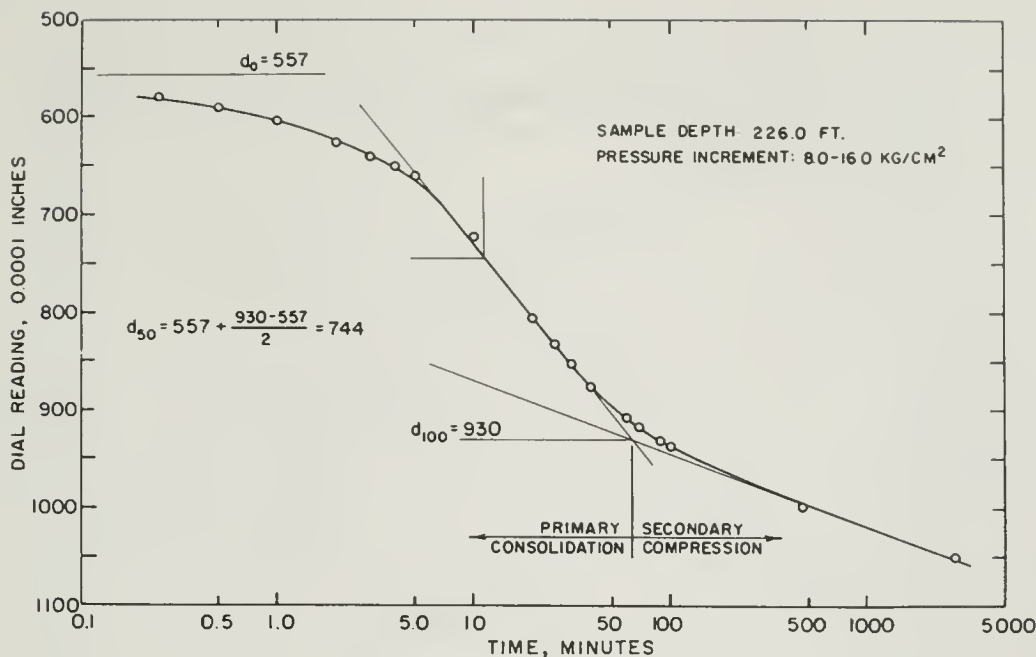
Fig. VI-15. Typical thickness change vs. time
curve during consolidation

actual time required for the sample to reach a degree of primary consolidation of 50 percent (11.2 minutes for the case shown in Figure VI-15), the coefficient of consolidation, c_v, is given by

$$c_v = \frac{T_{50} H^2}{t_{50}} = \frac{0.197 \, H^2}{t_{50}}$$

where T_{50} is a dimensionless time factor given by the theory and H is half the sample thickness for a sample drained at both top and bottom.

The coefficient of consolidation is related to other sample properties by

$$c_v = \frac{k(1 + e)}{a_v \gamma_w}$$

where k is the coefficient of hydraulic permeability, e is the void ratio, γ_w is the unit weight of water, and a_v is the coefficient of compressibility. The value of a_v is given by the slope, $-\Delta e/\Delta p$, of a plot of void ratio versus pressure at the average pressure corresponding to the pressure increment used. Since c_v, e, γ_w, and a_v are all known from the test results, the hydraulic permeability can be computed using the above equations.

This has been done for three of the consolidation test results obtained in this investigation for which direct permeability measurements were made and the soil type permitted calculation of the coefficient of consolidation. Figures VI-16, VI-17 and

-111-
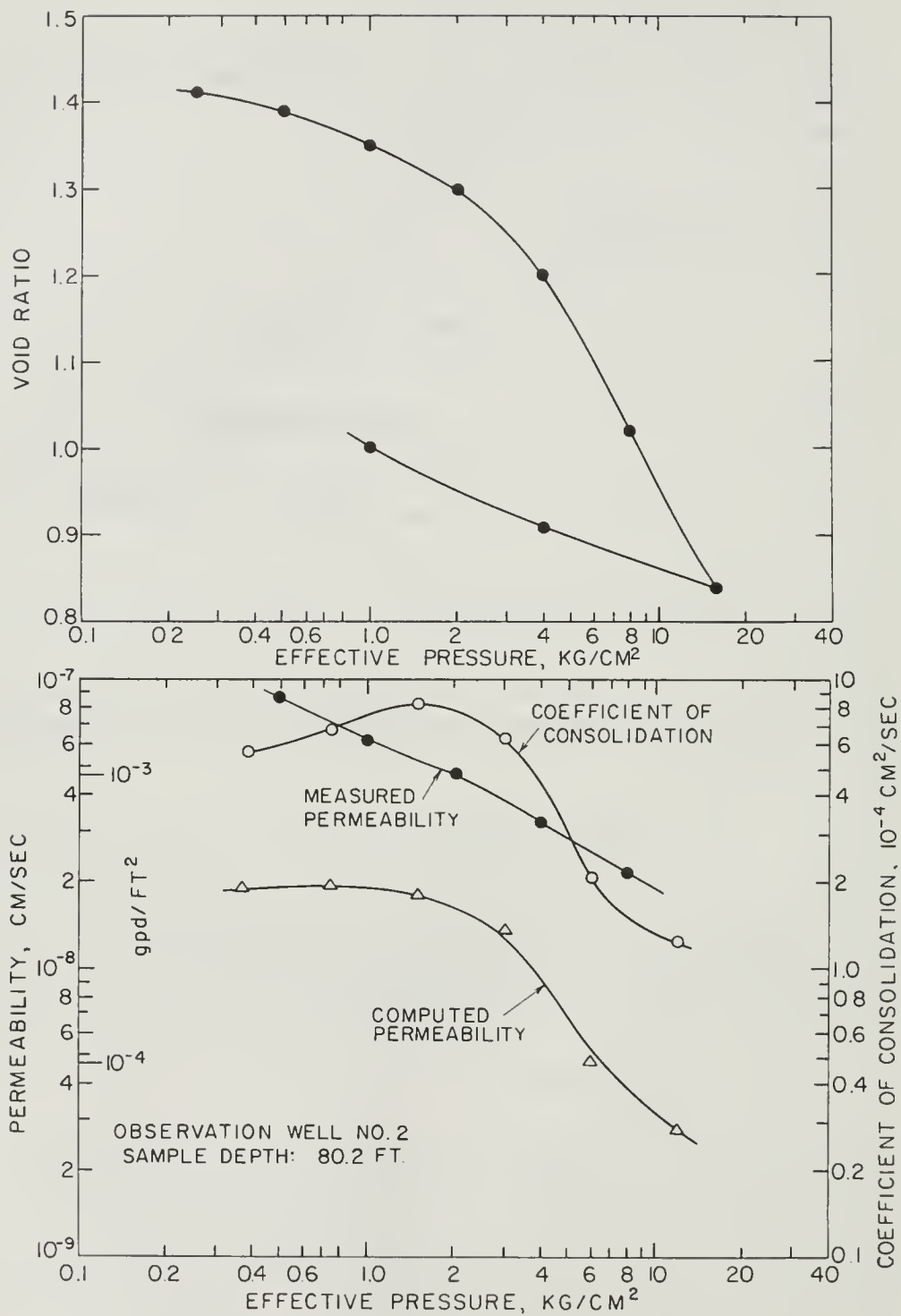
Fig. VI-16. Consolidation and permeability characteristics
of sample from 80.2 ft depth
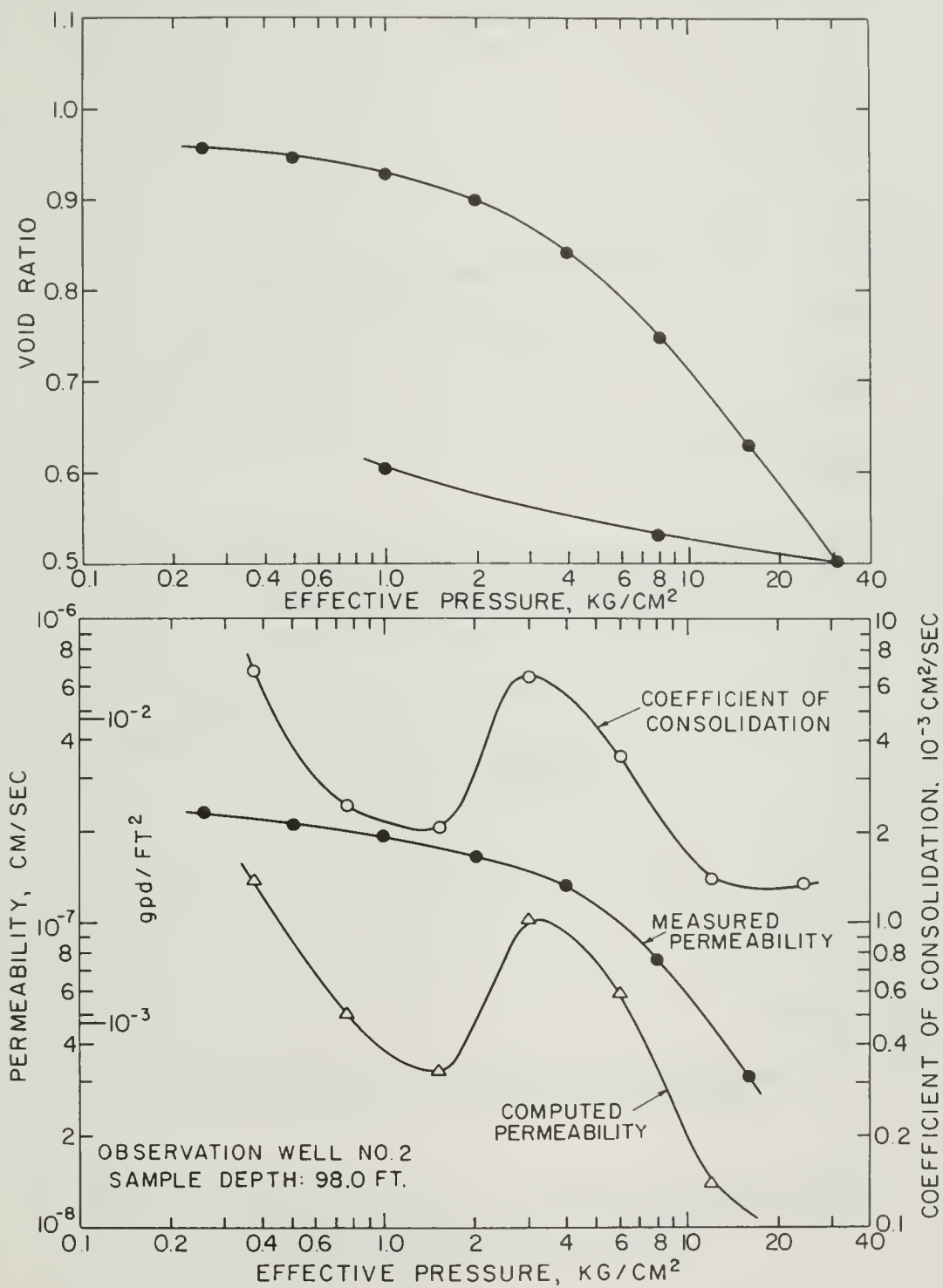
Figure VI-17. Consolidation and permeability characteristics
of sample from 98.0 ft depth
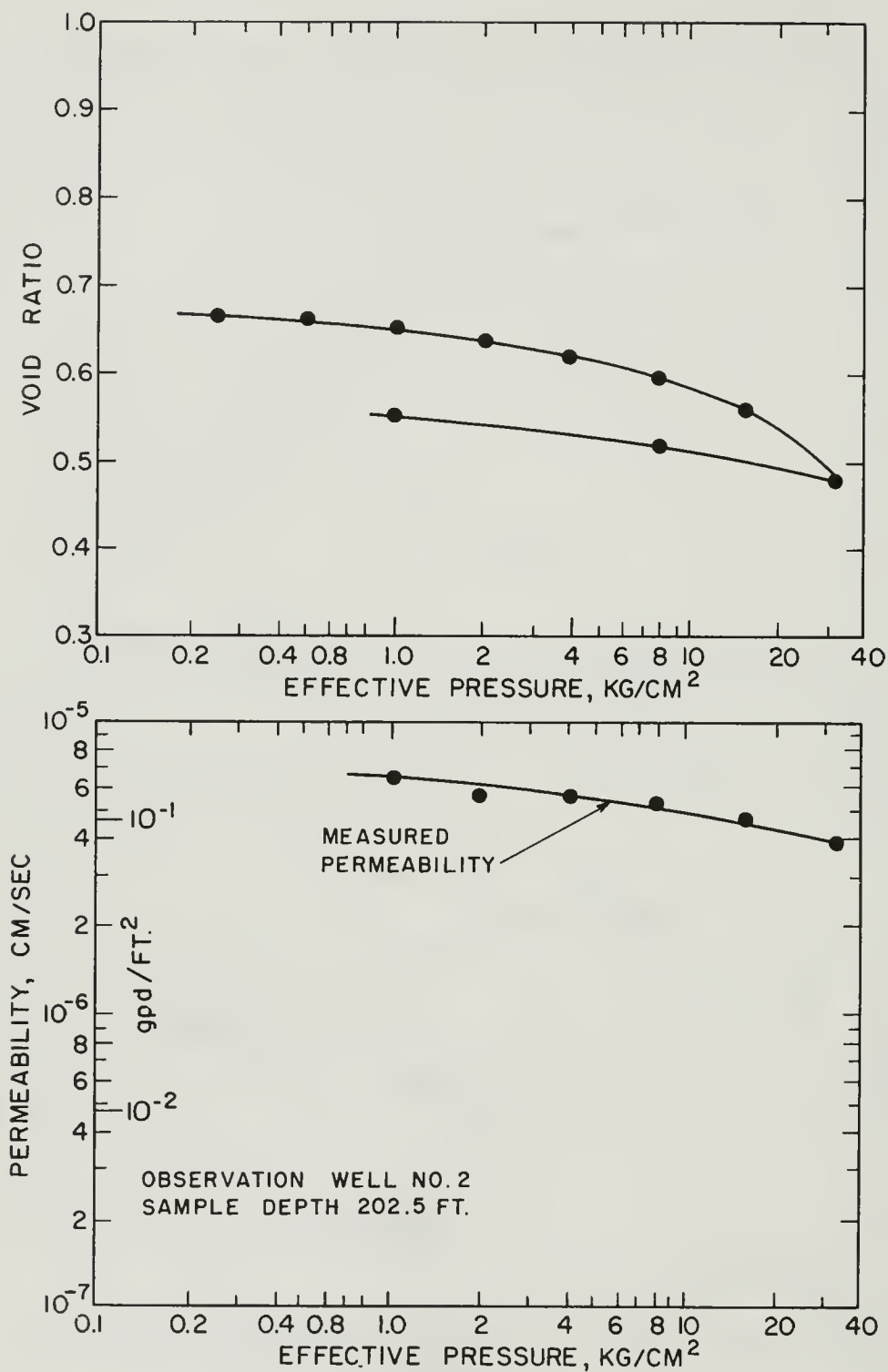
Fig. VI-18.   Consolidation and permeability characteristics
of sample from 202.5 ft depth
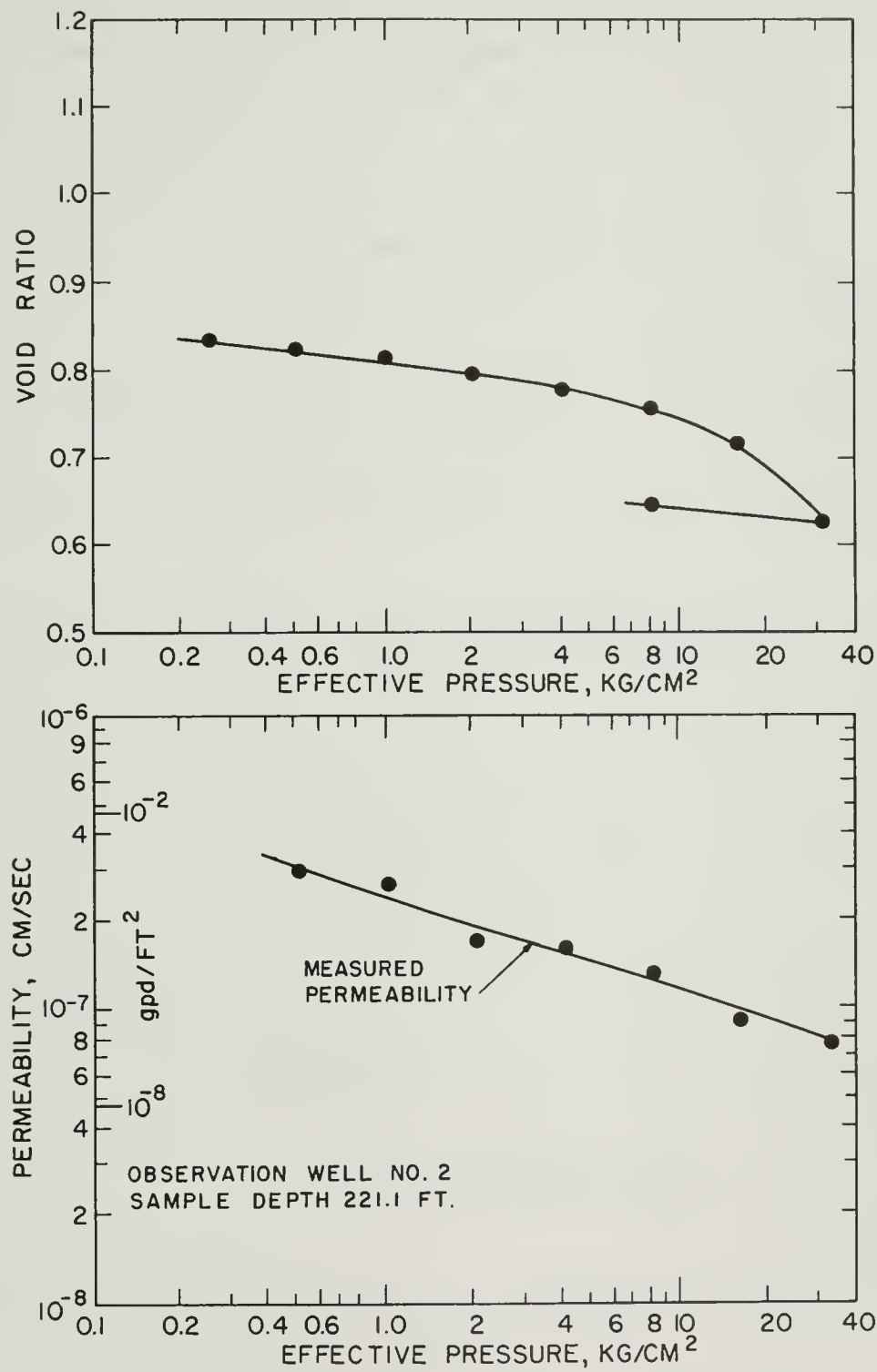
Fig. VI-19. Consolidation and permeability characteristics of sample from 221.1 ft depth

-115-
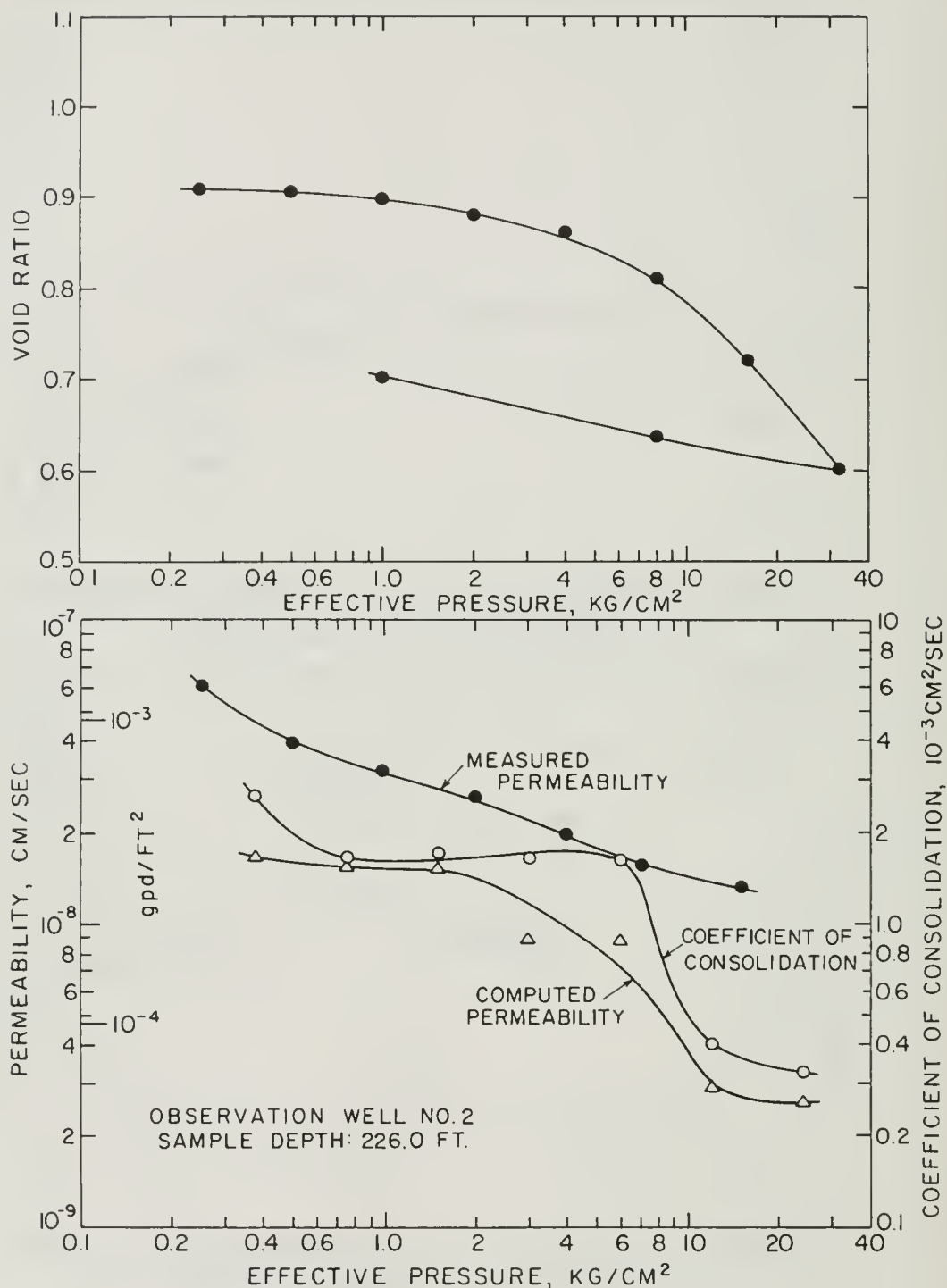
Fig. VI-20.   Consolidation and permeability characteristics
of sample from 226.0 ft depth

VI-20 show the variation of void ratio, coefficient of consolidation, measured permeability, and computed permeability with consolidation pressure for two samples from above the Oxnard aquifer and one sample from beneath the Oxnard aquifer. It may be seen from these figures that the agreement between the measured and computed values of permeability is not good. The computed values vary with consolidation pressure in a manner quite similar to the variation of coefficient of consolidation with pressure.

On the other hand, the actual permeability varies with pressure in the same general way as does the void ratio, which is a more reasonable relationship. Figures VI-18 and VI-19 show the variation of void ratio and measured permeability with consolidation pressure for two additional samples from depths greater than 200 feet.

It may be concluded from these comparisons that for these sediments it would be unwise to use values of permeability that have been computed from consolidation test results. Any estimates of flow quantities obtained using these values would be too low, and any estimates of the change in permeability due to consolidation would be considerably in error.

H. PROPERTY CHANGES ACCOMPANYING REPLACEMENT OF PORE WATER WITH SALT SOLUTIONS

The final phase of the laboratory investigation was a study to establish the sus-ceptibility of the aquitard properties to change as a result of salt water replacement of the pore fluid and to establish the significance of hydraulic and salt flows through these materials under the action of hydraulic gradients. Of particular interest was the effect of salt water replacement on the compression and permeability characteristics of the aquitard sediments.

Consolidation and direct permeability measurements were performed in the closed ring consolidometer shown in Figure VI-21. The closed ring consolidometer permitted direct permeability tests to be run at any stage of the consolidation test. The fluid chamber above the sample permitted the juxtaposition of solutions of any desired salt concentration against the top of the sample. The ports at the top and bottom of the sample allowed solutions to flow through the sample when a hydraulic gradient was induced across the sample. With proper adjustment of the applied load and back pressure in the pore water, hydraulic gradients could be induced while maintaining the soil structure at any desired average effective pressure level. As in the previous tests, permeability measurements were made at the equilibrium void ratios corresponding to the standard effective pressure increments and at the equilibrium void ratio corresponding to the present effective overburden pressure. At the in-situ effective overburden pressure, permeability measurements were made both before and after leaching with the salt solution. The control board used for flow measurements is described by Mitchell and Younger [1966]. Back pressure was maintained in the water throughout the tests in order to more closely

-117-
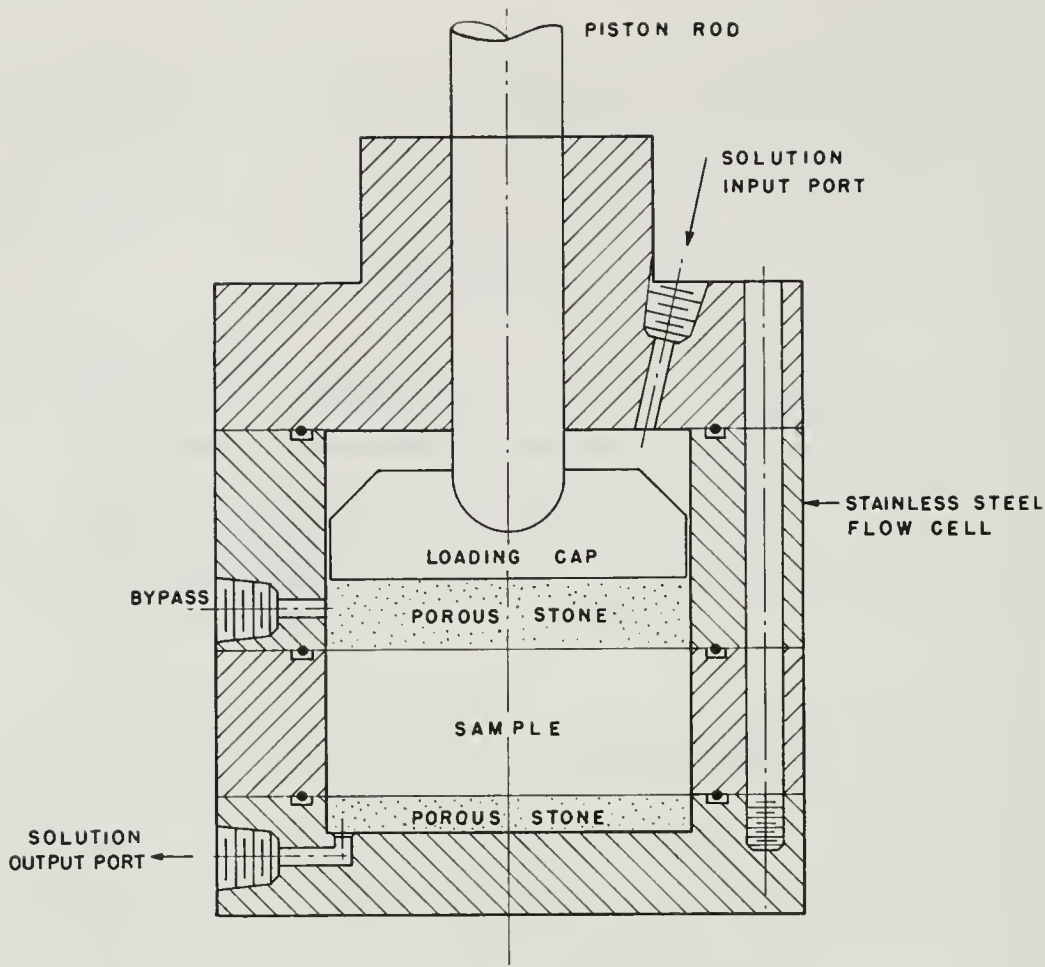
Fig. VI-21.   Closed ring consolidometer

approximate field conditions and to insure saturation of the sample.

   In permeability measurements flow was from the bottom of the sample to the top.
The gradient was induced by reducing the back pressure in the water at the top of the
sample. Pressure differences used resulted in hydraulic gradients of from 8 to 118. The
calculated value of permeability in centimeters per second was taken as the average of
several runs at different hydraulic gradients within the range given above. The upper
limit of hydraulic gradient for a given effective consolidation pressure was that corres-
ponding to a pressure difference of five percent of the effective consolidation pressure.

   After the sample had been consolidated under the standard sequence of pressures to
the computed effective overburden pressure, they were leached with 0.6N sodium chloride
solution. Prior to this, the water in the chamber above the sample was distilled. After
all primary consolidation had occurred and the final dial reading noted, the salt solution
was introduced into the chamber at the top of the sample. The solution was made to flow
through the sample from top to bottom under a hydraulic gradient induced by increasing the
fluid back pressure in the chamber above the sample. Hydraulic gradients from 8 to 16

-118-

were used. Flow through the samples was maintained for up to two weeks.

The samples were considered leached when the solution flowing out of the sample had a salt concentration of that flowing in, e.g. 0.6N, as determined by electrical conductivity measurements on the effluent. After a sample was leached and the change in void ratio at constant effective pressure noted, a direct permeability test was run as described above. Because of limitations inherent in the flow measurement apparatus, the solution used for permeability measurements was distilled water, both before and after leaching. Finally, the consolidation-permeability measurement sequence was resumed using standard consolidation test effective pressure increments.

The results of the consolidation permeability tests on leached samples are shown in Figures VI-22 through VI-25. Also plotted on these figures are the results of consolidation-permeability tests on unleached samples from adjacent depths.

If the data shown on the figures can be considered to reflect only the effects of leaching on the aquitard material, the following conclusions may be drawn:

(1) Substitution of salt solutions of the same concentration as sea water for distilled water in the pores of the samples tested resulted in a small decrease in void ratio at constant effective pressure. It should be noted that at the start of leaching distilled water had largely replaced the natural pore fluid as a result of previous direct permeability measurements at lower values of effective pressure.

(2) Replacement of the water in the pores by salt solution resulted in a decrease in the coefficient of permeability. In the absence of physico-chemical factors, that is, if the effect of changes in cation type and concentration in the pore water are not considered, then this result could be attributed to the decrease in void ratio.

(3) For at least two and possibly three of the four samples (samples from depths 80.2, 226.4, and 103.4 ft) replacement of distilled water in the pores by salt water resulted in an apparent reduction in permeability at effective pressures greater than the effective overburden pressure. This conclusion is tentative and is based on a comparison of the slopes of the permeability-effective pressure curves for the leached samples with those of the unleached samples from approximately the same depths. This conclusion is thus qualified by the previously emphasized observed variation in properties of the soils within small depth intervals. Furthermore, the leached sample from depth 97.5 showed the opposite effect when compared to the unleached sample from depth 98.0 ft.

(4) Replacement of distilled water in the pores by a 0.6N sodium chloride solution did not significantly change the compressibility characteristics of the samples as defined for instance by the compression index, i.e. the slope of the virgin consolidation curve. Again this conclusion is qualified by the observed

-119-
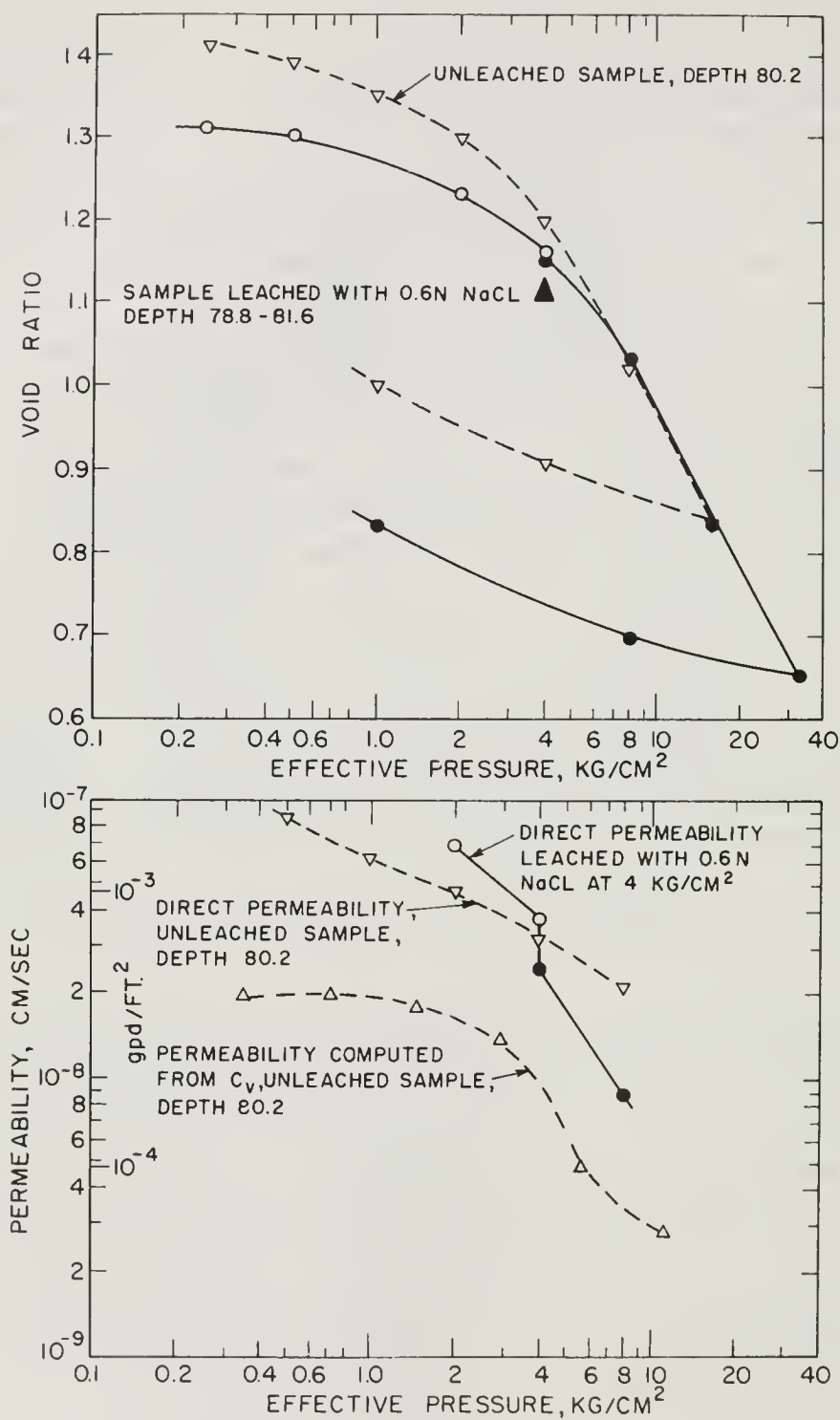
Fig. VI-22. Consolidation and permeability characteristics of two samples from depth range 78.0 to 82.0; leached and unleached
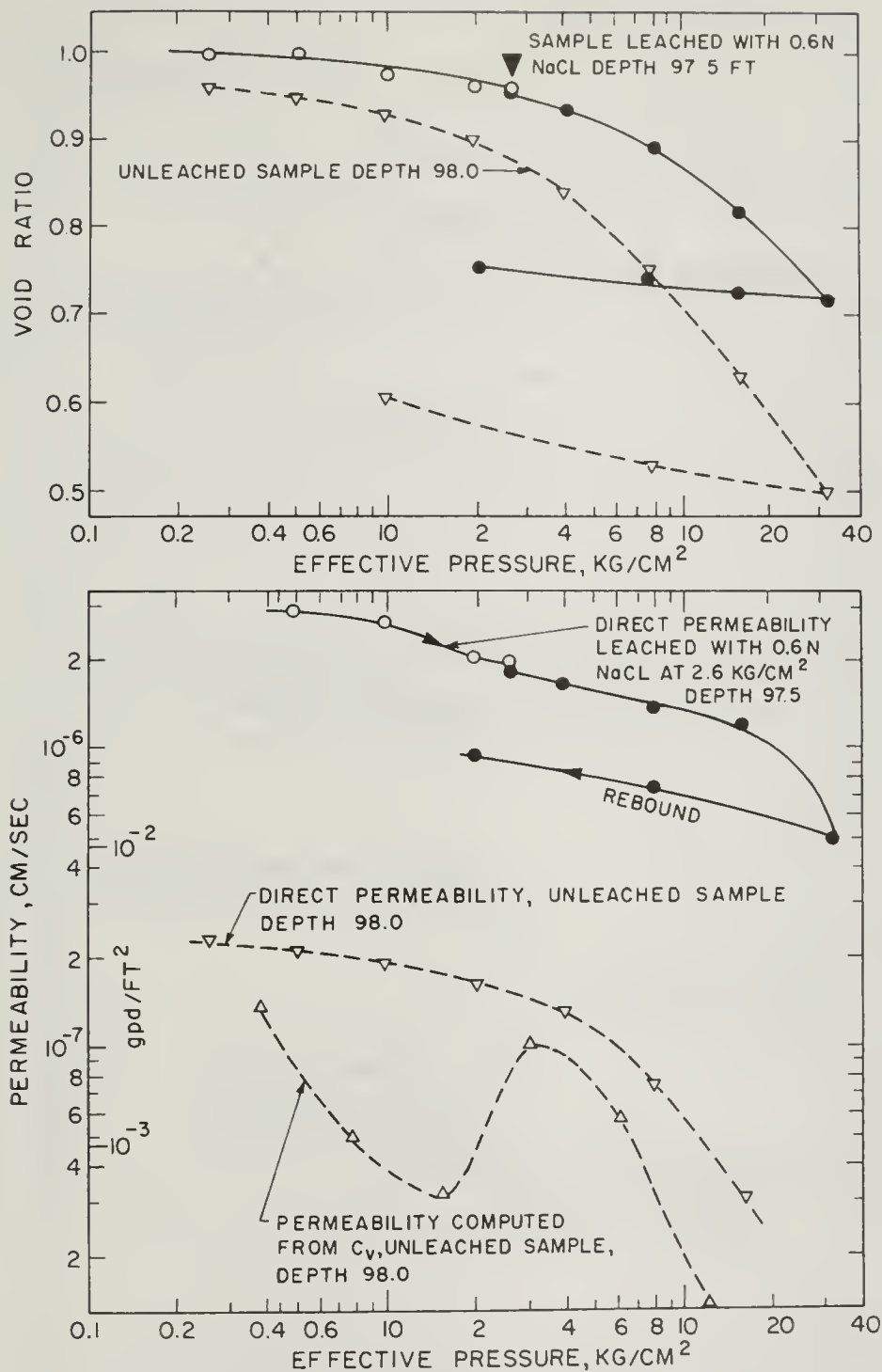
Fig. VI-23.   Consolidation and permeability characteristics
of two samples from depth range 97.0 to 98.0;
leached and unleached

-121-
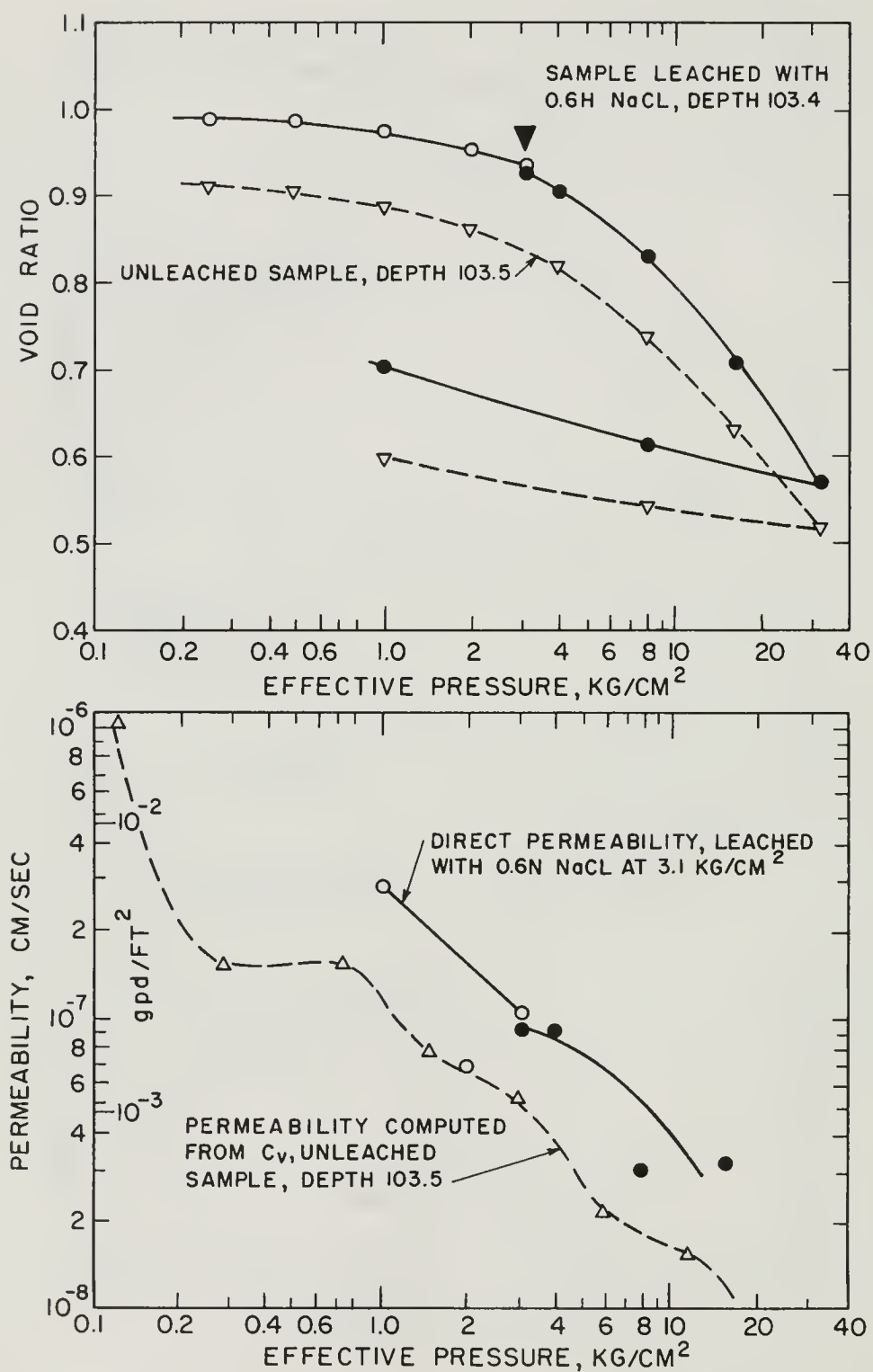
Fig. VI-24. Consolidation and permeability characteristics of two samples from the depth range 103.0 to 104.0; leached and unleached
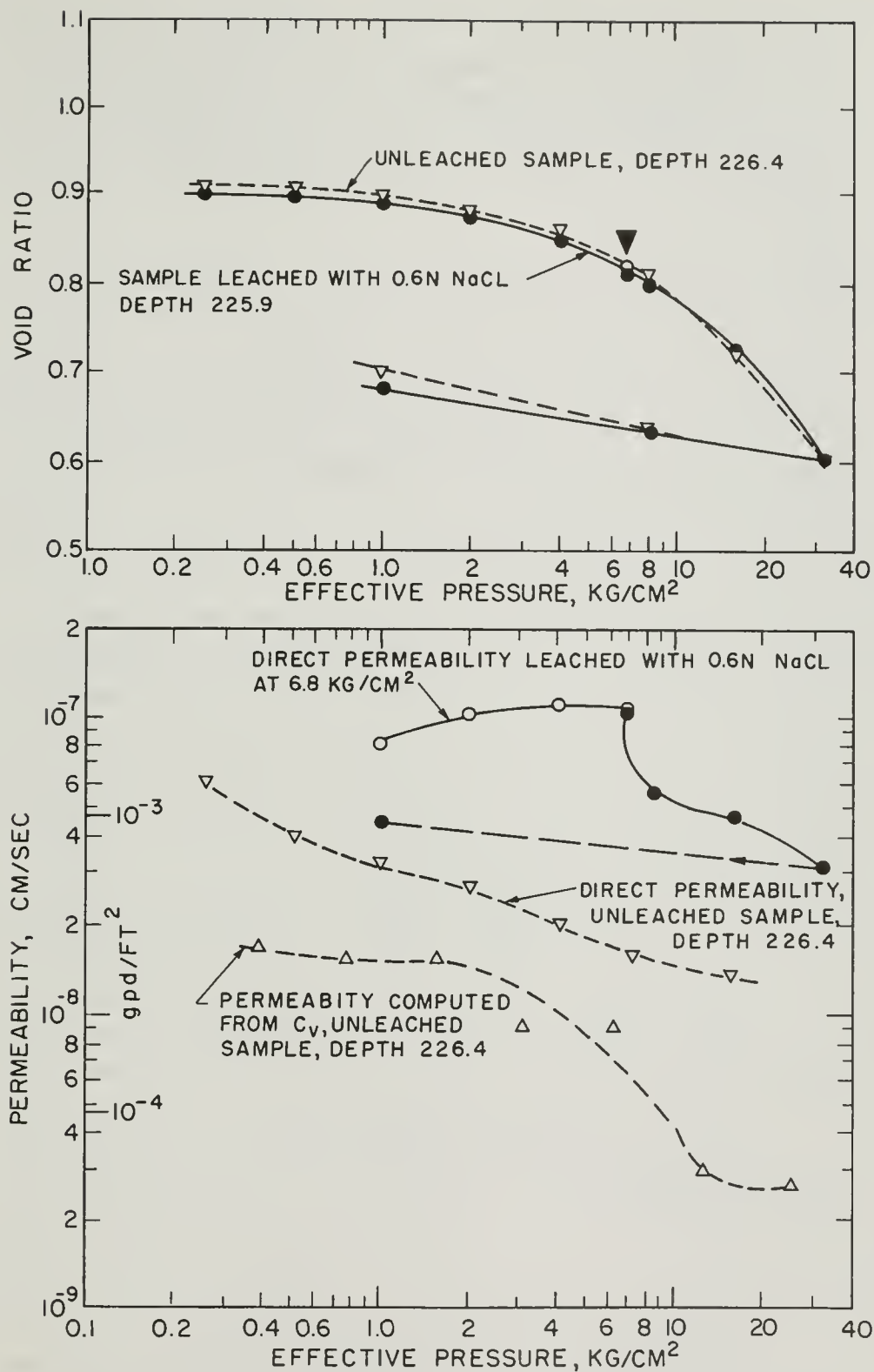
Fig. VI-25. Consolidation and permeability characteristics
of two samples from depth range 225.0 to 227.0;
leached and unleached

variability of the aquitard sediments. Furthermore, because permeability measurements were made with distilled water, the pore fluid largely reverted to distilled water once permeability measurements were initiated after leaching. Thus the test results may reflect the effects of exchanging monovalent sodium ions for the divalent calcium and magnesium ions naturally absorbed on the clay rather than an increased electrolyte concentration in the pore fluid.

(5) For the sample from the depth range 78.8 to 81.6 (Figure VI-22), replacement of the distilled water in the pores with a salt solution resulted in an increase in the liquid limit from 63 to 85 percent. The possibility that this represents an apparent increase due to the variability of the sediments is remote since the natural liquid limit of the samples tested in no case exceeded 79 percent. For the depth range 78.4 to 81.6 natural liquid limits did not exceed 69 percent.

The increase in liquid limit was perhaps due to the substitution of sodium ions fo the naturally absorbed calcium and magnesium cations. Mesri [1969] and Salas and Serratos [1953] report that for all pore fluid electrolyte concentrations, sodium monmorillonite ha considerably higher liquid limits than calcium montmorillonite. In view of the fact that the liquid limit determination was made after several direct permeability measurements wer made, the possibility that the increase in liquid limit was also partly a result of a decrease in electrolyte concentration cannot be discounted. Mesri, however, found that an electrolyte concentration decrease from 1N to 0.001N with calcium as the cation caused the liquid limit to increase from 201 to 207 percent. The same pure montmorillonite with sodium as the absorbed cation had a liquid limit of 1140.

The difficulty in fitting the results of the consolidation-permeability tests on leached samples into a consistant pattern is primarily due to the variability of the samples within narrow depth ranges. Clay content and cation exchange capacity vary over wide limits. The presence of organic material in all the samples may contribute to non-clay plasticity. The net result is that changes in properties attributed to leaching may in fact be due to the natural variability of the soils or the test method used.

In any case, the observed changes were small and are most probably due to the exchange of sodium ions for calcium and magnesium ions as the absorbed cation on the fine grained fraction of the sediments. The changes in void ratio for the four samples tested are summarized in Figure VI-26. Also given in the figure is an extremely approximate calculation of the settlements which could occur as a result of complete replacement of the natural pore fluid with a salt solution of the concentration of sea water. A reliable estimation of the settlements which may occur requires the testing of many more samples to adequately represent the compressible layers in the aquitards, as well as improvements in test methods and equipment. While the calculation is presented to serve as an example

-124-
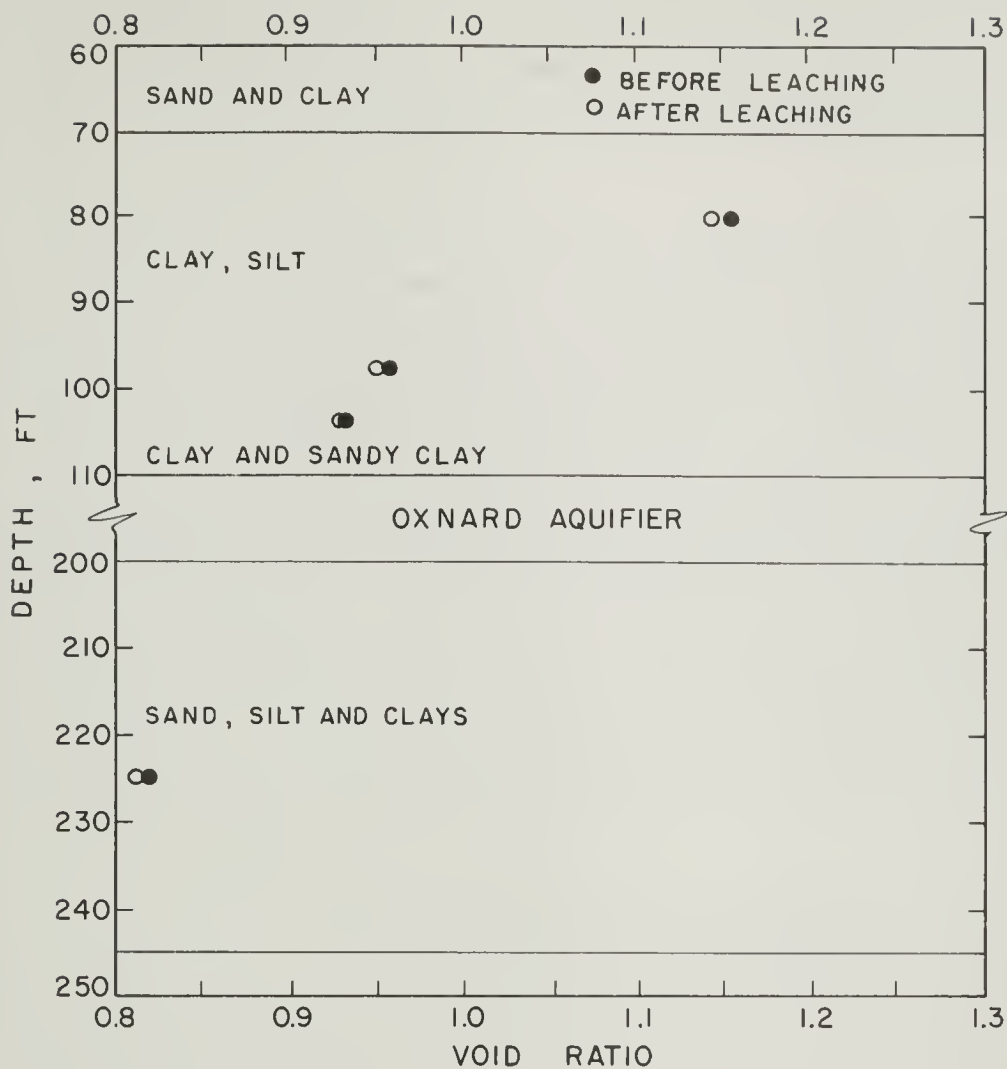
"SETTLEMENT"; DEPTH 70.0 TO 110.0 Δe_{avg} = 0.006

$e_{o \, avg}$ = 1.014

ΔH = $\frac{\Delta e}{1+e_{o}}$ H = 1.5 inches

DEPTH 198.0 TO 227.4 Δe_{avg} = 0.006

$e_{o \, avg}$ = 0.818

ΔH = $\frac{\Delta e}{1+e_{o}}$ H = 0.97 inches

Fig. VI-26.   Change in void ratio due to leaching
with 0.6N sodium chloride solution
at constant effective pressure

only, it is significant in that it indicates that for aquitards with montmorillonite clay contents higher than the rather low values for the Oxnard area aquitards, settlements due to sodium chloride solution replacement of natural pore fluids containing divalent cations in low concentration might be noticeable.

I. SUMMARY

The purpose of this chapter has been to present the results of laboratory studies of the fine-grained aquitard sediments that overlie the Oxnard aquifer and the sediments which separate this aquifer from the underlying Mugu aquifer. Data are presented on the classification, composition, consolidation and permeability of the sediments as well as on the effects of the replacement of the natural pore fluid with salt water.

The sediments throughout these aquitard layers are predominantly made up of silt-size particles, which are mainly composed of quartz and mica or mica-like materials. The clay content is generally low, amounting to 20 percent or less by weight of the whole material in most cases. Montmorillonite is the dominant clay mineral in the clay fraction, with lesser amounts of a kaolin mineral, quartz, and a hydrous mica or illite. The cation exchange capacity of these soils is high relative to the amount of clay mineral present, amounting to 20 to 45 milliequivalents per hundred grams of dry soil. The silt fraction was found to possess a cation exchange capacity of more than 20 milliequivalents per hundred grams.

The present pore fluid salinity is relatively low, amounting to 1300 to 1900 ppm. Magnesium and calcium are the dominant cations in solution.

Although the material properties vary erratically with depth, almost all samples can be classified as silts of low or high plasticity, with the exception of materials between 200 and 224 ft depth, which are mainly sands. In general the in-situ water content is significantly lower than the liquid limit. The materials are moderately compressible, with compression index values ranging from 0.2 to 0.6.

The hydraulic permeability varies erratically with depth over the range from about 10^{-5} to less than 10^{-7} cm/sec (0.1 to less than 0.001 gpd/ft^2). This variation of permeability cannot be simply accounted for in terms of any single factor. The variation of permeability with consolidation pressure and void ratio has been established from consolidation tests and direct measurement. Since permeability values computed from consolidation test results do not agree well with directly measured values, only values established by direct measurement should be used for estimating ground water flows.

Data from consolidation and permeability tests on samples leached with 0.6N sodium chloride solutions have been compared to tests on unleached samples from the same depth ranges. Substitution of the salt solution for the natural pore fluid in the pores of the sediments resulted in a small decrease in void ratio at constant effective consolidation

pressure. The effect of leaching on the permeability of the sediments was inconclusive
due to the variability of the aquitard soils. Leaching with salt solutions did not
significantly change the observable compressibility characteristics of the samples tested.
This conclusion is also qualified by the variability of the samples. The changes that
were observed are attributed to substitution of sodium ions for calcium and magnesium
ions as the absorbed cation during leaching.

The properties of the aquitard separating the Oxnard and Mugu aquifers have not
been well defined by this study. The samples recovered from a zone thought to be re-
presentative of this aquitard were in fact predominantly sand. Samples were not taken
from depths greater than 227.4 ft; thus, the total thickness of any clay-like materials
that may exist remains unknown.

Additional sampling and testing are required to properly define the properties
of the aquitard separating the Oxnard and Mugu aquifers as well as to completely identify
the parameters which control the response of aquitard materials to the intrusion of salt
water.

CHAPTER VII. THEORETICAL ANALYSIS OF CHEMICO-OSMOTIC
DIFFUSION AT OXNARD SITE

J. A. Greenberg and J. K. Mitchell

A. INTRODUCTION

Up to this point, the emphasis has been on the movement of fluids in the multiple-aquifer system of the Oxnard coastal basin solely by virtue of hydraulic gradients. The presence of sea water in the Oxnard aquifer, however, while fresh water is still present in other layers of the system, raises the question as to the importance of the chemical gradients. The work of Olsen [1969, 1970] shows that there may be a coupling across aquitard layers between solute (or salt) concentration gradient and ground water flow, and another between pore pressure gradient and solute flow; both of which can sometimes be fairly significant in the diffusion of ground water and dissolved solutes. In particular there is a possibility that these coupling effects could lead to unexpected intrusion into the Mugu aquifer because of salt flow across the aquitard that separates this aquifer from the overlying Oxnard.

The coupling between solute concentration gradient and ground water flow, i.e. the mechanism by which a salt concentration gradient causes ground water flow and a hydraulic gradient causes a salt flow, is referred to as chemico-osmotic coupling. In addition, Olsen's work suggests that a solute concentration increase in a solution in contact with a soil layer could cause the soil layer to consolidate chemico osmotically. Hence there is the possibility that the aquitards in contact with the Oxnard aquifer could consolidate, and cause ground subsidence.

A study was undertaken to (1) develop general solutions for coupled hydraulic and solute flows in fine-grained sediments and (2) to determine if chemico-osmotic effects are of significance at the Oxnard site. The results of this study are summarized here, and presented in more detail in Appendix D.[*]

B. OSMOSIS

Osmosis, which is one manifestation of chemico-osmotic coupling, has been studied

---

[*]Note that the terms soil and sediment are taken as synonymous in Appendix D.

since the middle of the 18th Century. The body of literature which has grown around this phenomenon is vast, and contains much information which aids in our understanding of chemico-osmotic coupling in fine-grained sediments. This literature was therefore searched, and we present here a short summary of our findings.

The basis of osmosis and chemico-osmotic coupling is that some membranes have the ability to retard or prevent the flow of solute (i.e., the salt), but not the flow of solvent (i.e., the water) in a solution. A membrane which has this ability is called semi-permeable with respect to the solution. If the membrane completely prevents all flows of solute, it is referred to as a non-leaky, semi-permeable membrane. If the membrane partially prevents flow of the solute, it is referred to as a leaky semi-permeable membrane. If the membrane is so leaky as to not retard or inhibit flow of the solute in any way, it is not semi-permeable.

Examination of the primary mechanisms of semi-permeability, and the chemico-osmotic properties of sediments leads to the conclusion that certain sediments may behave as semi-permeable membranes. In particular the fine-grained sediments above and below the Oxnard aquifer contain clay layers which are probably leaky, semi-permeable membranes with respect to sea water.

C. THEORY OF CHEMICO-OSMOTIC DIFFUSION

A theoretical framework was developed to provide a comprehensive means for quantitatively analyzing chemico-osmotic diffusion problems; including the situation at Oxnard. The theory was developed in three stages: Firstly, equations were derived which describe the simultaneous flow of solute and solutions in a sediment. These equations are referred to as the flow equations. Secondly, the equations of continuity were derived for solute and solution. Finally, the flow equations and continuity equations were combined to yield two diffusion equations; one describing the diffusion of solute and the other describing the diffusion of solution in a sediment solution system subject to both hydrostatic pressure and solute concentration gradients (for the details of these developments see Chapter II of Appendix D.)

1. Assumptions

The mathematical model considered was an open system consisting of a solute and solution in the pores of a porous compressible sediment in which we assume:
  (1) Isotropy and homogeneity
  (2) Isothermal conditions
  (3) No electrical or electro-magnetic gradients
  (4) No ion-exchange during diffusion

(5) The solute acts as a single species; i.e. it does not dissociate so that different species act independently.

(6) The solution is dilute enough for "ideal solution" relationships to be valid assumptions, and for the volume flow rate of solution to be essentially equal to the volume flow rate of solvent.

(7) Saturated sediment.

(8) The postulates of irreversible thermodynamics are applicable to the process. For experimental substantiation of this assumption, see the work of Abd-El-Aziz and Taylor [1964] and Olsen [1969, 1970].

2. Development of the Flow Equations

From the first postulate of irreversible thermodynamics it can be shown that the irreversible diffusional flow of solute and solution in the pores of a sediment will generate entropy Φ per unit volume which is given by

$$\Phi = \bar{J}_L V_L \ \text{grad} \ (-U) + \bar{J}_d \frac{RT}{c_s} \ \text{grad} \ (-c_s) \tag{VII-1}$$

where Φ = dissipation function

$\bar{J}_L$ = vector rate of flow of solution

$\bar{J}_d$ = vector rate of flow of solute relative to the vector rate of flow of solution

V_L = volume of solution per mole of solution

U = hydrostatic excess pressure

R = gas constant

T = absolute temperature

c_s = number of moles of solute per unit volume of solution

Flow equations can be derived from equation VII-1 by using the second postulate of irreversible thermodynamics.

These equations are

$$\bar{J}_L = L_{11} V_L \ \text{grad} \ (-U) + L_{12} \frac{RT}{c_s} \ \text{grad} \ (-c_s) \tag{VII-2}$$

$$\bar{J}_d = L_{21} V_L \ \text{grad} \ (-U) + L_{22} \frac{RT}{c_s} \ \text{grad} \ (-c_s)$$

The third postulate of irreversible thermodynamics establishes the reciprocal relationship

$$L_{21} = L_{12} \tag{VII-4}$$

The L-coefficients are phenomenological coefficients which depend on the particular sediment solution system being considered.

In practice it is convenient to use the vector flow rate of solute relative to the fixed sediment, $\bar{J}_s$ defined as

$$\bar{J}_s = \bar{J}_d + \frac{c_s}{c_L} \bar{J}_L \tag{VII-5}$$

3. Development of the Continuity Equations

Application of the law of conservation of mass to the solution in the pores of the sediment yields the continuity equation for solution

$$\bar{\nabla} \bar{J}_L = - \frac{\partial \gamma_L}{\partial t} \tag{VII-6}$$

Application of the same principle to solute gives

$$\bar{\nabla} \bar{J}_s = - \frac{\partial \gamma_s}{\partial t} \tag{VII-7}$$

where γ_L = number of moles of solution per unit volume of soil

γ_s = number of moles of solute per unit volume of soil

4. Diffusion Equations

The diffusion equations are generated by combining flow equations VII-2 and VII-3 with continuity equations VII-6 and VII-7 yielding

$$- \frac{\partial \gamma_L}{\partial t} = \bar{\nabla} \cdot \{L_{11} V_L \text{ grad } (-U) + L_{12} \frac{RT}{c_s} \text{ grad } (-c_s)\} \tag{VII-8}$$

$$- \frac{\partial \gamma_s}{\partial t} = \bar{\nabla} \cdot \{(L_{21} V_L + \frac{c_s}{c_L} L_{11} V_L) \text{ grad } (-U) + (L_{22} \frac{RT}{c_s} + \frac{L_{12} RT}{c_L}) \text{ grad } (-c_s)\} \tag{VII-9}$$

Equations VII-8 and VII-9 provide a completely general description of the coupled hydraulic-chemical flow process. They are not, however, in a form that is suitable for direct application to real problems. Thus, it was necessary to adapt the equations as follows. The L-coefficients are related to soil and solution properties according to

$$L_{11} = \frac{K'}{V_L^2 \gamma_w} \qquad\qquad L_{22} = \frac{c_s}{RT} D$$

$$\tag{VII-10}$$

$$L_{12} = \frac{c_s}{RT\, V_L} k_{hc} \qquad\qquad L_{21} = \frac{x}{V_L\, \gamma_w} k_{hc}$$

-132-

where γ_w = specific weight of water

      D = diffusion constant of solute

      k_{hc} and k_{ch} = chemico-osmotic coupling coefficients

      x = c_s/c_{sm} is the maximum value of c_s expected during the process

      K' = hydraulic permeability of the sediment

Details of the derivation of equations VII-10 are given in Chapter II-C, Appendix D.

It was assumed that change in void ratio and pore pressure within the aquitard are related by

$$\Delta e = a_v \, \Delta U \qquad\qquad (VII-11)$$

where ΔU = change in pore pressure

      Δe = corresponding change in void ratio

      a_v = coefficient of compressibility of the sediment

Finally it was assumed that the total volume of the aquitard, the molar density of the pure water, and the diffusion coefficient for salt are constants during the chemico-osmotic diffusion process (details are given in Chapter II-C of Appendix D).

With these assumptions and equations VII-10 and VII-11, the one dimensional forms of the diffusion equations VII-8 and VII-9 become

$$\frac{\partial U}{\partial t} = c_v \frac{\partial^2 U}{\partial y^2} + \frac{1 + e}{a_v} k_{hc} \frac{\partial^2 c_s}{\partial y^2} \qquad\qquad (VII-12)$$

and

$$e \frac{\partial c_s}{\partial t} = \frac{1 + e}{\gamma_w} K_{ch} \frac{\partial}{\partial y} \left(x \frac{\partial U}{\partial y} \right) + (1 + e) \, D' \frac{\partial^2 c_s}{\partial y^2} - a_v \, c_s \frac{\partial U}{\partial t} \qquad\qquad (VII-13)$$

where $K_{ch} = k_{ch} + c_{sm}K'$

      $D' = D + c_s k_{hc}$

Comparison of theoretical predictions for pore pressure and salt concentration vs. time from equations VII-12 and VII-13 with existing data provided satisfactory agreement and confidence that the theory is consistent with physical reality.

D. ANALYSIS OF THE OXNARD SITE

As mentioned above, sea water has invaded the Oxnard aquifer for several miles inland. The aquitard between the Oxnard and the next lowest aquifer, the Mugu aquifer, can be thought of as a layer of fine-grained sediment having fresh water as pore water, and in contact with an aquifer (the Oxnard) in which the originally fresh pore water has

-133-

been replaced by sea water. This replacement of fresh water by sea water is equivalent to a solute (predominately NaCl) concentration increase at the upper boundary of the aquitard. Since the clay members of the aquitard are leaky and semi-permeable with respect to sea water, increasing the NaCl concentration at the upper boundary could have two possible consequences.

(1) It could induce an osmotic pressure drop at the boundary which would suck pore fluid out of the aquitard, and hence induce chemico-osmotic consolidation which would manifest itself as surface subsidence.

(2) The increase of NaCl concentration in the Oxnard aquifer imposes a NaCl concentration drop across the aquitard which tends to drive NaCl down into, and through the aquitard by diffusion. Consequently the aquitard and the Mugu aquifer would tend to become contaminated by NaCl.

The theory described above was used to analyze the one dimensional chemico-osmotic diffusion of NaCl solutions across the aquitard separating the invaded Oxnard which was assumed to contain a salt concentration of 0.6 normal (~36,000 ppm), from the fresh waters of the Mugu. Since the laboratory investigation of the pore fluids in the aquitard materials revealed salt concentrations of 1340 to 1920 ppm (see Chapter IV-D), it was assumed that initially all of the fluids in the aquitard had uniform salt concentrations of 0.03 normal (~1,800 ppm). For the first analyses the aquitard was assumed to be 30 feet thick, and later smaller thicknesses were also examined.

To demonstrate the effects of chemico-osmotic diffusion, the aquitard material was assumed to have sufficient clay so that the basic constants would be as follows: hydraulic permeability, $K' = 10^{-7}$ cm/sec (2.2×10^{-3} gpd/ft^2); coefficient of compressibility, $a_v = 3.5 \times 10^{-2}$ cm^2/kg; coefficient of consolidation, $c_v = 10^{-3}$ cm^2/sec, coupling coefficient, $k_{hc} = 2 \times 10^{-7}$ cm^2/sec, and diffusion constant, $D = 10^{-5}$ cm^2/sec. Reference to Tables VI-7 and VI-8 will show that the above values for a_v, c_v, and K' are typical for the clay samples tested in the laboratory. However, 10^{-7} cm/sec is roughly ten times smaller than the permeability found during the pumping tests (see Table V-6) due to the greater proportion of silt and sand layers within the aquitard in the field. The results presented below must therefore be viewed in terms of what the situation would be if 30 feet of this type of clay material were separating the Oxnard and Mugu aquifers.

Two cases were considered. The first was that of no pumping from either aquifer so that initially no hydraulic gradient exists. The second case was that of pumping fresh water from the Mugu only, and two different values of drawdown, 10 and 30 feet, were examined.

The analyses were made using finite difference forms of equations VII-12 and VII-13. The various chemico-osmotic parameters cited above were deduced from a comparison of laboratory measured properties of the aquitard materials with sediments that Olsen [1969, 1970] had previously investigated. The results of the analyses are presented in more

detail in Chapter VI of Appendix D. Here, we shall confine our attention to the most pertinent results of the analyses.

Figure VII-1 presents a curve of average chemico-osmotically induced pore pressure drop (expressed as a percentage of the maximum chemico-osmotically induced pore pressure drop) versus time. Because of equation VII-11 above, Figure VII-1 can be thought of as a curve of chemico-osmotically induced consolidation (or reduction in void ratio) versus time. From Figure VII-1 we observe that the chemico-osmotic consolidation increases for about 25 years. At this point the amount of chemico-osmotic consolidation is .001 ft (see Section VI-C, Appendix D) which is negligibly small. After 25 years the chemico-osmotic consolidation ceases, and the aquitard rebounds as the chemico-osmotic pore pressure drop decreases to zero. However the aquitard does not rebound to its original thickness. Figure VI-13 in Chapter VI of this report shows that the aquitard is more compressible during consolidation than rebound. Consequently the aquitard will only recover a fraction of the consolidation. The size of this fraction depends on the ratio of expansibility to compressibility.

The explanation for this initial chemico-osmotic consolidation followed by re-bound is that initially the high NaCl concentration in the Oxnard aquifer causes water to be sucked out of the aquitard by chemico-osmosis. This causes chemico-osmotic con-solidation for about 25 years. After 25 years, diffusion of NaCl into the aquitard becomes appreciable. The result is a chemico-osmotic suction of sea water back into the aquitard which causes the consolidation to cease and the rebound to begin. This is discussed in more detail in Chapter III-C of Appendix D.

Figure VII-2 shows the amount of consolidation that can occur if, in addition to the chemico-osmotic effects, there is a drawdown of 10 and 30 feet in the hydraulic head of the Mugu aquifer. In both cases, we see that it takes about 25 years for the consol-idation to be completed, and the amount varies linearly with the amount of pumping. A final consolidation of 0.1 ft is induced by a drawdown of 10 ft, and 0.3 ft by a drawdown of 30 ft. Both of these consolidations are considerably larger than the chemico-osmotic consolidation (0.001 ft) discussed above, implying that chemico-osmotic coupling does not induce consolidation of any consequence. Both types of consolidation take essentially the same length of time to reach the steady state because in each case, the rate is controlled mainly by the hydraulic permeability.

Figure VII-3 depicts curves of the inflows with time of NaCl into (or rate of degradation of) the aquitard expressed as a percentage of the amount of inflow of NaCl into the aquitard in the equilibrium steady state when there is no drawdown in the Mugu aquifer. Note that initially the percentage of NaCl inflow is about 17%, not 0%. This is because there is an initial NaCl concentration of 0.03 normal in the aquitard. In addition to this there is an inaccuracy inherent in the finite difference approximation method which causes initial values of NaCl inflow to be overestimated. Note also that
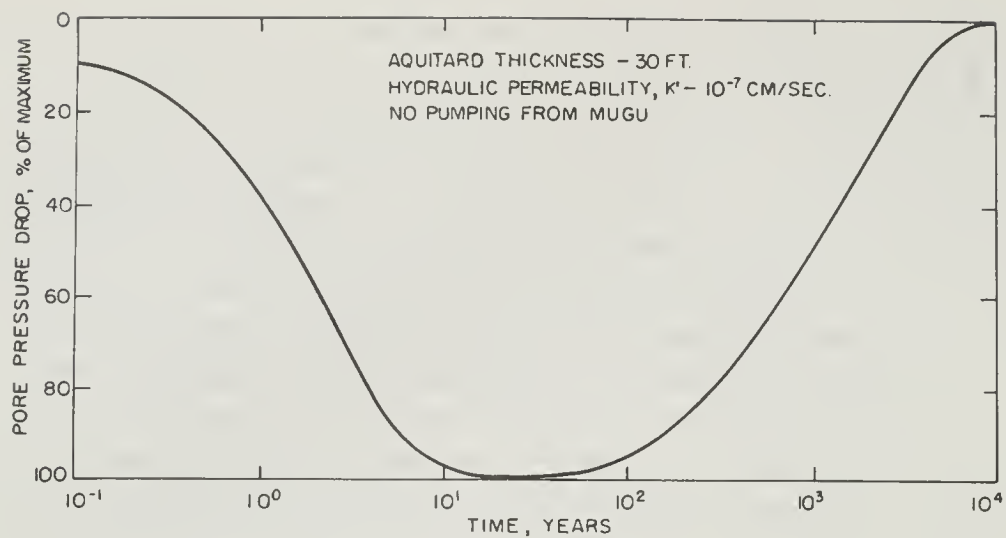
Fig. VII-1. Average pore pressure drop in aquitard versus time
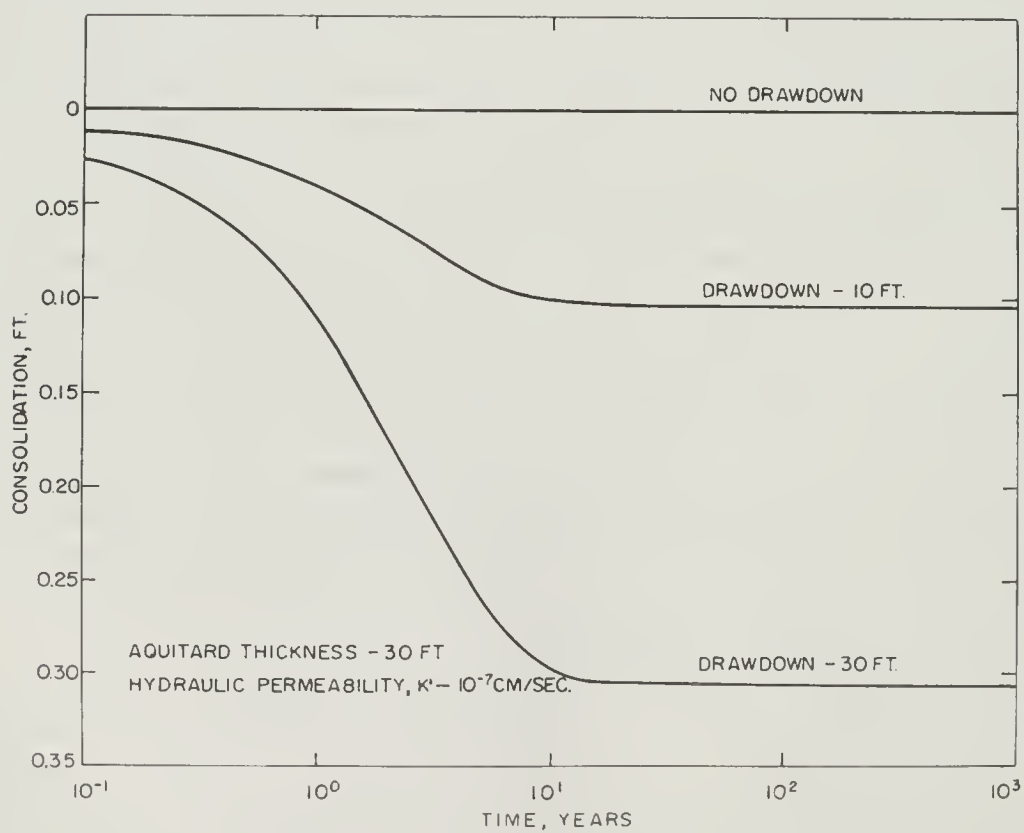
Fig. VII-2. Effect of drawdown on consolidation in aquitard
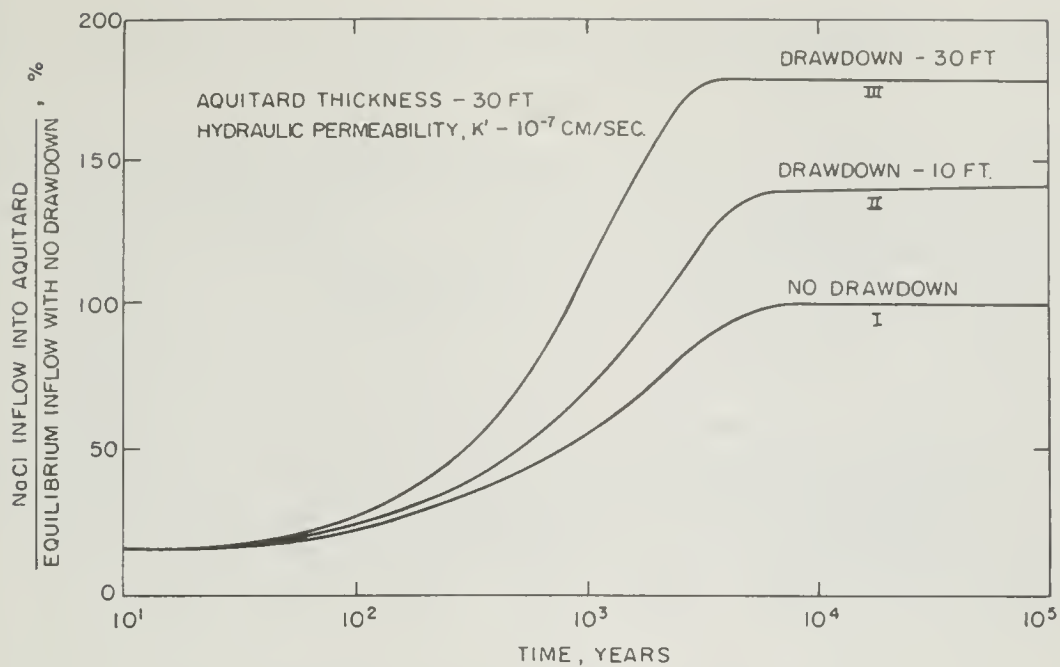
Fig. VII-3. NaCl inflow into aquitard showing effect
of drawdown in Mugu aquifer
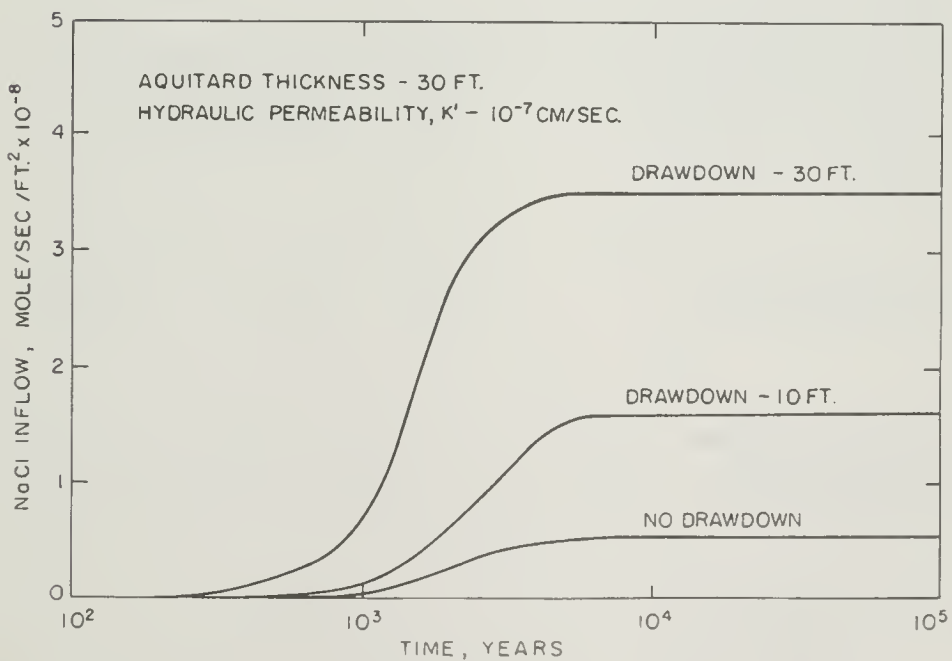
Fig. VII-4. NaCl inflow into Mugu aquifer showing
effect of drawdown

the non-steady state lasts for several thousands of years before a final steady state movement of NaCl is established.

A comparison of curve I for no drawdown in the Mugu with curves II and III for drawdowns of 10 and 30 feet, respectively, shows how the rate of NaCl inflow into the aquitard is greatly increased as a result of pumping. The explanation is that pumping from the Mugu causes a downward flow of sea water into and through the aquitard thus producing a more rapid as well as higher level of degradation.

As the NaCl moves through the aquitard, it eventually will reach the fresh water in the Mugu, and the time for this to occur is shown in Figure VII-4. Here one sees that the effect of drawdown in the Mugu causes a disproportionate increase in inflow as pumping increases. Table VII-1 summarizes results from Figures VII-3 and VII-4. It is apparent from these results that an aquitard that is 30 feet in thickness and has the properties assumed above acts as an effective barrier to NaCl movement from the Oxnard into the Mugu for long periods of time.

Table VII-1. Effect of drawdown in Mugu aquifer on rate of NaCl movement through 30 feet of aquitard

	Drawdown in Mugu, feet		
	0	10	30
Years to reach significant inflow into aquitard	25	25	25
Years to reach maximum inflow into aquitard	7000	5000	3000
Years to reach Mugu aquifer	800	250	170
Years to reach maximum inflow into Mugu	7000	5000	4000

To illustrate the effects of a reduced thickness, the above calculations were repeated for aquitard thicknesses of 10 feet and 1 foot using the same chemico-osmotic parameters and the same hydraulic gradient of 1/3. Figure VII-5 shows the rate of NaCl inflow into the aquitard, and Figure VII-6 shows the effect in the Mugu. Table VII-2 summarizes the results. One notes immediately that the rates of inflow in both the aquitard and the Mugu aquifer are very sensitive to the thickness of the aquitard. In effect, these rates vary as the square of the thickness of the aquitard. Thus, an aquitard only 1 foot thick offers little or no protection from degradation by sea water even though it may be of very low permeability. This is of considerable importance where the aquitard thicknesses are non-uniform, because it is obvious that the overall
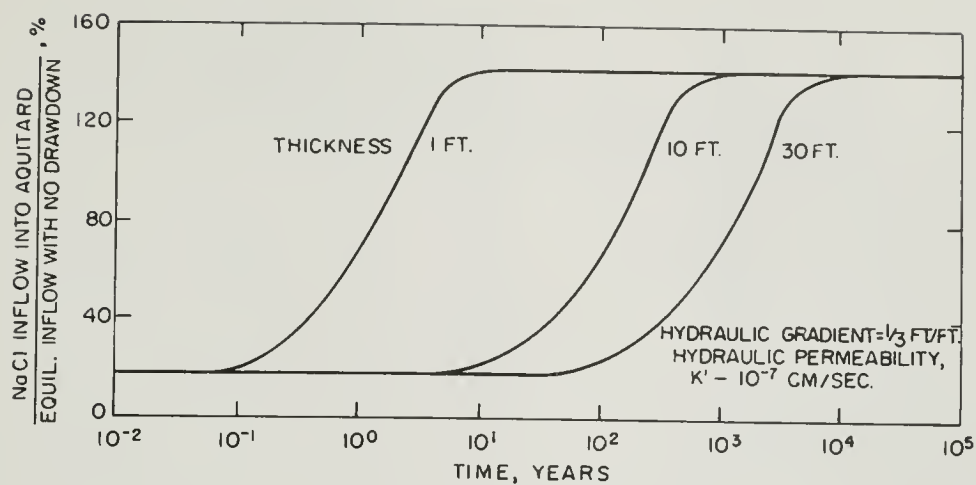
Fig. VII-5. NaCl inflow into aquitard showing effect
of aquitard thickness
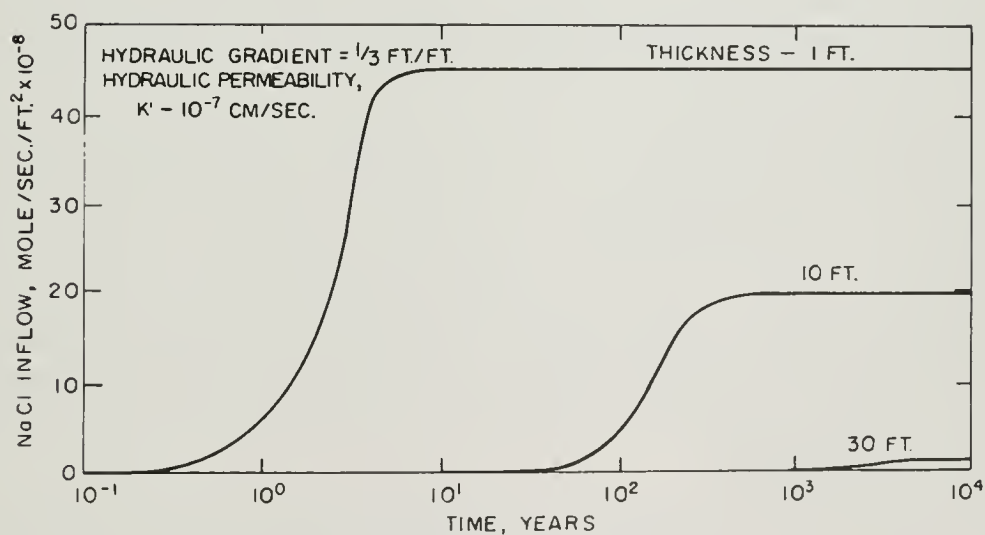
Fig. VII-6. NaCl inflow into Mugu aquifer showing
effect of aquitard thickness

Table VII-2. Effect of aquitard thickness on rate
of NaCl movement into Mugu
(Hydraulic gradient = 1/3 ft/ft)

	Aquitard thickness, feet		
	1	10	30
Years to reach significant inflow into aquitard	0.05	5	45
Years to reach maximum inflow into aquitard	15	1,500	13,000
Years to reach Mugu aquifer	0.3	30	250
Years to reach maximum inflow into Mugu	5.6	550	5,000

effectiveness of a barrier between fresh and salt water will be critically dependent on knowing the location of the thinnest sections.

To obtain some measure of the importance of the amount of NaCl that enters the Mugu aquifer, an attempt was made to relate it to the time for degradation of Mugu waters to reach a total solids content of 1,500 ppm. For the purposes of these calculations, it was assumed that the Mugu is 100 feet thick and has an average porosity of 30%. It was further assumed that the salt solutions being transported into the Mugu are able to mix thoroughly with the aquifer waters at all times. Knowing the rate of NaCl inflow into the Mugu as shown on Figures VII-4 and VII-6, the time for degradation to reach 1,500 ppm was calculated as shown in Table VII-3. These results further confirm the fact that as the thickness of an aquitard decreases, the time for diffusion to move significant quantities of salt water into fresh water systems can be relatively short.

As mentioned earlier, the analyses presented above assume the aquitard separating the Oxnard and Mugu aquifers is a homogeneous clay layer. In actuality, the aquitard is poorly defined and contains many silt and sand lenses interspersed with clay layers. As a result, the field tests indicate the aquitard permeability is at least ten times that used in the above calculations.

Since the field results suggest a higher permeability, what are the implications for chemico-osmotic effects at Oxnard? The rate of field consolidation, both chemico-osmotic, and that due to drawdown in the Mugu, is inversely proportional to the coefficient of consolidation, c_v. Since c_v will increase as permeability increases, the field rate of consolidation will occur faster than predicted. Chemico-osmotic coupling is inversely proportional to hydraulic permeability, and therefore the amount of chemico-osmotic consolidation, which has already been shown to be very small, will be further decreased.

Table VII-3. Time for degradation of Mugu
waters to reach 1,500 ppm
(Hydraulic gradient = 1/3 ft/ft)

Aquitard Conditions		Years to reach 1,500 ppm
Thickness ft	Hyd. Grad. ft/ft	
30	0.0	1700
30	0.33	1050
30	1.0	500
10	0.33	70
1	0.33	4

Due to the fact that the aquitard contains silt and sand lenses, the compressibility of the aquitard is probably also lower than was assumed in the above calculations. Since consolidation is proportional to compressibility, one can expect the calculated values shown in Figure VII-2 to be on the high side. More discussion on the implications of the actual permeability of the aquitard materials on sea water migration will be given in Chapter VIII.

CHAPTER VIII.   DISCUSSION OF RESULTS

P. A. Witherspoon and J. K. Mitchell

A.   OXNARD LEAKY AQUIFER SYSTEM

The results of the field pumping tests have definitely proven that the Oxnard aquifer and its associated confining beds constitute a leaky aquifer system. This is easily seen on Figure V-6 from the manner in which the drawdown data deviate from the Theis curve after about one day.

The question can therefore be asked whether conventional methods of analyzing leaky aquifers could be used at Oxnard. If the pumping test had been run for only one day, the effects of leakage would probably have been overlooked because they do not become pronounced until after two days of pumping. However, assuming a sufficient period of pumping, the data plotted on Figure V-6 could have been compared to the r/B solution (see Chapter IV-C), and one would obtain a value of r/B = 0.5. This is reasonably close to the value that can be calculated for the observation well of Figure V-6. The radial distance for this well is 502 ft, and using the results given in Chapter V, one can compute that r/B = 0.2.

Once an answer has been obtained using the conventional r/B method of analysis, the difficult question arises as to which aquitard is leaking. The field results using piezometers placed above and below the Oxnard clearly indicate that both aquitards are leaking. The results of our analysis using the ratio method reveal that the permeability of the underlying aquitard is about twice that of the overlying bed. It is impossible to extract this kind of information from the r/B method of analysis. Thus, it would be clear from the results that a leaky aquifer exists, but a more precise determination would not be possible. The ratio method, on the other hand, gives quantitative answers to this problem without ambiguity.

B.   SEA WATER INTRUSION IN COASTAL BASINS

Having obtained values for the hydraulic properties of sediments in the Oxnard Basin, what are the implications with regard to the widespread problem of sea water intrusion? If the various coastal basins contain aquitards with permeabilities approaching those found at Oxnard, the problems of intrusion may be more complicated than originally

believed. The general concept that the path of intrusion is essentially horizontal through the aquifer being pumped needs to be broadened to take into account the effects of vertical water movement.

To consider this problem, let us examine a generalized cross-section of a coastal basin as shown in Figure VIII-I. Originally this basin contained three fresh water aquifers that are separated from each other and from the ocean by aquitards. With reference to the Oxnard area: Aquifer A represents the semiperched zone; Aquifer B, the Oxnard aquifer; and Aquifer C, the Mugu aquifer.

We shall assume that as a result of overpumpage, sea water has intruded Aquifer B at point 1 (Figure VIII-1) and moved well inland. If Aquifer C is to be used for withdrawal purposes because water in the overlying Aquifer B is no longer potable, the question can be raised as to the magnitude of intrusion that can occur by vertical migration through the aquitard at point 2. Suppose that Aquifer C has been pumped sufficiently to develop a steady state vertical gradient of 1 ft/ft across the aquitard, whose permeability is the same as that found at Oxnard (i.e. 0.02 gpd/ft^2 or 10^{-6} cm/sec). Using the simple formula, Q = K i A, one can quickly calculate that the vertical migration across a square mile of aquitard under these conditions would amount to 560,000 gpd.

The problems that could develop from such intrusion would depend on the extent of water withdrawal from Aquifer C beneath this same square mile. If the average pumping rate is only 1,000 gpm, a vertical intrusion of 560,000 gpd represents 39 percent of the pumpage and might be a serious source of degradation. On the other hand, if the area can sustain yields of 10,000 gpm, the same intrusion represents only four percent of pumpage and might be tolerated. If the vertical gradient is less than 1 ft/ft, the rate of migration would be proportionately decreased. Nevertheless, the important fact remains that once sea water has intruded Aquifer B, the possibility of vertical migration through an adjacent aquitard cannot be disregarded.

We have assumed in the above discussion that fresh water in Aquifer B was degraded by sea water intruding the system at point 1 (Figure VIII-1). This is probably the case in the Oxnard Basin because the Oxnard aquifer outcrops close to land, perhaps one mile from shore, along submarine canyons. The Mugu aquifer, on the other hand, is believed to outcrop much further out on the continental shelf.

Nevertheless, in view of the preceding discussion, the question should be raised as to the possible effects of vertical migration into Aquifer B at point 3. Here, sea water just offshore could pass directly through the aquitard and mix with fresh waters moving landward under the gradients developed by excessive pumping. Depending on the circumstances and the distances involved, such migration might occur long before intrusion at point 1 could reach the shore line.

Whether such intrusion can cause a significant degradation of fresh water in Aquifer B depends on the conditions. If the average downward gradient across the
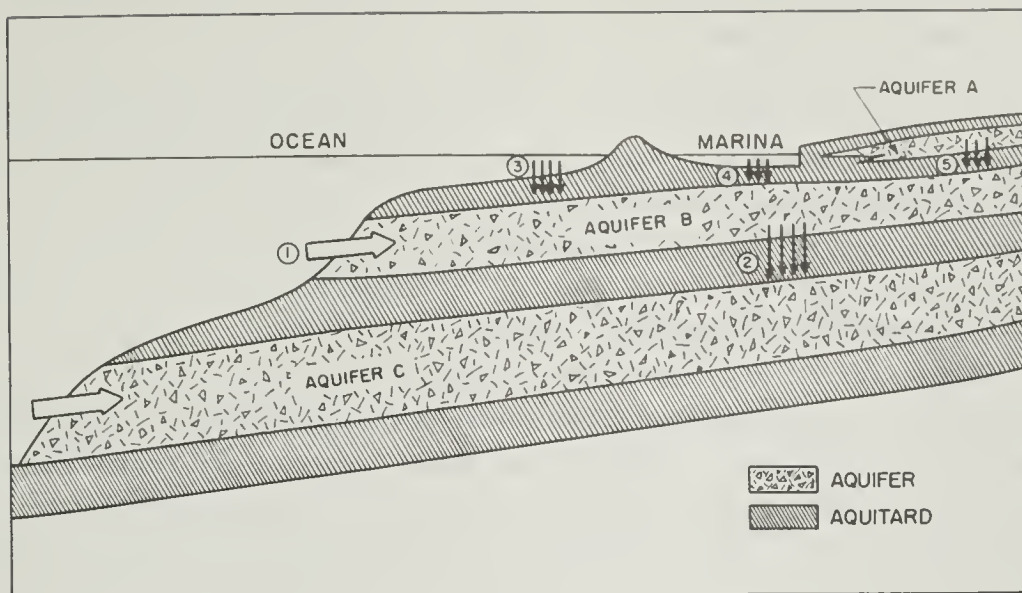
Fig. VIII-1. Generalized cross-section of a
multiple aquifer system in a
coastal basin

overlying aquitard should reach 1 ft/ft over significant areas adjacent to the shore
line and the vertical permeability is the same as assumed above (0.02 gpd/ft^2), then
the downward migration of sea water would again be 560,000 gpd per square mile of
exposed aquitard. Since this volume would enter Aquifer B just offshore and the
producing wells are onshore, the extent of degradation of fresh water sources would
depend largely on the rate of horizontal movement in the aquifer.

Onshore gradients in the Oxnard Basin have sometimes been of the order of 10 ft/
mile. If we assume Aquifer B is 100 ft thick and has a permeability comparable to that
of the Oxnard (i.e. 1,400 gpd/ft^2), a hydraulic gradient of this magnitude would move
1,400,000 gpd through a vertical cross-section that is a mile long and 100 ft high. In
such a case, an offshore intrusion of 560,000 gpd would amount to 40 percent of the flow.

Of course, this is an oversimplification because the vertical gradients in the
aquitard will diminish in the seaward direction; and as the gradient diminishes, so also
does the rate of migration. However, if Aquifer B extends far enough out on the shelf
before outcropping, leakage of sea water into Aquifer B will simply mix and accumulate
in the aquifer waters as they move landward. Therefore, one need only consider greater
distances out under the ocean than the one mile assumed above to realize that significant
intrusion could occur in this manner.

The crux of the matter depends on the magnitude of sea water intrusion relative
to the volume of fresh water moving landward. If horizontal movement in the aquifer is

-145-

the same as computed above and vertical gradients in the aquitard never exceed 0.1 ft/ft
out under the ocean, the intrusion of sea water into Aquifer B at point 3 may never
reach troublesome levels. On the other hand, if either the transmissibility of the
aquifer or the onshore gradient in this layer is significantly less than assumed above,
vertical gradients in the overlying aquitard would not have to reach 1 ft/ft to cause
degradation. This is a potential problem that cannot be ignored by those planning to
pump significant amounts of water from a coastal basin.

C. SEA WATER INTRUSION BENEATH MARINAS

A comparable situation arises on a smaller scale when a marina is constructed
in a coastal basin. As indicated at point 4 on Figure VIII-1, the natural barrier
between sea water and Aquifer B can be significantly reduced by a marina. Under virgin
conditions, any leakage through this aquitard is vertically upward from the fresh toward
the saline environment because in the undisturbed state, the hydraulic head in Aquifer B
normally exceeds that of the ocean. As long as such conditions prevail, excavation of
the aquitard during construction of the marina harbor will not result in sea water
intrusion into Aquifer B.

Once withdrawal of water from this aquifer begins, however, the hydraulic gra-
dients can be reversed. Then the excavation of a harbor could lead to a potential
problem of intrusion. For example, if the marina covers an area of 100 acres, a downward
gradient of 1 ft/ft can move 87,000 gpd of sea water across the aquitard at point 4
assuming a permeability of 0.02 gpd/ft^2.

The seriousness of this intrusion will depend on the volume of leakage relative
to the volume of fresh water moving landward. As has been demonstrated above, horizontal
movement in Aquifer B can be estimated knowing the transmissibility and effective gradient
in the aquifer. Intrusion of this kind is much more localized and only threatens pumping
wells near the marina.

D. DEGRADATION FROM POOR QUALITY WATER

Water of poor quality often accumulates in semiperched aquifers overlying fresh
water systems. Abnormally high concentrations of constituents such as arsenic, boron,
or nitrate can render such waters particularly dangerous. If the hydraulic head in the
semiperched zone exceeds that of the underlying aquifers, as is normally the case, the
poor quality water moves downward. This is shown on Figure VIII-1 by the movement from
Aquifer A to Aquifer B at point 5.

Even a small downward movement of poor quality water can create a potential
problem. For example, in March 1970, the hydraulic head at the test site in the Oxnard

Basin exceeded that of the underlying Oxnard aquifer by 13 ft (Figure V-11). The aquitard between the two has a thickness of about 40 ft and a permeability of 0.02 gpd/ft^2. The steady state gradient of 0.3 ft/ft was therefore able to move 165,000 gpd vertically downward through each square mile of aquitard.

It would not be unusual for total dissolved solids in the semiperched zone to build up to a level 10 times the accepted limits for drinking water. If such water began leaking into the Oxnard aquifer at the rate of 165,000 gpd over only one square mile, a horizontal flow of 1,650,000 gpd of fresh water would have to sweep through this particular area to dilute the poor quality water down to acceptable levels. As the area of contamination in the semiperched zone increased, the flow needed to sufficiently dilute the degraded water would increase proportionately.

The maximum horizontal gradients that have been noted in the Oxnard area have usually been able to move such volumes of water through the Oxnard aquifer. Gradients of 10 to 15 ft/mile have been observed, and with a permeability of 1,400 gpd/ft^2, such gradients can move from 1,400,000 to 2,100,000 gpd through a vertical cross-section that is one mile wide and 100 ft high. Thus, at the moment, poor quality water in the semiperched zone does not appear to pose a problem in the Oxnard area as long as these waters do not accumulate undesirable elements in concentrations more than 10 times the accepted limits.

If such concentrations should become too high, however, there would be a potential problem of serious degradation that could not be ignored. Concentrations of 20 to 50 times the accepted limit for dangerous elements such as arsenic, boron, or nitrate would pose a real threat. Under such circumstances, an aquitard with permeabilities as high as those found in the Oxnard Basin could not be considered an effective barrier to migration of poor quality waters.

E. GROUND WATER RECHARGE

The above discussion has focussed on the difficulties that arise when aquitards are leaky, but such beds can also play a significant role in recharging ground water into a basin. For example, if the vertical gradient across the aquitard overlying the Oxnard aquifer is only 0.1 ft/ft and the permeability is 0.02 gpd/ft^2, the volume of vertical recharge per square mile of aquifer amounts to 56,000 gpd, or about 63 acre-feet per year.

If this rate of recharge through the aquitard persists through the 95 or so square miles of Oxnard Basin that include the Oxnard aquifer, the total inflow from this source would be about 6,000 acre-feet per year. This amounts to 13 percent of the annual ground water supply of 46,000 acre-feet that has been reported in California Department of Water Resources, Bulletin 119-17 [1965].

Another important source of water can come from storage in the aquitard layers. This is due to the fact that S_s, the coefficient of storage per foot of thickness, is generally much higher in fine grained sediments than in the coarse grained aquifers. In the area of the test site in this investigation, S_s for the Oxnard aquifer was found to be 1.2×10^{-6} ft^{-1}, whereas in the overlying aquitard, S_s' was found to be 2.4×10^{-4} ft^{-1}, or 200 times higher (Table V-6).

Drawdowns in the aquifer will always be greater than those in the aquitard, but a factor of 200 will more than offset such differences in terms of water release. For example, one foot of drawdown in an aquitard only one foot thick will release as much water as 10 ft of drawdown in a 20-foot thick aquifer. Thus, in multiple aquifer systems where the combined thickness of the aquitards is much greater than that of the aquifers, the contribution of water from storage in the former will clearly dominate. Using the storage values cited above, a square mile of a 50-foot thick aquitard will release 7.7 acre-feet of water per foot of drawdown; an adjacent 10-foot aquifer, only 0.008 acre-feet.

This is not an important factor in the Oxnard Basin because hydraulic heads do not continue to fall year after year but fluctuate depending on the relative magnitudes of annual withdrawal and ground water recharge. In multiple aquifer systems, however, where the withdrawals continually exceed the annual rate of recharge, the contributions from storage within the fine grained sediments can be a dominant factor in the overall water supply.

One must, of course, keep in mind that the rate at which water is released from storage in an aquitard relative to the horizontal rate of movement in the much more permeable aquifer will determine the importance of aquitard contributions to ground water supply. Nevertheless, those who prepare hydraulic budgets should not overlook the role of aquitards either from the standpoint of their storage capacity or from the standpoint of the communication they provide with other parts of a multiple aquifer system.

F. RATE OF MOVEMENT ACROSS AN AQUITARD

At this point, the question can be raised that if the permeability of an aquitard is of the order of 0.02 gpd/ft^2 (~10^{-6} cm/sec), how long will sea water or some other nonpotable fluid take to move across such a bed.

The first problem is the length of time that must pass before the steady state is reached. One dimensional, non-steady flow across any bed essentially ends when dimensionless time ($t_D = \alpha' t / H'^2$) reaches a value of 0.1 to 1.0 [Carslaw and Jaeger, 1959, p. 101]. We shall consider a bed that is 30 ft thick and from Table V-3, we note that a hydraulic diffusivity ($\alpha' = K'/S_s'$) of 0.15 cm/sec is appropriate for a permeability of

0.02 gpd/ft^2. When $t_D = 0.1$, we can calculate the time to reach steady state from

$$t = \frac{H'^2 t_D}{\alpha'} = \frac{(30 \times 30.48)^2 (0.1)}{(0.15)} = 557,000 \text{ sec}$$

$$= 6.5 \text{ days (or 65 days, if } t_D = 1.0)$$

Thus, if head changes suddenly on one side of an aquitard in the Oxnard Basin, steady state flow conditions can be attained in a matter of days. The field pumping tests verify this calculation (see Figures V-9 and V-10).

        After the steady state is reached, an estimate of the time for fluids to move across an aquitard can be made by calculating velocities from $v = K\ i$. Table VII-1 presents some results for two different permeabilities.

Table VIII-1. Time for fluids to flow across aquitards
under steady-state conditions

Case	Permeability gpd/ft^2	Hydraulic gradient ft/ft	Velocity ft/day$\cdot 10^4$	Years to flow across aquitard with thickness of		
				10 ft	30 ft	50 ft
1	0.02	1.00	26.73	10	30	50
2	0.02	0.33	8.81	30	90	160
3	0.02	0.10	2.67	100	310	510
4	0.002	1.00	2.67	100	310	510
5	0.002	0.33	0.88	310	920	1550
6	0.002	0.10	0.27	1020	3070	5120

        If vertical gradients across the aquitard remain at values of 1 ft/ft and permeabilities are of the order of 0.02 gpd/ft^2, the time required for degradation to begin is relatively short (i.e. 10 to 50 years). This period of time happens to be essentially the same as that over which the various sea water intrusion problems in the coastal basins of California have developed. One wonders whether the observed degradation has always followed the traditional concept of horizontal movement from the aquifer outcrops out on the continental shelf, or whether there might be some instances where aquitard leakage was a contributing factor. This could probably be checked by investigating compositional changes in the pore waters of offshore aquitard samples. Until such investigations are made, a reliable answer to this problem will not be possible.

-149-

Table VIII-1 also shows that if either the gradients or the permeabilities are decreased, the time for pollution to occur is increased substantially. However, a decreased permeability implies a higher clay content and with it, the greater likelihood that chemico-osmotic diffusion must be considered. This kind of coupled flow has been discussed in Chapter VII, and examples have been worked out for an aquitard having a permeability of 0.002 gpd/ft^2 (~10^{-7} cm/sec).

One should bear in mind that movement of salt ions is always present when sea water is on one side and fresh water is on the other side of an aquitard. The process, however, is complex because at first, the fresh water in the aquitard moves toward the salt water and impedes the movement of salt ions into the aquitard. Later, this fluid movement diminishes and the salt migration toward the fresh water begins to control. As a result, movement by chemico-osmotic diffusion alone is very slow. This is demonstrated by the results given in Table VII-1, where one sees that 800 years are required for salt ions to diffuse from the Oxnard to the Mugu through 30 feet of an aquitard having a permeability of 0.002 gpd/ft^2.

The process can be significantly speeded up if, in addition to the chemico-osmotic effect, there is also a hydraulic gradient acting in the same direction as the concentration gradient. In the above example, a drawdown of 30 ft in the Mugu could shorten the transit time to 170 years (see Table VII-1).

By comparison, the steady state results of Table VIII-1 indicate that salt water moving only under the influence of a hydraulic gradient of the same magnitude (1.0 ft/ft) would take 310 years to move across 30 feet of the same permeability aquitard. The steady state result is almost twice too high because this approach neglects the fact that movement under the combined action of chemical and hydraulic gradients produces a more rapid rate of salt migration than can be taken into account by the simplified approach. Thus, in attempting to calculate movement of sea water across low permeability aquitards (<0.001 gpd/ft^2), the steady state approach can lead to results that are in error on the optimistic side.

Whether the transit time is 170 or 800 years may not pose a practical problem, but as the thickness of the aquitard diminishes, the transit times for salt to pass through the layer are drastically reduced. This has been brought out in Table VII-2, where it was shown that transit time varies directly with the square of the aquitard thickness. For example, the 170 years cited above for a 30-foot aquitard would become only 19 years for a 10-foot aquitard.

On the other hand, increasing the permeability of the aquitard up to the levels found for the Oxnard Basin (K = 0.02 gpd/ft^2) means that the migration will be much more dominated by the hydraulic gradients that develop. Movement by diffusion will remain at a relatively low level because this process is mainly dependent on: (a) the magnitude of the diffusion constant for NaCl in water (D $\cong$ 10^5 cm^2/sec), and (b) the concentration

gradient that develops when sea water (or some other non-potable fluid) comes in contact with one boundary of an aquitard. These two factors are not affected by an increase in permeability.

If a coastal basin has aquitard permeabilities as high or higher than those found at Oxnard, the process most likely to cause significant amounts of non-potable waters to move across an aquitard will probably be that of movement due to a hydraulic gradient. On the other hand, as the aquitards become clay-rich and their permeabilities fall to levels of the order of 0.001 gpd/ft^2, the migration will be controlled by chemico-osmotic diffusion. In this case, the only danger points will be where the aquitards that must serve as barriers to the movement of fluids are too thin. In either circumstance, careful control of hydrologic conditions must be maintained in any given area if sea water intrusion through aquitards is to be eliminated. Such controls will, of course, have to be integrated with any other operations that are required to prevent the usual landward migration of sea water due to over pumpage.

G. DETERIORATION AND SUBSIDENCE OF AQUITARD MATERIALS

As sea water invades an aquitard, there is the problem that a deterioration of the clays may lead to an increase in permeability. In the field of petroleum, "swelling" clays can cause a marked reduction in the permeability of sandstone in the presence of fresh water, and this effect is easily reversed by replacing the fresh by salt water. As discussed in Chapter VI, a number of leaching tests were performed on aquitard core samples, but the results were inconclusive. Part of the difficulty was the variability of the aquitard samples which ranged from clay to fine sand (Table VI-1).

Table VI-4 shows that the predominant clay mineral found in the clay-size fraction was montmorillonite. Sodium montmorillonite is one of the swelling clays, but an analysis of pore waters from the aquitard cores at Oxnard revealed calcium and magnesium to be the dominant cations present. Since calcium montmorillonite does not exhibit much of a swelling tendency, this may be part of the explanation for a lack of change in permeability due to leaching.

The question of subsidence is, of course, dependent on the degree of consolidation that the aquitard materials will undergo. As was brought out in the theoretical calculations of Chapter VII, consolidation due to chemico-osmotic effects is negligible compared to that induced by a change in hydraulic head on one side of the aquitard. After 25 years, a drawdown of 30 ft was able to produce a total consolidation of 0.3 ft over a 30-foot aquitard. This probably would not constitute a troublesome factor in the typical coastal basin. Of course, subsidence is largely irreversible, and if a basin has thick deposits of aquitards, the cumulative effect of continued lowering of hydraulic heads could lead to significant settlements over long periods of time. This has been found to be the case

in a number of instances [Poland and Davis, 1969].

H. NEED FOR FIELD OBSERVATIONS

All of these considerations lead one to the more general problem of the level of field observation that is necessary in multiple aquifer basins where leakage across aquitards poses a threat to ground water resources. Obviously, one must first know the magnitude of the aquitard permeabilities; otherwise reliable estimates of leakage through such beds will not be possible. In untested areas, this will require field investigations and a certain amount of laboratory measurements similar to that of this work. As the range of permeabilities that is possible for aquitard materials becomes better known, it should be possible to develop correlations between permeability and other more easily determined parameters. For example, such factors as grain size distribution and bulk density, which can be obtained during the drilling of water wells, may lead to estimates of aquitard permeabilities that are sufficiently accurate for most purposes.

Once the permeability of the aquitards (and presumably of the aquifers as well) is known, appropriate measurements of hydraulic head across the particular aquitard that is expected to act as a barrier must be made as often as one needs to know the degree of leakage. Locations where critical problems of fresh water degradation may occur should be equipped with enough observation wells so there can be no question as to the magnitude of vertical communication. These wells should be placed in the aquitard under consideration as well as in adjacent aquifers above and below.

Finally, it is concluded that in utilizing the ground water resources of coastal basins, such as those of California, the ability of aquitards to control sea water intrusion on the one hand, and to contribute to recharge on the other, must be carefully evaluated in any effective program of water resource management.

NOTATION

a_v Coefficient of compressibility, LT^2M^{-1}

B_{ij} $\sqrt{K_i H_i H_j'/K_j'}$, L

C_c Compression index

c_L Moles of solution per unit volume of solution, moles L^{-3}

c_s Moles of solute per unit volume of solution, moles L^{-3}

c_{sm} Maximum value of c_s expected during process, moles L^{-3}

c_v Coefficient of consolidation, L^2T^{-1}

D Diffusion constant of solute, L^2T^{-1}

e Void ratio

H Thickness of aquifer, L

H' Thickness of aquitard, L

$\bar{J}_d$ Vector flow of solute relative to flow of solution, moles $T^{-1}L^{-2}$

$\bar{J}_L$ Vector flow of solution, moles $T^{-1}L^{-2}$

J_o Zero order Bessel function of first kind

$\bar{J}_s$ Vector flow of solute, moles $T^{-1}L^{-2}$

K Permeability of aquifer, LT^{-1}

K' Permeability of aquitard, LT^{-1}

K_v Vertical permeability of aquitard, LT^{-1}

k Permeability of aquitard, LT^{-1}

k_{ch} Coupling coefficient, moles LT^{-1}

k_{hc} Coupling coefficient, moles LT^{-1}

p' Pressure, $ML^{-1}T^{-2}$

p_o' Initial pressure, $ML^{-1}T^{-2}$

Q Rate of discharge from aquifer, L^3T^{-1}

R Gas constant, ML^2T^{-2} mole^{-1} °K^{-1}

r Radial distance from pumping well, L

S Storage coefficient of aquifer

S_s Specific storage of aquifer, L^{-1}

S_s' Specific storage of aquitard, L^{-1}

s Drawdown in aquifer, L

s' Drawdown in aquitard, L

s_D Dimensionless drawdown, $4\pi Ts/Q$

T Transmissibility of aquifer, L^2T^{-1}

T	Absolute temperature, $^\circ K$
t	Time, T
t_D	Dimensionless time in aquifer, $\alpha t/r^2$
t_D'	Dimensionless time in aquitard, $\alpha' t/z^2$
U	Pore water pressure, $ML^{-1}T^{-2}$
V_L	Volume of solution per mole of solution, $L^3 \, mole^{-1}$
x	Dimensionless ratio, c_s/c_{sm}
z	Vertical coordinate, L
α	Hydraulic diffusivity of aquifer, $L^2 T^{-1}$
α'	Hydraulic diffusivity of aquitard, $L^2 T^{-1}$
β_{ij}	$\dfrac{r}{4H_i}\sqrt{\dfrac{K_j' S_{sj}'}{K_i S_{si}}}$
γ_L	Number of moles of solution per unit volume of sediment, $moles \, L^{-3}$
γ_s	Number of moles of solute per unit volume of sediment, $moles \, L^{-3}$
γ_w	Specific weight of water, $ML^{-2}T^{-2}$
Φ	Dissipation function, $ML^{-1}T^{-3}$

REFERENCES

Abd-El-Aziz, M. and Taylor, S. A. "Simultaneous Flow of Water and Salt through Unsaturated Porous Media. I. Rate Equations." Proceedings, Soil Science Society of America, Vol. 29, No. 2, p. 141. 1964.

Aravin, V. I. and Numerov, S. N. "Theory of Fluid Flow in Undeformable Porous Media." Israel Program for Scientific Translations, Jerusalem. 511 pp 1965.

American Society of Agronomy. "Methods of Soil Analysis." Agronomy No. 9. Madison, Wisconsin. 1965.

Bruington, A. E. and Seares, F. D. "Operating a Sea Water Barrier Project." Journal of the Irrigation and Drainage Division, ASCE, Vol. 91, No. IR1, Proc. Paper 4264, p. 117. March 1965.

California Department of Water Resources. "Investigation of Ground Water Pollution of Bolsa Chica Mesa-Sunset Beach, California." Office Report. January 1958.

----. "Sea-Water Intrusion in California." Bulletin No. 63. November 1958.

----. "Quality of Ground Waters in California, 1955 through 1959." Bulletins Nos. 66-55 through 66-59. June 1958 through February 1963.

----. "Intrusion of Salt Water into Ground Water Basins of Southern Alameda County." Bulletin No. 81. December 1960.

----. "Feasibility of Serving the Ventura County Flood Control District from the State Water Project." Bulletin No. 119-17. July 1965.

----. "Sea-Water Intrusion, Oxnard Plain of Ventura County." Bulletin No. 63-1. October 1965.

----. "Sea-Water Intrusion, Bolsa-Sunset Area Orange County." Bulletin 63-2. January 1968.

----. "Sea-Water Intrusion, Pismo-Guadalupe Area." Bulletin No. 63-3. February 1970.

----. "Sea-Water Intrusion Lower Salinas Valley, Progress Report 1968-1969." June 1970.

Carslaw, H. S. and Jaeger, J. C. "Conduction of Heat in Solids." Oxford University Press, London. 1959.

Casagrande, A. "The Determination of the Preconsolidation Load and its Practical Significances." Proceedings, International Conference Soil Mechanics, Vol. III, Harvard University, 1936.

Chapman, H. D. "Cation-Exchange Capacity." Chapter 57, "Methods of Soil Analysis." Agronomy No. 9, American Society of Agronomy, Madison, Wisconsin. 1965.

DeGlee, G. J. "Over Grondwaterstromingen by Wateronttrekking by Middel van Putten." T. Waltman Jr., Delft. 1930.

DeWiest, R. J. M. "On the Theory of Leaky Aquifers." Journal Geophysical Research, Vol. 66, p. 4257. 1961.

----. "Flow to an Eccentric Well in a Leaky Circular Aquifer with Varied Lateral Replenishment." Geofis. Pura Appl., Vol. 54, p. 87. 1963.

----. "Geohydrology" 336 pp. John Wiley, New York. 1965.

Ferris, J. G., Knowles, D. B., Brown, R. H., and Stallman, R. W. "Theory of Aquifer Tests; A Summary of Lectures." U. S. Geological Survey Water Supply Paper 1536-E. 1962.

Gill, H. E. "Hydrologic Significance of Confining Layers in the Artesian Potomac-Raritan-Magothy Aquifer System in New Jersey." Geological Society of America Annual Meeting, Atlantic City, New Jersey, Abstracts. p. 78. 1969.

Girinsky, N. K. "Nekotorye Voprosy Dinamiki Podzemnykh Vod." in Gidrogeologiya i Inzhenernaya Gelogiya, Sbornik Statei, Moscow. 1947.

Glebov, P. D. "Pritok Infiltratsionnoi Vody k Kolodtsam pri Gorizontalom Zaleganii Gruntov Razlichnoi Vodopronitsaemosti." Trudy Leningrad Industrial Institute, Vol. 1. 1940.

Hantush, M. S. "Plain Potential Flow of Ground Water with Linear Leakage." Ph.D. Dissertation, University of Utah, Salt Lake City. 1949.

----. "Analysis of Data from Pumping Tests in Leaky Aquifers." Transactions American Geophysical Union, Vol. 37, p. 702. 1956.

----. "Nonsteady Flow to a Well Partially Penetrating an Infinite Leaky Aquifer." Proceedings Iraq Scientific Society, Vol. 1, p. 10. 1957.

----. "Nonsteady Flow to Flowing Wells in Leaky Aquifers." Journal Geophysical Research, Vol. 64, p. 1043. 1959.

----. "Modification of the Theory of Leaky Aquifers." Journal Geophysical Research, Vol. 65, p. 3713. 1960a.

----. "Tables of the Function $H(u,\beta)$." Document 6427, U. S. Library of Congress. Washington, D. C. 1960b.

----. "Drainage Wells in Leaky Water-Table Aquifers." Proceedings American Society of Civil Engineers, Vol. 88, HY2, p. 123. 1962.

----. "Depletion of Storage, Leakage, and River Flow by Gravity Wells in Sloping Sands." Journal Geophysical Research, Vol 69, p. 2551. 1964.

----. "Flow of Ground Water in Relatively Thick Leaky Aquifers." Water Resources Research, Vol. 3, No. 2, p. 583. 1967a.

----. "Flow to Wells in Aquifers Separated by a Semipervious Layer." Journal Geophysical Research, Vol. 72, No. 6, p. 1709. 1967b.

Hantush, M. S. and Jacob. C. E. "Plane Potential Flow of Ground Water with Linear Leakage." Transactions American Geophysical Union, Vol. 35, p. 917. 1954.

----. "Nonsteady Green's Functions for an Infinite Strip of Leaky Aquifers." Transactions American Geophysical Union, Vol. 36, p. 101. 1955a.

----. "Nonsteady Radial Flow in an Infinite Leaky Aquifer." Transactions American Geophysical Union, Vol. 36, p. 95. 1955b.

----. "Flow to an Eccentric Well in a Leaky Circular Aquifer." Journal Geophysical Research, Vol. 65, p. 3425. 1960.

Jacob, C. E. "Radial Flow in a Leaky Artesian Aquifer." Transactions American Geophysical Union, Vol. 27, p. 198. 1946.

Javandel, I. and Witherspoon, P. A. "Analysis of Transient Fluid Flow in Multi-Layered Systems." Water Resources Center Contribution No. 124, University of California, Berkeley. 1968.

Johnson, A. I., Moston, R. P. and Morris, D. A. "Physical and Hydrologic Properties of Water-Bearing Deposits in Subsiding Areas in Central California." U. S. Geological Survey Professional Paper 497-A. 1968.

Lambe, T. W. "Soil Testing for Engineers." John Wiley and Sons, New York. 1951

Lambe, T. W. and Whitman, R. V. "Soil Mechanics." John Wiley and Sons, New York. 1969.

Mesri, G. "Engineering Properties of Montmorillonite." Thesis submitted in partial fulfillment of the requirements for the Doctor of Philosophy degree to the University of Illinois, Urbana. 1969.

Mitchell, J. K. "Physical and Hydrological Properties of the Aquitard Layers in the Oxnard California Area." Geotechnical Engineering Publication Number T. E. 69-2, University of California, Berkeley. 1969.

Mitchell, J. K., Hooper, D. R. and Campanella, R. G. "Permeability of Compacted Clay." Journal of the Soil Mechanics and Foundations Division, ASCE, Vol. 91, No. SM4, Proceeding Paper 4392, p. 41. July 1965.

Mitchell, J. K. and Younger, J. S. "Abnormalities in Hydraulic Flow through Fine-Grained Soils." Symposium on Permeability and Capillarity, 69th Annual Meeting of the American Society for Testing and Materials, Atlantic City, New Jersey. July 1966.

Myatiev, A. N. "Deistvie Kolodtsa v Napornom Basseine Podzemnykh Vod." Izvestia Turkmenia Filiala Akad. Nauk SSSR, Vol. 3-4. 1946.

----. "Napornyi Kompleks Podzemnykh Vod i Kolodtsy." Izvestia Akad. Nauk SSSR, Otdelenie Tekhnologiya Nauk, Vol. 9. 1947.

Narasimhan, T. N. "Ratio Method for Determining Characteristics of Ideal, Leaky and Bounded Aquifers." Bulletin International Association of Scientific Hydrology, Vol. 13, No. 1, p. 70. 1968.

Neuman, S. P. and Witherspoon, P. A. "Theory of Flow in Aquicludes Adjacent to Slightly Leaky Aquifers." Water Resources Research, Vol. 4, No. 1, p. 103. 1968.

Olsen, H. "Simultaneous Fluxes of Liquid and Charge in Saturated Kaolinite." Soil Science Society of America Proceedings. Vol 33, No. 3. May-June 1969.

----. "Liquid Movement through Kaolinite under Hydraulic Electrical and Osmotic Gradients." to appear in American Association of Petroleum Geology volume on "Membrane and Mass Transport Phenomena in the Geologic Environment." ed. F. Berry. 1970, in press.

Poland, J. F. and Davis, G. H. "Land Subsidence Due to Withdrawal of Fluids." in Reviews in Engineering Geology II. Geological Society of America, Boulder. p. 187. 1969.

Polubarinova-Kochina, P. Ya. "Theory of Ground Water Movement." Princeton University Press, Princeton. 613 p. 1962.

Rankin, W. L. "Tentative Method of Test for Organic Matter in Soils." Proposed to Committee D-18, ASTM. 1968. unpublished.

Salas, J. A. and Serratosa, J. M "Compressibility of Clays." Proceedings of the 3rd International Conference on Soil Mechanics and Foundation Engineering, Vol. 1, p. 192. Zurich. 1953.

Slater, R. J. "Application and Limitations of Pumping Tests." Inst. Water Engineers Journal, Vol. 17, No. 3, p. 189. 1963.

Steggeventz, J. H. and Van Nes, B. A. "Calculating the Yield of a Well Taking Account of Replenishment of the Ground Water from Above." Water and Water Engineering, Vol. 41, p. 561, 1939.

Taylor, D. W. "Fundamentals of Soil Mechanics." John Wiley and Sons, New York. 1948.

Terzaghi, K. and Peck, R. B. "Soil Mechanics in Engineering Practice." 2nd Ed., John Wiley and Sons, New York. 1967.

Walton, W. C. "Leaky Artesian Aquifer Conditions in Illinois." 27 pp. Illinois State Water Survey Report of Investigation 39, Urbana, Illinois. 1960.

----. "Selected Analytical Methods for Well and Aquifer Evaluation." 81 pp. Illinois State Water Survey Bulletin 49, Urbana, Illinois. 1962

----. "Ground-Water Recharge and Runoff in Illinois." 55 pp. Illinois State Water Survey, Report of Investigation 48. 1965.

Witherspoon, P. A., Javandel, I., Neuman, S. P. and Freeze, R. A. "Interpretation of Aquifer Gas Storage Conditions from Water Pumping Tests." American Gas Association, Arlington. 273 pp. 1967.

Witherspoon, P. A., Mueller, T. D. and Donovan, R. W. "Evaluation of Underground Gas-Storage Conditions in Aquifers through Investigations of Ground Water Hydrology." Transactions AIME, Vol 225, p. 555, 1962.

Witherspoon, P. A. and Neuman, S. P. "Evaluating a Slightly Permeable Caprock in Aquifer Gas Storage, I. Caprock of Infinite Thickness." Transactions AIME, Vol. 240, p. 949. 1967.

Wolff, R. G. "Field and Laboratory Determination of the Hydraulic Diffusivity of a Confining Bed." Water Resources Research, Vol. 6, No. 1, p. 194. 1970.

Yotov, I. G. "On Drawdown Around Wells in Leaky Water Table Aquifer." Doklady Bolgarskoi Akad. Nauk, Vol. 21, No. 8, p. 765. 1968.

APPENDIX A

TRANSIENT FLOW OF GROUND WATER TO WELLS

IN MULTIPLE-AQUIFER SYSTEMS

by

Shlomo P. Neuman

and

Paul A. Witherspoon

ABSTRACT

This work is an attempt to make a comprehensive investigation of transient fluid flow to a well in a multiple-aquifer system

Analytical solutions have been developed for the problem of flow toward a well of infinitesimal radius that discharges at a constant rate and completely penetrates an aquifer in a system composed of two aquifers and one aquitard. Solutions for a system composed of three aquifers and two aquitards have also been derived. In addition, asymptotic solutions for small values of time have been obtained that give the drawdown distribution in an aquifer which is enclosed between two aquitards. The solutions for the two-aquifer system, together with the asymptotic solutions have been evaluated using the Zonneveld-Adams-Moulton numerical method of integration and the results are presented in graphical form.

A complete solution to the problem described by Hantush in Case 1 of his "Modification of the Theory of Leaky Aquifers" has been developed, giving the drawdown distribution in the aquifer at arbitrary values of time since Hantush's solutions are only valid at small and large values of time.

The finite element method has been reviewed and was used to investigate the behavior of a two-aquifer system. The method was also used to obtain an independent check on the analytical solutions and to examine the basic assumption made in the analytical approach that the direction of flow is essentially horizontal in the aquifers and vertical in the aquitards. It was found that this assumption will probably hold in most field situations.

A review of the methods that are currently being used to evaluate the results of pumping tests in leaky aquifers has disclosed that these methods are limited in application. A new approach to the problem of evaluating multiple-aquifer systems that is based on the results of this investigation is outlined. This method needs further investigation before it can be applied in the field.

TABLE OF CONTENTS

a	=	Parameter of Hankel transform	
c_i	=	Compressibility of i-th aquifer	$L^2 F^{-1}$
$c_j{}^{\cdot}$	=	Compressibility of j-th aquitard	$L^2 F^{-1}$
erfc (x)	=	Complimentary error function of x	
Ei (x)	=	Exponential integral of x	
H_i	=	Thickness of i-th aquifer	L
$H_j{}^{\cdot}$	=	Thickness of j-th aquitard	L
$H_0{}^{(1)}$	=	First zero order Hankel function	
$H_0{}^{(2)}$	=	Second zero order Hankel function	
$H^*[f(r)]$	=	Zero order infinite Hankel transform of f(r)	
$H^{-1}[F(a)]$	=	Inverse Hankel transform of F(a)	
$I_0 (x)$	=	Zero order modified Bessel function of the first kind	
$J_0 (x)$	=	Zero order Bessel function of the first kind	
$J_1 (x)$	=	First order Bessel function of the first kind	
k_i	=	Specific permeability of i-th aquifer	L^2
k_j'	=	Specific permeability of j-th aquitard	L^2
K_i	=	$\dfrac{k_i \gamma}{\mu}$, Coefficient of permeability of i-th aquifer	LT^{-1}
K_j'	=	$\dfrac{k_j' \gamma}{\mu}$, Coefficient of permeability of j-th aquitard	LT^{-1}
$K_0 (x)$	=	Zero order modified Bessel function of the second kind	
$K_1 (x)$	=	First order modified Bessel function of the second kind	
$L[f(t)]$	=	Laplace transform of f(t)	
$L^{-1}[F(p)]$	=	Inverse Laplace transform of F(p)	
p	=	Parameter of Laplace transform	
Q_i	=	Rate of discharge from i-th aquifer	$L^3 T^{-1}$
r	=	Radial distance from pumping well	L

$$r/B_{ij} = r\sqrt{\frac{K_j'}{K_i H_i H_j'}} = \sqrt{\eta_{ij}}$$

s_i = Drawdown in i-th aquifer   L

s_j' = Drawdown in j-th aquitard   L

$\bar{s}$ = Laplace transform of s

$\bar{\bar{s}}$ = Hankel transform of $\bar{s}$

$s_D = \dfrac{4\pi T_i}{Q_i}s$, Dimensionless drawdown

$S_{s_i} = \gamma\varphi_i c_i$, Specific storage of i-th aquifer L^{-1}

$S_{s_j}' = \gamma\varphi_j' c_j'$, Specific storage of j-th aquitard L^{-1}

t = Time since pumping started   T

$t_{D_i} = \dfrac{\alpha_i t}{r^2}$, Dimensionless time in pumped aquifer

$\bar{t}_{D_j} = \dfrac{\alpha_j' t}{H_j'^2} = t_{D_i}\theta_{ij}$ where i refers to pumped aquifer

Δt = Time interval   T

$T_i = K_i H_i$, Transmissibility of i-th aquifer $L^2 T^{-1}$

$u_i = 1/4\, t_{D_i}$

z = Vertical coordinate   L

$\alpha_i = \dfrac{k_i}{\varphi_i\mu c_i} = \dfrac{K_i}{S_{s_i}}$, Hydraulic diffusivity of i-th aquifer $L^2 T^{-1}$

$\alpha_j' = \dfrac{k_j'}{\varphi_j'\mu c_j'} = \dfrac{K_j'}{S_{s_j}'}$, Hydraulic diffusivity of j-th aquitard $L^2 T^{-1}$

$\beta_{ij} = \dfrac{r}{4H_i}\sqrt{\dfrac{K_j'\varphi_j' c_j'}{K_i\varphi_i c_i}} = \dfrac{r}{4H_i}\sqrt{\dfrac{K_j' S_{s_j}'}{K_i S_{s_i}}} = \dfrac{\eta_{ij}}{4\sqrt{\theta_{ij}}}$

γ = Specific weight of liquid FL^{-3}

$\eta_{ij} = \dfrac{K_j' r^2}{T_i H_j'}$

$\theta_{ij} = \dfrac{\alpha_j' r^2}{\alpha_i H_j'^2}$

x

λ = Complex variable used to replace p during inversion of Laplace transform

μ = Dynamic viscosity of liquid $\quad FTL^{-2}$

ν_{ij} = $\sqrt{\theta_{i1}/\theta_{ij}}$

φ_i = Porosity of i-th aquifer

φ_j' = Porosity of j-th aquitard

ACKNOWLEDGMENTS

I. INTRODUCTION

When one is concerned with the flow of water to a well that is completed in a single aquifer, there is a tendency to focus attention on the effects to be expected in that particular aquifer. If the aquifer is effectively enclosed by impermeable confining beds, the well known methods based on the Theis (42) solution are easily applicable. More often, however, the aquifer from which water is being withdrawn is part of a more complex geohydrological system. Such systems can be thought of as a series of aquifers with intervening beds of relatively low permeability. From a theoretical standpoint, at least, we cannot confine our attention to the single aquifer that is being pumped but must consider the effects of flow in the entire system.

We shall refer to such a geohydrological situation as a "multiple-aquifer" system. When the flow of water through the confining beds is such that the effects can be detected by observations of drawdown in the aquifer being pumped, these beds are called "aquitards" and the aquifer is referred to as being "leaky". When these effects cannot be detected within the aquifer, the confining beds are called "aquicludes", and the aquifer is termed "slightly leaky" (35). No matter how small the permeabilities of the aquicludes that enclose a slightly leaky aquifer, the behavior of the entire system cannot be understood if the aquicludes are considered impermeable and if the aquifer is regarded as an independent hydrological unit. In nature, all aquifers are leaky or slightly leaky and all aquicludes have some degree of permeability.

The fact that aquifers are part of more complex geohydrological systems has long been recognized by ground water hydrologists. The phenomenon of leakage into an aquifer was first analyzed by the Dutch engineer DeGlee in 1930 (4), and by Steggeventz and Van Nes in 1939 (40). Polubarinova Kochina (38, p. 377-395) describes work that was done on the subject in the Soviet Union during 1946-1947 by Myatiev (32, 33) and by Girinsky (10). In 1946, Jacob (28) developed solutions to problems involving both steady and non-steady

flow in an aquifer with vertical leakage. The approach used by all of these
authors is based on the following assumptions:

1. The permeabilities of the aquifers are much larger than those of the
   aquitards, so that flow is essentially horizontal in the aquifers and
   vertical in the aquitards.

2. The rate of leakage into the aquifer being pumped is proportional to
   the potential drop across the aquitard, which implies that under tran-
   sient conditions the storage capacity of the aquitard is being neglected.

3. Head in the unpumped aquifers remains constant at all values of pump-
   ing time (Polubarinova-Kochina has also investigated the influence of
   pumping in one aquifer on the head in an adjacent aquifer under con-
   ditions of steady state when the aquifers are separated by an aquitard).

Employing these assumptions, Jacob and others were able to incorporate
the boundary conditions at the interfaces between the aquifer being pumped and
the aquitards into the differential equation which describes flow in the aquifer.
This step greatly facilitated mathematical treatment of the problem and as a
result, between the years 1949 and 1960, Hantush (13,17,18,19) and Hantush
and Jacob (14,15,16,20) have used this approach to develop a large number of
solutions to various problems involving flow in aquifers with vertical leakage.
One of these solutions (16) describes non-steady radial flow to a well completely
penetrating an infinite leaky aquifer and discharging at a constant rate. This
particular solution has been extensively tabulated (17), and the resulting type
curves are being widely used by groundwater hydrologists to evaluate the pro-
perties and the yield of leaky aquifers (7,8,39,43,44,47, p. 51-56,68-70). The
results of this solution are usually presented in terms of a dimensionless para-
meter r/B and the type curves are known as the r/B curves.

In 1960 Hantush (21) published a modified version of the differential
equations for flow in a leaky system, in which for the first time, consider-
ation was given to storage within the aquitards. The modified differential

equations have been applied by Hantush to the problem of non-steady radial flow to a well completely penetrating an infinite leaky aquifer and discharging at a constant rate. He was able to develop asymptotic solutions for the drawdown in the aquifer, which apply only at small and large values of pumping time. Hantush's solutions for small values of time have been extensively tabulated (22) in terms of a dimensionless parameter β, while his solutions for large values of pumping time, for the case when the unpumped aquifers have non-zero permeabilities, are similar in form to the r/B curves mentioned earlier. However, since Hantush was unable to describe the flow in the aquifer at intermediate values of pumping time, his modified approach has not received proper attention and was not used in subsequent works on leaky aquifers. Between the years 1961-1967, Hantush (23, 24, 26, 27) and DeWiest (5, 6) analyzed various problems involving flow in leaky aquifers but in all of these works, storage of water in the aquitards was consistently neglected.

Prior to 1962, ground water hydrologists were mostly preoccupied with the conditions in the aquifer being pumped and had given little consideration to the effect of pumping on the confining beds and on the unpumped aquifers in a multiple-aquifer system. The importance of observing the drawdown in an aquiclude which overlies a slightly leaky aquifer was pointed out first by Witherspoon et al. (48) in connection with underground storage of natural gas in aquifers. In 1966 Neuman and Witherspoon (34, 35) developed analytical solutions for the transient conditions in an aquiclude adjacent to a slightly leaky aquifer which is being pumped at a constant rate. In their development, the authors assumed that drawdown in the aquifer being pumped is prescribed by the Theis solution (42), and that drawdown in the unpumped aquifers remains zero at all values of pumping time. The authors took into account the storage capacity of the aquiclude and assumed that flow in this layer is essentially vertical. An independent check on these solutions was obtained with the aid of a finite difference model in which the direction of flow was unrestricted in the aquiclude (34). The results have been extensively tabulated (47) and the

authors have shown how these can be used to evaluate the permeability of an aquiclude using field data from a pumping test (49, 47, p. 62-68, 72-83, 86-92).

The problem of the steady state behavior of two aquifers that are separated by an aquitard, when the drawdown in the unpumped aquifer is not necessarily zero, was studied by Polubarinova-Kochina (38, p. 385-390), as mentioned previously. In 1967 Hantush (27) described the transient conditions in such aquifers for a case in which a well of infinitesimal radius completely penetrates one of these layers and discharges at a constant rate. In this work, Hantush again assumed that leakage is proportional to the potential drop across the intervening aquitard.

Thus far, all the work that has been concerned with the problem of non-steady flow in leaky aquifers has either neglected storage in the aquitards or ignored drawdown in the unpumped aquifers, or both. The assumption of no storage in the confining beds implies that hydraulic gradients across these beds are always linear. However, this is certainly not the case at small values of pumping time because the disturbance created by pumping propagates much faster through the aquifer than it does through the confining beds that enclose it. At large values of pumping time, gradients in these beds may eventually become linear, provided that the system reaches a quasi-steady state situation (35, Eq. 18). On the other hand, the effect of drawdown in the unpumped aquifers may be negligible at small values of pumping time, but at large values of time this effect may be quite significant. Therefore, a complete understanding of flow in multiple-aquifer systems requires that due consideration be given to storage of water in the confining beds and to the variation in drawdown at each point in the system.

A description of flow in multiple-aquifer systems may be of importance to a variety of engineering problems. In groundwater hydrology, there is the need for a new method of pump-testing complex geohydrological systems which enables one to effectively evaluate the properties of all the layers involved. The methods that are currently being used by groundwater hydrologists are limited in application and may often lead to misleading results.

In the case when a coastal aquifer has been invaded by sea water, there is the danger of leakage through the aquitards and degradation of potable waters in the adjacent aquifers. A similar problem arises in connection with underground disposal of industrial and nuclear wastes. An understanding of the behavior of multiple-aquifer systems under conditions of pumping should be helpful in planning underground waste disposal and in designing adequate pumping patterns for groundwater basins in which one or more aquifers have already been polluted or invaded by sea water.

The withdrawal of water from unconsolidated clay beds due to intensive pumping of the adjacent aquifers sometimes results in subsidence (36,37) which can be detrimental to structures on the surface. A knowledge of the flow patterns in such clays may help the soils engineer to predict and control the amount of subsidence that occurs at a given location as a result of pumping.

In underground storage of natural gas, which is a new technology that has gained acceptance in the United States and Europe during recent years, the engineer must make certain that gas will not leak through the aquiclude that overlies an intended storage reservoir. The problem of determining the permeability of such an aquiclude is critical for the success of the project, and an understanding of flow in this layer is therefore essential (35,47,48,49).

In the present work, we shall present an analytical approach to the problem of flow in two-aquifer and three-aquifer systems. In our development, we shall assume that flow is vertical in the aquitards and horizontal in the aquifers and that the systems are enclosed between layers of relatively negligible permeability. We will allow the drawdown at each point in the system to vary with time and will take into consideration storage of water in the aquitards.

The problem of flow in a two-aquifer system will also be investigated with the aid of the finite element method of analysis, which is a new numerical technique that has recently been adapted to problems of transient flow in porous media by Javandel and Witherspoon (29). The results obtained in this fashion will provide

us with an independent check on the analytical solutions and will help us to investigate flow patterns in systems in which the direction of flow in unrestricted in each layer.

Finally, the knowledge gained through these studies will be utilized in developing a new approach to field testing multiple-aquifer systems. The new method involves the use of a family of type curves which require that observation wells be placed both in the aquifer being pumped and in the aquicludes or aquitards that enclose it. The method may require the use of highly sensitive pressure transducers which must be lowered into the observation wells to detect, with a minimum of time lag, the extremely small changes in water pressure that take place in the confining beds at small values of pumping time.

II. ANALYTICAL SOLUTIONS

A. GENERAL MODEL OF A MULTIPLE-LAYER SYSTEM

The first step in developing analytical solutions to problems involving flow in porous media is to adopt some generalized conceptual model for the system being investigated. The model must be as simple as possible in order to yield to the present day tools of mathematical treatment and still remain representative of the actual physical problems involved. In problems that deal with the flow of groundwater in layered systems, most acceptable schematic models will usually fall into two major categories:

1. Models constructed for the purpose of studying flow fields that develop on a regional scale;

2. Models constructed for the purpose of studying the propagation of local disturbances, in an existing flow field, created by such diverse natural or artificial means as rivers, canals, ditches, drains, wells, artificial recharge facilities, etc. .

If the investigator is interested in studying the regional aspects of a groundwater flow system, his model should include the regional boundaries of that system. Therefore, models that describe regional flow patterns are characterized by finite geometrical boundaries. On the other hand, a model of infinite or semi-infinite extent may be more convenient when dealing with the propagation of local disturbances. In this type of problem, it is mainly the effect near and around the source of disturbance that is of primary interest. For example, in the case of a pumping well, a zone of disturbance will be created around the wellbore. This zone will grow with time as the disturbance propagates away from the wellbore in all directions. As long as the zone of disturbance has not reached the outer boundaries of the system, the disturbance may be regarded as local and the system as infinite or semi-infinite. Infinite and semi-infinite

models have the advantage of involving a relatively smaller number of variables and boundary conditions that are easier to treat mathematically.

In the present work, we will be studying flow fields that develop around a pumping well situated within a multiple aquifer system. We will restrict ourselves to the case of a line sink that completely penetrates one of the aquifers, and assume that the pump operates at some constant rate of discharge, Q.

As a most general approach, consider a system of N horizontal layers as shown on Fig. II-1. We assume that the layers are homogeneous, isotropic, uniform in thickness, and infinite in radial extent. We also assume that at any point within the system the flow is governed by Darcy's law, that the system is an elastic porous medium completely saturated with a single-phase, homogeneous, slightly compressible liquid, and that the coefficient of storage remains essentially constant during the entire period of pumping.

With these assumptions, a complete mathematical description of the flow within our system can be
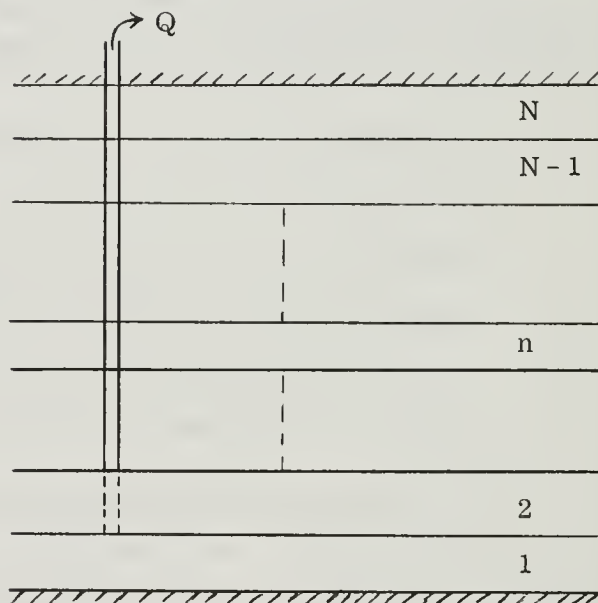
Fig. II-1. Multiple-layer system.

given by writing for each layer, n, the governing partial differential equation[*]

$$\frac{\partial^2 s_n}{\partial r^2} + \frac{1}{r}\frac{\partial s_n}{\partial r} + \frac{\partial^2 s_n}{\partial z^2} = \frac{1}{\alpha_n}\frac{\partial s_n}{\partial t} \tag{II-1}$$

_____

[*]See Nomenclature for definition of all symbols (note difference in subscripts).

the initial condition

$$s_n(r, z, 0) = f_n(r, z)$$ (II-2)

where $f_n(r, z)$ is not necessarily zero, the boundary condition

$$s_n(\infty, z, t) = 0$$ (II-3)

and the interface conditions

$$s_n(r, z_{n,n+1}, t) = s_{n+1}(r, z_{n,n+1}, t)$$ (II-4a)

$$K_n \left. \frac{\partial s_n}{\partial z} \right|_{z = z_{n,n+1}} = K_{n+1} \left. \frac{\partial s_{n+1}}{\partial z} \right|_{z = z_{n,n+1}}$$ (II-4b)

For the layer being pumped, we also have to consider the condition at the wellbore

$$\lim_{r \to 0} 2 \pi K_n \int_0^{H_n} r \frac{\partial s_n}{\partial r} \, dz = -Q$$ (II-5)

Eqs. II-1 through II-5 describe the initial boundary value problem for a multiple-layer system that is being pumped at a constant rate.

B. MODIFIED MODEL OF A MULTIPLE-AQUIFER SYSTEM

The solution of Eqs. II-1 through II-5 becomes extremely difficult whenever the number of layers N in Fig. II-1 exceeds one. Several attempts to solve this problem for two layers (N = 2) have resulted in solutions that are very difficult, if not impossible, to evaluate numerically. It is therefore essential that

-181-

the model described in the previous section be somewhat modified before any further attempt to solve the problem is made.

In the following discussion, we will adopt a model similar to the one employed by Hantush in his treatment of the modified "leaky aquifer" problem (21). This model is especially suitable for systems which involve layers with alternating high and low permeabilities. In such systems the model includes a minimum number of restricting conditions and, as will be shown later, yields results of a fairly general nature.

Consider a system of N highly permeable layers (aquifers) that are separated from each other by N – 1 layers with relatively low permeabilities (aquitards). A well of infinitesimal radius completely penetrates one of the aquifers and discharges at some constant rate Q. All the assumptions mentioned in Section II-A with regard to the geometry and flow properties of the individual layers will also be adopted here. The system is illustrated in Fig. II-2.

The basic assumption involved in this approach can be stated as follows: if the permeability contrast between any two adjoining layers in the system is sufficiently large, flow will be essentially horizontal in the aquifers and vertical in the aquitards whenever one of the aquifers is being pumped.
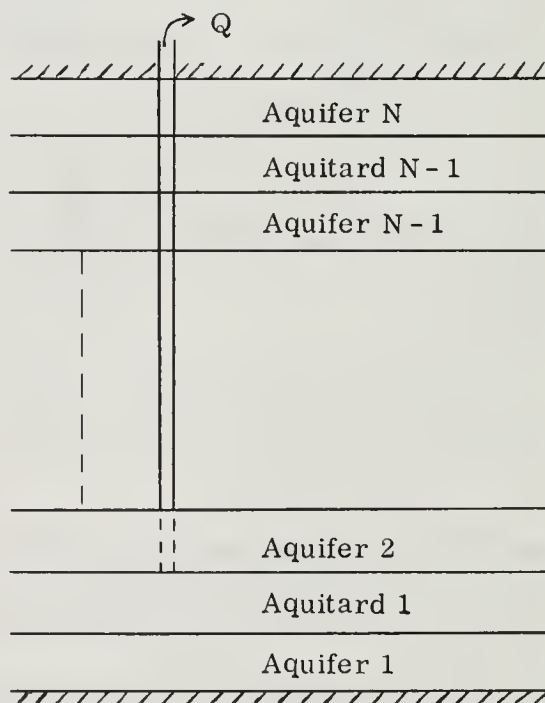
Fig. II-2. Multiple-aquifer system.

One immediate implication of this assumption is that all unpumped aquifers must be thin enough so that the drawdown across their thickness may at any time t be regarded as constant. The principle here is somewhat similar to that

of a cooling fin (1, p. 141). No restriction on the thickness of the aquifer being pumped is necessary since radial gradients that develop in this layer as a result of pumping are much larger than vertical gradients due to leakage from the adjacent aquitards. The effect of these assumptions on the overall quality of the solutions will be discussed in Chapter IV.

Since there are no vertical gradients in the aquifers, Eq. II-4b cannot be used and Eqs. II-1 through II-5 are inadequate to characterize the flow in such a system. A new mathematical formulation of the problem is therefore necessary to suit the modified model.

Consider an aquifer of permeability K_i and thickness H_i that is overlain and underlain by two aquitards of permeabilities K_{j+1}' and K_j', respectively. An infinitesimal element of the aquifer is shown in Fig. II-3. We assume that flow in the aquifer is horizontal and directed toward the vertical z axis, which acts as a line sink. Flow directed into the element is considered positive.

According to Darcy's law, flow rate into the element through its x and y faces is given by
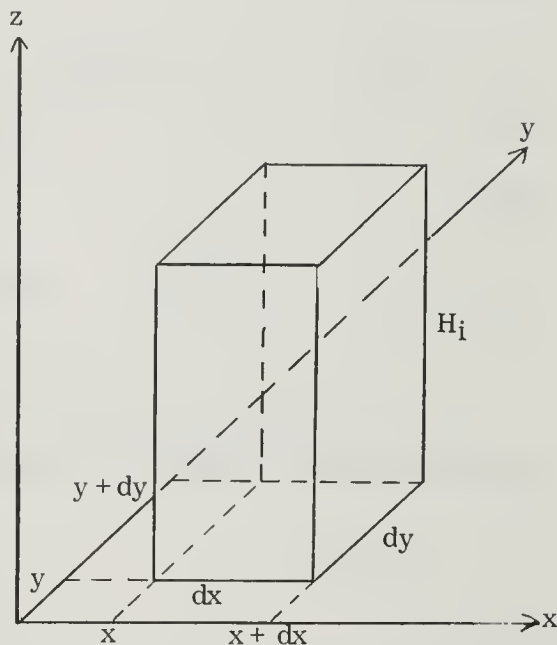
Fig. II-3. Infinitesimal aquifer element.

$$Q_x = K_i \frac{\partial s_i}{\partial x} H_i \, dy \qquad \text{and} \qquad Q_y = K_i \frac{\partial s_i}{\partial y} H_i \, dx$$

respectively. It should be remembered that for this case, both $\partial s_i/\partial x$ and $\partial s_i/\partial y$ are negative. The inflow rate at the x + dx and y + dy faces is

$$Q_{x+dx} = -K_i \frac{\partial s_i}{\partial x} H_i dy - \frac{\partial Q_x}{\partial x} dx$$

$$= -K_i \frac{\partial s_i}{\partial x} H_i dy - K_i \frac{\partial^2 s_i}{\partial x^2} H_i dx dy$$

and

$$Q_{y+dy} = -K_i \frac{\partial s_i}{\partial y} H_i dx - K_i \frac{\partial^2 s_i}{\partial y^2} H_i dx dy$$

In the z direction, leakage rate into the element from the adjacent aquitards is

$$Q_{z=H_i} = -K_{j+1}' \frac{\partial s_{j+1}'}{\partial z} \bigg|_{z=H_i} dx dy$$

and

$$Q_{z=0} = K_j' \frac{\partial s_j'}{\partial z} \bigg|_{z=0} dx dy$$

Storage within the element decreases at the rate of

$$S_i \frac{\partial s_i}{\partial t} dx dy$$

and the continuity equation for the element may be expressed in the form

$$Q_x + Q_y + Q_{x+dx} + Q_{y+dy} + Q_{z=H_i} + Q_{z=0} = -S_i \frac{\partial s_i}{\partial t} dx dy$$

Substituting for the values of Q and simplifying, we obtain

$$\frac{\partial^2 s_i}{\partial x^2} + \frac{\partial^2 s_i}{\partial y^2} + \frac{K_{j+1}'}{T_i} \frac{\partial s_{j+1}'}{\partial z} \bigg|_{z=H_i} - \frac{K_j'}{T_i} \frac{\partial s_j'}{\partial z} \bigg|_{z=0} = \frac{1}{\alpha_i} \frac{\partial s_i}{\partial t}$$

because $\alpha_i = S_i / T_i$.

Using radial coordinates, a complete description of the flow within the system can now be given as follows.

Flow in the i-th aquifer:

$$\frac{\partial^2 s_i}{\partial r^2} + \frac{1}{r} \frac{\partial s_i}{\partial r} + \left. \frac{K_{j+1}'}{T_i} \frac{\partial s_{j+1}'}{\partial z} \right|_{z_{i,j+1}} - \left. \frac{K_j'}{T_i} \frac{\partial s_j'}{\partial z} \right|_{z_{i,j}}$$

$$= \frac{1}{\alpha_i} \frac{\partial s_i}{\partial t} \tag{II-6}$$

$$s_i(r,z,0) = s_{0i}(r,z) \tag{II-2}$$

$$s_i(\infty,z,t) = 0 \tag{II-3}$$

$$\lim_{r \to 0} 2\pi K_i H_i r \frac{\partial s_i}{\partial r} = -Q_i \tag{II-7}$$

where $z_{i,j}$ is the value of z at the interface between the i-th aquifer and the j-th aquitard.

Flow in the j-th aquitard:

$$\frac{\partial^2 s_j'}{\partial z^2} = \frac{1}{\alpha_j'} \frac{\partial s_j'}{\partial t} \tag{II-8}$$

$$s_j'(r,z,0) = s_{0j}'(r,z) \tag{II-2}$$

$$s_j'(r,z_{i,j},t) = s_i(r,z_{i,j},t) \tag{II-4a}$$

The main advantage of posing the problem in this way is that the interface condition (Eq. II-4b) has been incorporated within the partial differential equation (Eq. II-6). The new initial boundary value problem obtained in this

fashion is easier to handle analytically than the problem defined by Eqs. II-1 through II-5, and will therefore be adopted throughout this work.

C. SOLUTION OF TWO-AQUIFER PROBLEM

In the previous section, we discussed the way in which an initial boundary value problem for a multiple-aquifer system can be formulated mathematically. We now turn to the solution of a particular case where the system is composed of only two aquifers separated by an aquitard. Our approach will be as follows. After formulating the problem for the two-aquifer system, a succession of Laplace and Hankel transforms will be applied to the differential equations and their corresponding initial, interface, and boundary conditions. The resulting ordinary differential equation will be solved to obtain solutions in terms of the double transform. The inverse Hankel and Laplace transforms of these results will yield the desired solutions.

1. Formulation of Problem

Consider a system of two aquifers separated by an aquitard as shown in Fig. II-4. A well of infinitesimal radius completely penetrates the lower aquifer and discharges at some constant rate Q. Each layer is horizontal, homogeneous, isotropic, and infinite in radial extent. The system is satur-
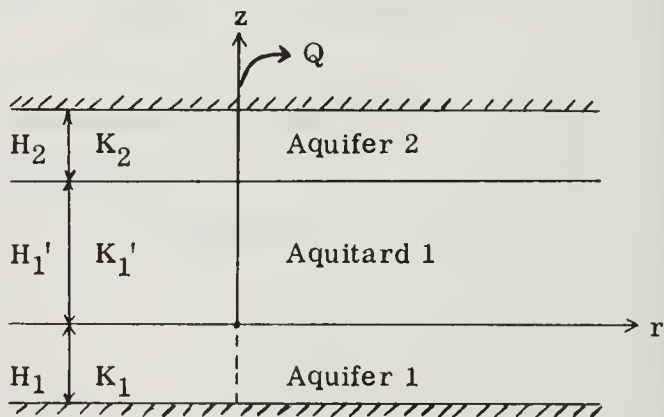
Fig. II-4. Two-aquifer system.

ated with a homogeneous, single-phase, slightly compressible liquid, and may itself be regarded as an elastic porous medium. Darcy's law applies everywhere in the system, and the storage coefficient in each layer remains constant with time. We assume that $K_1' \ll K_1$, $K_1' \ll K_2$, and that H_2 is sufficiently small so

that drawdown across the thickness of Aquifer 2 is constant at any time t. If the initial drawdown is zero everywhere in the system, we can use the results of Section II-B to formulate the problem as follows:

$$\frac{\partial^2 s_1}{\partial r^2} + \frac{1}{r}\frac{\partial s_1}{\partial r} + \frac{K_1'}{T_1}\frac{\partial s_1'}{\partial z}\bigg|_{z=0} = \frac{1}{\alpha_1}\frac{\partial s_1}{\partial t} \qquad \text{(a)}$$

$$s_1(r,0) = 0 \qquad \text{(b)}$$

$$s_1(\infty,t) = 0 \qquad \text{(c)}$$

$$\lim_{r\to 0} r\frac{\partial s_1}{\partial r} = -\frac{Q}{2\pi T_1} \qquad \text{(d)}$$

$$\left.\begin{array}{r}\end{array}\right\} \text{Aquifer 1 (pumped)} \quad \text{(II-9)}$$

$$\frac{\partial^2 s_1'}{\partial z^2} = \frac{1}{\alpha_1'}\frac{\partial s_1'}{\partial t} \qquad \text{(a)}$$

$$s_1'(r,z,0) = 0 \qquad \text{(b)}$$

$$s_1'(r,0,t) = s_1(r,t) \qquad \text{(c)}$$

$$s_1'(r,H_1',t) = s_2(r,t) \qquad \text{(d)}$$

$$\left.\begin{array}{r}\end{array}\right\} \text{Aquitard 1 \quad (II-10)}$$

$$\frac{\partial^2 s_2}{\partial r^2} + \frac{1}{r}\frac{\partial s_2}{\partial r} - \frac{K_1'}{T_2}\frac{\partial s_1'}{\partial z}\bigg|_{z=H_1'} = \frac{1}{\alpha_2}\frac{\partial s_2}{\partial t} \qquad \text{(a)}$$

$$s_2(r,0) = 0 \qquad \text{(b)}$$

$$s_2(\infty,t) = 0 \qquad \text{(c)}$$

$$\lim_{r\to 0} r\frac{\partial s_2}{\partial r} = 0 \qquad \text{(d)}$$

$$\left.\begin{array}{r}\end{array}\right\} \text{Aquifer 2 (not pumped)} \quad \text{(II-11)}$$

Eqs. II-9 through II-11 define the initial boundary value problem for the two-aquifer case.

2. Transformation of Problem

Let us apply the Laplace transform to Eq. II-10a, using the initial condition (Eq. 10b). We obtain

$$\frac{\partial^2 \bar{s}_1{}'}{\partial z^2} - \frac{P}{\alpha_1{}'} \bar{s}_1{}' = 0 \tag{II-12}$$

If we now operate on Eq. II-12 with the zero order infinite Hankel transform (see definition of Hankel transform in Appendix A), the result is

$$\frac{\partial^2 \bar{\bar{s}}_1{}'}{\partial z^2} - \frac{P}{\alpha_1{}'} \bar{\bar{s}}_1{}' = 0 \tag{II-13}$$

This is an ordinary differential equation that can be easily solved for $\bar{\bar{s}}_1{}'$

$$\bar{\bar{s}}_1{}' = c_1 \exp\left(\sqrt{p/\alpha_1{}'}\, z\right) + c_2 \exp\left(-\sqrt{p/\alpha_1{}'}\, z\right) \tag{II-14}$$

where c_1 and c_2 are arbitrary real constants. The double Laplace and Hankel transforms of Eqs. II-10c and II-10d are given by

$$\bar{\bar{s}}_1{}'(a, 0, p) = \bar{\bar{s}}_1(a, p) \tag{II-15}$$

and

$$\bar{\bar{s}}_1{}'(a, H_1{}', p) = \bar{\bar{s}}_2(a, p) \tag{II-16}$$

When Eqs. II-15 and II-16 are substituted in Eq. II-14, we obtain two equations in the two unknowns, c_1 and c_2

$$\bar{\bar{s}}_1(a, p) = c_1 + c_2$$

and

$$\bar{\bar{s}}_2(a, p) = c_1 \exp\left(\sqrt{p/\alpha_1{}'}\, H_1{}'\right) + c_2 \exp\left(-\sqrt{p/\alpha_1{}'}\, H_1{}'\right)$$

Solving for c_1 and c_2 and substituting the results in Eq. II-14 will yield the double transform of the drawdown in the aquitard,

$$\bar{\bar{s}}_1' = \frac{\sinh \left(\sqrt{p/\alpha_1'} \ z \right)}{\sinh \left(\sqrt{p/\alpha_1'} \ H_1' \right)} \bar{\bar{s}}_2 + \frac{\sinh \left[\sqrt{p/\alpha_1'} \ (H_1' - z) \right]}{\sinh \left(\sqrt{p/\alpha_1'} \ H_1' \right)} \bar{\bar{s}}_1 \qquad \text{(II-17)}$$

The Laplace transforms of II-9a and II-11a, considering II-9b and II-11b, can be written as

$$\frac{1}{r} \frac{\partial}{\partial r} \left(r \frac{\partial \bar{s}_1}{\partial r} \right) - \frac{P}{\alpha_1} \bar{s}_1 + \frac{K_1'}{T_1} \frac{\partial \bar{s}_1'}{\partial z} \Bigg|_{z=0} = 0 \qquad \text{(II-18)}$$

and

$$\frac{1}{r} \frac{\partial}{\partial r} \left(r \frac{\partial \bar{s}_2}{\partial r} \right) - \frac{P}{\alpha_2} \bar{s}_2 - \frac{K_1'}{T_2} \frac{\partial \bar{s}_1'}{\partial z} \Bigg|_{z=H_1'} = 0 \qquad \text{(II-19)}$$

respectively. The Laplace transforms of II-9d and II-11d are

$$\lim_{r \to 0} r \frac{\partial \bar{s}_1}{\partial r} = - \frac{Q}{2 \pi T_1 P} \qquad \text{(II-20)}$$

and

$$\lim_{r \to 0} r \frac{\partial \bar{s}_2}{\partial r} = 0 \qquad \text{(II-21)}$$

The Hankel transform H^* of the first term in Eqs. II-18 and II-19 is given by Eq. A-9 in Appendix A as

$$H^* \left[\frac{1}{r} \frac{\partial}{\partial r} \left(r \frac{\partial \bar{s}}{\partial r} \right) \right] = - a^2 \bar{\bar{s}} - \lim_{r \to 0} r \frac{\partial \bar{s}}{\partial r} \qquad \text{(II-22)}$$

Applying the Hankel transform to Eqs. II-18 and II-19 and considering Eqs. II-20, II-21, and II-22, we obtain the two equations

$$- a^2 \, \bar{\bar{s}}_1 + \frac{Q}{2 \pi T_1 p} - \frac{p}{\alpha_1} \, \bar{\bar{s}}_1 + \frac{K_1{'}}{T_1} \left. \frac{\partial \bar{\bar{s}}_1{'}}{\partial z} \right|_{z=0} = 0 \qquad \text{(II-23)}$$

and

$$- a^2 \, \bar{\bar{s}}_2 - \frac{p}{\alpha_2} \, \bar{\bar{s}}_2 - \frac{K_1{'}}{T_2} \left. \frac{\partial \bar{\bar{s}}_1{'}}{\partial z} \right|_{z=H_1{'}} = 0 \qquad \text{(II-24)}$$

The derivative of Eq. II-17 with respect to z is

$$\frac{\partial \bar{\bar{s}}_1{'}}{\partial z} = \sqrt{p/\alpha_1{'}} \left[\frac{\cosh (\sqrt{p/\alpha_1{'}} \, z)}{\sinh (\sqrt{p/\alpha_1{'}} \, H_1{'})} \, \bar{\bar{s}}_2 - \frac{\cosh [\, \sqrt{p/\alpha_1{'}} \, (H_1{'} - z) \,]}{\sinh (\sqrt{p/\alpha_1{'}} \, H_1{'})} \, \bar{\bar{s}}_1 \right]$$

so that

$$\left. \frac{\partial \bar{\bar{s}}_1{'}}{\partial z} \right|_{z=0} = \sqrt{p/\alpha_1{'}} \left[\frac{\bar{\bar{s}}_2}{\sinh (\sqrt{p/\alpha_1{'}} \, H_1{'})} - \bar{\bar{s}}_1 \coth (\sqrt{p/\alpha_1{'}} \, H_1{'}) \right] \qquad \text{(II-25)}$$

and

$$\left. \frac{\partial \bar{\bar{s}}_1{'}}{\partial z} \right|_{z=H_1{'}} = \sqrt{p/\alpha_1{'}} \left[\bar{\bar{s}}_2 \coth (\sqrt{p/\alpha_1{'}} \, H_1{'}) - \frac{\bar{\bar{s}}_1}{\sinh (\sqrt{p/\alpha_1{'}} \, H_1{'})} \right] \qquad \text{(II-26)}$$

Substituting II-25 in II-23 and II-26 in II-24, we obtain two equations in the two unknowns, $\bar{\bar{s}}_1$ and $\bar{\bar{s}}_2$:

$$- a^2 \bar{\bar{s}}_1 + \frac{Q}{2 \pi T_1 p} - \frac{p}{\alpha_1} \bar{\bar{s}}_1$$

$$+ \frac{K_1' \sqrt{p/\alpha_1'}}{T_1} \left[\frac{\bar{\bar{s}}_2}{\sinh (\sqrt{p/\alpha_1'}\ H_1')} - \bar{\bar{s}}_1 \coth (\sqrt{p/\alpha_1'}\ H_1') \right] = 0 \quad \text{(II-27)}$$

and

$$- a^2 \bar{\bar{s}}_2 - \frac{p}{\alpha_2} \bar{\bar{s}}_2$$

$$- \frac{K_1' \sqrt{p/\alpha_1'}}{T_2} \left[\bar{\bar{s}}_2 \coth (\sqrt{p/\alpha_1'}\ H_1') - \frac{\bar{\bar{s}}_1}{\sinh (\sqrt{p/\alpha_1'}\ H_1')} \right] = 0 \quad \text{(II-28)}$$

Let us define the functions

$$\left. \begin{aligned}
A_1(p) &\equiv \frac{p}{\alpha_1} + \frac{K_1' \sqrt{p/\alpha_1'}}{T_1}\ \coth (\sqrt{p/\alpha_1'}\ H_1') \\[2em]
A_2(p) &\equiv \frac{p}{\alpha_2} + \frac{K_1' \sqrt{p/\alpha_1'}}{T_2}\ \coth (\sqrt{p/\alpha_1'}\ H_1') \\[2em]
B_1(p) &\equiv \frac{K_1' \sqrt{p/\alpha_1'}}{T_1 \sinh (\sqrt{p/\alpha_1'}\ H_1')} \\[2em]
B_2(p) &\equiv \frac{K_1' \sqrt{p/\alpha_1'}}{T_2 \sinh (\sqrt{p/\alpha_1'}\ H_1')} \\[2em]
C(p) &\equiv \frac{Q}{2 \pi T_1 p}
\end{aligned} \right\} \quad \text{(II-29)}$$

Using these definitions, Eqs. II-27 and II-28 can be rearranged in the form

$$\left. \begin{aligned}
(a^2 + A_1) \bar{\bar{s}}_1 - B_1 \bar{\bar{s}}_2 &= C \\[1.5em]
B_2 \bar{\bar{s}}_1 - (a^2 + A_2) \bar{\bar{s}}_2 &= 0
\end{aligned} \right\} \quad \text{(II-30)}$$

Solving Eq. II-30 for $\bar{\bar{s}}_1$ and $\bar{\bar{s}}_2$ will give us the double transforms of the drawdowns in the aquifers

$$\bar{\bar{s}}_1 = \frac{C\,(a^2 + A_2)}{(a^2 + A_1)\,(a^2 + A_2) - B_1 B_2} \qquad\qquad \text{(II-31)}$$

and

$$\bar{\bar{s}}_2 = \frac{C\,B_2}{(a^2 + A_1)\,(a^2 + A_2) - B_1 B_2} \qquad\qquad \text{(II-32)}$$

3. Inversion of Hankel Transform

The next step in our development is to invert the double transforms in Eqs. II-17, II-31, and II-32 back into the domain of the Laplace transform. For this purpose, let us define the functions

$$\left.\begin{aligned}
D(p) &\equiv \sqrt{4\,B_1(p)\,B_2(p) + [A_1(p) - A_2(p)]^2} \\[2mm]
\xi_1{}^2(p) &\equiv \tfrac{1}{2}\,[A_1(p) + A_2(p) - D(p)] \\[2mm]
\xi_2{}^2(p) &\equiv \tfrac{1}{2}\,[A_1(p) + A_2(p) + D(p)]
\end{aligned}\right\} \qquad \text{(II-33)}$$

The denominator in Eqs. II-31 and II-32 can be rearranged so that

$$(a^2 + A_1)\,(a^2 + A_2) - B_1 B_2 = \left(a^2 + \frac{A_1 + A_2}{2}\right)^2 - \frac{D^2}{4}$$

With this in mind, Eqs. II-31 and II-32 may be expanded in the forms

$$\bar{\bar{s}}_1 = \frac{C(a^2 + A_2)}{D} \left(\frac{1}{a^2 + \xi_1{}^2} - \frac{1}{a^2 + \xi_2{}^2} \right) \qquad \text{(II-34)}$$

and

$$\bar{\bar{s}}_2 = \frac{C B_2}{D} \left(\frac{1}{a^2 + \xi_1{}^2} - \frac{1}{a^2 + \xi_2{}^2} \right) \qquad \text{(II-35)}$$

Using Eq. A-8 in Appendix A, the inverse Hankel transforms of II-34 and II-35 can immediately be written as

$$\bar{s}_1(r,p) = \frac{C(A_2 - \xi_1{}^2)}{D} K_0(\xi_1 r) - \frac{C(A_2 - \xi_2{}^2)}{D} K_0(\xi_2 r) \qquad \text{(II-36)}$$

and

$$\bar{s}_2(r,p) = \frac{C B_2}{D} [K_0(\xi_1 r) - K_0(\xi_2 r)] \qquad \text{(II-37)}$$

where A, B, C, D, and ξ are functions of the Laplace transform parameter p as defined in Eqs. II-29 and II-33. The inverse Hankel transfor of Eq. II-17 is simply

$$\bar{s}_1{}'(r,z,p) = \frac{\sinh(\sqrt{p/\alpha_1{}'}\ z)}{\sinh(\sqrt{p/\alpha_1{}'}\ H_1{}')} \bar{s}_2(r,p) + \frac{\sinh[\sqrt{p/\alpha_1{}'}\ (H_1{}' - z)]}{\sinh(\sqrt{p/\alpha_1{}'}\ H_1{}')} \bar{s}_1(r,p) \quad \text{(II-38)}$$

Eqs. II-36, II-37, and II-38 give the Laplace transforms of the draw-downs for each layer in the system.

4. Inversion of Laplace Transform

The inversion of Eqs. II-36 and II-37 can be accomplished with the aid of Mellin's inversion formula

$$s(r,t) = \frac{1}{2\pi i} \int_{\gamma - i\infty}^{\gamma + i\infty} (e^{\lambda t} - 1)\ \bar{s}(r,\lambda)\ d\lambda \qquad \text{(II-39)}$$

-193-

which can be written in this form due to the initial condition $s(r,0) = 0$. Here γ is some real positive constant, λ is a complex variable replacing p in the expressions for $\bar{s}(r,p)$, and $i = \sqrt{-1}$.

a. Determining Positions of Singularities

In order to apply Mellin's inversion formula to our problem, it is necessary that we determine the poles and branch points of the functions $\bar{s}_1(r,\lambda)$ and $\bar{s}_2(r,\lambda)$ in the complex domain of λ. From the definition of $C(p)$ in Eq. II-29, we immediately see that both of these functions have at least a simple pole at $\lambda = 0$. We also know from the definition of $K_0(\xi r)$ that this function has branch points at all values of λ that are roots of the equations $\xi_1(\lambda) = 0$ and $\xi_2(\lambda) = 0$. Our first step therefore will be to determine the roots of the equations

$$\xi_1^{\,2}(\lambda) \;=\; \frac{1}{2}\,[A_1(\lambda) + A_2(\lambda) - D(\lambda)] \;=\; 0 \qquad\qquad \text{(II-40)}$$

and

$$\xi_2^{\,2}(\lambda) \;=\; \frac{1}{2}\,[A_1(\lambda) + A_2(\lambda) + D(\lambda)] \;=\; 0 \qquad\qquad \text{(II-41)}$$

where A_1 and A_2 are defined in Eq. II-29 and D, ξ_1, and ξ_2 are defined in Eq. II-33.

Eqs. II-40 and II-41 can be written in the form

$$(A_1 + A_2)^2 \;=\; D^2 \;=\; 4\,B_1 B_2 + (A_1 - A_2)^2$$

so that

$$A_1 A_2 - B_1 B_2 \;=\; 0$$

Using the definitions in Eq. II-29, this can also be written as

-194-

$$\frac{\lambda^2}{\alpha_1 \alpha_2} + \frac{\lambda}{\alpha_1} \frac{K_1' \sqrt{\lambda/\alpha_1'}}{T_2} \coth(\sqrt{\lambda/\alpha_1'} \, H_1') + \frac{\lambda}{\alpha_2} \frac{K_1' \sqrt{\lambda/\alpha_1'}}{T_2} \coth(\sqrt{\lambda/\alpha_1'} \, H_1')$$

$$+ \frac{K_1'^2 \, \lambda/\alpha_1'}{T_1 T_2} \coth^2(\sqrt{\lambda/\alpha_1'} \, H_1') - \frac{K_1'^2 \, \lambda/\alpha_1'}{T_1 T_2 \, \sinh^2(\sqrt{\lambda/\alpha_1'} \, H_1')} = 0 \quad \text{(II-42)}$$

Let us define the complex variable

$$z \equiv \sqrt{\lambda/\alpha_1'} \; H_1' \qquad\qquad\qquad\qquad\qquad\qquad \text{(II-43)}$$

and the real positive constants

$$\left. \begin{aligned} a &\equiv \frac{\alpha_2 H_1' K_1'}{\alpha_1' T_2} \\[1em] b &\equiv \frac{\alpha_1 H_1' K_1'}{\alpha_1' T_1} \end{aligned} \right\} \qquad\qquad\qquad \text{(II-44)}$$

and

Multiplying Eq. II-42 throughout by $\dfrac{\alpha_1 \alpha_2 H_1'^4}{\alpha_1'^2} \sinh z$, and considering the identity $\cosh^2 z - 1 = \sinh^2 z$, this equation becomes

$$z^2 \left[(ab + z^2) \sinh z + z(a + b) \cosh z \right] = 0$$

which imples that either $z = 0$ or that the term in the brackets is zero. One can easily verify that $\lambda = 0$ is a solution of Eq. II-40 but not of Eq. II-41. Thus, $\lambda = 0$ is a branch point of $K_0(\xi_1 r)$ and is not a branch point of $K_0(\xi_2 r)$.

If $z \neq 0$, the term inside the brackets must vanish and we have

$$(ab + z^2)(e^z - e^{-z}) + z(a + b)(e^z + e^{-z}) = 0$$

When this is multiplied by e^z and solved for e^{2z}, the result is

$$e^{2z} = \frac{z^2 + ab - z(a+b)}{z^2 + ab + z(a+b)} \tag{II-45}$$

Let $z = x + iy$, where x and y are real variables. The modulus of e^{2z} is e^{2x}, so that from Eq. II-45 we will have

$$e^{2x} = \frac{|(x + iy)^2 + ab - (x + iy)(a+b)|}{|(x + iy)^2 + ab + (x + iy)(a+b)|}$$

Evaluating the moduli in this equation and taking the square of the result, we obtain

$$e^{4x} = \frac{[x^2 - y^2 + ab - x(a+b)]^2 + y^2[a+b-2x]^2}{[x^2 - y^2 + ab + x(a+b)]^2 + y^2[a+b+2x]^2} \tag{II-46}$$

where all the terms are real.

If $x > 0$ then $e^{4x} > 1$, but the numerator in Eq. II-46 is smaller than the denominator because the constants a and b are positive by definition. This is a contradiction, so $x \not> 0$.

If $x < 0$ then $e^{4x} < 1$, but the numerator in Eq. II-46 is larger than the denominator, which again is a contradiction. Therefore, $x \not< 0$.

The only possibility left is $x = 0$, in which case z is purely imaginary and Eq. II-46 is obviously satisfied. Eq. II-43 therefore implies that the roots of Eqs. II-40 and II-41 are all real, non-positive values of the form

$$\lambda = -y^2 \frac{\alpha_1'}{H_1'^2}$$

Substituting in Eqs. II-40 and II-41 will reveal that there is an infinite number of solutions y_n to these equations. We therefore conclude that each of the

equations $\xi_1(\lambda) = 0$ and $\xi_2(\lambda) = 0$ has at most an infinite number of distinct real, non-positive roots, λ_n, where $n = 1, 2, 3, \ldots$.

Our next step is to show that the equation $D(\lambda) = 0$ does not have any real roots. For this purpose let

$$z \equiv \sqrt{\lambda/\alpha_1'} \; H_1'$$

$$a \equiv \frac{\alpha_1' \sqrt{T_1 T_2}}{2 K_1' H_1'} \left(\frac{1}{\alpha_1} - \frac{1}{\alpha_2} \right)$$

$$b \equiv \frac{\sqrt{T_1 T_2}}{2} \left(\frac{1}{T_1} - \frac{1}{T_2} \right)$$

where z is a complex variable and a and b are real constants. When the expression for $D^2(\lambda)$ in Eq. II-33 is multiplied by $(T_1 T_2 H_1'^2)/(4 K_1'^2)$ and equated to zero, one obtains

$$\frac{z^2}{\sinh^2 z} + a^2 z^4 + 2 a b z^3 \coth z + b^2 z^2 \coth^2 z = 0$$

Multiplying by $\sinh^2 z$ and solving for a, we get

$$a = \frac{- b \cosh z \pm i}{z \sinh z} \tag{II-47}$$

Suppose that z is real and let $z = x$. Since a is real, the imaginary term in Eq. II-47 must vanish so that

$$\frac{1}{x \sinh x} = 0$$

This is impossible when x is finite, so z cannot be real. If z is imaginary, let $z = i y$. Eq. II-47 then becomes

-197-

$$a = \frac{b \cos y \pm i}{2 y \sin y}$$

and since a is real, we require that

$$\frac{1}{2 y \sin y} = 0$$

which again is impossible. Therefore z is not imaginary, and $\lambda = z^2 \alpha_1' / H_1'^2$ is not real. Thus, the equation $D(\lambda) = 0$ has no roots along the real axis.

Suppose that there exists some $\lambda = \lambda_0$ which satisfies the equation $D(\lambda) = 0$. Using the definitions in Eq. II-33, Eq. II-36 can be written in the form

$$\bar{s}_1(r, \lambda) = \frac{C}{2 D} \left[(A_2 - A_1 + D) K_0(\xi_1 r) - (A_2 - A_1 - D) K_0(\xi_2 r) \right]$$

where A_1, A_2, C, D, ξ_1, and ξ_2 are all functions of λ. Since

$$\lim_{D \to 0} \xi_1 = \lim_{D \to 0} \xi_2$$

we see that both numerator and denominator in this equation tend to zero as D approaches zero. In order to apply L'Hospital's rule to our problem we note that

$$\frac{d K_0(z)}{d z} = - K_1(z)$$

and

$$\frac{d K_0(\xi_1 r)}{d D} = \frac{d K_0(\xi_1 r)}{d(\xi_1 r)} \frac{d(\xi_1 r)}{d D}$$

$$= - K_1(\xi_1 r) \frac{(- r/2)}{2 \xi_1} \xrightarrow{D \to 0} \left. \frac{r K_1(\xi_1 r)}{4 \xi_1} \right|_{\lambda = \lambda_0}$$

which is finite because λ_o is not real and therefore is not a root of $\xi_1(\lambda) = 0$. Similarly,

$$\frac{d K_0(\xi_2 r)}{d D} \xrightarrow{D \to 0} - \left. \frac{r K_1(\xi_2 r)}{4 \xi_2} \right|_{\lambda = \lambda_o}$$

which is also finite. Using L'Hospital's rule, the limit of $\bar{s}_1(r, \lambda)$ as λ approaches λ_o can be written as

$$\lim_{\lambda \to \lambda_o} \bar{s}_1(r, \lambda) = \frac{Q}{4 \pi T_1 \lambda_o} \lim_{D \to 0} \left[K_0(\xi_1 r) + (A_2 - A_1 + D) \frac{d K_0(\xi_1 r)}{d D} \right.$$

$$\left. + K_0(\xi_2 r) - (A_2 - A_1 - D) \frac{d K_0(\xi_2 r)}{d D} \right]$$

$$= \frac{Q}{4 \pi T_1 \lambda_o} \left[K_0(\xi_1 r) + K_0(\xi_2 r) \right.$$

$$\left. + \frac{r}{4} (A_2 - A_1) \left(\frac{K_1(\xi_1 r)}{\xi_1} + \frac{K_1(\xi_2 r)}{\xi_2} \right) \right]_{\lambda = \lambda_o}$$

which is finite because λ_o is not zero and is not a root of $\xi_1(\lambda) = 0$ nor of $\xi_2(\lambda) = 0$.

In the same way we can treat Eq. II-37 using L'Hospital's rule to show that

$$\lim_{\lambda \to \lambda_o} \bar{s}_2(r, \lambda) = \frac{Q}{4 \pi T_1 \lambda_o} B_2 \Bigg|_{\lambda = \lambda_o} \lim_{D \to 0} \left[\frac{d K_0(\xi_1 r)}{d D} - \frac{d K_0(\xi_2 r)}{d D} \right]$$

$$= \frac{Q}{4 \pi T_1 \lambda_o} \left[B_2 \frac{r}{4} \left(\frac{K_1(\xi_1 r)}{\xi_1} + \frac{K_1(\xi_2 r)}{\xi_2} \right) \right]_{\lambda = \lambda_o}$$

which is also finite. Therefore, the roots λ_0 of $D(\lambda)$ are not singular points of $\bar{s}_1(r, \lambda)$ or of $\bar{s}_2(r, \lambda)$.

Multiplying numerators and denominators in Eqs. II-36 and II-37 by $\sinh(\sqrt{\lambda/\alpha_1'}\ H_1')$ will reveal that the roots of $\sinh(\sqrt{\lambda/\alpha_1'}\ H_1') = 0$ are removable singularities of $\bar{s}_1(r, \lambda)$ and $\bar{s}_2(r, \lambda)$.

b. Solutions in Aquifers

We have shown above that the only singularities in Eqs. II-36 and II-37 occur at values of λ that are singular points of the terms $K_0(\xi_1 r)/\lambda$ and $K_0(\xi_2 r)/\lambda$. In applying Mellin's inversion formula to our problem we can therefore perform the integration along the contour shown in Fig. II-5 where Γ_n and Γ_n' are semicircles of radii ε about the roots of either $\xi_1(\lambda) = 0$ or
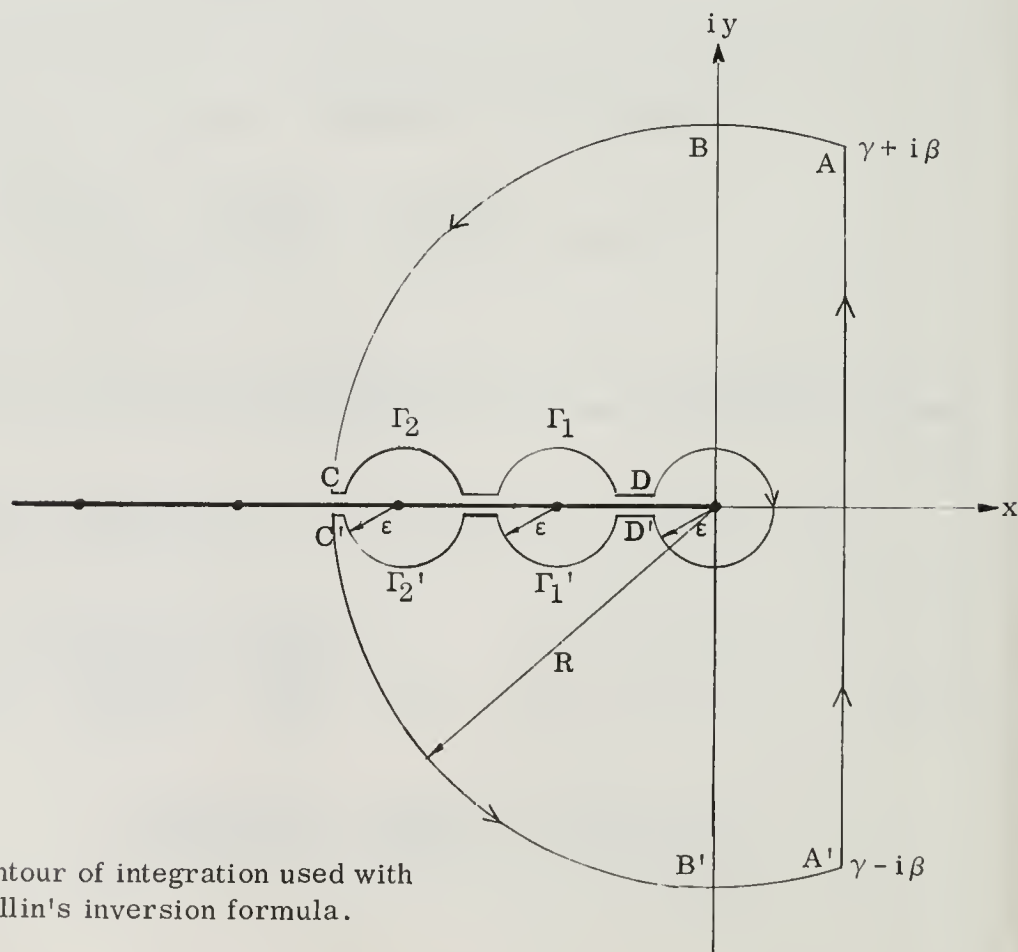
Fig. II-5. Contour of integration used with Mellin's inversion formula.

$\xi_2(\lambda) = 0$. We agree to choose our branch line along the negative real axis and to perform the integration in a counterclockwise fashion.

If we omit the constant $Q/(2\pi T_1)$ in Eq. II-36, then the first term becomes

$$\frac{A_2 - \xi_1^2}{D} \quad \frac{K_0(\xi_1 r)}{\lambda}$$

Let I_{AC} denote the integral with respect to λ of

$$(e^{\lambda t} - 1) \frac{A_2 - \xi_1^2}{D} \quad \frac{K_0(\xi_1 r)}{\lambda}$$

along the AC portion of the contour, let I_{Γ_n} be the corresponding integral along Γ_n, and so on. According to Cauchy's theorem, the integral along the entire contour vanishes, and at the limit as $\varepsilon \to 0$ and $R \to \infty$ we can write

$$-\int_{\gamma - i\infty}^{\gamma + i\infty} (e^{\lambda t} - 1) \frac{A_2 - \xi_1^2}{D} \quad \frac{K_0(\xi_1 r)}{\lambda} =$$

$$\lim_{\substack{\varepsilon \to 0 \\ R \to \infty}} \left[I_{AC} + I_{CD} + I_{DD'} + I_{D'C} + I_{C'A'} + \sum_{n=1}^{\infty} (I_{\Gamma_n} + I_{\Gamma_n'}) \right] \quad \text{(II-48)}$$

We now proceed to evaluate the limit of each integral on the right hand side of this equation. On the DD' portion of the contour, let $\lambda = \varepsilon\, e^{i\theta}$ so that

$$I_{DD'} = i \int_{\pi}^{-\pi} [\exp(\varepsilon\, e^{i\theta} t) - 1] \frac{A_2(\varepsilon\, e^{i\theta}) - \xi_1^2(\varepsilon\, e^{i\theta})}{D(\varepsilon\, e^{i\theta})} K_0[\xi_1(\varepsilon\, e^{i\theta})r]d\theta \quad \text{(II-49)}$$

-201-

The function $K_0(\lambda)$ can be expanded in the form

$$K_0(\lambda) = -\left[\overline{\gamma} + \ln(\tfrac{\lambda}{2})\right] I_0(\lambda) + \sum_{n=1}^{\infty} \frac{(\lambda/2)^{2n}}{(n!)^2}\left[1 + \frac{1}{2} + \frac{1}{3} + \ldots + \frac{1}{r}\right] \qquad \text{(II-50)}$$

where $\overline{\gamma}$ is Euler's constant and

$$I_0(\lambda) = \sum_{n=0}^{\infty} \frac{(\lambda/2)^{2n}}{(n!)^2}$$

We therefore see that as ε approaches zero, all the terms in the expanded series of $K_0[\xi_1(\varepsilon\, e^{i\theta})\, r]$ vanish or remain finite, except for those terms that involve $\ln \xi_1$. A glance at Eqs. II-29 and II-33 will reveal that the function $\xi_1^2(\lambda)$ is analytic everywhere except at the roots $\lambda_m = -m^2\, \pi^2\, \alpha_1'/{H_1'}^2$ of the equation $\sinh(\sqrt{\lambda/\alpha_1'}\ H_1') = 0$, where $m = 1, 2, \ldots$. Thus, there exists some neighborhood around $\lambda = 0$ in which $\xi_1^2(\lambda)$ is analytic and can be expanded in the Maclaurin series

$$\xi_1^2(\lambda) = a_m \lambda^m + a_{m+1} \lambda^{m+1} + \ldots$$

where a_m is the first non-zero coefficient in the expansion. We can therefore write

$$\lim_{\lambda \to 0} (e^{\lambda} - 1)\, \ln[\xi_1^2(\lambda)] = \lim_{\lambda \to 0} (e^{\lambda} - 1)\, \ln(a_m \lambda^m + a_{m+1} \lambda^{m+1} + a_{m+2} \lambda^{m+2} + \ldots)$$

$$= \lim_{\lambda \to 0} (e^{\lambda} - 1)\, [m \ln \lambda + \ln(a_m + a_{m+1} \lambda + a_{m+2} \lambda^2 + \ldots)]$$

$$= 0 \qquad \text{(II-51)}$$

because

$$\lim_{\lambda \to 0} (e^{\lambda} - 1) \ln \lambda = 0$$

while the second term in the brackets remains finite.

If we now make DD' in Fig. II-5 sufficiently small so that it is within the neighborhood in which $\xi_1^2(\lambda)$ is analytic, then from Eq. II-50 we have

$$\lim_{\lambda \to 0} \left| I_{DD'} \right| \leq \lim_{\lambda \to 0} \left| (e^{\lambda t} - 1) \frac{A_2(\lambda) - \xi_1^2(\lambda)}{D(\lambda)} K_0(\xi_1 r) \right| 2\pi =$$

$$2\pi \left| \frac{A_2(0) - \xi_1^2(0)}{D(0)} \right| \lim_{\lambda \to 0} \left| (e^{\lambda t} - 1) \ln \lambda \right| = 0$$

because $\lambda = 0$ is not a root of $D(\lambda) = 0$. Therefore

$$\lim_{\varepsilon \to 0} I_{DD'} = 0 \tag{II-52}$$

On Γ_n let $\lambda = \lambda_n + \varepsilon e^{i\theta}$ where λ_n is a root of $\xi_1(\lambda) = 0$. The integral then becomes

$$I_{\Gamma_n} = i\varepsilon \int_\pi^0 \{ \exp[\lambda_n + \varepsilon e^{i\theta})t] - 1 \} \frac{A_2(\lambda_n + \varepsilon e^{i\theta}) - \xi_1^2(\lambda_n + \varepsilon e^{i\theta})}{D(\lambda_n + \varepsilon e^{i\theta})}$$

$$\cdot K_0(\xi_1 r) \frac{e^{i\theta} d\theta}{\lambda_n + \varepsilon e^{i\theta}} \tag{II-53}$$

Using the same argument as before, we can say that $\xi_1^2(\lambda)$ has a Taylor expansion in some small neighborhood around $\lambda = \lambda_n$ of the form

$$\xi_1^2(\lambda) = a_m(\lambda - \lambda_n)^m + a_{m+1}(\lambda - \lambda_n)^{m+1} + \ldots \tag{II-54}$$

-203-

where a_m is the first non-zero coefficient in the series. From what was said earlier, we immediately conclude that

$$\lim_{\varepsilon \to 0} \varepsilon K_0(\xi_1 r) = \lim_{\varepsilon \to 0} \varepsilon \ln (\xi_1^2 r^2) = \lim_{\substack{\varepsilon \to 0 \\ \text{or } \lambda \to \lambda_n}} \varepsilon \{ m \ln (\lambda - \lambda_n) +$$

$$+ \ln [a_m + a_{m+1}(\lambda - \lambda_n) + a_{m+2}(\lambda - \lambda_n)^2 + \ldots] + \ln r^2 \} = 0 \quad \text{(II-55)}$$

because the term in brackets remains finite. Again, if we make Γ_n small enough so that it is within the neighborhood of Γ_n in which $\xi_1^2(\lambda)$ is analytic, then from Eqs. II-53 and II-55 we have

$$\lim_{\substack{\varepsilon \to 0 \\ \text{or } \lambda \to \lambda_n}} \left| I_{\Gamma_n} \right| \leq \lim_{\varepsilon \to 0} \left| \{ \exp[(\lambda_n + \varepsilon e^{i\theta}) t] - 1 \} \right.$$

$$\cdot \frac{A_2(\lambda_n + \varepsilon e^{i\theta}) - \xi_1^2(\lambda_n + \varepsilon e^{i\theta})}{D(\lambda_n + \varepsilon e^{i\theta})} \frac{e^{i\theta}}{\lambda_n + \varepsilon e^{i\theta}} K_0(\xi_1 r) \left| \varepsilon \pi \right.$$

$$= \pi \left| (e^{\lambda_n t} - 1) \frac{A_2(\lambda_n) - \xi_1^2(\lambda_n)}{D(\lambda_n)} \frac{1}{\lambda_n} \right| \lim_{\varepsilon \to 0} \left| \varepsilon K_0(\xi_1 r) \right| = 0$$

because $\lambda = \lambda_n$ is not a root of $D(\lambda) = 0$. Therefore

$$\lim_{\varepsilon \to 0} I_{\Gamma_n} = 0 \qquad\qquad\qquad\qquad\qquad\qquad \text{(II-56)}$$

and similarly it can be shown that

$$\lim_{\varepsilon \to 0} I_{\Gamma_n'} = 0 \qquad\qquad\qquad\qquad\qquad\qquad \text{(II-57)}$$

On AC let $\lambda = R\,e^{i\theta}$ and

$$I_{AC} = \int_{AC} (e^{\lambda t} - 1) \frac{A_2(\lambda) - \xi_1^2(\lambda)}{D(\lambda)} \frac{K_0(\xi_1 r)}{\lambda}\, d\lambda \qquad \text{(II-58)}$$

From Eq. II-33 we have

$$\left| \frac{A_2 - \xi_1^2}{D} \right| = \left| \frac{A_2 - A_1 + D}{2D} \right| = \left| \frac{A_2 - A_1}{2\sqrt{4B_1 B_2 + (A_1 - A_2)^2}} + \frac{1}{2} \right| \,,$$

which remains finite as $R \to \infty$ unless $D(R) \to 0$. However, the latter possibility can be disregarded because we have shown earlier that the roots of $D(\lambda) = 0$ are not singular points of $\bar{s}_1(r, \lambda)$ and $\bar{s}_2(r, \lambda)$. We can therefore, for the sake of convenience, assume that $D(\lambda)$ has no roots at all and that the above expression remains finite as $R \to \infty$. (Note that this is only necessary because we treat the two parts of $\bar{s}_1$ separately.)

The modulus $|\xi_1(\lambda)|$ approaches infinity as R approaches infinity. The argument of $\xi_1(\lambda)$, which according to Eqs. II-33 and II-29 is the same as the argument θ of λ, is within the limits $-\pi < \theta \le \pi$ on AC. Therefore, for large values of R, we can use the asymptotic expression

$$K_0(\xi_1 r) \approx \sqrt{\frac{\pi}{2\xi_1 r}}\, e^{-\xi_1 r} \qquad \text{(II-59)}$$

On this basis we can now conclude that there exists some real constant M such that

$$\left| \frac{A_2(\lambda) - \xi_1^2(\lambda)}{D(\lambda)} \frac{K_0(\xi_1 r)}{\lambda} \right| \approx \left| \frac{A_2(\lambda) - \xi_1^2(\lambda)}{D(\lambda)} \right| \frac{\sqrt{\pi/2}}{R} \frac{1}{\left| \sqrt{\xi_1 r}\, e^{\xi_1 r} \right|} < M R^{-1}$$

-205-

because all the expressions that appear here are bounded. We can therefore use the lemma on p. 76 in Carslaw and Jaeger (2) to conclude that

$$\lim_{R \to \infty} I_{AC} = 0 \qquad (II-60)$$

Similarly, it can be shown that

$$\lim_{R \to \infty} I_{C'A'} = 0 \qquad (II-61)$$

On CD, let $\lambda = x^2 e^{i\pi}$ in the first term of Eq. II-36 and let $\xi_1^* \equiv \xi_1(x^2 e^{i\pi})$. Defining the function

$$D(x) \equiv r^2 D(x^2 e^{\pm i\pi}) = r^2 \left\{ \frac{4 K_1'^2 x^2}{T_1 T_2 \alpha_1' \sin^2 (x H_1'/\sqrt{\alpha_1'})} \right.$$

$$\left. + \left[\left(\frac{1}{\alpha_1} - \frac{1}{\alpha_2} \right) x^2 + \left(\frac{1}{T_2} - \frac{1}{T_1} \right) \frac{K_1' x}{\sqrt{\alpha_1'}} \cot (x H_1'/\sqrt{\alpha_1'}) \right]^2 \right\}^{1/2} \qquad (II-62)$$

and noting that $\pm i \, x \coth (\pm i \, x H_1'/\sqrt{\alpha_1'}) = x \cot (x H_1'/\sqrt{\alpha_1'})$, we can write the first term in Eq. II-36 as

$$f(x) \equiv \frac{A_2(x^2 e^{\pm i\pi}) - \xi_1^2(x^2 e^{\pm i\pi})}{D(x^2 e^{\pm i\pi})}$$

$$= \frac{r^2}{2 D(x)} \left[\left(\frac{1}{\alpha_1} - \frac{1}{\alpha_2} \right) x^2 + \left(\frac{1}{T_2} - \frac{1}{T_1} \right) \frac{K_1' x}{\sqrt{\alpha_1'}} \cot (x H_1'/\sqrt{\alpha_1'}) \right] + \frac{1}{2} \qquad (II-63)$$

where $f(x)$ is an even function of x. We can then write

$$\lim_{\substack{\varepsilon \to 0 \\ R \to \infty}} I_{CD} = 2 \int_{-\infty}^{0} (e^{-x^2 t} - 1) \, f(x) \, K_0(\xi_1^* r) \frac{dx}{x} \qquad (II-64)$$

Now let us consider the integral of the first term in Eq. II-36 along D'C', and let $\lambda = x^2 e^{-i\pi}$ and $\xi_1^{**} \equiv \xi_1 (x^2 e^{-i\pi})$. Using these definitions together with Eq. II-63 we have

$$\lim_{\substack{\varepsilon \to 0 \\ R \to \infty}} I_{D'C'} = 2 \int_0^\infty (e^{-x^2 t} - 1) f(x) K_0 (\xi_1^{**} r) \frac{dx}{x} \qquad (II-65)$$

Let us define a new function

$$\omega_1^2 (x) \equiv \frac{r^2}{2} \left[\left(\frac{1}{\alpha_1} + \frac{1}{\alpha_2} \right) x^2 - \left(\frac{1}{T_1} + \frac{1}{T_2} \right) \frac{K_1' x}{\sqrt{\alpha_1'}} \cot (x H_1'/\sqrt{\alpha_1'}) \right] + \frac{1}{2} D(x) \qquad (II-66)$$

and note that

$$\cosh \left(\frac{x H_1' e^{\pm i\pi/2}}{\sqrt{\alpha_1'}} \right) = \cos \left(\frac{x H_1'}{\sqrt{\alpha_1'}} \right)$$

and $\qquad (II-67)$

$$\frac{x e^{\pm i\pi/2}}{\sinh \left(\frac{x H_1' e^{\pm i\pi/2}}{\sqrt{\alpha_1'}} \right)} = \frac{-x e^{\pm i\pi}}{\sin \left(\frac{x H_1'}{\sqrt{\alpha_1'}} \right)}$$

Using Eqs. II-66 and II-67 together with II-33 and II-29, we can write

$$(r \xi_1^*)^2 = \omega_1^2 (x) e^{i\pi}$$

and $\qquad (II-68$

$$(r \xi_1^{**})^2 = \omega_1^2 (x) e^{-i\pi}$$

Obviously, $\omega_1^2 (x)$ is real and takes on both positive and negative values as x changes between zero and $\pm \infty$. Eqs. II-68 therefore suggest

$$\left. \begin{array}{l} \arg{(r\,\xi_1{}^*)}^2 \;=\; \pi \\[2mm] \arg{(r\,\xi_1{}^{**})}^2 \;=\; -\,\pi \end{array} \right\} \qquad \text{when } \omega_1{}^2\,(x) \,>\, 0$$

and

$$\arg{(r\,\xi_1{}^*)}^2 \;=\; \arg{(r\,\xi_1{}^{**})}^2 \;=\; 0 \;\; \text{when } \omega_1{}^2\,(x) \,<\, 0 \left. \phantom{\frac{1}{2}} \right\} \tag{II-69}$$

One can easily verify that

$$I_0\,(z\,e^{\pm\,i\,\pi/2}) \;=\; J_0\,(z)$$

so that from II-68 we have

$$I_0\,(r\,\xi_1{}^*) \;=\; I_0\,(r\,\xi_1{}^{**}) \;=\; J_0\!\left(\omega_1\,(x)\right) \tag{II-70}$$

Considering the fact that the numerical values of even powers of $(r\,\xi_1{}^*)$ and $(r\,\xi_1{}^{**})$ are identical and using Eqs. II-50, II-69, and II-70, we see that

$$K_0\,(r\,\xi_1{}^{**}) \,-\, K_0\,(r\,\xi_1{}^*) \;=\; \frac{1}{2}\,\ell n\,(r\,\xi_1{}^*)^2\,I_0\,(r\,\xi_1{}^*) \,-\, \frac{1}{2}\,\ell n\,(r\,\xi_1{}^{**})^2\,I_0\,(r\,\xi_1{}^{**})$$

$$=\; \frac{i}{2}\,J_0\!\left(\omega_1\,(x)\right)\left[\,\arg{(r\,\xi_1{}^*)}^2 \,-\, \arg{(r\,\xi_1{}^{**})}^2\,\right]$$

$$=\; \begin{cases} i\,\pi\,J_0\!\left(\omega_1\,(x)\right) & \text{when } \omega_1{}^2\,(x) \,>\, 0 \\[3mm] 0 & \text{when } \omega_1{}^2\,(x) \,<\, 0 \end{cases} \tag{II-71}$$

Combining this with Eqs. II-64 and II-65 gives for the first term in Eq. II-36

$$\lim_{\substack{\varepsilon \to 0 \\ R \to 0}}\,(I_{CD} + I_{D'C'}) \;=\; -\,2\int_0^{-\infty}(1 - e^{-x^2 t})\,f\,(x)\,[\,K_0\,(r\,\xi_1{}^{**}) - K_0\,(r\,\xi_1{}^*)\,]\,\frac{dx}{x}$$

$$=\; -\,2\,\pi\,i\int_0^{\infty}(1 - e^{-x^2 t})\,f\,(x)\,J_0\!\left(\omega_1\,(x)\right)\,\frac{dx}{x} \tag{II-72}$$

where the function $J_0\left(\omega_1(x)\right)$ must be set to zero when $\omega_1^2(x) < 0$. Substituting this result together with Eqs. II-52, II-56, II-57, II-60, and II-61 into Eq. II-48 and dividing throughout by $2\pi i$, we obtain

$$\frac{1}{2\pi i} \int_{\gamma-i\infty}^{\gamma+i\infty} (e^{\lambda t} - 1) \frac{A_2(\lambda) - \xi_1^2(\lambda)}{D(\lambda)} \frac{K_0\left(\xi_1(\lambda)\,r\right)}{\lambda} \, d\lambda$$

$$= \int_0^\infty (1 - e^{-x^2 t}) \, f(x) \, J_0\left(\omega_1(x)\right) \frac{dx}{x} \tag{II-73}$$

The second term in Eq. II-36 can be treated in a completely analogous fashion. Let us define the function

$$\omega_2^2(x) \equiv \omega_1^2(x) - D(x) \tag{II-74}$$

and note that

$$\frac{A_2(x^2 e^{\pm i\pi}) - \xi_2^2(x^2 e^{\pm i\pi})}{D(x^2 e^{\pm i\pi})} = f(x) - 1$$

From Eq. II-74 one can easily show by analogy to the previous development that

$$\frac{1}{2\pi i} \int_{\gamma-i\infty}^{\gamma+i\infty} (e^{\lambda t} - 1) \frac{A_2(\lambda) - \xi_2^2(\lambda)}{D(\lambda)} \frac{K_0\left(\xi_2(\lambda)\,r\right)}{\lambda} \, d\lambda$$

$$= \int_0^\infty (1 - e^{-x^2 t}) \, [\, f(x) - 1 \,] \, J_0\left(\omega_2(x)\right) \frac{dx}{x} \tag{II-75}$$

We are now in a position to obtain the inverse Laplace transform of $\bar{s}_1(r,p)$ in Eq. II-36. For this purpose let

$$G(x) \equiv 1 - 2\,f(x) \tag{II-76}$$

such that $[1 - G(x)] = 2\,f(x)$ and $[1 + G(x)] = 2\,[1 - f(x)]$. Substituting Eq. II-36 in Mellin's inversion formula II-39 and using Eqs. II-73, II-75, and II-76, we immediately obtain

$$
s_1(r,t) = \frac{Q}{4\pi T_1} \int_0^\infty (1 - e^{-x^2 t}) \Big[\big[1 - G(x) \big]\, J_0\big(\omega_1\,(x)\big)
$$
$$
+ \big[1 + G(x) \big]\, J_0\big(\omega_2\,(x)\big) \Big]\,\frac{dx}{x} \tag{II-77}
$$

where the Bessel functions must be set to zero when their arguments are not real.

In order to invert Eq. II-37, let us define the function

$$
g(x) \equiv \frac{B_2(x^2 e^{\pm i\pi})}{D(x^2 e^{\pm i\pi})} = \frac{r^2\,K_1'\,x}{T_2\,\sqrt{\alpha_1'}\ D(x)\,\sin(x\,H_1'/\sqrt{\alpha_1'}\,)} \tag{II-78}
$$

Following the same development as before, we arrive at the inverse Laplace transform of $\bar{s}_2(r,p)$

$$
s_2(r,t) = \frac{1}{2\pi i} \int_{\gamma - i\infty}^{\gamma + i\infty} (e^{\lambda t} - 1)\frac{Q}{2\pi T_1}\frac{B_2(\lambda)}{D(\lambda)} \Big[K_0\big(\xi_1(\lambda)\,r\big) - K_0\big(\xi_2(\lambda)\,r\big) \Big]\frac{d\lambda}{\lambda}
$$
$$
= \frac{Q}{4\pi T_1} \int_0^\infty (1 - e^{-x^2 t})\,2\,g(x) \Big[J_0\big(\omega_1\,(x)\big) - J_0\big(\omega_2\,(x)\big) \Big]\frac{dx}{x} \tag{II-79}
$$

where the Bessel functions must be set to zero when their arguments are not real.

In order to write Eqs. II-77 and II-79 in a more convenient form, let us define a new variable

$$y \equiv \frac{x H_1'}{\sqrt{\alpha_1'}}$$

and the dimensionless parameters

$$\left.\begin{aligned}
\bar{t}_{D_1} &\equiv \frac{\alpha_1' t}{H_1'^2} \\[4pt]
\theta_{11} &\equiv \frac{\alpha_1' r^2}{\alpha_1 H_1'^2} \\[4pt]
\theta_{21} &\equiv \frac{\alpha_1' r^2}{\alpha_2 H_1'^2} \\[4pt]
\eta_{11} &\equiv \frac{K_1' r^2}{T_1 H_1'} \\[4pt]
\eta_{21} &\equiv \frac{K_1' r^2}{T_2 H_1'}
\end{aligned}\right\} \tag{II-80}$$

The functions defined in Eqs. II-62, II-63, II-66, II-74, and II-76 may now be written in the form

$$\left.\begin{aligned}
D(y) &= \left\{ \frac{4 \eta_{11} \eta_{21} y^2}{\sin^2 y} + \left[(\theta_{11} - \theta_{21}) y^2 + (\eta_{21} - \eta_{11}) y \cot y \right]^2 \right\}^{1/2} \\[6pt]
\omega_1^2(y) &= \frac{1}{2} \left[(\theta_{11} + \theta_{21}) y^2 - (\eta_{11} + \eta_{21}) y \cot y + D(y) \right] \\[6pt]
\omega_2^2(y) &= \omega_1^2(y) - D(y) \\[6pt]
G(y) &= \frac{1}{D(y)} \left[(\theta_{21} - \theta_{11}) y^2 + (\eta_{11} - \eta_{21}) y \cot y \right]
\end{aligned}\right\} \tag{II-81}$$

In terms of these definitions, Eq. II-77 becomes

$$s_1(r,t) = \frac{Q}{4\pi T_1} \int_0^\infty (1 - e^{-y^2 \bar{t} D_1}) \left[\left(1 - G(y) \right) J_0\left(\omega_1 (y) \right) \right.$$

$$\left. + \left(1 + G(y) \right) J_0\left(\omega_2 (y) \right) \right] \frac{dy}{d} \tag{II-82}$$

The function in II-78 will become $g(y) = \eta_{21} y / (D(y) \sin y)$ so that Eq. II-79 may be written as

$$s_2(r,t) = \frac{Q}{4\pi T_1} \int_0^\infty (1 - e^{-y^2 \bar{t} D_1}) \frac{2\eta_{21}}{D(y)} \left[J_0\left(\omega_1 (y) \right) - J_0\left(\omega_2 (y) \right) \right] \frac{dy}{\sin y} \tag{II-83}$$

In both of these equations it is understood that the respective Bessel functions must vanish when $\omega_1^2 (y) < 0$ and $\omega_2^2 (y) < 0$.

c. Solution in Aquitard

To obtain the solution for the aquitard, it is necessary to invert the expression in Eq. II-38. From tables of Laplace transforms we know that

$$L^{-1} \left[\frac{\sinh (\sqrt{p/\alpha_1'}\ z)}{\sinh (\sqrt{p/\alpha_1'}\ H_1')} \right]$$

$$= \frac{2\pi \alpha_1'}{H_1'^2} \sum_{n=1}^\infty (-1)^n n \exp(-n^2 \pi^2 t \alpha_1'/ H_1'^2) \sin \frac{n\pi z}{H_1'} \tag{II-84}$$

and

$$L^{-1} \left[\frac{\sinh [\sqrt{p/\alpha_1'}\ (H_1'- z)]}{\sinh (\sqrt{p/\alpha_1'}\ H_1'} \right]$$

$$= \frac{2\pi \alpha_1'}{H_1'^2} \sum_{n=1}^\infty (-1)^n n \exp(-n^2 \pi^2 t \alpha_1'/H_1'^2) \sin \left[n\pi \left(1 - \frac{z}{H_1'} \right) \right] \tag{II-85}$$

The convolution of the functions $(1 - e^{-y^2 \bar{t} D1})$ and $e^{-n^2 \pi^2 \bar{t} D1}$ is

$$(1 - e^{-y^2 \bar{t} D1}) * e^{-n^2 \pi^2 \bar{t} D1} = \int_0^t \left(1 - e^{-y^2(\alpha_1' T/H_1'^2)}\right) \exp[-n^2 \pi^2 \alpha_1'(t - T)/H_1'^2] \, dT$$

$$= \frac{H_1'^2}{\alpha_1'} \int_0^{\bar{t} D_1} (1 - e^{-y^2 v}) \exp[-n^2 \pi^2 (\bar{t}_{D_1} - v)] \, dv$$

$$= \frac{H_1'^2}{\alpha_1'} \left[\frac{1 - e^{-n^2 \pi^2 \bar{t} D1}}{n^2 \pi^2} + \frac{e^{-y^2 \bar{t} D1} - e^{-n^2 \pi^2 \bar{t} D1}}{y^2 - n^2 \pi^2} \right] \quad \text{(II-86)}$$

where the dummy variable of integration T has been replaced by the dummy variable $v = T \alpha_1' / H_1'^2$.

We must now use the Convolution Theorem (2, p. 7) which can be stated as follows. If $\bar{x}_1(p)$ and $\bar{x}_2(p)$ are the Laplace transforms of $x_1(t)$ and $x_2(t)$, then $\bar{x}_1(p) \bar{x}_2(p)$ is the transform of

$$x_1(t) * x_2(t) = \int_0^t x_1(T) x_2(t - T) \, dT = \int_0^t x_1(t - T) x_2(T) \, dT$$

Applying this theorem to Eq. II-38 using Eqs. II-82 through II-86, we obtain

$$s_1'(r, z, t) = \frac{Q}{4 \pi T_1} 2 \pi \sum_{n=1}^{\infty} (-1)^n n \left\{ \sin \frac{n \pi z}{H_1'} \int_0^{\infty} \left[\frac{1 - e^{-n^2 \pi^2 \bar{t} D1}}{n^2 \pi^2} \right. \right.$$

$$\left. + \frac{e^{-y^2 \bar{t} D1} - e^{-n^2 \pi^2 \bar{t} D1}}{y^2 - n^2 \pi^2} \right] \frac{2 \eta_{21}}{D(y)} \left[J_0(\omega_1(y)) - J_0(\omega_2(y)) \right] \frac{dy}{\sin y}$$

$$+ \sin \left[n \pi \left(1 - \frac{z}{H_1'} \right) \right] \int_0^{\infty} \left[\frac{1 - e^{-n^2 \pi^2 \bar{t} D1}}{n^2 \pi^2} + \frac{e^{-y^2 \bar{t} D1} - e^{-n^2 \pi^2 \bar{t} D1}}{y^2 - n^2 \pi^2} \right]$$

$$\cdot \left[(1 - G(y)) J_0(\omega_1(y)) + (1 + G(y)) J_0(\omega_2(y)) \right] \frac{dy}{y} \right\}$$

Noting that

$$\sin\left[n\pi\left(1-\frac{z}{H_1'}\right)\right] = -(-1)^n \sin\frac{n\pi z}{H_1'}$$

we can multiply and divide the above equation by $n^2\pi^2$ so that upon rearranging it becomes

$$s_1'(r,z,t) = \frac{Q}{4\pi T_1}\frac{2}{\pi}\sum_{n=1}^{\infty}\frac{1}{n}\sin\frac{n\pi z}{H_1'}\int_0^{\infty}\left[1-e^{-n^2\pi^2 t_{D1}}+\frac{e^{-y^2 t_{D1}}-e^{-n^2\pi^2 t_{D1}}}{y^2/(n^2\pi^2)-1}\right]$$

$$\cdot\left\{\left[\frac{2\eta_{21}(-1)^n y}{D(y)\sin y}+G(y)-1\right]J_0\left(\omega_1(y)\right)-\left[\frac{2\eta_{21}(-1)^n y}{D(y)\sin y}+G(y)+1\right]\right.$$

$$\left.\cdot J_0\left(\omega_2(y)\right)\right\}\frac{dy}{y} \tag{II-87}$$

where it is understood that the Bessel functions vanish when the square of their arguments are negative.

Eqs. II-82, II-83, and II-87 together with the definitions in II-80 and II-81 give the drawdown at any point within the two-aquifer system at any time t when the lower aquifer is being pumped at a constant rate Q. All that one has to do in order to use these equations when the upper aquifer is being pumped is to turn the model in Fig. II-4 upside down without making any changes in the notation and numbering used in that figure.

d. Solutions for Case when Aquifers Have Identical Properties

In the special case when the two aquifers have similar hydraulic diffusivities α and transmissibilities T, the functions defined in Eq. II-81 reduce to

$$D(y) = \frac{2\eta y}{\sin y}$$

$$\omega_1{}^2(y) = \theta y^2 - \eta y \cot y + \frac{\eta y}{\sin y}$$

$$\omega_2{}^2(y) = \theta y^2 - \eta y \cot y - \frac{\eta y}{\sin y}$$

$$G(y) = 0$$

where $\theta = (\alpha_1' r^2)/(\alpha H_1'^2)$ and $\eta = (K_1' r^2)/(T H_1')$. With these definitions, Eqs. II-82, II-83, and II-87 become

$$s_1(r,t) = \frac{Q}{4\pi T} \int_0^\infty (1 - e^{-y^2 \bar{t} D_1}) \left[J_0\!\big(\omega_1(y)\big) + J_0\!\big(\omega_2(y)\big) \right] \frac{dy}{y} \qquad \text{(II-88)}$$

$$s_2(r,t) = \frac{Q}{4\pi T} \int_0^\infty (1 - e^{-y^2 \bar{t} D_1}) \left[J_0\!\big(\omega_1(y)\big) - J_0\!\big(\omega_2(y)\big) \right] \frac{dy}{y} \qquad \text{(II-89)}$$

$$s_1'(r,z,t) = \frac{Q}{4\pi T} \frac{2}{\pi} \sum_{n=1}^\infty \frac{1}{n} \sin\frac{n\pi z}{H_1'} \int_0^\infty \left[1 - e^{-n^2\pi^2 \bar{t} D_1} + \frac{e^{-y^2 \bar{t} D_1} - e^{-n^2\pi^2 \bar{t} D_1}}{y^2/(n^2\pi^2) - 1} \right]$$

$$\cdot \left\{ \left[(-1)^n - 1\right] J_0\!\big(\omega_1(y)\big) - \left[(-1)^n + 1\right] J_0\!\big(\omega_2(y)\big) \right\} \frac{dy}{y} \qquad \text{(II-90)}$$

where the Bessel functions must be set to zero when the squares of their arguments are negative.

5. Reduction to Theis Solution

When the permeability K_1' in the aquitard becomes zero, Eq. II-82 reduces to the Theis solution. In order to show this, we first rewrite Eq. II-82 in terms of the variable

$$x = y \sqrt{\alpha_1'} / H_1'$$

Let

$$L_1^2 = \frac{1}{2}\left[\frac{1}{\alpha_1} + \frac{1}{\alpha_2} + \left|\frac{1}{\alpha_1} - \frac{1}{\alpha_2}\right|\right]$$

and

$$L_2^2 = \frac{1}{2}\left[\frac{1}{\alpha_1} + \frac{1}{\alpha_2} - \left|\frac{1}{\alpha_1} - \frac{1}{\alpha_2}\right|\right]$$

(II-91)

From Eqs. II-62, II-66, and II-74 we see that when $K_1' = 0$ then

and

$$\omega_1^2(x) = (rxL_1)^2$$

$$\omega_2^2(x) = (rxL_2)^2$$

(II-92)

From Eq. II-76 we have $G(x) = 1 - 2f(x)$ and when this is combined with Eqs. II-62 and II-63, we obtain

$$G = -\frac{1/\alpha_1 - 1/\alpha_2}{\left|1/\alpha_1 - 1/\alpha_2\right|}$$

so that Eq. II-82 becomes

$$s_1(r,t) = \frac{Q}{4\pi T_1}\int_0^\infty (1-e^{-x^2 t})\left\{\left[1 + \frac{1/\alpha_1 - 1/\alpha_2}{\left|1/\alpha_1 - 1/\alpha_2\right|}\right] J_0(rxL_1)\right.$$

$$\left. + \left[1 - \frac{1/\alpha_1 - 1/\alpha_2}{\left|1/\alpha_1 - 1/\alpha_2\right|}\right] J_0(rxL_2)\right\}\frac{dx}{x}$$

(II-93)

In the special case when $\alpha_1 = \alpha_2$, the second term in brackets vanishes and Eq. II-91 gives

$$rxL_1 = rxL_2 = rx/\sqrt{\alpha_1}$$

Let us define a new variable

$$y \equiv xr/\sqrt{\alpha_1}$$

so that Eq. II-93 can be rewritten in the form

$$s_1(r,t) = \frac{Q}{2 \pi T_1} \int_0^\infty (1 - e^{-y^2 t_{D_1}}) J_0(y) \frac{dy}{y}$$ (II-94)

where $t_{D_1} = \alpha_1 t / r^2$. Let us also define the function

$$\gamma(c,x) \equiv \int_0^x e^{-t} t^{c-1} dt$$

where x is a variable and Re c > 0. From tables of definite integrals
(11, p. 731) we have

$$\int_0^\infty y^{\nu-1} e^{-ay^2} J_\nu(by) dy = 2^{\nu-1} b^{-\nu} \gamma(\nu, \frac{b^2}{4a})$$

where b > 0, Re a > 0, and Re ν > 0. The limit of $\gamma(c,x)$ as c approaches zero is

$$\lim_{c \to 0} \gamma(c,x) = \int_0^x \frac{e^{-t}}{t} dt$$

and we can therefore write

$$\int_0^\infty (1 - e^{-y^2 t_{D_1}}) J_0(y) \frac{dy}{y} = \lim_{\substack{a \to 0 \\ \nu \to 0}} \int_0^\infty y^{\nu-1} e^{-ay^2} J_\nu(y) dy - \lim_{\substack{a \to t_{D_1} \\ \nu \to 0}} \int_0^\infty y^{\nu-1} e^{-ay^2} J_\nu(y) dy$$

$$= \frac{1}{2} \int_0^\infty \frac{e^{-t}}{t} dt - \frac{1}{2} \int_0^{u_1} \frac{e^{-t}}{t} dt$$

$$= \frac{1}{2} \int_{u_1}^\infty \frac{e^{-t}}{t} dt = -\frac{1}{2} Ei(-u_1)$$ (II-95)

where $u_1 = 1 / 4 t_{D_1}$. Combining Eqs. II-94 and II-95, we obtain

$$s_1(r,t) = \frac{Q}{4 \pi T_1} \text{Ei} (-u_1)$$

which is the Theis solution.

In the case that $\alpha_2 > \alpha_1$, the second term in Eq. II-93 vanishes and from Eq. II-91 we obtain

$$r x L_1 = r x / \sqrt{\alpha_1}$$

If we again change variables to $y \equiv x r / \sqrt{\alpha_1}$, Eq. II-93 will reduce to II-94 which is equivalent to the Theis solution, as was shown above.

When $\alpha_2 < \alpha_1$, the first term in Eq. II-93 vanishes and from Eq. II-91 we have

$$r x L_2 = r x / \sqrt{\alpha_1}$$

so that we again obtain the Theis solution for Aquifer 1.

Thus, the solution in the aquifer being pumped reduces to the Theis solution when the permeability of the aquitard becomes zero. Obviously, it is possible to use the development in Section II-C to derive the Theis solution directly from Eq. II-9 simply by letting K_1' approach zero. We have therefore inadvertently shown how the Theis solution can be obtained with the aid of Laplace and Hankel transforms.

D. SOLUTION OF THREE-AQUIFER PROBLEM

1. Formulation of Problem

Consider a system of three
horizontal aquifers separated by two
aquitards as shown in Fig. II-6.
Aquifers 1 and 2 are completely pene-
trated by wells of infinitesmal radii
that discharge at some constant rates
Q_1 and Q_2, respectively. Each layer
is homogeneous, isotropic and infinite
in radial extent. The system is an
elastic porous medium completely
saturated with a homogeneous, single-
phase, slightly compressible liquid.
Darcy's law applies everywhere in the
system, and the storage coefficients
in each layer remain constant with
time. We assume that $K_1' \ll K_1$,
$K_1' \ll K_2$, $K_2' \ll K_2$, and $K_2' \ll K_3$.
In addition, the thickness of each

Fig. II-6. Three-aquifer system.

unpumped aquifer must be sufficiently small so that drawdown across the thickness
of such an aquifer is constant at any time t.

If the initial drawdown in the system is zero, we can use the results of
Section II-B to formulate the problem as follows:

$$\frac{\partial^2 s_1}{\partial r^2} + \frac{1}{r}\frac{\partial s_1}{\partial r} + \frac{K_1'}{T_1}\frac{\partial s_1'}{\partial z}\bigg|_{z=0} = \frac{1}{\alpha_1}\frac{\partial s_1}{\partial t} \qquad \text{(a)}$$

$$s_1(r,0) = 0 \qquad \text{(b)}$$

$$s_1(\infty,0) = 0 \qquad \text{(c)}$$

$$\lim_{r\to 0} r\frac{\partial s_1}{\partial r} = -\frac{Q_1}{2\pi T_1} \qquad \text{(d)}$$

Aquifer 1 (pumped) (II-96)

$$\frac{\partial^2 s_1'}{\partial z^2} = \frac{1}{\alpha_1'}\frac{\partial s_1'}{\partial t} \qquad \text{(a)}$$

$$s_1'(r,z,0) = 0 \qquad \text{(b)}$$

$$s_1'(r,0,t) = s_1(r,t) \qquad \text{(c)}$$

$$s_1'(r,H_1',t) = s_2(r,t) \qquad \text{(d)}$$

Aquitard 1 (II-97)

$$\frac{\partial^2 s_2}{\partial r^2} + \frac{1}{r}\frac{\partial s_2}{\partial r} - \frac{K_1'}{T_2}\frac{\partial s_1'}{\partial z}\bigg|_{z=H_1'}$$

$$+ \frac{K_2'}{T_2}\frac{\partial s_2'}{\partial z}\bigg|_{z=z_1} = \frac{1}{\alpha_2}\frac{\partial s_2}{\partial t} \qquad \text{(a)}$$

$$s_2(r,0) = 0 \qquad \text{(b)}$$

$$s_2(\infty,t) = 0 \qquad \text{(c)}$$

$$\lim_{r\to 0} r\frac{\partial s_2}{\partial r} = -\frac{Q_2}{2\pi T_2} \qquad \text{(d)}$$

Aquifer 2 (pumped) (II-98)

$$\frac{\partial^2 s_2'}{\partial z^2} = \frac{1}{\alpha_2'} \frac{\partial s_2'}{\partial t} \qquad \text{(a)}$$

$$s_2'(r,z,0) = 0 \qquad \text{(b)}$$

$$s_2'(r,z_1,t) = s_2(r,t) \qquad \text{(c)}$$

$$s_2'(r,z_2,t) = s_3(r,t) \qquad \text{(d)}$$

Aquitard 2   (II-99)

$$\left. \frac{\partial^2 s_3}{\partial r^2} + \frac{1}{r} \frac{\partial s_3}{\partial r} - \frac{K_2'}{T_3} \frac{\partial s_2'}{\partial z} \right|_{z=z_2} = \frac{1}{\alpha_3} \frac{\partial s_3}{\partial t} \qquad \text{(a)}$$

$$s_3(r,0) = 0 \qquad \text{(b)}$$

$$s_3(\infty,t) = 0 \qquad \text{(c)}$$

$$\lim_{r \to 0} r \frac{\partial s_3}{\partial r} = 0 \qquad \text{(d)}$$

Aquifer 3   (II-100)
(not pumped)

Eqs. II-96 through II-100 define the initial boundary value problem for the three-aquifer case.

2. Transformation of Problem

Let us apply the Laplace transform to Eq. II-97a using the initial condition (Eq. 97b). Following the procedure outlined in Eqs. II-12 through II-17, we obtain the double transform of s_1',

$$\bar{\bar{s}}_1' = \frac{\sinh(\sqrt{p/\alpha_1'}\ z)}{\sinh(\sqrt{p/\alpha_1'}\ H_1')} \bar{\bar{s}}_2 + \frac{\sinh[\sqrt{p/\alpha_1'}\ (H_1' - z)]}{\sinh(\sqrt{p/\alpha_1'}\ H_1')} \bar{\bar{s}}_1 \qquad \text{(II-101)}$$

By analogy, application of Laplace and Hankel transforms to II-99 will result in the double transform

$$\bar{\bar{s}}_2{}' = \frac{\sinh\left[\sqrt{p/\alpha_2{}'}\ (z-z_1)\right]}{\sinh\left(\sqrt{p/\alpha_2{}'}\ H_2{}'\right)}\,\bar{\bar{s}}_3 + \frac{\sinh\left[\sqrt{p/\alpha_2{}'}\ (z_2-z)\right]}{\sinh\left(\sqrt{p/\alpha_2{}'}\ H_2{}'\right)}\,\bar{\bar{s}}_2 \tag{II-102}$$

Here $\bar{\bar{s}}_1{}'$ and $\bar{\bar{s}}_2{}'$ are functions of a, z, and p, and $\bar{\bar{s}}_1$, $\bar{\bar{s}}_2$, and $\bar{\bar{s}}_3$ are functions of a and p.

If we apply Laplace and Hankel transforms to Eqs. II-96, II-98, and II-100 and follow the procedure outlined in Eqs. II-18 through II-24, we obtain

$$\left.
\begin{aligned}
&-a^2\bar{\bar{s}}_1 + \frac{Q_1}{2\pi T_1 p} - \frac{p}{\alpha_1}\bar{\bar{s}}_1 + \frac{K_1{}'}{T_1}\left.\frac{\partial\bar{\bar{s}}_1{}'}{\partial z}\right|_{z=0} = 0\\[2mm]
&-a^2\bar{\bar{s}}_2 + \frac{Q_2}{2\pi T_2 p} - \frac{p}{\alpha_2}\bar{\bar{s}}_2 - \frac{K_1{}'}{T_2}\left.\frac{\partial\bar{\bar{s}}_1{}'}{\partial z}\right|_{z=H_1{}'} + \frac{K_2{}'}{T_2}\left.\frac{\partial\bar{\bar{s}}_2{}'}{\partial z}\right|_{z=z_1} = 0\\[2mm]
&-a^2\bar{\bar{s}}_3 - \frac{p}{\alpha_3}\bar{\bar{s}}_3 - \frac{K_2{}'}{T_3}\left.\frac{\partial\bar{\bar{s}}_2{}'}{\partial z}\right|_{z=z_2} = 0
\end{aligned}
\right\} \tag{II-103}$$

As in Eqs. II-25 and II-26, the derivatives of Eqs. II-101 and II-102 at the various interfaces are

$$\left.\frac{\partial\bar{\bar{s}}_1{}'}{\partial z}\right|_{z=0} = \sqrt{p/\alpha_1{}'}\left[\frac{\bar{\bar{s}}_2}{\sinh\left(\sqrt{p/\alpha_1{}'}\ H_1{}'\right)} - \bar{\bar{s}}_1\coth\left(\sqrt{p/\alpha_1{}'}\ H_1{}'\right)\right]$$

$$\left.\frac{\partial\bar{\bar{s}}_1{}'}{\partial z}\right|_{z=H_1{}'} = \sqrt{p/\alpha_1{}'}\left[\bar{\bar{s}}_2\coth\left(\sqrt{p/\alpha_1{}'}\ H_1{}'\right) - \frac{\bar{\bar{s}}_1}{\sinh\left(\sqrt{p/\alpha_1{}'}\ H_1{}'\right)}\right]$$

$$\left.\frac{\partial\bar{\bar{s}}_2{}'}{\partial z}\right|_{z=z_1} = \sqrt{p/\alpha_2{}'}\left[\frac{\bar{\bar{s}}_3}{\sinh\left(\sqrt{p/\alpha_2{}'}\ H_2{}'\right)} - \bar{\bar{s}}_2\coth\left(\sqrt{p/\alpha_2{}'}\ H_2{}'\right)\right]$$

$$\left.\frac{\partial\bar{\bar{s}}_2{}'}{\partial z}\right|_{z=z_2} = \sqrt{p/\alpha_2{}'}\left[\bar{\bar{s}}_3\coth\left(\sqrt{p/\alpha_2{}'}\ H_2{}'\right) - \frac{\bar{\bar{s}}_2}{\sinh\left(\sqrt{p/\alpha_2{}'}\ H_2{}'\right)}\right]$$

Let us define the functions

$$A_1(p) \equiv \frac{p}{\alpha_1} + \frac{K_1' \sqrt{p/\alpha_1'}}{T_1} \coth(\sqrt{p/\alpha_1'} \; H_1')$$

$$A_2(p) \equiv \frac{p}{\alpha_2} + \frac{K_1' \sqrt{p/\alpha_1'}}{T_2} \coth(\sqrt{p/\alpha_1'} \; H_1')$$

$$+ \frac{K_2' \sqrt{p/\alpha_2'}}{T_2} \coth(\sqrt{p/\alpha_2'} \; H_2')$$

$$A_3(p) \equiv \frac{p}{\alpha_3} + \frac{K_2' \sqrt{p/\alpha_2'}}{T_3} \coth(\sqrt{p/\alpha_2'} \; H_2')$$

$$B_1(p) \equiv \frac{K_1' \sqrt{p/\alpha_1'}}{T_1 \sinh(\sqrt{p/\alpha_1'} \; H_1')}$$

$$B_2(p) \equiv \frac{K_1' \sqrt{p/\alpha_1'}}{T_2 \sinh(\sqrt{p/\alpha_1'} \; H_1')}$$

$$B_3(p) \equiv \frac{K_2' \sqrt{p/\alpha_2'}}{T_2 \sinh(\sqrt{p/\alpha_2'} \; H_2')}$$

$$B_4(p) \equiv \frac{K_2' \sqrt{p/\alpha_2'}}{T_3 \sinh(\sqrt{p/\alpha_2'} \; H_2')}$$

$$C_1(p) \equiv \frac{Q_1}{2\pi T_1 p}$$

$$C_2(p) \equiv \frac{Q_2}{2\pi T_2 p}$$

(II-104)

Substituting these definitions together with the above derivatives into II-103 and rearranging, we obtain

$$(a^2 + A_1)\, \bar{\bar{s}}_1 - B_1 \bar{\bar{s}}_2 = C_1$$

$$B_2 \bar{\bar{s}}_1 - (a^2 + A_2)\, \bar{\bar{s}}_2 + B_3 \bar{\bar{s}}_3 = -C_2$$

$$B_4 \bar{\bar{s}}_2 - (a^2 + A_3)\, \bar{\bar{s}}_3 = 0$$

-223-

These equations can be solved for $\bar{\bar{s}}_1$, $\bar{\bar{s}}_2$, and $\bar{\bar{s}}_3$:

$$\bar{\bar{s}}_1 = \frac{C_1}{M} [(a^2 + A_2)(a^2 + A_3) - B_3 B_4] + \frac{C_2}{M} B_1 (a^2 + A_3) \qquad \text{(II-105)}$$

$$\bar{\bar{s}}_2 = \frac{C_1}{M} B_2 (a^2 + A_3) + \frac{C_2}{M} (a^2 + A_1)(a^2 + A_3) \qquad \text{(II-106)}$$

$$\bar{\bar{s}}_3 = \frac{C_1}{M} B_2 B_4 + \frac{C_2}{M} B_4 (a^2 + A_1) \qquad \text{(II-107)}$$

where

$$M \equiv (a^2 + A_1)(a^2 + A_2)(a^2 + A_3) - (a^2 + A_1) B_3 B_4 - (a^2 + A_3) B_1 B_2 \qquad \text{(II-108)}$$

3. Inversion of Hankel Transform

In order to invert the Hankel transform, it is desirable to rearrange Eqs. II-105, II-106, and II-107 in a form such that we can employ Eq. A-8 of Appendix A. Let us define

$$m \equiv A_1 + A_2 + A_3$$

$$q \equiv A_1 A_3 + A_2 A_3 + A_1 A_2 - B_1 B_2 - B_3 B_4 \qquad \text{(II-109)}$$

$$n \equiv A_1 A_2 A_3 - A_1 B_3 B_4 - A_3 B_1 B_2$$

so that M in Eq. II-108 becomes

$$M \equiv a^6 + m a^4 + q a^2 + n \qquad \text{(II-110)}$$

Let

$$
\left.
\begin{aligned}
x &\equiv a^2 + \frac{m}{3} & U &\equiv \left[-\frac{\delta^2}{2} + \sqrt{\frac{\delta^2}{4} + \frac{\gamma^3}{27}} \right]^{1/3} \\[6pt]
\gamma &\equiv \frac{1}{3}(3q - m^2) & & \\[6pt]
\delta &\equiv \frac{1}{27}(2m^3 - 9mq + 27n) & V &\equiv \left[-\frac{\delta}{2} - \sqrt{\frac{\delta^2}{4} + \frac{\gamma^3}{27}} \right]^{1/3}
\end{aligned}
\right\} \quad \text{(II-111)}
$$

and consider the cubic equation

$$M = x^3 + \gamma x + \delta = 0$$

The roots of this equation are

$$x_1 = -\frac{U+V}{2} + \frac{U-V}{2}\sqrt{-3}$$

$$x_2 = -\frac{U+V}{2} - \frac{U-V}{2}\sqrt{-3}$$

$$x_3 = U+V$$

which in terms of a^2 become

$$\left.\begin{aligned}
a_1{}^2 &= -\frac{U+V}{2} + \frac{U-V}{2}\sqrt{-3} - \frac{m}{3} \\[2mm]
a_2{}^2 &= -\frac{U+V}{2} - \frac{U-V}{2}\sqrt{-3} - \frac{m}{3} \\[2mm]
a_3{}^2 &= U+V - \frac{m}{3}
\end{aligned}\right\} \qquad \text{(II-112)}$$

We can therefore write

$$\frac{1}{M} = \frac{X}{a^2 + m/3 + 1/2\,[U+V-\sqrt{-3}\,(U-V)]}$$

$$+ \frac{Y}{a^2 + m/3 + 1/2\,[U+V+\sqrt{-3}\,(U-V)]} + \frac{Z}{a^2 + m/3 - (U+V)}$$

where X, Y, and Z are unknown coefficients still to be determined. By bringing
the right hand side of this equation to a common denominator, we can equate
numerators on both sides,

$$X \left[a^4 + \frac{2}{3} a^2 m - \frac{1}{2} a^2 (U+V) + \frac{1}{2} a^2 \sqrt{-3} (U-V) + \frac{m^2}{9} - \frac{m}{6} (U+V) + \frac{m}{6} \sqrt{-3} (U-V) \right.$$

$$\left. - \frac{1}{2} (U+V)^2 - \frac{\sqrt{-3}}{2} (U^2 - V^2) \right] + Y \left[a^4 + \frac{2}{3} a^2 m - \frac{1}{2} a^2 (U+V) \right.$$

$$\left. - \frac{1}{2} a^2 \sqrt{-3} (U-V) + \frac{m^2}{9} - \frac{m}{6} (U+V) - \frac{m}{6} \sqrt{-3} (U-V) - \frac{1}{2} (U+V)^2 \right.$$

$$\left. + \frac{\sqrt{-3}}{2} (U^2 - V^2) \right] + Z \left[a^4 + \frac{2}{3} a^2 m + a^2 (U+V) + \frac{m^2}{9} + \frac{m}{3} (U+V) \right.$$

$$\left. + \frac{1}{4} (U+V)^2 + \frac{3}{4} (U-V)^2 \right] = 1$$

If we equate coefficients of equal powers of a on both sides of this equation, we obtain

$$X + Y + Z = 0$$

$$X \left[\frac{2}{3} m - \frac{1}{2} (U+V) + \frac{\sqrt{-3}}{2} (U-V) \right] + Y \left[\frac{2}{3} m - \frac{1}{2} (U+V) - \frac{\sqrt{-3}}{2} (U-V) \right]$$

$$+ Z \left[\frac{2}{3} m + U + V \right] = 0$$

$$X \left[\frac{m^2}{9} - \frac{m}{6} (U+V) + \frac{m}{6} \sqrt{-3} (U-V) - \frac{1}{2} (U+V)^2 - \frac{\sqrt{-3}}{2} (U^2 - V^2) \right]$$

$$+ Y \left[\frac{m^2}{9} - \frac{m}{6} (U+V) - \frac{m}{6} \sqrt{-3} (U-V) - \frac{1}{2} (U+V)^2 + \frac{\sqrt{-3}}{2} (U^2 - V^2) \right]$$

$$+ Z \left[\frac{m^2}{9} - \frac{m}{3} (U+V) + \frac{1}{4} (U+V)^2 + \frac{3}{4} (U-V)^2 \right] = 1$$

These are three equations in three unknowns that can be solved for X, Y, and Z:

$$X = \frac{\sqrt{-3} (V-U) - 3 (U+V)}{6 \sqrt{-3} (U^3 - V^3)}$$

$$Y = \frac{\sqrt{-3} (V-U) + 3 (U+V)}{6 \sqrt{-3} (U^3 - V^3)}$$

$$Z = \frac{U-V}{3 (U^3 - V^3)}$$

Let us define

$$\xi_1^2(p) \equiv \frac{m}{3} + \frac{1}{2} [U + V + \sqrt{-3} (V - U)]$$

$$\xi_2^2(p) \equiv \frac{m}{3} + \frac{1}{2} [U + V - \sqrt{-3} (V - U)] \tag{II-113}$$

$$\xi_3^2(p) \equiv \frac{m}{3} - U - V$$

Using these definitions together with the above values of X, Y, and Z, the expression for $1/M$ can be written as

$$\frac{1}{M} = \frac{\sqrt{-3}\,(V - U) - 3\,(U + V)}{6\,\sqrt{-3}\,(U^3 - V^3)\,(a^2 + \xi_1^2)} + \frac{\sqrt{-3}\,(V - U) + 3\,(U + V)}{6\,\sqrt{-3}\,(U^3 - V^3)\,(a^2 + \xi_2^2)}$$

$$+ \frac{U - V}{3\,(U^3 - V^3)\,(a^2 + \xi_3^2)} \tag{II-114}$$

We are now in a position to invert Eqs. II-105 through II-107 back into the Laplace transform domain. In order to simplify matters, we will consider the following cases: (a) drawdown in Aquifers 1 and 2 when only Aquifer 2 is being pumped $(C_1 = 0)$ and (b) drawdown in each aquifer when only Aquifer 1 is being pumped $(C_2 = 0)$. In the first case, the inverse Hankel transform H^{-1} of Eq. II-105 can be obtained by combining this equation with Eq. II-114 and using Eq. A-8 in Appendix A. We obtain

$$\bar{s}_1 = \frac{C_2 B_1}{6\,\sqrt{-3}\,(U^3 - V^3)}\, H^{-1}\left\{ [\sqrt{-3}\,(V - U) - 3\,(U + V)]\,\frac{a^2 + A_3}{a^2 + \xi_1^2} \right.$$

$$+ [\sqrt{-3}\,(V - U) + 3\,(U + V)]\,\frac{a^2 + A_3}{a^2 + \xi_2^2} + 2\,\sqrt{-3}\,(U - V)\,\left.\frac{a^2 + A_3}{a^2 + \xi_3^2} \right\}$$

$$= \frac{C_2 B_1}{6\,\sqrt{-3}\,(U^3 - V^3)}\left\{ [\sqrt{-3}\,(V - U) - 3\,(U + V)]\,(A_3 - \xi_1^2)\,K_0(\xi_1 r) \right.$$

$$+ [\sqrt{-3}\,(V - U) + 3\,(U + V)]\,(A_3 - \xi_2^2)\,K_0(\xi_2 r)$$

$$+ 2\,\sqrt{-3}\,(U - V)\,(A_3 - \xi_3^2)\,K_0(\xi_3 r)\Bigg\} \tag{II-115}$$

Similarly, the inverse of Eq. II-106 is

$$\bar{s}_2 = \frac{C_2}{6\sqrt{-3}\,(U^3 - V^3)} \left\{ [\sqrt{-3}\,(V - U) - 3(U + V)] [A_1 A_3 - (A_1 + A_3)\,\xi_1^2 + \right.$$

$$+ \xi_1^4] K_0(\xi_1 r) + [\sqrt{-3}\,(V - U) + 3(U + V)] [A_1 A_3 - (A_1 + A_3)\,\xi_2^2$$

$$+ \xi_2^4] K_0(\xi_2 r) + 2\sqrt{-3}\,(U - V) [A_1 A_3 - (A_1 + A_3)\,\xi_3^2$$

$$\left. + \xi_3^4] K_0(\xi_3 r) \right\} \tag{II-116}$$

In the second case, the inverse Hankel transforms of Eqs. II-105 through II-107 can be immediately written as

$$\bar{s}_1 = \frac{C_1}{6\sqrt{-3}\,(U^3 - V^3)} \left\{ [\sqrt{-3}\,(V - U) - 3(U + V)] [A_2 A_3 - B_3 B_4 - (A_2 + A_3)\,\xi_1^2 \right.$$

$$+ \xi_1^4] K_0(\xi_1 r) + [\sqrt{-3}\,(V - U) + 3(U + V)] [A_2 A_3 - B_3 B_4 - (A_2 + A_3)\,\xi_2^2$$

$$+ \xi_2^4] K_0(\xi_2 r) + 2\sqrt{-3}\,(U - V) [A_2 A_3 - B_3 B_4 - (A_2 + A_3)\,\xi_3^2$$

$$\left. + \xi_3^4] K_0(\xi_3 r) \right\} \tag{II-117}$$

$$\bar{s}_2 = \frac{C_1 B_2}{6\sqrt{-3}\,(U^3 - V^3)} \left\{ [\sqrt{-3}\,(V - U) - 3(U + V)] (A_3 - \xi_1^2) K_0(\xi_1 r) \right.$$

$$+ [\sqrt{-3}\,(V - U) + 3(U + V)] (A_3 - \xi_2^2) K_0(\xi_2 r)$$

$$\left. + 2\sqrt{-3}\,(U - V) (A_3 - \xi_3^2) K_0(\xi_3 r) \right\} \tag{II-118}$$

$$\bar{s}_3 = \frac{C_1 B_2 B_4}{6\sqrt{-3}\,(U^3 - V^3)} \left\{ [\sqrt{-3}\,(V - U) - 3(U + V)] K_0(\xi_1 r) \right.$$

$$\left. + [\sqrt{-3}\,(V - U) + 3(U + V)] K_0(\xi_2 r) + 2\sqrt{-3}\,(U - V) K_0(\xi_3 r) \right\} \tag{II-119}$$

In all of these equations, A, B, and C are functions of the Laplace transform parameter p as defined in Eqs. II-104 and U, V, and ξ are functions of A, B, and C as defined in Eqs. II-109, II-111, and II-113.

The inverse Hankel transforms of Eqs. II-101 and II-102 are simply

$$\bar{s}_1{}' = \frac{\sinh(\sqrt{p/\alpha_1{}'}\ z)}{\sinh(\sqrt{p/\alpha_1{}'}\ H_1')}\ \bar{s}_2 + \frac{\sinh[\sqrt{p/\alpha_1{}'}\ (H_1' - z)]}{\sinh(\sqrt{p/\alpha_1{}'}\ H_1')}\ \bar{s}_1 \qquad \text{(II-120)}$$

and

$$\bar{s}_2{}' = \frac{\sinh[\sqrt{p/\alpha_2{}'}\ (z - z_1)]}{\sinh(\sqrt{p/\alpha_2{}'}\ H_2')}\ \bar{s}_3 + \frac{\sinh[\sqrt{p/\alpha_2{}'}\ (z_2 - z)]}{\sinh(\sqrt{p/\alpha_2{}'}\ H_2')}\ \bar{s}_2 \qquad \text{(II-121)}$$

Eqs. II-115 through II-121 give the Laplace transforms of the solutions in a three-aquifer system when one of the aquifers is being pumped. It is obvious that the solution in any layer due to pumping of any aquifer in the system can be obtained from these equations by symmetry and superposition.

4. Inversion of Laplace Transform

The inversion of Eqs. II-115 through II-119 can be accomplished with the aid of Mellin's inversion formula (II-39). In order to apply this formula to our problem we must first determine the poles and branch points of the functions $\bar{s}_1(r, \lambda)$, $\bar{s}_2(r, \lambda)$, and $\bar{s}_3(r, \lambda)$ in the complex domain of λ. From the definitions of $C_1(p)$ and $C_2(p)$ in II-104, we see that all of these functions have at least a simple pole at $\lambda = 0$. In addition, the function $K_0(\xi r)$ has branch points at all values of λ that are roots of the equation $\xi(\lambda) = 0$. It would therefore appear necessary that we determine the roots of the equations $\xi_1(\lambda) = 0$, $\xi_2(\lambda) = 0$, $\xi_3(\lambda) = 0$, and $U^3(\lambda) - V^3(\lambda) = 0$ before applying Mellin's inversion formula to Eqs. II-115 through II-119.

A glance at Eqs. II-111 and II-113 will reveal, however, that the expressions for $\xi(\lambda)$, $U(\lambda)$, and $V(\lambda)$ are very complicated, which makes it extremely difficult to determine the roots of the above equations analytically. We have shown that in the two-aquifer case the equations $\xi(\lambda) = 0$ had at most an infinite number of distinct non-positive real roots, and that the only terms in the expressions for $\bar{s}(r, \lambda)$ that could become singular were of the form $K_0(\xi r)/\lambda$.

-229-

Since the three-aquifer problem is merely an extension of the two-aquifer case, it seems reasonable to assume that the behavior of the functions $\bar{s}(r,\lambda)$ is essentially similar in both cases. Therefore, in our following development we will assume that the equations $\xi_1(\lambda) = 0$, $\xi_2(\lambda) = 0$, and $\xi_3(\lambda) = 0$ have at most an infinite number of distinct non-positive real roots, and that the roots of $U^3(\lambda) - V^3(\lambda) = 0$ are not singular points of $\bar{s}(r,\lambda)$.

a. Solutions in Aquifers

Since all the singularities are assumed to lie at $\lambda = 0$ or on the negative real axis, in applying Mellin's inversion formula to our problem we can use the same contour of integration as in Fig. II-5. Therefore, by analogy to the two-aquifer case, we can immediately conclude that

$$\lim_{\substack{\varepsilon \to 0 \\ R \to \infty}} \int_{DD',\,\Gamma_n,\,\Gamma_n',\,AC,\,C'A'} (e^{\lambda t} - 1)\,\bar{s}(r,\lambda)\,d\lambda \;=\; 0 \qquad\qquad \text{(II-122)}$$

for all functions $s(r,\lambda)$ in Eqs. II-115 through II-119. We can now let $\lambda = x^2 e^{i\pi}$ on CD and $\lambda = x^2 e^{-i\pi}$ on D'C'. Multiplying the expressions in II-104 by r^2 and considering Eqs. II-67, we are led to the following definitions:

$$
\begin{aligned}
A_1(x) &\equiv r^2\left[-\frac{x^2}{\alpha_1} + \frac{K_1' x}{T_1\sqrt{\alpha_1'}}\,\cot\frac{x H_1'}{\sqrt{\alpha_1'}} \right] \\[2ex]
A_2(x) &\equiv r^2\left[-\frac{x^2}{\alpha_2} + \frac{K_1' x}{T_2\sqrt{\alpha_1'}}\,\cot\frac{x H_1'}{\sqrt{\alpha_1'}} + \frac{K_2' x}{T_2\sqrt{\alpha_2'}}\,\cot\frac{x H_2'}{\sqrt{\alpha_2'}} \right] \\[2ex]
A_3(x) &\equiv r^2\left[-\frac{x^2}{\alpha_3} + \frac{K_2' x}{T_3\sqrt{\alpha_2'}}\,\cot\frac{x H_2'}{\sqrt{\alpha_2'}} \right] \\[2ex]
B_1(x) &\equiv \frac{K_1' r^2 x}{T_1\sqrt{\alpha_1'}\,\sin(x H_1'/\sqrt{\alpha_1'})} \qquad\qquad B_3(x) \equiv \frac{K_2' r^2 x}{T_2\sqrt{\alpha_2'}\,\sin(x H_2'/\sqrt{\alpha_2'})} \\[2ex]
B_2(x) &\equiv \frac{K_1' r^2 x}{T_2\sqrt{\alpha_1'}\,\sin(x H_1'/\sqrt{\alpha_1'})} \qquad\qquad B_4(x) \equiv \frac{K_2' r^2 x}{T_3\sqrt{\alpha_2'}\,\sin(x H_2'/\sqrt{\alpha_2'})}
\end{aligned}
\right\} \quad \text{(II-123)}
$$

Let $\xi_1^* \equiv \xi_1(x^2 e^{i\pi})$, $\xi_1^{**} \equiv \xi_1(x^2 e^{-i\pi})$, and

$$
\left.
\begin{aligned}
\omega_1^2 &\equiv -\frac{m}{3} - \frac{1}{2}\left[U + V + \sqrt{-3}\,(V - U)\right] \\[2ex]
\omega_2^2 &\equiv -\frac{m}{3} - \frac{1}{2}\left[U + V - \sqrt{-3}\,(V - U)\right] \\[2ex]
\omega_3^2 &\equiv -\frac{m}{3} + U + V
\end{aligned}
\right\}
\tag{II-124}
$$

where m, U, and V are the same as before except that the values of A and B in Eq. II-109 are as defined in Eqs. II-123. One can easily verify that

$$
\left.
\begin{aligned}
(r\xi_1^*)^2 &= \omega_1^2(x)\, e^{i\pi} \\[3ex]
(r\xi_1^{**})^2 &= \omega_2^2(x)\, e^{-i\pi}
\end{aligned}
\right\}
\tag{II-125}
$$

and

which is similar to Eq. II-68. Following the same argument as in Eqs. II-68 through II-71, we obtain

$$
K_0(r\xi_1^{**}) - K_0(r\xi_1^*) =
\begin{cases}
i\pi J_0\!\left(\omega_1(x)\right) & \text{when } \omega_1^2(x) > 0 \\[2ex]
0 & \text{when } \omega_1^2(x) < 0
\end{cases}
\tag{II-126}
$$

If for the first term in II-115 we let

$$
f(x) \equiv \frac{B_1(x)}{6\sqrt{-3}\,(U^3 - V^3)}\left[\sqrt{-3}\,(V - U) - 3(U + V)\right]\left[A_3(x) + \omega_1^2(x)\right]
$$

where U and V are functions of x, then by analogy to Eq. II-73 we will have

$$\frac{1}{2\pi i} \int_{\gamma - i\infty}^{\gamma + i\infty} (e^{\lambda t} - 1) \frac{B_1(\lambda) \left[\sqrt{-3}\,(V - U) - 3\,(U + V) \right] \left[A_3(\lambda) - \xi_1^2(\lambda) \right]}{6\sqrt{-3}\,(U^3 - V^3)} K_0(\xi_1 r)\, d\lambda$$

$$= \int_0^\infty (1 - e^{-x^2 t})\, f(x)\, J_0 \Big| \omega_1(x) \Big| \frac{dx}{x} \tag{II-127}$$

where U and V are functions of λ, and $J_0\Big|\omega_1(x)\Big|$ must vanish when $\omega_1^2(x) < 0$. This is the inverse of the first term in Eq. II-115. Before writing down the entire inverse of II-115, let us define a new variable

$$y \equiv x H_1' / \sqrt{\alpha_1'}$$

and the dimensionless quantities

$$\left.\begin{aligned}
\bar{t}_{D_1} &\equiv \frac{\alpha_1' t}{H_1'^2} \\[2mm]
\theta_{ij} &\equiv \frac{\alpha_j' r^2}{\alpha_i H_j'^2} \\[2mm]
\eta_{ij} &\equiv \frac{K_j' r^2}{T_i H_j'} \\[2mm]
\nu_{22} &\equiv \sqrt{\theta_{21}/\theta_{22}}
\end{aligned}\right\} \tag{II-128}$$

The functions in II-123 can now be written as

$$\left.\begin{aligned}
A_1(y) &= -\theta_{11} y^2 + \eta_{11} y \cot y \\[1mm]
A_2(y) &= -\theta_{21} y^2 + \eta_{21} y \cot y + \eta_{22} \nu_{22} y \cot(\nu_{22} y) \\[1mm]
A_3(y) &= -\theta_{32} \nu_{22}^2 y^2 + \eta_{32} \nu_{22} y \cot(\nu_{22} y) \\[1mm]
B_1(y) &= \eta_{11} y / \sin y \qquad B_3(y) = \eta_{22} \nu_{22} y / \sin(\nu_{22} y) \\[1mm]
B_2(y) &= \eta_{21} y / \sin y \qquad B_4(y) = \eta_{32} \nu_{22} y / \sin(\nu_{22} y)
\end{aligned}\right\} \tag{II-129}$$

Using II-127 as an example, the inverse Laplace transforms of Eqs. II-115 through II-119 can be immediately written as follows for the case when only Aquifer 2 is pumped ($C_1 = 0$):

$$
s_1(r,t) = \frac{Q_2}{6\,\pi\,T_2} \left\{ \int_0^\infty (1-e^{y^2\bar{t}D_1}) \frac{B_1\,[\sqrt{-3}\,(V-U)-3\,(U+V)]\,(A_3+\omega_1^2)}{2\,\sqrt{-3}\,(U^3-V^3)} J_0(\omega_1)\frac{dy}{y} \right.
$$

$$
+ \int_0^\infty (1-e^{-y^2\bar{t}D_1}) \frac{B_1\,[\sqrt{-3}\,(V-U)+3\,(U+V)]\,(A_3+\omega_2^2)}{2\,\sqrt{-3}\,(U^3-V^3)} J_0(\omega_2)\frac{dy}{y}
$$

$$
\left. + \int_0^\infty (1-e^{-y^2\bar{t}D_1}) \frac{B_1\,(U-V)\,(A_3+\omega_3^2)}{U^3-V^3} J_0(\omega_3)\frac{dy}{y} \right\} \tag{II-130}
$$

$$
s_2(r,t) = \frac{Q_2}{6\,\pi\,T_2} \left\{ \int_0^\infty (1-e^{-y^2\bar{t}D_1}) \frac{[\sqrt{-3}\,(V-U)-3\,(U+V)]\,(A_1+\omega_1^2)(A_3+\omega_1^2)}{2\,\sqrt{-3}\,(U^3-V^3)} J_0(\omega_1)\frac{dy}{y} \right.
$$

$$
+ \int_0^\infty (1-e^{-y^2\bar{t}D_1}) \frac{[\sqrt{-3}\,(V-U)+3\,(U+V)]\,(A_1+\omega_2^2)(A_3+\omega_2^2)}{2\,\sqrt{-3}\,(U^3-V^3)} J_0(\omega_2)\frac{dy}{y}
$$

$$
\left. + \int_0^\infty (1-e^{-y^2\bar{t}D_1}) \frac{(U-V)\,(A_1+\omega_3^2)(A_3+\omega_3^2)}{U^3-V^3} J_0(\omega_3)\frac{dy}{y} \right\} \tag{II-131}
$$

For the case when only Aquifer 1 is pumped ($C_2 = 0$),

$$
s_1(r,t) = \frac{Q_1}{6\,\pi\,T_1} \left\{ \int_0^\infty (1-e^{-y^2\bar{t}D_1}) \frac{[\sqrt{-3}\,(V-U)-3\,(U+V)]\,[(A_2+\omega_1^2)(A_3+\omega_1^2)-B_3B_4]}{2\,\sqrt{-3}\,(U^3-V^3)} \right.
$$

$$
\cdot J_0(\omega_1)\frac{dy}{y} + \int_0^\infty (1-e^{-y^2\bar{t}D_1}) \frac{[\sqrt{-3}\,(V-U)+3\,(U+V)]\,[(A_2+\omega_2^2)(A_3+\omega_2^2)-B_3B_4]}{2\,\sqrt{-3}\,(U^3-V^3)}
$$

$$
\left. \cdot J_0(\omega_2)\frac{dy}{y} + \int_0^\infty (1-e^{-y^2\bar{t}D_1}) \frac{(U-V)\,[(A_2+\omega_3^2)(A_3+\omega_3^2)-B_3B_4]}{U^3-V^3} J_0(\omega_3)\frac{dy}{y} \right\} \tag{II-132}
$$

$$s_2(r,t) = \frac{Q_1}{6\pi T_1}\left\{ \int_0^\infty (1-e^{-y^2\bar{t}D_1})\,\frac{B_2\,[\sqrt{-3}\,(V-U)-3\,(U+V)]\,(A_3+\omega_1^2)}{2\sqrt{-3}\,(U^3-V^3)}\,J_0(\omega_1)\,\frac{dy}{y}\right.$$

$$+\int_0^\infty (1-e^{-y^2\bar{t}D_1})\,\frac{B_2\,[\sqrt{-3}\,(V-U)+3\,(U+V)]\,(A_3+\omega_2^2)}{2\sqrt{-3}\,(U^3-V^3)}\,J_0(\omega_2)\,\frac{dy}{y}$$

$$\left.+\int_0^\infty (1-e^{-y^2\bar{t}D_1})\,\frac{B_2\,(U-V)(A_3+\omega_3^2)}{U^3-V^3}\,J_0(\omega_3)\,\frac{dy}{y}\right\} \qquad (\text{II-133})$$

$$s_3(r,t) = \frac{Q_1}{6\pi T_1}\left\{ \int_0^\infty (1-e^{-y^2\bar{t}D_1})\,\frac{B_3 B_4\,[\sqrt{-3}\,(V-U)-3\,(U+V)]}{2\sqrt{-3}\,(U^3-V^3)}\,J_0(\omega_1)\,\frac{dy}{y}\right.$$

$$+\int_0^\infty (1-e^{-y^2\bar{t}D_1})\,\frac{B_3 B_4\,[\sqrt{-3}\,(V-U)+3\,(U+V)]}{2\sqrt{-3}\,(U^3-V^3)}\,J_0(\omega_2)\,\frac{dy}{y}$$

$$\left.+\int_0^\infty (1-e^{-y^2\bar{t}D_1})\,\frac{B_3 B_4\,(U-V)}{U^3-V^3}\,J_0(\omega_3)\,\frac{dy}{y}\right\} \qquad (\text{II-134})$$

In all of these equations, A and B are as in II-129 and U, V, and ω are as in II-111 and II-124, respectively. Obviously, A, B, U, V, and ω are all functions of y. In addition, the Bessel functions in these equations are understood to vanish when the squares of their corresponding arguments, ω^2, are negative.

b. Solutions in Aquitards

To obtain the inverse Laplace transforms of II-120 and II-121 we will use the convolution theorem together with Eqs. II-84 through II-86 and II-130 through II-134. In analogy to Eq. II-87, the required inverses are immediately obtained as follows for the case when only Aquifer 2 is pumped ($C_1 = 0$):

$$s_1'(r,z,t) = \frac{Q_2}{6\pi T_2} \frac{2}{\pi} \sum_{n=1}^{\infty} \frac{1}{n} \sin\frac{n\pi z}{H_1'} \int_0^{\infty} \left[1 - e^{-n^2\pi^2\bar{t}D_1} + \frac{e^{-y^2\bar{t}D_1} - e^{-n^2\pi^2\bar{t}D_1}}{(y^2/n^2\pi^2) - 1} \right] \frac{1}{U^3 - V^3}$$

$$\cdot \left\{ \frac{[\sqrt{-3}\,(V-U) - 3\,(U+V)]}{2\sqrt{-3}} \left[(-1)^n (A_1 + \omega_1^2)(A_3 + \omega_1^2) - B_1(A_3 + \omega_1^2) \right] J_0(\omega_1) \right.$$

$$+ \frac{[\sqrt{-3}\,(V-U) + 3\,(U+V)]}{2\sqrt{-3}} \left[(-1)^n (A_1 + \omega_2^2)(A_3 + \omega_2^2) - B_1(A_3 + \omega_2^2) \right] J_0(\omega_2)$$

$$+ (U-V) \left[(-1)^n (A_1 + \omega_3^2)(A_3 + \omega_3^2) - B_1(A_3 + \omega_3^2) \right] J_0(\omega_3) \bigg\} \frac{dy}{y} \qquad \text{(II-135)}$$

The drawdown $s_2'(r,z,t)$ in Aquitard 2 can be obtained from Eq. II-135 by symmetry and there is no need to write it down explicitly.

For the case when only Aquifer 1 is pumped ($C_2 = 0$), we have

$$s_1'(r,z,t) = \frac{\bar{Q}_1}{6\pi T_1} \frac{2}{\pi} \sum_{n=1}^{\infty} \frac{1}{n} \sin\frac{n\pi z}{H_1'} \int_0^{\infty} \left[1 - e^{-n^2\pi^2\bar{t}D_1} + \frac{e^{-y^2\bar{t}D_1} - e^{-n^2\pi^2\bar{t}D_1}}{(y^2/n^2\pi^2) - 1} \right] \frac{1}{U^3 - V^3}$$

$$\cdot \left\{ \frac{[\sqrt{-3}\,(V-U) - 3\,(U+V)]}{2\sqrt{-3}} \left[(-1)^n B_2(A_3 + \omega_1^2) + B_3 B_4 - (A_2 + \omega_1^2)(A_3 + \omega_1^2) \right] J_0(\omega_1) \right.$$

$$+ \frac{[\sqrt{-3}\,(V-U) + 3\,(U+V)]}{2\sqrt{-3}} \left[(-1)^n B_2(A_3 + \omega_2^2) + B_3 B_4 - (A_2 + \omega_2^2)(A_3 + \omega_2^2) \right] J_0(\omega_2)$$

$$+ (U-V) \left[(-1)^n B_2(A_3 + \omega_3^2) + B_3 B_4 - (A_2 + \omega_3^2)(A_3 + \omega_3^2) \right] J_0(\omega_3) \bigg\} \frac{dy}{y} \qquad \text{(II-136)}$$

$$s_2'(r,z,t) = \frac{Q_1}{6\pi T_1} \frac{2}{\pi} \sum_{n=1}^{\infty} \frac{1}{n} \sin\frac{n\pi z'}{H_2'} \int_0^{\infty} \left[1 - e^{-n^2\pi^2\bar{t}D_1} + \frac{e^{-y^2\bar{t}D_1} - e^{-n^2\pi^2\bar{t}D_1}}{(y^2/n^2\pi^2) - 1} \right] \frac{1}{U^3 - V^3}$$

$$\cdot \left\{ \frac{[\sqrt{-3}\,(V-U) - 3\,(U+V)]}{2\sqrt{-3}} \left[(-1)^n B_3 B_4 - B_2(A_3 + \omega_1^2) \right] J_0(\omega_1) \right.$$

$$+ \frac{[\sqrt{-3}\,(V-U) + 3\,(U+V)]}{2\sqrt{-3}} \left[(-1)^n B_3 B_4 - B_2(A_3 + \omega_2^2) \right] J_0(\omega_2)$$

$$+ (U-V) \left[(-1)^n B_3 B_4 - B_2(A_3 + \omega_3^2) \right] J_0(\omega_3) \bigg\} \frac{dy}{y} \qquad \text{(II-137)}$$

where $z' = z - (H_1' + H_2)$.

Eqs. II-130 through II-137 give the complete solution to the three-aquifer problem as defined in Eqs. II-96 through II-100. It is understood that in all of these solutions, $J_0(\omega) = 0$ whenever $\omega^2 < 0$. The functions $A(y)$, $B(y)$, $U(y)$, $V(y)$, and $\omega(y)$ have been completely defined in Eqs. II-123, II-109, II-111, and II-124.

c. Remark on Nature of Solutions

Although the above solutions include complex numbers under the integral signs (like $\sqrt{-3}$, for example), it is easy to show that the integrands in these equations are always real. From Eq. II-111 we see that when $(\delta^2/4 + \gamma^3/27) < 0$, then U and V are conjugate complex functions

$$U = a + ib$$
$$V = a - ib$$

where a and b are some real functions of y. In such a case $(U^3 - V^3)$ is imaginary, $(V - U)$ is imaginary, and $(U + V)$ is real. Thus $(U - V)/(U^3 - V^3)$ and $[\sqrt{-3}(V - U) \pm 3(U + V)]/\sqrt{-3}(U^3 - V^3)$ are both real so that ω_1^2, ω_2^2, and ω_3^2 are real. Consequently, all the integrals in Eqs. II-130 through II-137 are real.

When $(\delta^2/4 + \gamma^3/27) \geq 0$, then both U and V are real. Thus ω_3^2 is real whereas ω_1^2 and ω_2^2 are conjugate complex functions, and so are $[\sqrt{-3}(V - U) \pm 3(U + V)]/\sqrt{-3}$. Consequently, all the integrals involving ω_3 are real. Let

$$J_0(\omega_1) = u + iv$$
$$J_0(\omega_2) = u - iv$$

$$\frac{\sqrt{-3}(V - U) - 3(U + V)}{2\sqrt{-3}} = a + ib$$

$$\frac{\sqrt{-3}(V - U) + 3(U + V)}{2\sqrt{-3}} = a - ib$$

where u, v, a, and b are some real functions of y. Consider Eq. II-136 as an example and write $(c + id)$ for the brackets in front of $J_0(\omega_1)$ and $(c - id)$ for those in front of $J_0(\omega_2)$. The first and second terms within the $\{ \}$ parentheses become

$$(a + ib)(c + id)(u + iv) + (a - ib)(c - id)(u - iv)$$

which is real. The same argument can be used to show that all the integrands in Eqs. II-130 through II-137 are always real.

5. Reduction to Two-Aquifer Solutions

When the permeability K_2' in Aquitard 2 is zero (see Fig. II-6), the drawdown in Aquifer 3 must also be zero, which is the same as letting K_3 in this aquifer approach infinity. In such a case from Eq. II-129 we will have

$$A_2(y) = -\theta_{21} y^2 + \eta_{21} \cot y$$

$$A_3(y) = B_3(y) = B_4(y) = 0$$

From II-109 we therefore have

$$m = A_1 + A_2$$

$$q = A_1 A_2 - B_1 B_2$$

$$n = 0$$

and Eq. II-110 becomes

$$M = a^2(a^4 + m a^2 + q)$$

The roots of $M = 0$ are

$$a_1^2 = \frac{-m + \sqrt{m^2 - 4q}}{2} \qquad a_2^2 = \frac{-m - \sqrt{m^2 - 4q}}{2} \qquad a_3^2 = 0$$

However, the roots of $M = 0$ are also given by II-112. Equating these roots we obtain

$$a_1^2 = -\frac{U+V}{2} + \frac{U-V}{2}\sqrt{-3} - \frac{m}{3} = -\frac{m}{2} + \frac{D}{2}$$

$$a_2^2 = -\frac{U+V}{2} - \frac{U-V}{2}\sqrt{-3} - \frac{m}{3} = -\frac{m}{2} - \frac{D}{2}$$

$$a_3^2 = U + V - \frac{m}{3} = 0$$

where $D = \sqrt{m^2 - 4q} = \sqrt{(A_1 + A_2)^2 - 4(A_1 A_2 - B_1 B_2)} = \sqrt{4 B_1 B_2 + (A_1 - A_2)^2}$ is the same as in II-81. Solving these equations for U and V we obtain

$$U = \frac{m}{6} + \frac{D}{2\sqrt{-3}}$$

$$V = \frac{m}{6} - \frac{D}{2\sqrt{-3}}$$

$$U + V = \frac{m}{3}$$

$$\frac{U-V}{2}\sqrt{-3} = \frac{D}{2}$$

We can therefore write

$$\sqrt{-3}\,(U^3 - V^3) = \sqrt{-3}\left[\left(\frac{m}{6}\right)^3 + 3\left(\frac{m}{6}\right)^2\left(\frac{D}{2\sqrt{-3}}\right) + 3\left(\frac{m}{6}\right)\left(\frac{D}{2\sqrt{-3}}\right)^2 + \left(\frac{D}{2\sqrt{-3}}\right)^3\right.$$

$$\left. - \left(\frac{m}{6}\right)^3 + 3\left(\frac{m}{6}\right)^2\left(\frac{D}{2\sqrt{-3}}\right) - 3\left(\frac{m}{6}\right)\left(\frac{D}{2\sqrt{-3}}\right)^2 + \left(\frac{D}{2\sqrt{-3}}\right)^3\right]$$

$$= \frac{D}{12}(m^2 - D^2) = \frac{D}{3}(A_1 A_2 - B_1 B_2)$$

Using these values of U, V, and m together with Eq. II-124, we obtain

$$\omega_1{}^2 = -\frac{1}{2}(A_1 + A_2 - D)$$

$$\omega_2{}^2 = -\frac{1}{2}(A_1 + A_2 + D)$$

$$\omega_3{}^2 = 0$$

From Eq. II-129 we see that $\omega_1{}^2$ and $\omega_2{}^2$ are the same as in Eq. II-81.

Consider Eq. II-132. The third integral vanishes because $A_3 = B_3 = \omega_3{}^2 = 0$. The first integral becomes

$$\int_0^\infty (1 - e^{-y^2 \bar{t} D_1}) \frac{-(D + A_1 + A_2)\left[-\frac{1}{2}(A_1 A_2 + A_2{}^2 - A_2 D) + \frac{1}{4}(A_1 + A_2)^2 - \frac{1}{2}(A_1 + A_2)D + \frac{D^2}{4}\right]}{\frac{D}{3}(A_1 A_2 - B_1 B_2)} J_0(\omega_1)\frac{dy}{y}$$

where the numerator of the fractional term may be expanded as follows:

$$\frac{1}{2}(D + A_1 + A_2)(-A_1{}^2 + A_1 D + A_1 A_2 - 2B_1 B_2)$$

$$= A_1 A_2{}^2 - A_1{}^2 A_2 + A_1 B_1 B_2 - A_2 B_1 B_2 + D A_1 A_2 - B_1 B_2 D$$

$$= (A_1 A_2 - B_1 B_2)(A_2 \quad A_1 + D)$$

Upon substitution in the above integral it becomes

$$\frac{3}{2}\int_0^\infty (1 - e^{-y^2 \bar{t} D_1}) \frac{A_2 - A_1 + D}{D} J_0(\omega_1)\frac{dy}{y}$$

and similarly the second integral in II-132 becomes

$$\frac{3}{2}\int_0^\infty (1 - e^{-y^2 \bar{t} D_1}) \frac{A_1 - A_2 + D}{D} J_0(\omega_2)\frac{dy}{y}$$

From Eqs. II-81 and II-129 we see that

$$\frac{A_2 - A_1 + D}{D} = 1 - G$$

$$\frac{A_1 - A_2 + D}{D} = 1 + G$$

so that Eq. II-132 becomes

$$s_1(r,t) = \frac{Q_1}{4\pi T_1} \int_0^\infty (1 - e^{-y^2 \bar{t} D_1}) [(1 - G) J_0(\omega_1) + (1 + G) J_0(\omega_2)] \frac{dy}{y}$$

which is the same as Eq. II-82 for the two-aquifer case.

Let us now consider Eq. II-133. The third integral vanishes because $A_3 = \omega_3^2 = 0$. The first integral becomes

$$\frac{3}{2} \int_0^\infty (1 - e^{-y^2 \bar{t} D_1}) \frac{- B_2 (D + A_1 + A_2) \left[-\frac{1}{2} (A_1 + A_2 - D) \right]}{D (A_1 A_2 - B_1 B_2)} J_0(\omega_1) \frac{dy}{y}$$

and since

$$\frac{1}{2} (A_1 + A_2 + D)(A_1 + A_2 - D) = 2 (A_1 A_2 - B_1 B_2)$$

it reduces to

$$\frac{3}{2} \int_0^\infty (1 - e^{-y^2 \bar{t} D_1}) \frac{2 B_2}{D} J_0(\omega_1) \frac{dy}{y}$$

Similarly, the second integral becomes

$$- \frac{3}{2} \int_0^\infty (1 - e^{-y^2 \bar{t} D_1}) \frac{2 B_2}{D} J_0(\omega_2) \frac{dy}{y}$$

Since $B_2 = \eta_{21} y / \sin y$, Eq. II-133 reduces to

$$s_2(r,t) = \frac{Q_1}{4 \pi T_1} \int_0^\infty (1 - e^{-y^2 \bar{t}_{D_1}}) \frac{2 \eta_{21}}{D} [J_0(\omega_1) - J_0(\omega_2)] \frac{dy}{\sin y}$$

which is the same as Eq. II-83 for the two-aquifer case.

Eq. II-136 for Aquitard 1 obviously reduces to Eq. II-87 for the two-aquifer case, the proof being the same as for Eqs. II-132 and II-133. Using a similar approach one can now easily verify that Eqs. II-130 and II-131 reduce to the symmetric counterparts of Eqs. II-82 and II-83, as expected. This becomes obvious by inspection since Eqs. II-130 and II-131 are similar in form to Eqs. II-133 and II-132, respectively. The same is true with respect to Eq. II-135 which reduces to the symmetric counterpart of II-87.

Thus, the solutions for the three-aquifer case reduce to those for the two-aquifer case when the permeability of Aquitard 2 becomes zero.

E. ASYMPTOTIC SOLUTIONS FOR SMALL VALUES OF TIME

The solutions obtained in Sections C and D for the drawdown in two- and three-aquifer systems have complicated forms and are difficult to evaluate numerically at small values of pumping time. To overcome this difficulty, we will develop asymptotic solutions for small values of time that have relatively simple forms and are easy to evaluate numerically.

Consider the dimensionless terms

$$\bar{t}_{D_1} = \frac{t \alpha_1'}{H_1'^2} \qquad \text{and} \qquad \bar{t}_{D_2} = \frac{t \alpha_2'}{H_2'^2}$$

relative to the two aquitards in Fig. II-6. Since p and t in the Laplace transform are inversely related to each other, we can say that

$$\sqrt{p/\alpha_1{}'}\ H_1{}' > \sqrt{10} \qquad \text{and} \qquad \sqrt{p/\alpha_2{}'}\ H_2{}' < \sqrt{10}$$

whenever $\bar{t}_{D_1} < 0.1$ and $\bar{t}_{D_2} < 0.1$. In such a case

$$\coth\left(\sqrt{p/\alpha_1{}'}\ H_1{}'\right) \approx 1 \qquad \text{and} \qquad \coth\left(\sqrt{p/\alpha_2{}'}\ H_2{}'\right) \approx 1$$

and substituting in Eq. II-104 we obtain

$$
\left.
\begin{aligned}
A_1(p) &\approx \frac{p}{\alpha_1} + \frac{K_1{}'\sqrt{p/\alpha_1{}'}}{T_1} \\[2mm]
A_2(p) &\approx \frac{p}{\alpha_2} + \frac{K_1{}'\sqrt{p/\alpha_1{}'}}{T_2} + \frac{K_2{}'\sqrt{p/\alpha_2{}'}}{T_2} \\[2mm]
A_3(p) &\approx \frac{p}{\alpha_3} + \frac{K_2{}'\sqrt{p/\alpha_2{}'}}{T_3}
\end{aligned}
\right\} \qquad \text{(II-138)}
$$

Consider Eqs. II-105 and II-106. Since $a^2 > 0$, it is obvious that when $C_2 = 0$ these equations can be approximated by

$$
\left.
\begin{aligned}
\bar{\bar{s}}_1 &\approx \frac{C_1}{a^2 + A_1} \\[2mm]
\bar{\bar{s}}_2 &\approx \frac{C_1 B_2}{(a^2 + A_1)(a^2 + A_2)}
\end{aligned}
\right\} \qquad \text{(II-139)}
$$

where $\bar{\bar{s}}_1 \gg \bar{\bar{s}}_2$. Similarly, if $C_1 = 0$, then

$$
\left.
\begin{aligned}
\bar{\bar{s}}_1 &\approx \frac{C_2 B_1}{(a^2 + A_1)(a^2 + A_2)} \\[2mm]
\bar{\bar{s}}_2 &\approx \frac{C_2}{a^2 + A_2} \\[2mm]
\bar{\bar{s}}_3 &\approx \frac{C_2 B_4}{(a^2 + A_2)(a^2 + A_3)}
\end{aligned}
\right\} \qquad \text{(II-140)}
$$

where $\bar{\bar{s}}_2 \gg \bar{\bar{s}}_1$ and $\bar{\bar{s}}_2 \gg \bar{\bar{s}}_3$.

Using Eq. A-8 in Appendix A we see that the inverse Hankel transform of $\bar{\bar{s}}_2$ in Eq. II-140 is

$$\bar{s}_2(r,p) \approx \frac{Q_2}{2\pi T_2} \frac{K_0(r\sqrt{A_2})}{p} \tag{II-141}$$

and the inverse of $\bar{\bar{s}}_1$ in Eq. II-139 is

$$\bar{s}_1(r,p) \approx \frac{Q_1}{2\pi T_1} \frac{K_0(r\sqrt{A_1})}{p} \tag{II-142}$$

From tables of definite integrals we have

$$K_0(x) = \frac{1}{2} \int_0^\infty \exp\left(-y - \frac{x^2}{4y}\right) \frac{dy}{y}$$

and therefore Eq. II-141 can also be written in the form

$$\bar{s}_2(r,p) \approx \frac{Q_2}{4\pi T_2 p} \int_0^\infty \exp\left(-y - \frac{r^2 A_2}{4y}\right) \frac{dy}{y}$$

$$= \frac{Q_2}{4\pi T_2} \int_0^\infty \frac{e^{-y}}{y} \bar{h}(p)\, dy \tag{II-143}$$

where

$$\bar{h}(p) = \frac{1}{p} \exp\left(-p \frac{r^2}{4\alpha_2 y}\right) \exp\left[-\sqrt{p}\left(\frac{K_1' r^2}{T_2 \sqrt{\alpha_1'}} + \frac{K_2' r^2}{T_2 \sqrt{\alpha_2'}}\right) \frac{1}{4y}\right]$$

From tables of Laplace transforms we know that

$$L^{-1}\left[\frac{1}{p} \exp(-c\sqrt{p})\right] = \operatorname{erfc}\left(\frac{c}{2\sqrt{t}}\right) \tag{II-144}$$

where $c > 0$. Using this together with Theorem V in Carslaw and Jaeger (2, p. 7) we obtain

$$L^{-1}[\bar{h}(p)] = \begin{cases} 0 & \text{when } t \le \dfrac{r^2}{4\,\alpha_2\,y} \\[3mm] \text{erfc }[f(y)] & \text{when } t > \dfrac{r^2}{4\,\alpha_2\,y} \end{cases} \qquad \text{(II-145)}$$

where

$$f(y) = \left(\frac{K_1'\, r^2}{T_2\, \sqrt{\alpha_1'}} + \frac{K_2'\, r^2}{T_2\, \sqrt{\alpha_2'}} \right) \Bigg/ \left(8\,y\, \sqrt{t - \frac{r^2}{4\,\alpha_2\,y}} \right)$$

If we define the new dimensionless variable

$$\beta_{ij} \equiv \frac{r}{4\,H_i}\, \sqrt{\frac{K_j'\,\varphi_j'\,c_j'}{K_i\,\varphi_i\,c_i}} \qquad \text{(II-146)}$$

then

$$f(y) = \frac{(\beta_{21} + \beta_{22})\,\sqrt{u_2}}{\sqrt{y\,(y - u_2)}}$$

where $u_2 = r^2/4\,\alpha_2\,t$. Using Eq. II-145, the inverse Laplace transform of II-143 can immediately be written in the form

$$s_2(r,t) = \frac{Q_2}{4\,\pi T_2} \int_{u_2}^{\infty} \frac{e^{-y}}{y}\, \text{erfc}\left[\frac{(\beta_{21} + \beta_{22})\,\sqrt{u_2}}{\sqrt{y\,(y - u_2)}} \right]\, dy \qquad \text{(II-147)}$$

which is equivalent to Hantush's solution for the so called "leaky aquifer" problem (21, p. 3723).

The inverse of Eq. II-142 is

$$s_1(r,t) = \frac{Q_1}{4\,\pi T_1} \int_{u_1}^{\infty} \frac{e^{-y}}{y}\, \text{erfc}\left[\frac{\beta_{11}\,\sqrt{u_1}}{\sqrt{y\,(y - u_1)}} \right]\, dy \qquad \text{(II-148)}$$

-244-

In order to obtain asymptotic solutions for the aquitards, let us consider the case when Aquifer 2 is being pumped $(Q_1 = 0)$. We have seen in Eq. II-140 that $\bar{\bar{s}}_2$ is much larger than both $\bar{\bar{s}}_1$ and $\bar{\bar{s}}_3$. It therefore follows from Eqs. II-101 and II-102 that for points that are not in the immediate vicinity of the unpumped aquifers, we can write

$$\bar{s}_1'(r,z,p) \approx \frac{Q_2}{2\pi T_2 p} \frac{\sinh(\sqrt{p/\alpha_1'}\,z)}{\sinh(\sqrt{p/\alpha_1'}\,H_1')} K_0(r\sqrt{A_2})$$

(II-149)

$$\bar{s}_2'(r,z,p) \approx \frac{Q_2}{2\pi T_2 p} \frac{\sinh[\sqrt{p/\alpha_2'}\,(z_2 - z)]}{\sinh(\sqrt{p/\alpha_2'}\,H_2')} K_0(r\sqrt{A_2})$$

At small values of time such that $\sqrt{p/\alpha_2'}\,H_2' > \sqrt{10}$, we have

$$\frac{\sinh[\sqrt{p/\alpha_2'}\,(H_2' - z')]}{\sinh(\sqrt{p/\alpha_2'}\,H_2')} \approx \frac{\exp[\sqrt{p/\alpha_2'}\,(H_2' - z')] - \exp[-\sqrt{p/\alpha_2'}\,(H_2' - z')]}{\exp(\sqrt{p/\alpha_2'}\,H_2')}$$

$$= \exp(-\sqrt{p/\alpha_2'}\,z') - \exp[\sqrt{p/\alpha_2'}\,(z' - 2H_2')]$$

where $z' = z - (H_1' + H_2)$. Using this together with Eq. II-143, the second equation in II-149 can be written in the form

$$\bar{s}_2'(r,z,p) \approx \frac{Q_2}{4\pi T_2} \int_0^\infty \frac{e^{-y}}{y} \bar{g}(p)\,dy$$

(II-150)

where

$$\bar{g}(p) = \frac{1}{p} \exp\left(-p\frac{r^2}{4\alpha_2 y}\right)\left\{\exp\left[-\sqrt{p}\left(\frac{K_1' r^2}{4 T_2 \sqrt{\alpha_1'}\,y} + \frac{K_2' r^2}{4 T_2 \sqrt{\alpha_2'}\,y} + \frac{z'}{\sqrt{\alpha_2'}}\right)\right]\right.$$

$$\left. - \exp\left[-\sqrt{p}\left(\frac{K_1' r^2}{4 T_2 \sqrt{\alpha_1'}\,y} + \frac{K_2' r^2}{4 T_2 \sqrt{\alpha_2'}\,y} + \frac{2H_2' - z'}{\sqrt{\alpha_2'}}\right)\right]\right\}$$

Using Eq. II-144 together with Theorem V in Carslaw and Jaeger (2, p. 7) we obtain

$$L^{-1}[\bar{g}(p)] = \begin{cases} 0 & \text{when } t \leq \dfrac{r^2}{4\,\alpha_2\,y} \\[3em] \text{erfc}\,[f_1(y)] - \text{erfc}\,[f_2(y)] & \text{when } t > \dfrac{r^2}{4\,\alpha_2\,y} \end{cases} \qquad (\text{II-151})$$

where

$$f_1(y) \;=\; f(y) + \frac{z'/\sqrt{\alpha_2'}}{2\sqrt{t - r^2/(4\,\alpha_2\,y)}}$$

$$f_2(y) \;=\; f(y) + \frac{(2\,H_2' - z')/\sqrt{\alpha_2'}}{2\sqrt{t - r^2/(4\,\alpha_2\,y)}}$$

and $f(y)$ is the same as in Eq. II-145. In terms of β and $\bar{t}_D$ these functions can also be expressed as

$$\left. \begin{aligned} f_1(y) &= \frac{(\beta_{21} + \beta_{22})\sqrt{u_2} \;+\; y\,(z'/H_2')/\sqrt{4\,\bar{t}_{D2}}}{\sqrt{y\,(y - u_2)}} \\[2em] f_2(y) &= \frac{(\beta_{21} + \beta_{22})\sqrt{u_2} \;+\; y\,(2 - z'/H_2')/\sqrt{4\,\bar{t}_{D2}}}{\sqrt{y\,(y - u_2)}} \end{aligned} \right\} \qquad (\text{II-152})$$

Using this together with Eq. II-150 and II-151, the inverse Laplace transform of $\bar{s}_2'(r,z,p)$ is obtained in the form

$$\begin{aligned} s_2'(r,z,t) \;=\; \frac{Q_2}{4\,\pi\,T_2} \int_{u_2}^{\infty} \frac{e^{-y}}{y} \Bigg[& \text{erfc}\left(\frac{(\beta_{21} + \beta_{22})\sqrt{u_2} \;+\; y\,(z'/H_2')/\sqrt{4\,\bar{t}_{D2}}}{\sqrt{y\,(y - u_2)}} \right) \\[1.5em] & - \text{erfc}\left(\frac{(\beta_{21} + \beta_{22})\sqrt{u_2} \;+\; y\,(2 - z'/H_2')/\sqrt{4\,\bar{t}_{D2}}}{\sqrt{y\,(y - u_2)}} \right) \Bigg]\, dy \quad (\text{II-153}) \end{aligned}$$

where $z' = z - (H_1' + H_2)$. By analogy the inverse of $\bar{s}_1'(r,z,p)$ in Eq. II-149 is

$$s_1'(r,z,t) = \frac{Q_2}{4\pi T_2} \int_{u_2}^{\infty} \frac{e^{-y}}{y} \left[\mathrm{erfc}\left(\frac{(\beta_{21}+\beta_{22})\sqrt{u_2} + y(1-z/H_1')/\sqrt{4\bar{t}_{D_1}}}{\sqrt{y(y-u_2)}} \right) \right.$$

$$\left. - \mathrm{erfc}\left(\frac{(\beta_{21}+\beta_{22})\sqrt{u_2} + y(1+z/H_1')/\sqrt{4\bar{t}_{D_1}}}{\sqrt{y(y-u_2)}} \right) \right] dy \quad \text{(II-154)}$$

In the case when Aquifer 1 is being pumped, the solution in Aquitard 1 is

$$s_1'(r,z,t) = \frac{Q_1}{4\pi T_1} \int_{u_1}^{\infty} \frac{e^{-y}}{y} \left[\mathrm{erfc}\left(\frac{\beta_{11}\sqrt{u_1} + y(z/H_1')/\sqrt{4\bar{t}_{D_1}}}{\sqrt{y(y-u_1)}} \right) \right.$$

$$\left. - \mathrm{erfc}\left(\frac{\beta_{11}\sqrt{u_1} + y(2-z/H_1')/\sqrt{4\bar{t}_{D_1}}}{\sqrt{y(y-u_1)}} \right) \right] dy \quad \text{(II-155)}$$

When H_1' approaches infinity, the second part in Eq. II-155 vanishes and the expression reduces to Hantush's asymptotic solution for a semi-infinite aquitard (34, p. 35, Eq. 54).

Eqs. II-147, II-148, II-153, II-154, and II-155 are asymptotic solutions for the drawdown in an aquifer that is being pumped at a constant rate and in its adjacent aquitards. They hold when $\bar{t}_{D_1} < 0.1$ and $\bar{t}_{D_2} < 0.2$ and when z is not in the immediate vicinity of the unpumped aquifers. This is the same as saying that the above asymptotic solutions hold as long as the effect of pumping has not become significant in the unpumped aquifers.

F. COMPLETE SOLUTION TO HANTUSH'S MODIFIED "LEAKY AQUIFER" PROBLEM

The term "leaky aquifer", as it is generally used by groundwater hydrologists, refers to an aquifer that is overlain or underlain by aquitards which permit a significant amount of water to leak into the aquifer as it is being pumped. In Case 1 of his "Modification of the Theory of Leaky Aquifers," Hantush (21) treated the problem of a leaky aquifer where the supply of leakage to the aquitards

comes from some highly permeable source layers. Hantush assumed that these source layers are able to maintain a constant potential during the entire period of pumping. On the basis of this assumption, he was able to obtain the Laplace transform of the solution in the aquifer (21, p. 3722),

$$\bar{s}_2(r,p) = \frac{Q_2}{2\pi T_2 p} K_0(r\sqrt{A})$$ (II-156)

where

$$A(p) = \frac{p}{\alpha_2} + \frac{K_1'}{T}\sqrt{\frac{p}{\alpha_1'}} \coth\left(H_1'\sqrt{\frac{p}{\alpha_1'}}\right) + \frac{K_2'}{T}\sqrt{\frac{p}{\alpha_2'}} \coth\left(H_2'\sqrt{\frac{p}{\alpha_2'}}\right)$$

Here Q_2, T_2, and α_2 refer to the aquifer being pumped, K_2', H_2', and α_2' to the overlying aquitard, and K_1', H_1', and α_1' to the underlying aquitard.

Instead of developing the general inverse Laplace transform of $\bar{s}(r,p)$, Hantush restricted himself to asymptotic solutions for small and large values of pumping time. In order to develop the general inverse of Eq. II-156, it is first necessary that we determine the roots of the equation $A(\lambda) = 0$ where the parameter p has been replaced by the complex variable λ. For this purpose let

$$z \equiv \sqrt{\lambda/\alpha_1'}\, H_1'$$

be a new complex variable. Multiplying $A(\lambda)$ in II-156 by $\alpha_2 H_1'^2/\alpha_1'$ and equating the result to zero, we obtain

$$z^2 + a z \coth z + b z \coth(cz) = 0$$

where a, b, and c are real, positive constants. Since $z = 0$ obviously does not satisfy this equation, we can divide all the terms by z and write

$$z + a\frac{e^{2z}+1}{e^{2z}-1} + b\frac{e^{2cz}+1}{e^{2cz}-1} = 0$$ (II-157)

If $z = x + iy$ where x and y are real, then

$$\frac{e^{2cz} + 1}{e^{2cz} - 1} = \frac{e^{2cx}(\cos 2cy + i\sin 2cy) + 1}{e^{2cx}(\cos 2cy + i\sin 2cy) - 1} \cdot \frac{(e^{2cx}\cos 2cy - 1) - ie^{2cx}\sin 2cy}{(e^{2cx}\cos 2cy - 1) - ie^{2cx}\sin 2cy}$$

$$= \frac{(e^{4cx} - 1) - i2e^{2cx}\sin 2cy}{e^{4cx} + 1 - 2e^{2cx}\cos 2cy}$$

The sum of the real terms in Eq. II-157 must be zero, so that

$$x + a\frac{e^{4x} - 1}{e^{4x} + 1 - 2e^{2x}\cos 2y} + b\frac{e^{4cx} - 1}{e^{4cx} + 1 - 2e^{2cx}\cos 2cy} = 0 \qquad \text{(II-158)}$$

If $x > 0$, then $e^{4cx} - 1 > 0$, and

$$e^{4cx} + 1 - 2e^{2cx}\cos 2cy \geq e^{4cx} + 1 - 2e^{2cx} = (e^{2cx} - 1)^2 > 0$$

so that all the terms in Eq. II-158 are positive, which is impossible. If $x < 0$, then $e^{4cx} - 1 < 0$, the denominators remain positive, so that all the terms in II-158 are negative, which again is impossible. The only remaining possibility is that $x = 0$ and z is imaginary, so that

$$\lambda = -y^2\frac{\alpha_1'}{H_1'^2}$$

We can therefore conclude that the equation $A(\lambda) = 0$ has at most an infinite number of distinct, real, negative roots. This immediately suggests that in applying Mellin's inversion formula (Eq. II-39) to Eq. II-156, the integration can be performed along the contour shown in Fig. II-5 where Γ_n and Γ_n' are semicircles of radii ϵ about the roots of $A(\lambda) = 0$.

Let I_{AC} denote the integral with respect to λ of

$$(e^{\lambda t} - 1)\frac{K_0(r\sqrt{A})}{\lambda}$$

along the AC portion of the contour, let I_{Γ_n} be the corresponding integral along Γ_n, and so on. According to Cauchy's theorem, we can write

$$-\int_{\gamma-i\infty}^{\gamma+i\infty} (e^{\lambda t}-1)\,\frac{K_0(r\sqrt{A})}{\lambda}\,d\lambda$$

$$= \lim_{\substack{\varepsilon\to 0 \\ R\to\infty}} \left[I_{AC} + I_{CD} + I_{DD'} + I_{D'C'} + I_{C'A'} + \sum_{n=1}^{\infty} (I_{\Gamma_n} + I_{\Gamma_n'}) \right] \qquad \text{(II-159)}$$

If we let $f(x)$ in Eq. II-63 be equal to 1, then the results in Eqs. II-52, II-56, II-57, II-60, II-61, and II-72 are directly applicable to our problem and Eq. II-159 becomes

$$-\int_{\gamma-i\infty}^{\gamma+i\infty} (e^{\lambda t}-1)\,\frac{K_0(r\sqrt{A})}{\lambda}\,d\lambda \;=\; -2\pi i \int_0^{\infty} (1-e^{-x^2 t})\,J_0\!\left|\omega(x)\right|\,\frac{dx}{x} \qquad \text{(II-160)}$$

where

$$\omega^2(x) \;=\; \frac{r^2 x^2}{\alpha_2} \;-\; \frac{r^2 K_1' x}{T_2\sqrt{\alpha_1'}}\,\cot\,(x\,H_1'/\sqrt{\alpha_1'}) \;-\; \frac{r^2 K_2' x}{T_2\sqrt{\alpha_2'}}\,\cot\,(x\,H_2'/\sqrt{\alpha_2'})$$

and where it is understood that $J_0(\omega) = 0$ when $\omega^2(x) < 0$.

If we define a new variable

$$y \equiv x\,H_1'/\sqrt{\alpha_1'}$$

and use the definitions in Eq. II-128, then from Eqs. II-39, II-156, and II-160 we obtain

$$s_2(r,t) \;=\; \frac{Q_2}{2\pi T_2} \int_0^{\infty} (1-e^{-y^2 \bar{t} D_1})\,J_0\!\left|\omega(y)\right|\,\frac{dy}{y} \qquad \text{(II-161)}$$

where

$$\omega^2(y) \;=\; \theta_{21}\,y^2 \;-\; \eta_{21}\,y\cot y \;-\; \eta_{22}\,\nu_{22}\,y\cot\,(\nu_{22}\,y)$$

and where the Bessel function must be set to zero when $\omega^2(y) < 0$.

Eq. II-161 is the general solution to the problem described by Hantush in Case 1 of his "Modification of the Theory of Leaky Aquifers" (21).

G. REDUCTION OF THREE-AQUIFER SOLUTION TO THE COMPLETE SOLUTION OF HANTUSH'S MODIFIED "LEAKY AQUIFER" PROBLEM

Consider a special case of the three-aquifer problem described in Section D where the permeabilities K_1 and K_3 in Aquifers 1 and 3 approach infinity. In such case, the drawdowns in these aquifers remain zero when Aquifer 2 is being pumped at a constant rate. This situation is the same as that described in Section F, and the solution to this problem is given by Eq. II-161. One therefore expects that Eq. II-131 should reduce to Eq. II-161 when $K_1 \to \infty$ and $K_3 \to \infty$.

From Eq. II-129 we see that when K_1 and K_3 approach infinity, then

$$A_1(y) = A_3(y) = B_1(y) = B_4(y) = 0$$

so that m, q, and n in Eq. II-109 become

$$m = A_2(y)$$
$$q = 0$$
$$n = 0$$

Substituting these values in Eq. II-111 we get

$$\gamma = -A_2^2/3 \qquad\qquad \delta = 2A_2^3/27$$

so that $U = V = -A_2/3$. Using these values in Eq. II-124, we get

$$\omega_1^2 = -\frac{A_2}{3} - \frac{1}{2}\left(-\frac{A_2}{3} - \frac{A_2}{3}\right) = 0$$

$$\omega_2^2 = \omega_1^2 = 0$$

$$\omega_3^2 = -\frac{A_2}{3} - \frac{A_2}{3} - \frac{A_2}{3} = -A_2$$

Thus, the first and second integrals in Eq. II-131 cancel each other, and we remain only with the third integral. Now

$$\frac{(U-V)\,\omega_3{}^4}{U^3-V^3} = \frac{\omega_3{}^4}{U^2+V^2+UV} = \frac{A_2{}^2}{\dfrac{A_2{}^2}{9}+\dfrac{A_2{}^2}{9}+\dfrac{A_2{}^2}{9}} = 3$$

so that Eq. II-131 reduces to

$$s_2(r,t) = \frac{Q_2}{2\,\pi T_2} \int_0^\infty (1-e^{-y^2\bar{t}D_1})\,J_0\,(\omega_3)\,\frac{dy}{y}$$

where

$$\omega_3{}^2\,(y) = -A_2(y) = \theta_{21}\,y^2 - \eta_{21}\,y\cot y - \eta_{22}\,\nu_{22}\,y\cot(\nu_{22}\,y)$$

which is exactly the same as Eq. II-161.

H. RELATIONSHIP BETWEEN DIMENSIONLESS QUANTITIES USED AND THEIR SIGNIFICANCE

All the solutions that were developed in this chapter can be written in the general form

$$s = \frac{Q_p}{4\,\pi T_p}\,s_D \tag{II-162}$$

where

    s drawdown

    Q_p rate of discharge

    T_p transmissibility of aquifer being pumped

and s_D is a dimensionless quantity that will be referred to as "dimensionless drawdown". For example, Eq. II-161 can be written as

$$s_2(r,t) = \frac{Q_2}{4\pi T_2} s_D$$

where

$$s_D = 2 \int_0^\infty (1 - e^{-y^2 \bar{t}_{D1}}) J_0\big(\omega(y)\big) \frac{dy}{y}$$

Similarly, the Theis solution can be written in the form of Eq. II-162 so that the dimensionless drawdown for this solution is

$$s_D = \int_{1/4t_D}^\infty \frac{e^{-y}}{y} \, dy$$

The quantity t_D will be referred to as "dimensionless time in the aquifer being pumped," or simply as "dimensionless time".

In the case of a one-layer system composed of a single aquifer, the drawdown at any point is given by the Theis solution. In such case, s_D is a function of only one dimensionless quantity

$$s_D = f(t_D) \tag{II-163}$$

Since the functional relationship (Eq. II-163) between s_D and t_D is known, one can use matching techniques to determine values of s_D and t_D that correspond to some known values of drawdown s and pumping time t that were obtained through measurements in the field. Assuming that the geometry of the system is known, one can now use Eq. II-162 together with the definition

$$t_D = \frac{\alpha t}{r^2} = \frac{kt}{\varphi c \mu r^2}$$

to determine the unknown quantities k and φc for the aquifer. Thus, in the case of a single-layer system, the Theis solution provides us with two dimensionless

quantities, s_D and t_D, that enable us to determine the two unknown properties of the aquifer, k and φc.

In a multiple-aquifer system there exist two unknown quantities in each layer that are of interest to the hydrologist: (a) the permeability k, which is indicative of the flow properties of the layer, and (b) φc, which is related to the ability of the layer to store liquid and to the elasticity of the saturated medium. A complete solution to the problem of flow in a multiple-aquifer system must therefore involve a number of dimensionless quantities that are twice the number of layers in the system. In addition, these quantities must be such that they enable one to uniquely determine the values of k and φc for each layer in the system.

We saw that in the case of a single-layer system, the solution was given in terms of the two dimensionless quantities s_D and t_D. Consider now the two-aquifer system shown in Fig. II-4. The drawdowns in each layer of this system are given by Eqs. II-82, II-83, and II-87 and all of these solutions depend on the dimensionless quantities defined in Eq. II-80. One can easily verify that when Aquifer 1 is being pumped, then $\bar{t}_{D_1} = \theta_{11} t_D$. Therefore, it follows that the solutions in all of these three layers are given in terms of the six dimensionless quantities

$$s_D, \ t_D, \ \theta_{11}, \ \theta_{21}, \ \eta_{11}, \ \text{and } \eta_{21}$$

Obviously, knowing the values of these quantities will give us six equations in six unknowns that can be solved for k and φc in each layer. Similarly, Eq. II-129 shows that the solutions for the three-aquifer case depend on the ten quantities

$$s_D, \ t_D, \ \theta_{11}, \ \theta_{21}, \ \theta_{22}, \ \theta_{32}, \ \eta_{11}, \ \eta_{21}, \ \eta_{22}, \ \text{and } \eta_{32}$$

because the system here consists of five different layers.

Consider now a multiple-aquifer system that is composed of n different layers. If one plots the dimensionless drawdown s_D at some point in the system versus the dimensionless time t_D in the aquifer being pumped, one obtains a curve that is characterized by (n - 1) values of θ_{ij} and by (n - 1) values of η_{ij}. In the case of the Theis solution, n = 1 and the curve of s_D versus t_D is unique. Since the drawdown s is directly proportional to s_D and pumping time t is directly proportional to t_D, one can use graphical matching techniques to determine the values of s_D and t_D that correspond to some known values of s and t as measured in the field. However, when the number of layers in the system is larger than one, there will be no unique relationship between s_D and t_D. Instead, one will obtain an infinite number of such curves, each corresponding to some given values of θ_{ij} and η_{ij}.

An interesting feature of the asymptotic solutions for small values of time that were developed in Section II-E is that they always involve a maximum of four dimensionless quantities. For example, Eq. II-153 involves the quantities

$$s_D, \ t_D, \ \bar{t}_{D_2}, \ \text{and} \ (\beta_{21} + \beta_{22})$$

and Eq. II-148 involves only

$$s_D, \ t_D, \ \text{and} \ \beta_{11}$$

This fact will be utilized in Chapter V to develop practical methods of evaluating multiple-aquifer systems with the aid of pumping tests.

Using the definitions in Eqs. II-128 and II-146, one can easily verify that the following relationships always hold:

$$\left.\begin{aligned}
\bar{t}_{D_j} &= \theta_{ij} t_{D_i} \\
\beta_{ij} &= \eta_{ij} / 4 \sqrt{\theta_{ij}} \\
r/B_{ij} &= \sqrt{\eta_{ij}}
\end{aligned}\right\} \qquad (\text{II-164})$$

where r/B_{ij} has been defined in the nomenclature. The reason that we are using β_{ij} and r/B_{ij} in this work is that these quantities have been introduced into the literabure by Hantush and Jacob (16,21) and are now widely accepted by ground-water hydrologists.

Eq. II-164 shows that solutions written in terms of θ_{ij} and η_{ij} can also be expressed in terms of the corresponding quantities β_{ij} and r/B_{ij}. Therefore, from now on we will express all the solutions that were developed in this work in terms of the dimensionless quantities

$$s_D, \ t_D, \ \beta_{ij}, \ \text{and} \ r/B_{ij}$$

which will make these solutions directly comparable to those of Hantush and Jacob.

I. NUMERICAL EVALUATION OF SOLUTIONS

The solutions for the two-aquifer case and the asymptotic solutions for small values of time have been evaluated numerically using the Zonneveld-Adams Moulton numerical method of integration. The particular program employed in the evaluation was developed by Dr. Loren P. Meissner, Lawrence Radiation Laboratory, University of California, Berkeley, and it is available from the Computer Center Library at the University upon request.

The method has been applied to evaluate Eqs. II-82, II-83, II-87, II-148, and II-155. Except for Eq. II-87, the evaluation of these equations with the aid of the above program is straight forward and does not require any further comment.

To evaluate Eq. II-87, it is useful to note that the integral in this equation converges to two different limits as n approached infinity; one limit for odd values of n and the other for even values of n. It was found by experience that in most cases this convergence is so rapid that the integrals for odd and even values of n may be considered constant after just a few terms in the series. If, in addition, one also considers the fact that the integral is independent of z/H' and that the

term $\sin(n \pi z/H')$ repeats itself in cyclic order for any given value of z/H', one may be able to reduce the computer time necessary for the evaluation of this equation to a minimum.

In most cases the asymptotic solutions, Eqs. II-148 and II-155, can be evaluated much faster than the general solutions, Eqs. II-82, II-83, and II-87, because they do not involve oscillating functions.

The numerical results obtained in evaluating the two-aquifer solutions will be discussed in Chapter IV.

III. FINITE ELEMENT METHOD

In the previous chapter, two separate mathematical models of a multiple-aquifer system were discussed. The first model, described in Section II-A, had relatively simple geometry but involved complex boundary conditions which made the problem intractable analytically. We therefore had to resort to further simplification by imposing certain restrictions on the directions of flow in various parts of the system and limiting the thicknesses of the unpumped aquifers. This laid the ground work for a modified mathematical model which, although less representative of the actual situation, could nevertheless be solved analytically (Section II-B).

However, the use of a simplified model raised two questions: (a) To what extent do the analytical solutions represent the true behavior of a multiple-aquifer system and (b) what is the true behavior of such a system? Our ability to answer these questions seems to depend on the development of numerical techniques which are well adapted to modern digital computers and require a minimum number of restrictions on the geometry and flow properties of the system.

Thus far, none of the conventional finite difference techniques seem to completely satisfy these requirements. Recently, however, a powerful new numerical technique has been introduced into the field of groundwater hydrology. This technique is especially well adapted to high speed digital computers and can easily handle problems that involve flow in anisotropic, heterogeneous porous media with complex boundary conditions. We are referring to the little known finite element method of analysis which, although new to the field, has already demonstrated its usefulness on several occasions (29,41,46,50,51).

The history of the finite element method and its development from the direct stiffness scheme, initially employed in the aircraft industry and various branches of structural engineering, to the present use of variational principles

in conjunction with the finite element discretization, have been reviewed by Javandel and Witherspoon (29). Attention is directed here only to those works which pertain directly to heat conduction in solids and to fluid flow in porous media. Zienkiewicz and Cheung were the first to apply the finite element method to problems of steady state heat conduction in isotropic solids (50). Later, Zienkiewicz, et al. (51), used the method to investigate steady state flow of fluids in anisotropic porous media. The method was further extended by Taylor and Brown (41) to account for free surface boundaries in steady state seepage. In 1964 Gurtin (12) developed the variational principle for linear initial value problems which enabled Wilson and Nickel (46) in 1966 to apply the finite element method to problems involving transient heat conduction in aniso-tropic, heterogeneous solids of arbitrary geometry and complex boundary conditions. Their approach was further modified and adapted to flow of slightly compressible fluids in porous media by Javandel and Witherspoon (29) in 1968.

In the present work the finite element method was used to obtain a numerical solution for the problem of transient flow in multiple-aquifer systems described by Eqs. II-1 through II-5. The results were then utilized to investigate the true behavior of such systems and to obtain an independent check on the analytical solutions developed in Chapter II.

A general description of the mathematical principles that underlie the finite element method was given by Javandel and Witherspoon (29), using matrix notation. In the following discussion we shall present in detail, from a some-what different view point, those aspects of the theory which pertain to the partic-ular computer program employed in this work. Indicial notation will be used and particular emphasis will be given to the explicit evaluation of all the matrices which enter into the computer program.

A. VARIATIONAL PRINCIPLE FOR INITIAL VALUE PROBLEMS INVOLVING FLOW IN POROUS MEDIA

Let us consider a saturated, anisotropic porous medium whose permeability, K_{ij}, is a symmetric 3 x 3 matrix which may be a function of the space coordinates*. The average flow velocity vector, v_i, at any point in the medium, is given by Darcy's generalized formula

$$v_i = -K_{ij} \frac{\partial s}{\partial x_j} \; ; i, j = 1, 2, 3 \tag{III-1}$$

The equation of continuity for a small element in the medium can be expressed as

$$\frac{\partial (\gamma \, v_i)}{\partial x_i} = -\frac{\partial (\gamma \, \varphi)}{\partial t} \tag{III-2}$$

Eqs. III-1 and III-2 may be combined to obtain the partial differential equation which governs flow in the porous medium. In the particular case when the liquid is slightly compressible, the governing equation becomes

$$\frac{\partial}{\partial x_i} \left(K_{ij} \frac{\partial s}{\partial x_j} \right) = S_s \frac{\partial s}{\partial t} \tag{III-3}$$

Eq. III-3 together with the initial condition

$$s(x_i, 0) = s_o(x_i) \tag{III-4}$$

define the initial value problem for flow of slightly compressible liquids in porous media.

---

*For a short discussion of the indicial notation, refer to Appendix B

Gurtin (12) showed that Eqs. III-3 and III-4 can be translated into a variational problem. To show how this is done, we first define the convolution of two functions, $f_1(t)$ and $f_2(t)$, as

$$f_1(t) * f_2(t) \equiv \int_0^t f_1(t-T) f_2(T) \, dT = \int_0^t f_1(T) f_2(t-T) \, dT \qquad \text{(III-5)}$$

Using this definition, Gurtin arrived at the following

Lemma: A function $s(x_i, t)$ satisfies the initial value problem defined by

$$\frac{\partial}{\partial x_i} \left(K_{ij} \frac{\partial s}{\partial x_j} \right) = S_s \frac{\partial s}{\partial t} \qquad \text{(III-3)}$$

$$s(x_i, 0) = s_o(x_i) \qquad \text{(III-4)}$$

if and only if it satisfies

$$\frac{\partial}{\partial x_i} \left(K_{ij} * \frac{\partial s}{\partial x_j} \right) = S_s(s - s_o) \qquad \text{(III-6)}$$

Proof: Assuming that Eqs. III-3 and III-4 hold, we can use Eq. III-5 to write

$$\frac{\partial}{\partial x_i} \left(K_{ij} * \frac{\partial s}{\partial x_j} \right) = \frac{\partial}{\partial x_i} \int_0^t K_{ij} \frac{\partial}{\partial x_j} s(x_i, T) \, dT$$

$$= \int_0^t \frac{\partial}{\partial x_i} \left[K_{ij} \frac{\partial}{\partial x_j} s(x_i, T) \right] dT = S_s \int_0^t \frac{\partial}{\partial T} s(x_i, T) \, dT$$

$$= S_s \left[s(x_i, t) - s(x_i, 0) \right] = S_s (s - s_o)$$

which shows that Eq. III-6 is satisfied.

We can now reverse the argument to demonstrate that if Eq. III-6 holds, then

$$\int_0^t \frac{\partial}{\partial x_i} [K_{ij} \frac{\partial}{\partial x_j} s(x_i, T)] d T = \frac{\partial}{\partial x_i} (K_{ij} * \frac{\partial s}{\partial x_j})$$

$$= S_s(s - s_o) = S_s \int_0^t \frac{\partial}{\partial t} s(x_i, T) d T$$

which completes the proof of the lemma.

The lemma leads to the following.

Corollary: The variational principle for the initial value problem, defined by Eqs. III-3 and III-4, is the same as the variational principle for the problem defined by Eq. III-6.

On the basis of this corollary, Gurtin proved the following.

Theorem: Let $\mathcal{F}$ be the set of all functions $s(x_i, t)$ which, together with their first derivatives, are continuous in some region R and satisfy the boundary conditions

$$s(A_1, t) = U \tag{III-7}$$

where $A = A_1 + A_2$ is the boundary of the region R, and U is a prescribed function. We will refer to $\mathcal{F}$ as the set of "admissible functions," since they satisfy all the constraints of the variational problem.

For any admissible functions $s \, \epsilon \, \mathcal{F}$, at any time $t \, \epsilon \, [0, \infty)$, we define the functional

$$\Omega(s) \equiv \int_V \left[S_s s * s + K_{ij} * \frac{\partial s}{\partial x_i} * \frac{\partial s}{\partial x_j} - 2 S_s s * s_o \right] d V$$

$$- 2 \int_{A_2} K_{ij} * \overline{U} * s \, d A_2 \tag{III-8}$$

-263-

where V is the volume of the region R and $\overline{U}$ is a prescribed function such that

$$\frac{\partial s}{\partial n}\bigg|_{A_2} = \overline{U} \;;\; n - \text{outer normal to } A_2 \tag{III-9}$$

The variation, $\delta\Omega(s)$, of this functional vanishes at a particular function $s \in \mathcal{F}$ if and only if s is the solution to the following initial boundary value problem:

$$\left.\begin{array}{l} \dfrac{\partial}{\partial x_i}\left(K_{ij}\dfrac{\partial s}{\partial x_j}\right) = \dfrac{\partial s}{\partial t} \\[12pt] s(x_i, 0) = s_0(x_i) \\[12pt] s(A_1, t) = U \\[12pt] \dfrac{\partial s}{\partial n}\bigg|_{A_2} = \overline{U} \end{array}\right\} \tag{III-10}$$

The details of the proof have been given by Javandel and Witherspoon (29) and will not be repeated here.

The immediate result of this theorem can be stated as follows. Suppose that one is able to find an admissible function, $s(x_i, t)$, which minimizes the functional $\Omega(s)$ in Eq. III-8. One would then have the solution for the initial boundary value problem defined by Eq. III-10. Thus, instead of dealing with a problem that involves partial differential equations, one can now deal with another problem that involves searching for some admissible function which minimizes the functional $\Omega(s)$. We shall refer to such a function as the "minimizing function". It should be mentioned that in the case of real physical problems, the existence of a minimizing function is always guaranteed through the known existence of a solution to the corresponding initial boundary value problem.

B. PRINCIPLES OF THE FINITE ELEMENT METHOD

In the previous section, we have defined our variational problem and have shown that its solution may be obtained in the form of a minimizing function. We will now turn our attention to the "direct variational methods" of finding such a function for a given variational problem.

Most direct variational methods involve the construction of a minimizing sequence

$$\{ s_n \} = s_1, s_2, \dots, s_n \tag{III-11}$$

of admissible functions $s \in \mathcal{F}$, such that

$$\lim_{n \to \infty} s_n = s \tag{III-12}$$

where s is the minimizing function, and

$$\Omega(\lim_{n \to \infty} s_n) = \lim_{n \to \infty} \Omega(s_n) = \Omega(s) \tag{III-13}$$

where $\Omega(s)$ is the greatest lower bound of Ω taken over all the admissible functions $s \in \mathcal{F}$. From Eqs. III-12 and III-13 we see that if s is the solution to the variational problem then the functions of the sequence $\{ s_n \}$ can be considered as approximate solutions to the problem (9).

In the well known Rayleigh-Ritz method, which is of particular interest for the following discussion, the functions of the minimizing sequence $\{ s_n \}$ are taken as the linear combination of a finite number of linearly independent admissible functions, $u_i \in \mathcal{F}$,

$$s_n = a_1 u_1 + a_2 u_2 + \dots + a_n u_n \tag{III-14}$$

where a_i are arbitrary real coefficients. When s_n from Eq. III-14 is substituted for the minimizing function, s, in the functional $\Omega(s)$, the latter becomes a function of the n independent variables a_1, a_2, ... , a_n. The next step is to choose the values of a_1, a_2, ... , a_n in such a way as to minimize the functional $\Omega(s_n)$. This is done by differentiating $\Omega(s_n)$ with respect to each coefficient a_i and equating the results to zero,

$$\frac{\partial \Omega(s_n)}{\partial a_i} = 0 \; ; i = 1, 2, \ldots , n \qquad \text{(III-15)}$$

Eq. III-15 represents a set of n simultaneous linear algebraic equations in the n unknowns a_i. Solving these equations and substituting the results in Eq. III-14 will yield an approximate solution to the variational problem at hand. As previously mentioned, the exact solution is given by the limit of the sequence $\{ s_n \}$ as n approaches infinity.

Usually, the more complex the boundary conditions of a given variational problem, the more difficult it is to find a sequence $\{ s_n \}$ which satisfies these boundary conditions. One way of simplifying the problem is to divide the region into a finite number of elements (or subregions) and define the functions s_n separately for each element. The finite element idealization is particularly helpful because (a) it is usually much easier to find a sequence of functions $\{ s_n \}$ which satisfy the constraints of a problem defined over a small region with simple boundary conditions than of a problem defined over a large region with complex boundary conditions and (b) the smaller the domain of definition of a given sequence of functions $\{ s_n \}$, the faster this sequence approaches the minimizing function. In other words, the smaller the elements, the fewer the terms needed in Eq. II-14 in order for s_n to be a sufficient approximation of the exact solution. This means that there are two ways for the minimizing sequence to converge to the true solution: (a) by increasing the number of functions u_n in Eq. III-14 and (b) by decreasing the size of the elements while keeping the number of functions u_n in Eq. III-14 constant.
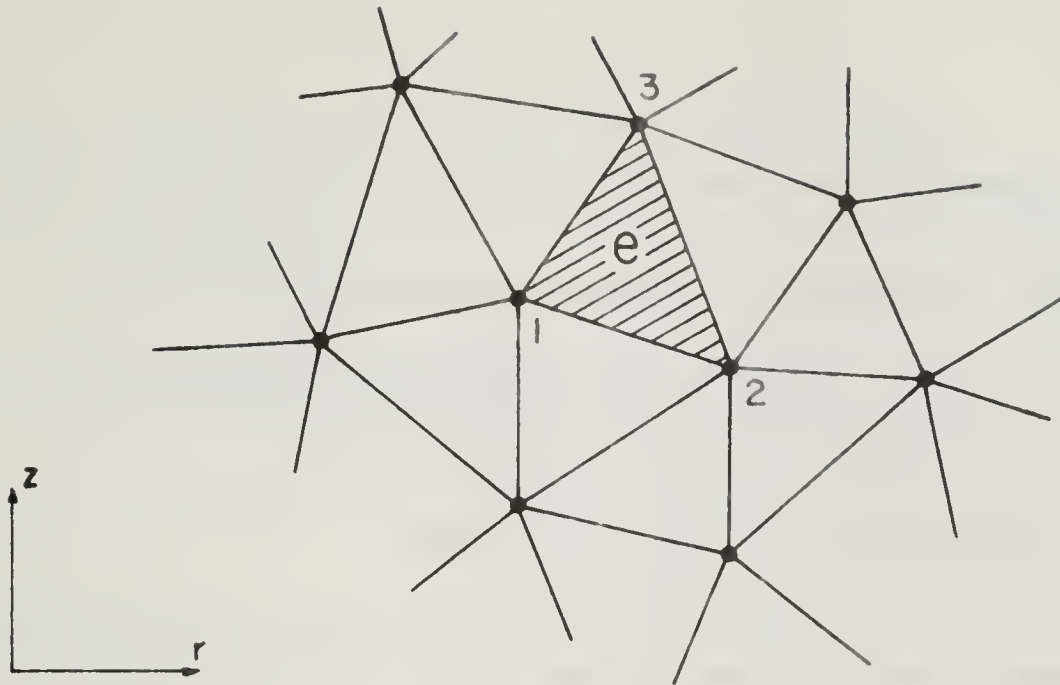
Fig. III-1. Two dimensional triangular elements.
[After Zienkiewicz (50)]
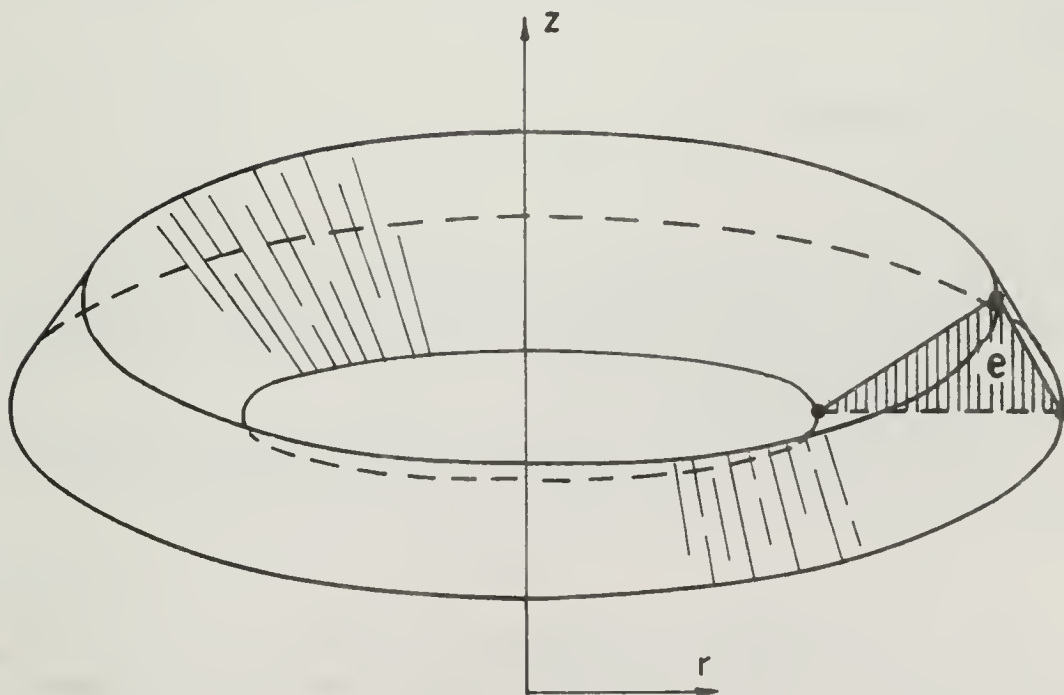
Fig. III-2. Axisymmetric element with constant triangular
cross-section.

In the following analysis, the Rayleigh-Ritz method will be used in conjunction with the finite element discretization to solve the variational problem defined by Eqs. III-7 through III-9 for two dimensional and axisymmetric porous media. The medium will be divided into triangular elements in the two dimensional case (Fig. III-1) and into concentric rings of constant triangular cross-section in the axisymmetric case (Fig. III-2). In both cases, the solution will be a function of only two space coordinates, r and z.

C. CONSTRUCTION OF MINIMIZING SEQUENCE

Since we are dealing with real physical problems, the solutions in each element are analytic and can be expanded in a power series. It is therefore convenient to construct the minimizing sequence $\{s_n\}$ (Eq. III-14) for any element e in the form

$$s_n = a_1 + a_2 r + a_3 z + a_4 r^2 + a_5 r z + a_6 z^2 + a_7 r^3 + \ldots + a_n r^{m-k} z^k \quad (III-16)$$

where

$$n = \frac{(m+1) m}{2} + k + 1 ,$$

s_n is a function of r, z, and t, and a_i are functions of t. The values of a_i for each element must be chosen in such a way that the functions s_n satisfy the boundary conditions for their respective elements and minimize the functional $\Omega(s_n)$ over the entire medium.

If the elements are sufficiently small, drawdown within each element may be approximated by a linear function and Eq. III-16 reduces to

$$s = a + b r + c z \quad (III-17)$$

Considering a typical triangle (Figs. III-1 and III-2), let s_1, s_2. and s_3 be the values of drawdown at the nodal points 1, 2, and 3, respectively. Since s in Eq. III-17 must satisfy these boundary conditions, we can write

$$s_1 = a + b\,r_1 + c\,z_1$$

$$s_2 = a + b\,r_2 + c\,z_2 \qquad \text{(III-18)}$$

$$s_3 = a + b\,r_3 + c\,z_3$$

Solving for a, b, and c and substituting in Eq. III-17, we obtain

$$s = \frac{1}{2\,\Delta}\,[(a_1 + b_1\,r + c_1\,z)s_1 + (a_2 + b_2\,r + c_2\,z)s_2 + (a_3 + b_3\,r + c_3\,z)s_3] \qquad \text{(III-19)}$$

where

$$
\begin{array}{lll}
a_1 = r_2\,z_3 - r_3\,z_2 & \quad b_1 = z_2 - z_3 & \quad c_1 = r_3 - r_2 \\[2mm]
a_2 = r_3\,z_1 - r_1\,z_3 & \quad b_2 = z_3 - z_1 & \quad c_2 = r_1 - r_3 \qquad \text{(III-20)} \\[2mm]
a_3 = r_1\,z_2 - r_2\,z_1 & \quad b_3 = z_1 - z_2 & \quad c_3 = r_2 - r_1
\end{array}
$$

and

$$2\,\Delta = \begin{vmatrix} 1 & r_1 & z_1 \\ 1 & r_2 & z_2 \\ 1 & r_3 & z_3 \end{vmatrix} = \text{twice area of triangle 1, 2, 3} \qquad \text{(III-21)}$$

Obviously, s is still a function of r, z, and t, while s_1, s_2, and s_3 are functions of t only. Since s in Eq. III-19 satisfies all the constraints of the variational problem for any element e, it may be considered as an admissible function for that particular element.

D. MINIMIZATION OF THE FUNCTIONAL

The next step is to determine the values of the drawdowns s_1, s_2, and s_3 at the nodal points of all the elements in the medium so as to minimize the functional $\Omega(s)$ in Eq. III-8. For this purpose we again choose a representative element, e, (Figs. III-1 and III-2), and define the 1 x 3 matrix

$$N_n \equiv \frac{1}{2\Delta} \, (a_n + b_n \, r + c_n \, z) \tag{III-22}$$

for that element. Using this definition. Eq. III-19 can be rewritten in the form

$$s = N_n \, s_n \tag{III-23}$$

Substituting Eq. III-23 in Eq. III-8, the functional $\Omega^e (s)$ for the element becomes

$$\Omega^e (s) = \int_{V^e} \left[S_s \, N_n \, s_n \cdot N_m \, s_m + K_{ij} \cdot \frac{\partial N_n}{\partial x_i} \, s_n \cdot \frac{\partial N_m}{\partial x_j} \, s_m - 2 \, S_s \, N_n \, s_n \cdot N_m \, s_{o_m} \right] dV^e$$

$$- 2 \int_{A^e} K_{ij} \cdot \bar{U} \cdot N_n \, s_n \, dA^e \tag{III-24}$$

where V^e is the volume of the element and A^e is the surface area across which $\bar{U}$ has been prescribed.

The functional for the entire medium, $\Omega(s)$, is the sum of the functionals for the individual elements, $\Omega^e (s)$:

$$\Omega(s) = \sum_e \Omega^e (s) \tag{III-25}$$

Let us suppose that the nodal points in the medium have been numbered in sequential order from 1 to N, where N is the total number of nodal points. We now want to determine the values of s_n so as to minimize the functional $\Omega(s)$. Remembering that s_n are functions of time and that $\Omega(s)$ involves integration with respect to time as well with respect to the space coordinates, Eq. III-15 cannot be directly applied to our problem. In order to minimize $\Omega(s)$ with respect to s_n, we replace $s_n(t)$ by $s_n(t) + \varepsilon \, \eta(t)$ where ε is an arbitrary constant and $\eta(t)$ is a continuously differentiable function which vanishes at $t = 0$ and $t = t$. The functional in Eq. III-25 now becomes

$$\Omega_n(\varepsilon) = \sum_e \left\{ \int_{V^e} \int_0^t \left[S_s N_n \left(s_n(T) + \varepsilon \eta(T) \right) N_m s_m(t-T) + \right. \right.$$

$$+ K_{ij} * \frac{\partial N_n}{\partial x_i} \left(s_n(T) + \varepsilon \eta(T) \right) \frac{\partial N_m}{\partial x_j} s_m(t-T) -$$

$$\left. - 2 S_s N_n \left(s_n(T) + \varepsilon \eta(T) \right) N_m s_{om} \right] dT \, dV^e -$$

$$\left. - 2 \int_{A^e} \int_0^t K_{ij} * \overline{U} N_n \left(s_n(T) + \varepsilon \eta(T) \right) dT \, dA^e \right\} \qquad (\text{III-26})$$

The minimum value of this functional with respect to s_n is obtained when

$$\left. \frac{d\Omega_n(\varepsilon)}{d\varepsilon} \right|_{\varepsilon=0} = 0$$

Thus,

$$\left. \frac{d\Omega_n(\varepsilon)}{d\varepsilon} \right|_{\varepsilon=0} = 2\eta * \sum_e \left\{ \int_{V^e} \left[S_s N_n N_m s_m + K_{ij} * \frac{\partial N_n}{\partial x_i} \frac{\partial N_m}{\partial x_j} s_m - \right. \right.$$

$$\left. \left. - S_s N_n N_m s_{om} \right] dV^e - \int_{A^e} K_{ij} * \overline{U} N_n \, dA^e \right\} = 0$$

Since η is arbitrary, we obtain N equations of the form

$$\sum_e \left\{ \int_{V^e} \left[S_s N_n N_m s_m + K_{ij} * \frac{\partial N_n}{\partial x_i} \frac{\partial N_m}{\partial x_j} s_m - S_s N_n N_m s_{om} \right] dV^e - \right.$$

$$\left. - \int_{A^e} K_{ij} * \overline{U} N_n \, dA^e \right\} = 0 \qquad (\text{III-27})$$

which involve N unknown values of the nodal drawdowns, s_m.

Obviously, the above integrals vanish for all elements which do not include the nth nodal point. Thus, only those elements which are shared by the nth nodal point will contribute to the nth equation in Eq. III-27. The resulting set of equations will therefore be sparse, a fact which greatly facilitates the application of digital computers to the finite element method.

If we define the 3 x 3 matrices

$$D_{nm}{}^e \equiv S_S \int_{V^e} N_n N_m \, d V^e \qquad \text{(III-28)}$$

and

$$AA_{nm}{}^e \equiv K_{ij} \int \frac{\partial N_n}{\partial x_i} \frac{\partial N_m}{\partial x_j} \, d V^e \qquad \text{(III-29)}$$

and substitute them in Eq. III-27, the nth equation becomes

$$\sum_e \left[D_{nm}{}^e (s_m - s_{o_m}) + AA_{nm}{}^e * s_m - \int_{A^e} K_{ij} * \overline{U} N_n \, d A^e \right] = 0 \quad \text{(III-30)}$$

From Eq. C-3 in Appendix C we know that

$$D_{nm}{}^e = \begin{cases} \dfrac{S_S \Delta}{12} & \text{if } n \neq m \\[3mm] 2 \dfrac{S_S \Delta}{12} & \text{if } n = m \end{cases} \qquad \text{(III-31)}$$

for a planar triangle, and

$$D_{nm}{}^e = \begin{cases} 2 \pi \bar{r} \dfrac{S_S \Delta}{12} & \text{if } n \neq m \\[3mm] 4 \pi \bar{r} \dfrac{S_S \Delta}{12} & \text{if } n = m \end{cases} \qquad \text{(III-32)}$$

for a concentric ring with triangular cross-section, where $\bar{r}$ is the average value of r for the triangle and Δ^e is its area.

To determine the form of $AA_{nm}{}^e$ for a planar triangle, we write

$$AA_{nm}{}^e = \int_\Delta K_{ij} \frac{\partial N_n}{\partial x_i} \frac{\partial N_m}{\partial x_j} \, d\Delta$$

$$= \int_\Delta \left(K_{rr} \frac{\partial N_n}{\partial r} \frac{\partial N_m}{\partial r} + K_{rz} \frac{\partial N_n}{\partial r} \frac{\partial N_m}{\partial z} + K_{zr} \frac{\partial N_n}{\partial z} \frac{\partial N_m}{\partial r} + K_{zz} \frac{\partial N_n}{\partial z} \frac{\partial N_m}{\partial z} \right) dr \, dz$$

$$= \int_\Delta \frac{1}{4\Delta^2} (K_{rr} b_n b_m + K_{rz} b_n c_m + K_{zr} c_n b_m + K_{zz} c_n c_m) \, dr \, dz$$

$$= \frac{1}{4\Delta} (K_{rr} b_n b_m + K_{rz} b_n c_m + K_{zr} c_n b_m + K_{zz} c_n c_m) \qquad \text{(III-33)}$$

For a concentric ring with triangular cross-section this becomes simply

$$AA_{nm}{}^e = 2\pi \bar{r} \frac{1}{4\Delta} (K_{rr} b_n b_m + K_{rz} b_n c_m + K_{zr} c_n b_m + K_{zz} c_n c_m) \qquad \text{(III-34)}$$

The integral over A^e in Eq. III-30 is directly proportional to the flow rate through the boundaries of the element. Since flow from any element, A, into some adjacent element, B, is equal to but opposite in sign to the flow from B to A, these integrals cancel at all internal points in the medium which do not act as sinks (or sources) and vanish at all impermeable or constant potential boundaries. The forms of the integrals for elements whose boundaries act as sinks (or sources) will depend on the nature and geometry of these sinks.

We now turn our attention to the case of a well of radius r_w located at the axis of an axisymmetric medium and operating at some prescribed rate of discharge, Q (t). The well, together with a typical axial element, e, is shown in Fig. III-3. Let us assume that the discharge from the element into the well, Q^e (t), is evenly distributed along the z axis, such that $\partial s/\partial r$ at $r = r_w$
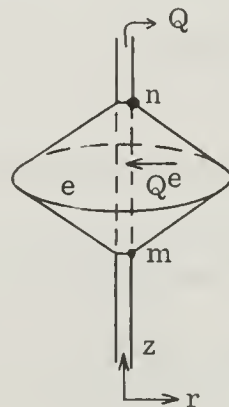
Fig. III-3. Well with typical axial element.

is not a function of z in this element. Remembering that N_n is a linear function of z, that $N_n(n) = 1$ and $N_n(m) = 0$ (see Eq. C-2 in Appendix C), and using the definition of $\overline{U}$ in Eq. III-9, we can write

$$\int_{A^e} K_{ij} * \overline{U} N_n \, dA^e = K_{rr} * \int_{z_m}^{z_n} \left. \frac{\partial s}{\partial r} \right|_{r=r_W} N_n \, 2\pi r_W \, dz$$

$$= K_{rr} \left. \frac{\partial s}{\partial r} \right|_{r=r_W} 2\pi r_W (z_n - z_m) * \frac{N_n(n) + N_n(m)}{2}$$

$$= \frac{1}{2} * Q^e(t) \tag{III-35}$$

Eqs. III-31 through III-35 give us the explicit forms of the element matrices inside the brackets in Eq. III-30.

Let us define the 1 x N matrix

$$Q_n(t) \equiv \sum_e \frac{1}{2} Q^e(t) \tag{III-36}$$

where the summation is taken over the elements adjacent to the n-th nodal point, and the N x N matrices

$$D_{nm} \equiv \sum_e D_{nm}^e$$

$$AA_{nm} \equiv \sum_e AA_{nm}^e \tag{III-37}$$

We can then rewrite Eq. III-30 in the form

$$D_{nm}(s_m - s_{o_m}) + AA_{nm} * s_m - 1 * Q_n = 0 \tag{III-38}$$

During a sufficiently small time interval, Δt, the functions s_m and Q_n can be assumed to vary linearly with time. We therefore have for Δt

$$1 * s_m = \int_{t-\Delta t}^{t} s_m(\tau) \, d\tau \approx \frac{\Delta t}{2} \left[s_m(t) + s_m(t - \Delta t) \right] \qquad \text{(III-39)}$$

and

$$1 * Q_n \approx \frac{\Delta t}{2} \left[Q_n(t) + Q_n(t - \Delta t) \right] = \Delta t \, \overline{Q}_n \qquad \text{(III-40)}$$

where $\overline{Q}_n$ is the average value of Q_n during the interval Δt. Substituting in Eq. III-38 and rearranging, we obtain

$$\frac{1}{2} \left[s_m(t) + s_m(t - \Delta t) \right] \left[D_{nm} + \frac{\Delta t}{2} AA_{nm} \right] = \frac{\Delta t}{2} \overline{Q}_n + D_{nm} \, s_m(t - \Delta t) \qquad \text{(III-41)}$$

Defining the new matrices

$$A_{nm} \equiv D_{nm} + \frac{\Delta t}{2} AA_{nm}$$

$$B_n \equiv \frac{\Delta t}{2} \overline{Q}_n + D_{nm} \, s_m(t - \Delta t) \qquad \text{(III-42)}$$

$$x_m \equiv \frac{1}{2} \left[s_m(t) + s_m(t - \Delta t) \right]$$

Eq. III-41 can be rewritten in a concise form as

$$A_{nm} x_m = B_n \qquad \text{(III-43)}$$

Eqs. III-43 are a set of N simultaneous linear algebraic equations which can be solved for the N unknowns, x_m, provided that the values of $s_m(t - \Delta t)$ at all the nodal points are known. At the beginning of the first time step, Δt_1, these values are given by the initial conditions, $s_m(0) = s_{0m}$. Thus, Eqs. III-43 may be used to calculate the values of x_m and $s_m(t_1)$ at the end of this time step. The newly obtained nodal drawdowns, $s_m(t_1)$, can then be substituted for $s_m(t - \Delta t)$ in Eq. III-42 and used in calculating these values of x_m and $s_m(t_2)$ at the end of the second time step, Δt_2. This procedure can be continued until the drawdowns prior to any desired value of time have all been determined.

As stated earlier, the set of Eqs. III-43 is sparse, and the matrix A_{nm} is banded. Thus, if each nodal point, n, in the finite element network is shared by not more than M - 1 triangles, there will not be more than M non-zero values of A_{nm} for each value of n. The number M is usually referred to as the "band width" of the matrix A_{nm}.

E. CONSTANT DRAWDOWN BOUNDARY CONDITIONS

If drawdown at some nodal point k remains constant at all values of time, we will have

$$s_k(t) = s_k(t - \Delta t) = s_k$$

where s_k is constant. Eq. III-41 can therefore be written in the form

$$\frac{1}{2} [s_m(t) + s_m(t - \Delta t)] [D_{nm} + \frac{\Delta t}{2} AA_{nm}] = \frac{\Delta t}{2} [\bar{Q}_n - AA_{nk} s_k] + D_{nm} s_m(t - \Delta t)$$

where $m \neq k$. In general, one can account for constant drawdown boundaries in Eqs. III-43 by simply redefining

$$D_{nk} \equiv 0$$

$$A_{nk} \equiv 0 \qquad\qquad\qquad\qquad\qquad\qquad\qquad\qquad\qquad\text{(III-44)}$$

$$B_n \equiv \frac{\Delta t}{2} \left[\bar{Q}_n - \sum_k AA_{nk} s_k \right] + D_{nm} s_m(t - \Delta t) ; \quad m \neq k$$

where k represents all the nodal points at which the drawdown remains constant. With these definitions, Eqs. III-43 can now be used unaltered.

If there are K constant drawdown nodes in the network, Eqs. III-43 will represent a set of N simultaneous linear algebraic equations in N - K unknowns. Since some of these equations are redundant, the total number of equations may be reduced from N to N - K.

F. WELL OF CONSTANT DISCHARGE IN A NON-UNIFORM FLOW FIELD

Let us assume that a well of radius r_w which has been completed at the center of an axisymmetric porous medium is pumped at a constant rate, Q. When the flow field near the axis is uniform, the discharge is evenly distributed along the wellbore and the contributions of the axial elements, Q^e, to the total discharge, Q, are directly proportional to the vertical dimensions of these elements at the center of the medium. When the flow field is not uniform, as in the case of multiple-layered media, the values of Q^e become time dependent and the distribution of discharge along the wellbore becomes uneven. This variable inner boundary condition was first incorporated into the finite element method by Javandel and Witherspoon (29), using the theory of super-position. A detailed review of this approach is given in the following discussion.

Consider a well that is surrounded by $K - 1$ axial elements with triangular cross-sections so that the total number of nodal points along the well is K. As indicated by Eqs. III-36 and III-40, at each time step, Δt, these nodal points can be associated with some average nodal discharges, $\overline{Q}_n$, which can be expressed in the form

$$\overline{Q}_n = \sum_e \frac{1}{2} \overline{Q}^e \qquad \text{(III-45)}$$

where $\overline{Q}^e = \frac{1}{2} [Q^e(t) + Q^e(t - \Delta t)]$.

The summation in the above equation is taken over the two axial elements shared by the n-th nodal point and $\overline{Q}^e$ represents the average discharge from the element e during the interval Δt. The values of $\overline{Q}_n$ and $\overline{Q}^e$ are constant during any given time step, but they may change from one time step to another.

During any time step, Δt, the total discharge, Q, may be expressed as the sum of the average nodal discharges, $\overline{Q}_n$:

$$Q = \sum_{n=1}^{K} \bar{Q}_n \qquad\qquad\qquad \text{(III-46)}$$

If the discharge is not uniformly distributed along the wellbore, the values of $\bar{Q}_n$ cannot be determined from the dimensions of the axial element. Thus, Eqs. III-43 will give us N equations in N + K unknowns, which is impossible to solve.

If we assume that the drawdown in the wellbore is uniform at any given time, t, the number of unknowns can be reduced from N + K to N + 1. The number of unknowns can be further reduced from N + 1 to N by guessing at the value of $\bar{Q}_K$ during the first time step, Δt_1. This makes it possible to solve the N equations in Eqs. III-43 for the N - K + 1 unknown nodal drawdowns, $s_m(t_1)$, and the remaining K - 1 nodal discharges at the wellbore, $\bar{Q}_n(\Delta t_1)$. The actual total discharge during this time step is given by

$$Q_1 = \sum_{n=1}^{K} \bar{Q}_n(\Delta t_1)$$

For the next time step, Δt_2, the estimate of $\bar{Q}_K$ can be improved with the formula

$$\bar{Q}_K(\Delta t_i) = \frac{Q}{Q_{i-1}} \bar{Q}_K(\Delta t_{i-1}) \qquad\qquad \text{(III-47)}$$

where Q is the prescribed discharge at the well. (This procedure can be repeated after each time step.) Solving Eqs. III-43 for $s_m(t_2)$ and $\bar{Q}_n(\Delta t_2)$, the actual total discharge for the second time step may be calculated from

$$Q_2 = \sum_{n=1}^{K} \bar{Q}_n(\Delta t_2)$$

The discharge profile for the entire period of pumping is shown in Fig. III-4.
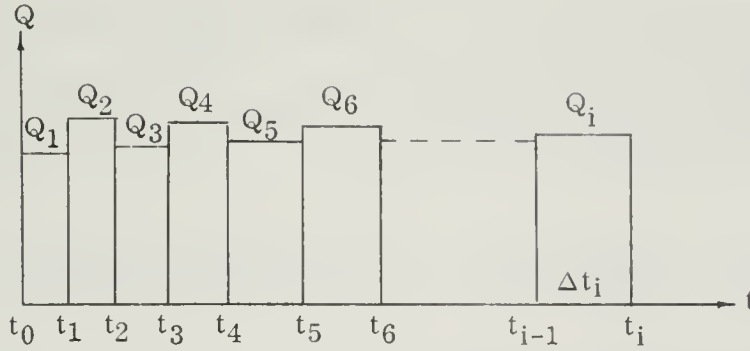
Fig. III-4. Variation of average total rate of discharge with time.

It is well known that drawdown at any point in a porous medium, at any time, t, is directly proportional to the strength of the sink that operates in that medium. Thus, for each nodal point, m, there exists a function, $f_m(\Delta t)$, such that

$$s_m(t) - s_m(t_0) = Q \, f_m(t - t_0) \qquad \text{(III-48)}$$

If Q changes from time step to time step as in Fig. III-4, we can use the principle of superposition to write

$$s_m(t_1) - s_m(t_0) = Q_1 \, f_m(t_1 - t_0)$$

$$s_m(t_2) - s_m(t_0) = Q_1 \, f_m(t_2 - t_0) + (Q_2 - Q_1) \, f_m(t_2 - t_1)$$

.
.
.

$$s_m(t_i) - s_m(t_0) = Q_1 \, f_m(t_i - t_0) + (Q_2 - Q_1) \, f_m(t_i - t_1)$$
$$+ (Q_3 - Q_2) \, f_m(t_i - t_2) + \cdots$$
$$\cdots + (Q_i - Q_{i-1}) \, f_m(t_i - t_{i-1}) \qquad \text{(III-49)}$$

Let us denote the solutions of Eqs III-43 for the first time step, Δt_1, by $\bar{s}_m(t_1)$. As mentioned earlier, these solutions correspond to the discharge Q_1 which is not necessarily the same as the prescribed discharge Q. Multiplying

-279-

the values of $\bar{s}_m(t_1)$ by Q/Q_1 while assuming that $s_m(t_0) = 0$ for all values of m (drawdown initially zero) and using Eq. III-49, we obtain a new set of solutions, $s_m(t_1)$, which correspond to the prescribed discharge, Q, during the first time step:

$$\frac{Q}{Q_1} \bar{s}_m(t_1) = \frac{Q}{Q_1} [Q_1 f_m(t_1 - t_0)] = Q f_m(t_1 - t_0) = s_m(t_1) \qquad (III-50)$$

Using the corrected solutions, $s_m(t_1)$, we can solve Eqs. III-43 for the second time step, Δt_2, to obtain the drawdowns $\bar{s}_m(t_2)$ which correspond to the discharges Q during Δt_1 and Q_1 during Δt_2. Using Eq. III-49 we can write

$$\bar{s}_m(t_2) = Q f_m(t_2 - t_0) + (Q_2 - Q) f_m(t_2 - t_1)$$

If we choose t_2 in such a way that $\Delta t_2 = t_1 - t_0$, this equation becomes

$$\bar{s}_m(t_2) = s_m(t_2) + \frac{Q_2 - Q}{Q} s_m(t_1)$$

and the corrected drawdowns, $s_m(t_2)$, corresponding to the discharge Q, will be given by

$$s_m(t_2) = \bar{s}_m(t_2) - \frac{Q_2 - Q}{Q} s_m(t_1) \qquad (III-51)$$

Using these values to calculate the solutions at the end of the third time step, we obtain

$$\bar{s}_m(t_3) = Q f_m(t_3 - t_0) + (Q_3 - Q) f_m(t_3 - t_2)$$

where $\bar{s}_m(t_3)$ corresponds to the discharges Q during Δt_1 and Δt_2 and Q_3 during Δt_3. We now have two possibilities: either choose t_3 such that $\Delta t_3 = t_1 - t_0$, in which case the corrected solutions are given by

$$s_m(t_3) = \bar{s}_m(t_3) - \frac{Q_3 - Q}{Q} s_m(t_1) \qquad (\text{III-52})$$

or choose t_3 such that $\Delta t_3 = t_2 - t_0$, in which case the corrected solutions can be obtained from

$$s_m(t_3) = \bar{s}_m(t_3) - \frac{Q_3 - Q}{Q} s_m(t_2) \qquad (\text{III-53})$$

In general, the solutions may be corrected for Q using the recurrence formula

$$s_m(t_i) = \bar{s}_m(t_i) - \frac{Q_i - Q}{Q} s_m(t_j) \qquad (\text{III-54})$$

where

$t_j - t_0 = \Delta t_i = t_i - t_{i-1}; \qquad j < i$

Q_i = actual discharge during Δt_i

$s_m(t_i)$ = drawdown at nodal point m and time $t = t_i$ due to pumping with constant discharge Q during the interval $[t_0, t_i)$

$\bar{s}_m(t_i)$ = drawdown at nodal point m and time $t = t_i$ due to pumping with constant discharges Q during the interval $[t_0, t_{i-1})$ and Q_i during the time step Δt_i

Eq. III-54 can be used to calculate the drawdown at any nodal point m at any time, $t = t_i$, due to a well that discharges at a constant rate Q during the interval $[t_0, t_i)$ in a non-uniform flow field.

In the next chapter, the finite element method will be used to examine the behavior of a two-aquifer system and to obtain an independent check on the analytical solutions developed in Chapter II.

IV. BEHAVIOR OF MULTIPLE-AQUIFER SYSTEMS

A. INVESTIGATION OF A TWO-AQUIFER SYSTEM

The analytical solutions and finite element technique described in
Chapters II and III, respectively, can be used to investigate flow fields around
pumping wells in multiple-aquifer systems. As a basic approach to such an
analysis, we will study the behavior of a system consisting of only two aquifers,
separated by a single aquitard. We assume that the layers are homogeneous,
isotropic, uniform in thickness and infinite in radial extent. A well of infini-
tesimal radius completely penetrates one of the aquifers and discharges at
a constant rate Q. The system which is saturated with water and is in a static
condition prior to pumping, is illustrated in Fig. II-4.

1. Approach to Problem

Our primary objective here is to develop an understanding of the
transient flow patterns in the vicinity of a pumping well that operates in a
two-aquifer system. For this purpose, we must be able to determine the
values of the dimensionless drawdowns, s_D, at each point in the system at
all values of pumping time, t. One way of obtaining such data is to evaluate
numerically the analytical solutions in Section II-C (Eqs. II-82, II-83 and
II-87) for various values of the dimensionless parameters t_D, β_{ij} and r/B_{ij}.
Another possibility is to divide the system into a network of finite elements
and use the method described in Chapter III to calculate the dimensionless
drawdowns at the nodal points of the mesh, at various values of pumping time,
t. The advantages and disadvantages of each of these methods will be dis-
cussed below.

Our analytical solutions were developed with the assumption that flow
is essentially horizontal in the aquifers and vertical in the aquitard. These
solutions are therefore theoretically limited to systems in which the unpumped
aquifer is relatively thin, and in which the permeability of the aquitard is

-283-

much smaller than the permeabilities of both aquifers. The finite element method, on the other hand, is free from such limitations and can be used to investigate two-aquifer systems with arbitrary thicknesses and permeabilities. This suggests that flow patterns obtained with the finite element method should be more representative of the actual situation than those obtained from the analytical solutions.

To demonstrate the importance of the analytical solutions, it should be remembered that the dimensionless drawdown, s_D, at a given point (r, t) in the two-aquifer system is a function of the following thirteen variables: t, K_1, K_1', K_2, φ_1, φ_1', φ_2, c_1, c_1', c_2, H_1, H_1', H_2. In Section II-H it was shown that under the limitations for which the analytical solutions were developed, the values of s_D depend on only five dimensionless quantities, t_D, β_{11}, r/B_{11}, β_{21}, r/B_{21}. Obviously, values of s_D obtained with the finite element method in the absence of these limitations can also be expressed in terms of dimensionless quantities. However, the form of these quantities is unknown, and to determine them would require that we investigate the effect on the solutions of all possible dimensionless combinations of the above thirteen variables, which is impractical. Thus, the analytical solutions have an advantage over the finite element method in that they enable us to express the dimensionless drawdown at any point within the system in terms of a minimum number of parameters.

Since neither the analytical approach nor the finite element method is by itself sufficient to analyze the problem, we will use a combination of those methods to investigate the behavior of a two-aquifer system. Our approach will be as follows: (a) various two-aquifer systems with different properties will be studied using the finite element technique, (b) each system will be subdivided into a network of finite elements, and values of the dimensionless drawdown, s_D, at each nodal point will be calculated at different values of pumping time, t, (c) at a selected number of nodal points, the values of s_D will be plotted on logarithmic paper versus the corresponding values of

t_D, β_{ij} and r/B_{ij} and (d) the resulting curves will then be compared to results obtained through numerical evaluation of the analytical solutions at similar values of t_D, β_{ij} and r/B_{ij}.

As long as the permeability ratios K_1/K_1' and K_2/K_1' are sufficiently large, and the thickness H_2 of the unpumped aquifer is sufficiently small, the dimensionless drawdown s_D for practical values of time at any given values of t_D, β_{ij} and r/B_{ij} should be the same whether determined from the finite element or the analytical approach. We will then gradually decrease the ratios of K_1/K_1' and K_2/K_1', without changing the values of t_D, β_{ij} and r/B_{ij}, until the two sets of solutions will no longer coincide. In this way, we will be able to determine the limiting values of K_1/K_1' and K_2/K_1' below which the dimensionless drawdowns will cease to be unique functions of t_D, β_{ij} and r/B_{ij}. At this point the analytical solutions will have to be discarded, and the system studied with the aid of the finite element method alone. The effect of the thickness, H_2, on the applicability of the analytical solutions will also be investigated in a similar manner.

The distribution of curves of equal drawdown around the pumping well in different systems and at various values of pumping time will also be plotted from results obtained with the finite element method. Here the analytical solutions are of little use, since they assume that flow is unidirectional within each layer.

Finally, the functional relationships between s_D, t_D, β_{ij} and r/B_{ij} will be utilized to develop practical methods of evaluating multiple-aquifer systems in the field with the aid of pumping tests.

2. Design of Finite Element Network

A typical finite element network used to investigate two-aquifer systems is illustrated in Fig. IV-1. The network represents a radial cross-section through the three-dimensional axisymmetric medium, so that each triangle and rectangle in the figure is a part of a concentric ring of constant cross-

-285-
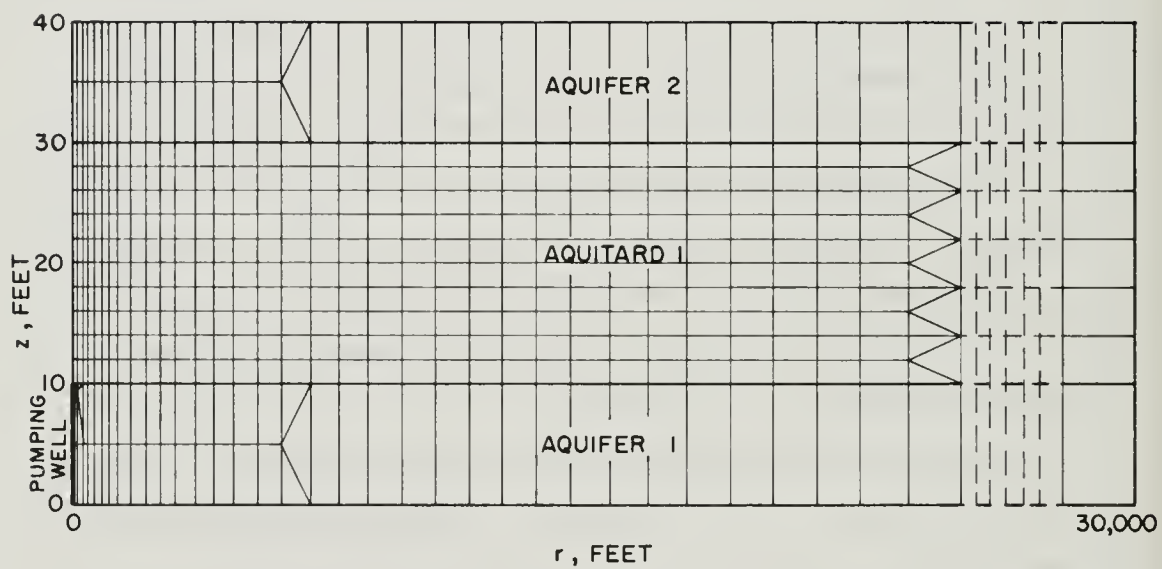
Fig. IV-1. Network of finite elements used to investigate a two-aquifer system.

section. The computer program automatically divides each rectangle into triangles. The network consists of 542 nodal points and of 501 elements. The pumping well coincides with the axis and removes fluid only from the bottom three axial elements. The external radius of the network is 30,000 feet, and the elements increase in size along the radial dimension from the axis outward. The thicknesses and properties of the individual layers in the system vary from problem to problem.

For any problem, the solutions at the end of each time step are obtained both in the form of drawdowns, s (feet of water), and in the form of dimensionless drawdowns, s_D. By definition, the values of β_{ij} and r/B_{ij} at any point are directly proportional to the radial distance, r, from the pumping well. This means that the ratios between the values of β_{ij} and r/B_{ij} are the same at all nodal points in any given problem. In addition, each nodal value of s_D at the end of any given time step can be associated with some known values of t_D, β_{ij} and r/B_{ij}. Therefore, at each nodal point, one obtains a unique functional relationship between the dimensionless drawdown, s_D, and the dimensionless parameters, t_D, β_{ij} and r/B_{ij}. By carefully choosing the properties of the individual layers in the system, one can always fix the values of β_{ij} and r/B_{ij} at the various nodal points as desired. This greatly facilitates comparison of the results with those obtained from the analytical solutions, and enables one to design the network so as to develop curves of s_D versus t_D for arbitrary values of β_{ij} and r/B_{ij}.

3. <u>Curves of Dimensionless Drawdown Versus Dimensionless Time</u>

A convenient way of presenting the numerical results is to plot on logarithmic paper the dimensionless drawdown, s_D, at any point in the system versus the dimensionless time, t_D, in the aquifer being pumped, for various values of the parameters β_{ij} and r/B_{ij}. In the case of a two-aquifer system, each curve of s_D versus t_D is a function of the four dimensionless parameters β_{11}, β_{21}, r/B_{11} and r/B_{21}, so that there exists an infinite number of such curves. Therefore, in presenting the results for this case, one must, for practical

reasons, limit himself to a small sample of this infinite population of possible curves. The combinations of β_{ij} and r/B_{ij} that have been considered in this work are listed in Table IV-1

Table IV-1   List of Figures Showing Values of β_{ij} and r/B_{ij} Investigated

Figure	β_{11}	r/B_{11}	β_{21}	r/B_{21}
IV - 2	0.01	0.01	0, 0.01	0, 0.01
IV - 3	0 1	0.1	0, 0.1	0, 0.1
IV - 4	1.0	1.0	0, 1.0	0, 1.0
IV - 5	0.01	0.02	0, 0.01	0, 0.02
IV - 6	0.05	0.1	0, 0 05	0, 0.1
IV - 7	0.1	0.2	0, 0.1	0, 0.2
IV - 8	0 01	0.1	0.01	0.1
IV - 9	0.1	1.0	0, 0.1	0, 1.0
IV - 10	0 1	0.1	0, 0.00316, 0.01, 0.02, 0.0316, 0 05 0.1, 0.316, 1.0, ∞	0, 0.02, 0.0316, 0.05 0.1, 0.316, 1.0, ∞

Each figure listed in the table shows curves of s_D versus t_D for points in the system which are all at the same radial distance from the pumping well, but at different vertical elevations. From top to bottom, the curves on any given figure correspond to. (a) aquifer being pumped, (b) $z/H_1' = 0.2$ in aquitard, (c) $z/H_1' = 0.5$ d) $z/H_1' = 0.8$, and (e) unpumped aquifer. If one plots the values of s_D as a function of the elevation across any vertical line in these figures, corresponding to some given value of t_D, one obtains the vertical profile of the dimensionless drawdown at some particular values of t_D and r

Each curve in Figs. IV-2 through IV-10 is composed of a steep portion at small values of t_D, and of a relatively flatter portion at large values of t_D.
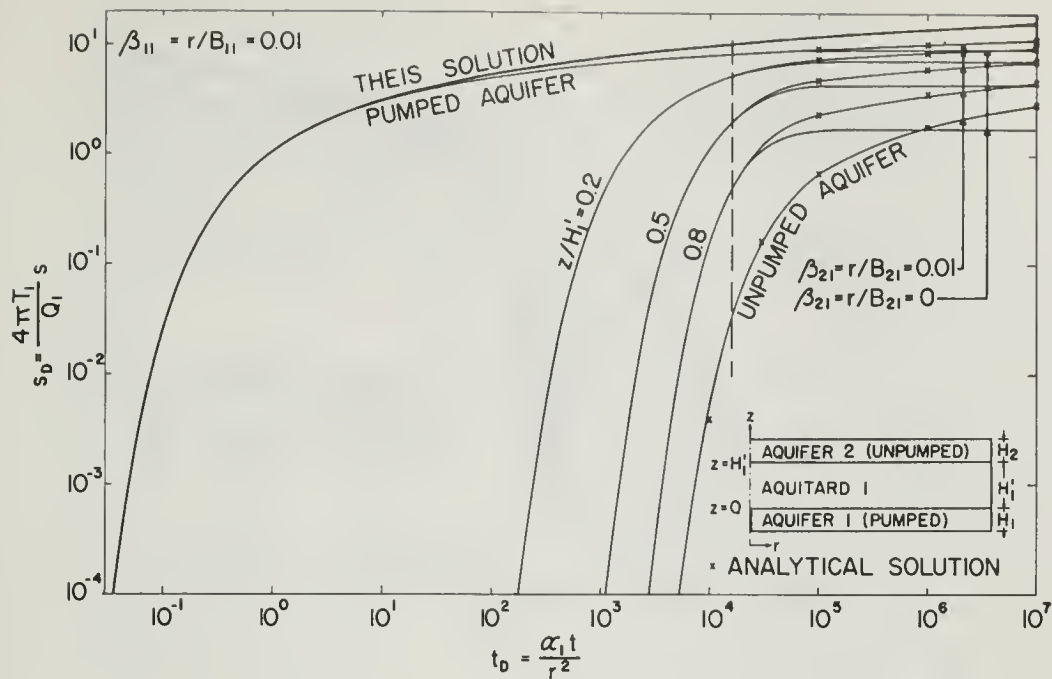
Fig. IV-2. Dimensionless drawdown versus dimensionless time
in a two-aquifer system. ($\beta_{11} = r/B_{11} = 0.01$;
$\beta_{21} = r/B_{21} = 0.01$ and $\beta_{21} = r/B_{21} = 0$)
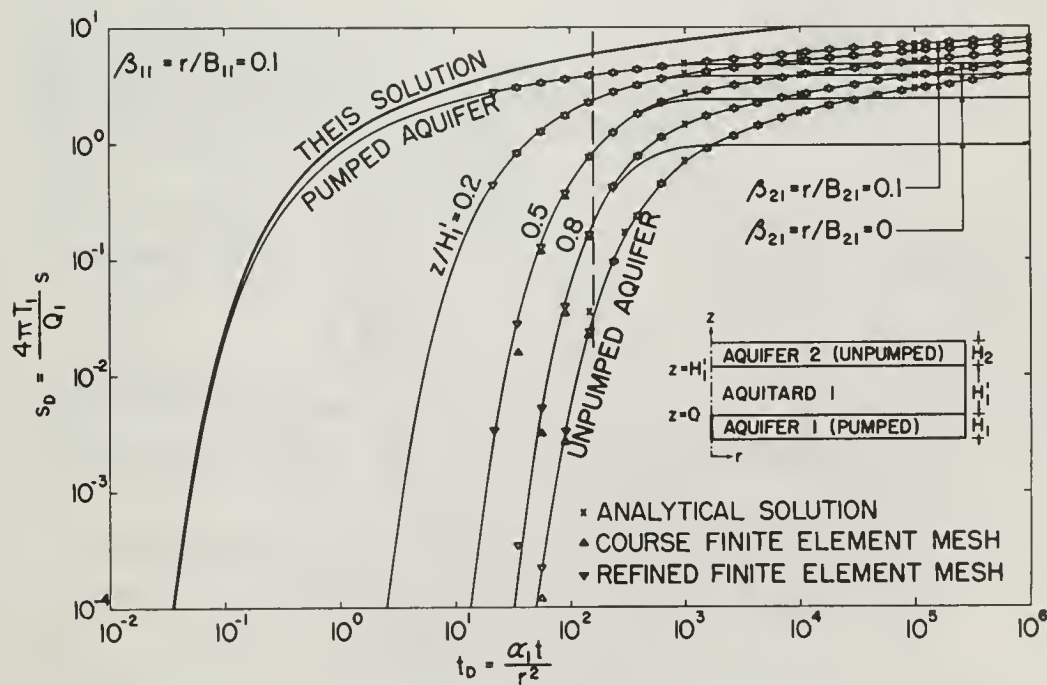
Fig. IV-3. Dimensionless drawdown versus dimensionless time
in a two-aquifer system. ($\beta_{11} = r/B_{11} = 0.1$;
$\beta_{21} = r/B_{21} = 0.1$ and $\beta_{21} = r/B_{21} = 0$)
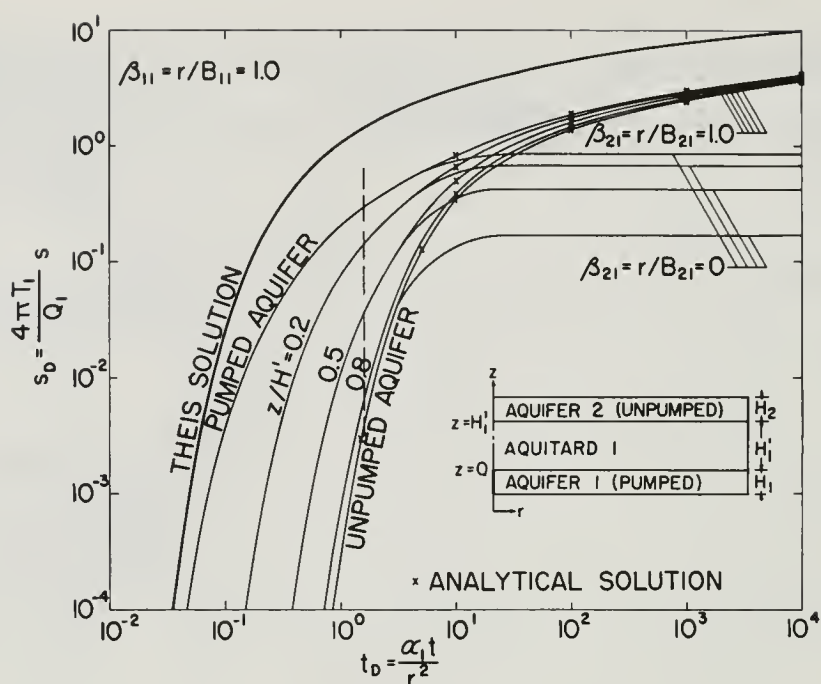
Fig. IV-4. Dimensionless drawdown versus dimensionless time in a two-aquifer system. ($\beta_{11} = r/B_{11} = 1.0$; $\beta_{21} = r/B_{21} = 1.0$ and $\beta_{21} = r/B_{21} = 0$)
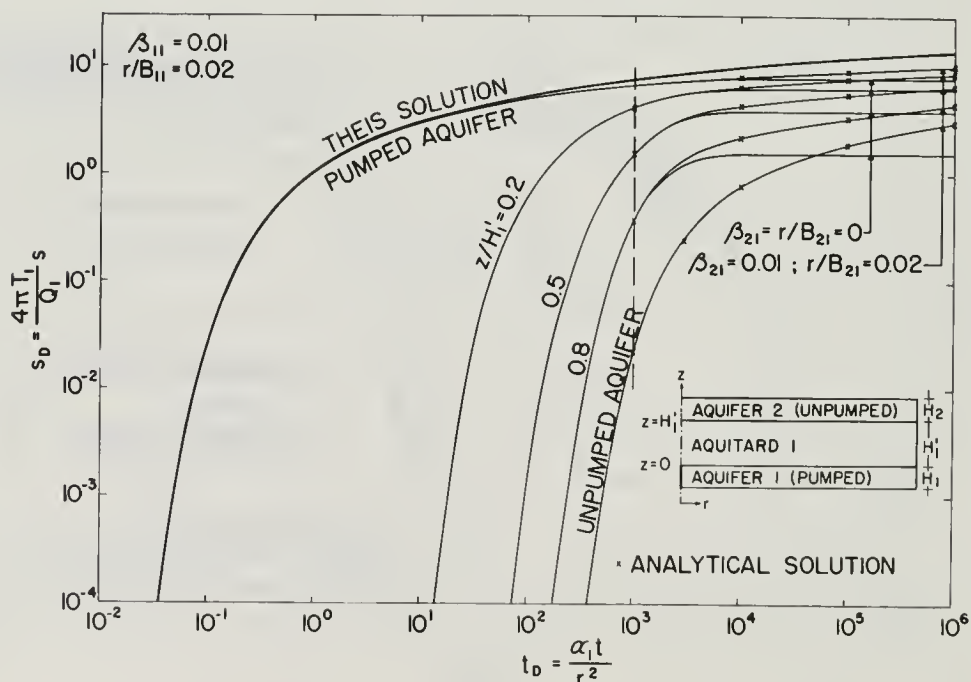
Fig. IV-5. Dimensionless drawdown versus dimensionless time in a two-aquifer system. ($\beta_{11} = 0.01$, $r/B_{11} = 0.02$; $\beta_{21} = 0.01$, $r/B_{21} = 0.02$ and $\beta_{21} = r/B_{21} = 0$)
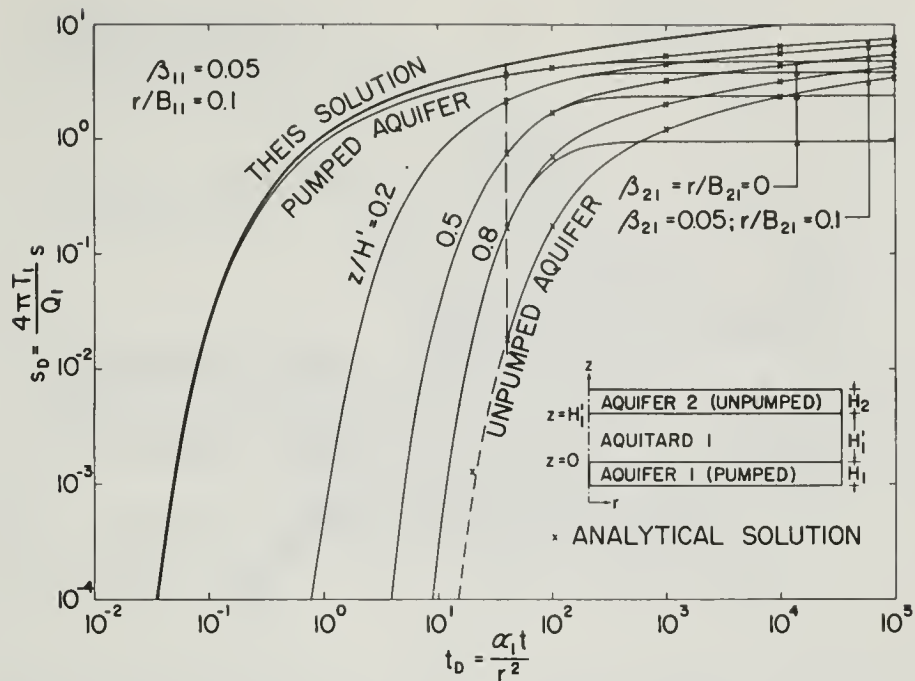
Fig. IV-6. Dimensionless drawdown versus dimensionless time
in a two-aquifer system. ($\beta_{11} = 0.05$, $r/B_{11} = 0.1$;
$\beta_{21} = 0.05$, $r/B_{21} = 0.1$ and $\beta_{21} = r/B_{21} = 0$)
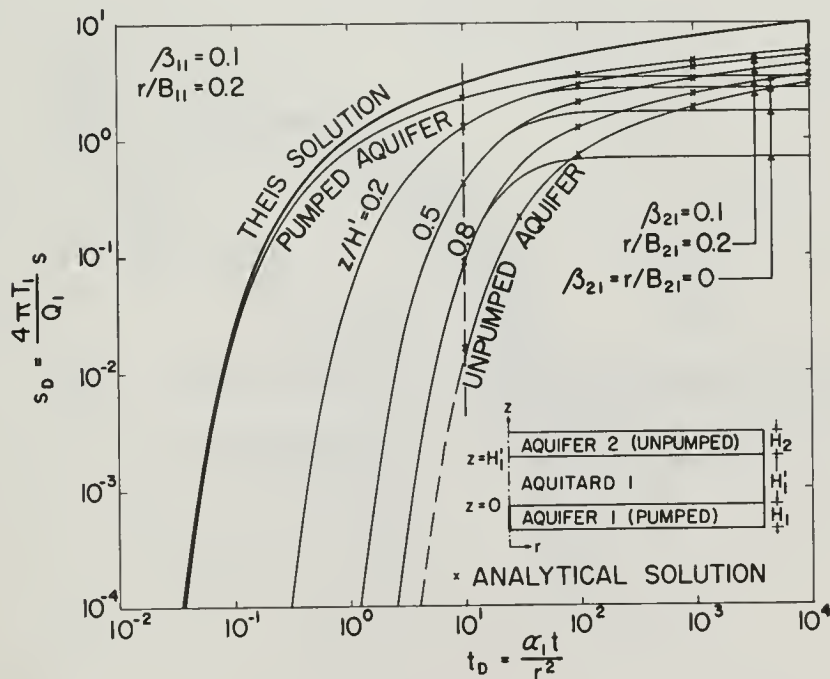
Fig. IV-7. Dimensionless drawdown versus dimensionless time
in a two-aquifer system. ($\beta_{11} = 0.1$, $r/B_{11} = 0.2$;
$\beta_{21} = 0.1$, $r/B_{21} = 0.2$ and $\beta_{21} = r/B_{21} = 0$)
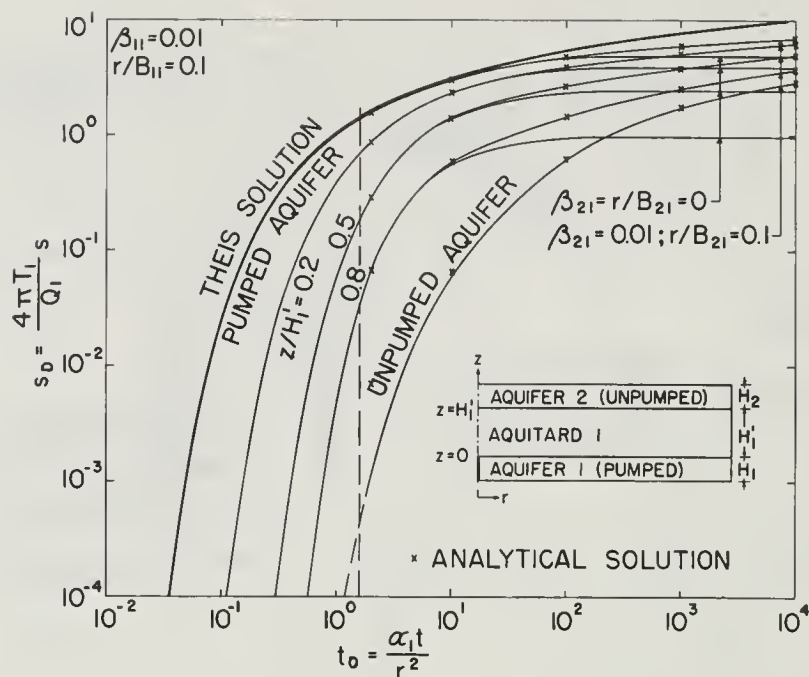
Fig. IV-8. Dimensionless drawdown versus dimensionless time in a two-aquifer system. ($\beta_{11} = 0.01$, $r/B_{11} = 0.1$; $\beta_{21} = 0.01$, $r/B_{21} = 0.1$ and $\beta_{21} = r/B_{21} = 0$)
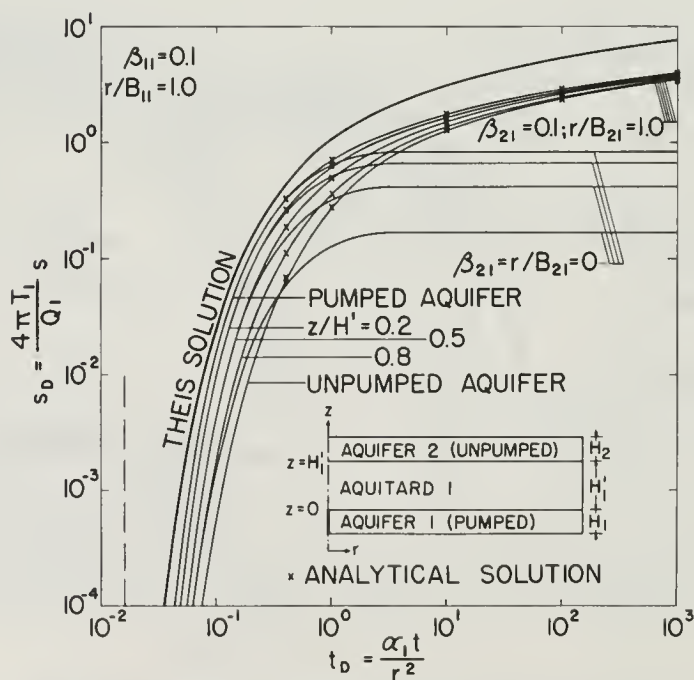
Fig. IV-9. Dimensionless drawdown versus dimensionless time in a two-aquifer system. ($\beta_{11} = 0.1$, $r/B_{11} = 1.0$; $\beta_{21} = 0.1$, $r/B_{21} = 1.0$ and $\beta_{21} = r/B_{21} = 0$)
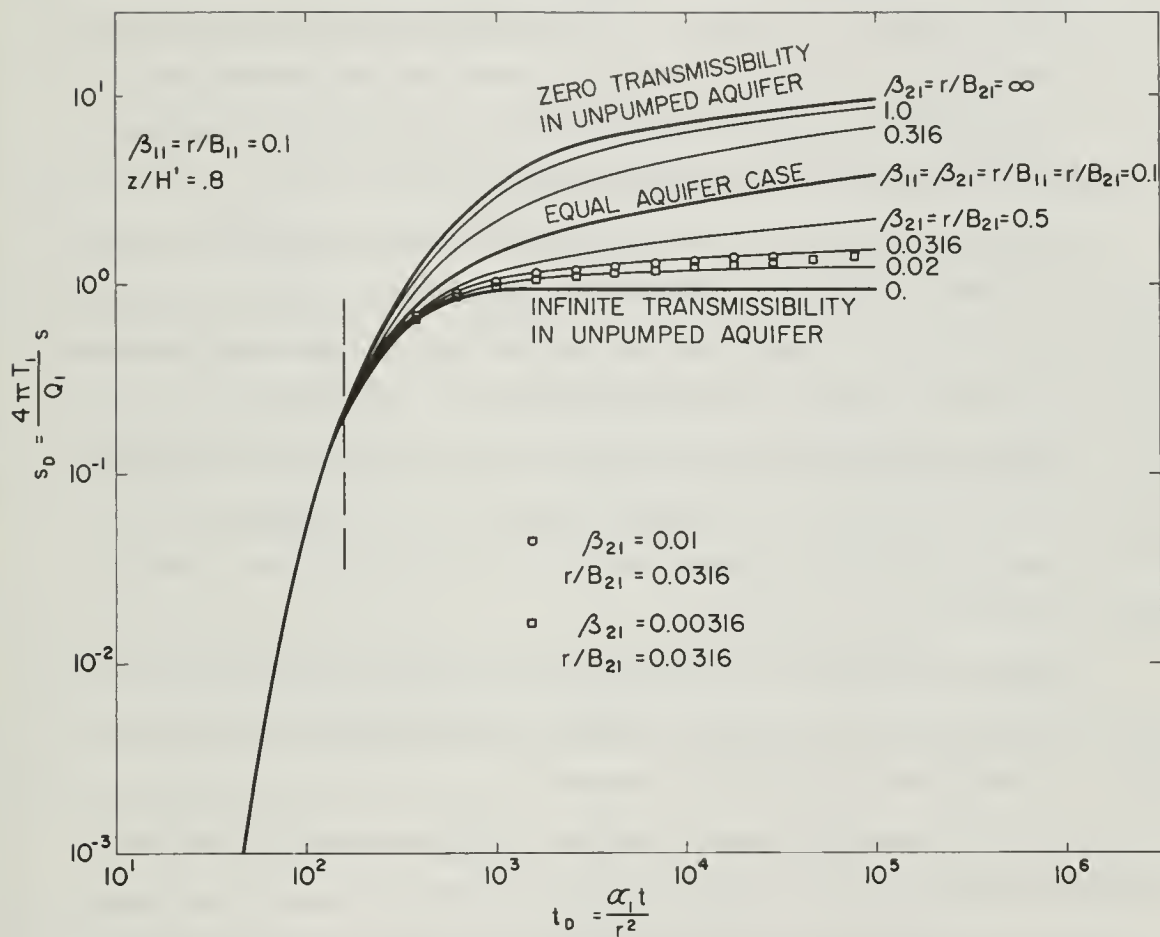
Fig. IV-10. **Effect** of unpumped **aquifer on** dimensionless drawdown in aquitard at $z/H_1' = 0.8$ in a two-aquifer system with $\beta_{11} = r/B_{11} = 0.1$.

The flatter portions of these curves were plotted from results obtained with the finite element method at relatively large permeability ratios, K_1/K_1' and K_2/K_1', and at relatively small values of H_2. In order to compare with the analytical solutions, Eqs. II-82, II-83 and II-87 were evaluated numerically for selected values of t_D, β_{ij} and r/B_{ij}, and these results are indicated by an x on the figures. It is seen that the results obtained by both methods are practically identical along the flatter portions of the curves.

The steep portions of the curves are based almost entirely on results obtained through numerical evaluation of the analytical solutions. Exceptions are the curves for the unpumped aquifer because at small values of dimensionless time, Eq. II-83 could not be evaluated numerically. The finite element method, when used with the network shown in Fig. IV-1, failed to yield satisfactory results along the steep portions of the curves; the results started to deviate from the analytical solutions as the curves became steeper, and they became negative at low values of t_D.

However, in Section IV-A-4c, it will be shown that whenever the results obtained with the two methods deviate from each other due to reasons such as an insufficient permeability contrast between the aquifers and the aquitard, this deviation increases as the value of t_D increases. It will be shown that at small values of pumping time the system is closer to conditions of unidirectional flow in the individual layers than at larger values of time. This suggests that, since in Figs. IV-2 through IV-9 the results are identical along the flatter portions of the curves, they should certainly be identical along the steep portions. Where this was not the case, the reason probably was due to the computer program used in evaluating the analytical solution for the unpumped aquifer, or the coarse mesh used in the finite element approach.

Indeed, when the network in Fig. IV-1 was refined, the finite element results were considerably improved. For example, Fig. IV-3 shows results obtained with the normal network used in this study and another special network

-294-

containing a much larger number of elements This special network consisted of 34 nodal points along the vertical axis, with a total of 857 nodal points and 839 elements. It will be noted on Fig. IV-3 that results from the refined network give much better agreement with the analytical solutions as dimensionless time decreases.

This can be explained from the development of the finite element method in Chapter III. We know that this method will not yield correct results unless the hydraulic gradient is constant across each element in the network. When the vertical gradient across the aquitard is very large, which is the case when the curves are steep, the only way to obtain near constant gradients in all elements is to divide the aquitard vertically into a large number of small elements. The smaller these elements are, the more accurate are the finite element results. Since there is a practical limit to the number of elements that one can use, we were forced to construct the steep portions of our curves solely on the basis of the analytical solutions. This can be theoretically justified as long as the analytical solutions match the finite element results at the flatter portions of the curves, which is the case in Figs. IV-2 through IV-9.

Fig. IV-10 has been constructed entirely on the basis of results obtained with the finite element method, for the purpose of studying the effects of variations in β_{21} and r/B_{21} on the solutions. It will be discussed in detail in Section IV-A-4b.

4. Behavior of a Two-Aquifer System

a. Small Values of Time

In Section II-E, asymptotic solutions have been developed which give the drawdowns in the aquitard and in the aquifer being pumped at small values of time. In a two-aquifer system, the criterion for small values of time was defined as

$$\bar{t}_{D_1} \leq 0.1 \tag{IV-1}$$

since $t_{D_1} = \theta_{11} t_D$ and $\theta_{11} = (r/B_{11})^4/16 \beta_{11}^2$, this criterion can also be written in terms of the dimensionless time t_D in the aquifer being pumped as

$$t_D \leq \frac{1.6 \beta_{11}^2}{(r/B_{11})^4} \tag{IV-2}$$

Thus, for each pair of the dimensionless parameters β_{11} and r/B_{11} there exists some limiting value of t_D below which the asymptotic solutions can be considered to be good approximations for the actual drawdown in the system, provided that we are not in the immediate vicinity of the unpumped aquifer. These limiting values of t_D are shown by dashed vertical lines on Figs. IV-2 through IV-10.

For small values of pumping time when Eq. IV-2 will be satisfied, dimensionless drawdown in the aquifer being pumped is given by

$$s_D = \int_{1/4\,t_D}^{\infty} \frac{e^{-y}}{y} \, \text{erfc} \left[\frac{\beta_{11} \sqrt{1/4\,t_D}}{\sqrt{y\,(y - 1/4\,t_D)}} \right] dy \tag{IV-3}$$

and dimensionless drawdown in the aquitard is given by

$$s_D = \int_{1/4\,t_D}^{\infty} \frac{e^{-y}}{y} \left\{ \text{erfc} \left[\frac{\beta_{11} \sqrt{1/4\,t_D} + y\,(z/H_1')/\sqrt{4\,t_{D1}}}{\sqrt{y\,(y - 1/4\,t_D)}} \right] \right.$$
$$\left. - \, \text{erfc} \left[\frac{\beta_{11} \sqrt{1/4\,t_D} + y\,(2 - z/H_1')/\sqrt{4\,t_{D1}}}{\sqrt{y\,(y - 1/4\,t_D)}} \right] \right\} dy \tag{IV-4}$$

-296-

Dimensionless drawdown in the unpumped aquifer is assumed to be negligibly small and an asymptotic solution for this part of the system is not available.

Eq. IV-3 shows that the dimensionless drawdown in the aquifer being pumped is a function of only two variables, t_D and β_{11}. According to Eq. IV-4, dimensionless drawdown at any given elevation z/H_1' in the aquitard is a function of the three variables t_D, β_{11} and r/B_{11} (which is implicit in $\bar{t}_D$). Thus, since the values of β_{21} and r/B_{21} do not appear in Eqs. IV-3 or IV-4, the solutions at small values of pumping time are independent of the properties of the unpumped aquifer. This means that when t_D satisfies Eq. IV-2, the aquitard and the aquifer being pumped may be considered as an independent two-layer system. This conclusion will prove to be of invaluable assistance in developing practical methods for evaluating real two-aquifer systems from field pumping tests.

The functional relationships between s_D and t_D for different values of β_{11} and r/B_{11} at small values of pumping time are shown at the left of the dashed vertical lines on Figs. IV-2 through IV-10. It is seen that the effects of β_{21} and r/B_{21} do not manifest themselves to the left of these vertical lines, but that they become quite evident at larger values of t_D. In addition, as one gets closer to the unpumped aquifer (i.e. $z/H_1' = 0.8$), the effect of this aquifer becomes evident at smaller values of time.

Since the values of s_D in the aquifer being pumped depend solely on t_D and β_{11}, we expect these curves to be identical in Figs. IV-2, IV-5 and IV-8 where $\beta_{11} = 0.01$, and in Figs. IV-3, IV-7 and IV-9 where $\beta_{11} = 0.1$. Indeed, when these graphs are superposed, one finds that the curves for the pumped aquifer coincide to the left of the particular dashed line whose value of t_D is smallest. On the other hand, the curves for the aquitard are different in each figure because they are functions of both β_{11} and r/B_{11}. In the unpumped aquifer, dimensionless drawdown depends on all four parameters, β_{ij} and r/B_{ij}, at all values of t_D.

As mentioned earlier, the vertical spread between the curves in Figs. IV-2 through IV-9 is indicative of the vertical hydraulic gradient in the aquitard at some given radial distance r from the pumping well. The horizontal spread is a direct measure of the time lag in the drawdown between points situated at different elevations at a given radial distance from the pumping well. We will show that there exists a relationship between the spread of these curves and the relative magnitudes of the parameters β_{11} and r/B_{11}.

In Figs. IV-3, IV-6, and IV-8, the values of r/B_{11} are fixed at 0.1 and we see that the spread between the curves of each graph is not the same. As β_{11} decreases from 0.1 on Fig. IV-3 to 0.01 on Fig. IV-8, the spread between the curves also decreases. Conversely, when β_{11} is fixed at 0.01 and r/B_{11} decreases from 0.1 to 0.01, the spread in these curves increases (see Figs. IV-2, IV-5, and IV-8). In addition, reference to Figs. IV-2, IV-3, and IV-4 will show that when β_{11} and r/B_{11} both increase from 0.01 to 1.0, while the ratio $\beta_{11}/(r/B_{11})$ remains unity, the spread in the curves decreases.

We can therefore say that, in general, the spread between these curves increases as the ratio

$$\frac{\beta_{11}}{r/B_{11}} = \frac{1}{4}\sqrt{\frac{\varphi_1' c_1' H_1'}{\varphi_1 c_1 H_1}} \qquad\qquad (IV-5)$$

increases, but decreases as the magnitudes of β_{11} and r/B_{11} increase for a given ratio.

In order to explain this relationship, we must consider the effect on the physical conditions in the system of each of the following quantities. H_1', H_1, $\varphi_1' c_1'$, $\varphi_1 c_1$, K_1'/K_1 and r. Obviously, increasing the values of H_1' and $\varphi_1' c_1'$ or decreasing the values of H_1 and $\varphi_1 c_1$ is the same as increasing the ratio $\beta_{11}/(r/B_{11})$. When the thickness H_1' of the aquitard increases, the time that is required for a disturbance in the aquifer to reach a point at some given value of z/H_1' also increases. This results in longer time lags, higher vertical gradients, and consequently in larger spreads between the curves. If the thickness H_1 of the pumped aquifer decreases while the rate of discharge remains unchanged, drawdowns in the aquifer are greater and gradients in the aquitard become larger. By increasing the value of $\varphi_1' c_1'$ we actually increase the storage capacity of the aquitard and decrease the drawdowns in this layer. Similarly, low values of $\varphi_1 c_1$ correspond to low storage capacity in the aquifer and therefore to higher drawdowns. In both cases the effect is longer time lags and higher gradients in the aquitard, which explains the effect of the ratio $\beta_{11}/(r/B_{11})$ on the spread of the curves.

Increasing the values of β_{11} and r/B_{11} for a given ratio of $\beta_{11}/(r/B_{11})$ is the same as increasing the values of r or K_1'/K_1. Since drawdown in the aquifer is smaller at larger values of r, vertical gradients tend to become smaller as one moves away from the pumping well. When K_1'/K_1 increases, the permeability of the aquitard approaches that of the aquifer, which again reduces vertical gradients in the aquitard. This explains why the spread for a given ratio of $\beta_{11}/(r/B_{11})$ decreases when the values of β_{11} and r/B_{11} become larger.

b. Large Values of Time

When the dimensionless time t_D in the aquifer being pumped is greater than $1.6\,\beta_{11}^2/(r/B_{11})^4$, Eq. IV-2 is not satisfied and the asymptotic formulas IV-3 and IV-4 do not apply. Instead, dimensionless drawdown everywhere in the system is now a function of the five variables t_D, β_{11}, r/B_{11}, β_{21} and r/B_{21}

-299-

and is given by Eqs. II-82, II-83 and II-87. Thus, each curve of s_D versus t_D in Figs. IV-2 through IV-10 that was uniquely defined by the parameters β_{11} and r/B_{11} to the left of the dashed vertical lines, has an infinite number of branches to the right of those lines, each branch corresponding to different values of β_{21} and r/B_{21}.

In Figs. IV-2 through IV-9, we have shown two branches for each curve. The upper branch corresponds to the special case when $\beta_{11} = \beta_{21}$ and $r/B_{11} = r/B_{21}$, which means that transmissibilities and hydraulic diffusivities are identical in both aquifers. This branch will therefore be referred to as the "equal-aquifer" branch. The lower branch represents the limiting case when $\beta_{21} = r/B_{21} = 0$, which means that the transmissibility, T_2, in the unpumped aquifer is infinitely large, so that the hydraulic head in this layer remains constant during the entire period of pumping. This corresponds to the case treated by Hantush in his modified theory of leaky aquifers (21) which will be discussed in more detail in Section IV-A-4e. For the time being, we will only mention that when the hydraulic head in the unpumped aquifer is constant, the entire system must eventually approach a steady state, and the curves of s_D versus t_D must become horizontal. At this stage, vertical hydraulic gradients within the aquitard become linear, and we obtain the relationship

$$\frac{s_D{}'}{s_D} = 1 - \frac{z}{H_1{}'} \tag{IV-6}$$

where $s_D{}'$ is dimensionless drawdown at $z/H_1{}'$ in the aquitard and s_D is dimensionless drawdown in the aquifer being pumped. Both $s_D{}'$ and s_D are measured at the same radial distance from the pumping well. One can easily verify Eq. IV-6 from the lower branches of the curves on Figs. IV-2 through IV-9.

When the transmissibility, T_2, of the unpumped aquifer increases, the values of β_{21} and r/B_{21} decrease, drawdown in this aquifer becomes less,

and therefore drawdowns in the entire system are diminished. On the other hand, by increasing the value of $\varphi_2 c_2$, we are actually increasing the storage capacity of the unpumped aquifer, decreasing the value of β_{21}, and at the same time decreasing the drawdown everywhere in the system. Therefore, the higher the values of T_2 and $\varphi_2 c_2$, or conversely, the lower the values of β_{21} and r/B_{21}, the flatter are the curves of s_D versus t_D at large values of pumping time.

To verify these conclusions, consider Fig. IV-10 which shows a family of curves for the particular elevation in the aquitard of $z/H_1' = 0.8$ and the situation where $\beta_{11} = r/B_{11} = 0.1$. The heavy lines in this figure correspond to the two limiting cases when $\beta_{21} = r/B_{21} = \infty$ (i. e. $T_2 = 0$) and $\beta_{21} = r/B_{21} = 0$ (i. e. $T_2 = \infty$), and the equal aquifer case where $\beta_{21} = \beta_{11}$ and $r/B_{21} = r/B_{11}$ (i. e. $T_1 = T_2$, $\alpha_1 = \alpha_2$). The branches for all intermediate values of β_{21} and r/B_{21} lie between these limits, either below the equal aquifer branch when $0 < \beta_{21} < \beta_{11}$ and $0 < r/B_{21} < r/B_{11}$, or above this branch when $\beta_{11} < \beta_{21} < \infty$ and $r/B_{11} < r/B_{21} < \infty$.

From figures IV-2 through IV-9 we see that the spread between the branches of different curves in any given figure is smallest in the aquifer being pumped and that it increases with z/H_1'. This could have been anticipated, since the effect of the unpumped aquifer is obviously more pronounced in the vicinity of this aquifer than it is at more distant points.

c. Effect of Permeability Contrasts

The analytical solutions in Chapter II were derived on the assumption that flow is essentially vertical in the aquitard and horizontal in the aquifers. We now want to determine what are the permeability contrasts that must be maintained in an actual two-aquifer system in order for the analytical solutions to apply. This problem can easily be investigated with the finite element method of analysis.

As mentioned earlier, the curves of s_D versus t_D in Figs. IV-2 through

IV-9 were in part composed of data obtained with the finite element method. Since the purpose of those curves was to demonstrate the behavior of a two-aquifer system when the contrast in permeability between the aquifers and aquitard is sufficiently large, we have not included in these figures any finite element results that did not fit the analytical solutions. Thus, in developing these curves, we always increased the values of K_1/K_1' and K_2/K_1' until the results were identical to those obtained through numerical evaluation of the analytical solutions and disregarded data that did not match these solutions. We can therefore investigate the effect of the permeability ratios on the analytical solutions by comparing the cuves in Figs. IV-2 through IV-9 with results obtained by the finite element method for similar values of β_{ij} and r/B_{ij}, but for lower values of K_1/K_1' and K_2/K_1'. Whenever these results deviate from the above curves, we will know that we have reached the limiting values of K_1/K_1' and K_2/K_1'. The amount of deviation will give an indication of the error introduced by using the analytical solutions with such permeability ratios.

To apply this approach, we have considered a system composed of two aquifers with identical transmissibilities and hydraulic diffusivities, in which

$$K_1 = K_2$$
$$H_1 = H_2 = 10 \text{ feet}$$
$$H_1' = 20 \text{ feet}$$
$$\frac{\varphi_1' c_1'}{\varphi_1 c_1} = \frac{\varphi_1' c_1'}{\varphi_2 c_2} = 8.0$$

and
$$\beta_{11} = r/B_{11} = \beta_{21} = r/B_{21} = \sqrt{\frac{K_1'}{200 K_1}} \, r$$

where r is being measured in feet. We studied the effect of the ratios $K_1/K_1' = K_2/K_1'$ on the drawdowns in this system by comparing values of s_D with those read from Figs. IV-2, IV-3 and IV-4 for $\beta_{ij} = r/B_{ij} = 0.01$, 0.1 and 1.0 respectively.

When $K_1/K_1' = K_2/K_1' = 5000$, our dimensionless parameters become $\beta_{ij} = r/B_{ij} = 10^{-3}r$. At $r = 100$ feet ($\beta_{ij} = r/B_{ij} = 0.1$) and at $r = 1000$ feet ($\beta_{ij} = r/B_{ij} = 1.0$), the finite element results were identical with the analytical solutions and were therefore used in constructing the curves of Figs. IV-3 and IV-4. At $r = 10$ feet ($\beta_{ij} = r/B_{ij} = 0.01$) the finite element results for the aquitard were no more than 5% below the curves in Fig. IV-2. The results for both aquifers were in excellent agreement with the curves of Fig. IV-2.

When $K_1/K_1' = K_2/K_1' = 500$, we have $\beta_{ij} = r/B_{ij} = 3.16 \times 10^{-3}r$. At $r = 31.6$ feet ($\beta_{ij} = r/B_{ij} = 0.1$) and at $r = 316$ feet ($\beta_{ij} = r/B_{ij} = 1.0$) the finite element results were identical with the curves in Figs. IV-3 and IV-4. At $r = 3.16$ feet ($\beta_{ij} = r/B_{ij} = 0.01$) the match was still very good in the aquifers, but in the aquitard the results were slightly below the curves of Fig. IV-2 on the right side of the dashed vertical line. The error was less than 5%.

When $K_1/K_1' = K_2/K_1' = 50$, then $\beta_{ij} = r/B_{ij} = 10^{-2}r$. At $r = 100$ feet ($\beta_{ij} = r/B_{ij} = 1.0$) the match was perfect at low values of t_D, but deviations of up to 5% from the curves in Fig. IV-4 occurred at $t_D > 10^2$. At $r = 10$ feet ($\beta_{ij} = r/B_{ij} = 0.1$) agreement was excellent in the aquifer being pumped, but deviations of up to 5% occurred in the unpumped aquifer. In the aquitard, deviations from the curves in Fig. IV-3 were less than 5% along the steep portions and less than 10% along the flatter portions. At $r = 1$ foot ($\beta_{ij} = r/B_{ij} = 0.01$) the match was still very good in the aquifer being pumped. In the unpumped aquifer, the deviations were less than 5%, but in the aquitard the finite element results were as much as 10% below the curves of Fig. IV-2.

Finally, when $K_1/K_1' = K_2/K_1' = 20$, we obtain $\beta_{ij} = r/B_{ij} = 1.581 \times 10^{-2}r$. At $r = 63.25$ feet ($\beta_{ij} = r/B_{ij} = 1.0$) the finite element results for the aquifers were less than 5% below the curves of Fig. IV-4. In the aquitard, the deviations were less than 5% at $t_D < 10^3$ and less than 10% at $t_D > 10^3$, and the error was larger at lower values of z/H_1' than at higher values.

At $r = 6.325$ feet ($\beta_{ij} = r/B_{ij} = 0.1$) deviations from the curves in Fig. IV-3 were less than 10% in the aquifers and less than 20% in the aquitard.

In all cases, the finite element results were either at or below the curves in Figs. IV-2 through IV-4, and the deviations increased as the values of t_D increased. Errors were always largest in the aquitard and smallest in the aquifer being pumped.

To illustrate the effect of permeability contrasts between the aquifers and the aquitard on the flow patterns in these layers, the finite element results were used to obtain the distribution of dimensionless drawdown in the system at various values of $K_1/K_1' = K_2/K_1'$ as shown in Figs. IV-11 through IV-14. These figures show that flow in the aquifer being pumped is always nearly horizontal, while in the aquitard and in the unpumped aquifer the flow fields tend to be less uniform. Except in the vicinity of the pumping well, the flow field in the unpumped aquifer is usually more uniform than it is in the aquitard. In general, flow becomes less horizontal in the aquifers and less vertical in the aquitard as pumping time increases and as the radial distance from the pumping well decreases. One also notes that flow in the aquitard is closer to the vertical when the permeability of the unpumped aquifer increases (compare Figs. IV-11 and IV-14). This explains why the error in the analytical solutions increases with time and decreases with radial distance from the pumping well, and why it is largest in the aquitard and smallest in the aquifer being pumped.

As a next step, we must examine the effect of changing the thickness of the various layers in our system on the flow fields in this system. Figs. IV-11 through IV-13 incicate that when the permeability contrasts between the aquifers and the aquitard are not less than one order of magnitude, the effect of leakage from the aquitard is concentrated along a thin portion of the aquifer being pumped in the vicinity of the interface. By decreasing the thick-
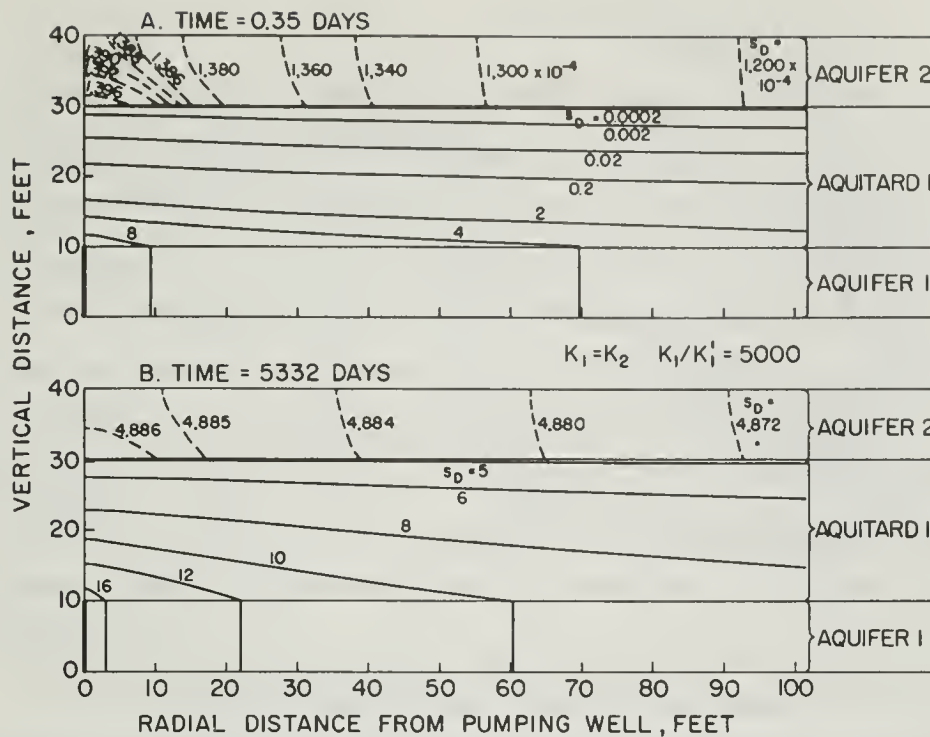
Fig. IV-11.   Distribution of dimensionless drawdowns in a two-
aquifer system with $K_1 = K_2$ and $K_1/K_1' = 5000$.
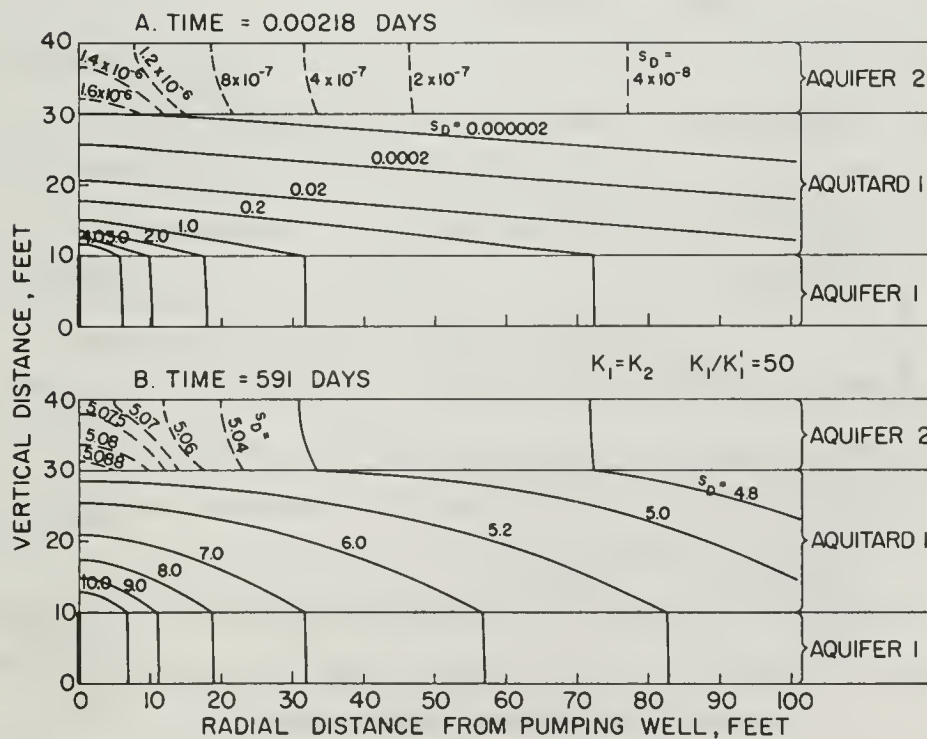
Fig. IV-12.   Distribution of dimensionless drawdowns in a two-
aquifer system with $K_1 = K_2$ and $K_1/K_1' = 50$.
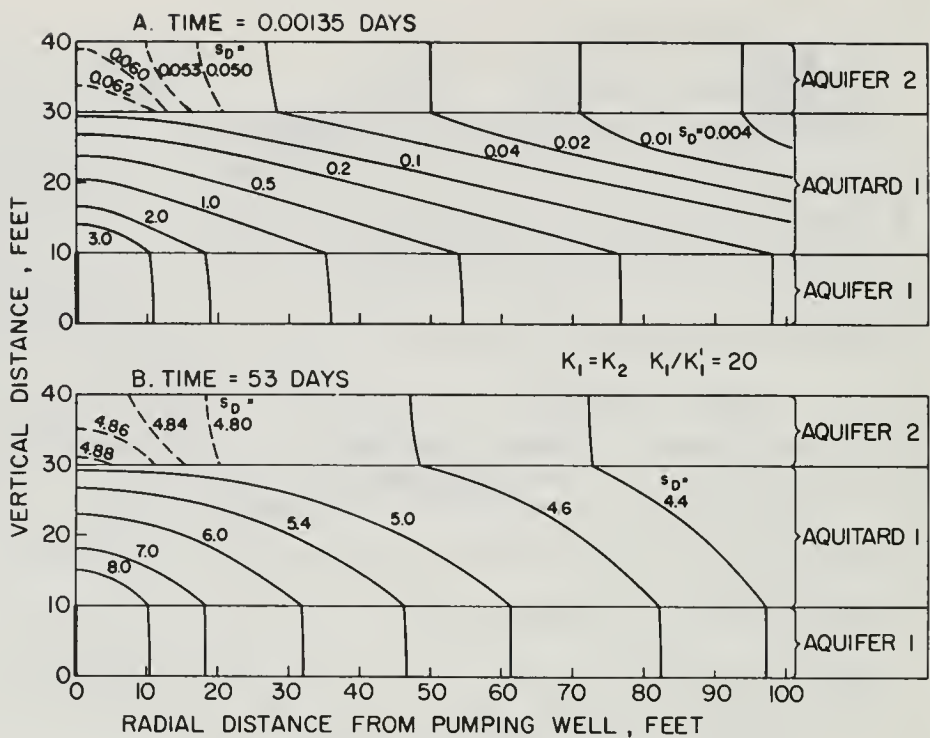
Fig. IV-13. Distribution of dimensionless drawdowns in a two-aquifer system with $K_1 = K_2$ and $K_1/K_1' = 20$.
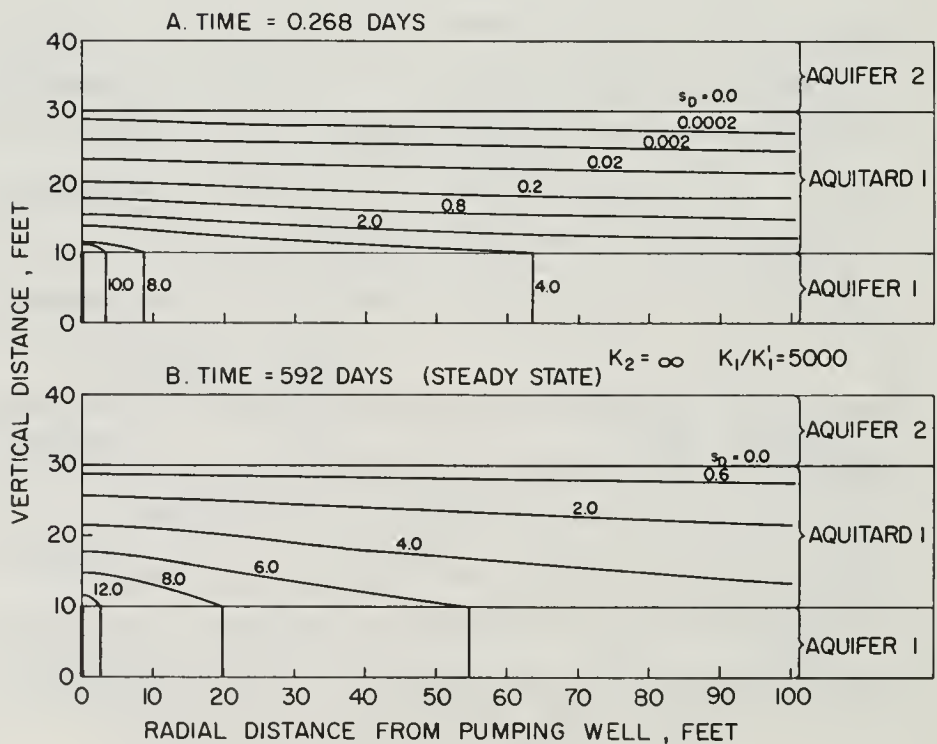
Fig. IV-14. Distribution of dimensionless drawdowns in a two-aquifer system with $K_2 = \infty$ and $K_1/K_1' = 5000$.

ness of this aquifer we would reduce the vertical components and increase the horizontal components of flow in this layer, thereby bringing the system closer to conditions of vertical flow in the aquitard and horizontal flow in the aquifers. Thus, the effect of reducing the thickness of the aquifer being pumped is to reduce the error in applying the analytical solutions to this problem. On the other hand, since vertical flow is confined to a thin portion of this aquifer, we can say that flow in the lower part of the aquifer is essentially horizontal. Thus, adding to the thickness of the aquifer being pumped would have little effect on the shapes of the flow fields in Figs. IV-11 through IV-13 since we would be merely adding horizontal flow lines to a horizontal flow field.

At small values of pumping time, the shape of the flow field in the aquitard is determined solely by the permeability ratio K_1/K_1', since the properties of the unpumped aquifer have little effect on the drawdown in the other layers. Thus, the error in using analytical solutions at the steep portions of the curves of s_D versus t_D should not be significantly influenced by the thicknesses of the aquitard and the unpumped aquifer. At larger values of time, the shape of the flow field in the aquitard will depend on the conditions at the interfaces, which are determined by the thicknesses and permeabilities of the two aquifers. Thus, the thickness of the aquitard should have less influence on the error introduced by the analytical solutions at large values of time than the permeability ratios at the interfaces.

The effect of the unpumped aquifer on the flow fields in the other two layers is negligible at small values of pumping time, as was shown above. In the next section, it will be shown that the influence of its thickness on these flow fields at large values of time is less significant than the permeability contrast between this aquifer and the aquitard. We can therefore conclude that, in general, the error introduced by the analytical solutions depends to a much larger degree on the permeability ratios than on the thicknesses of the individual layers.

Let us define "practical values of pumping time" as those values of t_D at which the relatively flatter portions of the curves of s_D versus t_D at any point in the system do not exceed a length of five logarithmic cycles. According to this definition, the curves in Figs. IV-2 through IV-10 never exceed the range of practical values of pumping time. It now seems that for real two-aquifer systems the results of our investigation may be generalized in the following manner:

1. When the permeabilities of the aquifers are at least three orders of magnitude larger than the permeability of the aquitard, the analytical solutions apply everywhere in the system at all practical values of pumping time. At points in the aquitard situated within a radius of about 30 feet from the pumping well the analytical solutions may eventually give errors of not more than 5%. When the permeability contrasts are larger than three orders of magnitude, even these errors become negligible.

2. When the permeabilities of the aquifers are two orders of magnitude larger than the permeability of the aquitard, the analytical solutions apply everywhere within the aquifer being pumped, at all practical values of pumping time. For points in the aquitard that are radially several tens of feet away from the pumping well, the analytical solutions may give errors of up to 5%. For points in the aquitard that are at least several feet away from the pumping well the errors are not more than 10%, but they can increase sharply at points closer to the well. In the unpumped aquifer, the errors are less than 5% everywhere except in the immediate vicinity (a few feet) of the pumping well.

3. When the permeabilities of the aquifers are one order of magnitude larger than the permeability of the aquitard, the errors involved in applying the analytical solutions to points that are at a radial distance of more than about 100 feet from the pumping well are less than 10%

-308-

in the aquitard and less than 5% in the aquifers, at all practical values of pumping time. These errors may double several tens of feet away from the pumping well, and they may be even larger for points in the aquitard that are within a radius of several feet from the pumping well.

4. When the permeabilities of the aquifers are less than one order of magnitude larger than the permeability of the aquitard, the errors in applying the analytical solutions may be very large and we can no more regard the system as composed of distinct aquifers and aquitards; these definitions would now lose all meaning.

5. At small values of pumping time, which in most cases are associated with the steep portions of the curves of s_D versus t_D, the error introduced by applying the analytical solutions to the aquitard and to the aquifer being pumped is practically independent of the permeability K_2 of the unpumped aquifer.

6. The error introduced by applying the analytical solutions to a two-aquifer system increases with pumping time and decreases with radial distance from the pumping well. It is largest in the aquitard and smallest in the aquifer being pumped.

d. Effect of Thickness of Unpumped Aquifer

The analytical solutions in Chapter II were derived on the assumption that the unpumped aquifer is thin enough so that drawdown across its thickness is uniform at any time t. Since the axis of the system must act as a vertical flow line, all flow lines in the vicinity of this axis must be inclined away from the horizontal. The distorting effect of the axis on the essentially horizontal flow field in the unpumped aquifer can be clearly seen in Figs. IV-11 through IV-13. These figures also show that in the aquitard, horizontal components of flow are larger near the aquifer being pumped than near the unpumped aquifer. This suggests that since the permeabilities of

both aquifers are the same, flow in the unpumped aquifer should be closer to horizontal than is flow in the aquifer being pumped. Since in the aquifer being pumped flow is essentially horizontal, we conclude that it is chiefly the effect of the axis that causes deviations from horizontal flow in the unpumped aquifer. Therefore, the larger the thickness of this aquifer, the wider is the distorted portion of its flow field. Thus, increasing the thickness of the unpumped aquifer results in larger errors when applying the analytical solutions to the system.

However, increasing the thickness of the unpumped aquifer also has an opposite effect: as the transmissibility increases, the drawdowns and hydraulic gradients in this aquifer become smaller. In the extreme case when the transmissibility is infinity, the drawdown in the unpumped aquifer is zero at all values of pumping time and the interface between this layer and the aquitard becomes an equipotential surface. This is illustrated in Fig. IV-14. Therefore, the larger the thickness of the unpumped aquifer, the smaller are the horizontal components of flow in the aquitard and the more uniform are the drawdowns within the aquifer. Consequently, the error in applying the analytical solutions to the system is smaller.

The two opposite effects of changing the thickness H_2 tend to cancel each other to some extent, and we can therefore say that the error involved in the analytical solutions depends to a much lesser degree on the thickness of the unpumped aquifer than on the permeability ratios between the layers. The magnitudes of these errors were discussed in the previous section.

e. Comparison with Hantush's Modified "Leaky Aquifer" Problem

In his "Modification of the Theory of Leaky Aquifers," Hantush (21) developed asymptotic solutions for the drawdown in an aquifer that is overlain and underlain by two aquitards. He assumed that the aquifer is completely penetrated by a well of infinitesimal radius, and that the drawdown along the upper and lower boundaries of this system remains zero when the well is being

pumped at a constant rate. In Section II-G, we have shown that the problem considered by Hantush is a special case of our three-aquifer problem, and that our three-aquifer system reduces to his "leaky aquifer" system when the transmissibilities of the unpumped aquifers approach infinity. A general solution to this problem was developed in Section II-F.

In the absence of a lower aquitard, Hantush's system becomes mathematically equivalent to a two-aquifer system in which the transmissibility of the unpumped aquifer is infinity and $\beta_{21} = r/B_{21} = 0$. His solution for small values of pumping time is therefore equivalent to Eq. IV-3. As mentioned previously, this solution is valid at all values of dimensionless time t_D which satisfy the condition

$$t_D \leq \frac{1.6 \, \beta_{11}^2}{(r/B_{11})^4} \tag{IV-2}$$

For large values of pumping time, Hantush (21) developed the equation

$$s_D = \int_{\delta_1 u}^{\infty} \exp\left[-y - \frac{(r/B_{11})^2}{4y}\right] \frac{dy}{y} \tag{IV-7}$$

in which $u = 1/4 t_D$ and $\delta_1 = 1 + \dfrac{\varphi_1' c_1' H_1'}{3 \varphi_1 c_1 H_1}$. According to Hantush, Eq. IV-7 is valid at all values of time that satisfy the condition $t > 5 H_1'^2/c_1'$. Since

$$\frac{t \, \alpha_1'}{H_1'^2} = \bar{t}_{D_1} = \theta_{11} t_D = \frac{(r/B_{11})^4}{16 \beta_{11}^2} \, t_D$$

we can rewrite this condition in terms of β_{11} and r/B_{11} as

$$t_D > \frac{80 \, \beta_{11}^2}{(r/B_{11})^4} \tag{IV-8}$$

The parameter δ_1 can also be expressed in terms of β_{11} and r/B_{11} as

$$\delta_1 = 1 + \frac{16}{3} \cdot \frac{\beta_{11}^2}{(r/B_{11})^2} \qquad \text{(IV-9)}$$

Eqs. IV-3, IV-5, IV-7, IV-8 and IV-9 indicate that Hantush's solutions, together with the ranges of t_D within which they are valid, are unique functions of the dimensionless parameters β_{11} and r/B_{11}. In addition, Eqs. IV-5 and IV-8 show that for given values of β_{11} and r/B_{11}, these solutions cover the entire range of dimensionless time, t_D, except for an interval whose length is less than two logarithmic cycles. Within this interval, Hantush's asymptotic solutions fail, and the dimensionless drawdown s_D must be obtained either by graphical interpolation or through numerical evaluation of the analytical solutions developed in this work.

Hantush has apparently overlooked the unique relationship that exists between the parameters β_{11} and r/B_{11} and the ranges of t_D within which his solutions are valid. Consequently, he was unable to develop dimensionless type curves of s_D versus t_D (or u) that would apply to all values of pumping time. Instead, he has presented his solutions separately for small values of time (in terms of β_{11} only) and large values of time (in terms of r/B_{11} only). Since his solution for large values of time depends on β_{11} and r/B_{11}, and since the range of t_D (or u) within which his solutions are valid is a function of both β_{11} and r/B_{11}, Hantush's well known β curves and r/B curves have limited application in analyzing leaky aquifer systems. We will now show how these two sets of curves can be integrated into one unified family of curves.

Figs. IV-15 through IV-20 show curves of dimensionless drawdown in the aquifer being pumped versus dimensionless time t_D, for different values of β_{11} and r/B_{11}. Each curve corresponds to a given value of β_{11} and r/B_{11} for the case when $\beta_{21} = r/B_{21} = 0$, and is divided by parentheses into three sections. The section enclosed within the parentheses corresponds to the interval within which, according to Eqs. IV-5 and IV-8, Hantush's solutions are not valid. The values of s_D in this section were obtained through numerical
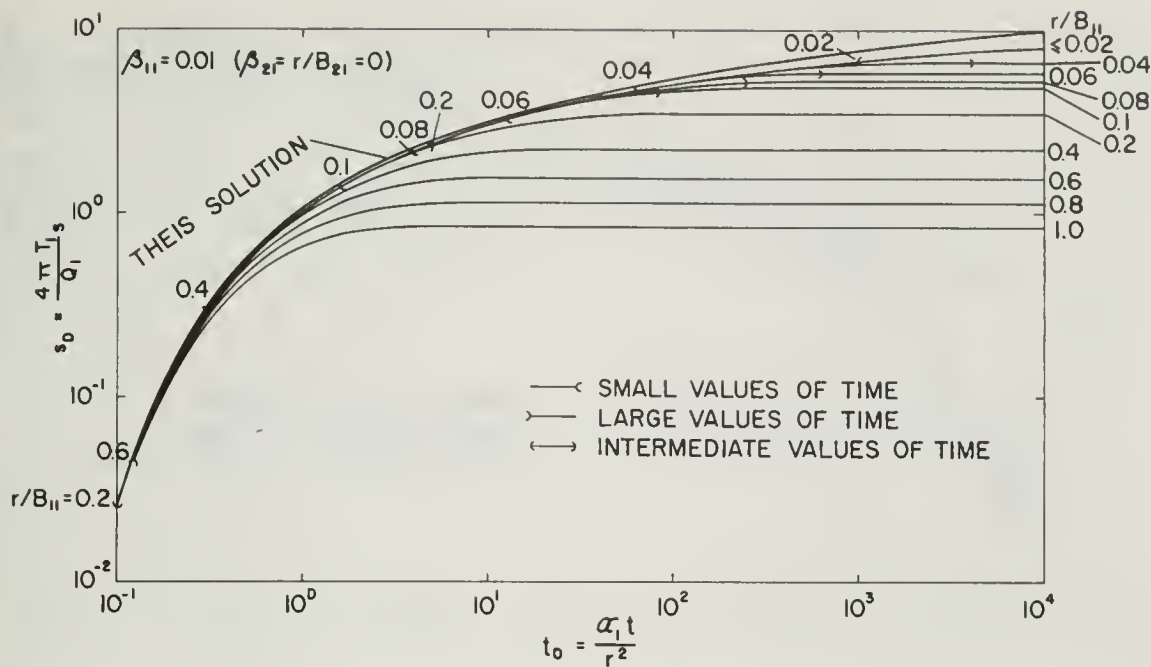
Fig. IV-15. Dimensionless drawdown versus dimensionless time in pumped aquifer of a two-aquifer system with zero drawdown in unpumped aquifer. $(\beta_{11} = 0.01)$
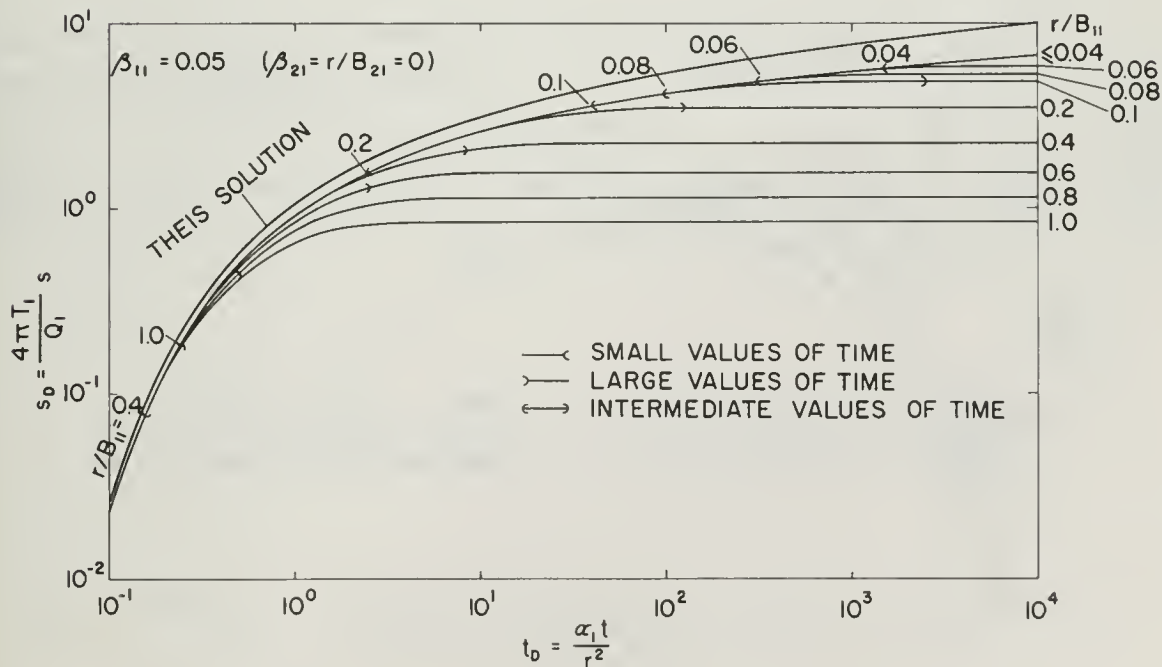
Fig. IV-16. Dimensionless drawdown versus dimensionless time in pumped aquifer of a two-aquifer system with zero drawdown in unpumped aquifer. $(\beta_{11} = 0.05)$
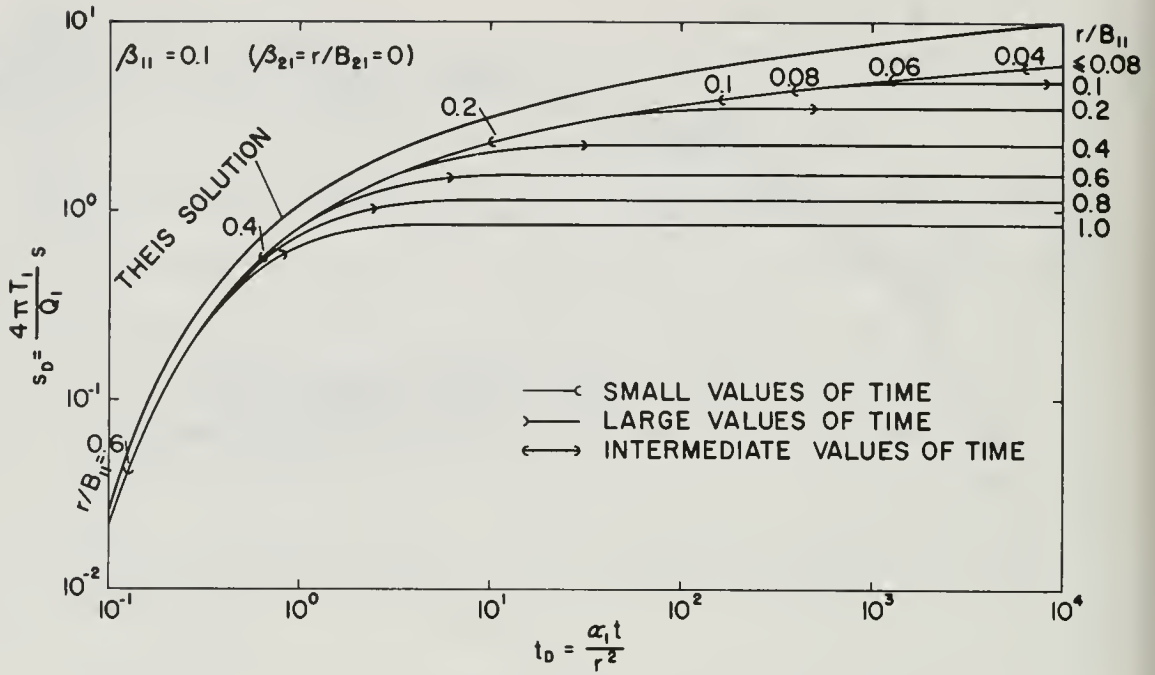
Fig. IV-17. Dimensionless drawdown versus dimensionless time
in pumped aquifer of a two-aquifer system with zero
drawdown in unpumped aquifer. ($\beta_{11} = 0.1$)
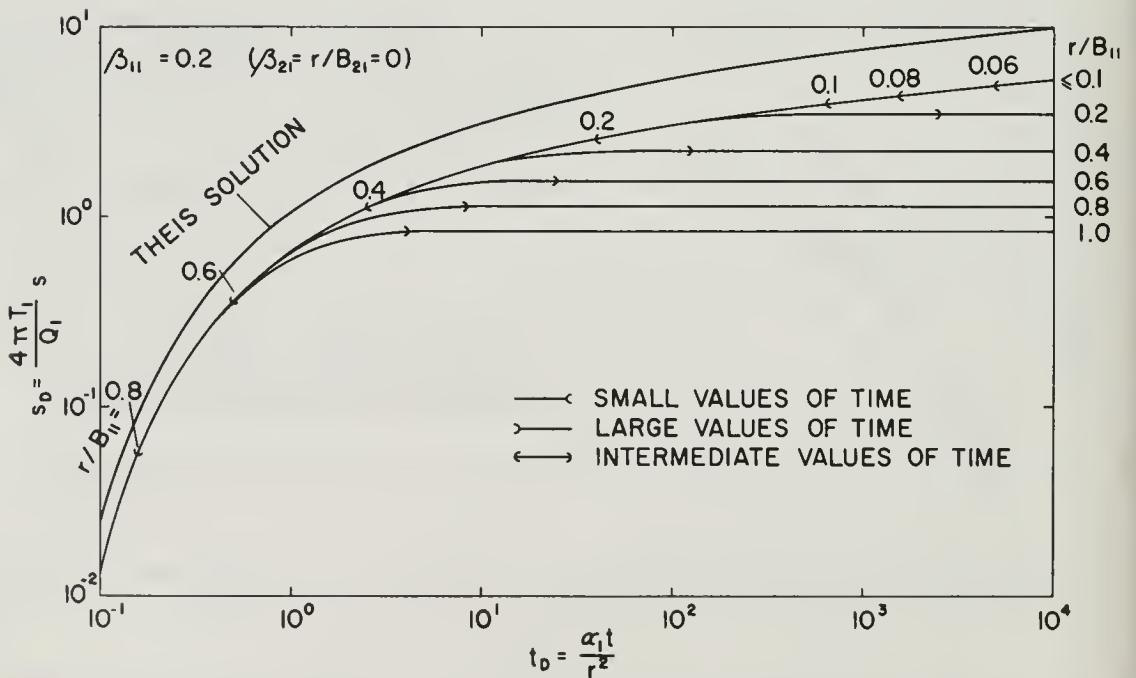
Fig. IV-18. Dimensionless drawdown versus dimensionless time
in pumped aquifer of a two-aquifer system with zero
drawdown in unpumped aquifer. ($\beta_{11} = 0.2$)
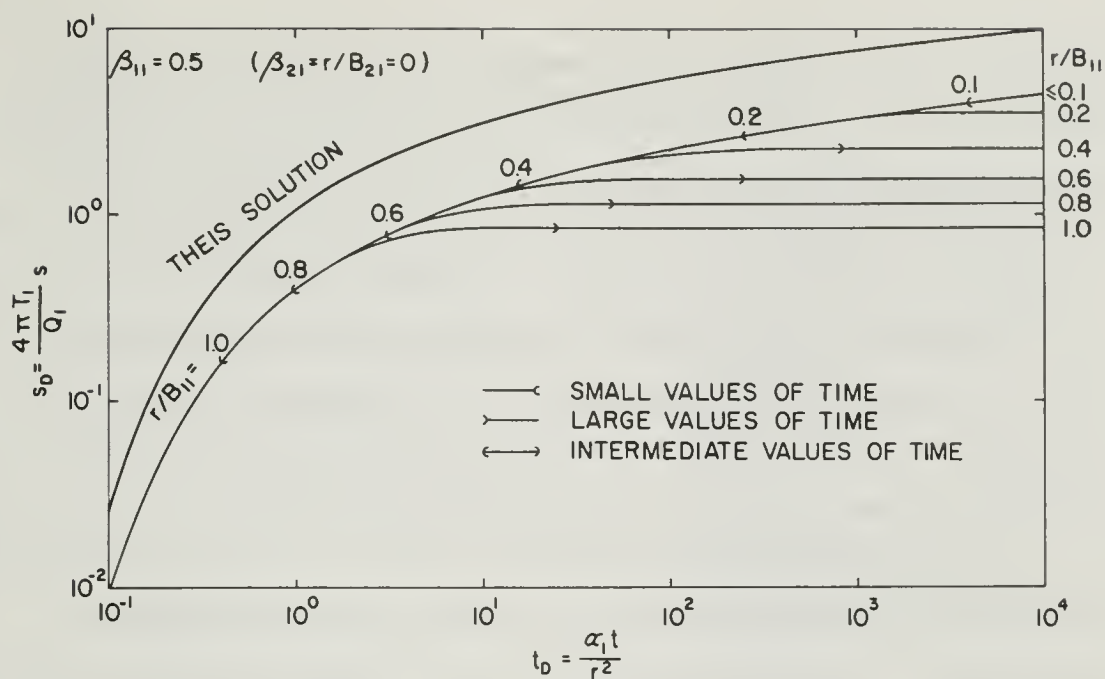
Fig. IV-19. Dimensionless drawdown versus dimensionless time in pumped aquifer of a two-aquifer system with zero drawdown in unpumped aquifer. ($\beta_{11} = 0.5$)
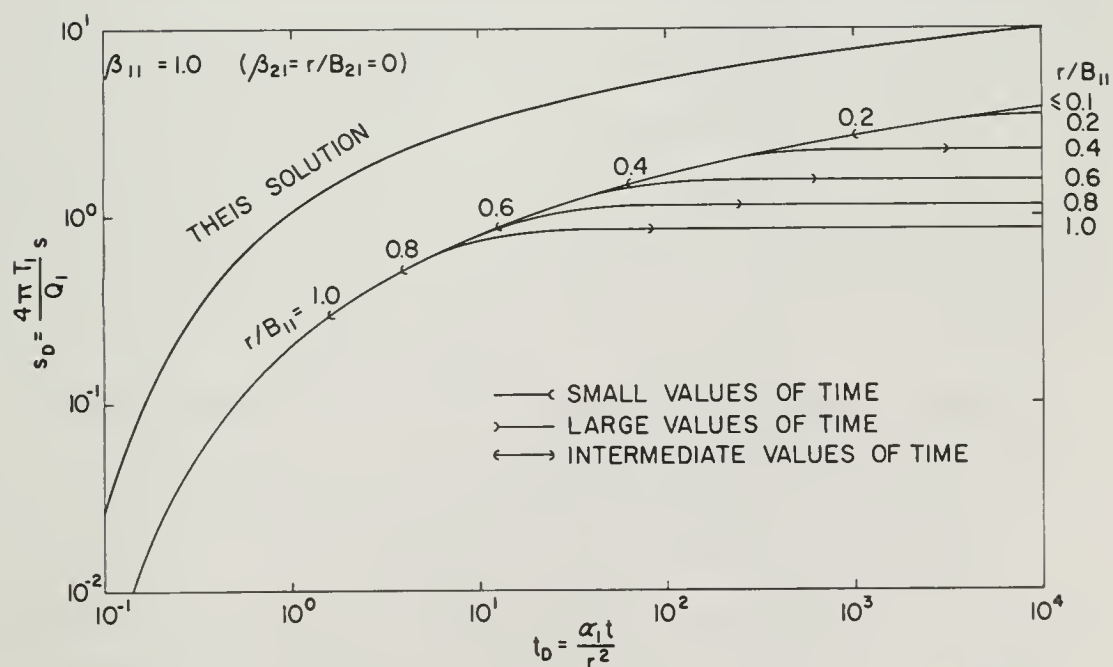
Fig. IV-20. Dimensionless drawdown versus dimensionless time in pumped aquifer of a two-aquifer system with zero drawdown in unpumped aquifer. ($\beta_{11} = 1.0$)

evaluation of the analytical solutions developed in Chapter II (Eqs. II-82 and II-161). The other two sections correspond to small and large values of pumping time and were obtained through numerical evaluation of Eqs. IV-3 and IV-7 respectively. Although all portions of these curves could be obtained from Eqs. II-82 and II-161, we preferred to use Eqs. IV-3 and IV-7 when applicable, because they require relatively little computer time. It is seen on these figures that the restrictions on the validity of Hantush's solutions, as defined in IV-5 and IV-8, are on the conservative side and are therefore sufficient for all practical purposes.

At small values of time, the curves in Figs. IV-15 through IV-20 are identical with the curves in Figs. IV-2 through IV-9 for corresponding values of β_{11} . At large values of time, these curves become invalid whenever the transmissibility of the unpumped aquifer is not many times larger than that of the aquifer being pumped. Since in reality the transmissibility of the aquifer being pumped is usually larger, we conclude that Hantush's solutions have limited application in predicting the behavior of real two aquifer systems at large values of pumping time.

B. GENERALIZATION TO MULTIPLE-AQUIFER SYSTEMS

The knowledge gained in the investigation of a two-aquifer system can be used to develop a partial understanding of the behavior of multiple-aquifer systems. As an example, we will consider a system that consists of five aquifers and four aquitards, as shown in Fig. IV-21.

In our example, let us assume that Aquifer 1 is being pumped at a constant rate. It was shown previously that the effect of Aquifer 2 on the flow in Aquifer 1 and Aquitard 1 is negligible at small values of time. Therefore, the behavior of Aquifer 1 and Aquitard 1

Fig. IV-21. Five-aquifer system.

at small values of time is independent of the rest of the system and is the same as in the two aquifer case. Drawdowns in these layers depend only on the parameters β_{11} and r/B_{11} and are given by Eqs. IV-3 and IV-4. They are represented by the steep portions of the curves in Figs. IV-2 through IV-10. Drawdowns in Aquifers 2 through 5 and in Aquitards 2 through 4 cannot be predicted on the basis of our previous results.

At large values of time, the effect of Aquifer 2 on the flow in Aquifer 1 and in Aquitard 1 is quite significant, as discussed in Section IV-A-4b. However, the behavior of Aquifer 2 is now being influenced by the properties of the overlying layers, so that drawdowns in Aquifers 1 and 2 and in Aquitard 1 need not be the same as in the two-aquifer case. On the other hand, the larger the transmissibility of Aquifer 2 with respect to that of Aquifer 1, the smaller the drawdown in Aquifer 2. Consequently, the influence of the overlying layers on the behavior of Aquifers 1 and 2 and of Aquitard 1 diminishes. When the

transmissibility of Aquifer 2 becomes infinity, the influence of the overlying layers disappears completely and the lowermost three beds behave like an independent two-aquifer system. In such cases the system eventually reaches a steady state, as shown in Figs. IV-2 through IV-10.

Next, let us assume that Aquifer 3 is being pumped at a constant rate. At small values of time, the effect of Aquifers 2 and 4 on the drawdowns in the pumped aquifer and in Aquitards 2 and 3 is negligible. We can therefore adopt Eqs. II-147, II-153 and II-154 to this problem simply by changing the parameters in these equations to $(\beta_{32} + \beta_{33})$, r/B_{32}, and r/B_{33}. Drawdown in Aquifer 3 is then given by

$$s_3(r,t) = \frac{Q_3}{4\pi T_3} \int_{u_3}^{\infty} \frac{e^{-y}}{y} \, \text{erfc} \left[\frac{(\beta_{32} + \beta_{33})\sqrt{u_3}}{\sqrt{y(y-u_3)}} \right] dy \qquad (\text{IV-10})$$

drawdown in Aquitard 2 is given by

$$s_2'(r,z,t) = \frac{Q_3}{4\pi T_3} \int_{u_3}^{\infty} \frac{e^{-y}}{y} \left[\text{erfc} \left(\frac{(\beta_{32} + \beta_{33})\sqrt{u_3} + y(1-z/H_2')/\sqrt{4\,t_{D2}}}{\sqrt{y(y-u_3)}} \right) \right.$$
$$\left. - \text{erfc} \left(\frac{(\beta_{32} + \beta_{33})\sqrt{u_3} + y(1+z/H_2')/\sqrt{4\,t_{D2}}}{\sqrt{y(y-u_3)}} \right) \right] dy \qquad (\text{IV-11})$$

and drawdown in Aquitard 3 is given by

$$s_3'(r,z,t) = \frac{Q_3}{4\pi T_3} \int_{u_3}^{\infty} \frac{e^{-y}}{y} \left[\text{erfc} \left(\frac{(\beta_{32} + \beta_{33})\sqrt{u_3} + y(z'/H_3')/\sqrt{4\,t_{D3}}}{\sqrt{y(y-u_3)}} \right) \right.$$
$$\left. - \text{erfc} \left(\frac{(\beta_{32} + \beta_{33})\sqrt{u_3} + y(2-z'/H_3')/\sqrt{4\,t_{D3}}}{\sqrt{y(y-u_3)}} \right) \right] dy \qquad (\text{IV-12})$$

where $z' = z - (H_2' + H_3)$ and z is being measured from the top of Aquifer 2 upward. Since the forms of these equations are comparable to those of Eqs. IV-3 and IV-4, the curves of s_D versus t_D for Aquifer 3 and Aquitards 2 or 3, for given values of $(\beta_{32} + \beta_{33})$ and r/B_{32} or r/B_{33}, are similar to the

-318-

curves on Figs. IV-2 through IV-10 for equivalent values of β_{11} and r/B_{11}.
For example, the steep portions of the curves on Fig. IV-2 represent the
solutions for the following cases: (a) $\beta_{11} = r/B_{11} = 0.01$ when Aquifer 1 is
being pumped, (b) $(\beta_{32} + \beta_{33}) = r/B_{32} = 0.01$ or $(\beta_{32} + \beta_{33}) = r/B_{33} = 0.01$
when Aquifer 3 is being pumped, etc. .

We see that the steep portions of the curves for the pumped aquifer and
for the aquitard on Figs. IV-2 through IV-10 are applicable to arbitrary
multiple-aquifer systems. If there is an impermeable boundary adjacent to
the aquifer being pumped, the curves are functions of the two parameters
β_{ij} and r/B_{ij} where i designates the aquifer and j the adjacent aquitard. If
there is no impermeable boundary, the curves depend on $(\beta_{ij} + \beta_{i,j-1})$ and
r/B_{ij} in the aquifer and in the j-th adjacent aquitard, or on $(\beta_{ij} + \beta_{i,j-1})$ and
$r/B_{i,j-1}$ in the aquifer and in the $(j-1)$-th adjacent aquitard.

In the special case when $\sqrt{K_j' \varphi_j' c_j'} \gg \sqrt{K_{j-1}' \varphi_{j-1}' c_{j-1}'}$ (i.e. $\beta_{ij} \gg \beta_{i,j-1}$),
the parameter $(\beta_{ij} + \beta_{i,j-1})$ can be replaced with β_{ij}. The effect is the same
as if the $(j-1)$-th aquitard was impermeable. For example, if $\sqrt{K_2' \varphi_2' c_2'} \ll$
$\sqrt{K_3' \varphi_3' c_3'}$ and $\sqrt{K_4' \varphi_4' c_4'} \ll \sqrt{K_3' \varphi_3' c_3'}$ (i.e. $\beta_{32} \ll \beta_{33}$ and $\beta_{34} \ll \beta_{33}$),
then Aquifers 3 and 4 together with Aquitard 3 can be considered as an indepen-
dent two-aquifer system. This shows that the definition of the boundaries of a
multiple-aquifer system is a relative matter, and that it depends on the accuracy
which one is willing to accept in applying our theory to the particular problem
at hand.

At large values of time, drawdown in the system can no longer be
predicted using analogy to the two-aquifer case. It can be obtained only through
numerical evaluation of the solutions for the three-aquifer case developed in
Section II-D, or through the application of numerical methods such as the finite
element technique described in Chapter III.

V. A PROPOSED APPROACH TO THE PROBLEM OF EVALUATING
MULTIPLE-AQUIFER SYSTEMS BY MEANS OF PUMPING TESTS

The importance of pump testing as a means of evaluating the properties of water bearing strata has long been recognized by groundwater hydrologists. As a result, a variety of methods have been developed to assist the engineer in analysing the results of such tests. Whereas in most of these methods the aquifer is treated as if it had no hydraulic communication with the adjoining layers, several procedures have also been developed for the case when the aquifer is being supplied with leakage from above or from below.

In the first part of our discussion, we shall briefly review the methods that are currently being used in evaluating the results of pumping tests in "leaky" aquifers. We will show that these methods have theoretical and practical limitations which may often lead to erroneous interpretation of the field data. This will demonstrate the need for a new method of field testing multiple-aquifer systems which would enable one to evaluate the permeabilities and storage coefficients of all the aquifers and aquitards in a given system. An approach to this problem will be outlined in the second part of this chapter.

A. REVIEW OF METHODS CURRENTLY USED TO ANALYSE RESULTS OF PUMPING TESTS IN LEAKY AQUIFERS

1. Steady State Method

In 1946 Jacob (28) described a solution for the steady drawdown in an infinite leaky aquifer that is being pumped at a constant rate. In his development, Jacob considered a two-aquifer system in which all layers are homogeneous, isotropic, horizontal and infinite in radial extent. The pumping well has an infinitesimal radius and completely penetrates one of the aquifers (Fig. V-1). Jacob assumed that flow is essentially horizontal in the pumped aquifer, vertical in the aquitard, and that drawdown in the unpumped aquifer remains

zero at all values of time. His solution can be written in the form

$$s_1 = \frac{Q_1}{2\pi T_1} K_0(r/B_{11}) \qquad \text{(V-1)}$$

According to Polubarinova Kochina (38, p. 382), a similar solution was developed by Myatiev in 1946 (32).

In his work, Jacob described a graphical procedure of analysing the results of pumping tests in leaky aquifers, using a semilogarithmic graph of $K_0(r/B_{11})$ versus r/B_{11}. A logarithmic graph of $K_0(r/B_{11})$ versus r/B_{11} was

Fig. V-1. Two-aquifer system with zero drawdown in unpumped aquifer.

used by Walton (43, 44) to investigate leaky aquifer conditions in Illinois. Still another method of analysing field data, based in part on Eq. V-1, was proposed by Hantush in 1956 (17). The details of these procedures have been summarized by DeWiest (7, p. 278-282). They enable the engineer to calculate the transmissibility, $T_1 = K_1 H_1$, of the aquifer being pumped, and the dimensionless parameter $r/B_{11} = r\sqrt{K_1'/(K_1 H_1 H_1')}$. Knowing the values of r, H_1 and H_1', it is then possible to determine the permeabilities, K_1 and K_1', of the aquifer and the aquitard, respectively.

This method has the following limitations:

    a. As all steady state solutions, the method does not enable one to obtain the storage coefficients of the aquifer or the aquitard.

    b. It was shown in Section IV-A-4b that steady state cannot be reached in the system, unless the transmissibility of the unpumped aquifer is much larger than that of the aquifer being pumped. In reality, the system will seldom reach steady state unless the aquitard is overlain by
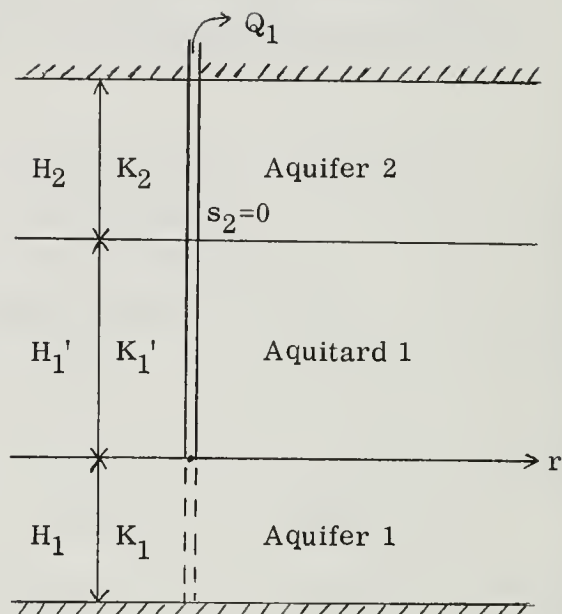
a body of water such as a lake, a reservoir, or a river, which can maintain a relatively constant head at the top of the aquitard.

Occasionally, the method may yield relatively good results even when the transmissibility of the unpumped aquifer is not larger than that of the pumped aquifer. For example, if $\beta_{11} = r/B_{11} = 0.01$, the curve of s_D versus t_D in the pumped aquifer (see Fig. IV-2) for the case when $T_1 = T_2$ (i.e. $\beta_{21} = \beta_{11}$ and $r/B_{21} = r/B_{11}$) is very close to the horizontal steady state curve. The error introduced by applying Eq. V-1 to this problem would therefore be relatively small. However, applying this equation to the case when $T_1 = T_2$ and $\beta_{11} = r/B_{11} = 1.0$ would lead to significant errors in the results, since the deviation between the curves in Fig. IV-4 is much larger than in Fig. IV-2.

2. The r/B Method

A solution for the non-steady state drawdown in an infinite leaky aquifer that is being pumped at a constant rate was obtained by Hantush and Jacob in 1955 (16). In their development, Hantush and Jacob adopted a two-aquifer system similar to the one shown in Fig. V-1. They again assumed that the layers are homogeneous, isotropic and infinite in radial extent; that a well of infinitesimal radius completely penetrates one of the aquifers; that flow is essentially horizontal in this aquifer and vertical in the aquitard; and that drawdown in the unpumped aquifer remains zero at all values of time. In addition, Hantush and Jacob neglected the storage of water in the aquitard. Their solution may be written in the form

$$s_1 = \frac{Q_1}{4\pi T_1} \int_{1/4t_D}^{\infty} \exp\left[-y - \frac{(r/B_{11})^2}{4y}\right] \frac{dy}{y} \tag{V-2}$$

where $t_D = \alpha_1 t / r^2$.

In 1956 Hantush (17) outlined a graphical procedure of analysing the results of pumping tests in leaky aquifers, based on Eq. V-2. His procedure involves the use of a family of type curves of s_D versus t_D where each curve corresponds to a given value of r/B_{11} (Fig. V-2). Observed values of drawdown in the pumped aquifer, s_1, at a given radial distance from the pumping well are plotted against the time, t, on logarithmic paper. Since s_1 is proportional to s_D and t is proportional to t_D, the field data can be matched graphically to one of the type curves, which determines the value of r/B_{11}. One then chooses a match point anywhere on the overlapping portion of the two sheets and records the values of s_1 and t that correspond to the coordinates s_D and t_D of the match point, respectively.

Knowing the values of Q_1 and H_1, the permeability K_1 of the aquifer can be determined from $s_1 = (Q_1/4 \pi T_1) \, s_D(t_D, r/B_{11})$. Since the values of r/B_{11}, r, H_1, H_1' and K_1 are now all known, the permeability K_1' of the aquitard can also be calculated from $r/B_{11} = r \sqrt{K_1'/(K_1 H_1 H_1')}$. In addition, the specific storage $S_s = \varphi_1 c_1 \gamma$ of the aquifer can be obtained from $t_D = K_1 t/(\varphi_1 c_1 \gamma r^2)$.

Despite its wide acceptance among ground water hydrologists (7,8, 39,43,44), the r/B method is limited in application and may often lead to erroneous results. Its main disadvantages are as follows:

a. The method does not enable one to obtain the specific storage of the aquitard.

b. The assumption of no drawdown in the unpumped aquifer implies that a steady state must eventually be established in the system. This is why the curves in Fig. V-2 become horizontal at large values of time. The limitations of this assumption have been discussed in Section V-A-1 in connection with the steady state method.

c. The steep portions of the curves in Fig. V-2 coincide with the Theis solution, implying that leakage at small values of time is negligible. However, from Section IV-A-4a and from Figs. IV-2 through IV-9

-324-
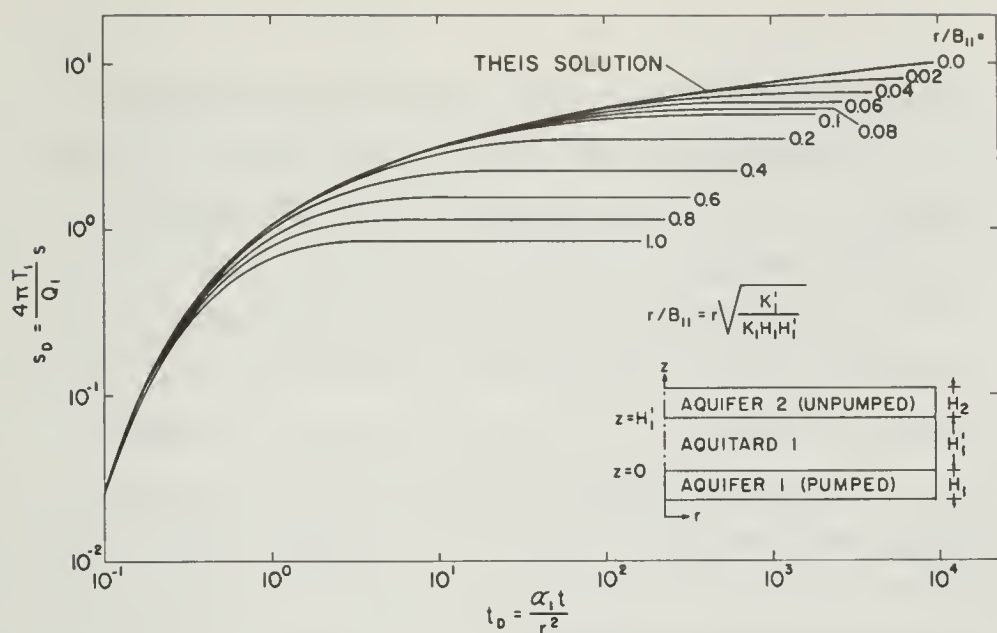
Fig. V-2. Dimensionless drawdown versus dimensionless time
from Hantush and Jacob (16) solution for infinite
leaky aquifer neglecting storage in aquitard. [After
Witherspoon et al. (47)]
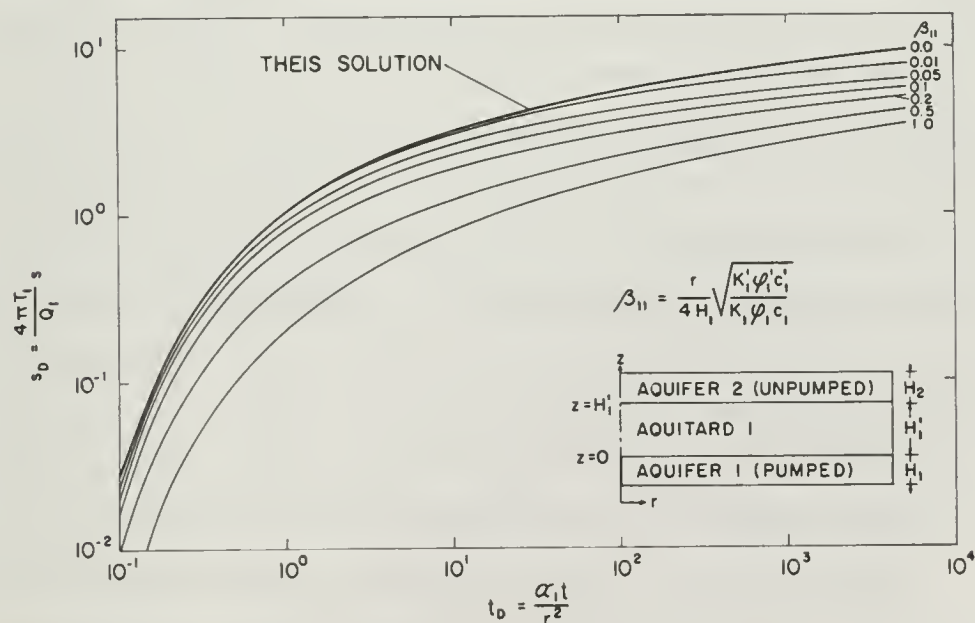
Fig. V-3. Dimensionless drawdown versus dimensionless time
from Hantush's (21) asymptotic solution for infinite
leaky aquifer considering storage in aquitard. Valid
at $t_D \leq 1.6\,\beta_{11}^2/(r/B_{11})^4$. [After Witherspoon et al. (47)]

we know that these portions of the curves are actually functions of β_{11}. For example, let us consider Figs. IV-4 and IV-9, in both of which $r/B_{11} = 1.0$. Comparing the curves for the pumped aquifer will reveal that they are different in both figures, simply because the values of β_{11} are not the same. In addition, the effect of leakage at small values of time depends on the magnitude of β_{11}; it is negligible when β_{11} is small, but it can be significant when β_{11} is large.

In the particular case when drawdown in the unpumped aquifer remains zero (i.e. $\beta_{21} = r/B_{21} = 0$), the curves in Figs. IV-4 and IV-9 become horizontal at large values of time and reach the same value of s_D as the corresponding curve for $r/B_{11} = 1.0$ on Fig. V-2. We therefore conclude that while the horizontal (steady state) portions of the curves in Fig. V-2 are correct (provided that there is no drawdown in the unpumped aquifer), the steeper (transient) portions of these curves are generally not. This may be explained as follows: During the first stage of the pumping operation, most of the leakage is derived from storage in the aquitard. At this stage, neglecting the effect of storage in the aquitard is similar to neglecting the effect of leakage in general. Since storage in the aquitard was neglected in the development of Eq. V-2, the resulting curves (Fig. V-2) do not show the effect of leakage at small values of time. As time goes on, the relative importance of water that comes from storage in the aquitard diminishes, while more and more leakage is contributed by the unpumped aquifer. By the time steady state is reached, all the leakage is supplied by the unpumped aquifer and the amount of water stored in the aquitard remains unchanged. At this stage, the storage capacity of the aquitard has practically no influence on the behavior of the system, and Eq. V-2 is correct.

d. Since the steep portions of the curves in Fig. V-2 are not correct unless β_{11} is very small, they should not be used indiscriminately

in the interpretation of field results. This means that since the field
data can only be matched with the horizontal portions of these curves,
the value of r/B_{11} cannot be determined uniquely. We conclude that
the r/B method may give correct results when β_{11} is sufficiently small,
but it may lead to erroneous results when β_{11} is large.

3. The β Method

In 1960, Hantush (21) developed asymptotic solutions to the same
problem that was discussed in Section V-A-2, except that this time he did
not neglect the effect of storage in the aquitard. In his work, Hantush also
treated the more general case of an aquifer that is enclosed between two aqui-
tards. His solutions have been discussed earlier in Section IV-A-4e.

In the case of a two-aquifer system such as in Fig. V-1, Hantush's
solution for small values of time (Eq. IV-3) can also be written in the form

$$ s_1 \quad = \quad \frac{Q_1}{4 \pi T_1} \; s_D \; (t_D, \beta_{11}) \qquad\qquad (V-3) $$

where $t_D = \alpha_1 t/r^2$. A graphical procedure of analysing the results of pumping
tests has been developed on the basis of this solution. The procedure involves
the use of type curves of s_D versus t_D such as in Fig. V-3, each curve cor-
responding to a given value of β_{11}. As in the r/B method, observed values
of drawdown, s_1, at a given radial distance from the pumping well are plotted
against the time, t, on logarithmic paper. The field data are then matched
graphically with one of the curves in Fig. V-3, which determines the value
of β_{11}. A match point is chosen anywhere on the overlapping portion of the
two sheets, and its dual coordinates, s_1, s_D and t, t_D, are recorded.

Knowing the values of Q_1 and H_1, the permeability K_1 of the aquifer
can be determined from Eq. V-3. The specific storage of the aquifer, $S_{s_1} = \varphi_1 c_1 \gamma$, is obtained from $t_D = K_1 t/(\varphi_1 c_1 \gamma r^2)$. Since β_{11} is known, the value of
$K_1' \varphi_1' c_1'$ can be calculated from

$$\beta_{11} = \frac{r}{4 H_1} \sqrt{\frac{K_1' \varphi_1' c_1'}{K_1 \varphi_1 c_1}}$$

This method is quite limited in application, its main disadvantages being as follows:

a. The shapes of the curves in Fig. V-3 are not too different from the Theis curve. Thus, it may be difficult to decide which of these curves should be used in matching the field data.

b. The curves bear no indication as to the range of t_D within which they are valid. As shown in Section IV-A-4e, this range depends not only on the value of β_{11}, but also on that of r/B_{11}. This is illustrated in Figs. IV-15 through IV-20. For example, Fig. IV-15 indicates that while the curve for $\beta_{11} = 0.01$ is valid up to $t_D \approx 5 \times 10^2$ when $r/B_{11} = 0.04$, its range of validity is reduced to $t_D \leq 1.5 \times 10^{-1}$ in the case when $r/B_{11} = 1.0$. Thus, one may have difficulties in deciding whether his field data fall within the range of validity of any particular curve in Fig. V-3.

c. The method does not enable one to obtain the permeability, K_1', and the storage coefficient, $S_{s_1}' = \varphi_1' c_1' \gamma$, of the aquitard, only the value of their product, $K_1' S_{s_1}'$.

B. A NEW APPROACH TO PUMP TESTING MULTIPLE-AQUIFER SYSTEMS

It is apparent from Section V-A that the conventional methods of pump testing leaky aquifers are often not adequate for their purpose and that they may lead to erroneous interpretation of the field data. We shall now outline a new approach to field testing multiple-aquifer systems, based on the theory developed in this work. The new procedure should be applicable to systems that contain an arbitrary number of aquifers, aquitards and aquicludes, and may possibly enable one to evaluate the properties of all the layers in such systems.

To start with a relatively simple problem, consider a system that consists of two aquifers and one aquitard, as shown in Fig. V-4. In order

to determine the properties of the aqui-
tard or the lower aquifer, a well that
has been drilled to the bottom of this
aquifer is completed as a pumping well.
In the same aquifer, another well is
drilled at a distance r_0 from the pumping
well and is completed as an observation
well. In addition, one or more obser-
vation wells are completed in the aqui-
tard, at the same radial distance r_0
from the pumping well, at different ele-
vations. In our example, we shall as-
sume that three such wells have been
completed in the aquitard and that the

Fig. V-4. Observation points in pump-
testing a two-aquifer system.

midpoints of their perforated sections are located at the elevations $z/H_1' =$
0.2, 0.5 and 0.8, respectively. Because of the relatively steep vertical gradients
that develop in the aquitard, the perforated sections of these wells should be short
enough so that the observed drawdowns are representative of the actual drawdowns
at the midpoints of these sections.

The next step consists of withdrawing water at a constant rate from the
pumping well and measuring the drawdowns that occur in the observation wells.
These drawdown data are then plotted on transparent logarithmic paper against
the time, t, and are compared with type curves of dimensionless drawdown versus
dimensionless time such as in Figs. IV-2 through IV-9. Obviously, these figures
are only a small sample of the large number of similar figures, corresponding to
different values of β_{11} and r/B_{11}, that must be developed prior to such a test.
The possibility of matching field data uniquely to only one family of such curves
needs further investigation. The curves for the unpumped aquifer in Figs. IV-2
through IV-9 are not needed in the interpretation of the field data and are not a
part of the type curves.

As one may recall from Chapter IV, the shapes of the type curves depend on the values of β_{11} and r/B_{11} at small values of time, and on the values of β_{11}, r/B_{11}, β_{21} and r/B_{21} at large values of time. Thus, at large values of time, the curves for any given values of β_{11} and r/B_{11} split into a large number of branches, each branch corresponding to different values of β_{21} and r/B_{21}. This was illustrated in Fig. IV-10. In Figs. IV-2 through IV-9, only two such branches were shown for each curve, and the same must be done in all the additional type curves that will be developed prior to the test. Superposition of the field data is done only along the relatively steep portions of the type curves, before these curves split in two. In this way, the type curves will be functions of only two parameters, β_{11} and r/B_{11}, and the need for additional type curves representing different values of β_{21} and r/B_{21} is avoided. Since superposition is based not only on the shapes of the type curves but also on the spread between these curves, there is an increased likelihood that the field data can be matched uniquely to only one family of type curves.

As an example, Fig. V-5 shows a set of hypothetical field data that were obtained from the pumping test described earlier. We assume that a unique graphical match between these data and the type curves in Fig. IV-5 ($\beta_{11} = 0.01$ and $r/B_{11} = 0.02$) was obtained by shifting the two plots while keeping their axes parallel, until the field data fell on the type curves prior to the points where these curves split in two. The field data need not coincide with the type curves to the right of the points where these curves split.

After the values of β_{11} and r/B_{11} have been determined from the type curves, a match point is selected anywhere on the overlapping portion of the two sheets, and the values of s_D and t_D that correspond to the drawdown s and time t at this point are recorded. In Fig. V-5, the values of these quantities at the match point are $s_D = 1.0$, $s = 0.5$ feet, $t_D = 10.0$ and $t = 2.5 \times 10^{-3}$ days.

With these data secured, the properties of the pumped aquifer and the aquitard can now be easily determined. Knowing the values of Q_1 and H_1, the permeability of the aquifer can be obtained from
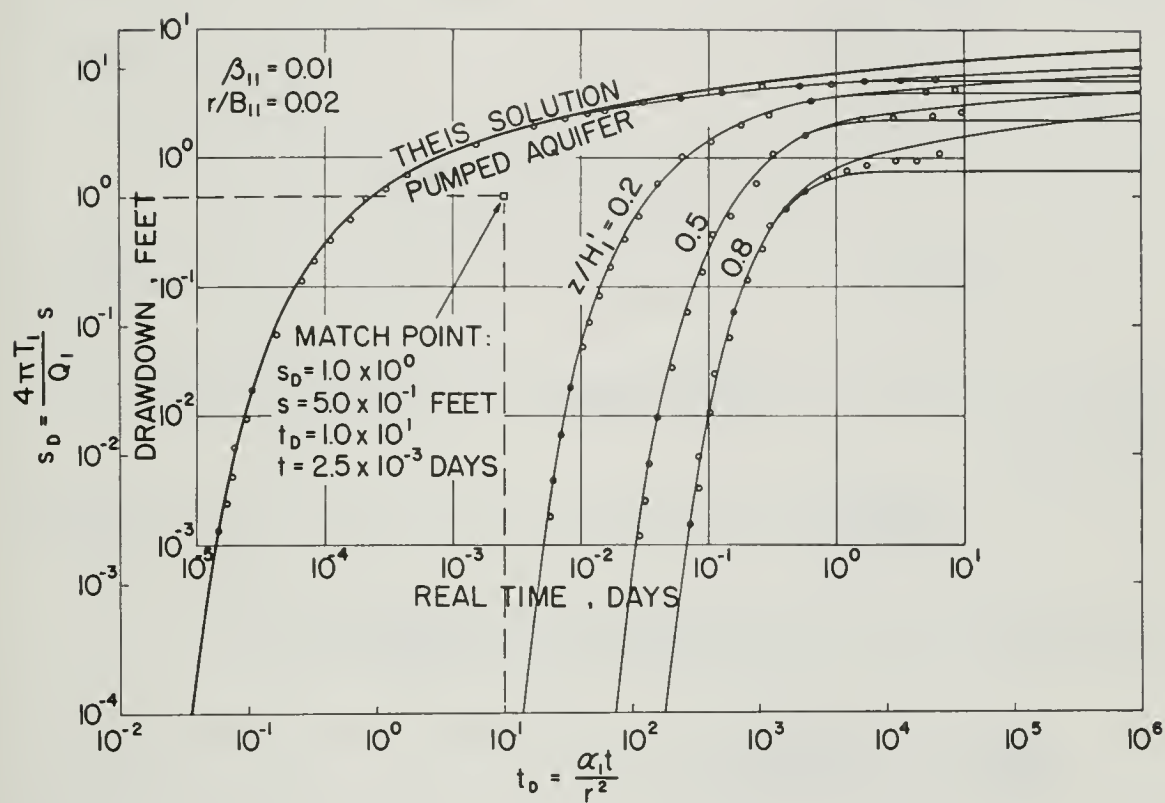
Fig. V-5. Comparison of hypothetical data from pumped aquifer and adjacent aquitard with theoretical solutions.

$$s = \frac{Q_1}{4 \pi K_1 H_1} s_D \qquad (V-4)$$

If Q is given in gpm, s and H_1 in feet, and K_1 in gpd/ft^2, one can rewrite this equation in the form

$$K_1 = \frac{114.6 \, Q_1 \, s_D}{H_1 \, s} \qquad (V-4a)$$

The specific storage of the aquifer is determined from

$$t_D = \frac{K_1 t}{S_{s1} \, r_o^2} \qquad (V-5)$$

and when t is in days, r_o in feet, K_1 in gpd/ft^2. and S_{s1} in feet^{-1}, this can also be written as

$$S_{s1} = \frac{K_1 t}{7.48 \, r_o^2 \, t_D} \qquad (V-5a)$$

The permeability of the aquitard can be calculated from

$$r/B_{11} = r_o \sqrt{\frac{K_1'}{K_1 H_1 H_1'}} \qquad (V-6)$$

which can be rewritten in the form

$$K_1' = \frac{(r/B_{11})^2 \, K_1 \, H_1 \, H_1'}{r_o^2} \qquad (V-6a)$$

Finally, the specific storage of the aquitard is obtained from

$$\beta_{11} = \frac{r_o}{4 H_1} \sqrt{\frac{K_1' S_{s1}'}{K_1 S_{s1}}} \qquad (V-7)$$

which can be expressed as

$$S_{s1}' = \frac{16 \beta_{11}^2 \, H_1^2 \, K_1 \, S_{s1}}{K_1' \, r_o^2} \qquad (V-7a)$$

In our example, let us assume that

H_1 = 100 feet r_o = 200 feet

H_1' = 200 feet Q_1 = 1000 gpm

We found from the type curves that

β_{11} = 0.01

r/B_{11} = 0.02

s = 0.5 feet when s_D = 1.0

t = 2.5 x 10^{-3} days when t_D = 10.0

From Eq. V-4a, the permeability of the aquifer is

$$K_1 = \frac{114.6 \times 1000 \times 1.0}{100 \times 0.5} = 2{,}292 \text{ gpd/ft}^2$$

From Eq. V-5a, the specific storage of the aquifer is obtained as

$$S_{s1} = \frac{2292 \times 2.5 \times 10^{-3}}{7.48 \times 200^2 \times 10} = 1.914 \times 10^{-6} \text{ ft}^{-1}$$

The dimensionless storage coefficient, S_1, of the aquifer is $S_1 = S_{s1} H_1$ = 1.914 x 10^{-6} x 100 = 1.914 x 10^{-4}. The permeability of the aquitard is determined from Eq. V-6a as

$$K_1' = \frac{0.02^2 \times 2292 \times 100 \times 200}{200^2} = 4.584 \times 10^{-1} \text{ gpd/ft}^2$$

Finally, from Eq. V-7a, the specific storage of the aquitard is found to be

$$S_{s1}' = \frac{16 \times 0.01^2 \times 100^2 \times 2292 \times 1.914 \times 10^{-6}}{4.584 \times 10^{-1} \times 200^2} = 3.827 \times 10^{-6} \text{ ft}^{-1}$$

In the above example we assumed that there were three observation wells in the aquitard at the elevations $z/H_1' = 0.2$, 0.5 and 0.8. Similar results could perhaps be obtained with only one or two such wells in the aquitard. However, it seems that the larger is the number of these wells, the easier it may be to match the field data uniquely to one of the families of type curves. Performing additional tests at different radial distances from the pumping well should increase the likelihood of obtaining a meaningful result by this procedure, but this has not been investigated.

As a more general case, let us consider a system that consists of an arbitrary number of aquifers and aquitards, a part of which is shown in Fig. V-6. One may recall from Section IV-B that at small values of time, drawdown in the i-th aquifer (if it is being pumped) is a function of the single parameter $(\beta_{i,j-1} + \beta_{ij})$. At the same time, drawdown in the overlying aquitard depends on the two parameters $(\beta_{i,j-1} + \beta_{ij})$ and r/B_{ij}, and in the underlying aquitard on $(\beta_{i,j-1} + \beta_{ij})$ and $r/B_{i,j-1}$. However, the forms of Eqs. IV-3 and IV-4 are comparable to those of Eqs. IV-10, IV-11 and IV-12, respectively. Therefore, as mentioned in Section IV-B, the relatively steep portions of the curves in Figs. IV-2 through IV-9 have the same shapes whether the pumped aquifer has an impermeable boundary or not. Thus, in order to adapt these type curves to arbitary multiple-aquifer systems one has only to replace the parameters β_{11} and r/B_{11} by the general parameters $(\beta_{i,j-1} + \beta_{ij})$ and r/B_{ij}
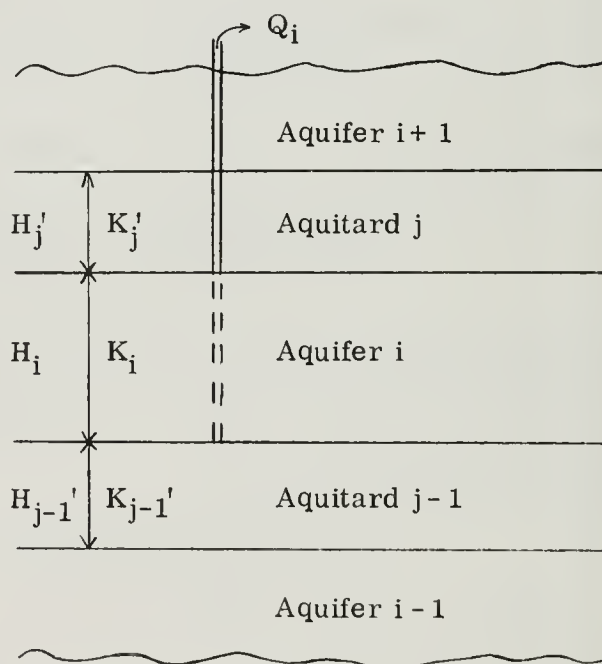
Fig. V-6. Portion of multiple-aquifer system.

(or $r/B_{i,j-1}$ if drawdown is being observed in the $(j-1)$-th aquitard). For example, instead of $\beta_{11} = 0.01$ and $r/B_{11} = 0.02$, Fig. IV-5 should be labeled $(\beta_{i,j-1} + \beta_{ij}) = 0.01$ and $r/B_{ij} = 0.02$.

If the pumping test is performed in the i-th aquifer while drawdown is being observed in the j-th aquitard, Eqs. V-4a, V-5a, and V-6a become

$$K_i = \frac{114.6\, Q_i\, s_D}{H_i\, s} \tag{V-8}$$

$$S_{si} = \frac{K_i\, t}{7.48\, r_o^2\, t_D} \tag{V-9}$$

$$K_j' = \frac{(r/B_{ij})^2\, K_i\, H_i\, H_j'}{r_o^2} \tag{V-10}$$

where K_i and K_j' are in gpd/ft^2, Q_i is in gpm, H_i, H_j', r_o, and s are in feet, t is in days, and S_{si} is in $feet^{-1}$. Eqs. V-8 through V-10 can be used to evaluate the properties of the i-th aquifer and the permeability of the adjacent j-th aquitard. If drawdown is being measured in the $(j-1)$-th aquitard, these equations are still applicable if one replaces the subscript j in V-10 by $j-1$. It is, of course, possible to pump the i-th aquifer and at the same time measure the drawdowns in both aquitards, $j-1$ and j. In this manner, one obtains two sets of field data from a single test; one set of data for the aquifer and the upper aquitard (i.e. $(\beta_{i,j-1} + \beta_{ij})$ and r/B_{ij}) and one set for the aquifer and the lower aquitard (i.e. $(\beta_{i,j-1} + \beta_{ij})$ and $r/B_{i,j-1}$). Since the values of r/B_{ij} and $r/B_{i,j-1}$ are not necessarily the same, the two sets of data may be matched to different familes of type curves and the values of $(\beta_{i,j-1} + \beta_{ij})$, r/B_{ij}, and $r/B_{i,j-1}$ can be determined from these curves. By choosing a match point for each set of data and following the procedure described earlier, one can then use Eqs. V-8 through V-10 to obtain the properties of the aquifer and the permeabilities of the enclosing aquitards.

In the two-aquifer case, Eqs. V-7 and V-7a were used to evaluate the specific storage of the single aquitard adjacent to the aquifer being pumped. However, in the more general case of an aquifer that is enclosed between two aquitards, such as in Fig. V-6, Eq. V-7 must be rewritten in the form

$$(\beta_{i,\,j-1} + \beta_{ij}) = \frac{r_o}{4\,H_i}\left[\sqrt{\frac{K_{j-1}{}'S_{s_{j-1}}{}'}{K_i\,S_{s_i}}} + \sqrt{\frac{K_j{}'S_{s_j}{}'}{K_i\,S_{s_i}}}\right] \tag{V-11}$$

Although the values of $(\beta_{i,\,j-1} + \beta_{ij})$, K_i, S_{s_i}, $K_j{}'$, and $K_{j-1}{}'$ have been previous-ly determined, the quantities $S_{s_{j-1}}$ and S_{s_j} cannot be obtained from Eq. V-11.

Occasionally, one may find that one of the aquitards is much less permeable than the other and its effect on the drawdown in the aquifer is relatively small. For example, if $\sqrt{K_{j-1}{}'} \ll \sqrt{K_j{}'}$, the first term on the right hand side of Eq. V-11 can in most cases be neglected, and the specific storage of the j-th aquitard can be calculated from

$$(\beta_{i,\,j-1} + \beta_{ij}) \approx \beta_{ij} = \frac{r_o}{4\,H_i}\sqrt{\frac{K_j{}'S_{s_j}{}'}{K_i\,S_{s_i}}} \tag{V-12}$$

In such case, the less permeable aquitard can be considered as one of the "impermeable" boundaries of the multiple-aquifer system.

When the permeabilities of the aquitards are such that none of them can be neglected, the only way to evaluate their specific storage by means of this procedure is to perform similar tests in additional aquifers. As an example, consider a system that consists of four aquifers and three aquitards as shown in Fig. V-7. We saw that the specific storage, $S_{s_2}{}'$, of Aquitard 2 cannot be determined from a single pumping test in Aquifers 2 or 3. However, it is possible to determine the value of $S_{s_2}{}'$ from two pumping tests, either in Aquifers 1 and 2 (with observation wells in Aquitards 1 and 2) or in Aquifers 3 and 4 (with observation wells in Aquitards 2 and 3). Thus, a test in Aquifer 1

will yield the values of β_{11} and r/B_{11}, which can be used to evaluate the properties of Aquitard 1, K_1' and S_{s1}'. A test in Aquifer 2 will yield the properties of this aquifer together with the values of $(\beta_{21} + \beta_{22})$ and r/B_{22}. Knowing the properties of Aquifer 2 and Aquitard 1, one can calculate the value of β_{21}. Since $(\beta_{21} + \beta_{22})$ is known, the value of β_{22} is obtained from $\beta_{22} = (\beta_{21} + \beta_{22}) - \beta_{21}$. Finally, knowing the values of β_{22} and r/B_{22}, together with the properties of Aquifer 2, enables one to use Eqs. V-8 through V-10 and Eq. V-12 in calculating the specific storage of Aquitard 2, S_{s2}'. A similar procedure can be used to

Fig. V-7. Four-aquifer system.

evaluate the properties of all the layers in any given system.

The success of the above method of pump testing multiple-aquifer systems may depend on our ability to detect, with a sufficient degree of accuracy and with a minimum of time lag, the extremely small changes in hydraulic head that take place in the system during the initial stages of the test. The answer to this problem seems to lie in the application of highly sensitive pressure transducers to the measurement of drawdowns in the observation wells. Further investigation into the practical aspects of the graphical matching procedure is needed before the method can be applied in the field.

VI. CONCLUSIONS

1. Analytical solutions for transient flow to a well of constant discharge in an infinite two-aquifer system have been obtained. These solutions have been evaluated numerically for selected values of the parameters β_{ij} and r/B_{ij}.

2. Analytical solutions for transient flow to a well of constant discharge in an infinite three-aquifer system have been developed, but the results have not been evaluated.

3. Asymptotic solutions for small values of time have been obtained for the pumped aquifer and the enclosing aquitards. These solutions are valid in multiple-aquifer systems and are relatively easy to evaluate numerically. The solution for the aquifer is the same as Hantush's modified solution for leaky aquifers (21).

4. A complete solution to the problem described by Hantush in Case 1 of his "Modification of the Theory of Leaky Aquifers" (21) has been developed. As one may recall, Hantush's solutions for this problem are restricted to the pumped aquifer and are valid only at small and large values of time.

5. It was shown that a solution for the above leaky aquifer problem can also be obtained from the solutions for flow in a three-aquifer system, simply by neglecting drawdown in the unpumped aquifers.

6. It was shown that when one of the two aquitards is impermeable, the solutions for the three-aquifer system reduce to those for the two-aquifer system. When the remaining aquitard is also impermeable, these solutions reduce to the Theis solution.

7. The finite element method, which was first adapted to problems of transient flow in porous media by Javandel and Witherspoon (29), has been used to investigate the behavior of a two-aquifer system and to obtain an independent check on the corresponding analytical solutions.

8. The analytical solutions were developed with the assumption that flow is essentially horizontal in the aquifers and vertical in the aquitards. The error involved in these assumptions was found to be a function of the ratios between the permeabilities of the aquifers and the adjacent aquitards; the larger these ratios, the more accurate the analytical solutions. In addition, the error was found to increase with time and decrease with radial distance from the pumping well.

9. When the permeabilities of the aquifers are at least two orders of magnitude larger than those of the adjacent aquitards, the error involved in the above assumption can be neglected everywhere except in the vicinity of the pumping well, at all practical values of time.

10. At small values of time, almost all of the water that leaks into the pumped aquifer is derived from storage in the adjacent aquitards. At this stage, neglecting the effect of storage in the aquitards is similar to neglecting the effect of leakage completely.

11. As time goes on, the relative importance of water that comes from storage in the aquitards diminishes while more and more leakage is contributed by the unpumped aquifers. If a quasi steady state is reached in the system, most of the leakage is supplied by the unpumped aquifers and storage in the aquitards may safely be neglected.

12.   The methods which are currently being used to evaluate the results of pumping tests in leaky aquifers are limited in application and may often lead to erroneous results.

13.   A new approach to the problem of evaluating multiple-aquifer systems by means of pumping tests has been proposed. The new procedure is based on the theory developed in this work and should enable one to evaluate the properties of all the aquifers and aquitards in a given system. Further investigation is needed before the method can be applied in the field.

The infinite Hankel transform of order zero, $F(a)$, of a function $f(r)$ is defined as

$$H^+ [f(r)] \ = \ F(a) \ = \ \int_0^\infty r \, J_0(a \, r) \, f(r) \, d \, r \tag{A-1}$$

The inverse of this transform is given by

$$f(r) \ = \ \int_0^\infty a \, J_0(r \, a) \, F(a) \, d \, a \tag{A-2}$$

A particular inverse Hankel transform that is needed in this work is that of the function

$$F(a) \ = \ \frac{a^{2n}}{a^2 + \xi^2} \tag{A-3}$$

where ξ is real and n is a non-negative integer.

To obtain the inverse of Eq. A-3, we will use Hankel functions of order zero defined as

$$H_0^{(1)} (z) \ = \ J_0(z) + i \, Y_0(z)$$
$$H_0^{(2)} (z) \ = \ J_0(z) - i \, Y_0(z) \tag{A-4}$$

where z is a complex variable. Consider the integral

$$\int \frac{z^{2n+1} \, H_0^{(1)} (r \, z)}{z^2 + \xi^2} \, d \, z \tag{A-5}$$

taken around the contour shown
in Fig. A-1. The integrand has
simple poles at $z = \pm\, i\,\xi$ and a
branch point at $z = 0$. We there-
fore choose the negative imaginary
axis as our branch line. Let

$z = R\,e^{i\theta}$ on Γ

$z = \varepsilon\,e^{i\theta}$ on γ

$z = x$ on the positive real axis

$z = x\,e^{i\pi}$ on the negative real axis
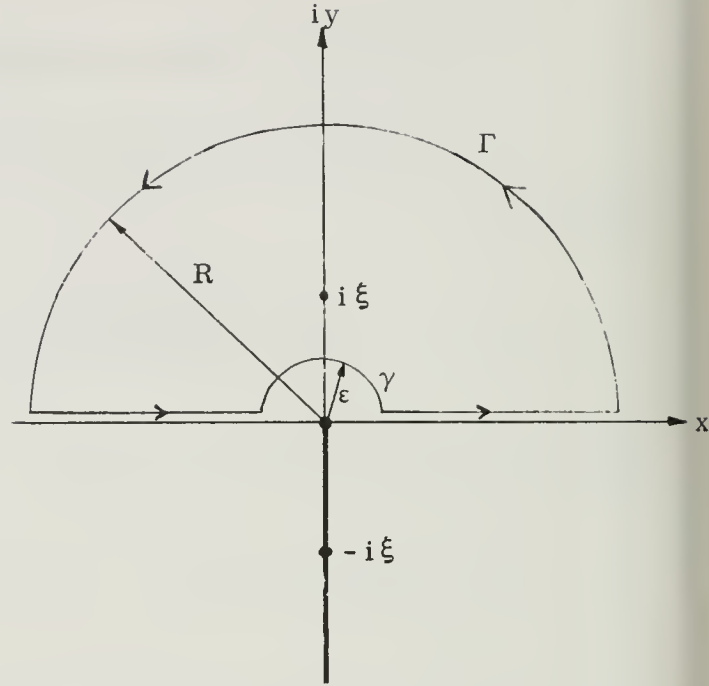
Fig. A-1. Contour of integration for Eq. A-5.

Applying the residue theorem to
Eq. A-5, we can write

$$\int_0^\infty \frac{x^{2n+1}\,H_0^{(1)}(r\,x)}{x^2 + \xi^2}\,dx + \lim_{R \to \infty} \int_\Gamma \frac{z^{2n+1}\,H_0^{(1)}(r\,z)}{z^2 + \xi^2}\,dz$$

$$+ \int_{-\infty}^0 \frac{(x\,e^{i\pi})^{2n+1}\,H_0^{(1)}(r\,x\,e^{i\pi})}{(x\,e^{i\pi})^2 + \xi^2}\,d(x\,e^{i\pi}) + \lim_{\varepsilon \to 0} \int_\pi^0 \frac{\varepsilon^{2n+1}\,e^{(2n+1)i\theta}\,H_0^{(1)}(r\varepsilon\,e^{i\theta})\,i\varepsilon\,e^{i\theta}}{\varepsilon^2\,e^{2i\theta} + \xi^2}\,d\theta$$

$= 2\,\pi\,i$ times (residue of integrand in Eq. A-5 at $z = i\,\xi$)   (A-6)

We can now use the relationship (31, p. 204)

$$K_0(z\,e^{-i\,\pi/2}) = \frac{i\,\pi}{2}\,H_0^{(1)}(z) \tag{A-7}$$

and the asymptotic formula

$$K_0(z) \approx \sqrt{\frac{\pi}{2\,z}}\;\,e^{-z}$$

for $\left| z \right| \to \infty$ and $-\pi < \arg z \le \pi$ to show that

$$\left| H_0^{(1)}(z) \right| \approx \sqrt{\frac{2}{\pi R}} \left| e^{-z e^{-i\pi/2}} \right|$$

when $\left| z \right| \to \infty$ and $-\pi/2 < \arg z \le 3\pi/2$. If I_Γ denotes the second integral in Eq. A-6 we therefore have

$$\lim_{R \to \infty} \left| I_\Gamma \right| \le \lim_{R \to \infty} \left| \frac{z^{2n+1} H_0^{(1)}(rz)}{z^2 + \xi^2} \right| \pi R \le \lim_{R \to \infty} \frac{\pi R^{2n+2}}{R^2 - \xi^2} \sqrt{\frac{2}{\pi R r}} \left| e^{-z r e^{-i\pi/2}} \right|$$

$$\le \lim_{R \to \infty} \frac{\pi R^{2n+2}}{R^2 - \xi^2} \sqrt{\frac{2}{\pi R r}} \ \frac{1}{1 - (rR) + \dfrac{(rR)^2}{2!} - \dfrac{(rR)^3}{3!} + \cdots} = 0$$

for any finite value of n.

The last integral in Eq. A-6 obviously vanishes at the limit as $\varepsilon \to 0$ because

$$\lim_{\varepsilon \to 0} \varepsilon\, J_0(\varepsilon) = 0$$

and

$$\lim_{\varepsilon \to 0} \varepsilon\, Y_0(\varepsilon) = \lim_{\varepsilon \to 0} \varepsilon\, \ln \varepsilon = 0$$

The residue of the integrand in Eq. A-5 at $z = i\xi$ can be evaluated with the aid of Eq. A-7,

$$\mathrm{Res} \left[\frac{z^{2n+1} H_0^{(1)}(rz)}{z^2 + \xi^2} \right]_{z = i\xi} = \frac{(i\xi)^{2n+1} H_0^{(1)}(ri\xi)}{2i\xi}$$

$$= \frac{(-1)^n}{2} \xi^{2n} H_0^{(1)}(ri\xi) = \frac{(-1)^n}{\pi i} \xi^{2n} K_0(r\xi)$$

-345-

The function $H_0^{(2)}(z)$ consists entirely of terms involving $\ln z$ and powers of z^2, and is therefore even with respect to real values of z. We also know (31, p. 199) that $H_0^{(1)}(z e^{i\pi}) = - H_0^{(2)}(z)$ for all values of z. Using these results, Eq. A-6 becomes

$$\int_0^\infty \frac{x^{2n+1} [H_0^{(1)}(rx) + H_0^{(2)}(rx)]}{x^2 + \xi^2} dx = 2(-1)^n \xi^{2n} K_0(r\xi)$$

Substituting the Hankel functions from A-4 in the above equation, we obtain the inverse Hankel transform of Eq. A-3 in the form

$$f(r) = H^{-1}\left[\frac{a^{2n}}{a^2 + \xi^2}\right] = \int_0^\infty \frac{x^{2n+1} J_0(xr)}{x^2 + \xi^2} dx = (-1)^n \xi^{2n} K_0(r\xi) \qquad \text{(A-8)}$$

Note that when $n = 0$, this reduces to an equation that was previously developed by Watson (45, p. 425).

A particular Hankel transform that is needed in this work is

$$H^*\left[\frac{1}{r} \frac{\partial}{\partial r}\left(r \frac{\partial \bar{s}(r,p)}{\partial r}\right)\right]$$

Using the relationships

$$\frac{d J_0(x)}{dx} = - J_1(x)$$

and

$$\frac{d}{dx}\left[x J_1(x)\right] = x J_0(x)$$

we can write

$$H^*[\bar{s}(r,p)] = \int_0^\infty r\, J_0(a\,r)\, \bar{s}(r,p)\, d r$$

$$= \frac{r}{a}\, J_1(a\,r)\, \bar{s}(r,p)\,\Big|_0^\infty - \int_0^\infty \frac{r}{a}\, J_1(a\,r)\, \frac{\partial}{\partial r}\, \bar{s}(r,p)\, d r$$

The integral term in this equation can be written as

$$\frac{1}{a}\int_0^\infty J_1(a\,r)\, r\, \frac{\partial}{\partial r}\, \bar{s}(r,p)\, d r$$

$$= \frac{1}{a}\left[-\frac{1}{a}\, J_0(a\,r)\, r\, \frac{\partial}{\partial r}\, \bar{s}(r,p)\,\Big|_0^\infty + \frac{1}{a}\int_0^\infty J_0(a\,r)\, \frac{\partial}{\partial r}\left(r\, \frac{\partial}{\partial r}\, \bar{s}(r,p) \right) d r \right]$$

$$= -\frac{1}{a}\left[\frac{1}{a}\, J_0(a\,r)\, r\, \frac{\partial}{\partial r}\, \bar{s}(r,p)\,\Big|_0^\infty - \frac{1}{a}\int_0^\infty r\, J_0(a\,r)\, \frac{1}{r}\, \frac{\partial}{\partial r}\left(r\, \frac{\partial}{\partial r}\, \bar{s}(r,p) \right) d r \right]$$

The last term is the required Hankel transform so that

$$H^*\left[\frac{1}{r}\, \frac{\partial}{\partial r}\left(r\, \frac{\partial}{\partial r}\, \bar{s}(r,p) \right) \right]$$

$$= \left[a\,r\, J_1(a\,r)\, \bar{s}(r,p) + J_0(a\,r)\, r\, \frac{\partial}{\partial r}\, \bar{s}(r,p) \right]_0^\infty - a^2\, H^*[\bar{s}(r,p)]$$

Using the boundary conditions

$$\lim_{r\to\infty} \bar{s}(r,p) = 0$$

$$\lim_{r\to\infty} r\, \frac{\partial}{\partial r}\, \bar{s}(r,p) = 0 \quad \text{(no flow at infinity)}$$

and noting that

$$\lim_{r \to \infty} J_0(a\,r) = 0$$

$$\lim_{r \to 0} J_0(a\,r) = 1$$

$$\lim_{\substack{r \to 0 \\ r \to \infty}} r\,J_1(a\,r) = 0$$

we finally obtain

$$H^* \left[\frac{1}{r} \frac{\partial}{\partial r} \left(r \frac{\partial}{\partial r} \bar{s}(r,p) \right) \right] = -a^2\,\bar{\bar{s}}(a,p) - \lim_{r \to 0} r \frac{\partial}{\partial r} \bar{s}(r,p) \tag{A-9}$$

APPENDIX B. INDICIAL NOTATION

In the indicial notation, matrices are represented by subscripted quantities which correspond to the individual terms of the matrix. The number of subscripts indicates the order of the matrix, and the range of each subscript must be specified in each case.

For example, the quantity N_i, where $i = 1, \ldots, I$, represents the first order $(1 \times I)$ matrix

$$(N_1 \quad N_2 \cdot \quad \cdot \quad \cdot \quad \cdot \quad \cdot \quad \cdot \quad N_I)$$

A_{ij} represents the second order $(I \times J)$ matrix

$$\begin{pmatrix} A_{11} & A_{12} & \cdot & \cdot & \cdot & \cdot & \cdot & A_{1J} \\ A_{21} & & & & & & & \cdot \\ \cdot & & & & & & & \cdot \\ \cdot & & & & & & & \cdot \\ \cdot & & & & & & & \cdot \\ A_{I1} & & & & & & & A_{IJ} \end{pmatrix}$$

B_{ijk} represents a third order $(I \times J \times K)$ matrix, and so on.

The advantage of the indicial notation is that it enables one to manipulate matrices in the same manner as regular algebraic quantities. This can be done by observing the following few simple rules.

1. Repeated subscripts indicate summation over those subscripts. For example,

$$N_i M_i \; = \; N_1 M_1 + N_2 M_2 + \ldots + N_I M_I$$

and

$$A_{ij} B_j \; = \; A_{i1} B_1 + A_{i2} B_2 + \ldots + A_{iJ} B_J$$

Thus, $N_i M_i$ is a (1 x 1) matrix, while $A_{ij} B_j$ is a (1 x I) matrix. This rule is known as the "summation convention".

2. No subscript should occur more than twice in any given matrix. Thus, the quantity $A_{ij} B_{jj}$ has no meaning in indicial notation, while the quantity $A_{ij} B_{jk}$ represents the second order (I x K) matrix

$$A_{ij} B_{jk} \; = \; A_{i1} B_{1k} + A_{i2} B_{2k} + \ldots + A_{iJ} B_{Jk}$$

3. Suppose that i and j represent the rows and the columns of a matrix respectively, or vice versa. The transpose of a first order matrix N_i can therefore be written as N_j, and the transpose of a second order matrix A_{ij} can be expressed as A_{ji}. Thus, to multiply the matrix N_i by another matrix M_i, one must first transpose M_i to M_j and then express the product in the form $N_i M_j$. Similarly, to multiply A_{ij} by B_j, the matrix B_j must be transposed to B_k and the product written as $A_{ij} B_k$. (Note that $A_{ij} B_j$ or $A_{ij} B_i$ indicate summation over j and i, respectively, and that they represent a reduction in the order of the matrix instead of the increase required by multiplication.)

4. Matrices can be added to (or subtracted from) other matrices only if they have similar subscripts. For example, the operations $A_i + B_j$ or $A_{ij} + B_{jk}$ have no meaning, while $A_i + B_i$ or $A_{ij} + B_{ij}$ are well defined. Similarly, it is incorrect to write $A_i B_j C_j - K_j$, but the operation $A_i B_j C_j - K_i$ is legitimate.

APPENDIX C

INTEGRAL OF THE FUNCTION $N_n N_m$ OVER THE AREA OF A TRIANGLE

Consider the function

$$N_n(r,z) = \frac{1}{2\Delta}(a_n + b_n r + c_n z)$$

where $n = 1, 2, 3$ corresponds to
the corners of the triangle on
Fig. C-1, a_n, b_n, and c_n are con-
stants depending on the values of r_n
and z_n at the corners of the triangle
as defined in Eq. III-20, and Δ is
the area of the triangle given by
Eq. III-21. Let $N_n(k)$ represent the
values of $N_n(r,z)$ at the k-th corner
where $r = r_k$ and $z = z_k$, such that

$$N_n(k) \equiv \frac{1}{2\Delta}(a_n + b_n r_k + c_n z_k)$$
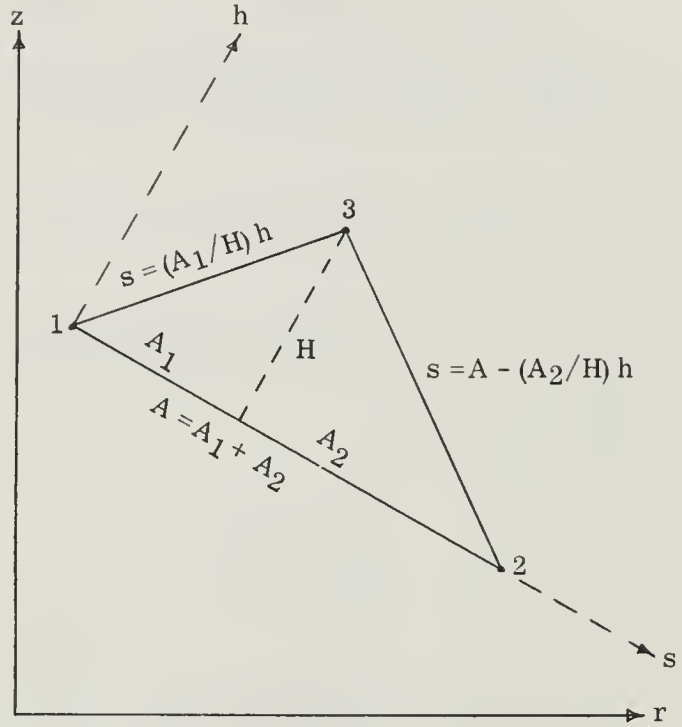
Fig. C-1. Cross section of triangular element.

The value of 2Δ can be
written explicitly, using Eq. III-21,
as

$$2\Delta = r_2 z_3 + r_1 z_2 + z_1 r_3 - r_2 z_1 - r_3 z_2 - z_3 r_1 \qquad (C\text{-}1)$$

Substituting for a_n, b_n, and c_n their actual values from Eq. III-20, we can now
evaluate the functions $N_n(k)$ as follows:

$$N_1(1) \quad = \quad \frac{1}{2\Delta} (a_1 + b_1 r_1 + c_1 z_1)$$

$$= \quad \frac{1}{2\Delta} (r_2 z_3 - r_3 z_2 + z_2 r_1 - z_3 r_1 + r_3 z_1 - r_2 z_1) \quad = \quad 1$$

$$N_1(2) \quad = \quad \frac{1}{2\Delta} (a_1 + b_1 r_2 + c_1 z_2)$$

$$= \quad \frac{1}{2\Delta} (r_2 z_3 - r_3 z_2 + z_2 r_2 - z_3 r_2 + r_3 z_2 - r_2 z_2) \quad = \quad 0$$

$$N_1(3) \quad = \quad \frac{1}{2\Delta} (a_1 + b_1 r_3 + c_1 z_3)$$

$$= \quad \frac{1}{2\Delta} (r_2 z_3 - r_3 z_2 + z_2 r_3 - z_3 r_3 + r_3 z_3 - r_2 z_3) \quad = \quad 0$$

and in general

$$N_n(k) \quad = \quad \begin{cases} 0 & \text{if } n \neq k \\ \\ 1 & \text{if } n = k \end{cases} \qquad\qquad (C\text{-}2)$$

Eq. C-2 indicates that $N_3(1) = N_3(2) = 0$ and $N_3(3) = 1$. Thus, since N_3 is a linear function of the orthogonal coordinates s and h (Fig. C-1), its value is zero everywhere along face 3 (opposite corner 3) of the triangle, and it can be expressed in the form

$$N_3(s,h) \quad = \quad \frac{h}{H}$$

Similarly, since $N_2(1) = N_2(3) = 0$ and $N_2(2) = 1$, the function N_2 is zero on face 2 of the triangle and can therefore be written in terms of s and h as

$$N_2(s,h) \quad = \quad \frac{1}{A} (s - \frac{A_1}{H} h)$$

Using these expressions, the integral of N_2N_3 over the area of the triangle, Δ, can now be easily evaluated. Thus,

$$\int_\Delta N_2 N_3 \, d\Delta = \int_0^H \int_{(A_1/H)h}^{A-(A_2/H)h} \frac{1}{A}\left(s - \frac{A_1}{H}\right) \frac{h}{H} \, ds \, dh$$

$$= \frac{1}{AH} \int_0^H \left[h \frac{A^2}{2} + h^2\left(-\frac{AA_2}{H} - \frac{AA_1}{H}\right) + h^3\left(\frac{1}{2}\frac{A_2^2}{H^2} + \frac{1}{2}\frac{A_1^2}{H^2} + \frac{A_1A_2}{H^2}\right) \right] dh$$

$$= \frac{AH}{24} = \frac{\Delta}{12}$$

The integral of N_3N_3 over the area of the triangle is

$$\int_\Delta N_3 N_3 \, d\Delta = \int_0^H \int_{(A_1/H)h}^{A-(A_2/H)h} \frac{h}{H} \frac{h}{H} \, ds \, dh$$

$$= \frac{1}{H^2} \int_0^H h^2\left(A - \frac{A_2}{H}h - \frac{A_1}{H}h\right) dh$$

$$= \frac{AH}{12} = 2\frac{\Delta}{12}$$

By appropriately changing the positions of the coordinates s and h so that s coincides with different faces of the triangle, it is possible to use the above two integrals to show that, in general,

$$\int_\Delta N_n N_m \, d\Delta = \begin{cases} \dfrac{\Delta}{12} & \text{if } n \neq m \\[2mm] 2\dfrac{\Delta}{12} & \text{if } n = m \end{cases} \tag{C-3}$$

If Δ represents the cross-section of an axisymmetric annular element of volume V, the functions N_n for any given element remain independent of the position of this element and may be expressed in terms of s and h only. The integral of $N_n N_m$ over the volume of the element can therefore be written as

$$\int_V N_n N_m \, dV = \int_0^{2\pi} \left[\int_\Delta N_n N_m \, d\Delta \right] \bar{r} \, d\theta = 2\pi\bar{r} \int_\Delta N_n N_m \, d\Delta$$

where

$$\bar{r} = \frac{r_1 + r_2 + r_3}{3}$$

With the aid of Eq. C-3, this becomes simply

$$\int_V N_n N_m \, dV = \begin{cases} (2\pi\bar{r}) \dfrac{\Delta}{12} & \text{if } n \neq m \\[2em] (2\pi\bar{r}) \, 2\dfrac{\Delta}{12} & \text{if } n = m \end{cases} \tag{C-4}$$

REFERENCES

1. Carslaw, H. S. and J. C. Jaeger, Conduction of Heat in Solids, Oxford University Press, London, 1959.

2. Carslaw, H. S. and J. C. Jaeger, Operational Methods in Applied Mathematics, Dover Publications, New York, 1963.

3. Churchill, R. V., Operational Mathematics, McGraw-Hill, New York, 1958.

4. DeGlee, G. J., Over Grondwaterstromingen by Wateronttrekking by middel van Putten, T. Waltman, Jr., Delft, 1930.

5. DeWiest, R. J. M., "On the theory of leaky aquifers," Jour. Geophys. Res., v. 66, p. 4257, 1961.

6. DeWiest, R. J. M., "Flow to an eccentric well in a leaky circular aquifer with varied lateral replenishment," Geofis. Pura Appl., v. 54, p. 87, 1963.

7. DeWiest, R. J. M., Geohydrology, John Wiley and Sons, New York, 1965.

8. Ferris, J. G., D. B. Knowles, R. H. Brown and R. W. Stallman, Theory of Aquifer Tests: A Summary of Lectures, U. S. Geol. Surv. Water-Supply Paper 1536-E, 1962.

9. Gelfand, I. M. and S. V. Fomin, Calculus of Variations, Prentice Hall, Englewood Cliffs, New Jersey, 1963.

10. Girinsky, N. K., "Nekotorye voprosy dinamiki podzemnykh vod," Gidrogeologiya i Inzhenernaya Geologiya, Sbornik Statei, n. 9, Moscow, 1947.

11. Gradshtein, I. S. and I. M. Ryzhik, Tablitsy Integralov, Summ, Ryadov i Proizvedenii, Gosudarstvennoe Izdatelstvo Fiziko-Matematicheskoi Literatury, Moscow, 1963.

12. Gurtin, M. E., "Variational principles for linear initial-value problems," Qtly. Appl. Math., v. 22, p. 252, 1964.

13. Hantush, M. S., Plain Potential Flow of Groundwater with Linear Leakage, Ph.D. Dissertation, University of Utah, 1949.

14. Hantush, M. S. and C. E. Jacob, "Plane potential flow of ground water with linear leakage," Trans. Am Geophys. Union, v. 35, p. 917, 1954.

15. Hantush, M. S. and C. E. Jacob, "Nonsteady Green's functions for an infinite strip of leaky aquifers," Trans. Am. Geophys. Union, v. 36, p. 101, 1955.

16. Hantush, M. S. and C. E. Jacob, "Nonsteady radial flow in an infinite leaky aquifer," Trans. Am. Geophys. Union, v. 36, p. 95, 1955.

17. Hantush, M. S., "Analysis of data from pumping tests in leaky aquifers," Trans. Am. Geophys. Union, v. 37, p. 702, 1956.

18. Hantush, M. S., "Nonsteady flow to a well partially penetrating an infinite leaky aquifer," Proc. Iraqui Sci. Soc., v. 1, p. 10, 1957.

19. Hantush, M. S., "Nonsteady flow to flowing wells in leaky aquifers," Jour. Geophys. Res., v. 64, p. 1043, 1959.

20. Hantush, M. S. and C. E. Jacob, "Flow to an eccentric well in a leaky circular aquifer," Jour. Geophys. Res., v. 65, p. 3425, 1960.

21. Hantush, M. S., "Modification of the theory of leaky aquifers," Jour. Geophys. Res., v. 65, p. 3713, 1960.

22. Hantush, M. S., Tables of the Function $H(u, \beta)$, Document 6427, U. S. Library of Congress, Washington, D. C., 1960.

23. Hantush, M. S., "Drainage wells in leaky water-table aquifers," Proc. Am. Soc. Civil Engrs., v. 88, HY2, p. 123, 1962.

24. Hantush, M. S., "Depletion of storage, leakage, and river flow by gravity wells in sloping sands," Jour. Geophys. Res., v. 69, p. 2551, 1964.

25. Hantush, M. S., "Hydraulics of wells," in Advances in Hydroscience, v. 1, V. T. Chow, editor, Academic Press, New York, 1964.

26. Hantush, M. S., "Flow of groundwater in relatively thick leaky aquifers," Water Resour. Res., v. 3, n. 2, p. 583, 1967.

27. Hantush, M. S., "Flow to wells in aquifers separated by a semipervious layer," Jour. Geophys. Res., v. 72, n. 6, p. 1709, 1967.

28. Jacob, C. E., "Radial flow in a leaky artesian aquifer," Trans. Am. Geophys. Union, v. 27, p. 198, 1946.

29. Javandel, I. and P. A. Witherspoon, Analysis of Transient Fluid Flow in Multi-Layered Systems, Water Resources Center Contribution No. 124, University of California, Berkeley, 1968.

30. McCracken, D. D. and W. S. Dorn, Numerical Methods and Fortran Programming, John Wiley and Sons, New York, 1964.

31. McLachlan, N. W., Bessel Functions for Engineers, Oxford University Press, London, 1961.

32. Myatiev, A. N., "Deistvie kolodtsa v napornom basseine podzemnykh vod," Izv. Turkmenskogo Filiala Am SSSR, No. 3-4, 1946.

33. Myatiev, A. N., "Napornyi kompleks podzemnykh vod i kolodtsy," Izv. An SSSR, Otd. Tekhn. Nauk, n. 9, 1947.

34. Neuman, S. P., Transient Behavior of an Aquifer with a Slightly Leaky Caprock, M. S. Thesis, University of California, Berkeley, 1966.

35. Neuman, S. P. and P. A. Witherspoon, "Theory of flow in aquicludes adjacent to slightly leaky aquifers," Water Resour. Res., v. 4, n. 1, p. 103, 1968.

36. Poland, J. F. and G. H. Davis, "Land subsidence due to withdrawal of fluids," in Rev. Eng. Geol., Geol. Soc. Am., v. 2, 1967.

37. Poland, J. F. and G. H. Green, Subsidence in the Santa Clara Valley, California - A Progress Report, U. S. Geol. Surv. Water-Supply Paper 1619-C, 1962.

38. Polubarinova-Kochina, P. Y. A., <u>The Theory of Ground Water Movement</u>, Princeton University Press, New Jersey, 1962.

39. Slater, R. J., "Application and limitations of pumping tests," <u>Instn. Water Engnrs. Jour.</u>, v. 17, n. 3, p. 189, 1963.

40. Steggeventz, J. H. and B. A. Van Nes, "Calculating the yield of a well taking account of replenishment of the groundwater from above," <u>Water and Water Engineering</u>, v. 41, p. 561, 1939.

41. Taylor, R. L. and C. B. Brown, "Darcy flow solutions with a free surface," <u>Jour. Hyd. Div. ASCE</u>, v. 93, HY2, p. 25, 1967.

42. Theis, C. V., "The relationship between the lowering of the piezometric surface and the rate and duration of discharge of a well using ground water storage," <u>Trans. Am. Geophys. Union</u>, v. 16, p. 519, 1935.

43. Walton, W. C., <u>Leaky Artesian Aquifer Conditions in Illinois</u>, Ill. State Water Surv. Rept. Invest. 39, Urbana, Illinois, 1962.

44. Walton, W. C., <u>Selected Analytical Methods for Well and Aquifer Evaluation</u>, Ill. State Water Surv. Bull. 49, Urbana, Illinois, 1962.

45. Watson, G. N., <u>Theory of Bessel Functions</u>, Macmillan, New York, 1944.

46. Wilson, E. L. and R. E. Nickell, "Application of finite element method to heat conduction analysis," <u>Nuclear Engineering and Design</u>, North Holland Publishing Co., Amsterdam, p. 276, 1966.

47. Witherspoon, P. A., I. Javandel, S. P. Neuman and R. A. Freeze, <u>Interpretation of Aquifer Gas Storage Conditions from Water Pumping Tests</u>, American Gas Association, New York, 1967.

48. Witherspoon, P. A., T. D. Mueller and R. W. Donovan, "Evaluation of underground gas-storage conditions in aquifers through investigations of ground water hydrology," <u>Trans. AIME</u>, v. 225, p. 555, 1962.

49. Witherspoon, P. A. and S. P. Neuman, "Evaluating a slightly permeable caprock in aquifer gas storage, I. Caprock of infinite thickness," <u>Trans. AIME</u>, v. 240, p. 949, 1967.

50. Zienkiewicz, O. C. and Y. K. Cheung, "Finite elements in the solution of field problems," The Engineer, p. 220, 1965.

51. Zienkiewicz, O. C., P. Mayer and Y. K. Cheung, "Solution of anisotropic seepage by finite elements," Jour. Engr. Mech. Div. ASCE, v. 92, EM2, p. 111, 1966.

52. Zienkiewicz, O. C. and Y. K. Cheung, The Finite Element Method in Structural and Continuum Mechanics, McGraw-Hill, London, 1967.

APPENDIX B

TABLE OF DRAWDOWN DATA

FROM PUMPING TESTS

Drawdown Data - First Pumping Test

Time Since Pumping Started minutes	Drawdown (in feet)									
	Mugu Aquifer	Lower Aquitard	Oxnard Aquifer					Upper Aquitard		Semiperched Aquifer
	Well No. 1A	Well No. 3	Well No. 1	Well No. 22H2	Well No. 22H5	Well No. 22K2	Well No. 23E2	Well No. 4	Well No. 5	Well No. 4A
A	B	C	D	E	F	G	H	I	J	K
0.5			1.08							
1			2.12	0.11						
2				0.40	0.06					
3			6.61	0.41						
4			6.96	0.53						
5				0.65			0.07			
6			5.50	0.76						
7			4.53	0.84						
8			4.63							
9				1.02		0.70				
10			4.82	1.08						
11				1.14						
12			4.98	1.21	0.81					
13				1.27						
14			5.14	1.33						
15				1.38			0.27			
16			5.23	1.44						
17				1.48						
18			5.33	1.53						
19				1.57						
20			5.44	1.61		1.24				
22				1.69						
22.5					1.16					
24				1.75						

Drawdown Data - First Pumping Test

A	B	C	D	E	F	G	H	I	J	K
25			5.62							
25.5							0.72			
26				1.81						
28				1.86						
30			5.81	1.92						
30.5						1.59				
33					1.44					
34		0.00								
35				1.95			0.97			
39.25						1.81				
40			6.05	2.18						
41		0.02								
42					1.64					
45				2.28						
46							1.11			
50			6.25	2.35						
50.5						2.00				
51		0.03								
53					1.83					
57							1.25			
60			6.37	2.51		2.15				
61		0.03								
62					1.92					
70				2.63			1.41			
75			6.55			2.31				
76		0.07								
80				2.74	2.12					
88							1.57			
90			6.67							
90.5						2.45				
91		0.10								
94					2.24					
95.5										
99						2.52	1.62			

-364-

Drawdown Data - First Pumping Test

A	B	C	D	E	F	G	H	I	J	K
105			6.78	2.90						
107		0.14			2.34					
111							1.70			
114.5						2.62				
116					2.37					
119							1.79			
121			6.88							
122		0.21				2.66				
124					2.41					
127							1.81			
130				3.04						
131						2.70				
150			7.00							
151		0.32								
152					2.52					
156							1.94			
159						2.83				
160				3.17						
180			7.14		2.62					
182		0.41					2.04			
185						2.93				
220				3.38						
240			7.29		2.80					
242							2.20			
244		0.82								
246						3.13				
300			7.44					0.0		
302		0.97								
308					2.96		2.38			
310						3.31				
317								0.03		
320				3.49						
360			7.59	3.74				0.06		
361	0.0									

Drawdown Data - First Pumping Test

A	B	C	D	E	F	G	H	I	J	K
363		1.22			3.11					
365							2.50			
369						3.43				
375								0.07		
390								0.09		
397		1.38	7.67					0.10		
405			7.70							
421	0.05	1.52	7.72					0.12		
426					3.23					
428							2.62			
430				3.86						
432						3.59				
451								0.14		
480	0.04	1.72	7.86					0.18		
486					3.34					
488							2.72			
490				3.98						
493						3.69				
544		1.97								
549			7.92							
550	0.08									
553	0.06									
555								0.27		
575				4.11						
608		2.24								
610			8.03							
619						3.93				
620								0.37		
730	0.13	2.58	8.17					0.58		
740				4.32			3.01			
850		2.92			3.65	4.01				
860	0.21		8.25	4.36				0.83		
865							3.10			
970		3.21			3.76	4.05				

Drawdown Data - First Pumping Test

A	B	C	D	E	F	G	H	I	J	K
980	0.28		8.30	4.42				1.11		
990							3.13			
1,110	0.37	3.44	8.36	4.47						
1,120								1.39		
1,130					3.81					
1,150						4.14	3.21			
1,180		3.64								
1,210	0.41			4.51						
1,220			8.41		3.86			1.63		
1,230							3.25			
1,240						4.17				
1,300		3.79								
1,340	0.50		8.44	4.54				1.94		
1,350					3.88					
1,370						4.19	3.30			
1,460			8.37							
1,520								2.37		
1,530		3.98								
1,570				4.55	3.92			2.51		
1,580	0.63		8.34							
1,590						4.18	3.32			
1,690								3.06		
1,700			8.42							
1,770		4.16								
1,810	0.75			4.59	3.94					
1,820			8.49				3.33	3.07		
1,940			8.56					3.35		
2,020		4.27								
2,050						4.42				
2,060	0.88		8.61		4.12					
2,070							3.52	3.60		
2,170								3.80		
2,180			8.57							
2,260		4.37								

Drawdown Data - First Pumping Test

A	B	C	D	E	F	G	H	I	J	K
2,290								4.06		
2,300	0.91		8.58		4.07	4.37			0.0	
2,310				4.73						
2,320							3.45			
2,410								4.30		
2,420			8.57						0.01	
2,500		4.42								
2,530						4.34		4.53		
2,540	1.07		8.59	4.62	4.06				0.02	
2,550							3.42			
2,650								4.71		
2,660									0.03	
2,690			8.60							
2,760		4.48								
2,780			8.57							
2,800	1.14				4.07					
2,810				4.71				4.97	0.03	
2,820						4.37	3.46			
2,890								5.11		
2,900			8.48						0.03	
2,970		4.50								
3,010	1.19			4.65	4.00	4.30				
3,020			8.41				3.42	5.30	0.04	
3,130								5.47		
3,140			8.51						0.05	
3,220		4.52								
3,250					4.02	4.31				
3,260	1.25		8.56	4.66				5.72	0.06	
3,270							3.41			
3,380			8.62	4.72				5.83	0.07	
3,450		4.52								
3,490	1.28									
3,500								5.99	0.07	
3,510							3.45			

Drawdown Data - First Pumping Test

A	B	C	D	E	F	G	H	I	J	K
3,520						4.38				
3,620			8.61							
3,630									0.08	
3,690		4.54								
3,740								6.01	0.10	
3,860			8.56							
3,930		4.57								
3,970	1.34				4.04	4.33				
3,980				4.69				6.37	0.13	
3,990							3.42			
4,100			8.63							
4,170		4.60								
4,220								6.80	0.14	
4,340			8.64							
4,420		4.60								
4,450	1.38				4.15	4.42				
4,460				4.77				7.03	0.16	
4,470							3.54			
4,690	1.42									
4,700								7.28	0.22	
4,820			8.67							
4,930	1.44				4.12	4.42				
4,940				4.76				7.49	0.24	
4,950							3.46			
5,060			8.69							
5,130		4.65								
5,170	1.46							7.76		
5,180									0.26	
5,410					4.06	4.35				
5,420	1.47			4.68				7.84	0.29	
5,430							3.43			
5,540			8.69							
5,610		4.65								
5,660	1.48							8.01	0.34	

Drawdown Data - First Pumping Test

A	B	C	D	E	F	G	H	I	J	K
6,090		4.64								
6,130	1.50				4.14					
6,140				4.77				8.35	0.42	
6,150						4.43	3.52			
6,570		4.59								
6,610	1.52				4.12					
6,620				4.81			3.50	8.63	0.50	
6,640						4.46				
6,980			8.71							
7,050		4.68								
7,090					4.19					
7,100	1.54			4.84				8.94	0.58	
7,120							3.61			
7,130						4.49				
7,460			8.78							
7,530		4.75								
7,570	1.55				4.27					
7,580				4.88			3.68	9.11	0.68	
7,590						4.53				
7,940			8.82							
8,010		4.90								
8,050	1.58				4.23					
8,060				4.90		4.56		9.47	0.81	
8,070							3.66			
8,410			8.87							
8,490		4.94								
8,530	1.61				4.28					
8,540				4.94			3.68	9.72	0.87	
8,570						4.58				
8,900			9.14							
8,970		4.98								
9,010	1.64				4.68					
9,020				5.28				9.72	1.09	
9,030							4.09			

Drawdown Data - First Pumping Test

A	B	C	D	E	F	G	H	I	J	K
9,050						4.69				
9,380			9.08							
9,450		5.08								
9,490	1.71				4.54					
9,500				5.17			3.96	9.96	1.09	
9,520						4.70				
9,870			8.98							
9,930		4.22								
9,970					4.49					
9,980				5.10						
9,990	1.76							10.17		
10,000						4.71	3.90		1.20	
10,380			9.32							
10,410		4.19								
10,450				5.50	4.90					
10,500	1.79					5.10	4.32	10.37	1.30	
10,820			9.24							
10,890		5.38								
10,940	1.87			5.38	4.77	5.01	4.18	10.60	1.43	
11,300			9.19							
11,370		5.64								
11,420	1.92			5.39	4.80	4.93	4.24	10.68	1.49	
11,760			9.92							
11,850		5.62								
11,900	1.96			6.21		5.65	5.21	10.81	1.64	
12,330		5.55	9.59							
12,380	2.04			5.78	5.18	5.35	4.60	10.94	1.77	
12,560										
12,770			9.42							
12,810		5.66								
12,870				5.90		5.44				
12,890	2.09						4.74	10.98	1.86	
13,230			9.87							
13,290		5.83								

Drawdown Data - First Pumping Test

A	B	C	D	E	F	G	H	I	J	K
13,350	2.15			6.15	5.63	5.62	5.15	11.20	1.99	
13,700			10.01							
13,770		5.92								
13,820	2.22			5.92			5.01	11.30	2.11	
13,870						5.58				
14,180			9.66							
14,250		5.98								
14,300	2.31			5.85	5.29		4.75	11.40	2.23	0.01
14,380						5.42				
14,660			10.25							
14,730		6.20								
14,780	2.37						5.67	11.49	2.35	0.04
14,830						6.01				
15,140			10.13							
15,210		6.36								
15,260	2.48			6.49	5.92		5.49	11.58	2.46	0.04
15,300						5.97				
15,620			10.07							
15,700		6.75								
15,740	2.61						5.33	11.65	2.58	0.04
15,790						5.84				
16,100			10.88							
16,220	2.68			7.23	6.70		6.23	11.72	2.68	0.03
16,580			10.79							
16,650		7.19								
16,700	3.01						6.14	11.80	2.83	0.04
16,750						6.61				
17,050			10.69							
17,130		7.62								
17,180	3.03			7.11	6.58		6.13	11.85	2.94	0.04
17,230						6.49				
17,540			11.96							
17,610		7.59								

Drawdown Data - First Pumping Test

A	B	C	D	E	F	G	H	I	J	K
17,660	3.22						7.64	11.94	3.04	0.07
17,710						7.83				
18,010			11.75							
18,140	3.48	7.68		7.89	7.64		7.13	12.03	3.15	0.08
18,190						7.53				
18,500		7.71	11.46							
18,620	3.75						6.82	12.11	3.29	0.08
18,670						7.20				
18,970			11.79							
19,050		7.73								
19,100	3.89			8.21	7.74		7.27	12.32	3.41	0.10
19,170						7.63				
19,450			11.72							
19,580	4.04						7.15	12.25	3.49	0.11
19,630						7.57				
19,940			11.66							
20,010		8.15								
20,060	4.12			8.05	7.56		7.07	12.34	3.62	0.10
20,110						7.51				
20,410			12.46							
20,490		8.44								
20,540	4.24						8.13	12.40	3.73	0.13
20,590						8.35				
20,890			12.44							
20,970		8.92								
21,020	4.50			8.99	8.62		8.21	12.38	3.82	0.13
21,070						8.38				
21,380			12.44							
21,500	4.57						8.27	12.35	3.96	0.12
21,550						8.27				
21,860			13,90							
21,930		9.42								
21,980	4.78			10.58	10.38		10.05	12.62	4.05	0.15

Drawdown Data - First Pumping Test

A	B	C	D	E	F	G	H	I	J	K
22,030						9.78				
22,320			14.30							
22,410		9.82								
22,440	4.91									0.12
22,460							9.80	12.69	4.13	
22,530						9.94				
22,820			14.09							
22,890		9.32								
22,940	4.96			10.09	9.74		9.51	12.76	4.19	0.08
23,020						9.26				
23,290			13.94							
23,370		9.05								
23,420	5.00						8.93	12.84	4.26	0.16
23,500						9.01				
23,770			13.42							
23,850		8.73								
23,900	5.15			9.63	9.45		8.76	12.92	4.38	0.21
23,980						8.93				
24,250			13.10							
24,330		8.78								
24,380	5.34						8.65	13.05	4.52	0.18
24,460						8.82				
24,730			12.78							
24,810		9.10								
24,860	5.48			9.39	8.96		8.53	13.15	4.66	0.19
24,940						8.72				
25,220			12.81							
25,290		9.30								
25,340	5.47						8.58	13.20	4.73	0.20
25,430						8.83				
25,720			13.02							
25,770		9.43								
25,820				9.54	9.12			13.26	4.86	
25,850	5.47						8.63			0.20

Drawdown Data - First Pumping Test

A	B	C	D	E	F	G	H	I	J	K
25,930						8.96				
26,180			13.55							
26,250		9.62								
26,300	5.53						9.43	13.35	4.96	0.21
26,390						8.52				
26,650			13.43							
26,730		9.65								
26,780	5.65			10.02	9.67		9.18	13.42	5.06	0.21
26,860						8.94				
27,140			13.38							
27,210		9.74								
27,260	5.82						8.97	13.48	5.16	0.22
27,340						9.34				
27,610			13.52							
27,690		9.83								
27,740	5.89			10.14	9.78		9.34	13.53	5.24	0.24
27,820						9.54				
28,100			13.57							
28,170		9.94								
28,220	6.12						9.41	13.60	5.33	0.25
28,310						9.57				
28,590			13.66							
28,650		10.21								
28,710	6.17			10.27	9.90		9.48	13.69	5.46	0.26
28,800						9.61				
29,060			14.19							
29,130		10.34								
29,190	6.26						10.12	13.70	5.52	0.26
29,270						10.12				
29,530			14.53							
29,660	6.37			10.73	10.27		9.86	13.76	5.58	0.25
29,740						9.96				
30,020			13.98		10.19					
30,140	6.45			10.70			9.73	13.83	5.72	0.29

Drawdown Data - First Pumping Test

A	B	C	D	E	F	G	H	I	J	K
30,220						9.99				
32,300	6.57	10.43	14.10	10.90	10.02	10.09	9.75	13.49	5.95	0.29
33,020	6.68	10.60	14.30	11.54	10.04	10.65	9.74	13.02	6.00	0.14
33,745	6.83	10.80	14.85	11.43	11.18	10.84	10.80	13.14	6.11	0.26
34,465	6.41	10.51	14.70	11.60	10.91	10.91	10.46	13.29	5.93	0.23
35,185	6.28	10.36	14.43	11.34	10.73	10.80	10.53	13.66	6.05	0.35
35,905	6.00	10.21	14.79	11.14	10.77	10.62	10.69	13.44	6.32	0.38
36,625	6.11	9.79	14.64	11.28	11.12	10.54	10.79	13.35	6.58	0.40
37,345	6.36	10.57	14.67	11.41	11.17	10.57	10.87	13.40	6.72	0.29
38,065	6.62	11.10	15.59	12.35	12.16	12.52	10.83	13.49	6.81	0.44
38,785	6.81	11.16	15.08	12.15	11.52	12.04	11.31	13.41	6.88	0.47
39,505	7.23	11.34	15.03	11.64	11.33	10.59	10.89	13.66	7.05	
40,225	7.30	11.06	14.47	11.17	10.84	11.46	10.44	13.70	7.15	

Drawdown Data - Second Pumping Test

Time Since Pumping Started minutes	Drawdown (in feet)								
	Mugu Aquifer	Lower Aquitard	Oxnard Aquifer				Upper Aquitard		Semiperched Aquifer
	Well No. 1A	Well No. 3	Well No. 1	Well No. 22H2	Well No. 22H5	Well No. 22K2	Well No. 4	Well No. 5	Well No. 4A
A	B	C	D	E	F	G	I	J	K
0.25			0.27						
0.5			0.81	0.06	0.08				
0.75			1.33	0.09	0.12				
1.0			1.74	0.13	0.14	0.14			
1.5			2.28						
1.75				0.24					
2			2.60	0.28	0.22	0.19			
2.5				0.36					
3			3.05	0.40	0.28	0.25			
4			3.33	0.51	0.36	0.33			
5			3.53	0.61	0.43	0.42			
6			3.69	0.71	0.50	0.49			
7			3.80	0.79	0.55	0.57			
8			3.92	0.87	0.59	0.64			
9			4.00	0.93	0.64	0.71			
10			4.09	0.99	0.70	0.75			
11			4.16	1.06	0.74	0.81			
12			4.21	1.12	0.80	0.86			
13			4.29	1.17	0.84	0.91			
14			4.34	1.23	0.88	0.97			
15			4.39	1.29	0.92	1.01			
16			4.45	1.32	0.92	1.05			
17						1.09			

Drawdown Data - Second Pumping Test

A	B	C	D	E	F	G	I	J	K
18			4.53	1.41	1.02	1.14			
20			4.61	1.47	1.10	1.21			
22			4.69	1.54	1.15	1.25			
24			4.77	1.61	1.22	1.32			
26			4.82	1.69	1.27	1.39			
28			4.87	1.73	1.31	1.44			
30			4.93	1.78	1.36	1.49			
35			5.07	1.90	1.46	1.61			
40			5.18	1.99	1.56	1.72			
45			5.27	2.09	1.66	1.81			
50			5.34	2.19	1.73	1.90			
55			5.42	2.27	1.82	1.97			
60			5.51	2.32	1.88	2.03			
70			5.66	2.48	2.03	2.17			
80		0.01	5.73	2.57	2.13	2.26			
90		0.03	5.83	2.68	2.24	2.36			
100		0.06	5.94	2.78	2.35	2.46			
110		0.07	6.02	2.87	2.44	2.54			
120		0.09	6.08	2.94	2.51	2.61			
130		0.12							
140		0.14	6.21	3.09	2.66	2.74			
150		0.17							
160		0.20	6.33	3.23	2.79	2.87			
170		0.23							
180		0.25	6.46			2.98			
190		0.29							
200		0.31	6.57			3.09			
210		0.36			3.09				
215				3.55					
220		0.40	6.65						
230						3.22			
235		0.46							
250		0.51	6.82						
265		0.57							

Drawdown Data - Second Pumping Test

A	B	C	D	E	F	G	I	J	K
280		0.63	6.92						
285				3.86	3.53	3.45			
295		0.70					0.01		
310		0.74	7.00				0.02		
325		0.81					0.03		
340		0.89	7.11				0.04		
350				4.09	3.69	3.68			
355		0.93					0.06		
370	0.01	0.99	7.23				0.07		
385		1.07					0.09		
400	0.01	1.11	7.33				0.10		
405				4.39	3.98	3.91			
415		1.18					0.13		
430	0.04	1.28	7.44				0.15		
445		1.32					0.16		
460	0.03	1.37	7.55				0.18		
465				4.57	4.20				
470						4.11			
475		1.44					0.22		
490	0.05	1.48	7.66				0.24		
505		1.56					0.25		
520	0.01	1.63	7.77				0.28		
525				4.80	4.45				
530						4.33			
550		1.75					0.31		
580	0.07	1.87	7.93	4.96			0.37		
600				4.99					
610		1.99				4.52	0.40		
640	0.09	2.10	7.97				0.48		
670		2.20			4.61		0.52		
700	0.13	2.30	7.96		4.54		0.58		
730		2.42		4.94		4.50	0.63		
760	0.16	2.66	7.87				0.69		
820		2.70	7.77	4.74			0.81		

Drawdown Data - Second Pumping Test

A	B	C	D	E	F	G	I	J	K
840					5.27	4.33			
880	0.23	2.86	7.67				0.93		
1,000	0.32	3.15	7.45	4.34			1.18		
1,020					4.85	4.03			
1,120	0.40	3.33	7.19				1.46	0.01	
1,140				4.08	3.53	3.80			
1,240	0.47	3.50	7.05	3.93	3.38	3.71	1.74	0.02	
1,390	0.54	3.50	7.24	4.15	3.70	3.93	2.02	0.03	
1,540	0.65	3.58	7.87	4.86	4.40	4.54	2.30	0.07	
1,720	0.73	3.76	8.39	5.53	4.97	5.04	2.63	0.04	
1,960	0.90	4.12	8.69	5.71	5.30	5.28	3.04	0.08	
2,260	1.09	4.51	8.32	5.29	4.95	5.00	3.65	0.12	
2,560	1.24	4.61	8.00	4.92	4.47	4.68	3.96	0.15	
2,800	1.48	4.63	7.79	4.67	4.17	4.42	4.38	0.19	
3,040	1.55	4.53	7.71	4.54	4.02	4.30	4.66	0.21	
3,280	1.61	4.41	7.52	4.37	3.83	4.11	4.94	0.25	0.02
3,520	1.64	4.30	7.44	4.29	3.76	4.02	5.21	0.29	0.02
3,760	1.67	4.18	7.36	4.21	3.69	3.93	5.48	0.32	0.02
4,000	1.74	4.06	7.34	4.05	3.61	3.86	5.74	0.36	0.03
4,240	1.63	3.90	7.64	4.29	3.71	4.05	5.99	0.42	0.05
4,600	1.59	3.92	7.93	4.94	4.44	4.60	6.18	0.49	0.06
4,960	1.61	4.22	8.06	5.02	4.53	4.67	6.45	0.55	0.06
5,320	1.64	4.33	7.65	4.54	4.07	4.24	6.54	0.60	0.06
5,680	1.69	4.09	6.95	3.73	3.25	3.59	6.92	0.70	0.06
6,040	1.60	3.87	7.39	4.32	3.85	3.98	7.12	0.77	0.07
6,400	1.54	3.90	7.73	4.66	4.22	4.27	7.29	0.84	0.07
7,120	1.50	3.91	7.05	3.91	3.40	3.62	7.72	1.02	0.10
7,600	1.42	3.83	7.42	4.33	3.83	4.02	7.83	1.13	0.11
8,080	1.40	3.76	6.99	3.82	3.25	3.58	8.04	1.25	0.09
8,560	1.30	3.45	6.62	3.53	3.06	3.15	8.68	1.38	0.11
9,040	1.22	3.70	8.58	5.65	5.28	5.12	8.33	1.50	0.13
9,520	1.35	4.44	8.30	5.29	4.81	4.95	8.48	1.61	0.13
10,000	1.51	4.42	7.43	4.39	3.85	4.12	8.57	1.73	0.14
10,480	1.59	4.32	7.97	4.95	4.48	4.58	8.82	1.87	0.16

Drawdown Data - Second Pumping Test

A	B	C	D	E	F	G	I	J	K
10,960	1.50	4.05	7.26	4.26	3.72	3.87	8.84	1.98	0.16
11,440	1.62	3.85	6.63	4.47	2.90	3.25	8.96	2.12	0.165
11,920	1.47	3.56	7.01	3.91	3.41	3.60	9.10	2.24	0.18
12,400	1.42	3.48	6.56	3.40	2.83	3.19	9.20	2.36	0.17
12,880	1.12	3.04	6.78	2.53	1.87	2.42	9.28	2.50	0.18
13,383	0.85	2.54	5.40	2.13	2.47	2.01	9.34	2.61	0.20

APPENDIX C

GRAIN SIZE DISTRIBUTION CURVES

All Samples from Observation Hole 2
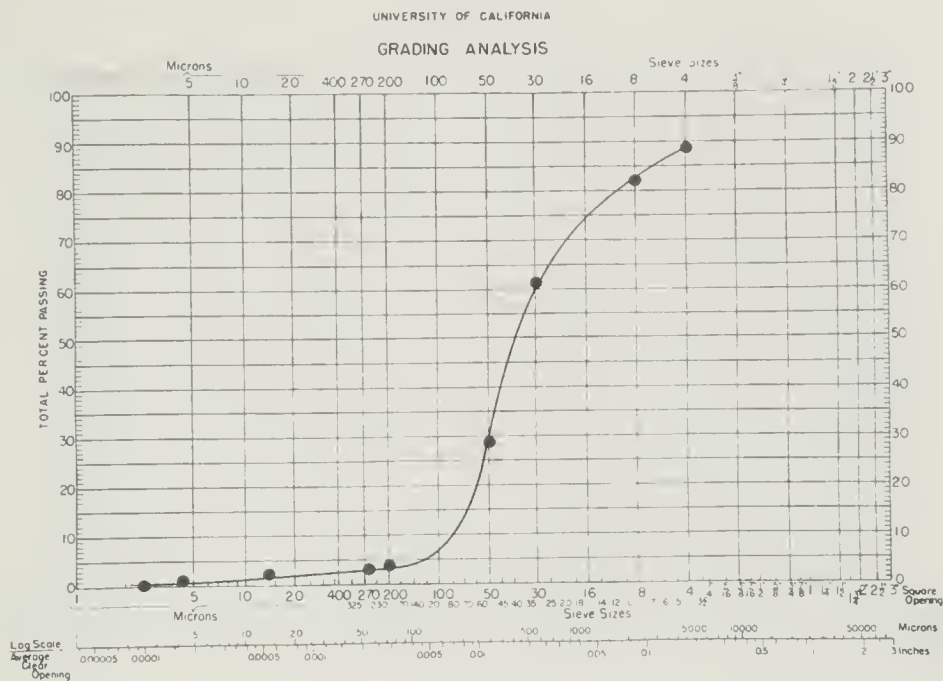
Fig. C-1.   Grain Size Distribution for Sample from 62.0 to 62.5 ft Depth
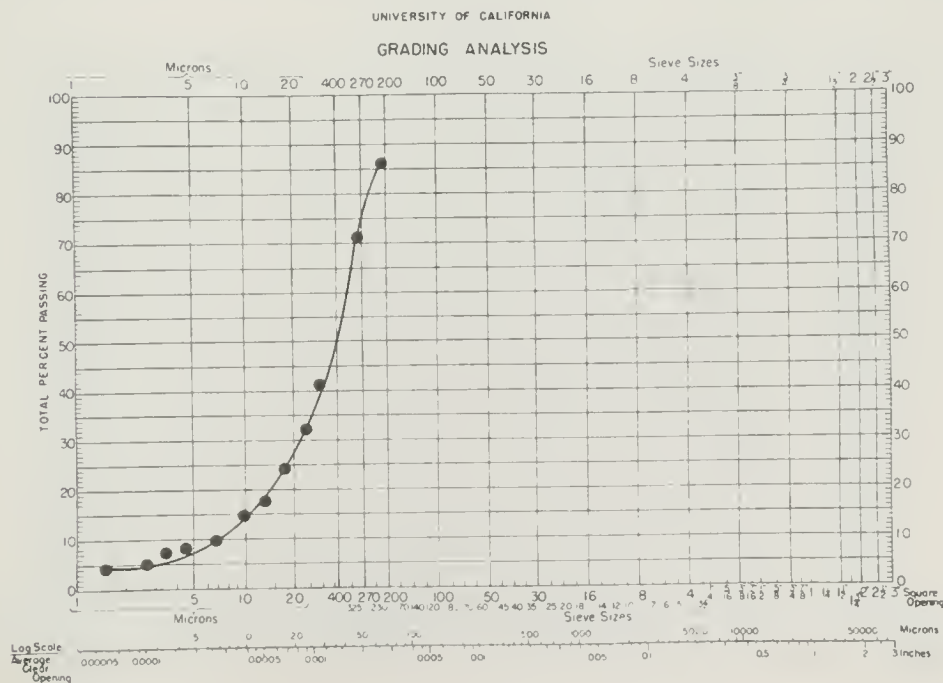
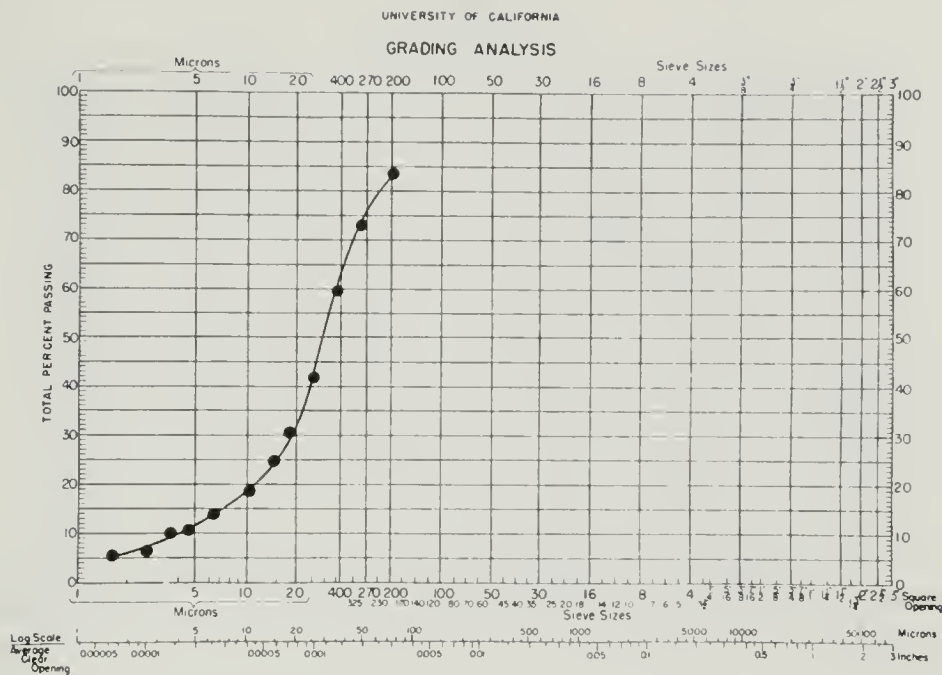Fig. C-2.   Grain Size Distribution for Sample from 69.8 to 70.3 ft Depth
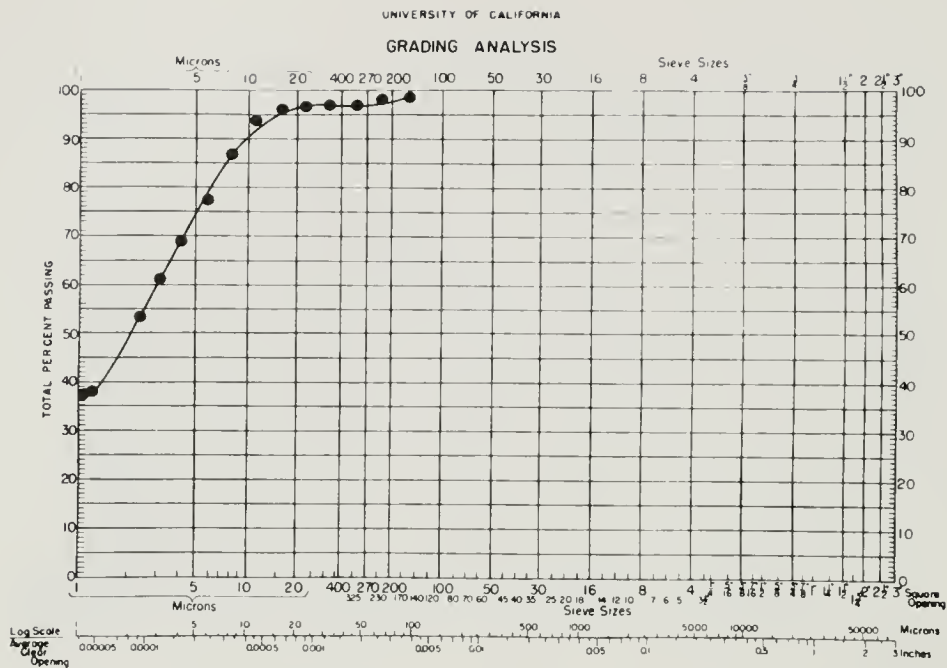
Fig. C-3. Grain Size Distribution for Sample from 70.3 to 73.1 ft Depth
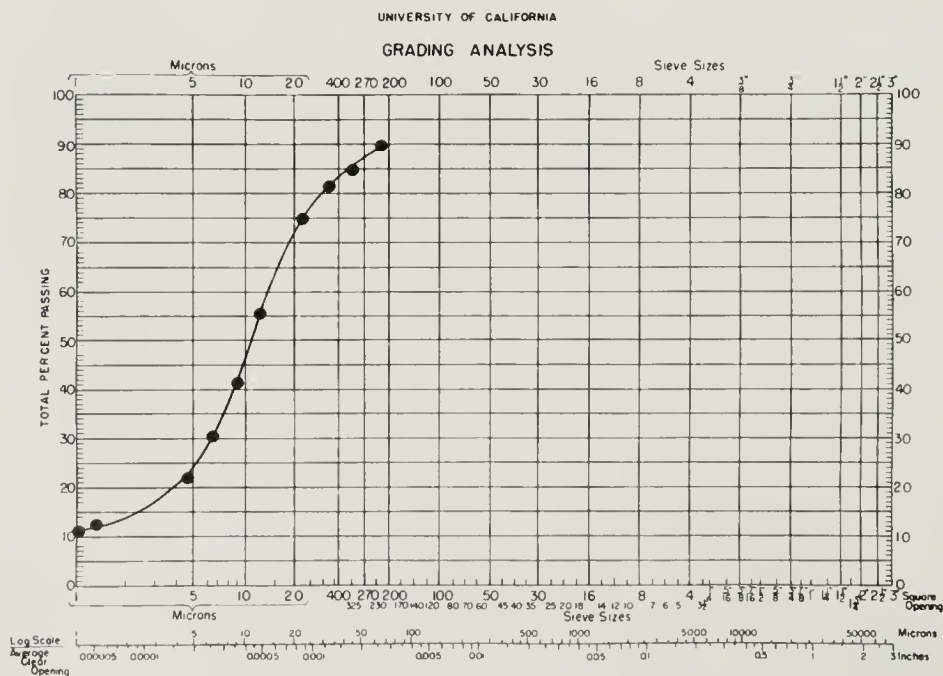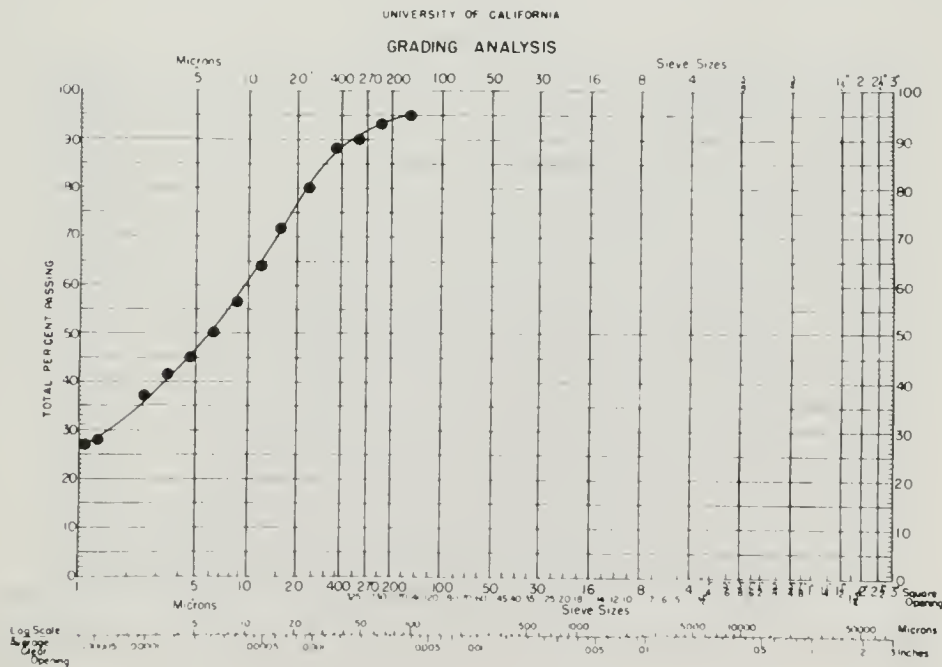

Fig. C-4. Grain Size Distribution for Sample from 72.5 to 73.1 ft Depth
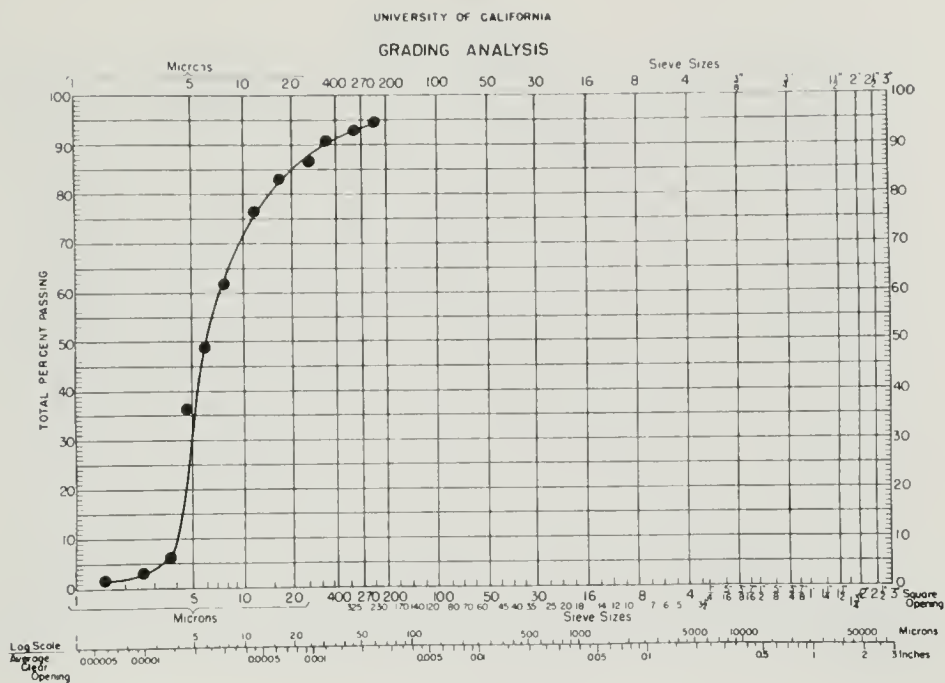
Fig. C-5. Grain Size Distribution for Sample from 78.0 to 78.8 ft Depth
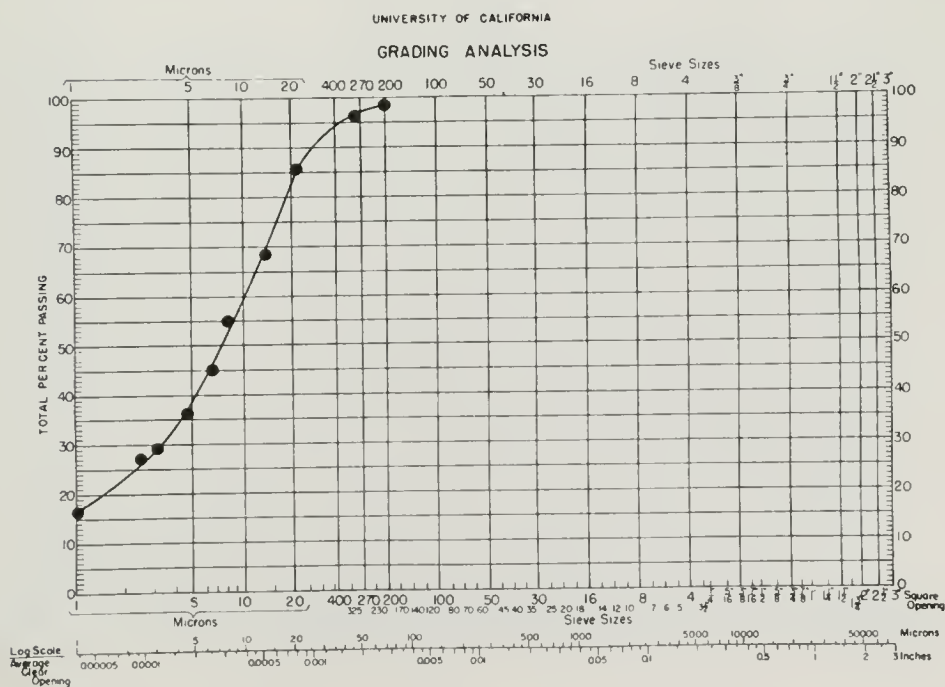
Fig. C-6. Grain Size Distribution for Sample from 78.0 to 78.8 ft Depth
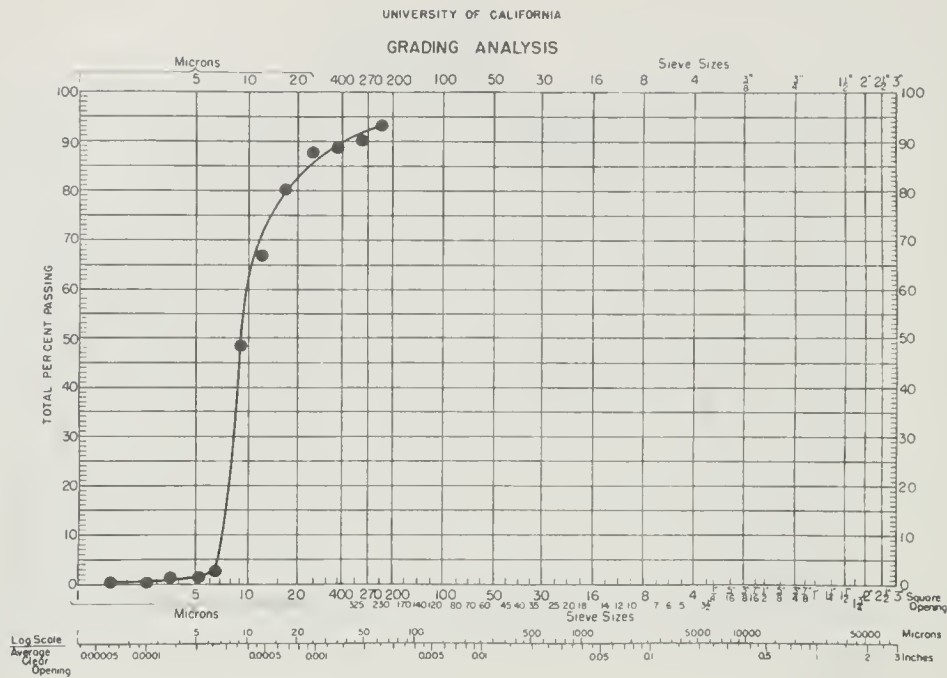
Fig. C-7. Grain Size Distribution for Sample from 83.6 to 84.4 ft Depth
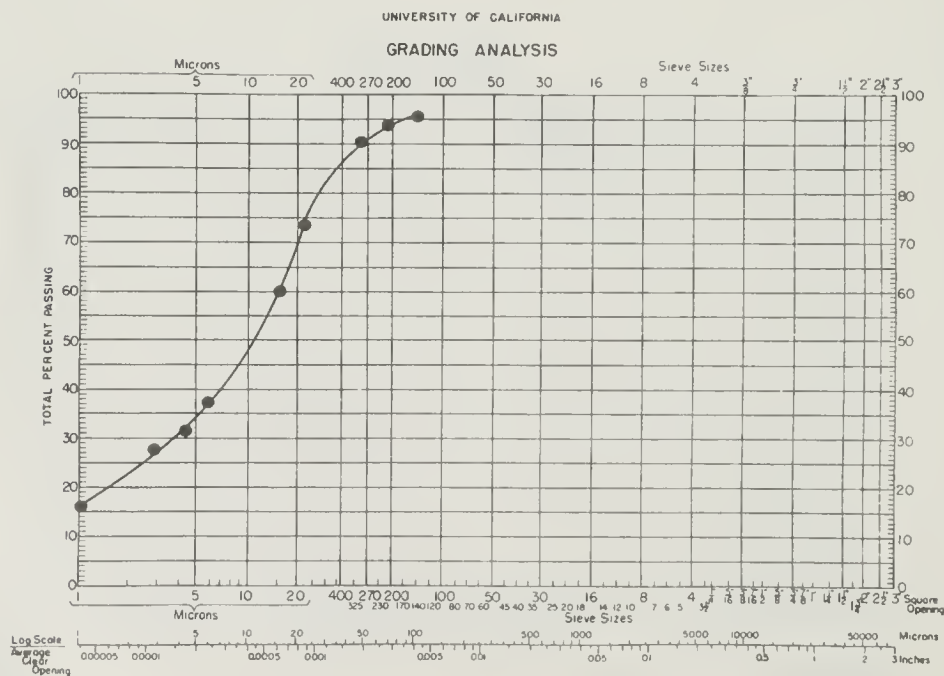
Fig. C-8. Grain Size Distribution for Sample from 83.6 to 84.4 ft Depth
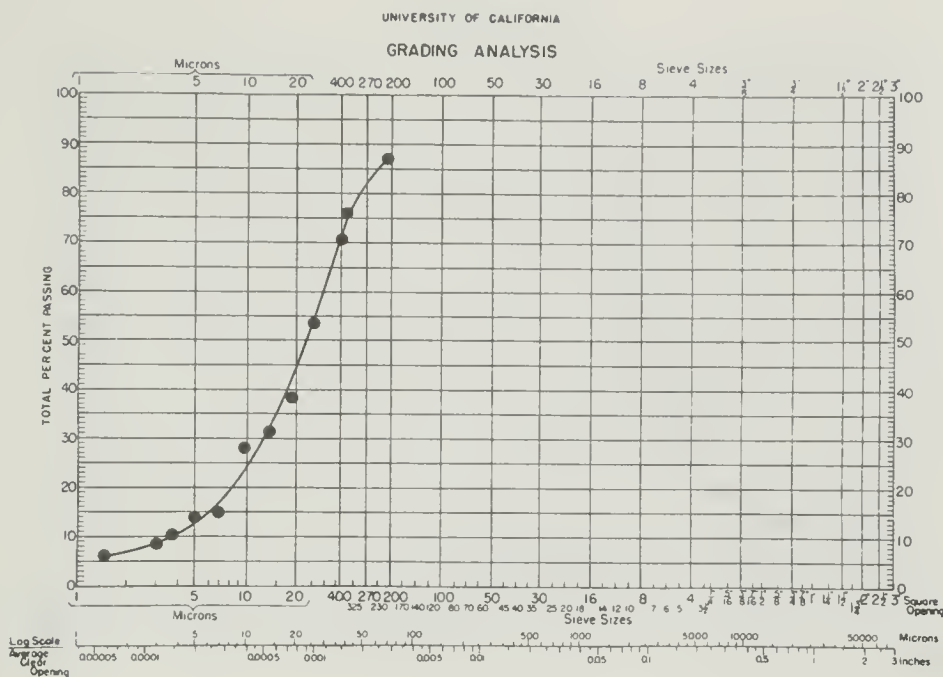
Fig. C-9. Grain Size Distribution for Sample from 91.0 to 92.0 ft Depth
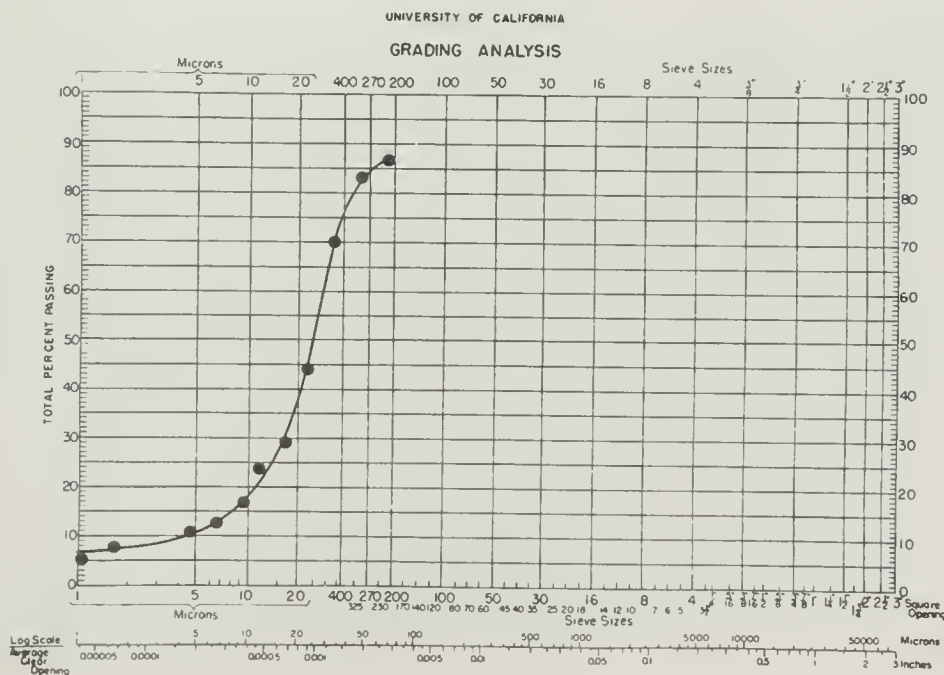
Fig. C-10. Grain Size Distribution for Sample from 91.0 to 92.0 ft Depth
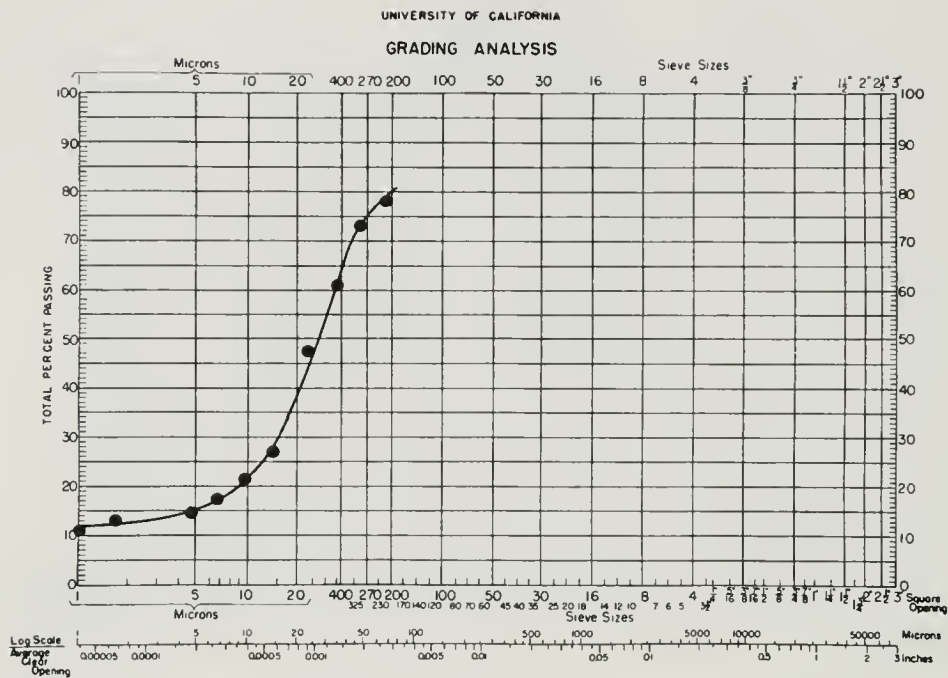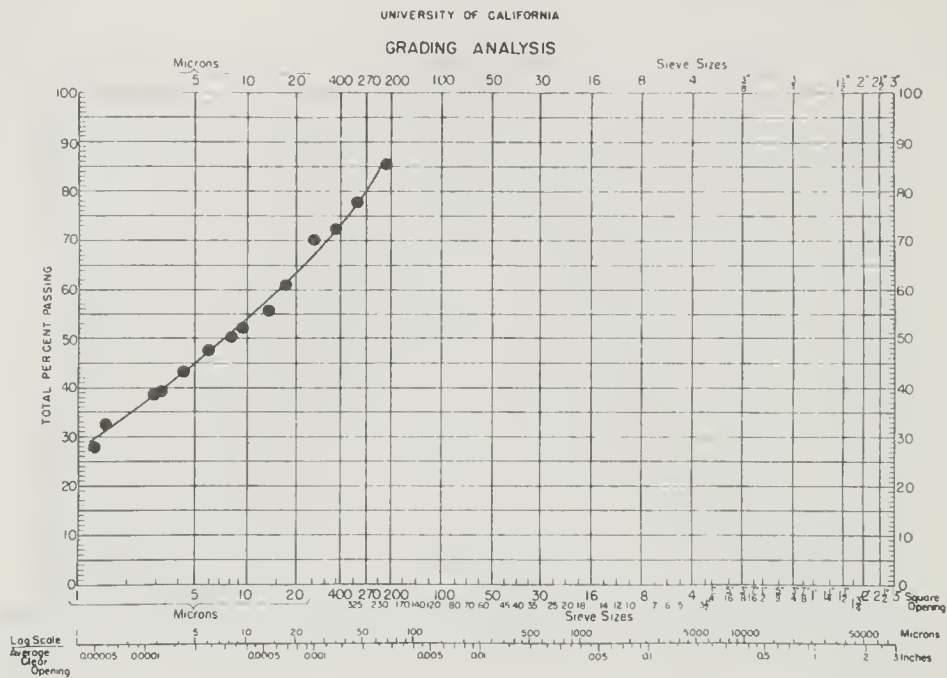
Fig. C-11. Grain Size Distribution for Sample from 96.0 to 96.5 ft Depth
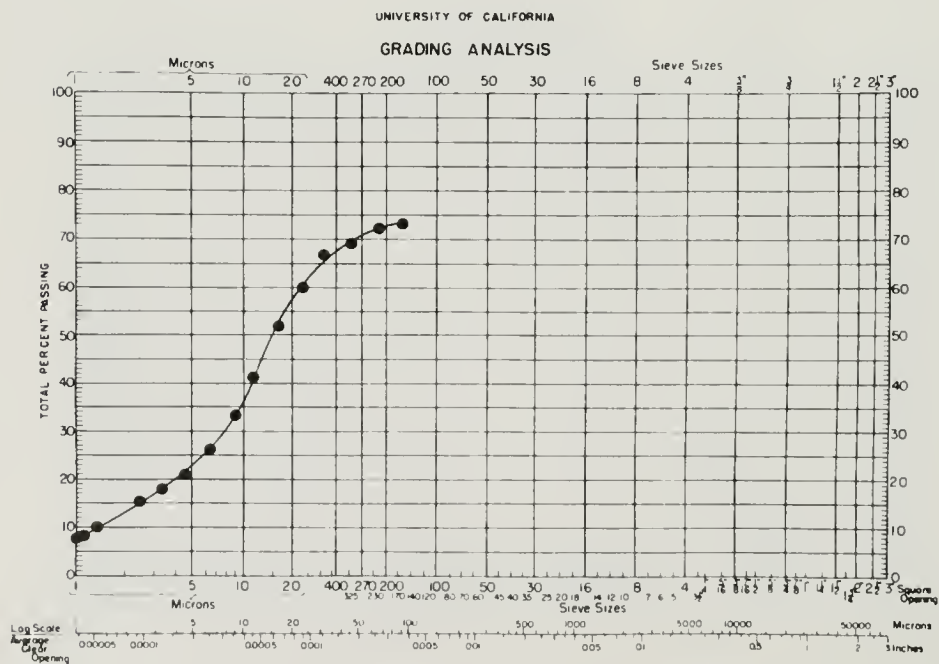
Fig. C-12. Grain Size Distribution for Sample from 96.5 to 99.3 ft Depth

Fig. C-13. Grain Size Distribution for Sample from 98.7 to 99.3 ft Depth

Fig. C-14. Grain Size Distribution for Sample from 102.1 to 104.9 ft Depth

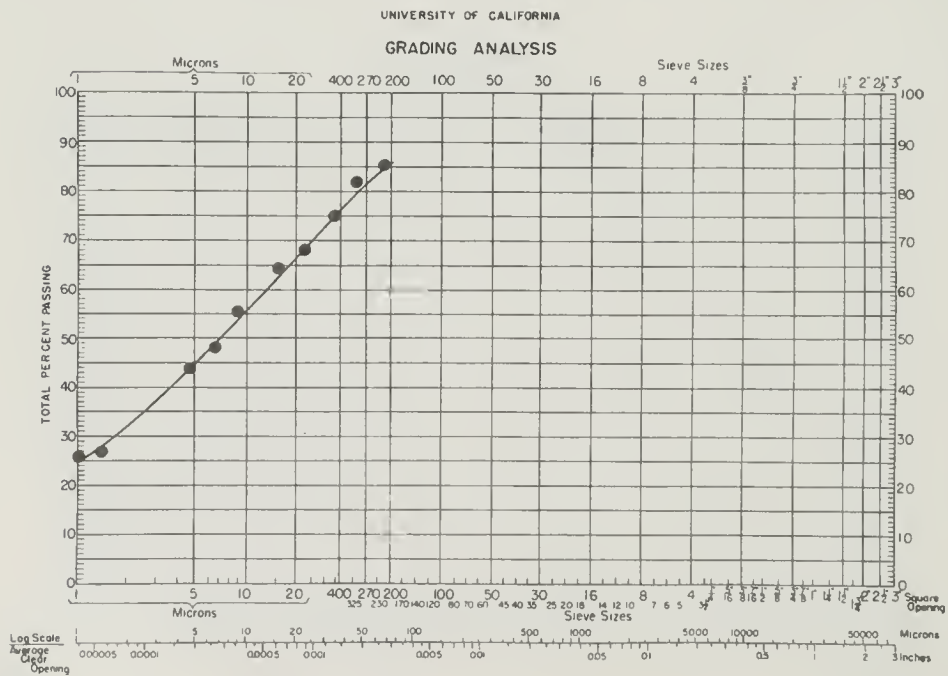Fig. C-15.   Grain Size Distribution for Sample from 104.0 to 104.9 ft Depth

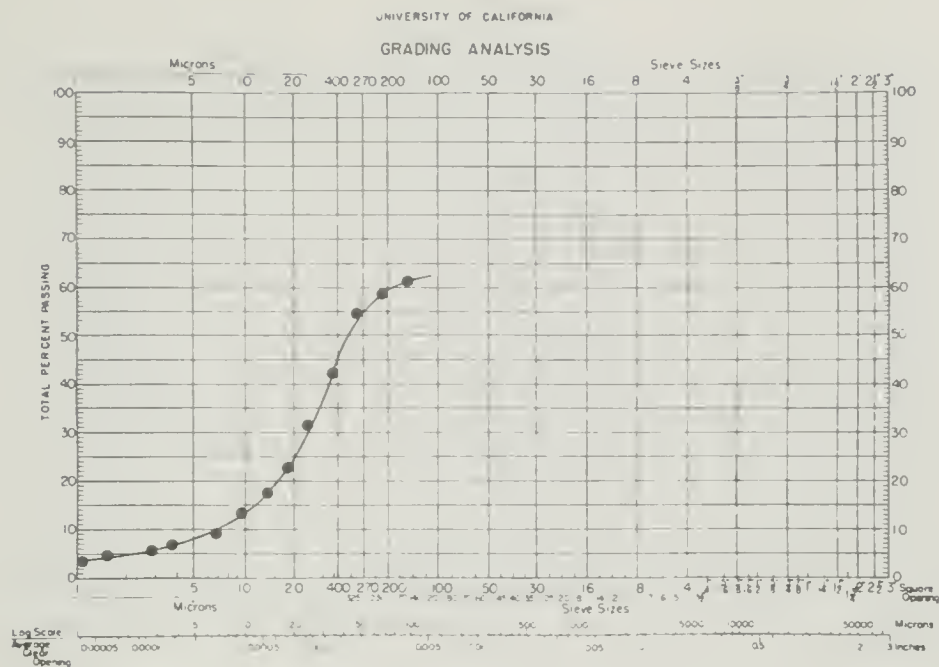Fig. C-16.   Grain Size Distribution for Sample from 104.0 to 104.9 ft Depth

Fig. C-17.   Grain Size Distribution for Sample from 201.0 to 204.0 ft Depth
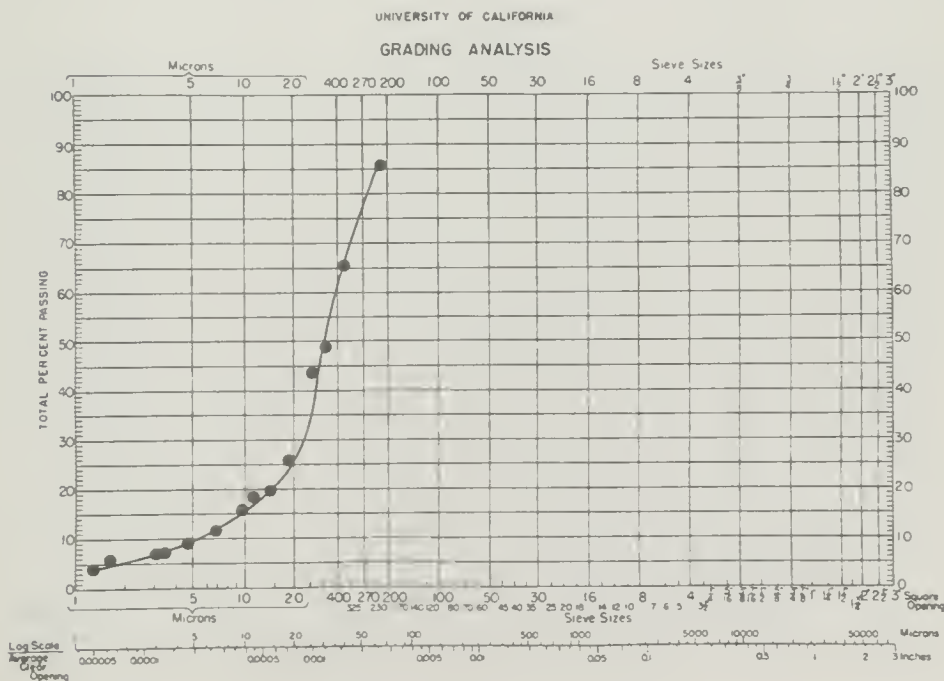

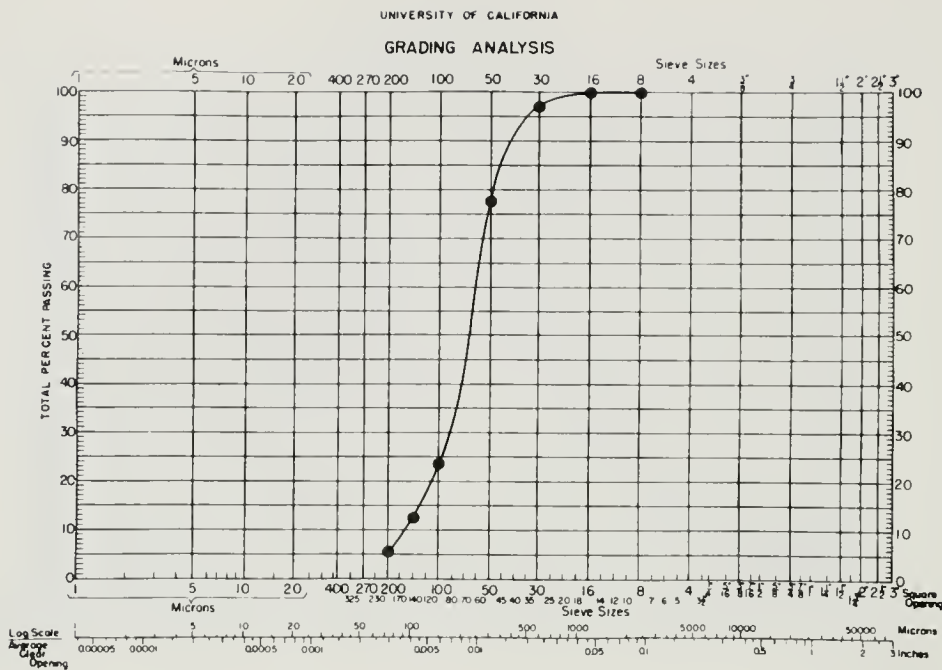Fig. C-18.   Grain Size Distribution for Sample from 203.4 to 204.0 ft Depth

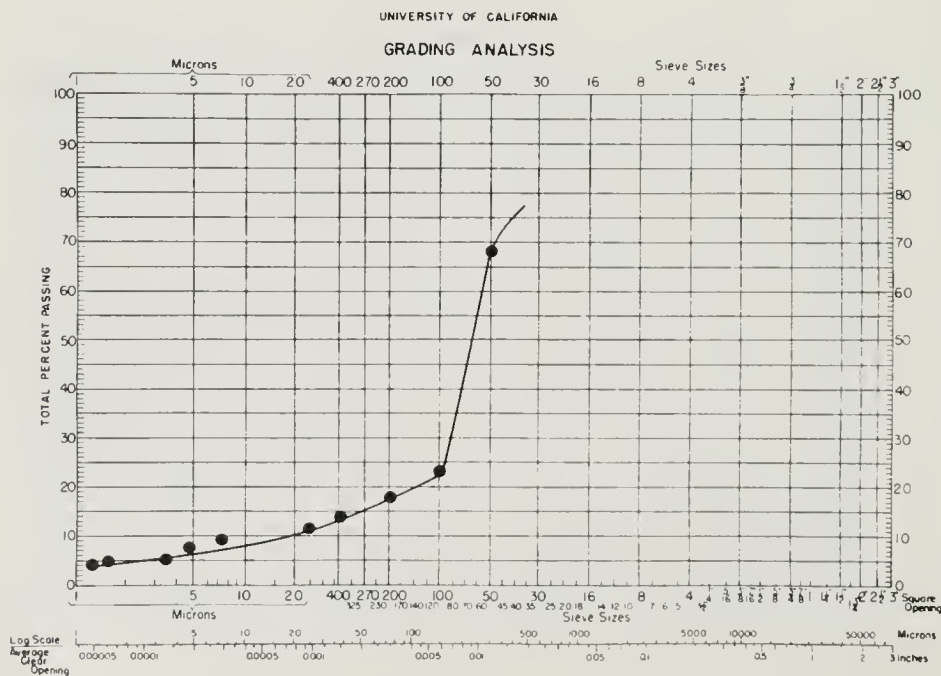Fig. C-19.   Grain Size Distribution for Sample from 207.0 to 211.5 ft Depth

Fig. C-20.   Grain Size Distribution for Sample from 218.5 to 219.0 ft Depth
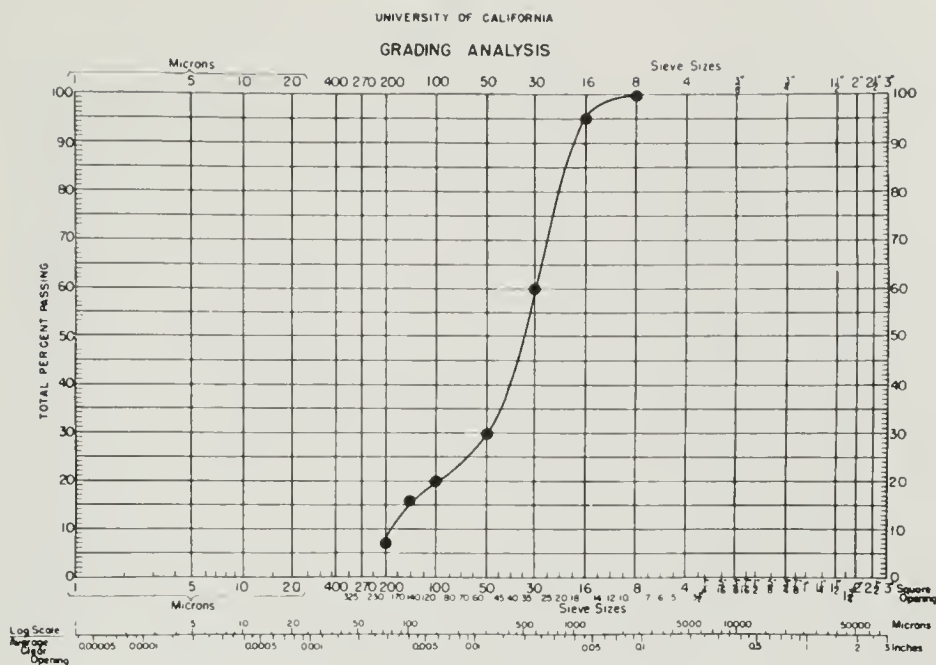
Fig. C-21. Grain Size Distribution for Sample from 219.0 to 221.8 ft Depth
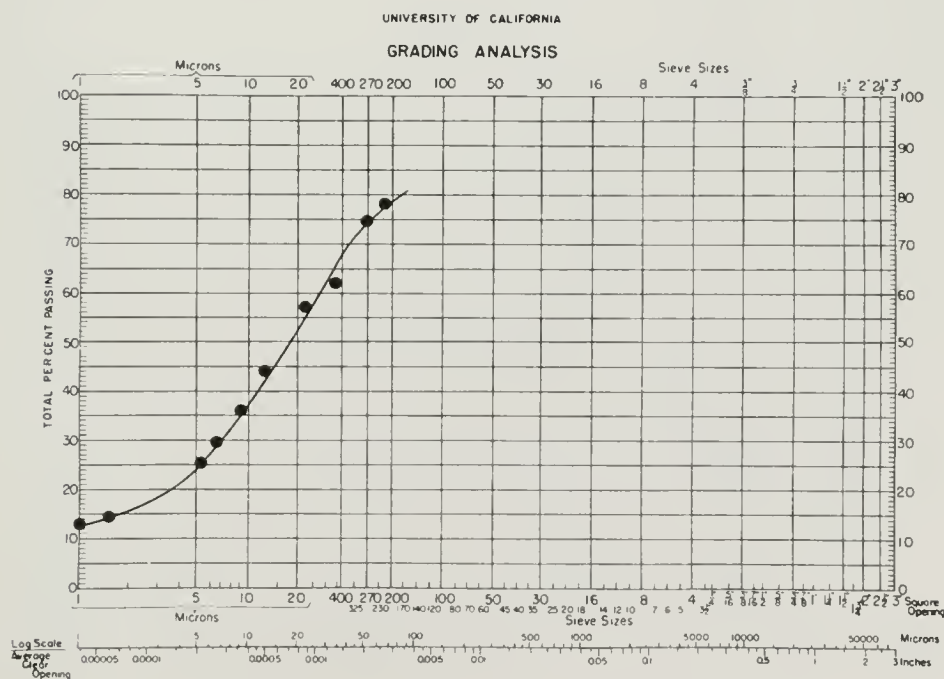

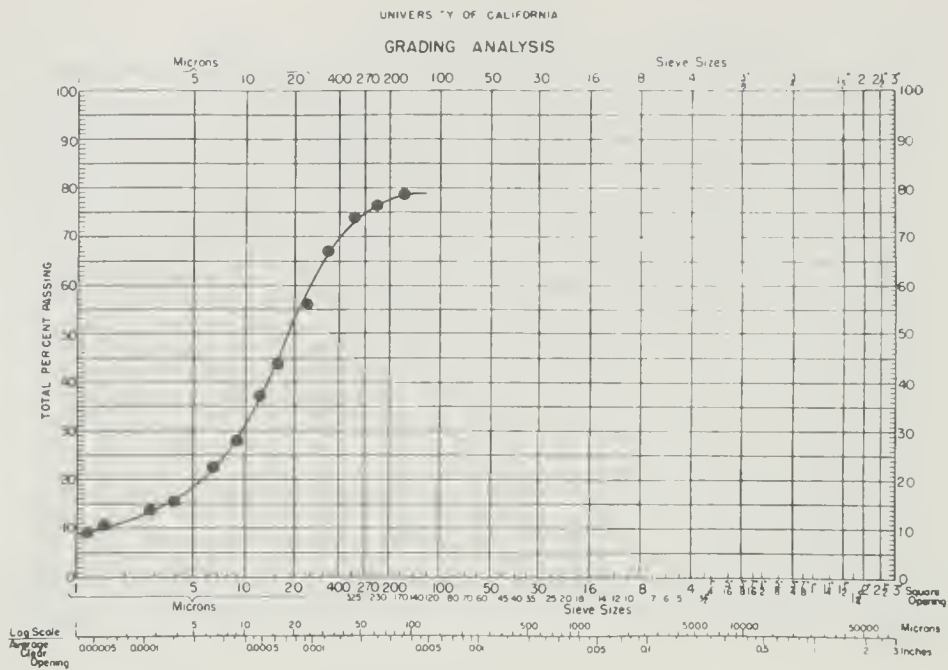Fig. C-22. Grain Size Distribution for Sample from 221.0 to 221.5 ft Depth

Fig. C-23. Grain Size Distribution for Sample from 221.8 to 224.6 ft Depth
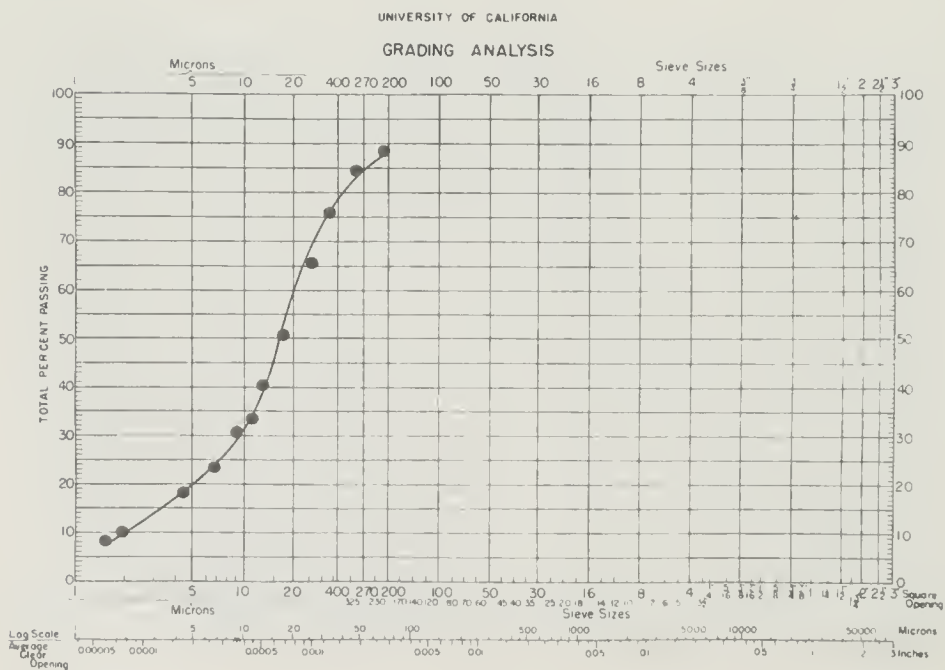

Fig. C-24. Grain Size Distribution for Sample from 224.0 to 224.6 ft Depth

APPENDIX D

DIFFUSIONAL FLOW OF SALT AND WATER

IN SOILS

by

James Greenberg

and

James K. Mitchell

ABSTRACT

Past studies have shown that there is likely to be a small but finite
chemico-osmotic coupling between the flow of salt and water in the pores
of a soil. A theory is presented which provides a detailed, comprehensive,
phenomenological description of the simultaneous coupled flow of salt and
water under the action of salt concentration and hydrostatic pressure
gradients in soils. A finite difference digital computer algorithm which
employed the theory to analyze the one dimensional coupled flow of salt
and water in a soil subjected to a sudden boundary salt concentration
increase is described. The algorithm was also used to analyze the one
dimensional coupled flow of NaCl and water in a horizontal fine-grained
aquitard at a site in Oxnard, California. Experimental investigation
provided verification of some aspects of the theory, and helped in
developing an understanding of the magnitude of chemico-osmotic phenomena
in soils.

The prime concern of this report is the nature and engineering signi-
ficance of chemico-osmotic effects in fine-grained soils. Existing data
indicate that the magnitude of these effects should increase as void
ratio decreases, size of clay fraction increases and molecular weight
of the dissolved salt increases.

The theory leads to two second order differential equations, which
were developed by applying the principles of irreversible thermodynamics
and the law of conservation of mass to an open continuous system of a
dissolved salt and water in the pores of a soil. The theory was tested
against available data, and found to include the Terzaghi diffusion
equation and Fick's law as limiting cases. It is also consistent with

van't Hoffs' law and provides a theoretical framework for analyzing and interpreting earlier work on the simultaneous flow of NaCl and water in kaolinite clay.

Consideration of the physical significance of the phenomenological coefficients appearing in the diffusion equations revealed that there are three types of coupling between the flow of salt and the flow of water in a soil: drag coupling which is a coupling between hydrostatic pressure gradient and flow of salt; chemico-osmotic coupling which is a coupling between salt concentration gradient and flow of water; and void ratio coupling which is a coupling between void ratio change and flow of salt.

Computer analysis of a normally consolidated clay sample subjected to a sudden boundary salt concentration increase indicates that the sample will first chemico-osmotically consolidate, then it will rebound to an equilibrium thickness less than the original sample thickness. Salt diffusion into the sample is a smooth process building steadily to equilibrium which is attained at the same time the sample thickness reaches equilibrium. The maximum amount of chemico-osmotic consolidation increases with increase in boundary salt concentration increase, increase in soil compressibility, increase in drag coupling and increase in void ratio coupling.

Computer analysis of salt and water flow in an aquitard due to lateral sea water invasion of the upper adjacent aquifer at the Oxnard Site, indicate that chemico-osmotic effects will cause only minor surface subsidence (.001 ft). NaCl contamination of the aquitard should be negligible for about 25 years after first arrival of the sea water, and thence become significant reaching a maximum in about 70 centuries. Pumping of water from the lower adjacent aquifer increases both the surface subsidence and rate of contamination of the aquitard and lower adjacent aquifer itself.

-400-

TABLE OF CONTENTS

LIST OF FIGURES

C	Degree of solute inflow
D	Diffusion coefficient (L^2/t)
G	Gibbs free energy $(M/L^2/t^2)$
R	Gas constant $(ML^2/t^2/mole/^\circ A)$
S	Entropy per unit volume of solution $(M/t^2/L/^\circ A)$
T	Absolute temperature $(^\circ A)$, or dimensionless time
U	Pore water pressure $(M/L/t^2)$
UO, UF	Initial and boundary values respectively of u
Z	Mole fraction of solute in solution
a	Activity of the solvent
c	Molar concentration of solute $(moles/L^3)$
e	Void ratio
h	Hydraulic pressure head (L)
t	Time variable (t)
u	U/U_{max}
v	$J_L V_L$ = flow velocity cf solution (L/t)
x	c_s/c_{sm}
y	Distance variable (L)
z	Dimensionless length variable
Φ	Dissipation function $(M/L/t^3)$
π	Osmotic pressure $(M/L/t^2)$
β	$\Delta t/\Delta z^2$ is a measure of the fineness of the finite difference grid
σ	Total stress $(M/L/t^2)$
μ	Chemical potential of solvent $(ML^3/t/mole)$

$\bar{J}_D$ Vector flow of solute relative to flow of solution ($moles/t/L^2$)

$\bar{J}_i$ Vector flow of ith component ($moles/t/L^2$)

$\bar{J}_L$ Vector flow of solution ($moles/t/L^2$)

$\bar{J}_L'$ Vector flow of solute ($moles/t/L^2$)

$\bar{J}_s$ Vector flow of solute ($moles/t/L^2$)

L_{ij} Phenomenological coefficient relating X_j to $\bar{J}_i$ ($moles^2 t/ML^3$)

R_1 First R coefficient

R_2 Chemico-osmotic coupling coefficient

R_3 Drag coupling coefficient

R_4 Fourth R coefficient

R_5 Void ratio coupling coefficient

T_c Value of dimensionless time at 100% chemico-osmotic consolidation

T_{s90} value of dimensionless time at 90% solute inflow

U_o Hydraulic pressure in pure solvent ($M/L/t^2$)

V_i Volume of component i per mole of solution ($L^3/mole$)

V_L Volume of solution per mole of solution ($L^3/mole$)

X_i Vector force due to ith component ($M/L/t^2$)

a_i Activity of component i in solution

a_v Coefficient of compressibility (Lt^2/M)

c_i Moles of component i per unit volume of solution ($moles/L^3$)

c_L Moles of solution per unit volume of solution ($moles/L^3$)

c_L' Moles of solvent per unit volume of solution ($moles/L^3$)

c_s Moles of solute per unit volume of solution ($moles/L^3$)

c_{sm} Maximum value of c_s expected during the process ($moles/L^3$)

c_v Coefficient of consolidation (L^2/t)

g_i Portion of μ_{ic} which depends only on T

k_h Hydraulic permeability (L/t)

k_{ch}, k_{hc} Coupling coefficients (moles L/t)

n_i Number of moles of component i in the solution (moles)

n_1 Number of moles of solution in the solution (moles)

n_2 Number of moles of solute in the solution (moles)

t_c Time at which 100% chemico-osmotic consolidation occurs (t)

t_{s90} Time at which 90% solute inflows occurs (t)

v_i Partial molar volume of component i in the solution ($L^3/moles$)

ΔT Size of dimensionless time interval in the finite difference grid

Δz Size of 3-interval in the finite difference grid

γ_L Number of moles of solution per unit volume of soil (moles/L^3)

γ_s Number of moles of solute per unit volume of soil (moles/L^3)

γ_w Specific weight of water ($M/t^2/L^2$)

μ_i Chemical potential of ith component ($ML^2/t^2/moles$)

μ_{ic} Chemical part of chemical potential of ith component ($ML^2/t^2/moles$)

μ_{Lc} Chemical part of chemical potential of solution ($ML^2/t^2/moles$)

$\mu_{L'c}$ Chemical part of chemical potential of solvent ($ML^2/t^2/moles$)

μ_{sc} Chemical part of chemical potential of solute ($ML^2/t^2/moles$)

σ^1 Effective stress ($M/L/t^2$)

ACKNOWLEDGMENTS

I. OSMOSIS AND SEMI-PERMEABILITY

A. INTRODUCTION

In soil mechanics it is usually assumed that pore water moves in response to two forces; the gravitational force and the hydrostatic pressure (or suction) force. Forces of electrical or chemical origin have conventionally been considered to be negligible.

Recent work (22, 23, 30) indicates that there are instances when both electrical and chemical forces can play a significant role in moving pore water, thus affecting soil behavior.

This report presents a comprehensive quantitative theoretical formulation for analyzing the coupled diffusion of salt and water in fine grained soils. The theory is used in a theoretical computer analysis of ground water pollution and surface subsidence resulting from sea water intrusion of a fresh water aquifer in Oxnard, California.

Chapter I provides a historical introduction and description of chemico-osmotic phenomena, and their place in soil mechanics. A comprehensive theory for the chemico-osmotic diffusion of one solute and solvent in a porous compressible medium is presented in Chapter II. Chapter III develops a finite difference algorithm for applying the theory in soil mechanics, and actually uses the algorithm to analyze chemico-osmotically induced consolidation. Chapter IV uses a slightly modified version of the algorithm to analyze

the movement of sodium chloride and water and the surface subsidence resulting from lateral invasion of sea water into a horizontal fresh water aquifer at a site in Oxnard, California.

B. HISTORICAL BACKGROUND

Osmosis is a phenomenon which has been studied since about the mid-18th century. Early experimenters used animal sacs e.g. pig, ox or fish bladders and intestines as osmotic membranes, and the first published experiments were those of Abbe Nollet in 1748 (5, 8). In 1867 Traube conducted the first osmosis tests on artifically prepared membranes, made of copper ferrocyamide precipited in the pores of porcelain. Probably the first good artificial membranes were paper parchmentized with 55° - 60° Bé sulphuric acid. Since those early pioneering days a multitude of osmotic pressure measurements have been made using many different types of membranes.

Today we find scientists in many disciplines investigating the osmotic characteristics of various natural membranes in our bodies, in animals and plants. This knowledge is used to understand the life process. For example the diffusion of oxygen through the wall of a lung into the bloodstream is an osmotic-type phenomenon. Plant nutrients may pass through various membranes by osmosis enroute from soil water to becoming a part of plant tissue.

Osmosis membranes are also being used to desalinate sea water by reverse osmosis (18, 26). In a similar vein they will probably find application for purification of water polluted with other impurities.

There is also a growing awareness on the part of water resource management agencies and geologists that osmotic effects are relevant when considering the purity and transport of underground water supplies (22).

C. THE NATURE OF OSMOSIS AND REVERSE OSMOSIS

a) Initial   b) Osmosis   c) Reverse Osmosis
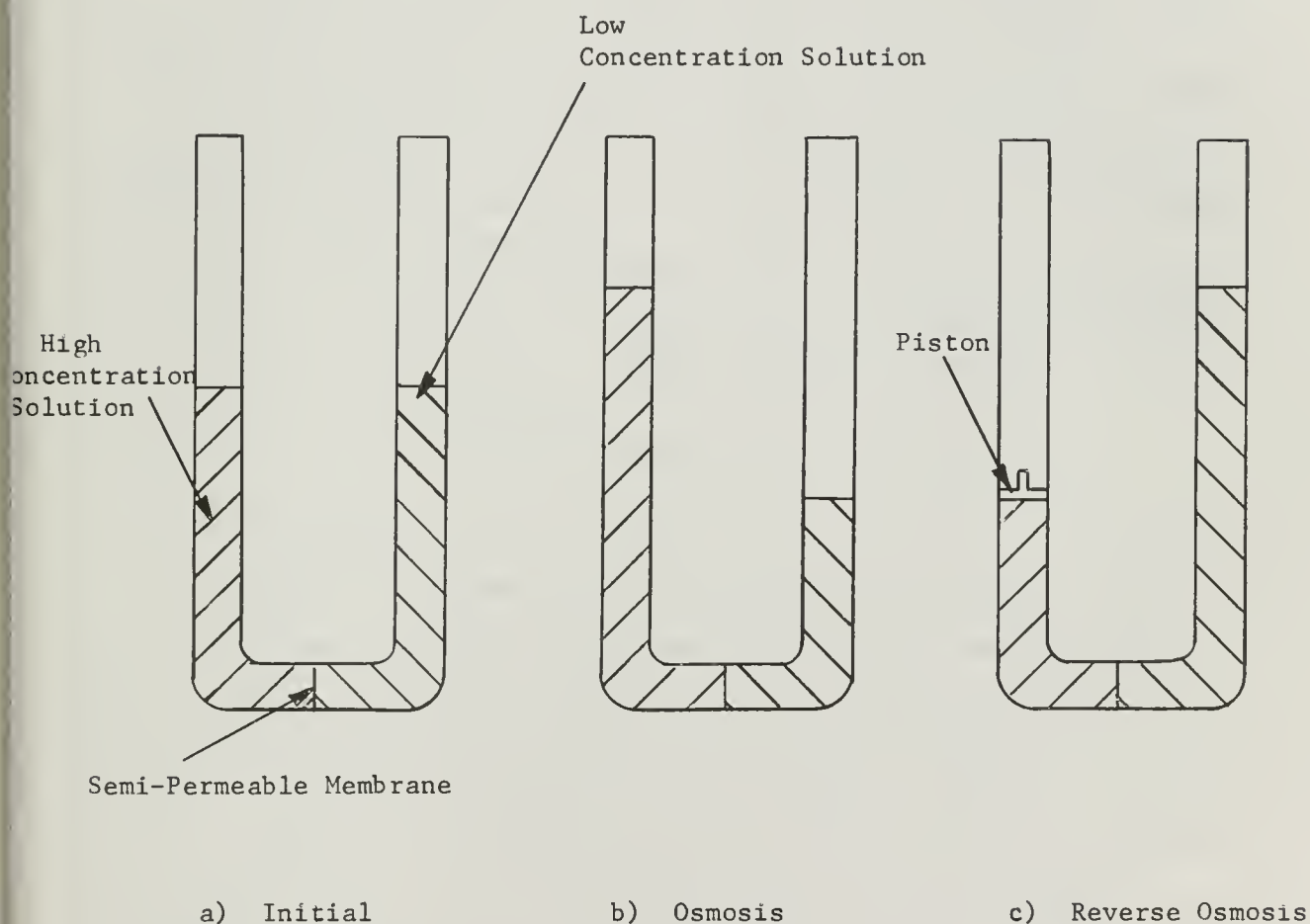
Fig. I-1. Simple Osmotic Phenomena

1. Osmosis

For the purpose of providing a simple description, we make reference to Fig. I-1. This depicts a U-tube containing a high concentration solution in one arm separated by a semi-permeable membrane from a solution of lower concentration (or pure solvent) in the other arm. If the levels of the two liquids are initially equal, as depicted in Fig. I-1a, solvent will flow from the low to the high concentration side by osmosis. Equilibrium will obtain when the hydraulic pressure difference across the membrane is equal to the osmotic pressure difference. This is depicted in Fig. III-1b. If the membrane is non-leaky, i.e. if it allows no solute whatever to pass through, the above description of osmosis is complete.

On the other hand if the membrane is leaky, i.e., if it does allow solute to pass through (even though it be only a small amount at a very slow rate), the above description is incomplete. While solvent flows from the low to the high concentration solution by osmosis, solute will flow from high to low concentration solution by simple diffusion. The osmotic pressure difference decreases as the concentration difference across the membrane decreases (see Chapter I-C). Consequently the pressure decreases as solute diffuses from the high to the low concentration side of the membrane. In this case the hydraulic pressure difference across the membrane builds up to a value less than if the membrane were non-leaky. As time passes and solute diffuses from high to low concentration solution, the hydraulic pressure difference decreases. The process reaches equilibrium when

both solutions are of equal concentration and the osmotic pressure or hydraulic pressure difference across the membrane is zero.

This description of osmosis is based on the classical method of measuring osmotic pressure. It represents one initial and boundary condition. In later discussions we will find occasion to consider different initial and boundary conditions, and will be interested in concentration and hydraulic changes within the membrane itself.

The basic driving mechanism in the osmotic process is the tendency for all things to move to a state of disorder, as formalized in the second law of thermodynamics. In terms of the concepts of thermodynamics, a concentration drop across the semi-permeable membrane represents order, whereas equal solute concentration on both sides of the membrane represents disorder.

2. Reverse Osmosis

Consider the set-up in Fig. I-1a where no osmosis has taken place, and the liquid levels are equal on both sides of the membrane. Imagine now that a pressure greater than the osmotic pressure is applied to the high concentration solution by means of a piston as shown in Fig. I-1c. This will cause solvent to flow from the high concentration solution to the low concentration solution. Hence the high concentration solution will become more concentrated and the low concentration solution will become less concentrated.

This process is known as reverse osmosis, hyperfiltration or ultra filtration (18). If the high concentration solution is seawater

and the low concentration solution is pure water, we have a simple
desalination machine. The less leaky the reverse osmosis (or semi-
permeable) membrane, the less will be the flow of salt through the
membrane, and the purer will be the effluent water. The more leaky
the membrane, the less pure the effluent water, and the more in-
efficient the desalination or seawater conversion process.

Much of the literature on desalination is concerned with
finding efficient reverse-osmosis membranes, i.e., membranes which
are non-leaky and which at the same time maintain a high permeability
to water.

D. THEORETICAL ASPECTS OF OSMOSIS

To obtain a better understanding of osmosis we present a development
of van't Hoff's Law, the classical osmotic pressure equation.

Consider the U tube and semi-permeable membrane depicted in
Fig. I-1. The Gibbs equation (18) tells us that if either hydraulic
pressure or solute concentration are changed in the solution in one
of the arms of the U tube, the corresponding change in free energy
will be given by

$$dG = VdU + \sum_{i=1}^{2} \mu i \, dn_i \qquad (I-1)$$

where G is the free energy of the solution

    V is the volume of the solution

U   is the hydraulic pressure in the solution

n_i is the number of moles of component i in the solution

μ_i is the chemical potential of component i in the solution,
given by

$$\mu_i = g_i + RT \ln a_i \tag{I-2}$$

where g_i is that part of the chemical potential depending on T only

R   is the gas constant

T   is absolute temperature

a_i is the activity of component i. By convention a = 1 for
pure solvent

From equation I-1

$$\mu_i = \frac{\partial G}{\partial n_i}$$

$$\therefore \frac{\partial \mu_i}{\partial U} = \frac{\partial^2 G}{\partial n_i \partial U} \tag{I-3}$$

Also from equation I-1

$$V = \frac{\partial G}{\partial U}$$

$$\frac{\partial V}{\partial n_i} = \frac{\partial^2 G}{\partial U \partial n_i} \tag{I-4}$$

-417-

From (I-3) and (I-4)

$$v_i = \frac{\partial V}{\partial n_i} = \frac{\partial \mu_i}{\partial U} \qquad (I-5)$$

where v_i is the partial molar volume of component i.

Imagine that there is pure solvent under a hydraulic pressure U_o, on both sides of the semi-permeable membrane in Fig. I-1.

From equation I-2 the chemical potential of the pure solvent is

$$g_o + RT \ln 1 = g_o$$

If solute is added to the solvent in one side of the membrane, the chemical potential of the solvent on the side increases to

$$g_o + RT \ln a$$

where a is the activity of the solvent

Hence the effect of adding solute is to increase the chemical potential by

$$RT \ln a \qquad (I-6)$$

To maintain equilibrium and prevent flow of solvent across the membrane we can apply a hydraulic pressure increase $U - U_o$, equal to the osmotic

pressure, to the solution

The increase in chemical potential due to this increase in hydraulic pressure is given by

$$\int_{U_o}^{U} \frac{\partial \mu}{\partial U} \, dU$$

where μ is the chemical potential of the solvents in the solution

From equation I-5 this becomes

$$\int_{U_o}^{U} v \, dU \qquad (I-7)$$

where v is the partial molar volume of solvent in the solution

At equilibrium the increase of chemical potential in equation I-6 must be counteracted by the increase of chemical potential in equation I-7, i.e.

$$\int_{U_o}^{U} v dU = - RT \ln a \qquad (I-8)$$

This equation gives us the osmotic pressure $U - U_o$ in terms of the

activity and partial molar volume of the solvent in the solution.   The

equation is theoretically exact and its accuracy is limited only by

the accuracy of the relationships between v and U and between a and

solute concentration used.

In practice it is usually adequate to assume that the solution is

incompressible, i.e. that v is a constant.   Thus equation I-8 becomes

$$U - U_o = - \frac{RT}{v} \ln a$$

i.e.

$$\pi = - \frac{RT}{v} \ln a \qquad\qquad (I-9)$$

where π is the osmotic pressure

In the event that the solution is of low concentration we may use Raoullt's

law which states that the activity of the solvents is equal to the mole

fraction of the solvent, i.e.,

$$a = 1 - Z$$

where Z is the mole fraction of the solute and is equal to the number of

moles of solute in the solution divided by the number of moles of solution.

In a low concentration solution we may further assume that

$$Z = \frac{n_2}{n_1}$$

where n_2 is the number of moles of solute in the solution

n_1 is the number of moles of solvent in the solution

Hence $a = 1 - \dfrac{n_2}{n_1}$, and substituting this in equation I-9 gives

$$\pi = - \frac{RT}{v} \ln \left(1 - \frac{n_2}{n_1} \right) = \frac{RT}{v} \frac{n_2}{n_1}$$

because $\ln \left(1 - \dfrac{n_2}{n_1} \right) = - \dfrac{n_2}{n_1}$ since $\dfrac{n_2}{n_1}$ is small

i.e.

$$\pi = RT \frac{n_2}{V}$$

because v is assumed to be constant.

Thus

$$\pi = RTC \tag{I-10}$$

where C is the molar concentration of solute in the solution

Equation I-10 is van't Hoff's law. It tells us that the value of the osmotic pressure is directly proportional to the solute concentration in the solution van't Hoff first deduced the law empirically from the data of Pfeffer (18). The equation gives accurate results for ideal dilute solutions only, because it neglects interactions between solute particles which occur in more concentrated solutions.

E. SEMI-PERMEABILITY

1. Basic Concepts

A porous membrane is said to be semi-permeable to a solution if the membrane retards the flow of solute more than the flow of solvent through its pores.* We will also refer to this retardation of flow of solute by a membrane as chemico-osmotic coupling. If the membrane completely prevents the solute from moving through its pores, the system is said to be semi-permeable and non-leaky. Such a system exhibits a high degree of chemico-osmotic coupling. If the membrane only retards the flow of solute very slightly relative to the flow of solvent, the system is said to be leaky and semi-permeable, and exhibits less chemico-osmotic coupling.

Semi-permeability depends not only on the characteristics of the membrane, but also on the properties of the solution. Factors such as temperature, pressure solute concentration can also have an effect on the semi-permeability characteristics of certain membrane-solution systems (18).

2. Mechanisms of Semi-Permeability

Primary mechanisms responsible for semi-permeability have been suggested, tested and discussed by many workers. We will present a summary of the most commonly accepted ideas.

To be able to retard the flow of solute a membrane must exert some sort of molecular frictional resistance to, or braking effect on

---

*Note that this definition includes the classical definition of a semi-permeable membrane, i.e. a membrane permeable only to solvent (18).

the movement of solute molecules. Johnson, Dresner and Krauss describe this process as follows (26).

> "The membrane must be able to affect the thermodynamic or transport properties of salts and water by forces."

One such force is a physical or molecular sieving. This microscopic sieving mechanism is analogous to macroscopic sieving, and is thought to occur when the pores or voids of the membrane are about the same size as, or smaller than the molecules themselves; so that the membrane has the ability to geometrically screen them. In systems where neither the membrane nor the solute molecules are charged, and where the membrane pores are saturated with solution, the microscopic sieving mechanism is the predominant cause of semi-permeability (26). For example, it is the predominant cause in systems of cellophane membranes and polymer solutions

Another mechanism which enables uncharged membranes to be semi-permeable to uncharged solute molecules is dialysis (28). To dialyse means literally to "dissolve through", and dialysis is envisaged as a migration or diffusion of solute molecules dissolved in the "solid state" of the membrane

A third phenomenon responsible for semi-permeability is the distillation mechanism. This mechanism was first suggested by Callendar (18), and is only operative if the membrane is partly saturated, and the solvent is more volatile than the solute. It can be envisaged as solvent molecules diffusion in the gas phase across air voids within the membrane pores. Solute molecules will also diffuse in this way, but at a slower rate than solvent because the solvent is more volatile.

-423-

If the membrane is electrically charged, semi-permeability is likely to be the result of an electrostatic effect. The microscopic forces at play are sometimes of the primary valence type, e.g., covalent or ionic bonds, sometimes they are secondary bonds, e.g., hydrogen bonds or short range Van der Vaals London forces; and sometimes they are tertiary or long range bonds, e.g. contombic forces.

At present we are not able to state which forces are active in which membrane-solution systems.

Membranes which exhibit semi-permeability due to electrical charge are called permselective. The fact that some membranes are semi-permeable to solutions of inorganic ions which are about the same size as water molecules (e.g. cellulose acetate membranes and Na^+, Cl^- solution) is held as confirmation that permselectivity is an electrostatic rather than a geometric screening effect.

If the membrane is positively charged, it is referred to as an anion exchange permselective membrane. The positive surface charge binds the solute anion; hence retarding the flow of solute.

If the membrane is negatively charged, it is referred to as a cation exchange permselective membrane. The mechanism of retardation of flow of solute is analogous to that for anion exchange permselective membranes.

Spiegler (26) has proposed a slightly different mechanism for the cellulose acetate membrane. It is called the hydrogen bonding mechanism, and is similar to dialysis except that the solute does not dissolve in the solid phase of the membrane. Rather, solute

molecules or ions diffuse in the noncrystalline portion of the membrane while being held there by hydrogen bonding.

F. SOILS AS SEMI-PERMEABLE MEMBRANES

A semi-permeable membrane can be thought of as a porous medium whose pores are continuous and which retards and hinders flow of solute more than the flow of solvent. Soil pores are continuous so soils can be thought of as membranes. The question is are soils semi-permeable membranes? Do they have the power of retarding or hindering flow of solute more than the flow of solvents?

We will attempt to answer this question by incorporating some of the ideas we have already established and supplementing them with available experimental data.

There are two possible causes of semi-permeability arising in a soil whose pores are saturated with a solution.

1. Permselectivity

The first is permselectivity, and would arise if the soil particles contained surface electrical charges and the solute particles were charged. In fact many clay size particles do contain surface electrical charges (7), and many solutes are charged dissociated ions; for example most inorganic molecules dissociate into anions and cations in water. Hence we can expect soils with a large clay fraction to be permselective to solutions of most inorganic salts in water

Of the three most common clay minerals found in natural soils, Montmorillonite has the highest volumetric charge density, Illite the

second and Kaolinite the lowest. Ion exchange capacity is a direct

measure of the volumetric charge density; and is about 100 milli-

equivalents* per 100 grams of soil for Montmorillonite, 40 for Illite

and 3 - 8 for Kaolinite (7). Hence we expect soils with a high

percentage of Montmorillonite to exhibit relatively more permselectivity

than soils with equal percentages of Illite and Kaolinite.

2. Sieving Mechanism

The second possible cause of semi-permeability in soils is the

sieving mechanism. For the soil to be able to hinder the flow of

solute by "microscopic sieving" the diameter of the solute ion, or

molecule, should be of the same order of magnitude as the average

diameter of the soil pores. In this event the soil could be a semi-

permeable membrane to the solution. If the diameter of the solute

ion or molecule is much larger than the average diameter of soil pores,

so that no solute can enter the soil, the soil-solution system will be

semi-permeable and non-leaky. If the diameter of the solute ion or

molecule is slightly larger than the average soil pore diameter, so

that the movements of solute through the soil is retarded, but not

totally inhibited, the system will be semi-permeable and leaky.

---

*One milli-equivalent is 10^{-3} equivalents. An equivalent is the number
of electronic charges in one mole of solution and equals 6×10^{23},
Avagadro's number. An exchange capacity of 10 milli-equilvalents
per 100 grams means that each 100 grams of soil particles can exchange
$10 \times 10^{-3} \times 6 \times 10^{23} = 6 \times 10^{21}$ electronic charges.

Clay particle diameters are generally less than 2 microns or 20,000 Å (25). Unfortunately it is not possible to specify a lower bound since not many measurements have been made on soil particle sizes below 20,000 Å. However, we do know that clay minerals are composed of sheets made of basic building blocks which are about 10 Å thick. Hence an estimate for the smallest clay particle thickness is about 10 Å.

The smallest solute particles are inorganic ions such as Na^+ or Cl^- which are about 1 to 10 Å in diameter. An example of a large diameter solute would be polyethylene glycol 20,000 which is a synthetic polymer composed of about 100 ethylene glocol molecules each of molecular weight 200 and about 5 Å long, bound together in a chain about 500 Å long. Another example is amylpectin which is one of the two component polymers of natural starch (3, 13). It is a branch-chain type of molecule composed of about 2,000 interlinked dextrose groups, each of molecular weight around 600 and length about 20 Å. It is difficult to estimate a diameter for these polymers, because they are neither round nor solid and are in a state of constant motion. For our purposes however it is probably adequate to assume that the "diameter" of a large polymer molecule increases as its molecular weight increases.

A cursory look at the sizes of clay particles and solute molecules presented above indicates that there can be an overlap between the two. This means that there is a possibility that soils with a large clay fraction will probably sieve solute molecules, especially

large polymer molecules, and hence be semi-permeable. If the soil were a pure clay of very low void ratio and the solute were a large polymer like amylpectin, the system could conceivably be non-leaky.

However it seems likely that systems composed of natural clayey soils and solutions with inorganic solutes will be leaky. In general we might say that factors which decrease the void ratio, increase the possibility of the soil being non-leaky, i.e., they increase the possibility of the system exhibiting chemico-osmotic coupling. Such factors are particle size distribution, maximum previous consolidation pressure, structure of the soil matrix, etc. We can also conclude that for a given soil, the larger the solute molecule the less leaky will be the system.

It is pertinent to note that there may be little value in considering molecules of ultra-large molecular weight, since there is only a finite amount of any solute that can be dissolved in a given volume of solution, depending on solubility of the solute, temperature, etc. If the molecular weight of the solute is very high, then this finite amount of solute may represent a very low molar concentration and hence only a very low osmotic pressure will be developed (see van't Hoff's law, equation I-10).

There is very little perceivable chemico-osmotic coupling in a soil solution system wherein osmotic pressures are very low. Consequently such systems, whether they be non-leaky or not, are of not much practical interest to us because we are concerned with systems exhibiting significant chemico-osmotic coupling.

3. Available Data

Little experimental work has been done on chemico-osmotic
effects in soils. Olsen (22, 23) has made some direct measurements of
chemico-osmotic coupling in a Kaolinite - NaCl solution system. His
experiments are described in some detail in Section II-D-3. We will
only mention pertinent aspects of his results here.

He found that for an increase in NaCl concentration from
10^{-3} normal to 10^{-2} normal the osmotic pressure varied from 0.6
centimeters of water at a consolidation pressure of 10 atmospheres
to 15 centimeters of water at a consolidation pressure of 700
atmospheres. A theoretical value for the osmotic pressure generated
by an increase in NaCl concentration from 10^{-3} normal to 10^{-2} normal
in a non-leaky semi-permeable membrane is obtained from van't Hoff's
law as 250 centimeters of water.

Hence we conclude that Kaolinite - NaC' solution systems are
semi-permeable and leaky. Also of significance is the fact that the
system becomes less leaky as the consolidation pressure increases,
i.e., as the void ratio decreases. The implication here is that the
microscopic sieving mechanism is chiefly responsible for the semi-
permeability. As we noted in Section I-E-1 the ion exchange capacity
of Kaolinite is low, hence we do not expect permselectivity to be a
large contributor to semi-permeability in this system.

The system exhibits a relatively large amount of leakiness
at a consolidation pressure of 10 atmospheres. Therefore we expect
that natural soils at consolidation pressures of about 10 atmospheres

and containing large clay fractions of Kaolinitic type material will be semi-permeable but relatively leaky to inorganic salt solutions such as seawater.

For example we expect the soil in the aquitards at the Oxnard site, discussed in Section III-D to be semi-permeable to seawater (see Section III-D) i.e., we expect it to exhibit some chemico-osmotic coupling in the presence of seawater.

Mokady and Low (20) conducted an experiment in which they imposed a NaCl solute concentration drop of .05 normal across a Bentonite sample of thickness 13.2 centimeters. They observed a flow of water of 2×10^{-5} milli moles per second through a 2.5 centimeter diameter sample from the low concentration to the high concentration solution.

If the hydraulic permeability of the Bentonite is assumed to be 10^{-9} cm/sec, this observed flow rate corresponds to an induced osmotic pressure of 97 centimeters of water. van't Hoff's law tells us that a solute concentration drop of .05 normal generates an osmotic pressure of 1300 centimeters of water. Our conclusion here is that the Bentonite - NaCl solution system was leaky and semi-permeable.

It is difficult to make an estimate of the degree of leakiness without having a measured value for the hydraulic permeability of the Bentonite. However Bentonite is usually more fine grained than Kaolinite and has a higher ion exchange capacity; hence both microscopic sieving and permselectivity should play a larger role in Bentonite than in Kaolinite. This we expect Bentonite to exhibit less leakiness to

NaCl solution than Kaolinite. The above data do not conclusively

support this contention, perhaps because our estimate of the hydraulic

permeability of the Bentonite is too crude.

4. Conclusions

    i. Available data indicate that clay - NaCl solution systems
are both semi-permeable and leaky.

    ii. We expect natural soils containing a large clay fraction to
exhibit leaky semi-permeability, or chemico-osmotic coupling.

    iii. The leakiness in a soil-solution system should decrease
as void ratio decreases.

    iv. Since the microscopic sieving mechanism is a component of
semi-permeability in soils, the degree of leakiness should decrease
as the size of the solute molecule increases and the size of the
clay fraction increases.

II.   THEORY OF CHEMICO-OSMOTIC DIFFUSION

A.   INTRODUCTION

This chapter considers theoretical aspects of chemico-osmotic
effects in soils. Firstly a generalized theory for the flow of
solute and solution in a compressible porous medium is presented.
The generalized theory is developed from the postulates of irreversible
thermodynamics and the law of conservation of mass applied to a gen-
eralized system of one solute and one solvent in a porous compressible
medium.

Subsequently the generalized theory is specialized to describe the
flow of solute and solvent in a soil. This is achieved by expressing
some of the variables in soil mechanics notation, by incorporating the
soil mechanics concept of effective stress and by using a constitutive
equation that relates void ratio to effective stress.

Kirkwood (14) developed a generalized theory for the transport of
several species through biological membranes, but did not attempt any
generalized solution. By incorporating some of the terminology and
principles of the discipline of soil mechanics, we have extended
Kirkwood's work and produced a theory capable of quantitatively
solving a wide range of chemico-osmotic flow problems.

Other workers (1, 22) have performed experiments which verify
some aspects of the generalized theory as we shall see in Chapter III;
but as yet no one has presented a comprehensive set of experimental
data which could be considered an empirical solution to the problem.

B. GENERALIZED THEORY

1. Assumptions

We consider an open system consisting of a solute and solution
in the pores of a porous compressible medium and we assume:

a. Isotropy and homogeneity

b. Isothermal conditions

c. No electrical or electromagnetic gradients

d. No ion exchange during diffusion

e. The solute acts as a single species; i.e., it does not
dissociate so that different ion species act independently

f. The solution is dilute enough for "ideal solution"
relationships to be valid, and for the flow of solvent and solution
to be considered synonymous

g. The pores of the medium are fully saturated with solution

h. The postulates of irreversible thermodynamics are applicable
to the process. For experimental substantiation of their validity in
soils see the work of Abd-El-Aziz and Taylor (1) and Olsen (22, 23)

2. Flow Equations

We consider the open system of solute and solution flowing under
the influence of hydraulic pressure and solute concentration gradients
in the porous medium.

The postulates of irreversible thermodynamics tell us that
these irreversible quasi-static flows will generate entropy at a rate
Φ given by (10):

$$\Phi = T \frac{dS}{dt} = \sum_{i=1}^{2} \bar{J}_i \cdot \text{grad} \, (- \mu_i) \qquad (II-1)$$

where

$$\text{grad} \, (- \mu_i) = v_i \, \text{grad} \, (- U) + \text{grad} \, (- \mu_{ic}) \qquad (II-2)$$

and

$$\mu_{ic} = g_i + RT \, \ell n \, c_i \qquad (II-3)$$

where g_i is a function of T only

In equations II-1, II-2, and II-3

    T   = absolute temperature

    S   = entropy per unit volume of the solution

    $\bar{J}_i$ = flow vector of ith component in moles per unit time per

          unit area

    t   = time

    μ_i = chemical potential of the ith component

    v_i = partial molar volume of the ith component

    U   = hydrostatic pressure in the solution

    μ_{ic} = chemical part of the chemical potential of the ith component

    R   = the gas constant

    c_i = number of moles of component i per unit volume of solution

According to the Gibbs-Duhem equation, the grad $(- \mu_{ic})$ are related by

$$\sum_{i}^{2} c_i \, \text{grad} \, (- \mu_{ic}) = 0 \qquad\qquad (II-4)$$

For the two component system under consideration (II-4) becomes

$$\text{grad} \, (- \mu_{L'c}) = - \frac{c_s}{c_{L'}} \, \text{grad} \, (- \mu_{sc}) \qquad\qquad (II-5)$$

where the subscripts L' and s refer to solvent and solute respectively.
From (II-1) and (II-2)

$$\Phi = \sum_{i=1}^{2} \bar{J}_i \, v_i \cdot \text{grad} \, (- U) + \sum_{i=1}^{2} \bar{J}_i \cdot \text{grad} \, (- \mu_{ic})$$

$$= \left(\sum_{i=1}^{2} \bar{J}_i \, v_i \right) \cdot \text{grad} \, (- U) + \bar{J}_s \cdot \text{grad} \, (- \mu_{sc})$$

$$+ \bar{J}_{L'} \cdot \text{grad} \, (- \mu_{L'c}) \qquad\qquad \text{from} \quad (II-5)$$

$$\sum_{i=1}^{2} J_i \, v_i$$ is the vector sum of the volume of solute and solvent
flowing through unit area in unit time, i.e., the volume flow
rate of solution.

Thus

$$\sum_{i = 1}^{2} \bar{J}_i \, v_i = \bar{J}_L \, v_L \qquad \text{(II-6)}$$

Since the flow rate of solution and solvent are nearly the same magnitude in an ideal dilute solution (as are also $c_{L'}$ and c_L), we may write

$$J_L = J_{L'} \quad \text{and} \quad c_L = c_{L'}$$

and substituting from equations II-5 and II-6, Φ becomes

$$\Phi = \bar{J}_L \, v_L \, \text{grad} \, (- \, U) + (\bar{J}_S - \frac{c_S}{c_L} \, \bar{J}_L) \, \text{grad} \, (- \, \mu_{sc})$$

From (II-3)

$$\text{grad} \, (- \, \mu_{sc}) = \text{grad} \, (- \, g_s) + RT \, \text{grad} \, (- \, \ln \, c_s)$$

$$= 0 + \frac{RT}{c_S} \, \text{grad} \, (- \, c_S) \qquad \text{(II-7)}$$

because g_s is dependent only on temperature. It may be noted that the quantity $(\bar{J}_S - \frac{c_S}{c_L} \bar{J}_L)$ represents the flow rate of solute relative to the flow rate of solution. If this quantity is denoted by $\bar{J}_D$, then with the aid of equation II-7, Φ becomes

-437-

$$\Phi = \bar{J}_L \, v_L \, \text{grad} \, (-\,U) + \bar{J}_D \, \frac{RT}{c_s} \, \text{grad} \, (-\,c_s) \qquad \text{(II-8)}$$

The postulates of irreversible thermodynamics tell us further that if the dissipation function, Φ, can be written in the form

$$\Phi = \sum_{i=1}^{n} \bar{J}_i \cdot x_i$$

for a given system, where $\bar{J}_i$ are generalized "flows" and x_i are generalized "forces", the forces and flows are related by

$$\bar{J}_i = \sum_{j=1}^{v} L_{ij} \, x_j$$

where L_{ij} are phenomenological constants. Onsagers reciprocal theorem tells us also that

$$L_{ij} = L_{ji}$$

i.e., the matrix of the phenomenological coefficients is symmetric.

In our case the "flows" are $\bar{J}_L$ and $\bar{J}_D$, while the "forces" are $v_L \, \text{grad} \, (-\,U)$ and $\frac{RT}{c_s} \, \text{grad} \, (-\,c_s)$, and they are related by

$$\bar{J}_L = L_{11} \, v_L \, \text{grad} \, (-\, U) + L_{12} \, \frac{RT}{c_s} \, \text{grad} \, (-\, c_s) \tag{II-9a}$$

$$\bar{J}_D = L_{21} \, v_L \, \text{grad} \, (-\, U) + L_{22} \, \frac{RT}{c_s} \, \text{grad} \, (-\, c_s) \tag{II-9b}$$

with

$$L_{12} = L_{21} \tag{II-9c}$$

Both "flows" have units of moles/L^2t and both "forces" have units of ML/moles t^2, thus the L_{ij} have units of moles^{2}t/M$\bar{L}^3$

Equations II-9 are the flow equations for a two-component system of one solute and solution. They can be expanded to describe a multi-solute solution and to incorporate electrical and temperature effects as well. In their present form they are suitable for application to the problems we will consider. For equations II-9 to be valid, the determinant of the coefficients L_{ij} must be positive definite (10) i.e.,

$$L_{11} \, L_{22} - L_{12} \, L_{21} \geqslant 0 \tag{II-10}$$

In Chapter III we will prove that this relationship is valid for soil-solution systems

In future developments, we deal more with $\bar{J}_s$ than $\bar{J}_D$, i.e., the flow of solute relative to the soil is of more significance than the flow of solute relative to the solvent. From the definition of $\bar{J}_D$ and using equations II-9a and II-9b:

$$\bar{J}_s = \bar{J}_D + \frac{c_s}{c_L}\,\bar{J}_L = L_{21}\,v_L\,\text{grad}\,(-U) + L_{22}\,\frac{RT}{c_s}\,\text{grad}\,(-c_s)$$

$$+\frac{c_s}{c_L}\left[\,L_{11}\,v_L\,\text{grad}\,(-U) + L_{12}\,\frac{RT}{c_s}\,\text{grad}\,(-c_s)\,\right]$$

which may be written

$$\bar{J}_s = \left(L_{21}\,v_L + \frac{c_s}{c_L}\,L_{11}\,v_L\right)\text{grad}\,(-U)$$

$$+\left(L_{22}\,\frac{RT}{c_s} + \frac{L_{12}RT}{c_L}\right)\text{grad}\,(-c_s) \tag{II-9d}$$

3. Continuity Equations

A continuity equation is a mathematical representation of the law of conservation of mass, and expresses the fact that matter can neither be created nor destroyed. Thus the rate of increase of mass density at any point must equal the rate at which matter flows towards that point.

For solution flowing in a porous medium this can be written as (1)

$$\bar{\nabla}\cdot\bar{J}_L = -\frac{\partial\gamma_L}{\partial t} \tag{II-10}$$

where γ_L is the number of moles of solution per unit volume of soil, and for solute

$$\bar{\nabla} \cdot \bar{J}_s = - \frac{\partial \gamma_s}{\partial t} \tag{II-11}$$

where γ_s is the number of moles of solute per unit volume of soil.

4. Diffusion Equations

The diffusion equation for the flow of solution is derived by substituting (II-9a) in (II-10) to give

$$- \frac{\partial \gamma_L}{\partial t} = \bar{\nabla} \cdot \{ L_{11} \ v_L \ \text{grad} \ (- \ U) + L_{12} \ \frac{RT}{c_s} \ \text{grad} \ (- \ c_s) \} \tag{II-12}$$

Similarly the diffusion equation for the flow of solute is obtained by substituting (II-9d) in (II-11)

$$- \frac{\partial \gamma_s}{\partial t} = \bar{\nabla} \cdot \{ (L_{21} \ v_L + \frac{c_s}{c_L} \ L_{11} v_L) \ \text{grad} \ (- \ U)$$

$$+ (L_{22} \ \frac{RT}{c_s} + \frac{L_{12} RT}{c_L}) \ \text{grad} \ (- \ c_s) \} \tag{II-13}$$

These equations are similar to those derived by Kirkwood (5). They are not amenable to quantitative solution because there are seven unknowns L_{11}, L_{12}, L_{22}, U, c_s, γ_L and γ_s and only two equations. In the next section, we will incorporate further relationships between these variables so that the problem will be solvable quantitatively.

C. SPECIALIZED THEORY

We now proceed to reduce the theory to a form suitable for
quantitative solution of a wide range of chemico-osmotic diffusion
problems. We will sacrifice detailed description of the many facets
of the phenomena in order to arrive at tenable usable conclusions.
The accuracy of our development should be comparable to that of the
development of the Terzaghi consolidation theory. Consideration is
first given to a derivation of simple functional relationships for
the L coefficients. Hence we draw on the postulates and methods
of soil mechanics to finally simplify equations II-12 and II-13 to
solvable form.

1. Functional Relationships for the L Coefficients

Consideration of the physical significance of the L-coefficients
enables us to interpret and derive relationships for them. The diffusion
process is a quasi-static non-equilibrium process so that the L-coefficients
are not necessarily constants but they do have to be continuous functions.

a. L_{11}

If the solute concentration gradient is zero, or if there is
no chemico-osmotic coupling (i.e. $L_{12} = L_{21} = 0$), the only "force" is
the hydrostatic pressure gradient and equation II-9a reduces to

$$\bar{J}_L = L_{11} \, v_L \, \text{grad} \, (-U)$$

This equation is of the same form as Darcy's law which we know describes

the flow of liquid under a hydraulic pressure gradient in a porous
medium.

Hence we can relate L_{11} to the hydraulic permeability of
the soil, and as a first approximation we assume that it is a constant

b. $\underline{L_{12}}$ $(= L_{21})$

If there is no hydrostatic pressure gradient, equation
II-9a reduces to

$$\bar{J}_L = L_{12} \frac{RT}{c_s} \text{ grad } (-c_s)$$

This equation relates the flow of solution $\bar{J}_L$ to the solute concentration
gradient. $L_{12} \frac{RT}{c_s}$ is the "permeability" factor relating the flow to the
gradient. As a first approximation we assume that an osmotically induced
flow of solution is independent of the solute concentration; i.e., we
assume that the "osmotic permeability" factor is a constant. This is
accomplished by assuming that L_{12} is a linear function of solute con-
centration in the form

$$L_{12} (= L_{21}) = \frac{c_s}{c_{sm}} L_1 = x L_1 \qquad\qquad (II-14)$$

where L_1 is a constant and

c_{sm} is the maximum solute concentration occuring during the
diffusion process.

c. $\underline{L_{22}}$

If there is no hydrostatic pressure gradient and no coupling,

equation II-9b reduces to

$$\bar{J}_s = L_{22} \frac{RT}{c_s} \text{ grad } (-c_s)$$

This equation has the same form as Fick's law for the flow of a solute under a solute concentration gradient.

Hence we can relate L_{22} to the diffusion coefficient D, and as a first approximation, we assume that D is a constant. This implies that L_{22} should be a linear function of solute concentration in the form

$$L_{22} = x \ L_2 \tag{II-15}$$

where L_2 is a constant.

All of the above relationships are to be regarded as reasonable first approximations, always amenable to re-evaluation if experimental data indicates the need.

If we define

$$D \quad = L_{22} \frac{RT}{c_s} \left(\frac{cm^2}{sec} \right)$$

$$k_h \quad = L_{11} \ v_L^{\ 2} \ \gamma_w \left(\frac{cm}{sec} \right)$$

$$k_{ch} = L_{21} \ v_L \ \frac{\gamma_w}{x} \left(\frac{moles}{sec \ cm^2} \right)$$

$$k_{hc} = L_{12} \; \frac{RT \; v_L}{c_s} \left(\frac{cm^5}{sec \; mole} \right)$$

$$K_{ch} = k_{ch} + c_{sm} \; k_h \left(\frac{moles}{sec \; cm^2} \right)$$

$$D' = D + c_s \; k_{hc} \left(\frac{cm^2}{sec} \right) \tag{II-16}$$

and substitute in the one dimensional forms of (II-9a) and (II-9d), we

obtain, after noting that $c_L = \frac{1}{v_L}$,

$$\bar{J}_L = - \frac{k_h}{v_L} \frac{\partial h}{\partial y} - \frac{k_{hc}}{v_L} \frac{\partial c_s}{\partial y} \tag{II-17a}$$

$$\bar{J}_s = - x \; K_{ch} \frac{\partial h}{\partial y} - D' \frac{\partial c_s}{\partial y} \tag{II-17b}$$

Notice that if there is no solute concentration gradient or
if there is no coupling (i.e., $k_{hc} = k_{ch} = 0$) in the system, (II-17a)
reduces to Darcys láw.

If there is no hydrostatic pressure gradient and there is
no chemico-osmotic coupling, equation II-17b reduces to Ficks law
because in this case $J_s = J_D$ and $D' = D$. From equations II-9c and
II-16 we can derive a relationship between k_{hc} and k_{ch}.

From equation II-16

$$L_{12} = \frac{k_{hc}\ c_s}{RT\ v_L}$$

$$L_{21} = \frac{k_{ch}\ x}{v_L\ \gamma_w}$$

From equation II-9c, $L_{12} = L_{21}$, and therefore

$$\frac{k_{ch}\ x}{v_L\ \gamma_w} = \frac{k_{hc}\ c_s}{RT\ v_L}$$

i.e.,

$$k_{ch} = \frac{\gamma_w\ c_{sm}}{RT}\ k_{hc} \tag{II-18}$$

2. Solvable Diffusion Equations

The following assumptions, most of them deriving from soil mechanics, are invoked

a. The constitutive relationship for one-dimensional compression of a soil is commonly taken as

$$\Delta e = -\ a_v\ \Delta\sigma' \tag{II-19}$$

where a_v, the coefficient of compressibility, is assumed constant for small changes of effective stress. This assumption is made in the development of the Terzaghi consolidation theory (27).

b.   The effective stress σ', is defined by

$$\sigma' = \sigma - U \qquad \text{(II-20a)}$$

In chemico-osmotic diffusion problems the total stress is a constant and
for this case equations II-19 and II-20a yield

$$\Delta e = a_v \, \Delta U \qquad \text{(II-20b)}$$

c. $1 + e$ is assumed constant during the chemico-osmotic diffusion
process.   This assumption is made in the development of the Terzaghi
consolidation theory and represents the fact that the soil volume changes
little during the process.

d. c_L is assumed to be a constant because the solution is dilute
i.e.,

$$\frac{dc_L}{dt} = 0 \qquad \text{(II-20c)}$$

e.   As a first approximation we assume that

$$D' = D + c_s \, k_{hc} \qquad \text{(II-20d)}$$

is a constant for a particular soil-solution system.

Now by definition

$$\gamma_s = c_s \frac{e}{1 + e}$$

since $\frac{e}{1 + e}$ is the porosity of the soil and is a direct measure of the volume of pores, or solution, per unit volume of the soil. Hence differentiating with respect to time and remembering that $1 + e$ is a constant we obtain

$$\frac{\partial \gamma_s}{\partial t} = \frac{c_s}{1 + e} \frac{\partial e}{\partial t} + \frac{e}{1 + e} \frac{\partial c_s}{\partial t} \qquad \text{(II-21)}$$

Also by definition

$$\gamma_L = c_L \frac{e}{1 + e}$$

Differentiating with respect to time and remembering that $1 + e$ is a constant and incorporating (II-20c) we obtain

$$\frac{\partial \gamma_L}{\partial t} = \frac{c_L}{1 + e} \frac{\partial e}{\partial t} \qquad \text{(II-22)}$$

Differentiating (II-20b) with respect to time yields

$$\frac{\partial e}{\partial t} = a_v \frac{\partial U}{\partial t} \qquad \text{(II-23)}$$

Substituting (II-22) into (II-12) and specializing to the case of one-dimensional flow in the y-direction we obtain

$$\frac{c_L}{1 + e} \frac{\partial e}{\partial t} = \frac{\partial}{\partial y} \left\{ L_{11} \, v_L \, \frac{\partial U}{\partial y} + L_{12} \, \frac{RT}{c_s} \, \frac{\partial c_s}{\partial y} \right\}$$

Using (II-23) and (II-16) this becomes

$$\frac{\partial U}{\partial t} = c_v \, \frac{\partial^2 U}{\partial y^2} + \frac{1 + e}{a_v} \, k_{hc} \, \frac{\partial^2 c_s}{\partial y^2} \qquad\qquad \text{(II-24a)}$$

where $c_v = \dfrac{k_h \, (1 + e)}{a_v \, \gamma_w}$, the coefficient of consolidation.

Substituting (II-21) into (II-13) and specializing to the case of one-dimensional flow in the y-direction we obtain

$$\frac{c_s}{1 + e} \frac{\partial e}{\partial t} + \frac{e}{1 + e} \frac{\partial c_s}{\partial t} = \frac{\partial}{\partial y} \left\{ (L_{21} v_L + \frac{c_s}{c_L} L_{11} \, v_L) \, \frac{\partial U}{\partial y} \right.$$

$$\left. + (L_{22} \, \frac{RT}{c_s} + L_{12} \, \frac{RT}{c_L}) \, \frac{\partial c_s}{\partial y} \right\}$$

Using equations II-23, II-20d and II-16 this becomes

$$e \, \frac{\partial c_s}{\partial t} = \frac{1 + e}{\gamma_w} \, K_{ch} \, \frac{\partial}{\partial y} \, [x \, \frac{\partial U}{\partial y}] + (1 + e) \, D' \, \frac{\partial^2 c_s}{\partial y^2} - a_v \, c_s \, \frac{\partial U}{\partial t}$$

$$\text{(II-24b)}$$

For a given soil, solute, and solvent there are only three unknowns in equations II-24, i.e., U, c_s and e. By using Equation II-20b we have a three equation three unknown system which is amenable to quantitative

solution as described in Chapter III.

If there is no solute concentration gradient or no coupling, equation II-24a reduces to

$$\frac{\partial U}{\partial t} = c_v \frac{\partial^2 U}{\partial y^2}$$

which is the usual Terzaghi diffusion equation for one-dimensional consolidation.

If there is no hydrostatic pressure gradient and no chemico-osmotic coupling then equation II-24b becomes

$$\frac{\partial c_s}{\partial t} = \left(\frac{1 + e}{e} \right) D \frac{\partial^2 c_s}{\partial y^2}$$

Except for the factor $\frac{1 + e}{e}$ this equation is the same as the well known solute diffusion equation. This factor is the inverse of the porosity of the material. It reflects the fact that the diffusion coefficient D relates to the flow rate of solute per unit cross sectional area of solution; and for flow through a soil, the available cross sectional area normal to the flow direction is proportional to the porosity of the soil. From a practical point of view this factor is not very significant, however, because whereas diffusion coefficients often vary by orders of magnitude, porosities seldom vary by more than a few percent.

D. CHECKS ON DEVELOPMENTS

Before proceeding to a description of the solution of equations
II-24, it is instructive to examine two special cases and some available
data on the magnitude of coupling coefficients.

1. Comparison with van't Hoff's Law

Here we apply the specialized theory to the special case of
the osmotic pressure test and compare the result with van't Hoff's law.
The osmotic pressure test is composed of a semi-permeable membrane
of thickness Δy,

a. across which there is no flow at equilibrium $(\bar{J}_L = 0)$

b. which separates two solutions of the same solute and solvent

c. across which there is a solute concentration difference
equal to C

d. across which there is an equilibrium hydrostatic pressure
drop equal to the osmotic pressure π

Integrating II-17a across this membrane we obtain for the conditions
described above

$$0 = -\frac{k_h}{\gamma_w}\,\frac{\pi}{\Delta y} - k_{hc}\,\frac{C}{\Delta y}$$

$$\pi = -\frac{k_{hc}}{k_h}\,\gamma_w\,C \tag{II-25}$$

Comparing this with van't Hoff's equation for dilute solutions $\pi = RTC$, we notice that equation II-25 contains a negative sign whereas van't Hoff's equation does not. The work of Katchalsky and Curran (10), Olsen (22) and Abd-El-Aziz and Taylor (1) shows however, that k_{hc} (and therefore k_{ch}, L_{12} and L_{21}) must be negative. Hence equation II-25 has the same form as van't Hoff's law.

If the soil behaves as an ideal semi-permeable membrane separating dilute solutions, we obtain an appropriate value for the ratio k_{hc}/k_h by equating the coefficients of C in equations II-25 and van't Hoff's law to obtain

$$- \frac{k_{hc}}{k_h} \gamma_w = RT$$

i.e.,

$$\frac{k_{hc}}{k_h} = - \frac{RT}{\gamma_w} \tag{II-26}$$

Since this relationship is valid only for the case when the soil behaves as a perfect semi-permeable membrane, it provides an upper bound estimate for the ratio k_{hc}/k_h. Any real fine-grained soil will not behave as a perfect membrane in that transfer of solute from one side of the membrane to the other will occur. In other words any real fine-grained soil will be a leaky semi-permeable membrane.

2. The Case of Negligible Chemico-Osmotic Effects

Consider the case of a solution of uniform concentration diffusing under a hydrostatic pressure gradient only. If there is no chemico-osmotic coupling, the solute concentration does not change at any point, i.e., $\frac{\partial c_s}{\partial t} = 0$ and hence the solute concentration remains uniform, i.e., $\frac{\partial c_s}{\partial y} = 0$. For this case equations II-24a becomes

$$\frac{\partial U}{\partial t} = c_v \frac{\partial^2 U}{\partial y^2} \qquad\qquad\qquad (II-27a)$$

and equation II-24b becomes

$$0 = \frac{(1 + e)K_{ch}}{\gamma_w} \times \frac{\partial^2 U}{\partial y^2} - a_v c_s \frac{\partial U}{\partial t}$$

i.e.,

$$\frac{\partial U}{\partial t} = \frac{(1 + e)K_{ch}}{a_v \gamma_w} \frac{x}{c_s} \frac{\partial^2 U}{\partial y^2} \qquad\qquad (II-27b)$$

From a comparison of equations II-27a and II-27b and the knowledge that there is only one equation needed to describe the diffusion of solution under hydrostatic pressure gradients if chemico-osmotic effects are negligible, we obtain

$$c_v = \frac{(1 + e)}{a_v \gamma_w} \frac{K_{ch}}{c_s} x$$

-453-

But, by definition of c_v and K_{ch}

$$\frac{(1 + e)\ k_h}{a_v\ \gamma_w} = \frac{(1 + e)}{a_v\ \gamma_w}\ \frac{(k_{ch} + c_{sm}\ k_h)}{c_{sm}}$$

Thus

$$k_{ch} = 0$$

and from equation II-18 therefore

$$k_{hc} = 0$$

i.e., the coupling coefficients are both zero in a system displaying no chemico-osmotic coupling. This statement might seem trite, but it provides us with confidence that the theory is consistent with physical reality.

3. Comparison with Previous Work

Olsen (22, 23) has made some direct experimental measurements on chemico-osmotic coupling effects in fine-grained soils. His experiments provide data verifying the applicability of the principles of irreversible thermodynamics to a low concentration NaCl solution in a pure Kaolinite matrix. He has also made measurements of certain parameters which enable us to examine equation II-26.

His experiment consisted of the application of a solute concentration drop $C_B - C_A$ across a sample of Kaolinite of thickness

L and cross sectional area A, and the measurement of the hydrostatic
head drop ΔH, required across the sample to prevent any flow of solution,
Q/t through the sample.

The equation Olsen used was

$$\frac{Q}{t} = k_h \ A \ \left(- \frac{\Delta H}{L} \right) + k_c \ A \ \ell n \frac{(C_B/C_A)}{L} \qquad (II-28)$$

where k_h is the hydraulic permeability and k_c is the coupling coefficient
for hydraulic flow under a solute concentration gradient. For no flow
of solution this equation becomes

$$0 = k_h \ A \ \left(- \frac{\Delta H}{L} \right) + k_c \ A \ \left(\ell n \ \frac{C_B/C_A}{L} \right)$$

i.e.,

$$k_c/k_h = \Delta H / \ell n \ (C_B/C_A) \qquad (II-29)$$

Hence by dividing the head drop ΔH by $\ell n \ (C_B/C_A)$ he obtained experimental
values for the ratio k_c/k_h.

We will use equation II-26 to deduce theoretical values for this
ratio and then compare them with Olsen's measured values. First however,
we need a relationship between the theoretical ratio and Olsen's
measured ratio.

Comparing Olsen's flow equation II-28 with our flow equation
II-17a we notice two fundamental differences

-455-

a.   Our equation is in terms of gradients while Olsen's equation is in terms of differences. This discrepancy can be eliminated by integrating II-17a over the thickness of the soil sample. This does not effect the relation between our ratio and Olsen's ratio.

b.   Equation II-17a is in terms of grad $(- c_s)$ while Olsen's equation is in terms of $\ln (C_B/C_A)$. Now

$$\text{grad} (- \ln c_s) = \frac{1}{c_s} \ln (- c_s)$$

Hence our ratio should be multiplied by c_s before a numerical comparison can be made between the theoretical ratio and Olsen's ratio, i.e.,

$$\text{theoretical ratio} = \frac{RT\ c_s}{\gamma_w}$$

The NaCl concentration within Olsen's sample was 10^{-3} N, i.e.,

$$c_s = 10^{-3} \text{ N} = 10^{-6} \text{ moles/cc}$$
$$R = \cdot \qquad 8.3 \times 10^7 \text{ erg/°K/mole}$$
$$T = \qquad 300 \text{ °K}$$
$$\gamma_w = \qquad 10^3 \text{ dynes/cc}$$

Thus numerically the theoretical ratio $= \dfrac{8.3 \times 10^7 \times 300 \times 10^{-6}}{10^3}$

$$= 26 \text{ cms of } H_2O$$

Olsen measured values of k_c/k_h of from about 0.6 cms of H_2O increasing

to about 15 cms of water as the consolidation pressure varied from 1

to about 700 atmospheres.

It should be noted that as the consolidation pressure increases,

the void ratio of the soil decreases and it becomes a less "leaky"

semi-permeable membrane. As we saw in Section II-D-1, the theoretical

value refers to a non-leaky semi-permeable membrane. Hence a comparison

should be made between the theoretical value and the value Olsen

measured at the high consolidation pressure of 700 atmospheres.

In fact agreement is evident. We conclude therefore that the the-

oretical ratio provides an order of magnitude estimate of the chemico-

osmotic coupling effect in real soil-solution systems of the Kaolinite

-NaCl type at very high consolidation pressure.

However, most natural soils are at conslidation pressure considerably

lower than 700 atmospheres and are therefore probably leaky (c.f. Section

I-E-2), if semi-permeable. The measured ratio of k_c/k_h is directly

proportional to the osmotic pressure developed in the system, and in

leaky systems the osmotic pressure developed is less than in a non-leaky

system. This is probably why Olsen's measured values were less at

low consolidation pressure than at high consolidation pressure.

Hence the theoretical value, which refers to a non-leaky

system provides an upper bound for natural soils. The less leaky

the system, the closer should be the actual ratio to our theoretical

ratio.

Olsen's results indicate that void ratio, as reflected by consolidation pressure, has a significant effect on the degree of leakiness in a Kaolinite-NaCl solution system. Hence when using the theory for quantitative computation, it will be most accurate to use a value of k_{ch}/k_h measured in the soil-solution system under consolidation loads expected in the situation being considered. If void ratio changes are expected to be small, it would probably be adequate to assume k_{ch}/k_h constant for the computation.

III. COMPUTER ANALYSIS OF CHEMICO-OSMOTIC

FLOW AND CONSOLIDATION

A. INTRODUCTION

Having completed our theoretical development, we proceed to a
computer analysis of certain chemico-osmotic problems. Our purpose
is two-fold: firstly, to gain insight into the relative importance
of the different coefficients in equations II-26, and secondly, to
explore the chemico-osmotic diffusion process itself.

The development of two computer programs is outlined in detail.
These programs are then used to analyze specific chemico-osmotic
diffusion problems.

B. DEVELOPMENT OF FINITE DIFFERENCE EQUATIONS

1. Dimensionless Equations

In order that the results of our computer analyses be as general
as possible, it is necessary to write equations II-26 in dimensionless
form.

Hence, we define dimensionless parameters:

$$z = \frac{y}{H}$$

where H = drainage path length for the diffusion process

$$u = \frac{U}{U_{max}}$$

where U_{max} = maximum value of U occurring in the diffusion process

$$R_1 = \frac{c_v}{c_v} = 1.0$$

$$R_2 = \frac{(1 + e)}{a_v \, U_{max}} k_{ch} \, c_{sm}/c_v = \frac{(1 + e)}{a_v \, U_{max}} k_{hc} \, c_{sm} \left/ \frac{(1 + e) \, k_h}{a_v \, \gamma_w} \right.$$

$$= \frac{k_{hc}}{k_h} \, \gamma_w \, \frac{c_{sm}}{U_{max}}$$

$$R_3 = \frac{(1 + e) \, K_{ch}}{\gamma_w} \frac{U_{max}}{c_{sm}} \left/ c_v \right. = \frac{(1 + e)}{\gamma_w} \frac{U_{max}}{c_{sm}} \left(c_{sm} + \frac{k_{ch}}{k_h} \right) k_h \left/ \frac{k_h \, (1 + e)}{a_v \, \gamma_w} \right.$$

$$= a_v \, U_{max} \, (1 + k_{ch}/k_h \, c_{sm})$$

$$R_4 = (1 + e) \, D'/c_v = (1 + e) \, (D + c_s \, k_{hc})/c_v$$

$$R_5 = a_v \, U_{max}$$

$$T = c_v t/H^2 \tag{III-1}$$

This last relationship is the same as the Terzaghi relation between the time factor T and time for one dimensional consolidation. Substituting equations III-1 into equations II-24, and recalling that $x = c_s/c_{sm}$, we get from (II-24a)

$$\frac{U_{max}}{H^2/c_v} \frac{\partial u}{\partial T} = \frac{c_v \, U_{max}}{H^2} \frac{\partial^2 u}{\partial z^2} + \frac{k_{hc} \, (1 + e)}{a_v} \frac{c_{sm}}{H^2} \frac{\partial^2 x}{\partial z^2}$$

i.e.,

$$\frac{\partial u}{\partial T} = R_1 \frac{\partial^2 u}{\partial z^2} + R_2 \frac{\partial^2 x}{\partial z^2} \qquad \text{(III-2a)}$$

from (II-24b)

$$\frac{e \, c_{sm}}{H^2/c_v} \frac{\partial x}{\partial T} = \frac{(1 + e) \, K_{ch}}{\gamma_w} \frac{U_{max}}{H^2} \frac{\partial}{\partial z} \left(x \, \frac{\partial u}{\partial z} \right) + \frac{D'(1 + e)c_{sm}}{H^2} \frac{\partial^2 x}{\partial z^2}$$

$$- a_v \, c_s \frac{U_{max}}{H^2/cv} \frac{\partial u}{\partial T}$$

i.e.,

$$e \, \frac{\partial x}{\partial T} = R_3 \frac{\partial}{\partial z} \left(x \, \frac{\partial u}{\partial z} \right) + R_4 \frac{\partial^2 x}{\partial z^2} - R_5 \, x \frac{\partial u}{\partial T} \qquad \text{(III-2b)}$$

2. Explicit Finite Difference Equations

Herein we present the development of a computer program which
uses equations III-2 and II-20b to analyze the one-dimensional diffusion
of solute and solution in a soil sample (or layer) of thickness 2H.

The basis of the computational procedure is the solution of
finite difference approximations of equations III-2 and II-20b at a
finite number of points within the soil. The process is one dimensional
so that it is only necessary to consider points along one vertical line

-461-

extending from the top to the bottom of the sample. We choose NZINT + 1

(NZINT being an integer defined below) points on this vertical line, one

at each boundary and the others (NZINT-1) equally spaced inside the

sample.

At the start of the process, the two independent variables U

and X are assigned values at each one of these NZINT + 1 points. The

finite difference equations are then used to calculate values of U

and X at each one of these points at some small value, of dimensionless

time, ΔT, later. The calculation is then repeated, using the values of

U and X calculated for dimensionless time ΔT, to calculate values of U

and X at each one of these points at dimensionless time $2\Delta T$. The

process is repeated for $3\Delta T$, $4\Delta T$, etc., and the computation can be

terminated at any value of dimensionless time desired.

We now proceed to a more detailed description of some of the

elements of the computer program itself.

a. The Z-T Grid

For purposes of description, we make reference to the Z-T

grid shown in Fig. III-1. Each vertical line on the grid represents

the vertical line extending from top to bottom of the sample, at

different value of T. The integer variable I denotes the NZINT + 1

points on this line and I extends from 1 at the top to NZINT + 1 at

the bottom of the sample. The spacing between any two of the NZINT

+ 1 points being denoted Δz, and depicted in Fig. II-1. NZINT is

defined as the number of Δz layers into which the sample is divided.

Because the sample is 2 units of z thick, $\Delta z = 2/NZINT$.
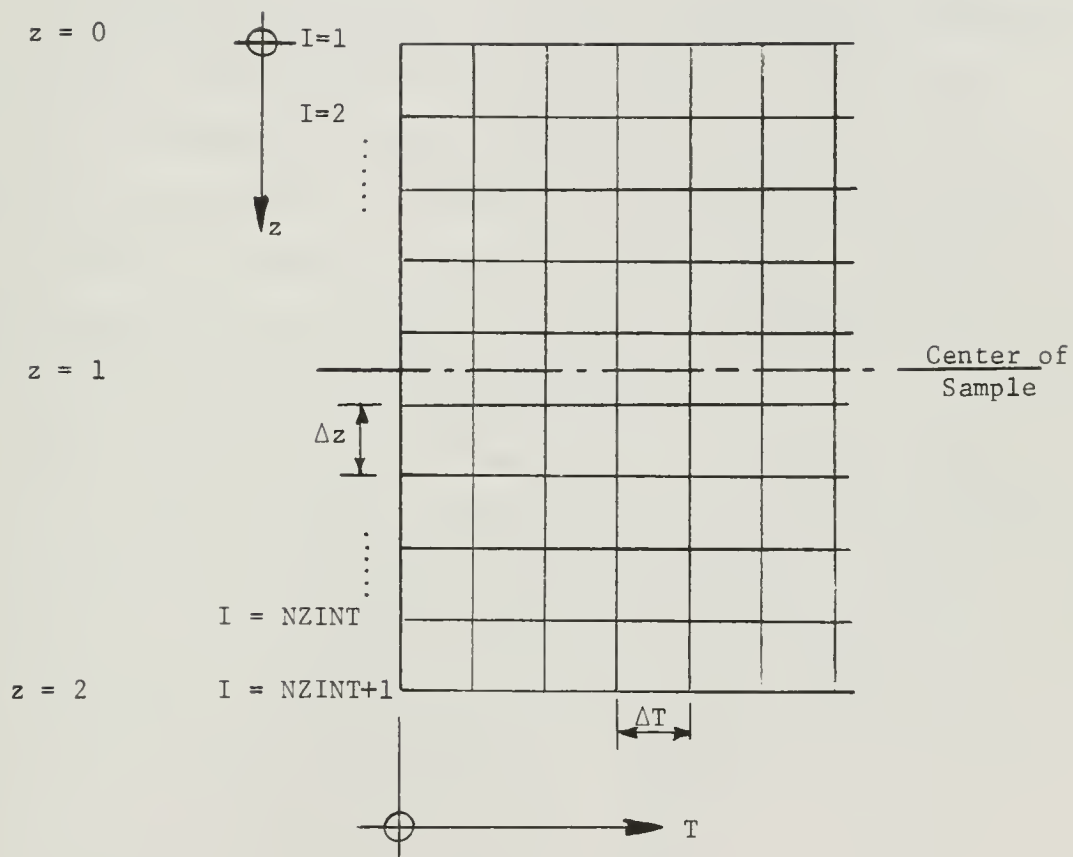
Fig. III-1.   The Z-T Grid

Adjacent vertical lines on the grid are separated by a small dimensionless time interval ΔT as depicted in Fig. III-1.

In any computation, values of ΔT and Δz have to be chosen small enough so that the approximations inherent in the finite difference method are good enough for the solution to be stable. This is discussed further later. A point of intersection of any two lines on the Z-T grid is known as a nodal point.
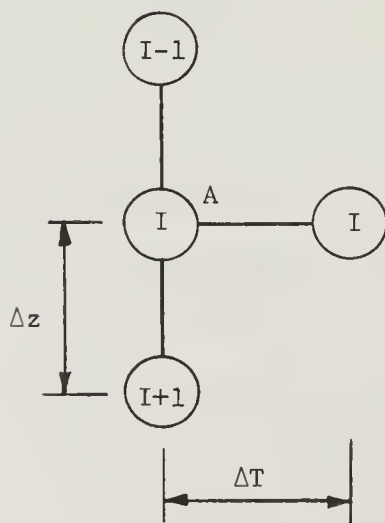
Fig. III-2. The Computational Molecule

To be able to write finite difference forms of equations III-2
which can be solved at any point on the Z-T grid (i.e., at any point
in the soil and at any time as ΔT and Δz tend to zero), we proceed
as follows.

The computational molecule in Fig.III-2 represents the config-
uration of nodal points on which the finite difference approximations
are based. The molecule is placed on the Z-T grid with its four atoms
on four grid nodal points. The molecule is moved up and down a vertical
line on the grid by varying the value of I in its atoms. It is moved
forward in time by replacing values of U and X in the atoms by those
calculated for later values of dimensionless time T.

When the molecule is at a general point, A, in the Z-T grid,
values of U are denoted by U(I-1), U(I) and U(I + 1) at the top middle
and lower atoms on the left; and by UV(I) at the atom on the right.
Corresponding values of X are X(I-1), X(I) and X(I + 1); and XV(I).

The various gradients of u and x at point A are approximated
by the following finite difference forms:

$$\frac{\partial u}{\partial T} = \Big(UV(I) - U(I) \Big)/\Delta T$$

$$\frac{\partial x}{\partial T} = \Big(XV(I) - X(I) \Big)/\Delta T$$

$$\frac{\partial x}{\partial z} = \Big(X(I + 1) - X(I - 1) \Big)/2\Delta z$$

$$\frac{\partial u}{\partial z} = \Big(U(I + 1) - U(I - 1) \Big)/2\Delta z$$

$$\frac{\partial^2 u}{\partial z^2} = \left[U(I + 1) - 2\,U(I) + U(I - 1) \right] / \Delta z^2$$

$$\frac{\partial^2 x}{\partial z^2} = \left[X(I + 1) - 2\,X(I) + X(I - 1) \right] / \Delta z^2$$

Also the following notation is used

$E(I)$ = void ratio at point A

$BETA = \Delta T / \Delta z^2$

Substitution of these finite difference forms into equations III-2 gives the finite difference approximations

$$UV(I) = U(I) + BETA \left\{ \left[U(I + 1) - 2U(I) + U(I-1) \right] \right.$$

$$\left. + R_2 \left[X(I + 1) - 2\,X(I) + X(I - 1) \right] \right\} \qquad \text{(III-3a)}$$

$$XV(I) = X(I) + \frac{BETA}{E(I)} \left\{ \frac{R3}{4} \left[\left(X(I + 1) - X(I - 1) \right)\left(U(I + 1) - U(I - 1) \right) \right. \right.$$

$$\left. + X(I) \left(U(I + 1) - 2\,U(I) + U(I - 1) \right) \right]$$

$$\left. + R_4 \left[X(I + 1) - 2\,X(I) + X(I - 1) \right] \right\} - \frac{R_5 X(I)}{E(I)} \left(UV(I) - U(I) \right)$$

$$\text{(III-3b)}$$

c. Solution Procedure

Firstly the initial values of U and X, U(I) and X(I)
I = 2, 3, ... NZINT; and the boundary values of U and X, U(I) and
X(I), I = 1 and NZINT + 1, are inserted on the Z-T grid.

Then values of U and X at T = ΔT, are calculated by
putting the computation molecule on the vertical line for T = 0
and calculating UV(I) and XV(I) from equations III-3 for I = 2, 3,
... NZINT.

Next UV(I) and XV(I) are renamed U(I) and XV(I) res-
pectively, for I = 2, 3 ... NZINT to save computer storage space.

The process is then repeated for T = 2ΔT, 3ΔT, etc.,
and is concluded whenever desired.

In order to keep the solution stable, it was found necessary
to keep Δz less than 0.2 and the parameter BETA = $\Delta T/\Delta z^2$ less than 0.5
(23, 27).

d. Computer program

A copy of an explicit finite difference computer program,
which solves the problem of chemico-osmotic diffusion of solute and
solution in a sample, with initial conditions

$$U(I) = UO$$
$$\qquad\qquad I = 2, 3 ... NZINT$$
$$X(I) = XO$$

and boundary conditions

```
U(I) = UF
                    I = 1 and NZINT + 1
X(I) = XF
```

is to be found in Appendix III-A. These boundary and initial conditions
represent the case of a horizontal soil sample or layer in which there
is initially no gradient of U or X; subject to a change of pore water
pressure (UF = UO) and solute concentration (XF - XO) at both its
boundaries.

It should be noted that this problem is symmetrical about
the centerline of the sample, and hence only half the sample is con-
sidered in the program. This is the reason for the appearance and
use of the parameter N (= (NZINT + 1)/2), through the program.

There are two variables in the program which require some
explanation. The first is the variable UC (appearing immediately after
statement 140 in the program) which is the dimensionless consolidation.
UC is denoted by U in Figs. III-4 to III-12, and is also sometimes
called the dimensionless solution inflow or excess pore pressure
dissipation, because by equations II-20b void ratio and pore water
pressure are linearly related. The value of UC at any time is defined
as the average pore pressure dissipation at that time divided by the
average pore pressure dissipation in the steady state. UC is analogous
to the degree of consolidation in normal soil mechanics usage.

The other variable is C which is the degree of solute inflow
and is denoted by C in Figs. III-4 to III-12. The value of C at any
time is defined as the amount of solute having flowed into the sample
at that time divided by the amount of solute having flowed into the
sample in the steady state.

The basis for calculating UC is now described. C is calculated in exactly the same manner. The pore pressure isochrone, ur u-z profile at some value of T is represented in Fig. III-3.
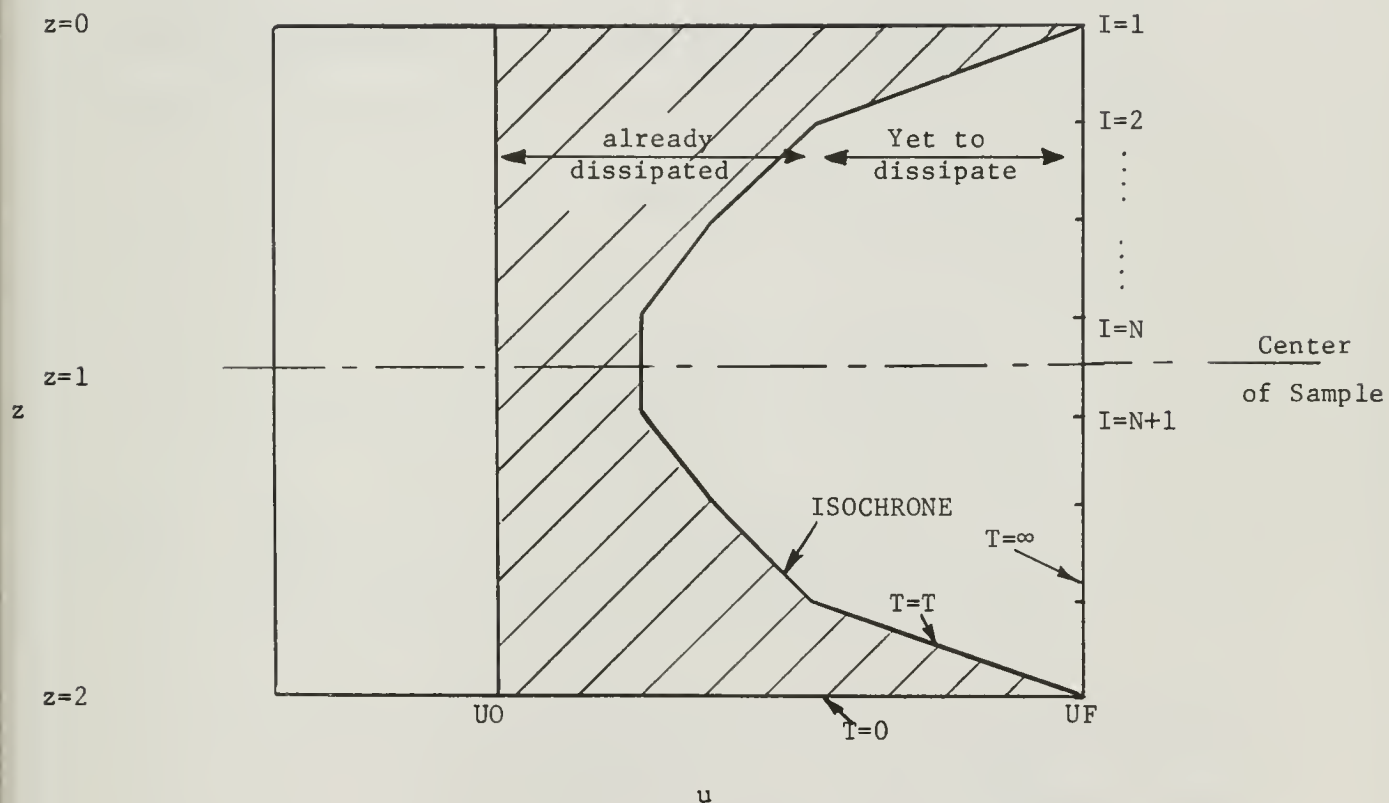
Fig. III-3. Isochrones in Chemico-Osmotic Consolidation

According to our above definition

$$UC = \frac{\text{shaded area}}{2.0 \ (UF - UO)}$$

Using the trapezoidal rule the shaded area is given by

$$2\Delta z \left(\frac{UF + U(1)}{2} + \frac{U(1) + U(2)}{2} + \ldots + \frac{U(N - 2) + U(N - 1)}{2} \right.$$

$$\left. + \frac{U(N) + U(N + 1)}{2} \right) - 2UO = 2 \ (UF - UO)$$

$$+ 2\Delta z \left[(1 - N) \ UF + \sum_{I = 2}^{N} U(I) \right]$$

$$UC = 1 - \frac{\Delta z}{(UF - UO)} \left[(N - 1) \ UF - \sum_{I = 2}^{N} U(I) \right] \qquad (III\text{-}4)$$

Equation III-4 is used for the calculation of both UC and C in the computer program.

The program is written so that it terminates calculation when both UC and C reach a value of .98. In other words the program terminates when both the dimensionless consolidation and the degree of solute inflow reach 98 percent.

3. Implicit Finite Difference Equations

At any point in the Z-T grid, the computational molecule in
Fig. III-2 yields two finite difference equations, (III-2) with two
unknowns UV(I) and XV(I). This two-equation two-unknown system can
be solved explicitly, or directly at any point in the grid. In the
development of the implicit method, we use the computational molecule
depicted in Fig. III-4. This molecule yields two finite difference
equations (III-6) produced below, with six unknowns UV(I - 1), UV(I),
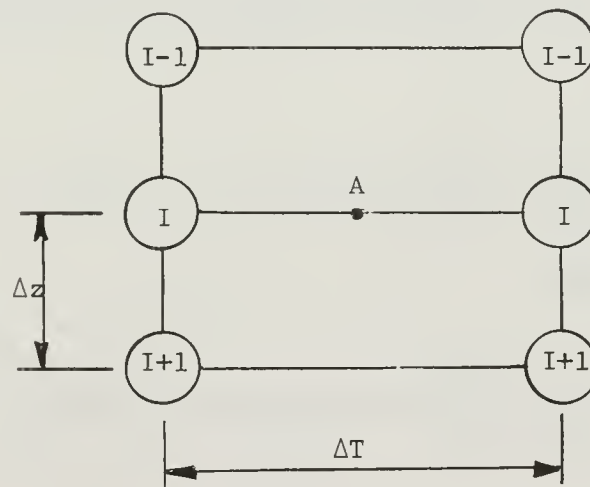
Fig. III-4. Implicit Computational Molecule

UV(I + 1), XV(I − 1), XV(I) and XV(I + 1). Hence equations III-6 cannot be solved explicitly at each point in the grid but have to be solved implicitly, or indirectly, as described in Appendix III-B.

In this case the finite difference approximations are based around point A and are

$$\frac{\partial U}{\partial T} = \left(UV(I) - U(I) \right) / \Delta T$$

$$\frac{\partial X}{\partial T} = \left(XV(I) - X(I) \right) / \Delta T$$

$$\frac{\partial U}{\partial z} = \frac{1}{2} \left\{ \frac{U(I + 1) - U(I - 1)}{2\Delta z} + \frac{UV(I + 1) - XV(I - 1)}{2\Delta z} \right\}$$

$$\frac{\partial X}{\partial z} = \frac{1}{2} \left\{ \frac{X(I + 1) - X(I - 1)}{2\Delta z} + \frac{XV(I + 1) - XV(I - 1)}{2\Delta z} \right\}$$

$$\frac{\partial^2 U}{\partial z^2} = \frac{1}{2} \left\{ \frac{U(I + 1) - 2U(I) + U(I - 1)}{\Delta z^2} \right.$$

$$\left. + \frac{UV(I + 1) - 2UV(I) + UV(I - 1)}{\Delta z^2} \right\}$$

-472-

$$\frac{\partial^2 X}{\partial z^2} = \frac{1}{2} \left\{ \frac{X(I + 1) - 2X(I) + X(I- 1)}{\Delta z^2} \right.$$

$$\left. + \frac{XV(I + 1) - 2XV(I) + XV(I - 1)}{\Delta z^2} \right\}$$

Substitution into equations III-2 yields

$$UV(I + 1) - 2(1 + \frac{1}{BETA}) \ UV(I) + UV(I - 1)$$

$$= - \ U(I + 1) - 2(1 - \frac{1}{BETA}) \ U(I) - U(I - 1)$$

$$+ \ 2R2 \ \{X(I + 1) - 2X(I) + X(I + 1)\} \qquad \text{(III-6a)}$$

and

$$\frac{XV(I - 1)}{2} \ \{R_4 - R_3 \ DEEU(I)\} \ - XV(I) \ \{R_4 - \frac{E(I)}{BETA} \}$$

$$+ \ \frac{XV(I + 1)}{2} \ \{R_4 + R_3 \ DEEU(I)\} = \frac{X(I - 1)}{2}\{-R_4 + R_3 \ DEEU(I)\}$$

$$+ \ X(I) \ \{R_4 + R_5 \ \cdot \ DEEUDT(I)/BETA$$

$$- \ E(I)/BETA - R_3 \ DEE2U(I)\}$$

$$- \ \frac{X(I + 1)}{2} \ \{R_4 + R_3 \ DEEU(I)\} \qquad \text{(III-6b)}$$

where $DEEU(I) = \frac{1}{8} \{U(I + 1) + UV(I + 1) - U(I - 1) - UV(I - 1)\}$

$$DEE2U(I) = \frac{1}{2} \{U(I + 1) + UV(I + 1) + U(I - 1) + UV(I - 1)$$

$$- 2U(I) - 2UV(I)\}$$

$$DEEUDT(I) = UV(I) - U(I)$$

Essentially the only difference between the computer program used for explicit finite difference equations, and that used for implicit finite difference equations, is in the method of solution of the finite difference equations. A copy of a program which uses equations III-6 to solve the chemico-osmotic diffusion problems described in the previous sections is presented in Appendix III-C.

Both the explicit and implicit computer programs were used to solve a few chemico-osmotic diffusion problems, and both gave exactly the same solutions. The implicit program, despite the greater complexity in its derivation, yielded the same solutions in about a quarter of the computation time because it provides stable solutions for values of BETA as large as 2.0. As noted above BETA cannot exceed 0.5 if the explicit program is to yield stable solutions.

4. Physical Interpretation of the R-Coefficients

The R-coefficients depend on the particular soil-solution system under consideration, and it is important that their physical significance be

explained, in order to be able to understand the results of the computer

analysis.

Equations III-2 depict these constants in their relationship to

the gradients effecting the diffusion process.

Equation III-2a

$$\frac{\partial u}{\partial T} = R_1 \frac{\partial^2 u}{\partial z^2} + R_2 \frac{\partial^2 x}{\partial z^2}$$

can be interpreted to mean that at any point in the soil-solution

system:

The rate of change of moles of solution per unit volume	=	The rate of change of moles of solution per unit volume due to solution flow under hydrostatic gradients	+	The rate of change of moles of solution per unit volume due to solution flow under solute concentration gradient

This interpretation derives from the fact that equation III-2a is actually

a statement of the law of conservation of mass applied to the solution.

In practice we measure pore water pressure rather than moles of solution

per unit volume and hence we usually interpret equation III-2a as

The rate of change of pore water pressure	=	The rate of change of pore water pressure due to solution flow under hydrostatic gradient	+	The rate of change of pore water pressure due to solution flow under solute concentration gradient

R_1 (= 1.0) is a constant for all systems, so that the larger R_2, the larger is the effect of a solute concentration gradient on the rate of change of pore water pressure relative to the effect of a hydrostatic pressure gradient on the rate of change of pore water pressure. This coupling between solute concentration gradient and the rate of change of pore water pressure is referred to as <u>chemico-osmotic coupling</u>. R_2 is referred to as the <u>chemico-osmotic coupling coefficient</u>. Now from Equation III-1

$$R_2 = \frac{k_{hc}}{k_h} \, \gamma_w \, \frac{c_{sm}}{U_{max}}$$

For given boundary conditions (i.e., a given ratio of $\frac{c_{sm}}{U_{max}}$) R_2 is proportional to $\frac{k_{hc}}{k_h}$. Hence R_2 can be considered as linearly dependent on the coupling coefficient k_{hc}, which is large for systems in which solute mobility is low; i.e., the chemico-osmotic coupling coefficient (and chemico-osmotic coupling) is high in non-leaky semi-permeable soil-solution systems.

Equation III-2b is

$$e \, \frac{\partial x}{\partial T} = R_3 \, \{\frac{\partial}{\partial z} \, (x \, \frac{\partial u}{\partial z})\} + R_4 \, \frac{\partial^2 x}{\partial z^2} - R_5 \, x \frac{\partial u}{\partial T}$$

and can be interpreted to mean that at any point in the soil-solution system,

The rate of change of moles of solute per unit volume of soil due to rate of change of moles of solute per unit volume of solution	=	The rate of change of moles of solute per unit volume of soil due to flow induced by hydrostatic pressure gradient	+	The rate of change of moles of solute per unit volume of soil due to flow induced by solute concentration gradient	−	The rate of change of moles of solute per unit volume of soil due to rate of increase of moles of solution per unit volume of soil because of rate of change of void ratio

Hence R_3, R_4 and R_5 are measures of the relative effects of hydrostatic pressure gradient, solute concentration gradient and change in void ratio, respectively, on the rate of change of moles of solute per unit volume of soil. From Equation III-1

$$R_3 = a_v\, U_{max}\, (1 + \frac{k_{ch}}{k_h\, c_{sm}})$$

For given boundary conditions, c_{sm} and U_{max} are fixed. In soil-solution systems which exhibit little coupling i.e., which are very leaky semi-permeable membranes, k_{ch} is very small so that the second term will be much smaller than unity.

Hence

$$R_3 \doteqdot a_v\, U_{max} \qquad\qquad\qquad (III-10a)$$

Now the larger R_3 the larger will be the rate of change of moles of solute induced by a hydrostatic pressure gradient. This together with equation

III-10a tells us that the larger the compressibility of soil, the larger will be the rate of change of moles of solute induced by a hydrostatic pressure gradient.

Physically this is because a flow of solution includes or "drags" solute with it, and thus contributes to the rate of change of moles of solute. This effect is known as drag coupling. The larger the compressibility of the soil, the larger will be the flow of solution induced by a given hydrostatic pressure gradient. Hence the larger will be the rate of change of moles of solute induced by drag coupling. In other words drag coupling increases as the soil compressibility increases. Drag coupling also increases as solute concentration increases simply because there is more solute to be "dragged" if the solute concentration is higher. R_3 is termed the drag coupling coefficient.

For soil-solution systems in which there is a large chemico-osmotic effect, i.e., for systems in which the soil is a non-leaky semi-permeable membrane, the term $\dfrac{k_{ch}}{k_h \, c_{sm}}$ will have a negative value smaller than unity; hence R_3 will be smaller than $a_v \, U_{max}$. Physically this means that drag coupling is low for systems in which the soil is a non-leaky semi-permeable membrane. This is because a given flow of solution "drags" less solute with it if the soil matrix acts as an efficient filter to the solute. In a perfectly non-leaky membrane there can be no drag coupling by definition, and hence R_3 should be zero. This is shown in the next section.

From physical considerations we expect the drag coupling coefficient, R_3, to remain positive because if this were not true, a flow of solution in one direction could induce a flow of, or "drag" solute in the opposite direction, a phenomenon which does not seem possible.

For R_3 to remain positive

$$a_v \, U_{max} \, (1 + \frac{k_{ch}}{k_h \, c_{sm}}) \geqslant 0$$

Since all the parameters in this inequality are positive except k_{ch}, it will be true if

$$k_h \geqslant | \frac{k_{ch}}{c_{sm}} | \qquad\qquad \text{(III-8)}$$

where $| \; |$ denotes the absolute value

From Equation III-1

$$R_4 = (1 + e) \, (D + c_s \, k_{hc})/c_v$$

For a soil in which there is negligible chemico-osmotic coupling, the term $c_s \, k_{hc}$ is very small so that

$$R_4 \; \fallingdotseq \; \frac{(1 + e) \, D}{c_v} \; ;$$

i.e., the larger the ratio of the diffusion constant D to the coefficient of consolidation c_v, the larger will be the rate of change of moles of

solute per unit volume of soil induced by the solute concentration

gradient. Physically this means that the higher the diffusion coefficient

D, the greater will be the flow of solute induced by a given solute

concentration gradient.

In the case where chemico-osmotic coupling is significant, the

term $c_s k_{hc}$ will be negative and less than unity, so that R_4 will be

smaller than $(1 + e) D/c_v$. Physically this means that a given solute

concentration gradient is less able to cause a flux of solute when the

soil matrix acts as a filter to the solute. As with R_3, we do not

expect R_4 to become negative i.e., we expect

$$D \geq c_s |k_{hc}| \qquad\qquad\qquad (III-9)$$

From Equation III-1

$$R_5 = a_v U_{max}$$

R_5 is a measure of the effect of the rate of change of void

ratio on the rate of change of moles of solute per unit volume of soil.

For given boundary conditions U_{max} is a constant so R_5 is directly

proportional to the compressibility of the system. Hence the greater

the compressibility the greater the effect of rate of change of void

ratio on the rate of change of moles of solute per unit volume of

soil.

Physically this coupling is due to the fact that a change in

void ratio causes a change in moles of solution per unit volume and

consequently a change in moles of solute per unit volume of soil.

We refer to the phenomenon as <u>void ratio coupling</u>; and to R_5 as the <u>void ratio coupling coefficient</u>. Essentially void ratio coupling can be considered as coupling between change in solute concentration per unit volume of soil due to change in void ratio. From the above discussion, we conclude that void ratio coupling increases as compressibility increases. For the same reason that drag coupling increases as solute concentration increases, void ratio coupling increases as solute concentration increases, even though the void ratio coupling coefficient is independent of solute concentration.

5. Numerical Values for R-Coefficients

Equations III-1 express the R-coefficients in terms of more basic parameters. We now assign numerical values to these parameters, and thereby calculate numerical values for the R-coefficients. The purpose of this is to find a range of values representative of real soil-solution systems so that the results of .our computer analyses will be realistic.

The most accurate method of obtaining qualitative results for a particular soil-solution system would of course be to measure k_h, D, k_{hc}, k_{ch}, c_v, U_{max}, and c_{sm} directly and thence to calculate the R-coefficients to be used in the computations. Values of k_h, D, U_{max}, c_v and c_{sm} are relatively easily determined for any given case, and typical ranges of k_h and c_v are quite well known for different soils. On the other hand little is known concerning the magnitudes of k_{hc} and k_{ch}. Olsen's data (22, 23) cited earlier, are all that are known to

the writer. Careful and complex experimentation is required for determination of k_{ch} and k_{hc}.

a. Direct Assumption of Values

Firstly we express the R-coefficients in terms of more basic parameters by substituting equations II-18 and II-26 in (III-1).

Note that (II-26) is based on Van't Hoffs law, i.e., it is based on the assumption of an ideal non-leaky semi-permeable membrane. Hence the values which we derive for the R-coefficients will represent an ideal non-leaky semi-permeable membrane.

Substitution of (II-18) and (II-26) into (III-1)

$$R_1 = 1.0$$

$$R_2 = \frac{k_{hc}}{k_h} \gamma_w \frac{c_{sm}}{U_{max}} = - \frac{RT \ c_{sm}}{U_{max}}$$

from (II-26),

$$R_3 = a_v \ U_{max} \left(1 + \frac{k_{ch}}{k_h \ c_{sm}}\right) = a_v \ U_{max} \left(1 + \frac{k_{hc}}{k_h} \frac{\gamma_w}{RT}\right)$$

from (II-18),

$$= a_v \ U_{max} \ (1 - 1)$$

from (II-26), i.e.,

-482-

$$R_3 = 0$$

$$R_4 = (1 + e)(D + c_s k_{hc})/c_v$$

$$= (1 + e)(D - RT \frac{c_s k_h}{\gamma_w})/c_v$$

from (II-26)

$$R_5 = a_v U_{max} \qquad\qquad\qquad\text{(III-1a)}$$

Note that R_3 is zero for an ideal non-leaky membrane, i.e., there is no drag coupling in a non-leaky membrane.

Next we assign numerical values to the quantities in the above equations

$\gamma_w \doteqdot 10^3$ dynes/cm^3

T = absolute temperature $\simeq 300°K$

R = gas constant $= 8.317 \times 10^7$ erg/mole/$°K$

a_v = coefficient of compressibility = 0.01 to 1.0 cm^2/kg

$\quad= 10^{-8}$ to 10^{-6} cm^2/dyne

D = diffusion coefficient $= 10^{-7}$ to 10^{-5} cm^2/sec (15, 12)

c_{sm} = highest change in solute

concentration occuring

during the diffusion process $= 10^{-3}$ to 1.0 N

$\quad= 10^{-6}$ to 10^{-3} mole/cc

U_{max} = maximum change in hydrostatic

pressure occurring during the

diffusion process $\quad\quad\quad\quad$ = .005 to 500 psi

$\quad\quad\quad\quad\quad\quad\quad\quad\quad\quad\quad\quad$ = 10^3 to 10^8 dynes/cm^2

$c_v\quad$ = 10^{-4} to 1.0 cm^2/sec

$k_h\quad$ = 10^{-9} to 10^{-6} cm/sec

Substituting these values into (III-1a) gives

R_1 = 1.0

$$R_2 = -\frac{8.317 \times 10^7 \times 300 \times (10^{-6} \text{ to } 10^{-3})}{(10^3 \text{ to } 10^8)} \sim -(.0001 \text{ to } 10,000)$$

R_3 = 0

$$R_4 \sim [(10^{-7} \text{ to } 10^{-5})$$

$$-\frac{3.817 \times 10^7 \times 300 \times (10^{-6} \text{ to } 10^{-3}) \times (10^{-9} \text{ to } -10^{-6})}{10^3}]$$

$$/(10^{-4} \text{ to } 10) = 0 \text{ to } + 0.1$$

$$R_5 = (10^{-8} \text{ to } 10^{-6}) (10^3 - 10^8) = .00001 \text{ to } 100$$

It should be remembered that these ranges of numerical values for the
R-coefficients are only intended as a rough guide to actual values.

b.   Values Based on Olsen's Empirical Data

Olsen (22, 23) has made some direct experimental measurements
of the coupling effects of NaCl and water flowing in Kaolinite.   We will
substitute Olsen's data into equation III-1 to obtain values for the R-
coefficients which refer to a NaCl solution-Kaolinite system

As described in II-D-3, Olsen measured the variation of k_h
and the ratio $\dfrac{c_s\, k_{hc}}{k_h}$ as a function of consolidation pressure ranging
from 1 to 700 atmospheres.   At low consolidation pressure (= 1 atmosphere)
he measured

$$-\frac{c_s\, k_{hc}}{k_h} \doteq -\,0.6 \ \text{cm} \ H_2O$$

$$k_h \doteq 10^{-6} \ \text{cm/sec}$$

$$\therefore \ c_s\, k_{hc} \doteq -\,0.6 \times 10^{-6} \ \text{cm}^2/\text{sec}$$

At high overburden pressure (= 700 atmospheres), he measured

$$\frac{c_s\, k_{hc}}{k_h} \doteq -\,30 \ \text{cm} \ H_2O$$

$$k_h \doteq 10^{-9} \ \text{cm/sec}$$

$$\therefore \ c_s\, k_{hc} \doteq -\,0.3 \times 10^{-7} \ \text{cm}^2/\text{sec}$$

The concentration of NaCl solution within Olsen's sample was 10^{-6} mole/cc

Substitution of these values and estimates of D, c_v, a_v, and U_{max} into equation III-1 gives, at low overburden pressure

$$R_1 = 1.0$$

$$R_2 = c_{sm} \frac{k_{hc}}{k_h} \frac{\gamma_w}{U_{max}} = -0.6 \times \frac{10^3}{10^3} = -0.6$$

$$R_3 = a_v U_{max} (1 + \frac{\gamma_w}{RT} \frac{c_s}{c_s} \frac{k_{hc}}{k_h} \qquad \text{from (II-18)}$$

$$= 10^{-6} \times 10^3 (1 = \frac{10^3}{8.317 \times 10^7 \times 300 \times 10^{-6}} \times 0.6)$$

$$= 10^{-3} (1 - .03) \sim 0.001$$

$$R_4 = (1 + e) (D + c_s k_{hc})/c_v \doteq (10^{-5} - 10^{-6})/10^{-2} \sim .001$$

$$R_5 = a_v U_{max} \doteq 10^{-6} \times 10^3 \sim .001$$

At high overburden pressure

$$R_1 = 1.0$$

$$R_2 = -30 \times \frac{10^3}{10^5} = -0.3$$

$$R_3 = 10^{-8} \times 10^5 (1 - \frac{10^3}{2 \times 10^4} \times 30) \sim .001$$

$$R_4 \doteq (10^{-7} - 0.3 \times 10^{-7})/10^{-4} \sim .001$$

$$R_5 \doteq 10^{-8} \times 10^{5} \sim .001$$

These numerical values for the R-coefficients will be used in the theoretical investigation of chemico-osmotic consolidation described in Section III-C and in the Oxnard Basin described in Chapter IV.

6. Proof that $L_{11} L_{22} - L_{12} L_{21} \geqslant 0$

As noted in Section II-B-2, the determinant of the matrix of the L-coefficients must be positive definite if Onsager's reciprocal relation is to be valid for the system, i.e., $L_{11} L_{22} - L_{12} L_{21} \geqslant 0$ must be true. We substitute the relations

$$L_{11} = k_h/v_L^2 \, \gamma_w$$

$$L_{22} = D \, c_s/RT$$

$$L_{12} = k_{hc} \, c_s/RT$$

$$L_{21} = k_{ch} \, x/v_L \, \gamma_w$$

From equation II-17 into the above inequality to obtain:

$$\frac{k_h}{v_L^2 \, \gamma_w} \frac{D \, c_s}{RT} - \frac{k_{hc} \, c_s}{RT \, v_L} \frac{k_{ch} \, x}{v_L \, \gamma_w} \geqslant 0$$

or

$$k_h \, D - k_{hc} \, k_{ch} \, x \geqslant 0$$

-487-

Thus

$$k_h \, D \geqslant k_{hc} \, k_{ch} \, x$$

and

$$k_h \, D \geqslant c_s \left| k_{hc} \right| \frac{\left| k_{ch} \right|}{c_{sm}} \qquad\qquad (III\text{-}10)$$

because both k_{hc} and k_{ch} are negative.

To prove that $L_{11} \, L_{22} - L_{12} \, L_{21} \geqslant 0$ we have to prove equation III-10.

Multiplying equation III-8 by D we get

$$k_h \, D \geqslant D \frac{\left| k_{ch} \right|}{c_{sm}}$$

and using equation III-9 we obtain

$$k_h D \geqslant c_s \left| k_{hc} \right| \frac{\left| k_{ch} \right|}{c_{sm}}$$

We have called upon our experience of the chemico-osmotic diffusion process to derive (III-8) and (III-9) and hence deduced (III-10), i.e., we have used physical arguments to show that the determinant of the L-coefficients must be positive definite for soil-solution systems.

C. CHEMICO-OSMOTIC CONSOLIDATION

Chemico-osmotic consolidation is induced when the concentration of the solution in contact with a boundary of a soil mass initially in equilibrium with its environment is increased. If the soil-solution system exhibits chemico-osmotic coupling, this tends to "suck" solution out of the soil pores by chemico-osmotic diffusion, and hence the soil tends to consolidate. If the flow of solute and solution is one-dimensional, the process can be referred to as one-dimensional chemico-osmotic consolidation.

One dimensional chemico-osmotic consolidation was simulated on the computer by using the implicit computer program (c.f. Section III-B-2) with initial conditions

$$x = XO < 1.0 \text{ for } o < z < 2$$
$$u = UO = 1.0 \qquad t = 0$$

and boundary conditions

$$x = XF = 1.0 \text{ for } z = 0, z = 2$$
$$u = UF = 1.0 \qquad t \geqslant 0$$

(see Section III-B-2) i.e., there is no change in hydrostatic pressure at the boundaries, but there is a solute concentration increase at the boundaries at time zero.

ΔT was chosen as .05 and the number of Δz intervals on the grid in Fig. III-1 was chosen as 9. The process was simulated for various types of soils by varying R_2, R_3, R_4 and R_5, and for different initial conditions by varying XO.

1. Results of Analysis of Chemico-Osmotic Consolidation

The results of the computer analysis are presented in the form of U vs log T and C vs log T curves in Figs. III-5 and III-7 to III-11. Note that U is a measure of consolidation and C is a measure of the degree of solute inflow. (Both of these parameters were defined exactly in Section III-B-3.) The ranges of variation of the R-coefficients in Figs. III-5 and III-7 to III-11 are

$$R_2 \ : \ - \ .01 \ \text{to} \ - \ 1.0$$
$$R_3 \ : \ .00001 \ \text{to} \ 0.1$$
$$R_4 \ : \ .000001 \ \text{to} \ 0.1$$
$$R_5 \ : \ .0001 \ \text{to} \ 0.1$$

These ranges are within those deduced in Section III-B-4.

From the results in Figs. III-5 and III-7 to III-11, two general observations may be made. Firstly the solute diffusion process manifests itself as a smooth continuous flow of solute into the sample, i.e., smooth increase of C with T. It may be noted incidentally that C starts at 0.11 instead of 0.0 at very low values of T. This is because of the inaccuracy inherent

in the finite difference approximations in equation III-4.

Secondly chemico-osmotic consolidation as reflected by the variation of U with T builds smoothly to a maximum after which it tends to decrease smoothly to zero, reaching equilibrium at about the same time as the solute diffusion process; i.e., U first increases smoothly to a maximum value, and then decreases to zero again.

There are exceptions to this rule however. Curves 4, 5 and 6 in Fig. III-5 show a chemico-osmotic consolidation which increases smoothly to a maximum value and then stays there.

Curves 4, 5 and 6 in Fig. III-5 represent systems with very low values of R_3 and R_4, and high values of R_5. In other words they represent systems of very low drag coupling and solute diffusion, but high chemico-osmotic coupling. According to the concepts developed in Section III-B-6, such systems tend to behave as non-leaky semi-permeable membranes. Hence curves 4, 5 and 6 in Fig. III-5 represent non-leaky semi-permeable membranes and all the other curves in Figs. III-5 and III-7 to III-11 represent leaky semi-permeable membranes.

We now provide a description of the chemico-osmotic diffusion process responsible for the chemico-osmotic consolidation and solute inflow curves in Figs. III-5 and III-7 to III-11.

First we consider the non-leaky semi-permeable system represented by curve 4 in Fig. III-5. For this purpose we make reference to Fig. III-6a which shows isochrones corresponding to curves 4 in Fig. III-5. The pressure isochrones are plots of dimensionless pore water pressure, u vs

dimensionless sample thickness, z, for various values of dimensionless

time. T. The solute concentration isochrones concentration x are plots of

dimensionless solute vs. dimensionless sample thickness H, for various values

of dimensionless time, T. Both diagrams are symmetrical about the center line

of the soil sample (z = 1.0) because the initial and boundary conditions are

both symmetrical about the center line of the sample

$$\left.\begin{matrix} \text{Initially } u = 1.0 \\ \text{and} \qquad x = .01 \end{matrix}\right\} \quad \text{for all } z$$

In other words, there is a uniform initial pore pressure and solute

concentration in the sample. At the start of the process, T = 0, x

is increased from 0.01 to 1.0 at z = 0 and z = 2.0. In other words

the solute concentration is increased one hundred fold at both sample

boundaries. The effect of this is to create an osmotic pressure difference

between the solution just inside the sample boundary and the outside solution.

In Fig. 6a this is represented by a decrease in dimensionless pore pressure,

u, from 1.0 to 0.5. It is this osmotic pressure drop that results in con-

solidation.

The magnitude of osmotic pressure difference in any real case depends

on the coupling properties of the soil. In the case when the soil behaves

as a non-leaky but compressible membrane water will flow out until the

osmotic pressure tending to suck water out is balanced by a return hydrostatic

pressure gradient tending to cause flow in the reverse direction. At equi-

librium there will be no flow of solution and $\bar{J}_L = 0$ at the sample boundary.

Hence from equation II-17a

$$- \frac{k_h}{v_L \, \gamma_w} \, \Delta U' + \frac{k_{hc}}{v_L} \, \Delta c_s = 0$$

where $\Delta U' - h\gamma_w$ = difference in hydrostatic pressure between the solution

and interior of the membrane, and Δc_s is the concentration difference. Thus

$$\Delta U' = + \frac{k_{hc}}{k_h} \, \gamma_w \, \Delta c_s \qquad \qquad \text{(III-11a)}$$

The actual amount of consolidation accompanying this development of $\Delta U'$ will

depend on the soil compressibility, a_v. Equation III-11a indicates that

the chemico-osmotically induced pore pressure drop at the same boundary

is proportional to the coupling coefficient k_{hc}, and to the increase in

solute concentration at the sample boundary; it is inversely proportional

to the hydraulic permeability of the soil. It should be borne in mind that

$\Delta U'$ represents the pore pressure induced in a non-leaky or perfect semi-

permeable membrane. Since real soils will be leaky membranes, other

factors will influence the behavior as will be discussed in connection

with Figs. III-5 to III-11.

To derive an expression for the chemico-osmotically induced

dimensionless pore pressure drop at the sample boundary we recall that

$$\Delta u' = \Delta U'/U_{max}$$

and

$$\Delta x = \Delta c_s/c_{sm}$$

where U_{max} and c_{sm} are the maximum pore pressure and solute concentration respectively during the diffusion process. Substitution in equation III-11a yields

$$\Delta u' = \frac{k_{hc}}{k_h} \gamma_w \frac{U_{max}}{c_{sm}} \Delta x$$

i.e.,

$$\Delta u' = R_2 \Delta x \qquad \text{(III-11b)}$$

from equation III-1.

In Fig. III-6a $\Delta X = .99$ and $R_2 = 0.5$. Hence the chemico-osmotically induced dimensionless pore pressure drop at the sample boundary $\Delta u' = 0.5 \times .99 = 0.5$, as we noted above. The drop of pore pressure just inside the sample boundary does not change as time proceeds so that as far as the pore pressure conditions inside the sample are concerned, it is equivalent to a drop of u of 0.5 at the sample boundary at $T = 0$.

Hence as far as the diffusion process is concerned, the boundary conditions are

$$\left.\begin{array}{l} x = 1.0 \\ \\ u = 0.5 \end{array}\right\} \; z = 0, \; Z, \; T \geqslant 0$$

Thenceforth solute concentration remains unchanged because the system is non-leaky so that solute mobility is zero. Consequently the solute
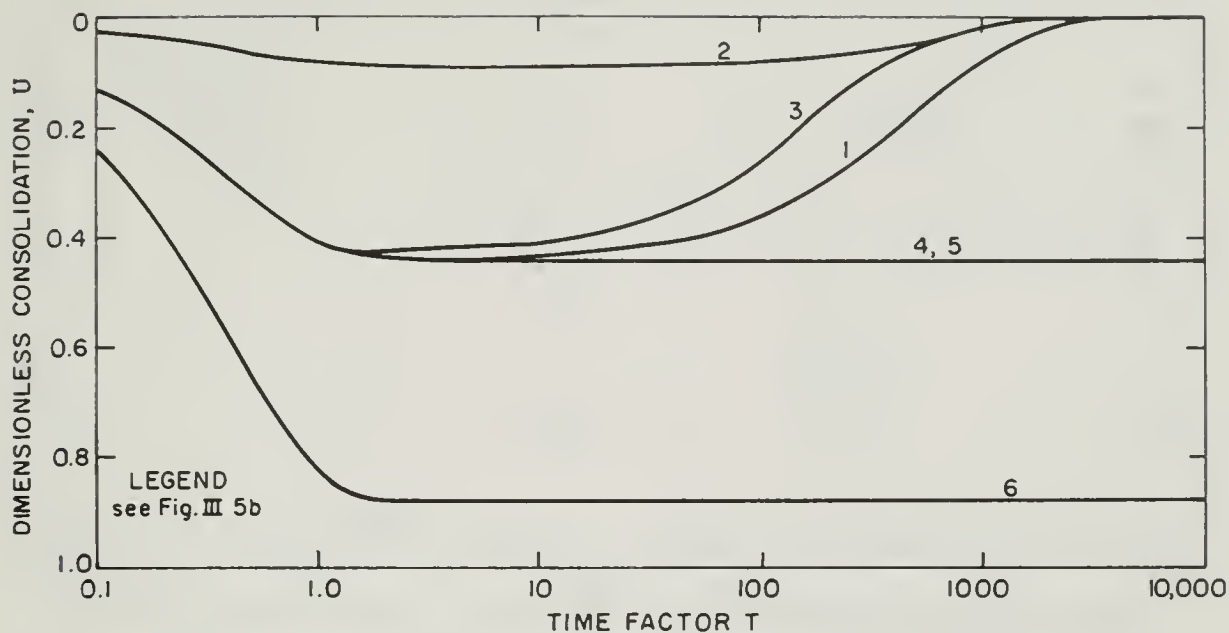
Fig. III-5a. Chemico-osmotic consolidation in leaky
and non-leaky soils
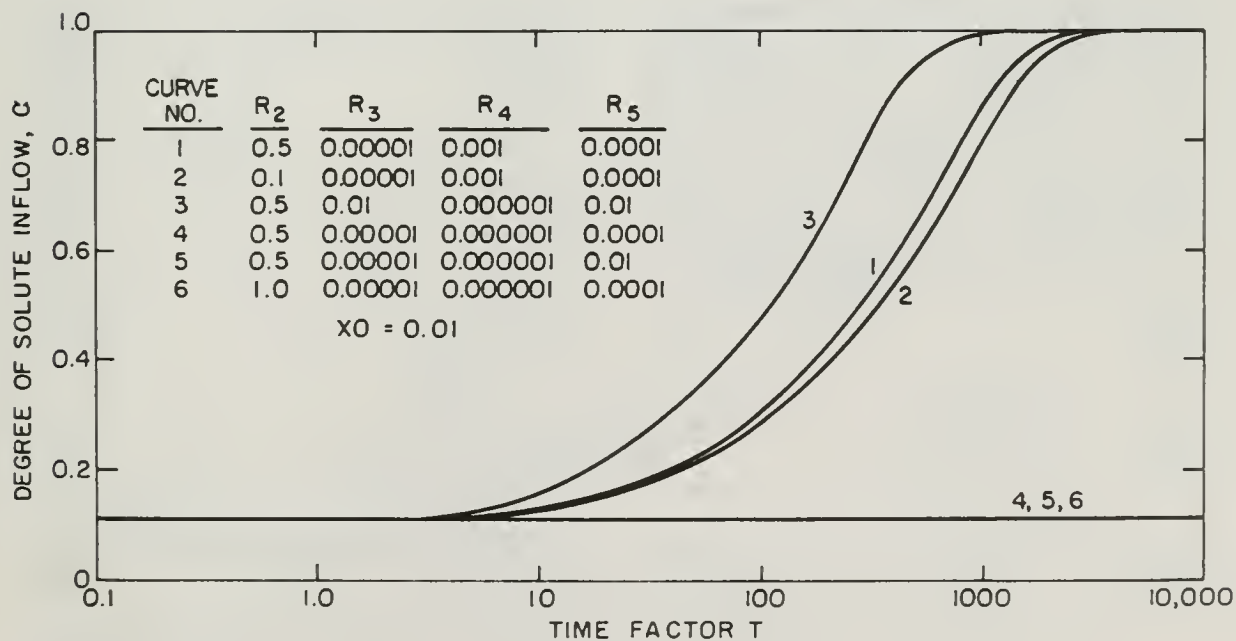
Fig. III-5b. Solute inflow in leaky and non-leaky soils
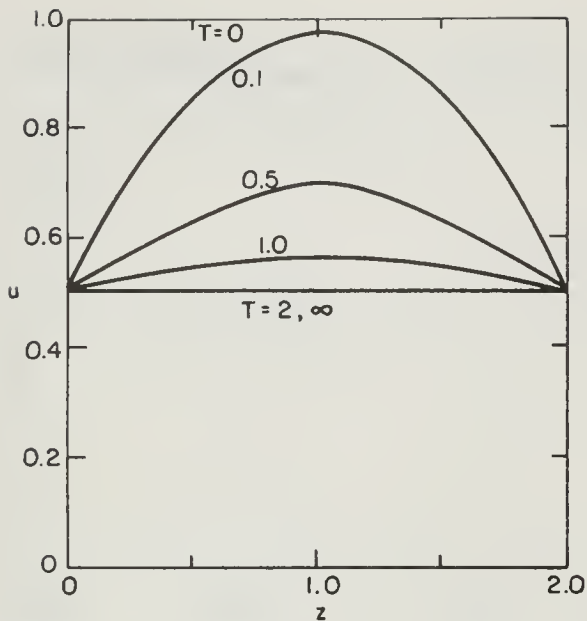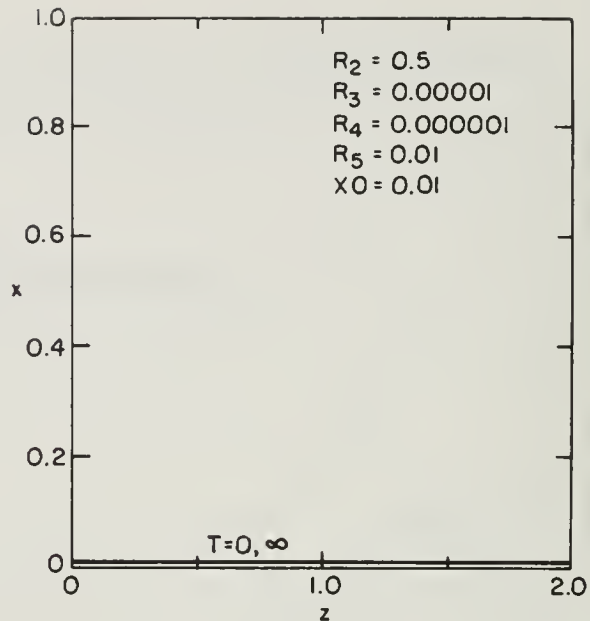
Fig. III-6a. Isochrones for a non-leaky semi-permeable system
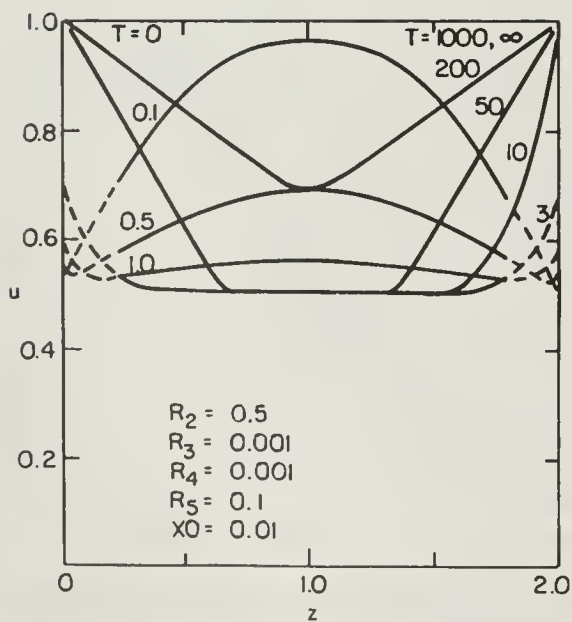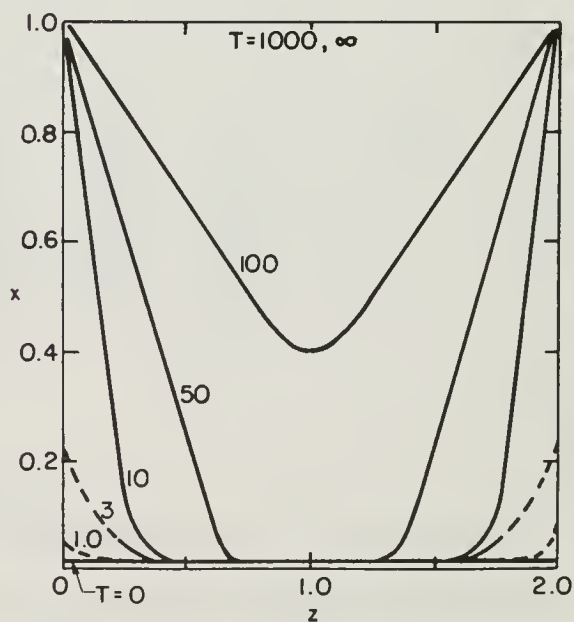
Fig. III-6b. Isochrones for a leaky semi-permeable system
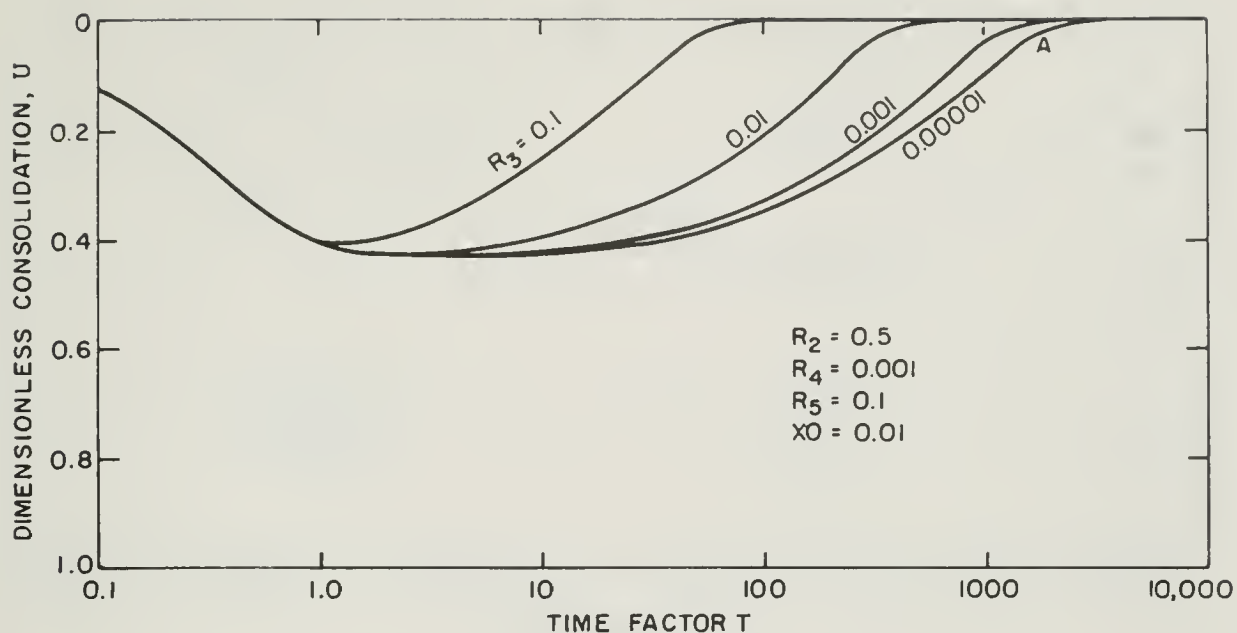
Fig. III-7a.   Effect of drag coupling on chemico-osmotic
consolidation
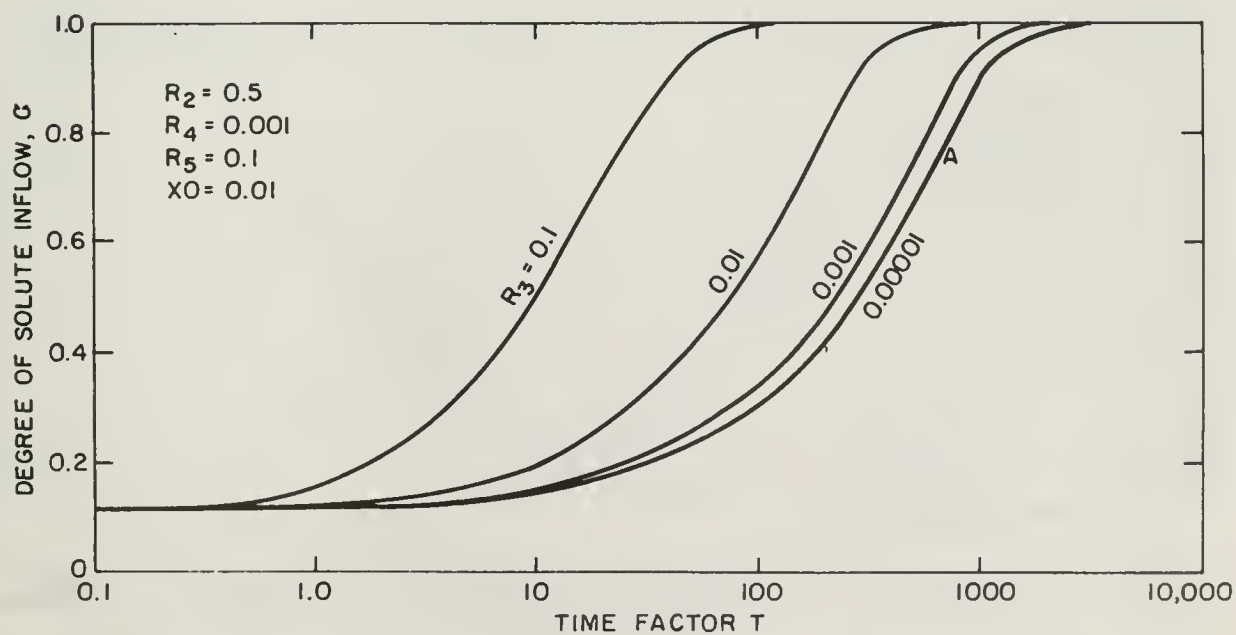
Fig. III-7b.   Effect of drag coupling on solute inflow
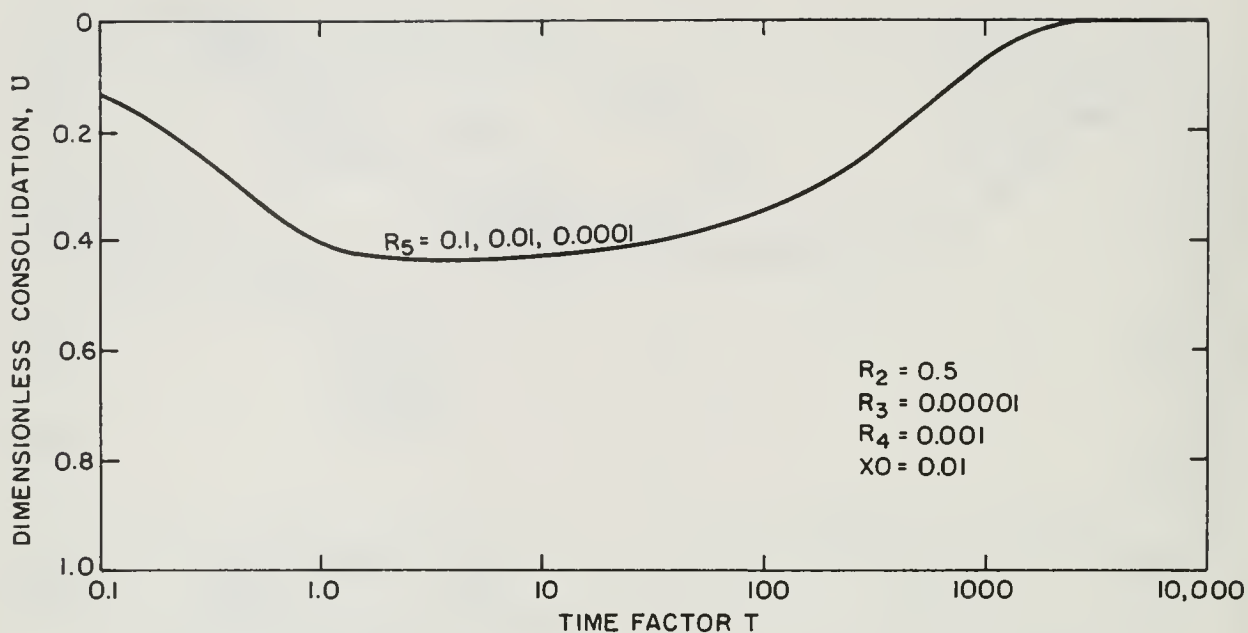
Fig. III-8a.   Effect of void ratio coupling on chemico-osmotic coupling
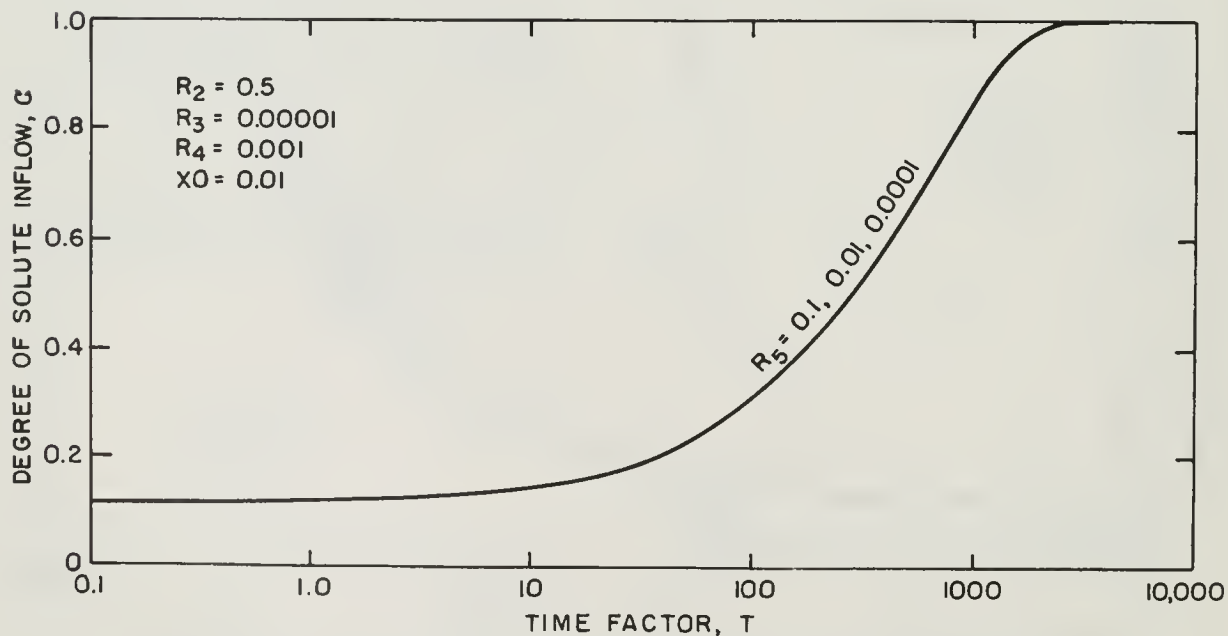
Fig. III-8b.   Effect of void ratio coupling on solute inflow
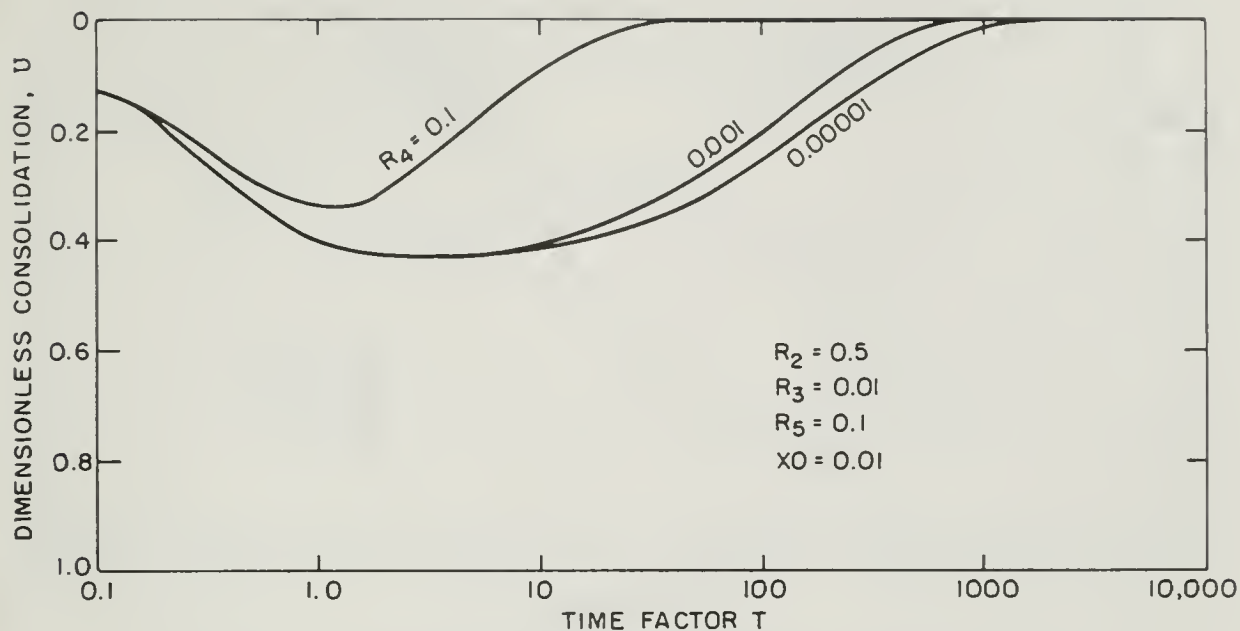
Fig. III-9a. Effect of diffusion constant on chemico-
osmotic consolidation
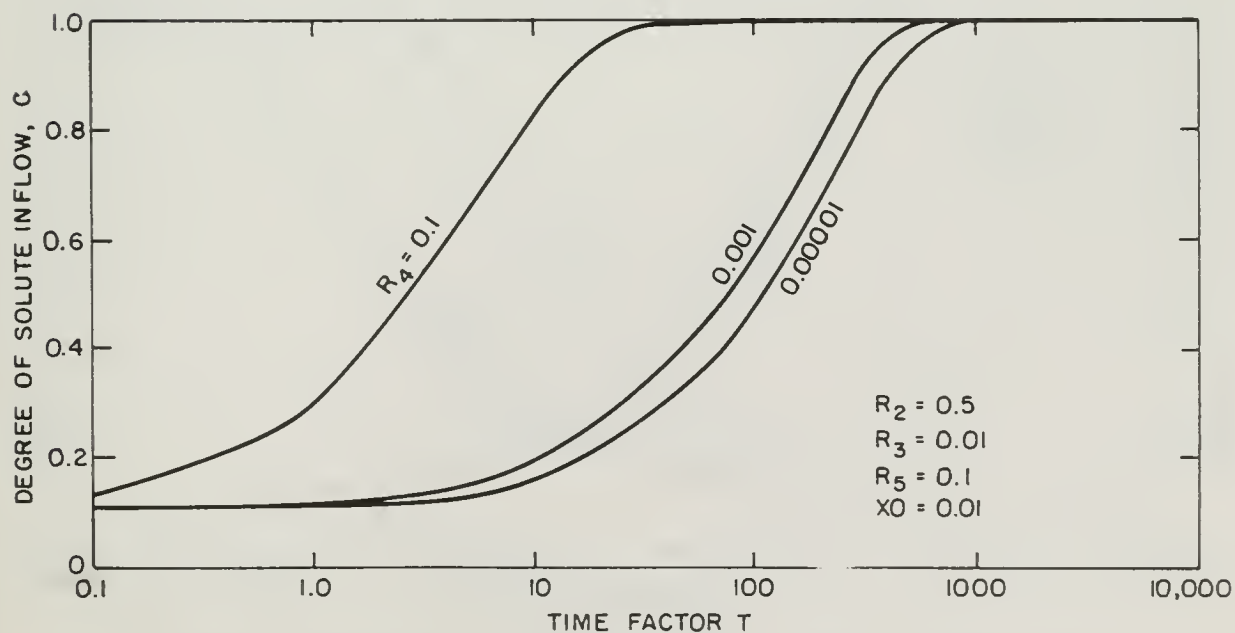
Fig. III-9b. Effect of diffusion constant on solute inflow
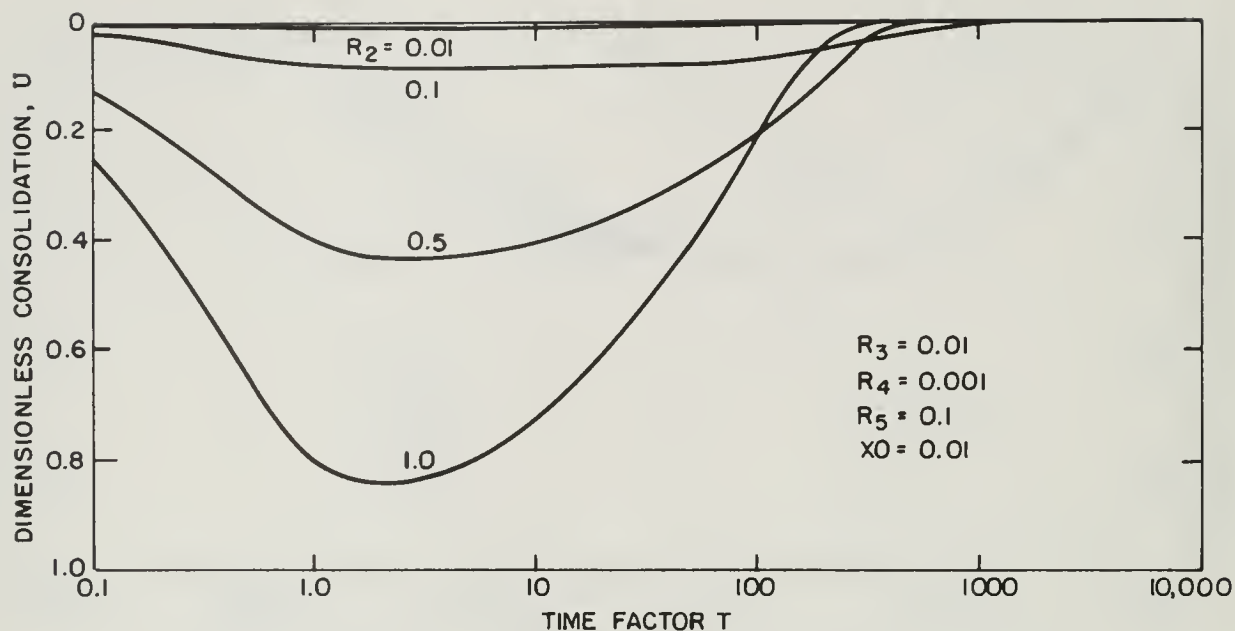
Fig. III-10a. Effect of chemico-osmotic coupling on chemico-osmotic consolidation
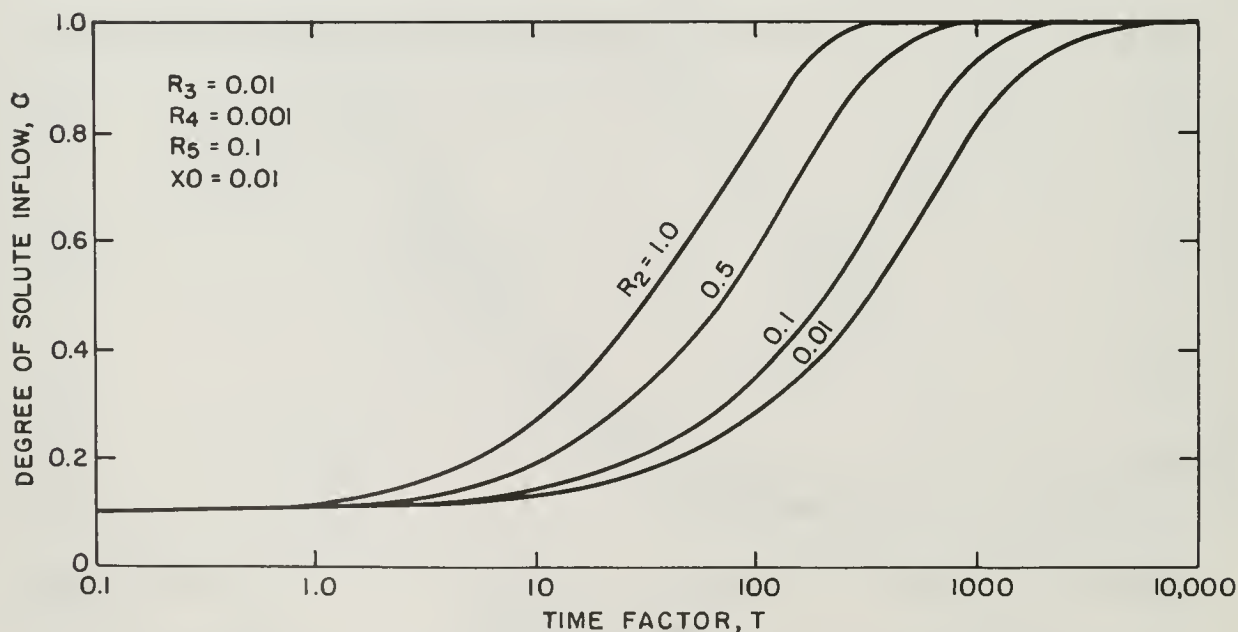
Fig. III-10b. Effect of chemico-osmotic coupling on solute flow
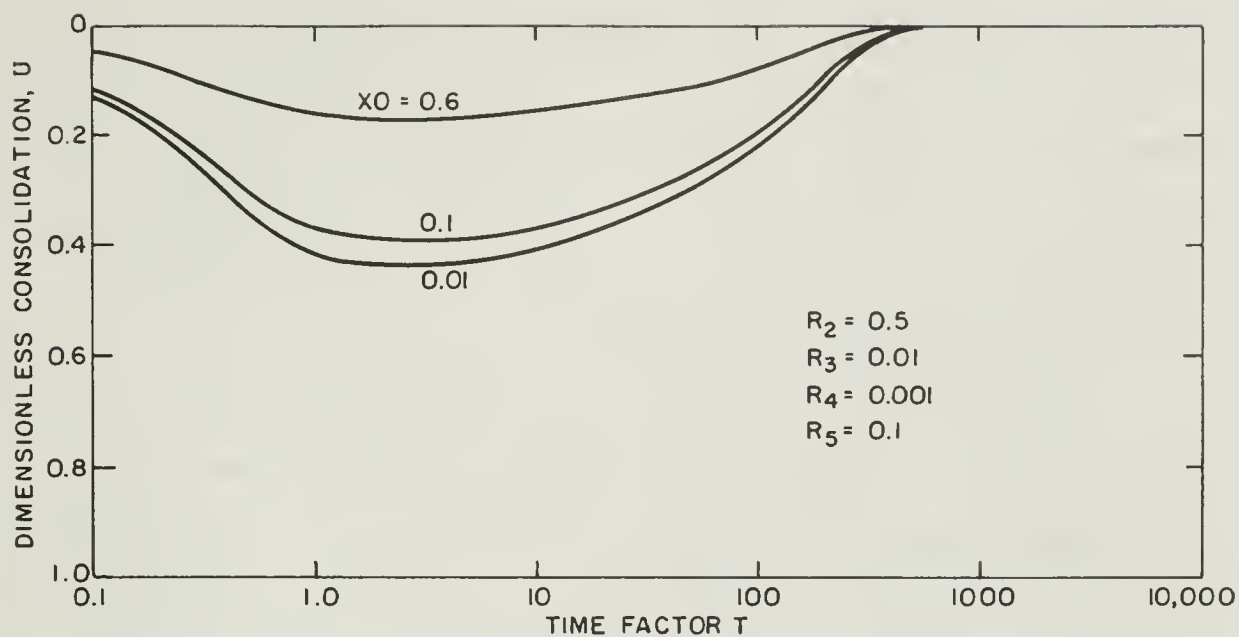
Fig. III-11a.   Effect of solute concentration increase on
chemico-osmotic consolidation
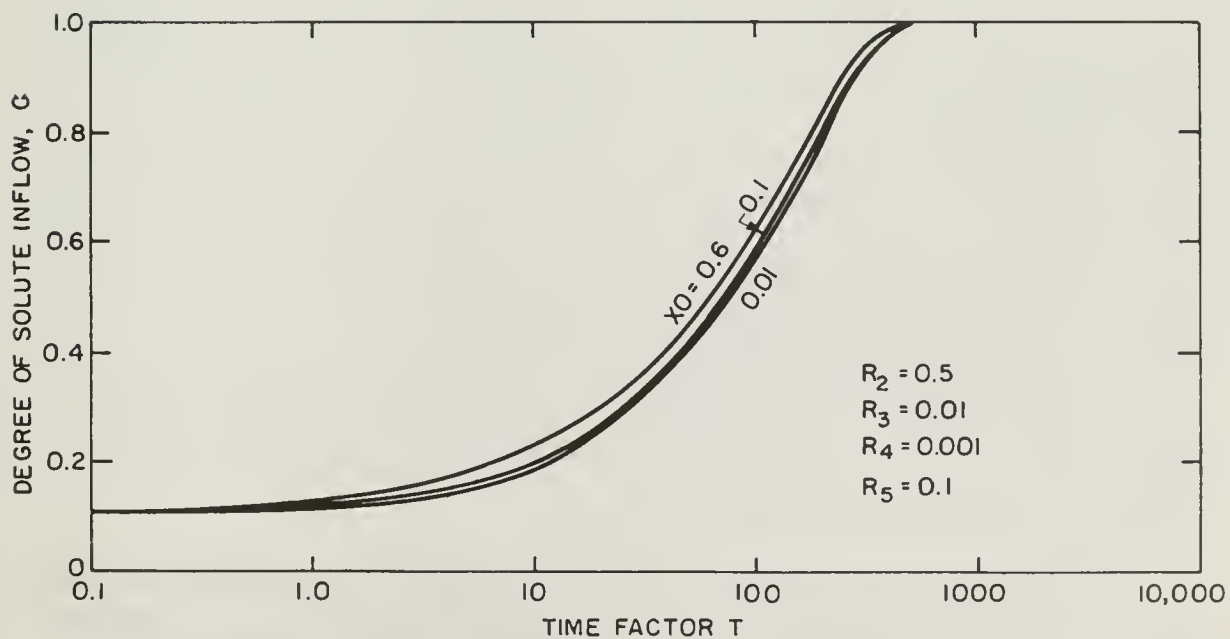
Fig. III-11b.   Effect of solute concentration increase on
solute inflow

concentration isochrone in Fig. III-6a, and the solute inflow curve 4 in Fig. III-5b do not change with T. On the other hand solvent is free to diffuse and does; it diffuses out of the sample under the influence of the chemico-osmotically induced drop in pore pressure at the sample boundary. The pore pressure isochrones in Fig. III-6 indicate u in the sample decreases with time.

The total stress is constant in the sample so that a drop in pore pressure corresponds to an increase in effective stress and a resulting decrease in void ratio, or consolidation. This consolidation is depicted by curve 4 in Fig. III-5a. The pore pressure continues dissipating until the pore pressure gradient is zero within the sample and u has dropped to 0.5 throughout the sample, as represented at T = 2.0 in Fig. III-6. At this point the diffusion process ends and the chemico-osmotic consolidation has reached its maximum, c. f. Fig. III-5a.

The solution diffusion process we have just described is exactly analogous to that described by the Terzaghi diffusion equation except that the drainage is caused by chemico-osmotic coupling rather than mechanical load. The chemico-osmotic consolidation curve 4 in Fig. III-5a is the same as the Terzaghi diffusion curve with T having the value .848 at 90% chemico-osmotic consolidation.

If we define T_c to be the value of T which 100% consolidation first occurs, Fig. III-5a and Figs. III-6 indicate that T_c is about 2.0 for a non-leaky semi-permeable system.

A physical description of the chemico-osmotic consolidation process in a non-leaky semi-permeable membrane system is that the increase in solute concentration at the sample boundary chemico-

-502-

osmotically "sucks" solution out of the sample. Equilibrium is reached

when the pore pressure throughout the sample has dropped by an amount

equal to the osmotic-pressure drop corresponding to the solute

concentration increase.

The process is more complicated if the system is a leaky

semi-permeable membrane system. In this case the increase of solute

concentration at the boundary does suck solution out of the sample,

but it also causes solute to diffuse into the sample. Pore pressure

dissipation is more rapid than solute diffusion. Thus by the time

the pore pressure has dropped by an amount equal to the osmotic

pressure drop, solute has just begun to penetrate regions of the sample

close to the boundary. Hence the osmotic pressure drop is less than

$\Delta u'$ at the boundary. In other words the boundary condition is no longer

$\Delta u' = 0.5$ (or $\Delta u' = k_{hc}/k_h \gamma_w \Delta c_s$) at $z = 0$ and $z = 2$, but $\Delta u'$ is some

smaller value which decreases to zero as time proceeds.

Fig. III-6b[*], which depicts isochrones for a "leaky" system

represented by curve 1 in Fig. III-5, shows this reduction in pore

pressure drop and increase in solute concentration near the sample

boundary by the time $T = 1.0$. As the process proceeds, the solute

continues to diffuse into the sample until solute concentration

throughout the sample is equal to the boundary value. The rate of

---

[*]Note that several of the isochrones are drawn dashed near the sample
 boundary. This is because the finite difference mesh was not fine
 enough to enable them to be located exactly. Their location was
 estimated.

solute inflow is depicted quantitatively by curve 1 in Fig. III-5b.

As the solute diffuses into the sample, it also continues to
reduce the osmotic pressure drop from the boundary inwards. This
causes a pore water pressure gradient which tends to suck solution
back into the soil. Hence the chemico-osmotic consolidation ceases
and swell begins as shown by curve 1 Fig. III-5a. Equilibrium is
reached when the hydrostatic pressure is equal to 1.0, the initial
value.

At this time the sample thickness is also equal to the initial
value ($u = 0$) if the soil is elastic and the coefficient of compressibility,
a_v, is the same for both consolidation and swelling. Figs. III-5a and
III-7a to III-11a are drawn on the basis of an elastic soil. However in
actual practice soils are not elastic and a_v is smaller for swelling
than for consolidation. In other words real soils will swell or rebound
less than they consolidate under the same change in effective stress.
Our analysis of chemico-osmotic consolidation has not incorporated this
aspect of real soil behavior, but could easily do so by assigning a
different value of a_v for consolidation and swelling. Real soils, which
are leaky membranes, will chemico-osmotically consolidate to a minimum
thickness and then swell to an equilibrium thickness less than the
original thickness.

The rate at which the solution diffuses back into the soil
depends on the rate at which the solute diffuses into the soil,
because it is the inward flow of solute which chemico-osmotically
"sucks" the solution back into the soil. This is the reason why

the solute inflow in Fig. III-5b and the degree of consolidation in Fig. III-5a reach equilibrium together.

We now proceed to discuss some of the further results in Figs. III-5 and III-7 to III-10. The value of T at which 90% solute inflow occurs is called T_{s90} and from Fig. III-7 we observe that as R_3, the drag coupling coefficient increases, T_{s90} decreases; i.e., the greater the drag coupling the greater is the rate of solute inflow. Hence drag coupling has a significant effect on solute diffusion.

On the other hand Fig. III-8 indicates that void ratio coupling has essentially no effect on either T_{s90} or the rate of solute diffusion. Fig. III-9 indicates that the larger R_4 the smaller T_{s90}. Increasing R_4 and keeping all else constant is equivalent to increasing the diffusion constant of the system (c.f. equations III-1). Hence Fig. III-9 tells us that solute inflow is more rapid if the diffusion constant is greater. We conclude that the diffusion constant is an important parameter for chemico-osmotic solute diffusion and consolidation.

All the chemico-osmotic consolidation curves in Fig. III-5a and III-7a to III-11a indicate that the value of T at which maximum, or 100%, chemico-osmotic consolidation first occurs T_c, is about 2.0.

The actual time at which the maximum amount of chemico-osmotic consolidation first occurs, t_c, is related to T_c by (c.f. equation III-1)

$$t_c = \frac{H^2 T_c}{c_v} = 2.0 \frac{H^2}{c_v}$$

where c_v is the coefficient of consolidation and H is the drainage

path length.

The important implication here is that the rate of chemico-osmotic consolidation is independent of all the coupling coefficients, type of solute, etc. It depends only on c_v and H.

From Figs. III-5a and III-10a, we see that the amount of chemico-osmotic consolidation increases as R_2 or chemico-osmotic coupling increases. We can interpret this result in terms of the description of chemico-osmotic consolidation we offered above: The higher the chemico-osmotic coupling, the less "leaky" is the system, and hence the greater the osmotic pressure drop that develops at the sample boundary for a given solute concentration increase at the boundary. This means a greater overall osmotic pressure drop throughout the sample at T_c, i.e., a great chemico-osmotic consolidation.

In Fig. III-11a we observe that the lower XO, i.e., the greater the increase of solute concentration at the sample boundary, the greater is the chemico-osmotic consolidation. This observation is easily explained if we remember that chemico-osmotic consolidation depends on osmotic pressure drop in the sample, which depends on the initial osmotic pressure drop at the sample boundary, which is directly proportional to the increase of solute concentration at the sample boundary (c.f. equation III-11a).

We should also note that for a given amount of chemico-osmotically induced overall drop in pore pressure, the amount of chemico-osmotic consolidation is proportional to the compressibility of the system (c.f. equation II-20b).

Finally we turn our attention to a consideration of the parameters which are important in determining the degree of leakiness of a particular system. To do this we confine our attention to Fig. III-5b where both leaky and non-leaky systems are represented.

Curves 1, 2 and 3 represent leaky systems. Curves 4, 5 and 6 represent non-leaky systems.

Curves 5 and 6 represent two systems displaying different void ratio couplings or R_5. The curves coincide exactly; hence we conclude that void ratio coupling is not particularly crucial in determining degree of leakiness.

The difference between curves 1 and 4 is that 1 represents a soil with a higher diffusion constant (R_4) than the soil represented by 4. Curve 1 represents a leaky system, while curve 4 represents a non-leaky system. Our conclusion is that a greater diffusion constant is associated with a higher degree of leakiness.

Curves 3 and 6 differ only in that the drag coupling coefficient R_3, is higher for curve 3 than for curve 6.[*] Curve 3 represents a leaky membrane while curve 6 represents a non-leaky membrane. Hence we conclude that drag coupling is an important parameter in determining the degree of leakiness of a system. The lower the drag coupling the lower the degree of leakiness.

It is also important to remember that implicit in R_3 and R_4 is the chemico-osmotic coupling effect. The larger the chemico-osmotic coupling effect, or R_2, or k_{hc} the smaller are both R_3 and R_4 (c.f.

---

[*] The values of R_5 also differ for these two cases; however this difference has no influence on behavior as shown by Fig. III-8.

equation III-1) and hence the less is the degree of leakiness of the system.

Summary of Results of Computer Analysis

(i) Solute inflow is a smooth process building steadily to equilibrium.

(ii) For a non-leaky system, chemico-osmotic consolidation builds rapidly and smoothly to equilibrium. For leaky systems, chemico-osmotic consolidation builds rapidly and smoothly to a maximum followed by a smooth swelling.

(iii) T_{s90} is greater for lower drag coupling and lower diffusion constant, but is not effected by void ratio coupling.

(iv) $T_c = 2.0$ and $t_c = 2.0 \ H^2/c_v$ i.e., chemico-osmotic consolidation reaches its maximum value at a time t_c which depends only on the drainage path length, H, and the coefficient of consolidation c_v.

(v) The maximum amount of chemico-osmotic consolidation increases with increase in chemico-osmotic coupling, increase in boundary solute concentration increase and increase in soil compressibility.

(vi) The degree of leakiness of a system decreases with decrease in drag coupling, increase in chemico-osmotic coupling but is not effected by void ratio coupling.

We should mention that the scope of these results is limited to the range of R coefficients used and may not apply to all semi-

permeable systems.

2. Implications for Experimentation

As mentioned in the introduction to Chapter II, the work of
Olsen (22, 23) and Abd-El-Aziz and Taylor (1) has provided data
substantiating the validity of certain assumptions inherent in the
development of our theory for chemico-osmotic diffusion in soils.
However, no experiments have been conducted on chemico-osmotic
consolidation per se.

The results of the computer analysis provide us with qualitative
guidelines for setting up experiments on chemico-osmotic consolidation.

Olsen's experiments (22, 23) indicate that there is very little
chemico-osmotic consolidation in a Kaolinite-NaCl solution system even
when the Kaolinite is at an effective overburden pressure of 700
atmospheres. At this extremely high overburden he observed a chemico-
osmotically induced pore pressure change of 20 centimeters of water for
XO = 0.1. To be able to successfully observe chemico-osmotic consolidation
in the laboratory would require a chemico-osmotically induced pore pressure
drop at least an order of magnitude higher than 20 centimeters of water.
Otherwise the amount of consolidation would be too small to measure with
any precision. We conclude therefore that

a. we require a soil-solution system exhibiting a much higher
chemico-osmotic coupling than a Kaolinite-NaCl solution system.

b. we should consider using as high a boundary solute
concentration increase as possible.

.

c. we should plan to use as compressible a soil as possible – certainly more compressible than Kaolinite under an effective stress of 700 atmospheres.

Another aspect in the observation of a complete chemico-osmotic consolidation curve is the time factor. The results of the computer analysis indicate that T_c is 2.0 and that T_{s90} is usually much larger than 2.0 (c.f. Figs III-5 to III-10). Thus observation of a complete chemico-osmotic consolidation curve will involve observing up to and including the (real) time corresponding to T_{s90}. Hence it would be desirable to use a soil-solution system for which T_{s90} is not too large.

We should therefore attempt to employ soil-solution systems for which

a. drag coupling is large

b. the diffusion constant is large

Drag coupling

$$R_3 = a_v \ U_{max} \left(1 + \frac{k_{ch}}{k_h \ c_{sm}} \right)$$

decreases as chemico-osmotic coupling increases (i.e., as the absolute magnitude of P_2 and k_{ch}, both of which are negative, increase). It also increases as compressibility increases. Hence we should attempt to employ a soil-solution system of high compressibility and low chemico-osmotic coupling.

The diffusion constant is usually low for soil-solution systems wherein chemico-osmotic coupling is high, because high chemico-osmotic

coupling is associated with low solute mobility. Hence again we conclude that for low T_{s90}, we should employ a soil-solution system of low chemico-osmotic coupling.

However, if the chemico-osmotic coupling is lower than in a Kaolinite-NaCl solution system, the amount of chemico-osmotically induced consolidation would probably be too small to measure with precision. Hence we conclude that we should employ a soil-solution system which exhibits an intermediate amount of chemico-osmotic coupling if we expect to measure a reasonably large amount of chemico-osmotic consolidation in a reasonably small time.

In summary, we should use a soil-solution system

a. exhibiting a higher chemico-osmotic coupling than a Kaolinite-NaCl solution system

b. exhibiting an intermediate degree of chemico-osmotic coupling

c. exhibiting a high compressibility

We should attempt to use as high a boundary solute concentration increase as possible. In a few words, we should attempt to put a highly compressible, non-leaky semi-permeable membrane in contact with a solution of very high concentration.

APPENDIX III-A

Explicit Finite Difference Computer Program

This Fortran program solves the one dimensional problem of the coupled diffusion of salt and water in a soil layer (or sample) of thickness 2.0 subject to various initial and boundary conditions. Solution proceeds by solving the two simultaneous finite difference equations for diffusion of salt and water at every point in the finite difference grid directly.

The data input, specifies:

a. The type of soil by defining the phenomenological constants R_1, R_2, R_3, R_4 and R_5; and the maximum and minimum void ratios, EF and EI respectively

b. The initial pore water pressure and salt concentration, UO and XO respectively, both constant throughout the sample. Boundary values of pore water pressure and salt concentration are both equal to 1.0.

c. The number of space intervals on the finite difference grid, XNZINT, and the value of the constant BETA (= $\Delta T/\Delta Z^2$). From the last two numbers the program calculates the size of the space and time intervals, ΔZ and ΔT respectively, on the finite difference grid. N.B. BETA should be less than 0.5 if the solution is to be stable.

The results are printed out at logarithmic intervals of dimensionless time, T, i.e., at T = .01, .02 . . . . .09, 0.1, 0.2, . . . 0.9, 1.0, 2.0, . . . 9.0, 10.0, 20.0, . . . 90.0, 100.0, 200.0, . . . etc.

Each printout consists of

a. T

b. Degree of pore pressure dissipation, UC

c. Degree of salt inflow, C

d. Pore pressure and salt concentration isochrones, in tabular form.

The program ceases calculating when both the degree of pore pressure dissipation and the degree of solute inflow are greater than or equal to 98%. After termination of calculation, the program will seek new data with which to begin another problem. If the data cards are blank the program terminates.

```
      SOLUTION OF SOLUTION AND SOLUTE DIFFUSION EXPLICIT METHOD
      DIMENSION U(50),UV(50),X(50),XV(50),E(50),INCR(50)
         ***********************(***********************************************
               **************MEANING OF SYMBOLS****************************
      U=PWP RATIO AT TIME T
      UV=PWP RATIO AT TIME T+DELTA-T
      X=SOLUTE CONC.RATIO AT TIME T
      XV=SOLUTE CONC. RATIO AT TIME T+DELTA-T
      E(I)=VOID RATIO AT TIME T
      R2,R3,R4, AND R5 ARE CONSTANTS IN DIFFUSION EQUATIONS
      UO =PWP RATIO AT TIME T=0
      XO =SOLUTE CONC. RATIO  AT TIME T=0
      EI =INITIAL VOID RATIO
      EF=FINAL VOID RATIO
      BETA =DELTA-T/DELT-Z SQUARED
      XNZINT =NO. OF Z INTERVALS
      DELT-Z=WIDTH OF Z-INTERVAL
      DELT= WIDTH OF TIME INTERVAL
      INT=NO. OF DELT IN 0.1
      UPR,CPR ARE DUMMY VARIABLES IN CALCULATION OF UC,C
      T=TIME FACTOR
      UC=DEGREE OF CONSOLIDATION
      C=DEGREE OF SOLUTE INFLOW
      XJ2,J2,J1 ARE DUMMY VARIABLES FOR KEEPING TIME
      INT,INTM1,INTM11 ETC. ARE DUMMY VARIABLES FOR KEEPING TIME
         ***************END OF SYMBOLS****************************************
         *******************************************************************
    1 FORMAT(7F10.4)
    2   FORMAT(3F10.4)
    3 FORMAT(//10X,2HT=,F10.4,5X,2HU=,F10.4,5X,2HC=,F10.4)
    4 FORMAT(10X,2HI=,I4,5X,2HU=,F10.4,5X,2HX=,F10.4)
**********READ CONSTANTS FOR CALCULATIONS****************************************
  100 READ 1,R2,R3,R4,R5,UO,XO,EI
      READ 2,EF,BETA,XNZINT
      PRINT 1,R2,R3,R4,R5,UO,XO,EI
*******CHECK IF THERE IS ANY DATA WITH WHICH TO CALCULATE***************
      IF(R2-0.)101,400,101
  101 PRINT 2,EF,BETA,XNZINT
*********************CALCULATE OTHER CONATANTS*************************
      DELTZ=2./XNZINT
      DELT=BETA*DELTZ*DELTZ
      N=(XNZINT+1.)/2.
      NPLUS1=N+1
      XNMIN1=N-1
      NMIN1 =XNMIN1
      DELTEE=EF-EI
      DELTX=1.-XO
      DELTU=1.-UO
      D=DELTEE/DELTU
      D1=DELTZ/DELTU
      D2=DELTZ/DELTX
      INT =.1/DELT
      J1=1
      J2=INT
      INTM1=INT-1 .
```

-515-

```
      INTM11=10*INT-1
      INTM12=100*INT-1
      INTM13=1000*INT-1
      DO 105 J=1,9
  105 INCR(J)=INTM1
      DO 106 J=10,18
  106 INCR(J)=INTM11
      DO 107 J=19,27
  107 INCR(J)=INTM12
      INCR(28)=INTM13
***********ESTABLISH INITIAL AND BOUNDARY CONDITIONS*********************
      DO 110 J=2,NPLUS1
      U(J)=UO
  110 X(J)=XO
      X(1)=1.
      U(1)=1.
      UV(1)=1.
      XV(1)=1.
*********************CALCULATIONS ACTUAL*****************************
      DO 300 JI=1,28
  115 DO 130 JR=J1,J2
      DO 120 I=2,N
      F(I)=EI+(1.-U(I))*D
      UV(I)=U(I)+BETA*           ((U(I+1)-2.*U(I)+U(I-1))-R2*(X(I+1)-2.*X(I)+
     1X(I-1)))
  120 CONTINUE
      DO 125 I=2,N
      XV(I)=X(I)+BETA/E(I)*(R3*((X(I+1)-X(I-1))*(U(I+1)-U(I-1))/4.+X(I)*
     1(U(I+1)-2.*U(I)+U(I-1)))+R4*(X(I+1)-2.*X(I)+X(I-1)))
     2                                      -R5*X(I)/E(I)*       (UV(I
     3)-U(I))
  125 CONTINUE
      U(NPLUS1)=UV(N)
      X(NPLUS1)=XV(N)
      DO 130 I=2,N
      U(I)=UV(I)
  130 X(I)=XV(I)
****************** CALCUCATION OF T,UC, AND C*****************************
      UPR=0.
      DO 140 I=2,N
  140 UPR=UPR+U(I)
      UC=1.-(XNMIN1-UPR)*D1
      CPR=0.
      DO 145 I=2,N
  145 CPR=CPR+X(I)
      C=1.-(XNMIN1-CPR)*D2
      XJ2=J2
      T=XJ2*DELT
      ****************PRINTOUT**********************************
      PRINT 3,T,UC,C
      DO 160 I=1,N
  160 PRINT 4,I,U(I),X(I)
    **************CHECK IF PROCESS IS EQUILIBRATED AND INCREMENT J1 AND
      J1=J2+1
      J2=J1+INCR(JI)
```
-516-

```
      IF(UC-.98)300,204,204
 204  IF(C-.98)300,350,350
 300  CONTINUE
 350  GO TO 100
 400  CONTINUE
      END
```

APPENDIX III-B

Solution of Implicit Finite Difference Equations

As mentioned in Section III-2c, equations III-6 cannot be solved explicitly at any point of the Z-T grid. In fact, they are solved implicitly using the method of Thomas (2, 6, 16) as outlined below.

We consider the specific problem of the horizontal sample with initial conditions

$$
\left.\begin{matrix} U(I) = UO \\ X(I) = XO \end{matrix}\right\} \quad I = 2, 3, \ldots, N + 1
$$

where

$$
N = \frac{NZINT + 1}{2}
$$

and boundary conditions

$$
U(1) = UF
$$

$$
X(1) = XF
$$

Note that this problem is exactly the same as that defined in Section III-2b-iv, and we specialize to the case UF = XV = 1.0. Only the upper half of the sample is considered because of symmetry about the center of the sample. NZINT is chosen odd so that U(N) = U(N + 1) and X(N) = X(N + 1).

By writing equation III-6a at all the nodal points between I = 2 and I = N + 1 for one value of T we obtain the following set of equations

$$- 2 \left(1 + \frac{1}{BETA}\right) \; UV(2) + UV(3) \qquad\qquad = CONSTU(2)$$

$$UV(2) - 2 \left(1 + \frac{1}{BETA}\right) UV(3) + UV(4) \quad = CONSTU(3)$$

.

.

.

.

$$UV(N - 2) - 2 \left(1 + \frac{1}{BETA}\right) UV(N - 1)$$

$$+ UV(N) \qquad\qquad = CONSTU(N - 1)$$

$$UV(N - 1) + (1 + \frac{2}{BETA}) \; UV(N) \qquad = CONSTU(N)$$

$$(C-1a)$$

where $CONSTU(I) = 2 \cdot U(I) \; (1 - \dfrac{1}{BETA}) \, U(I + 1) - U(I - 1) + 2 \cdot R2$

$\{X(I + 1) - 2 . X(I) + X(I - 1)\}$

$I = 3, \; 4 \; \ldots \; N$

and $CONSTU(2) = 2 . U(2) \; (1 - \dfrac{1}{BETA}) - U(3) . UF + 2 . R2 \{X(3) - 2 \; X(2)$

$+ XF\} - XF$

repeating the process for equation III-6b yields the following set of

equations

$$- \{R_4 + \frac{E(2)}{BETA} \} \ XV(2) + \{R_4 + R_3 \ . \ DEEU(2)\} \ \frac{XV(3)}{2} \qquad = CONST(3)$$

$$\frac{1}{2} \ \{R_4 - R_3 \ . \ DEEU(3)\} \ XV(2) - \{R_4 + \frac{E(3)}{BETA} \} \ \frac{XV(3)}{2} \ +$$

$$\frac{1}{2} \ \{R_4 + R_3 \ DEEU(3)\}XV(4) \qquad\qquad = CONSTX(3)$$

$$\frac{1}{2} \ \{R_4 - R_3 \ DEEU(N - 1) \ \} \ XV(N - 2) - \{R_4 + \frac{E(N - 1)}{BETA}\} \ XV(N - 1)$$

$$+ \frac{1}{2} \ \{R_4 + R_3 \ DEEU(N - 1)\} \ XV(N) \qquad\qquad = CONSTX \ (N - 1)$$

$$\frac{1}{2} \ \{R_4 - DEEU(N) \} \ XV(N - 1) + \{- \frac{R_4}{2} - \frac{E(N)}{BETA}$$

$$+ \ R_3 \ DEEU(N) \} \ XV(N) \qquad\qquad = CONSTX(N)$$

$$(C-1b)$$

where $CONSTX(2) = X(2) \ \{- \frac{E(2)}{BETA} - R_3 \cdot DEEU2(2) + R_4 + R_5 \ \frac{DEEUDT(2)}{BETA} \}$

$$- \frac{X(3)}{2} \ \{R_4 + R_3 \ . \ DEEU(2)\}$$

and $\quad CONSTX(I) = X(I) \ \{- \frac{E(I)}{BETA} - R_3 \ . \ DEEU2(I) + R_4 + R_5 \cdot \frac{DEEUDT(I)}{BETA} \}$

$$- \frac{X(I - 1)}{2} \ \{R_4 - R_3 \ . \ DEEU(I)\} - \frac{X(I + 1)}{2} \ \{R_4 + R_3 \ . \ DEEU(I)\}$$

Both sets of equations contain N - 1 equations and N - 1 unknowns and are therefore solvable. Consider now the general set of N - 1 linear equations with N - 1 unknowns in the form.

$$a_{22}\, x_2 + a_{23}\, x_3 \qquad\qquad\qquad\qquad = \text{const } 2$$

$$a_{32}\, x_2 + a_{33}\, x_3 + a_{34}\, x_4 \qquad\qquad\qquad = \text{const } 3$$

$$a_{43}\, x_3 + a_{44}\, x_4 + a_{45}\, x_5 \qquad\qquad = \text{const } 4$$

$$a_{54}\, x_4 + a_{55}\, x_5 + a_{56}\, x_6 \qquad = \text{const } 5$$

$$\cdot$$
$$\cdot$$
$$\cdot$$

$$a_{n-1\ n-2}\, x_{n-2} + a_{n-1\ n-1}\, x_{n-1} + a_{n-1\ n}\, x_n \qquad = \text{const } n-1$$

$$a_{n\ n-1}\, x_{n-1} + a_{nn}\, x_n \qquad = \text{const } n$$

$$(C-2a)$$

where a's are constant coefficients

x's are unknowns

const's are constants

This set of equations has the same form as both equations C-1a and C-1b, and is solvable by the Thomas method as follows:

Let

$$F_2 = a_{22}$$

$$F_3 = a_{33} - a_{23}\, a_{32}/F_2$$

$$F_4 = a_{44} - a_{34}\, a_{43}/F_3$$

$$\cdot$$
$$\cdot$$
$$\cdot$$

$$F_n = a_{nn} - a_{n-1\ n}\, a_{n\ n-1}/F_{n-1} \qquad\qquad (C\text{-}2b)$$

and let

$$D_2 = \text{const } 2$$

$$D_3 = \text{const } 3 - a_{32}\, D_2/F_2$$

$$D_4 = \text{const } 4 - a_{43}\, D_3/F_3$$

$$\cdot$$
$$\cdot$$
$$\cdot$$

$$D_n = \text{const } n - a_{n\ n-1}\, D_{n-1}/F_{n-1} \qquad\qquad (C\text{-}2c)$$

Hence the first equation of (C-2a) may be written

$$F_2 \, x_2 + a_{23} \, x_3 = D_2 \qquad\qquad\qquad \text{(C-3-1)}$$

Eliminating x_2 from (C-3-1) and the second equation of (C-2a)

$$\left(a_{33} - \frac{a_{23} \, a_{32}}{a_{22}}\right) x_3 + a_{34} \, x_4 = \text{const } 3 - \frac{a_{32}}{a_{22}} \ \text{const } 2$$

or $F_3 \, x_3 + a_{34} \, x_4 = D_3$ \qquad\qquad\qquad (C-3-2)

Eliminating x_3 from (C-3-2) and the third equation in (C-2a)

$$\left(a_{44} - \frac{a_{34} \, a_{43}}{F_3}\right) x_4 + a_{45} \, x_4 = \text{const } 4 - \frac{a_{43}}{F_3} \ D_3$$

or $F_4 \, x_4 + a_{45} \, x_5 = D_5$ \qquad\qquad\qquad (C-3-3)

.

.

.

$$F_{n-1} \, x_{n-1} + a_{n-1 \ n} \, x_n = D_{n-1} \qquad\qquad \text{(C-3-n-2)}$$

Eliminating x_{n-1} from (C-3-n-2) and the last equation of (C-2a)

$$a_{nn} - \frac{a_{n-1 \ n} \, a_{n \ n-1}}{F_{n-1}} \ x_n = \text{constn} - a_{n \ n-1} \frac{D_{n-1}}{F_{n-1}}$$

or

$$F_n \ x_n = D_n \qquad\qquad (C\text{-}3\text{-}n\text{-}1)$$

From equation   C-3-n-1   we solve for

$$x_n = \frac{D_n}{F_n}$$

Thence back substituting into equation C-3-n-2 we solve for x_{n-1}

$$x_{n-1} = \frac{D_{n-1} - a_{n-1 \ n}}{F_{n-1}} \ x_n \qquad\qquad (C\text{-}4\text{-}1)$$

Then back substituting into equation   C-3-n-3 we solve for x_{n-2}

$$x_{n-2} = \frac{D_{n-1} - a_{n-2 \ n-1} \ x_{n-1}}{F_{n-2}} \qquad\qquad (C\text{-}4\text{-}2)$$

.

.

.

$$x_2 = \frac{D_2 - a_{23} \ x_3}{F_2} \qquad\qquad (C\text{-}4\text{-}n\text{-}2)$$

Hence the equations are solved.

On the computer the process is actually fairly simple because the
kernel of the solution is equations C-2b, C-2c and C-4 which are

-525-

all calculated in do-loops.

The computer program which solves equations C-1a and C-1b using this procedure is presented in Appendix III-C.

APPENDIX III-C

Implicit Finite Difference Computer Program

This Fortran program solves the one dimensional problem of the coupled diffusion of salt and water in a soil layer (or sample) of thickness 2.0, subject to various initial and boundary conditions. Solution proceeds by solution of all the simultaneous finite difference equations for diffusion of salt and water at a value of T, using the method of Thomas.

The data input specifies

a. The type of soil by defining the phenomenological constants R_1, R_2, R_3, R_4 and R_5 and the maximum and minimum void ratios, EF and EI respectively.

b. The initial pore water pressure and salt concentration UO, and XO respectively; both constant throughout the sample. Boundary values of pore water pressure and salt concentration are both equal to 1.0.

c. The number of space intervals on the finite difference grid, XNZINT, and the size of the time interval on the finite difference grid, DELT.   N.B. DELT and XNZINT should be chosen so that BETA $(= \Delta T/\Delta Z^2)$ is less than or equal to 2.0.

The results are printed out at logarithmic intervals of dimensionless time T,i.e. at T = .01, .02, ...09, 0.1, 0.2, . . . 0.9, 1.0, 2.0, . . . 9.0, 10.0 20.0, . . . 90.0, 100.0, 200.0, . . . etc.

Each printout consists of:

a. T

b. Degree of pore pressure dissipation, UC

c. Degree of salt inflow, C

d. Pore pressure and salt concentration isochrones, in tabular form.

The program ceases calculating when both the degree of pore pressure dissipation and the degree of salt inflow are greater than or equal to 98%. After termination of calculation, the program will seek new data with which to begin another problem. If the data cards are blank the program terminates.

This program solves the same problems as the Implicit program, and requires less computational time to do so.

```
      CHEMICO-OSMOTIC CONSOL IMPLICIT  6-POINT
          ******************MEANING OF SYMBOLS******************************
      DIMENSION U(50),UV(50),X(50),XV(50),E(50),R(50),INCR(50),CONSTU(20
     1),CONSTX(20),FU(20),DU(20),DEEU(20),DEEU2(20),DEFUDT(20),CONST3X(2
     20),CONST4X(20),FX(20),DX(20)
          *****************(**************************************************
      U=PWP RATIO AT TIME T
      UV=PWP RATIO AT TIME T+DELTA-T
      X=SOLUTE CONC.RATIO AT TIME T
      XV=SOLUTE CONC. RATIO AT TIME T+DELTA-T
      E(I)=VOID RATIO AT TIME T
      R2,R3,R4, AND R5 ARE CONSTANTS IN DIFFUSION EQUATIONS
      UO =PWP RATIO AT TIME T=0
      XO =SOLUTE CONC. RATIO  AT TIME T=0
      FI =INITIAL VOID RATIO
      FF=FINAL VOID RATIO
      BETA =DELTA-T/DELT-Z SQUARED
      XNZINT =NO. OF Z INTERVALS
      DELT-Z=WIDTH OF Z-INTERVAL
      DELT= WIDTH OF TIME INTERVAL
      INT=NO. OF DELT IN 0.1
      UPR,CPR ARE DUMMY VARIABLES IN CALCULATION OF UC,C
      T=TIME FACTOR
      UC=DEGREE OF CONSOLIDATION
      C=DEGREE OF SOLUTE INFLOW
      XJ2,J2,J1 ARE DUMMY VARIABLES FOR KEEPING TIME
      INT,INTM1,INTM11 ETC. ARE DUMMY VARIABLES FOR KEEPING TIME
      CONSTU(I) ARE CONSTANTS IN THE LINEAR EQUATIONS BEING SOLVED
      CONSTX(I) ARE CONSTANTS IN THE LINEAR EQUATIONS BEING SOLVED
      CONST1,CONST2 ARE DUMMY VARIABLES IN CALCULATION OF UV(I)
      FU(I),DU(I) ARE CONSTANTS USED IN CALCULATING UV(I)
      DZ2T,DEFU(I),DEFU2(I),DEFUDT(I),CONST3X(I),CONST4X(I) ARE DUMMY
      VARIABLES IN CALCULATING XV(I)
      FX(I),DX(I) ARE CONSTANTS USED IN CALCULATION OF XV(I)
          ***************END OF SYMBOLS*************************************
          ****************************************************************
    1 FORMAT(7G10.4)
    2 FORMAT(3F10.4)
    3 FORMAT(//10X,2HT=,F10.4,5X,2HU=,F10.4,5X,2HC=,F10.4)
    4 FORMAT(10X,2HI=,I4,5X,2HU=,F10.4,5X,2HX=,F10.4)
***********READ CONSTANTS FOR CALCULATIONS****************************
  100 READ 1,R2,R3,R4,R5,UO,XO,EI
      READ 2,EF,DELT,XNZINT
      PRINT 1,R2,R3,R4,R5,UO,XO,EI
********CHECK IF THERE IS ANY DATA WITH WHICH TO CALCULATE***************
      IF(R2-0.)101,400,101
  101 PRINT 2,EF,DELT,XNZINT
********************CALCULATE OTHER CONATANTS************************
      DELTZ=2./XNZINT
      N=(XNZINT+1.)/2.
      NPLUS1=N+1
      XNMIN1=N-1
      NMIN1=XNMIN1
      DELTEE=EF-EI
      DELTX=1.-XO
```

-530-

```
      DELTU=1.-UO
      D=DELTEE/DELTU
      D1=DELTZ/DELTU
      D2=DELTZ/DELTX
      INT =.1/DELT
      J1=1
      J2=INT
      INTM1=INT-1
      INTM11=10*INT-1
      INTM12=100*INT-1
      INTM13=1000*INT-1
      INTM14=10000*INT-1
      DO 105 J=1,9
105   INCR(J)=INTM1
      DO 106 J=10,18
106   INCR(J)=INTM11
      DO 107 J=19,27
07    INCR(J)=INTM12
      DO 108 J=28,36
108   INCR(J)=INTM13
      INCR(37)=INTM14
********ESTABLISH INITIAL AND BOUNDARY CONDITIONS***********************
      DO 110 J=2,NPLUS1
      U(J)=UO
10    X(J)=XO
      U(1)=1.
      X(1)=1.
      UV(1)=1.
      XV(1)=1.
      DZ2T=DELTZ*DELTZ/DELT
      CONST1=2.*(1+DZ2T)
      CONST2=2.*(1-DZ2T)
      FU(2)=-CONST1
*********************CALCULATIONS ACTUAL****************************
      DO 300 JI=1,29
      ***************FIRSTLY SOLVE U/EQUATION ***************************
     *****************CALCULATION OF OTHER CONSTANTS*****************
      DO 130 JR=J1,J2
      DO 116 I=2,N
116   CONSTU(I)=U(I)*CONST2-U(I-1)-U(I+1)+2.*R2*(X(I+1)-2.*X(I)+X(I-1))
      CONSTU(2)=CONSTU(2)-1.
      DU(2)=CONSTU(2)
      DO 117 I=1,3
      FU(I)=-CONST1-1./FU(I-1)
117   DU(I)=CONSTU(I)-DU(I-1)/FU(I-1)
      FU(N)=FU(N)+1.
        **********CALCULATION OF UV,S *********************************
      UV(N)=DU(N)/FU(N)
      DO 118 I=2,NMIN1
118   UV(NPLUS1-I)=(DU(NPLUS1-I)-UV(N+2-I))/FU(NPLUS1-I)
      UV(NPLUS1)=UV(N)
        ***************CALCULATE E(I),S ****************************
      DO 119 I=2,N
119   E(I)=EF-(1.-(U(I)+UV(I))/2.)*DELTEE
        *********************SOLVE XV-EQUATIONS *******************
```

```
             ************** CALCULATION OF CONSTANTS ****************
      DO 120 I=2,N
      DEEU(I)=.125*(U(I+1)+UV(I+1)-U(I-1)-UV(I-1))
      DEEU2(I)=.5*(U(I+1)+UV(I+1)+U(I-1)+UV(I-1)-2.*U(I)-2.*UV(I))
      DEEUDT(I)=UV(I)-U(I)
      CONST3X(I)=.5*(R4-R3*DEEU(I))
      CONST4X(I)=.5*(R4+R3*DEEU(I))
  120 CONSTX(I)=X(I)*(-E(I)*DZ2T-R3*DEEU2(I)+R4+R5*DEEUDT(I)*DZ2T)-X(I-1
     1)*CONST3X(I)-X(I+1)*CONST4X(I)
      CONSTX(2)=CONSTX(2)-CONST3X(2)
      FX(2)=-(E(2)*DZ2T+R4)
      DX(2)=CONSTX(2)
      DO 121 I=3,N
      FX(I)=-(E(I)*DZ2T+R4)-CONST3X(I)*CONST4X(I-1)/FX(I-1)
  121 DX(I)=CONSTX(I)-(DX(I-1)/FX(I-1))*CONST3X(I)
      FX(N)=FX(N)+CONST4X(N)
          ***********************CALCULATION OF XV,S ********************
      XV(N)=DX(N)/FX(N)
      DO 122 I=2,NMIN1
  122 XV(NPLUS1-I)=(DX(NPLUS1-I)-XV(N+2-I)*CONST4X(NPLUS1-I))/FX(NPLUS1-
     1I)
      U(NPLUS1)=UV(N)
      X(NPLUS1)=XV(N)
      DO 130 I=2,N
      U(I)=UV(I)
  130 X(I)=XV(I)
 )*******************************PR/CEDURE FOR GETTING R FROM U*************
      DO 135 I=1,N
  135 R(I)=X(I)
          ***************************CALCULATION OF T,UC,RC AND C***********
      UPR=0.
      DO 140 I=2,N
  140 UPR=UPR+U(I)
      UC=1.-(XNMIN1-UPR)*D1
      CPR=0.
      DO 145 I=2,N
  145 CPR=CPR+X(I)
      C=1.-(XNMIN1-CPR)*D2
      XJ2=J2
      T=XJ2*DELT
         *****************PRINTOUT**********************************************
      PRINT 3,T,UC,C
      DO 160 I=1,N
  160 PRINT 4,I,U(I),X(I)
      ***************CHECK IF PROCESS IS EQUILIBRATED AND INCREMENT J1 AND.
      J1=J2+1
      J2=J1+INCR(JI)
      IF(UC-.98)300,204,204
  204 IF(C-.98)300,350,350
  300 CONTINUE
  350 GO TO 100
  400 CONTINUE
      END
```

IV. CHEMICO-OSMOTIC EFFECTS IN THE OXNARD BASIN

A. INTRODUCTION

There are five aquifers interbedded by layers of fine-grained sedimentary aquitard material in the geologic column beneath the Oxnard plain in Ventura County, Califonia. Seawater has intruded several miles inland into the uppermost aquifer, the Oxnard aquifer (see Chapter III of main report).

Computer analysis of conditions within the aquitard beneath the Oxnard aquifer can help us draw some conclusions concerning two problems of possible concern in the Oxnard Basin.

The first is the possibility of surface subsidence due to chemico-osmotic consolidation of the aquitard between the Oxnard and Mugu aquifers. The second is the possibility of aquifers deeper than the Oxnard becoming contaminated with seawater.

The analyses presented herein assume a homogeneous aquitard layer. In actuality the aquitard separating the Oxnard and Mugu aquifers is poorly defined, as discussed in Chapter VI of the main report. Field permeabilities are probably higher than those derived from laboratory tests; whereas the field compressibility may be lower than determined in the laboratory because of the presence of silted and sand lenses in the field. The following analyses use the results of laboratory measurements, so that the results of our analyses are biased as discussed at the end of Section IV-C-3.

Furthermore possible changes in aquitard properties as a result of
salt leaching have not been considered, although the test results
presented in Chapter VI of the main report indicate such effects are
small.

B. SURFACE SUBSIDENCE DUE TO CHEMICO-OSMOTIC CONSOLIDATION OF THE
AQUITARD

The aquitard between the Oxnard and Mugu aquifers can be thought of
as a layer of fine-grained material presently having fresh water as
pore water, and in contact with an aquifer (Oxnard aquifer) in which
the originally fresh pore water has been replaced by intruded seawater.
According to the concepts developed in Section III-D-1, we can expect
the solute (NaCl) concentration increase at a boundary of the aquitard
to induce a chemico-osmotic pressure drop at this boundary which tends
to "suck" water out of the aquitard. If there is significant chemico-
osmotic coupling in the aquitard soil-seawater system, we would expect
a compressible aquitard to undergo significant chemico-osmotic con-
solidation. Hence there is a possibility of a significant surface
subsidence.

To make an estimate of the amount of chemico-osmotic consolidation
to be expected in the aquitard, we need to have an estimate of the degree
of chemico-osmotic coupling inherent in the aquitard soil-seawater system.
This can only be done indirectly at this time, since direct testing of
the aquitard sediments for determination of the coupling coefficients
has not been possible.

Olsen (22, 23) has made some direct measurements of chemico-osmotic coupling in kaolinite-NaCl solution systems. By comparing data on the properties of the aquitard soil with data on the properties of kaolinite an attempt will be made to deduce the chemico-osmotic coupling characteristics of the aquitard soil.

From Chapter VI of the main report on the properties of the aquitard layers in the Oxnard area, we list the following data: The aquitard seems to be about an average of 30 feet thick. The hydraulic permeability of the aquitard soil varies between 10^{-7} and 10^{-5} cm/sec. The deposit appears very inhomogeneous, consisting predominantly of lenses of clayey silt interspersed with lenses of fine sand and silt. The cation exchange capacity of the soil is between 20 and 40 milli-equivalents per 100 grams of dry soil, and the clay content is generally less than 20% by weight, with montmorillonite the predominant clay mineral. The sediment was found to be moderately compressible, having an average compression index C_c, of 0.4. Consolidation tests revealed that the soil of the aquitard layer was overconsolidated, and the average maximum preconsolidation pressure corresponds to a depth of between 100 feet and 200 feet.

Olsen (22, 23) determined the hydraulic permeability of the kaolinite he tested to be about 10^{-7} cm/sec at an overburden pressure corresponding to a depth of 150 feet. This is at the lower end of the range of permeabilities (10^{-7} to 10^{-5} cm/sec) measured for the aquitard soil, and suggests that the kaolinite contains a higher percentage of fine-grained material than the aquitard soil. Most values of cation exchange

capacity in kaolinite, reported in the literature vary between 3 and 15 milli-equivalents per 100 grams of soil (7). This range is significantly lower than the range measured for the aquitard soil. Hence we conclude that even though the kaolinite contains a higher percentage of fine-grained material, the fine-grained fraction of the aquitard soil is probably far more active than kaolinite. The fact that the predominant clay mineral in the clay fraction of the aquitard soil is montmorillonite tends to lend support to this conclusion because montmorillonite is far more active than kaolinite (7).

We now make the assumption that cation exchange capacity, size of clay fraction and activity of a soil are crude indicators of the degree of chemico-osmotic coupling between that soil and a NaCl solution . On the basis of this assumption we conclude that as a first approximation the aquitard soil-seawater system and Olsen's kaolinite-NaCl solution system experience the same degree of chemico-osmotic coupling.

The present NaCl concentration within the aquitard soil was measured to be about .03 (see Table VI-6 of main report), and we assume that the NaCl concentration in the Oxnard aquifer prior to seawater invasion was also about 0.03 normal. The normality of NaCl in seawater is 0.6 so that the increase of NaCl concentration at the boundary of the aquitard is a factor of $\frac{0.6\ N}{.03\ N} = 20$.

At an overburden pressure corresponding to a depth of 150 feet, Olsen measured a chemico-osmotically induced pore pressure drop of 0.7 inches of water for a tenfold increase in external NaCl concentration.

(23), Olsen also showed empirically that the chemico-osmotically

induced pore pressure drop is proportional to the natural logarithm

of the increase in external NaCl concentration. Since log 20/log 10

= 1.3, the chemico-osmotically induced drop in pore pressure for a

twenty-fold increase in external NaCl concentration would be

$$0.7 \times 1.3 = 1 \text{ inch of water}$$

Hence we assume the chemico-osmotically induced drop in pore water

pressure in the aquitard to be equivalent to 1 inch of water.

To calculate the corresponding amount of chemico-osmotic consolidation

we assume:

1. The aquitard is a layer 30 feet thick

2. The chemico-osmotic pore pressure drop of 1 inch of water

(= .04 psi) corresponds to an increase in effective stress $\Delta\sigma'$ of

the same value acting over the whole aquitard.

3. The average coefficient of compressibility of the aquitard

layer, a_v can be derived from the average compression index via the

equation (31)

$$a_v = \frac{.435 \ C_c}{\sigma'} \qquad\qquad\qquad \text{(IV-1)}$$

where we take σ' to be the average maximum effective preconsolidation

pressure of about 75 psi and $C_c = 0.4$.

Then

$$a_v = \frac{.435 \times 0.4}{75} = .002$$

4. The amount of chemico-osmotic consolidation of the layer is given by (27)

$$\Delta H = a_v \ \Delta\sigma' \ H$$

$$= .002 \times .04 \times 30$$

$$\approx .002 \ \text{feet}$$

This value represents a negligible amount of consolidation.

It should be noted that we employed a value of a_v which was derived from an average value of C_c taken from the virgin portion of the e-log σ' curves rather than the recompression portion. This means that we have employed a value of a_v which is actually too high, because chemico-osmotic consolidation in the field would proceed along the recompression curve, since the actual aquitard soil is over consolidated. This means our estimate of ΔH is too high.

Hence we are safe in concluding that chemico-osmotic consolidation in the aquitard between the Oxnard and Mugu aquifers at Oxnard would only be significant if chemico-osmotic coupling and compressibility of the soil were both much greater than they actually appear to be.

C. POSSIBILITY OF DEEPER AQUIFERS BECOMING CONTAMINATED

There are two routes that seawater can take to reach aquifers lower than the Oxnard. The first is lateral invasion from the sea, as happened in the Oxnard aquifer. Since chemico-osmotic coupling is very low in aquifers, our theory provides no information on this process which cannot be deduced from ordinary hydraulic diffusion theory.

The second route is by one-dimensional downward diffusion of NaCl through the aquitard; the driving forces being the solute (NaCl) concentration drop across the aquitard and the hydraulic pressure drop which develops across the aquitard if there is pumping from the Mugu. As we deduced in Section III-D-1, there should be a fair amount of chemico-osmotic coupling in the Oxnard soil-NaCl system, so that ordinary solute diffusion theory is inadequate for describing the process. Hence we used our theory, which includes osmotic effects, to conduct a quantitative theoretical analysis of the process, and the results are presented in Figs. IV-1 to IV-8.

The problem solved was that of the one-dimensional diffusion of NaCl and water through a 30 foot thick aquitard under various boundary conditions. In all cases the initial conditions were a .03 normal NaCl concentration, and zero excess hydrostatic pressure throughout the aquitard and aquifers.

In mathematical terms for t = 0

$$
\left.
\begin{array}{l}
c_s = .03 \text{ normal} \\[20pt]
U \ = 0 \text{ feet of water}
\end{array}
\right\} \quad 0 \leqslant z \leqslant 30 \text{ feet}
$$

A slightly modified version of the program which solves the explicit form
of the finite difference equations, (c.f. III-B-2) with $\beta = 0.36$ and the
number of Z intervals equal to 12, was used for analysis of conditions
within the aquitard.

Two different cases were considered. The first was that of no
pumping from either aquifer. The second was that of pumping from the
Mugu aquifer, the Oxnard having presumably been abandoned after its
contamination by seawater. These two cases correspond to different
boundary conditions, and different R-coefficients, and will therefore
be discussed separately.

1. No Pumping

In the case of no pumping from either aquifer the boundary
conditions are for $t \geqslant 0$.

$c_S = 0.6$ normal $z = 0$

$c_S = 0.03$ normal $z = 30$ feet

$U = 0$ feet of water $z = 0$ and 30 feet

i.e., there is invasion of seawater in the Oxnard aquifer which causes
the NaCl concentration at the upper boundary ($z = 0$) of the aquitard to
increase from .03 to 0.6 normal, thus initiating the diffusion process.
The aquitard material was assumed to have the same chemico-osmotic
properties as the kaolinite which Olsen tested at low overburden
pressure (23), and the R-coefficients used were those calculated
in Section III-B-5 using Olsen's data

$R_1 = 1.0$

$R_2 = -0.6$

$R_3 = .001$

$R_4 = .001$

$R_5 = .001$

It is feasible to expect that the seawater diffusing in laterally along the Oxnard aquifer from the coastline might undergo a reduction in salt concentration as it moves inland and mixes with fresh water it encounters. If this were to happen, it would change the boundary conditions of our problem somewhat; and consequently it might change the nature of the ensuing diffusion. To investigate this possibility, an additional analysis was conducted assuming that the NaCl concentration in the Oxnard aquifer was 0.3 normal, i.e., half that of seawater.

To gain a feel for the influence of leakiness the aquitard soil, the case of 0.6 N NaCl concentration at the upper boundary was analyzed for a non-leaky soil ($R_1 = 1.0$, $R_2 = 0.6$, $R_3 = 0.0$, $R_4 = 0.0$ and $R_5 = .001$) and a perfectly leaky soil ($R_1 = 1.0$, $R_2 = 0.0$, $R_3 = .001$, $R_4 = .001$, $R_5 = .001$).

The results of these analyses are presented in Figs IV-1 to IV-5.

The results of the analysis for a non-leaky aquitard are shown in Figs. IV-1 and IV-2. Fig. IV-2 shows that there is no solute inflow.[*] This is to be expected if the aquitard is non-leaky, and implies that no contamination of the aquitard or Mugu aquifer would occur. Fig. IV-1 depicts the chemico-osmotic consolidation which would result if the aquitard were non-leaky, and Fig. IV-3 contains the corresponding pore pressure drop isochrones. The pore pressure drop isochrones, although the result of chemico-osmotic diffusion, are identical to those that would result if the process was an ordinary hydraulic diffusion process started by a pore pressure drop of 1 inch of water at the top surface of the aquitard. In other words the process is the same as an ordinary hydraulic diffusion process except that the driving force is chemical rather than physical in the form of an applied pressure to the water.

There is no salt flow in a non-leaky aquitard because solute cannot move or diffuse in response to drag coupling or "void ratio coupling"; consequently no solute concentration gradient can arise to cause solution to move due to chemico-osmotic coupling.

---

[*]
  Solute inflow is defined in Section III-B-2. Note also that initially the solute inflow is 17% not 0%. This is because there is initially a NaCl concentration of .03 normal in the aquitard, not 0 normal. In addition there is an inaccuracy inherent in the finite difference approximation method which causes initial values of solute inflow to be overestimated.
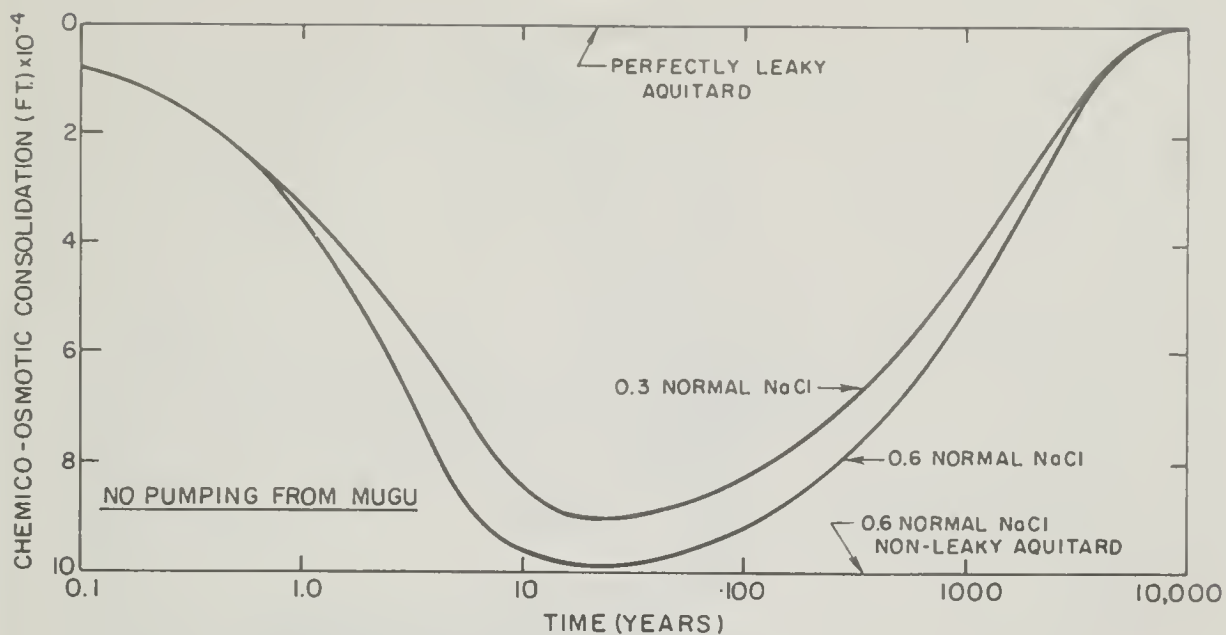
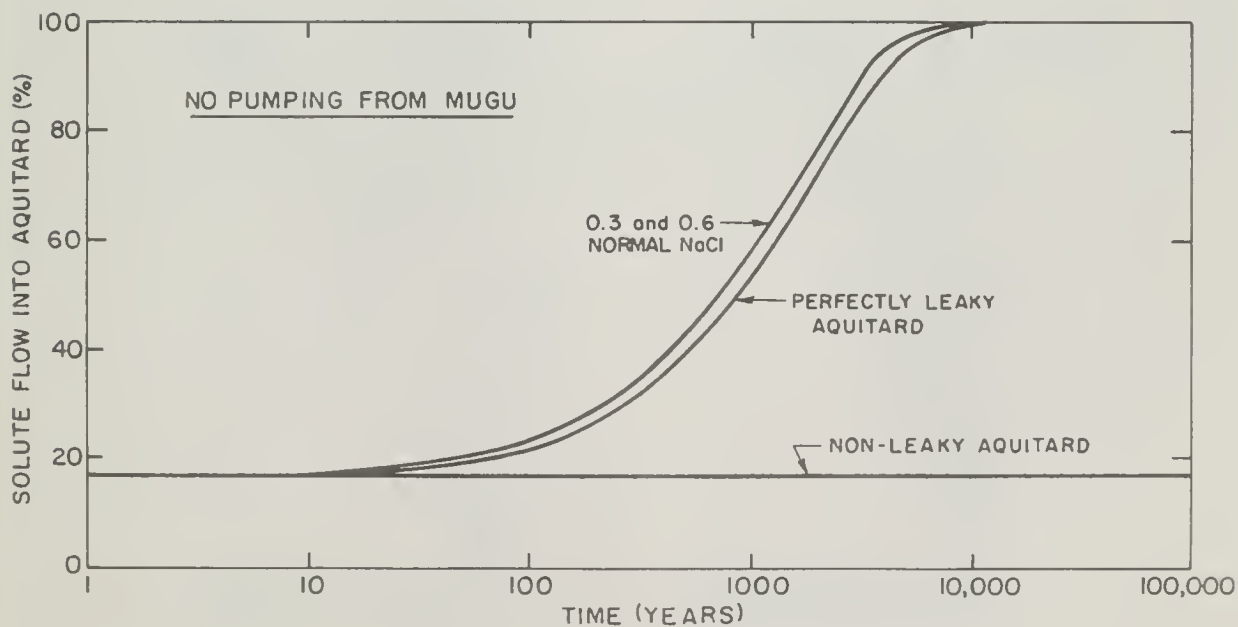Fig. IV-1. Chemico-osmotic consolidation in aquitard

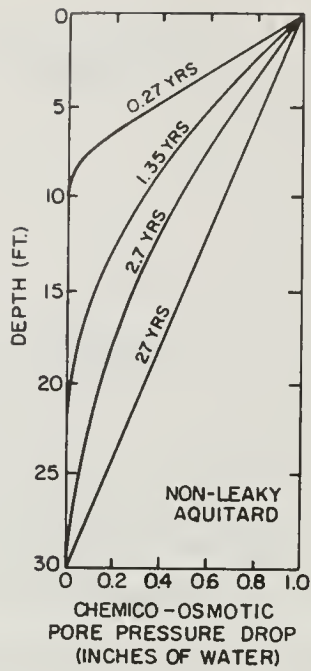Fig. IV-2. NaCl inflow curves - no pumping from Mugu

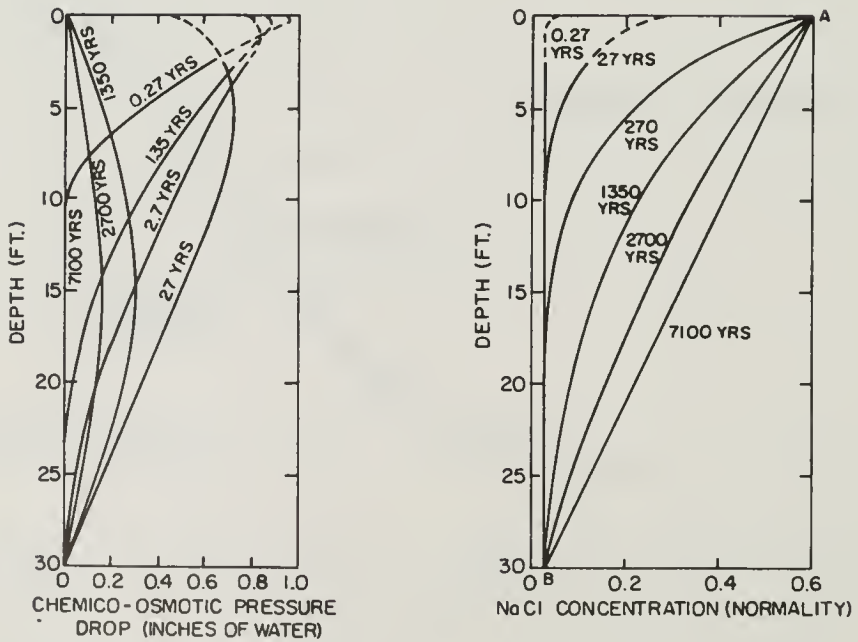Fig. IV-3.   Pore pressure isochrones - no pumping from Mugu

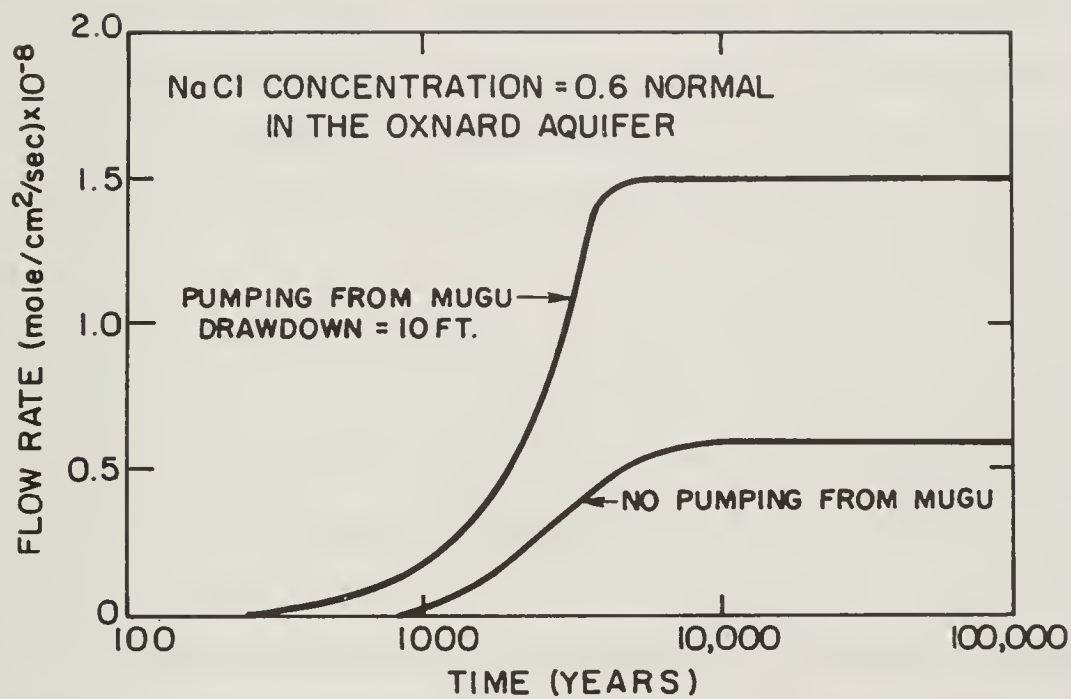Fig. IV-4.   Isochrones - no pumping from Mugu

Fig. IV-5. Downward diffusion of NaCl into Mugu aquifer

Fig. IV-1 indicates that the chemico-osmotic consolidation in the aquitard would reach a maximum value of .001 feet in about 25 years. This amount is half of the value estimated in the previous section. The reason for this is that the equilibrium pore pressure drop isochrone in Fig. IV-3 varies linearly from .001 inches of water at the top of the aquitard to zero at the bottom of the aquitard. Hence the average decrease in effective stress at equilibrium is 0.5 inches of water (.02 psi) rather than 1 inch of water (.04 psi) as assumed in the previous section.

Figs. IV-1 to IV-5 present the results of the analyses for the actual aquitard soil. The curves in Fig. IV-1 show that the chemico-osmotic consolidation increases to a maximum in about 25 years, after which rebound occurs. Physically the NaCl solute concentration increase at the boundary chemico-osmotically sucks water from the aquitard, and causes consolidation until "equilibrium" is reached after about 25 years. After 25 years the diffusion of NaCl into the aquitard begins to become significant, and it chemico-osmotically sucks water back into the aquitard, causing the aquitard to swell. Final equilibrium is attained after about 7000 years when the rate of NaCl diffusion into the aquitard reaches a steady-state.

Note that the chemico-osmotic consolidation curves in Fig. IV-1 have been drawn assuming that the coefficient of compressibility is the same for both consolidation and swell. Consequently the chemico-osmotic consolidation is zero at equilibrium (i.e., after about 5000 years). However, (as discussed in Section III-C-1) real soils exhibit a lower

coefficient of compressibility for swelling than consolidation. In

other words real soils will swell or rebound less than they consolidate

under the same change in pore pressure. Our analyses of chemico-osmotic

consolidation in the aquitard have not incorporated this aspect of

real soil behavior. If they did, the result would be that the curves

in Fig. IV-1 for the aquitard soil would consolidate to .001 feet in

about 25 years, and thence rebound to an amount less then .001 feet

in about 5000 years. In other words the aquitard will chemico-osmotically

consolidate for about 25 years and then swell to an equilibrium thickness

less than the original thickness.

The maximum amount of chemico-osmotic consolidation is slightly

less for an upper boundary NaCl concentration of 0.3 normal than for

0.6 normal. In both cases the maximum amount of chemico-osmotic con-

solidation induced is insignificant.

There is no chemico-osmotic consolidation if there is no chemico-

osmotic coupling. Analysis confirms this belief as can be seen in

Fig. IV-1.

Fig. IV-2 shows that the rate of NaCl inflow is slightly higher

in the actual aquitard than it would be in a perfectly leaky aquitard

subject to the same boundary conditions. To understand this requires

a discussion of the actual physical mechanisms comprising the chemico-

osmotic diffusion at Oxnard:

a. The increase of NaCl concentration at the upper surface of

the aquitard induces a chemico-osmotic pressure drop just beneath the

upper surface of the aquitard.

b.   This drop in pore water pressure at the surface causes water within the aquitard to diffuse upward and out of the aquitard. Consequently the pressure isochrones in Fig. IV-4 show the pore pressure dropping in the aquitard and the corresponding chemico-osmotic consolidation in Fig. IV-1 shows consolidation increasing with time up to about 25 years.

c.   The NaCl concentration isochrones in Fig. IV-4 show that NaCl starts slowly diffusing into the aquitard at the start of the process. Because of this there is a chemico-osmotic reduction in pore pressure drop near the upper boundary of the aquitard as indicated by the isochrones in Fig. IV-3. As time passes the rate of flow of NaCl into the aquitard increases so that the pore pressure drop near the upper boundary of the aquitard decreases further. This is the reason why the 27th year pore pressure drop isochrone in Fig. IV-4 drops to zero at the upper boundary of the aquitard, while the corresponding isochrone in Fig. IV-3 (for a non-leaky aquitard) shows no such drop.

d.   The result of the reduction in pore pressure drop at the upper boundary of the aquitard is that a counter hydraulic pressure gradient is created which causes seawater to diffuse into the aquitard. In an aquitard where there was no chemico-osmotic coupling (i.e., in a perfectly leaky aquitard) this effect would not occur. The result of this chemico-osmotically induced inflow of seawater therefore is to speed up the rate of inflow of NaCl above that occurring in a perfectly leaky aquitard. Fig. IV-2 shows that there is not much difference between the rate of solute inflow in the actual aquitard and rate of solute inflow in a perfectly leaky aquitard. In other words the rate

of contamination of the aquifer is almost the same as if the aquifer were perfectly leaky.

e. As the process proceeds, more NaCl diffuses into the aquitard, and chemico-osmotically causes more seawater to diffuse in. This inflow of NaCl and seawater which both contaminate the aquitard, becomes noticeable after about 25 years (see Fig. IV-2), eventually equilibrates after about 7000 years. Fig. IV-2 shows that the curve of degree of inflow of NaCl into the aquitard is the same for upper boundary NaCl concentrations of both 0.3 and 0.6 normal. From a practical point of view this implies that there is twice as much NaCl contaminating the aquifer if the upper boundary NaCl concentration is 0.6 normal than there is if the upper boundary NaCl concentration is 0.3 normal.

The NaCl concentration isochrones in Fig. IV-4 indicate that as the diffusion proceeds, a NaCl concentration gradient builds up at the bottom surface of the aquitard. This gradient induces a downward diffusional flow of NaCl into the Mugu aquifer. Consequently the Mugu begins to become contaminated. The downward diffusional flow of NaCl has been calculated assuming a diffusion constant of 10^{-5} cm^2/sec in the aquitard, and is plotted in Fig. IV-5 for an upper boundary NaCl concentration of 0.6 normal. For a non-leaky aquitard the flow rate would be zero. For a perfectly leaky aquitard the flow rate would be slightly less than for the real aquitard. The reason is the same as the reason for the NaCl inflow rate being slightly less in a perfectly leaky aquitard. For an upper boundary NaCl concentration of 0.3 normal, the flow rate would be half that shown in Fig. IV-5. Fig. IV-5 shows

that contamination of the Mugu aquifer begins after about 800 years and reaches its maximum rate after about 7000 years.

The whole process reaches equilibrium after about 7000 years, at which point there is no excess pore pressure gradient across the aquitard, but there is a finite and uniform NaCl concentration gradient across the aquitard. This NaCl concentration gradient causes a downward flow of NaCl into the Mugu aquifer (as shown in Fig. IV-5) and an upward flow of water into the Oxnard aquifer. Using equation II-17a we calculate that this upward flow of water is about 10^{-5} gallons/day/foot^2.

2. Pumping from the Mugu Aquifer

The second case analyzed was that of seawater invasion in the Oxnard aquifer and pumping of fresh water out from the Mugu aquifer.

The boundary conditions are for $t \geqslant 0$

$$c_s = 0.6 \text{ normal} \qquad z = 0$$

$$c_s = 0.03 \text{ normal} \qquad z = 30 \text{ ft}$$

$$U = 0 \text{ ft of water} \qquad z = 0 \text{ ft}$$

$$U = -10 \text{ ft of water} \qquad z = 30 \text{ ft}$$

i.e., we are assuming that the drawdown due to pumping is 10 feet of water. This drawdown is considerably greater than the chemico-osmotic pressure drop (1 inch of water) obtained in the previous case. The

R-coefficients, R_2, R_3, and R_5 contain the factor U_{max} (c.f. equations III-1), which is a measure of the maximum pressure drop occurring during the diffusion process. U_{max} is larger by the ratio 10 feet of water/1 inch of water for the case of pumping from the Mugu. To achieve the degree of accuracy required in this analysis we can take this ratio as 100. R_2 is inversely proportional to U_{max} and is therefore divided by this ratio to become $- 0.6/100 = - .006$. R_3 and R_5 are directly proportional to U_{max}, and are therefore multiplied by this ratio. They were both equal to .001 in the previous and hence become .001 x 100 = 0.1 in this case. Thus the R-coefficients used in this case are

$$R_1 = 1.0$$

$$R_2 = -.006$$

$$R_3 = 0.1$$

$$R_4 = 0.001$$

$$R_5 = 0.1$$

To provide additional information, analysis was also made for drawdowns of 5 and 10 feet of water. The results of these two analyses are depicted in Figs. IV-6 to IV-8. Several comments seem relevant.

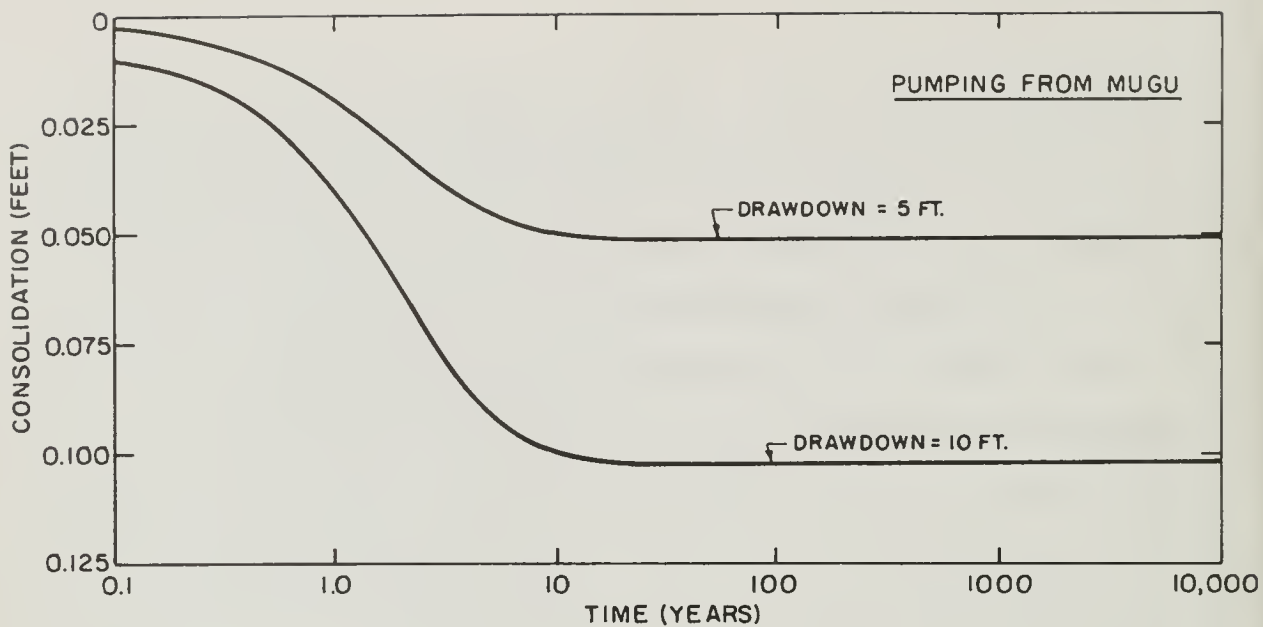a. Fig. IV-6 shows that consolidation occurs for about 25 years

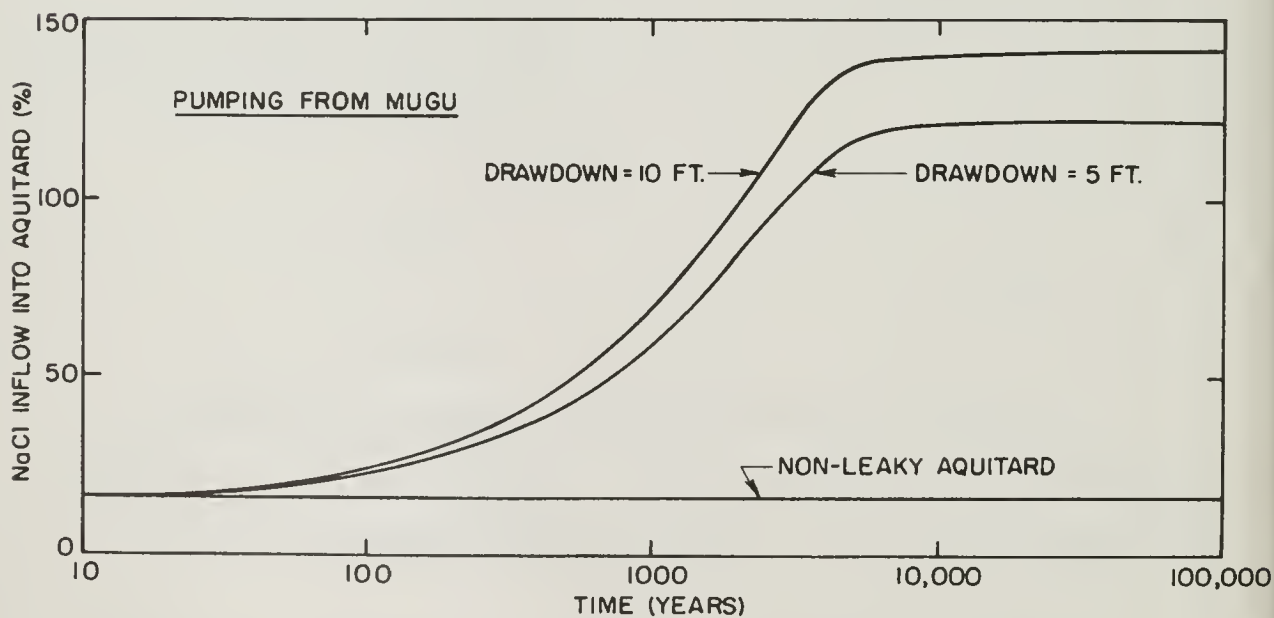Fig. IV-6.   Consolidation in aquitard
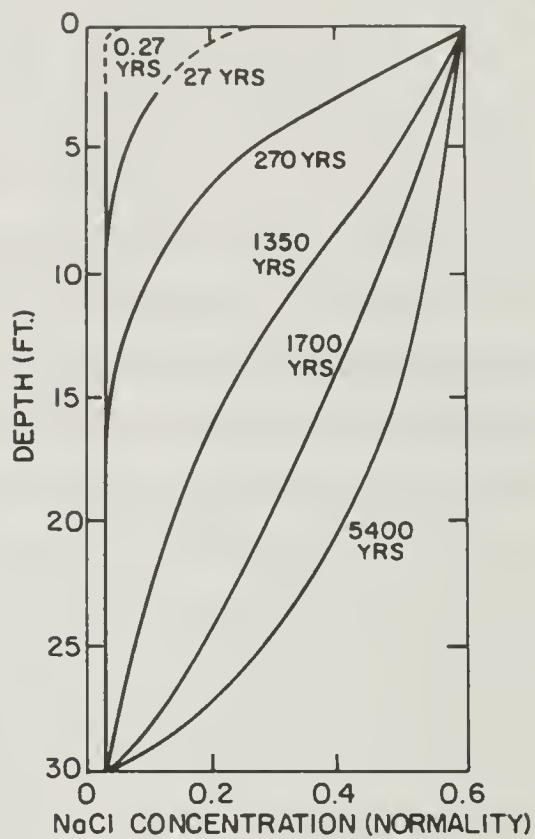

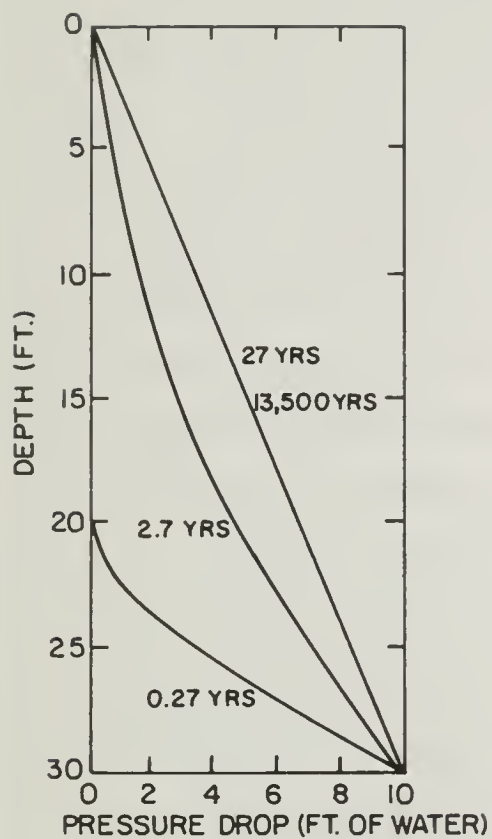Fig. IV-7.   NaCl inflow curves - pumping from Mugu

Fig. IV-8. Isochrones - pumping from Mugu

at which time it reaches, and thenceforth remains at a maxumum value. For drawdowns of 5 and 10 feet, the maximum consolidations are about 0.05 and 0.1 feet respectively. These consolidations are relatively small, but are about one hundred times as great as the chemico-osmotic consolidation discussed earlier. Indeed chemico-osmotic consolidation does occur in this case, and at the same rate as the consolidation due to pumping (see Section III-C-1). However chemico-osmotic consolidation constitutes only about one hundredth of the consolidation shown in Fig. IV-6, so that chemico-osmotic pressure reduction is an infintesimal fraction of the pressure drop shown in Fig. IV-8. In fact analyses conducted for a "perfectly leaky" aquitard and a non-leaky aquitard resulted in exactly the same consolidation curves as those in Fig. IV-6. Indicating again that for this sediment chemico-osmotic consolidation should be negligible compared to consolidation due to pumping from the Mugu aquifer.

b. The equilibrium pressure drop isochrone in Fig. IV-8, which is for a drawdown of 10 feet in the Mugu, represents a downward flow rate of water of about 10^{-2} gallons/day/foot^2 (10^{-6} cm/sec). This is in the opposite direction to, and far larger than the chemico-osmotically induced upward flow of about 10^{-5} gallons/day/foot^2 generated in the previous case.

c. The equilibrium NaCl concentration isochrone in Fig. IV-8 (5400 years) is significantly different from that in Fig IV-4 (7100 years). To explain this discrepancy we consider the flow of NaCl at equilibrium. There are two components of NaCl flow. The first

is diffusion under a NaCl concentration gradient, and the second is flow due to drag coupling. According to the law of conservation of mass these two components have to add up to the same value at every point in the aquitard at equilibrium, i.e., there is no storage or creation of NaCl within the aquitard after equilibrium is reached.

At equilibrium there is a constant downward flow of water of 10^{-2} gallons/day/foot^2 at all points in the aquitard. Hence the component of downward flow of NaCl due to drag coupling is proportional only to NaCl concentration in the aquitard. The NaCl concentration is high at the upper surface of the aquitard (0.6 normal) and much smaller at the lower surface (.03 normal). Therefore the component of downward flow of NaCl due to drag coupling is high near the top surface of the aquitard, and much smaller near the lower surface. This in turn implies that the component of downward NaCl flow due to diffusion under the NaCl concentration gradient is low near the top surface and much higher near the bottom surface of the aquitard (because the total downward flow of NaCl is a constant after equilibrium is reached). And consequently the NaCl concentration gradients should be low near the bottom surface of the aquitard.

Hence the equilibrium NaCl concentration isochrone in Fig. IV-8 should be concave upward and not linear like that in Fig. IV-4.

From a physical point of view: The downward flow of water due to pumping drags NaCl downward and increases the NaCl concentration in the aquitard above that in the case of no pumping.

The equilibrium NaCl concentration isochrone in Fig. IV-4

is linear because there is no drag coupling, since the pore water pressure gradient is zero at equilibrium in the case of no pumping from the Mugu.

d. This downward flow of NaCl due to drag coupling increases the rate of diffusional flow of NaCl into, and hence the rate of contamination of, the aquitard. This can be seen by comparing Fig. IV-2 and Fig. IV-7. The effect is slightly more pronounced for a drawdown of 10 feet than for a drawdown of 5 feet, the reason being that a higher pumping head causes a greater downward flow of solution and hence a higher downward flow of NaCl by drag coupling. From Fig. IV-7 we observe that contamination of the aquitard begins to be noticeable after about 25 years, and reaches a maximum after about 5000 years if the drawdown is 10 feet.

e. Fig. IV-5 shows that the rate of contamination of the Mugu aquifer is also speeded up by pumping from the Mugu. Here again it is the downward flow of NaCl by drag coupling which is responsible for the effect. The effect increases as the drawdown increases.[*] Fig. IV-5 shows that the contamination of the Mugu commences after about 250 years and reaches its maximum rate after about 5000 years if the drawdown is 10 feet.

Analysis of the case of pumping from the Mugu for drawdowns of both 5 feet and 10 feet, assuming a perfectly leaky aquitard, yielded solute inflow curves exactly the same as those in Fig. IV-7, and NaCl concentration isochrones exactly the same as those in Fig. IV-8. Hence

---

[*]
 The curve for a drawdown of 5 feet is omitted from Fig. IV-5 in order not to clutter the diagram.

the rate of contamination of the aquitard and the Mugu aquifer is exactly the same as if the aquitard was perfectly leaky. If, on the other hand, the aquitard was non-leaky, there would be no contamination of either the aquitard (c.f. Fig. IV-7) or the Mugu.

3. Summary

In summary we note that for the aquitard between the Oxnard and Mugu aquifers:

a. The maximum amount of chemico-osmotic consolidation is about .001 feet which is negligibly small. The amount of consolidation induced by pumping from the Mugu aquifer is about .1 foot. Both cases reach 100% consolidation in about 250 years.

b. The rate of inflow of NaCl into, or rate of contamination of the aquitard is almost the same as if the aquitard were perfectly leaky, and is increased by pumping from the Mugu aquifer. If there is no pumping from the Mugu aquifer, contamination starts to become significant after about 25 years and reaches its maximum in about 7000 years. If there is a drawdown of 10 feet in the Mugu, contamination starts to be significant after about 25 years and reaches a maximum in about 5000 years.

c. The rate of inflow of NaCl into, or rate of contamination of the Mugu is almost the same as if the aquitard were perfectly leaky, and is increased by pumping from the Mugu. If there is no pumping from the Mugu, contamination begins after about 800 years, and reaches its maximum rate in about 7000 years. If there is a drawdown of 10 feet

in the Mugu, the contamination begins after about 250 years and reaches its maximum rate in about 5000 years.

d. The rate of contamination of the aquitard is proportional to the NaCl concentration in the Oxnard aquifer. (Figs. IV-2 and IV-7 are plotted in terms of percentage of NaCl inflow rather than the actual amount of inflow.) Similarly the rate of contamination of the Mugu aquifer is proportional to the NaCl concentration in the Oxnard aquifer. The reason for this is that the flow of NaCl into the Mugu is almost totally due to diffusion, and diffusional flow is proportional to the NaCl concentration gradient, which in this case is proportional to the NaCl concentration in the Oxnard aquifer.

e. If there is no pumping, there is a chemico-osmotically induced upward flow of water in the aquitard, which builds up to a very small value of about 10^{-5} gallons/day/foot^2 in about 7000 years. If there is a drawdown of 10 feet in the Mugu, there is a downward flow of water in the aquitard which builds up to a maximum value of 10^{-2} gallons/day/foot^2 in about 25 years.

f. We observe that from a practical point of view there is no chemico-osmotic effect of any significance in the aquitards at Oxnard. The aquitards can be regarded as perfectly leaky membranes i.e., non semi-permeable.

g. As mentioned previously our analyses employ laboratory measurements of hydraulic permeability and coefficient of consolidation which are lower than those measured in the field. Consequently field consolidation, both chemico-osmotic, and that due to pumping from the

Mugu, will occur more rapidly than estimated in our analyses. Another effect is that chemico-osmotic coupling is reduced (because R_2 is inversely proportional to hydraulic permeability), so that there will be less chemico-osmotic consolidation than estimated. In addition the aquitard is not a homogeneous deposit of clay. Rather it is poorly defined, with many silt and sand lenses between clay lenses. The silt and sand lenses are less compressible than the clay tested in the laboratory. This tends to make our estimates of amount of consolidation, both chemico-osmotic, and that due to pumping from the Mugu, too large. It also reduces flow of NaCl by drag coupling because the drag coupling coefficient, R_3 is directly proportional to the coefficient of compressibility, a_v (see equation III-1). Consequently our analyses predict too rapid a flow of NaCl into or contamination of the aquitard and the Mugu aquifer.

D. PRACTICAL IMPLICATIONS OF THE ANALYSIS

From a practical point of view the most significant results of the analysis are:

1. Chemico-osmotic effects can be neglected at the Oxnard site.

2. For both cases analyzed there should be no significant contamination of the aquitard for about 25 years. Contamination of the aquitard reaches a maximum in about 7000 years if there is no pumping from the Mugu aquifer, and in a considerably shorter time if there is pumping from the Mugu.

3. Contamination of the Mugu takes slightly longer, beginning after about 800 years and reaching its maximum rate in about 7000

-559-

years. Pumping from the Mugu speeds up this contamination rather
significantly.

4. Due to the fact that we employed laboratory measured parameters
which are different from field measurements, our analyses overestimate
the amount of consolidation. They also estimate too slow a rate of
consolidation and too high a rate of contamination of the aquitard
and the Mugu aquifer.

Furthermore the above analyses take no account of possible transfer
of salt by direct communication through fissures, sand and silt lenses
etc. in the aquitard.

The effects of NaCl leaching on the physical properties of the
sediment have not been considered. As discussed in Chapter VI of the
main report, measurements have shown that these effects are negligible.

It should also be mentioned that these results make no claim to
generality. For example the deeper aquitards might exhibit a far higher
degree of chemico-osmotic coupling and hence act as more efficient
barriers between aquifers. If the solute were a radioactive waste or
some other form of disposed chemical, the amount and consequences of
chemico-osmotic coupling could also be quite different.

Each site has its own peculiarities, chemico-osmotic characteristics
and boundary conditions. These should be treated on their own merits
until we have greater experience with their relative effects.

V. SUMMARY, CONCLUSIONS, AND RECOMMENDATIONS

The objectives of this report were to investigate the nature and significance of chemico-osmotic effects in fine-grained soils.

A review of the literature revealed that there is likely to be a small but finite osmotic effect in most fine grained soils. This chemico-osmotic (or osmotic) effect manifests as a coupling between the flows of solvent and solute in the pores of a soil. The magnitude of this effect should increase as void ratio decreases, size of clay fraction increases and molecular weight of solute increases.

A theory describing the simultaneous flow of solute and solvent under the action of solute concentration and hydrostatic pressure gradients in soils was presented. The theory consists of two second order simultaneous differential equations, solution to which enables one to express solute concentration and pore water pressure as functions of time and position in the soil mass considered. The differential equations were developed by applying the principles of irreversible thermodynamics and the law of conservation of mass to an open, continuous system of one solute and solvent in the pores of a compressible medium. The following assumptions were made:

(1) Isotropy and homogeneity

(2) Isothermal conditions

(3) No electrical or electro magnetic gradients

(4) No ion exchange during diffusion

(5) The solute acts as a single species

(6) The solution is dilute enough for "ideal solution" relationships

to be valid and for the flow of solvent and solution to be considered

synonymous

(7) The pores of the medium are fully saturated

(8) The postulates of irreversible thermodynamics are applicable

to the process.

The theory was tested against available data and it was found that

the specialized one dimensional form of the diffusion equations

$$\frac{\partial U}{\partial t} = c_v \frac{\partial^2 U}{\partial y^2} + \frac{1 + e}{a_v} k_{hc} \frac{\partial^2 c_s}{\partial y^2} \tag{V-1a}$$

and

$$e \frac{\partial c_s}{\partial t} = \frac{1 + e}{\gamma_w} k_{ch} \frac{\partial}{\partial y} \left(x \frac{\partial U}{\partial y} \right) + (1 + e) D' \frac{\partial^2 c_s}{\partial y^2} - a_v c_s \frac{\partial U}{\partial t} \tag{V-1b}$$

where U = hydrostatic pressure

  c_s = solute concentration

  t = time

  c_v = coefficient of consolidation

  y = linear distance variable

  e = void ratio

  a_v = coefficient of compressibility

k_{hc}, k_{ch} = coupling coefficients

  γ_w = specific weight of water

  x = dimensionless solute concentration

  $D' = D + c_s k_{hc}$

and D = diffusion coefficient

-562-

include the Terzaghi diffusion equation and the solute diffusion

equation (Fick's Law) as limiting cases. The theory is consistent

with van't Hoff's Law, and also provides a framework for analyzing

and interpreting previous experimental work by Olsen (22,23) on the

simultaneous flow of salt and water in soils.

Consideration was given to the physical significance of the

phenomenological coefficients appearing in the diffusion equations.

It was shown that there are three types of coupling between the flow

of solute and solvent in a soil: Chemico-osmotic coupling, which is

a coupling between solute concentration gradient and flow of solvent;

drag coupling which is a coupling between hydrostatic pressure gradient

and flow of solute; and void ratio coupling which is a coupling between

void ratio change and flow of solute. Chemico-osmotic coupling increases

and drag coupling decreases as void ratio decreases, size of clay fraction

increases and molecular weight of solute increases. Drag coupling and

void ratio coupling increase as soil compressibility increases.

The theory was used as a basis for a computer investigation of the

one dimensional diffusional flow of solute and solvent in a soil sample

subjected to a sudden boundary solute concentration increase. Equations

V-1 were written in finite difference form and used to calculate solute

concentration isochrones, pore pressure isochrones and the resulting

consolidation (chemico-osmotic consolidation) in the soil sample. The

analyses included consideration of different initial and boundary solute

concentrations, and hydrostatic pressures, as well as different degrees

of chemico-osmotic, drag and void ratio coupling. There are very little

data available on the coupling coefficients (see Equations V-1). Ranges

of values for use in the theoretical analysis were deduced from the available data and also computed using reasonable assumed values for the other soil properties.

The results of the analysis indicate that:

(1) Solute inflow into the sample is a smooth process building steadily to equilibrium.

(2) Chemico-osmotic consolidation builds rapidly and smoothly to a maximum followed by rebound to an equilibrium thickness less than the original sample thickness.

(3) Chemico-osmotic consolidation reaches a maximum value at a time t_c given by

$$t_c = 2.0 \frac{H^2}{c_v} \qquad\qquad V-2$$

i.e., t_c depends only on the drainage path length H and the coefficient of consolidation c_v.

(5) Chemico-osmotically induced consolidation reaches a maximum value long before solute inflow into the sample becomes significant.

(5) The maximum amount of chemico-osmotic consolidation increases with increase in boundary solute concentration, increase in chemico-osmotic coupling and increase in soil compressibility.

(6) The magnitude of the chemico-osmotic effect increases with increase in drag coupling and chemico-osmotic coupling, but is not effected noticeably by change in void ratio coupling.

(7) The time taken for the process to attain equilibrium increases as drag coupling and diffusion constant decrease, and is not effected by change in void ratio coupling.

The theory was used in finite difference form to conduct computer analyses of the coupled flows of NaCl and water in a horizontal fine-grained aquitard at a site in Oxnard, California. The flows were induced by the lateral invasion of sea water in a contacting aquifer above the aquitard. Data on site conditions, including a physical description of the profile, and soil and pore fluid properties were taken from Chapter VI of the main report. Numerical values for the coupling coefficients (see equation V-1) were estimated from a comparison of the aquitard soil properties and the properties of a kaolinite for which Olsen measured coupling coefficients (22 23). The purpose of the investigation was to determine the relative effects of chemico-osmotic coupling and pumping drawdown in the aquifer beneath the aquitard on surface subsidence and rate of NaCl contamination of the aquitard and aquifer beneath the aquitard.

The results of the analyses indicated:

(1) Chemico-osmotic coupling is likely to cause only minor surface subsidence (.001 ft) and does cause the aquitard to become contaminated slightly more rapidly than if there was no chemico-osmotic coupling. However, both effects are negligibly small, and from a practical point of view it is adequate to neglect chemico-osmotic coupling at the Oxnard site.

(2) Assuming no fissures and no significant property changes with time in the aquitard clay, and no pumping from the aquifer below the aquitard, NaCl contamination of the aquitard should be negligible for about 25 years. After this time contamination becomes significant reaching a maximum in about 7000 years. Contamination of the aquifer

below the aquitard begins after about 800 years and reaches its maximum
rate of contamination in about 7000 years.

(3) Pumping of water from the aquifer below the aquitard increases
both surface subsidence and rates of contamination of aquitard and
aquifer below the aquitard. A drawdown of 10 feet of water may cause
a surface subsidence of 0.1 feet. Contamination of the aquitard becomes
significant after about 25 years and reaches a maximum in about 7000
years. Contamination of the aquifer below the aquitard begins after
about 250 years and reaches a maximum in about 5000 years.

(4) Both chemico-osmotic surface subsidence and surface subsidence
due to pumping from the aquifer below the aquitard reach maxima in
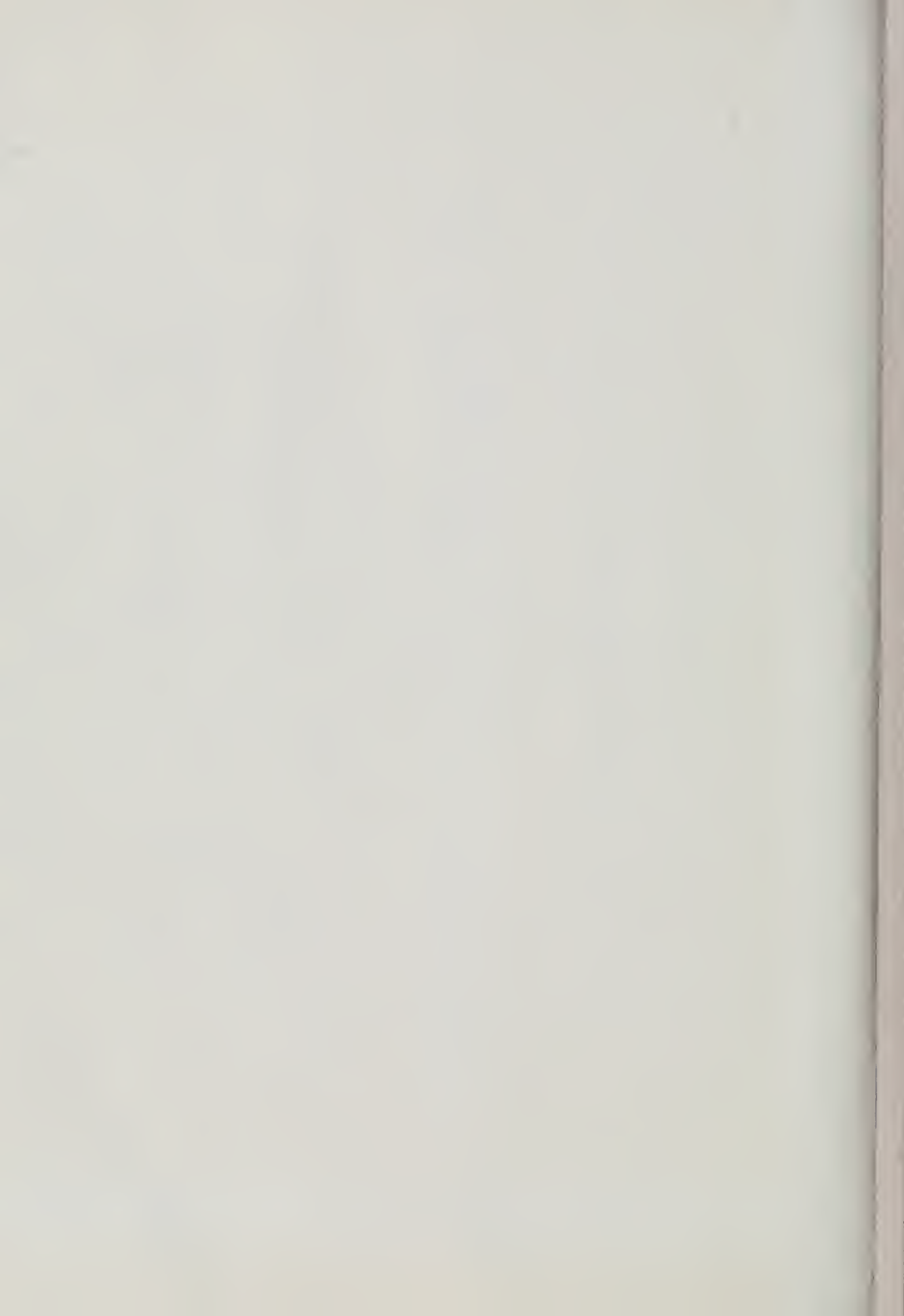about 25 years.

REFERENCES

1. Abd-El-Aziz, M. and Taylor, S. A. "Simultaneous flow of water and
    salt through unsaturated porous media: I. Rate equations", Proc.
    Soil Sci. Soc. Amer., v. 29, n. 2, p. 141, 1964.

2. Collatz, L. The numerical treatment of difference equations,
    Springer-Verlag, Berlin, 1959.

3. "Corn Starch" - a technical pamphlet issued by the Corn Industries
    Research Foundation, Inc., Washington, D. C. 1964.

4. deGroote, S. R. Thermodynamics of Irreversible Processes, North
    Holland, Amsterdam, 1952.

5. Findlay, A. Osmotic Pressure, Songmans Green and Company, New York,
    1913.

6. Greenberg, J. A. "An investigation of some parameters affecting the
    rate of heave in partly saturated soils", M. Sc. Thesis, University
    of the Witwatersrand, South Africa, 1966.

7. Grim, R. E. Clay Mineralogy, McGraw Hill, New York, 1953.

8. Houston, W. N. "Formation Mechanisms and Property Interrelationships
    in Sensitive Clays", Ph. D. Thesis, University of California,
    Berkeley, 1968.

9. Houston, W. N. - 270L Lecture Notes - Graduate course on Soil
    Testing, University of California, Berkeley, 1969.

10. Katchalsky, A. and Curran, P. F. Nonequilibrium Thermodynamics in
    Biophysics, Harvard University Press, 1967.

11. Kedem, D. and Katchalsky, A. "Thermodynamics analysis of the
    permeability of biological membranes to nonelectrolytes", Biochim,
    Biophys. Acta, v. 27, p. 229-246, 1958.

12. Kemper, W. and Van Schaik, K. "Diffusion of salts in clay-water
    systems", Proc. Soil Sci. Soc. Am., v. 30, p. 534.

13. Kerr, R. W. (ed.) Chemistry and Industry of Starch, Academic Press
    New York, 1950.

14. Kirkwood, J. G. "Transport of ions through bilogical membranes from
    the standpoint of irreversible thermodynamics" a paper in Ion
    Transport Across Membranes edited by H. Clarke, Academic Press,
    New York, 1954.

15. Lai, T. and Mortland, M. "Diffusion of ions in Bentonite and Vermiculite", <u>Proc. Soil Sci. Soc. Am.</u>, v. 25, p. 353.

16. Lax, P. D. and Richtmeyer, R. D. "Survey of Stability of Linear Finite difference equations", <u>J. Soc. Indus. Appl. Math.</u>, v. 4, p. 20-37, 1956.

17. Leonards, G. A. Foundation Engineering, Purdue University Press, 1967.

18. Metten, U. <u>Desalination by Reverse Osmosis</u>, M. I. T. Press, Cambridge, Massachusetts, 1966.

19. Mitchell, J. K. "Physical and hydrological properties of the aquitard layers in the Oxnard California area", Department of Civil Engineering Institute of Transportation and Traffic Engineering, University of California, Berkeley, TE Report 69-2, August 1969.

20. Mokady, R. S. and Low, P. F. "Simultaneous transport of water and salt through clays: I. Transport mechanisms", <u>Soil Sci.</u> v. 105, n. 2, 1966.

21. National Starch Products Inc. Technical Service Bull. No. 131, Rev. 1970.

22. Olsen, H. "Liquid movement through Kaolinite under hydraulic, electrical and osmotic gradients" to appear in Amer. Ass. Petr. Geol. volume on Membrane and Mass Transport Phenomena in the Geological Environment, ed. F. Berry, 1970, in press.

23. Olsen, H. "Simultaneous fluxes of liquid and charge in saturated Kaolinite" <u>Soil Sci. Soc. Am. Proc.</u>, v. 33, n. 3, May-June 1969.

24. Paduana, J. A. - "The effects of type and amount of clay on the strength and creep characteristics of clay-sand mixtures", University of California, Berkeley, January 1966.

25. Scott, Ronald F., <u>Principles of Soil Mechanics</u>, California Institute of Technology Press, 1962.

26. Spiegler, K. S., <u>Principles of Desalination</u>, Academic Press, New York, 1966.

27. Terzaghi, K., <u>Theoretical Soil Mechanics,</u> John Wiley and Sons, Inc. New York, 1959.

28. Tuwiner, S. B., <u>Diffusion and Membrane Technology</u>, Rheinhold Publishing Corporation, New York, 1962.

29.   Waldron, L. J. and Manbeian, T., "Moisture Characteristics by Osmosis" <u>Soil Sci.</u>, October 1970.

30.   Wan, Denis T. Y. "Consolidation of Soils by Electro-Osmosis", Ph. D. Thesis, University of California, Berkeley 1970.

31.   Wu, T. H. "Soil Mechanics", Allyn and Bacon, Inc., Boston 1967.